United States
Environmental Protection
Agency

Environmental Research
Laboratory
Duluth MN 55804

EPA-600/9-80-033
July 1980

Research and Development

EPA

Proceedings of the Second American-Soviet Symposium on the Use of Mathematical Models to Optimize Water Quality Mangement

RESEARCH REPORTING SERIES

Research reports of the Office of Research and Development, U.S. Environmental Protection Agency, have been grouped into nine series. These nine broad categories were established to facilitate further development and application of environmental technology. Elimination of traditional grouping was consciously planned to foster technology transfer and a maximum interface in related fields. The nine series are:

1. Environmental Health Effects Research
2. Environmental Protection Technology
3. Ecological Research
4. Environmental Monitoring
5. Socioeconomic Environmental Studies
6. Scientific and Technical Assessment Reports (STAR)
7. Interagency Energy-Environment Research and Development
8. "Special" Reports
9. Miscellaneous Reports

This document is available to the public through the National Technical Information Service, Springfield, Virginia 22161.

EPA-600/9-80-033
July 1980

PROCEEDINGS OF THE SECOND AMERICAN-SOVIET SYMPOSIUM ON THE USE OF MATHEMATICAL MODELS TO OPTIMIZE WATER QUALITY MANAGEMENT

Bloomfield Hills, Michigan, USA
August 27-30, 1979

Edited by

Wayland R. Swain
and
Virginia R. Shannon

ENVIRONMENTAL RESEARCH LABORATORY
OFFICE OF RESEARCH AND DEVELOPMENT
U.S. ENVIRONMENTAL PROTECTION AGENCY
DULUTH, MINNESOTA 55804

DISCLAIMER

This report has been reviewed by the Large Lakes Research Station, Environmental Research Laboratory-Duluth, Grosse Ile, Michigan, U.S. Environmental Protection Agency, and approved for publication. Mention of trade names or commercial products does not constitute endorsement or recommendation for use.

FOREWORD

The Environmental Research Laboratory-Duluth is concerned with the effects of pollutants on freshwater ecosystems, particularly the Laurentian Great Lakes. The development and verification of mathematical models describing the transport, fate and effects of pollutants in freshwater ecosystems are carried out at the Large Lakes Research Station at Grosse Ile, Michigan.

A part of this development, calibration and verification activity has been carried forward in cooperation with scientific personnel from the Soviet Union under the section entitled, Prevention of Pollution of Lakes and Estuaries under the Water Pollution Portion of the US-USSR Joint Agreement on Cooperation in the Field of Environmental Protection. The contributions to new knowledge contained in this volume clearly demonstrates the utility of joint scientific collaborations on an international basis.

Norbert Jaworski, Ph.D
Director
Environmental Research Laboratory
Duluth

PREFACE

This volume contains the proceedings of the papers presented at the Second US-USSR Symposium on the Use of Mathematical Models to Optimize Water Quality Management. All of the papers were presented either in English or in Russian with simultaneous interpretation into the corresponding language at the Cranbrook Institute of Science in Bloomfield Hills, Michigan, USA during August 27-30, 1979.

Identical copies of this volume are being simultaneously published in the Russian language under the direction of Dr. A.M. Nikavorov, Director of the Institute for Hydrochemistry at Rostov-on-Don in the USSR. This joint bilingual publication represents a reaffirmation of the continuing commitment pledged by both countries to cooperative environmental activities.

INTRODUCTION

The Joint US-USSR Agreement on Cooperation in the Field of Environmental Protection was established in May of 1972. These proceedings result from one of the projects, Project 02.02-12, Effects of Pollutants on Lakes and Estuaries.

As knowledge related to fate and transport of pollutants has grown, it has become increasingly apparent that local and even national approaches to solving pollution problems are insufficient. Not only are the problems themselves frequently international, but an understanding of alternate methodological approaches to the problem can avoid needless duplication of efforts. This expansion of interest from a local and national framework represents a logical and natural maturation from the provincial to a global concern for the environment.

In general, mankind is faced with very similar environmental problems regardless of the national or political boundaries which we have erected. While the problems may vary slightly in type or degree, the fundamental and underlying factors are remarkably similar. It is not surprising, therefore, that the interests and concerns of environmental scientists the world over are also quite similar. In this larger sense, we are our brother's brother, and have the ability to understand our fellowman and his dilemma, if we but take the trouble to do so. It is this singular idea of concerned scientists exchanging views with colleagues that provides the basic strength for this project. While our methods may vary, our goals are identical, and therein lies the value of such a cooperative effort.

Wayland R. Swain, Ph.D.
Project Officer, U.S. Side

CONTENTS

Foreword iii
Preface iv
Introduction v
Figures ix
Tables xviii
Acknowledgment xx

1. Basic Trends in the Study of Hydrochemical Fields and the Structure of Their Space-Time Heterogeneities
V.L. Pavelko, B.M. Vladimirskiy, I.T. Gavrilov and G.V. Tsytsarin 1

2. Modeling the Great Lakes - A History of Achievement
William C. Sonzogni and Thomas M. Heidtke 9

3. Data Management Requirements for Great Lakes Water Quality Modeling
William L. Richardson 37

4. Optimal Sampling for Long Term Trends in Lake Huron
David M. Dolan 58

5. A Model Approach to Estimating the Effects of Anthropogenic Influences on the Ecosystem of Lake Baikal
A.B. Gorstko, Yu.A. Dombrovskiy, V.V. Selyutin, F.A. Surkov, A.M. Nikanorov and A.A. Matveev 71

6. Species Dependent Mass Transport and Chemical Equilibria: Application to Chesapeake Bay Sediments
Dominic M. DiToro 85

7. Simulation of the Distribution of Polluted Water in Reservoirs From Concentrated Emissions
A.V. Karaushev and V.V. Romanovskiy 122

8. Results of a Joint USA/USSR Hydrodynamic Modeling Project for Lake Baikal
John F. Paul, Alexandr B. Gorstko and Anton A. Matveyev . . 129

9. The Structure of Hydrochemical Fields and Short-Term Prediction
A.M. Nikanorov, B.M. Vladimirskiy, V.L. Pavelko, Ye.V. Melnikov and K.L. Botsenyuk 156

10. Transport of Mining Waste in Lake Superior
M. Sydor, G.E. Glass and W.R. Swain 180

11. Principle of Organization of an Automated Information System
V.L. Pavelko 197

12. A Multi-Layered Nested Grid Model of Lake Superior
G.J. Oman and M. Sydor 207

13. A Review of Some Methods and Parameters Used in Assessing Effects of Water Intakes on Fish Populations
Richard L. Patterson 237

14. Control of the Water Resources of the Azov Sea Using the "Azov Problem" Family of Simulation Systems
A.B. Gorstko, F.A. Surkov, L.V. Epshteyn and A.A. Matveyev 252

15. The Transport of Contaminants in Lake Erie
Wilbert Lick 261

16. Self-Organization of Three-Dimensional Models of Water Pollution
A.G. Ivakhnenko and G.I. Krotov 306

17. A Spatially-Segmented Multi-Class Phytoplankton Model for Saginaw Bay, Lake Huron
Victor J. Bierman, Jr. and David M. Dolan 343

18. A Segmented Model of the Dynamics of the Ecosystem of Lake Baikal Considering Three-Dimensional Circulation of the Water
V.V. Menshutkin, O.M. Kozhova, L.Ya. Ashchepkova and V.A. Krotova 366

19. The Task of Optimal Planning of Discharge of Pollutants in a Dynamic Model of Self-Purification of a Body of Water
O.M. Kozhova and L.T. Aschepkova 379

FIGURES

Section		Page
1	Variation of level of study of a component with interval of sampling	5
3	Great Lakes modeling-management process	39
3	Large Lakes Research Station mini-Storet system	45
3	Summary of Lake Superior data from Storet water quality file	48
3	Summary of Lake Michigan data from Storet water quality file	49
3	Summary of Lake Huron data from Storet water quality file	50
3	Summary of Lake Erie data from Storet water quality file	51
3	Summary of Lake Ontario data from Storet water quality file	52
3	Summary of Connecting Channels data from Storet water quality file	53
4	The Lake Huron system	60
4	Simplified mass balance model	62
5	Diagram of surface currents in Baikal during the ice-free season	72
5	Time-series plots of concentrations of an arbitrary pollutant in the various regions of Lake Baikal	75
5	Concentration field of a pollutant in the 0-20 m layer near BCPC	77
5	Diagram of cycle of matter and energy in pelagic Lake Baikal	79

Section		Page
6	The vertical distribution of sediment organic carbon and nitrogen as percent dry weight	93
6	Chesapeake Bay Station 856: Observed and computed vertical distribution of total aqueous carbon dioxide, aqueous ammonia nitrogen and their ratio	98
6	Chesapeake Bay Station 856: Observed and computed vertical distribution of interstitial water	100
6	The effects of species dependent transport and solid phase reactions on net alkalinity	103
6	Characteristic shapes for net alkalinity	105
6	Chesapeake Bay Station 858C: Observed and computed vertical distributions of dissolved methane, mg carbon/l; total aqueous carbon dioxide, mg carbon/l; and total gas phase concentration, moles of gas/l of gas plus aqueous phase volume	108
6	Chesapeake Bay Station 858C: Observed and computed vertical distributions of dissolved nitrogen gas, mg nitrogen/l; dissolved argon, mg argon/l; and mole ratio	109
6	The effect of an upward gas phase velocity	111
6	The effect of an upward gas phase velocity with zero boundary conditions	112
6	The effect of an upward gas phase velocity with zero lower boundary conditions	113
7	Diagram for calculating the diffusion of pollutants in an aquatic ecosystem	124
8	Lake Baikal	131
8	Frequency of winds over Lake Baikal in the summer and autumn	137
8	Hydrodynamic model calculation for Lake Baikal with southwest wind	139
8	Hydrodynamic model calculation for Lake Baikal with southwest wind	140
8	Hydrodynamic model calculation for Lake Baikal with northwest wind	141

Section		Page
8	Hydrodynamic model calculation for Lake Baikal with northwest wind	142
8	Observed surface currents in the Selenga River Region of Lake Baikal	143
8	Lake Baikal whole lake dominant currents	145
8	Dispersion model calculation for Lake Baikal with southwest wind	146
8	Dispersion model calculation for Lake Baikal with southwest wind	147
8	Dispersion model calculation for Lake Baikal with southwest wind	148
8	Dispersion model calculation for Lake Baikal with southwest wind	149
8	Sample results from Hydromet cruise in Selenga Shallows on 28-29 May 1976	150
8	Sample results from Hydromet cruise in Selenga Shallows on 28-29 May 1976	151
8	Landsat satellite image of Lake Baikal	153
9	Berezina River at Gorval, 1951-1956	165
9	Berezina River at Gorval, 1951-1956	168
9	Berezina River at Bobruysk	170
9	Sula River at Zelenkova	171
10	Study area showing the outline of a deep trough where tailings are discharged and the discharge source location at Silver Bay	181
10	Comparison at Duluth of the measured winds and wind function used for modeling of Lake Superior for the November 1975 storm	184
10	Comparison at Duluth of the measured water level fluctuations with the fluctuations derived from the numerical model of Lake Superior for the November 1975 storm wind	185
10	Water transport due to westerly wind stress	187

Section		Page
10	Calculated transports for November 13, 1975 showing water movement for high fetch northeasterly winds	188
10	Numerical simulation of the plume of mining waste from point source at Silver Bay, Minnesota	190
10	Turbidity vs. Landsat Band 4 intensity above background . .	191
10	Turbidity plume derived from Landsat data for November 14, 1975	192
10	Discrete patches of upwelled tailings observed in Landsat data for July 2 and 3, 1973	195
11	Variation in number of errors v with time of continuous work t	203
12	Grids used in various models	208
12	Map of Lake Superior showing regions deeper than 200 m . .	215
12	Surface currents after 3 hours of constant easterly winds	216
12	Surface currents after 9 hours of constant easterly winds	217
12	Surface currents after 15 hours of constant easterly winds	218
12	Surface currents after 24 hours of constant easterly winds	219
12	Currents in layer 2 after 24 hours of constant easterly winds	220
12	Currents in layer 3 after 24 hours of constant easterly winds	221
12	Currents in layer 4 after 24 hours of constant easterly winds	222
12	Layer 2 downdwelling in western Lake Superior after 24 hours of constant easterly winds	223
12	Layer 2 upwelling in western Lake Superior after 24 hours of constant easterly winds	224
12	Surface currents in nested subgrid after 24 hours of constant easterly winds	225

Section		Page
12	Layer 2 currents in nested subgrid after 24 hours of constant easterly winds	226
12	Surface currents in nested subgrid after 24 hours of constant westerly winds	227
12	Layer 2 currents in nested subgrid after 24 hours of constant westerly winds	228
13	Box and arrow diagram summarizing transfers of fish biomass	240
14	Diagram of regions of the Azov Sea	256
14	Program structure of the "Azov Sea" SS	259
15	Lake Erie bottom topography	262
15	Settling velocity versus percent of suspended sediment for the Western Basin sediment	265
15	Side view of the flume	270
15	Example of the concentration time history data for the shallow-based sediment with τ_W = 0.92 dynes/cm^2 and a water content of 6.7%	272
15	The entrainment rate as a function of the average boundary shear stress for the shale-based, Western Basin, and Central Basin sediments	273
15	The entrainment rate as a function of shear stress of a linear scale for the Western Basin sediment	274
15	The reflectivity parameter as a function of shear stress for the shale-based, Western Basin, and Central Basin sediments	275
15	Friction coefficient as a function of Reynolds number for an oscillatory flow over a smooth bottom	277
15	Significant wave height in meters for a wind speed of 11.2 m/sec (25 mi/hr) and a southwest wind	278
15	Significant wave period in seconds for a wind stress of 11.2 m/sec (25 mi/hr) and a southwest wind	279
15	Bottom stress in dynes/cm^2 for a winds speed of 11.2 m/sec (25 mi/hr) and a southwest wind	280

Section		Page
15	Near-surface total suspended solids map for the Western Basin of Lake Erie on March 8, 1976	282
15	Observed surface sediment concentrations for the Western Basin of Lake Erie on March 11, 1976	283
15	Calculated surface sediment concentrations on the Western Basin of Lake Erie on March 11, 1976	284
15	Temperature distribution at 30 days for constant depth basin	287
15	Velocities (u and w) at 30 days for constant depth basin	288
15	Velocities perpendicular to cross-section at 30 days for constant depth basin	289
15	Temperature distribution at 90 days for constant depth basin	290
15	Velocities (u and w) at 90 days for constant depth basin	291
15	Velocities perpendicular to cross-section at 90 days for constant depth basin	292
15	Temperature distribution at 50 days for variable depth basin	294
15	Velocities (u and w) at 50 days for variable depth basin	295
15	Velocities perpendicular to cross-section at 50 days for variable depth basin	296
15	Temperature distribution at 80 days for variable depth basin	297
15	Temperature distribution at 120 days for variable depth basin	298
15	Temperature distribution at 150 days for variable depth basin	299
15	Temperature distribution at 180 days for variable depth basin	300
15	Contaminant concentration at 30 days after release at surface and 53 km from left side	302

Section		Page
16	Characteristic curves of change of external, mixed and internal criterion with increasing complexity of model structure	308
16	Use of simple models for extrapolation of the area of pollution between three measurement stations 1, 2 and 3 in the direction of the x-axis	313
16	Run-through of simple models and production of data tables for the prediction problem	316
16	Run-through of simple models of diagonal shape and production of data tables for the prediction problem	317
16	Selection of a model of optimal complexity based on the combined criterion	320
16	Change of emission and concentration of pollutants with time	331
16	Model I-1	332
16	Model II-1	333
16	Model II-2	335
16	Model II-3	336
16	Model III-1	337
16	Model III-2	339
16	Model III-3	340
17	Saginaw Bay and the spatial segmentation scheme used for the phytoplankton model	344
17	Sampling station network in Saginaw Bay	346
17	Gradient among spatial segments in annual average chloride concentration	348
17	Gradient among spatial segments in annual average phosphorus concentration	349
17	Gradient among spatial segments in summer average chlorophyll a concentration	350
17	Schematic diagram of principal model compartments and interaction pathways	351

Section		Page
17	Comparison between model output and field data for diatom biomass in segment two	354
17	Comparison between model output and field data for biomass of green algae in segment two	355
17	Comparison between model output and field data for biomass of non-N_2-fixing blue-greens in segment two . . .	356
17	Comparison between model output and field data for biomass of N_2-fixing blue-greens in segment two	357
17	Comparison between model output and field data for diatom biomass in segment four	358
17	Comparison between model output and biomass of green algae in segment four	359
17	Comparison between model output and field data for biomass of non-N_2-fixing blue-greens in segment four . .	360
17	Comparison between model output and field data for biomass of N_2-fixing blue-greens in segment four	361
17	Comparison between model output and field data for dissolved ortho-phosphorus in segment two	363
17	Comparison between model output and field data for dissolved ortho-phosphorus in segment four	364
18	Regionalization of Lake Baikal in the model and direction of horizontal transfer	368
18	Geostrophic circulation on the surface of Baikal and depth of circulation average for August-September 1925-1965	369
18	Diagram of horizontal exchange between segment in model	373
18	Horizontal distribution of phytoplankton throughout the year in the 0-50 m layer (generated by model)	375
18	Distribution of phytoplankton in Lake Baikal in the 0-25 m layer in 1964	376
19	$j_j = (j_1, j_2, j_3, j_4)$	383
19	Temperature curve	383

Section		Page
19	Subdivision of body of water into chambers	383
19	Diagram of water exchange	383
19	Picture of propagation of a pollutant through a body of water corresponding to optimal discharge levels	389

TABLES

Section		Page
2	Summary of Water Quality Model Relevant to the Great Lakes	11
2	Summary of Circulation/Transport Models Relevant to the Great Lakes	14
2	Summary of Available Heat Dispersion, Nonpoint Source, Toxic Substances and Miscellaneous Models Relevant to the Great Lakes	16
3	Summary of Principal Model Characteristics	42
3	Summary of Great Lakes Data in Storet	47
3	Storet Water Quality File Summary of Great Lakes Eutrophication Data	54
4	Lake Huron Major Inflows and Outflows	59
4	Chemical and Biological Indicators of Trophic Status - Main Lake Huron	61
4	Lake Huron Surveillance Plan Trend Detection Capabilities	65
4	Sensitivity Analysis for Standard Error in Southern Lake Huron for Total Phosphorus	67
4	Comparison of Stations Required by Different Strategies	68
5	Morphometric Characteristics of Lake Baikal	71
5	Biotic Balance of the Pelagic Ecosystem of Lake Baikal	78
6	Chemical Fast Reactants Structure and Aqueous Diffusion Coefficients	88
6	Chesapeake Bay Sediment Parameters	92
6	Sediment Electron and Nitrogen Stoichiometry	95

Section		Page
6	Station Sediment Parameters	96
8	Annual Average Water Balance for Lake Baikal During the Period 1901-1970	130
8	Parameters for Lake Baikal Hydrodynamic Model	136
9	Factor Solution for the Results of Chemical Analysis of Water Samples of the Gorky Reservoir in 1954-1958	158
9	Factor Solution for Results of Chemical Analysis of Water Samples of Tributaries of the Gorky Reservoir, 1954-1958	159
9	Factor Solution for Results of Chemical Analysis of Water Samples from Kuybyshev Reservoir, 1954-1961	160
9	Factor Solution for Results of Chemical Analysis of Water Samples from Kuybyshev Reservoir Taken Near Vyazovyye (Volga River) and Sokoli Gory (Kama River) and Near Komsomolskiy (Tailwater), 1958-1959	161
9	Factor Solution for Results of Chemical Analysis of Water Samples of Tributaries of the Volga River and Kuybyshev Reservoir, 1954-1961	162
9	Factor Solution for Results of Chemical Analysis of Water Samples from Volgograd Reservoir, 1954-1961	163
9	Factor Solution for Results of Chemical Analysis of Water Samples from Tributaries of Volga River Below Kuybyshev Reservoir, 1954-1961	164
9	Factor Solution for Results of Analysis of Water Samples of Gorval Tributary, Berezina River, 1951-1956	166
9	Factor Solution for Results of Analysis of Water Samples from Bobrusk Tributary of Berezina River, 1957-1973 . . .	167
10	Comparison of Currents Near Duluth	186
10	Comparison of Currents Near Silver Bay	186
10	Band Combinations for Signature Classification of Contaminants	193
17	Statistical Comparison Between Model Output and Field Data	353

ACKNOWLEDGMENTS

In any project of the scope and complexity of this effort, the Project Officers become increasingly indebted to a large number of individuals who contribute their time and effort with no thought of personal gain. Unfortunately, the list of persons who materially aided the effort is too extensive to allow a complete discussion. However, while those persons who made outstanding contributions to the success of this project are acknowledged below, the editors also wish to thank all those others, both Soviet and American, whose efforts and assistance smoothed the way to a satisfactory completion of this phase of the project.

Sincere thanks are extended to Mr. Igor Kozak, Mr. Igor Korobovsky, and Ms. Nina Ivanikiw whose assistance with translations and interpretation at the time of presentation have made possible the publication of this volume. The substantial contributions and tireless efforts of Ms. Debra Caudill to the preparation of the proceedings are acknowledged with deep appreciation.

It is also impossible to ignore the sustained interest and deep commitment to this effort made by Edward Lerchen, Acting President, and his staff at Cranbrook Institute of Science. Particularly, the planning of Dr. V. Elliott Smith and the implementation of efforts provided by Millicent Worrell were far above and beyond the call of duty. It was the contributions of these, and a host of others at the Cranbrook Institute which made the symposium so successful.

SECTION 1

BASIC TRENDS IN THE STUDY OF HYDROCHEMICAL FIELDS AND THE STRUCTURE OF THEIR SPACE-TIME HETEROGENEITIES

V.L. Pavelko[1], B.M. Vladimirskiy[1], I.T. Gavrilov[2] and G.V. Tsytsarin[2]

Currently the basic task of hydrochemical research is the development of prognostic and functional models of water quality. These models must correspond to the requirements not only of operational evaluation, but also of quality control, i.e., providing the necessary information for making the corresponding administrative and scientific-technical decisions. To do this, one must have full and representative data on the quality of water, and the nature of its changes in time and space to understand the processes which determine water quality. These data, naturally, should be obtained at minimum cost. This statement, while obvious, is still improper, due to the following factors:

a) The increasing difficulty of obtaining objective data describing mean and extreme values of water quality indices;

b) The set of tasks which must be performed, for which the concept of "water quality" is ambiguous, and in relationship to which the "completeness and representativeness" of the information must be evaluated, with an ever-increasing list of substances which are limited in terms of maximum allowable concentrations;

c) The lack of any scientifically well-founded criteria or methods for estimation of the "minimum cost".

Each of these factors is worthy of extensive discussion in both the theoretical and the practical aspects. In the present article, however, discussion is limited to the following considerations:

---

[1]Hydrochemical Institute, 192/3 Stachky Prospect; 344090 Rostov-on-Don, USSR.

[2]Moscow State University, Lennin Hills, Moscow, USSR.

1. Under natural conditions, water quality parameters usually vary in diurnal, seasonal or annual cycles, which may be disrupted by hydrochemical factors. The existing system of observations produces more or less reliable information. As the influence of man becomes stronger, the quality of water undergoes great changes, the amplitude of which increases greatly. In reservoirs and streams, flows of varying density with small degrees of mixing are seen. Thus, concentrations may vary by orders of magnitude when measured at points not greatly separated. Many pollutants do not move in the same way through bodies of water. The concept of "lag time" for water quality may differ significantly, since the speed of a stream varies greatly with depth. The hydrochemical lag time may also include a component of relaxation. Naturally, under these conditions the reliability of the information produced is determined in the first stage--as a sample is taken. Depending on the task at hand, the sampling system must assure either the maximum possible averaging over time and space coordinates, or the selection of samples in extreme situations. The development of such a system requires the accumulation of data on structures, and space-time heterogeneity of hydrochemical fields for typical aquatic systems.

2. The use of the concept of "minimum costs" involves the solution of optimization problems, but leaves unanswered a primary question: "Can new costs be correlated with old costs, or must the cost of losses prevented be considered as well?" A comparison with future costs may also be made, if mankind will be forced to rehabilitate or restore certain ecologic niches.

It follows then that optimization of the system of observations cannot be absolute and final, and that suboptimal solutions should be sought for specific problems which are pressing for the present period of development of society. These solutions should be systematically reviewed, following development and application of new achievements in science and technology. At the present time, obviously, it would be most expedient to:

a) limit consideration to the present level of costs, or plan increased costs within limits of the same scale;

b) consider that the functional weights of the observed components of chemical composition within the limits of the vector of states are characterized by a definite hierarchy, e.g., used in producing a generalized water quality index (Valner 1975).

Under these conditions, the task of equalization of the degree of hydrochemical study of components, locally homogeneous regions, and the significance of periods and phases of processes is formulated (equalization of residual entropy in space and time and with respect to weights of the components observed).

To perform this task, it is necessary to consider the following:

1) estimate the space and time study level of each component given the existing parameters of the observation system;

2) find the mean level of study, and estimate its sufficiency for the performance of the task at hand;

3) find the variation in the level of study with the space-time scanning step; and

4) redistribute the equipment of the observation network, in order to achieve a space-time level of study of each component agreeing with its weighted significance.

The practical achievement of these stages of the program requires massive detailed studies of typical hydraulic projects encompassing characteristic periods and phases of the operating mode, and the use of water quality indices. Bodies of water can be classified by means of pattern recognition algorithms, using data files which have been collected, a priori concepts from theoretical hydrochemistry, and the data used to classify sources of pollution. The selection of typical components of chemical composition can be based on the minimum mean-square deviation of the distance (X) of component (K) from the center of the grouping. The search for quasi-steady sections of a body of water, incorporating periods and phases can be conducted analogously (Rybnikov 1970; Borishanskiy 1970; Pavelko 1972).

These functions should be performed in the first stage of operation of the program. After standardization and selection of representative objects, their hierarchical ranking, evaluation of priorities, ordering of the investigation is planned in the second stage as a function of the significance of the object. Finally, the plans for development of the national economy, the degree of pollution of the water, the readiness of individual observation subdivisions, and the conduct of planned studies are incorporated as the third stage in the program.

The fourth stage consists of determination of the variation of the degree of study of a given component with the interval of sampling, and information in the coordinates of space and time, using the following arbitrary system:

x - distance along a stream or the longest axis of a body of water;
y - distance transverse or across the stream or body of water;
z - depth;
t - time.

The characteristics of the degree of study which have been suggested (Popov 1953; Linnik 1958; Margolin 1962; Margolin 1965; Pavelko 1972; Pavelko 1977) include the structural function, the spectral density of dispersion or an estimate such as:

$$\sigma_c = \sqrt{\frac{1}{2(n-1)} \sum_{i=1}^{n-1} (x_{i+1} - x_i)^2} \quad , \qquad (1)$$

which can be transformed to an estimate of the degree of study:

$$I = 1 - \frac{\sigma_c}{\sigma}, \tag{2}$$

where

$$\sigma = \sqrt{\frac{1}{n-1} \sum_{i=1}^{n} (x_i - \bar{x})^2} .$$

The graph of the variation of the degree of study (I) with the interval of sampling of information (τ) is shown in Figure 1.

Based on such functions for each of the components of a body of water which is studied, for its quasi-steady regions, for phases and periods, and considering the actual interval of sampling of information, it is possible to estimate the degree of heterogeneity of the level of study of a body of water for each component. This material can be used as a basis for development of recommendations for improvement of the observation system. The parameters of the observation systems can be adjusted to assure identical levels of study, e.g., equal to the average of all existing levels of study, or corresponding to some other comparative level, i.e., 0.7, 0.8 (see Figure 1), if this level is considered necessary and sufficient for the present stage. These functions can be used to select representative sections and times for sampling, and to provide a basis for the volume and degree of averaging of samples. It would be quite desirable to supplement the graphs of the level of study with the cost of observation, as a function of the frequency of sampling (interval of information collection), and the accuracy of measurements performed. This will allow a rather precise representation of the "value of information", which is necessary to solve the problem of cost minimization.

Obviously, these studies should be performed systematically in order to improve the system of observation and measurement for preventing pollution and for subsequent prediction. The most difficult and responsible stage will obviously be the third stage -- the conduct of studies.

The method of investigation must involve the collection of a large quantity of observed data on an expanding list of components in various bodies of water or parts of bodies of water during various periods and phases. Thus, the observation equipment must be highly productive, with low inertia and cost. The use of automated in situ, high time resolution equipment is desirable. The following systems can be used:

a) The "cross"-placement of a series of units of sensors along the x and y axes in a body of water at a fixed depth;

b) the "garland"-placement of sensors at various depths to perform synchronous observations along the z axis;

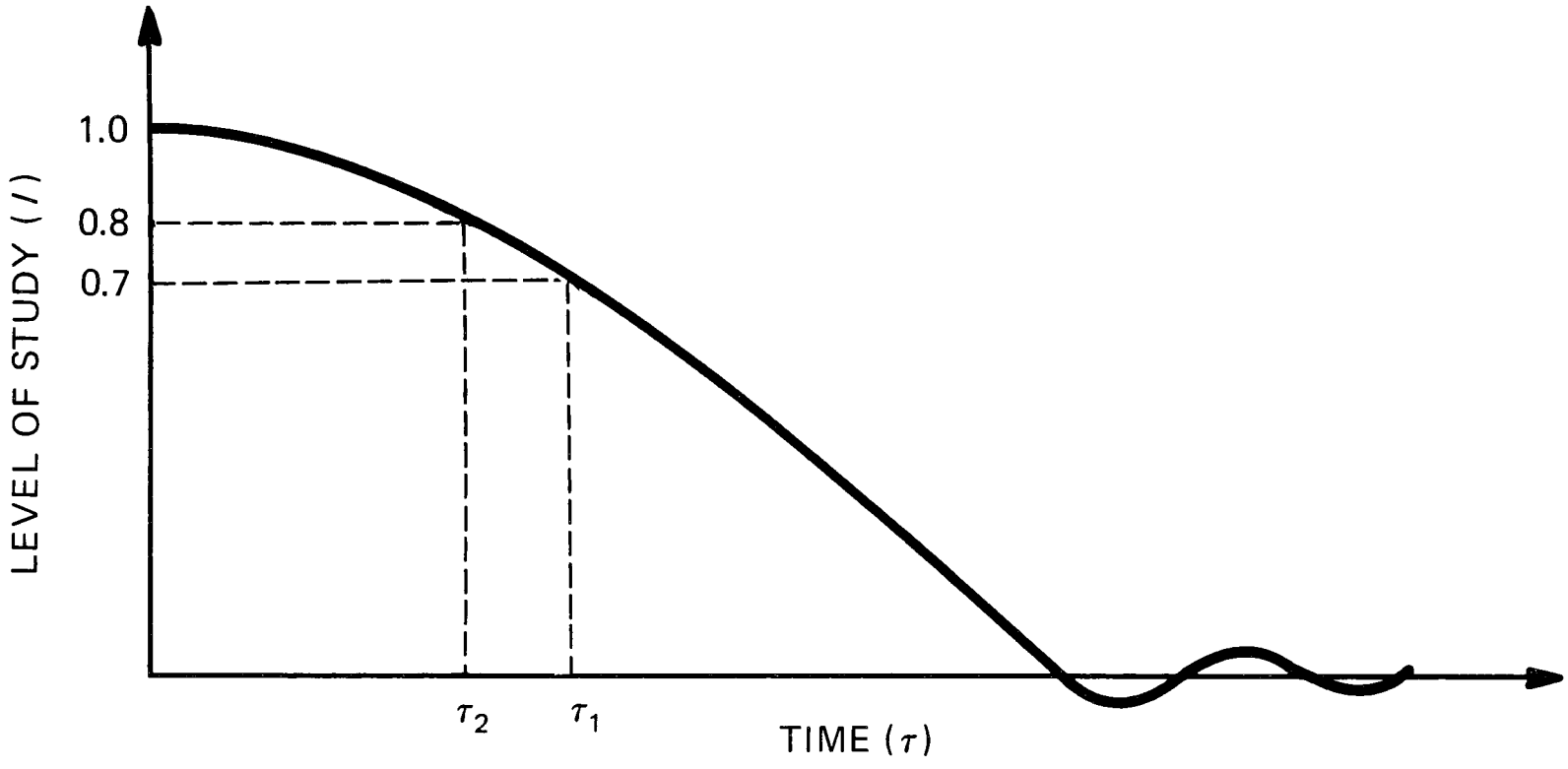

Figure 1. Variation of level of study of a component with interval of sampling.

c) the "cross-garland"-placement of a number of clusters of sensors at points along the x and y axes;

d) the "transverse-garland"-placement of sensor clusters across of a body of water;

e) an on-board automated continuous recording instrument for the conduct of observations in the x and y directions with fixed depth of sensors from a vessel. Depth observations (in the z direction) can also be made with the vessel on station by lowering and raising a group of sensors;

f) the mobile hydrochemical laboratory (truck and trailer with light boat), which may be shifted to any desired observation point. The boat is used to place the sensors, while the recording units are located in the trailer, and the laboratory is in the body of the truck.

The methods and techniques of in situ automated measurements, which form the basis of such systems, have been previously reported (Gavrilov 1977). A set of the hardware required has been tested in the Moscow River and in the reservoirs of this system. The data produced have shown that automated measurements in situ, even of a comparatively small number of parameters (5-7), can greatly increase the effectiveness of a system of observation and measurement of pollutants.

Calculations have shown that the area of spatial interpolation for various components differs by an order of magnitude. With identical density of the network and frequency of sampling, the spatial resolution of observations of oxygen and BOD may contain an error of up to 25 percent. When petroleum products are considered, the error may be up to 100 percent, and for other components, as high as 70 percent. The time resolution of observations of oxygen may sometimes contribute a significant degree of error. Automated observations have recorded a case in which, as an internal wave moved through a reservoir at a depth of 3 m, the oxygen content dropped in a period of one hour, from 20 mg/liter (over 200 percent supersaturation) to a life threatening 4 mg/liter (Tsytsarin 1975). These data confirm the need for performance of the studies described. It is suggested that reference points be created for the performance of studies in priority regions, from which methodologic and technical guidance could be provided. The observations would be performed by the efforts of special mobile hydrochemical detachments.

In the USSR, the planning and performance of observations, as well as the processing and interpretation of the data produced, should be performed with the participation of the Hydrochemical Institute, Moscow State University, and the Scientific Research Institute of Neurocybernetics of Rostov State University, since all of these organizations share common scientific views concerning the means and methods for performance of the task.

REFERENCES

Borishanskiy, L.S. 1970. The problem of effective placement of water temperature and sea level observation points in the littoral zone. Tr. GOIN-Statisticheskaya obrabotka okeanograficheskikh dannykh, Moscow, Gidrometeoizdat Press, No. 99, pp. 34-48.

Gavrilov, I.G. and G.G. Shinkar. 1977. Automated installation for in situ recording of certain physical-chemical properties of natural waters. Gidrokhimich. mat. vol. 70, Leningrad, pp. 75-83.

Linnik, Yu.V. and A.P. Khusu. 1958. Some considerations on statistical analysis of nonuniformity of a polished profile. Sb. Vzaimozamenyaemost', tochnost' i metody izmereniya v mashinostroyenii (Handbook on interchangeable, accuracy and methods of measurement in machine building), Mashgiz Press, 47, pp. 144-146.

Margolin, A.M. 1962. An analytic method of determination of the accuracy of mine-geometric plans. Vopr. marksheyderii i gornoy geometrii v neftegazodobyvayuschchey promyshlennosti (Problems of mine surveying and mine geometry in the oil and gas industry), Moscow, Gostoptekhizdat Press, pp. 210-226.

Margolin, A.M. 1965. Variability of oil and gas deposits and estimates of the error in results of their prospecting. Sb. Otsenka tochnosti opredeleniya parametrov zalezhey nefti i gaza (Estimate of the accuracy of determination of the parameters of oil and gas deposits), Moscow, Nedra Press, pp. 178-190.

Pavelko, V.L., V.M. Kalinchenko, and V.S. Baronov. 1972. Sovershenstvovaniye metodov marksheyderskikh rabot i geometrizatsii nedr (Improvement of methods of mine surveying and geometric measurements beneath the earth), Moscow, Nedra Press, pp. 269-279 and 238-246.

Pavelko, V.L. 1977. Variability and levels of study. Geometrizatsiya mestorozhdeniy poleznykh iskopayemykh (Geometric measurements of deposits of useful minerals), Ed. V.A. Bukhrinskiy and Yu.V. Korobchenko, Moscow, Nedra Press, pp. 95-113.

Popov, Ye.I. 1953. Estimating the accuracy of hipsometric plans of deposits. Zapiski Leningradskogo gornogo instituta, Vol. 37, No. 1.

Rybnikov, A.A., Ye.V. Markevich and N.V. Mertsalova. 1970. Methods of calculation of the discreteness of observations in the ocean. Tr. GOIN-Statisticheskaya obrabotka okeanograficheskikh dannykh, No. 99, pp. 5-24.

Tsytsarin, G.V. 1975. The reliability of estimates of water quality based on single samples. Vestn. MGU, ser. geografich., Moscow State University, No. 4, pp. 43-50.

Velner, Kh.A., V.I. Gurarii and A.S. Shayn. 1975. Determination of water quality criteria in streams for the control of water conservation systems. Materials of Soviet-American Symposium "Use of mathematical models for optimization of water quality control", Kharkov-Rostov n/D.

SECTION 2

MODELING THE GREAT LAKES - A HISTORY OF ACHIEVEMENT

William C. Sonzogni and Thomas M. Heidtke[1]

INTRODUCTION

The North American Great Lakes, which border the United States and Canada, are a unique system. The largest body of fresh water on earth, the Great Lakes contain 20 percent of the world's fresh water. Lake Superior, the largest of the North American Great Lakes, is the largest lake in the world in terms of surface area, and only Lake Baikal and Lake Tanganyika are larger in terms of total volume.

The watershed of the North American Great Lakes are heavily developed, at least in the southern portions. For this reason the lakes have been subject to considerable pollution. Since the lakes are a valuable natural resource and provide drinking water to 70 percent of the region's population (approximately 30 million), the governments of the United States and Canada have been sensitive to pollution problems. As a result, considerable effort has been devoted to the study of water quality/quantity phenomena in the Great Lakes basin. Mathematical modeling has played an important role in this research, as evidenced by the large number of different models which have been used to investigate various aspects of the lakes. In fact, the Great Lakes are among the most widely modeled bodies of water in the world.

Importantly, many of the modeling studies have been successful in terms of the valuable information and insights they have provided for making planning and management decisions. These applications of mathematical models to the Great Lakes system, which are likely to be relevant to the study of other large bodies of water throughout the world, have also influenced subsequent modeling research by revealing the limitations and shortcomings of existing modeling technology.

[1]Great Lakes Basin Commission, 3475 Plymouth Road, P.O. Box 999, Ann Arbor, Michigan 48106.

REVIEW OF PAST MODELING EFFORTS

As a first step in evaluating the capabilities and potential utility of mathematical models in the planning and management process for the Great Lakes, a literature review was initiated. The review focused on models and/or modeling activities which have been specifically designed for analysis of Great Lakes water quality/quantity problems, as well as those models which may be easily modified for application to the lakes. The primary objectives of this review were: (1) to supplement and update other Great Lakes modeling reviews completed several years ago (Hydroscience 1972; Tetra Tech 1974); and (2) to identify areas of relative strength and weakness in using current modeling technology to assist in the study of specific Great Lakes problems.

In order to isolate those models which may be appropriately applied to a particular water quality/quantity phenomena within a given region of the total basin, several broad categories were defined and used to group models having similar characteristics. These categories are:

1. Water Quality Models
2. Circulation/Transport Models
3. Heated Effluent Dispersion Models
4. Toxic Substances Models
5. Nonpoint Source Models
6. Other Models

Using these six headings for delineating model types, the results of the review indicated that well over a hundred mathematical models have been developed during the past 15 years. The major thrust of this modeling research has been in the areas of water quality (primarily eutrophication) and lake circulation or hydrodynamics. Because of the relatively large number of models which have been developed and applied in the study of Great Lakes water quality conditions and circulation patterns, these models have been further categorized in Table 1 through 3 on the basis of previous applications to specific lake basins. Tables 1 and 2 present summary information specifically on water quality and circulation/transport models, respectively. Table 3 incorporates information on heat dispersion, nonpoint source and toxic chemical models, as well as a number of miscellaneous models that are relevant to large lakes. It should be stressed that models listed under a given lake heading (Tables 1 and 2) have been calibrated and/or verified for this particular lake; this does not imply that the same model cannot be calibrated, verified and applied in the study of other lakes. A brief discussion of the modeling review is given below for each of the six different model classifications. Detailed information on each model covered by the review is contained in Heidtke (1979).

Water Quality Models

Examination of Table 1 reveals that water quality models have been most frequently applied to study eutrophication in Lake Ontario, Lake Michigan and Lake Huron. These models have been generally used to evaluate average, whole-lake effects for individual basins or their major embayments, e.g.,

TABLE 1. SUMMARY OF WATER QUALITY MODELS RELEVANT TO THE GREAT LAKES

Model Type	Lake Superior	Lake Michigan
Eutrophication Models Whole-Lake Effects	Great Lakes Total Phosphorus Model (Chapra 1977)	→
	Modified Great Lakes Total Phosphorus Model (Brandstetter *et al*. 1973)	→
		Grand Traverse Bay Phytoplankton Model (Canale *et al*. 1973)
		Phytoplankton-Based Food Web Model (Canale *et al*. 1976)
		Phosphorus Residence Time Model (Sonzogni, *et al*. 1976)
		Green Bay Water Quality Model - GBQUAL (Patterson, *et al*. 1975)
		MICH 01[1]
		Integral Primary Production Model (Fee, 1973)
Nearshore Effects		Grand Traverse Bay Phytoplankton Model (Canale *et al*. 1973)
		Green Bay Water Quality Model - GBQUAL (Patterson *et al*. 1975).
Conservative Substances	Great Lakes Chloride Model (O'Connor and Mueller 1970)	Lake Reactor Model[1]
Other Water Quality	Organic Carbon Budget Model (Maier and Swain 1978)	Grand Traverse Bay Coliform Model (Canale *et al*. 1973)

TABLE 1 (CONTINUED)

Lake Huron/Saginaw Bay	Lake Erie	Lake Ontario
Great Lakes Total Phosphorus Model (Chapra 1977)	→	→
Modified Great lakes Total Phosphorus Model (Brandstetter *et al*. 1973)	→	→
Vollenweider Nutrient Loading Model (Vollenweider 1968)	→	→
Modified Vollenweider Nutrient Loading Model (Vollenweider 1976; Vollenweider 1974)	→	→
BAY 5 (Richardson and Bierman 1976)	ERIE 01[1]	NOAA's Ecological Lake Ontario Model Scavia *et al*. 1976)
SMILE 1 (Bierman and Dolan 1976)	Phytoplankton Model of Western Lake Erie (O'Connor *et al*. 1975)	
SMILE 5[1]		
HURO 1 (Brandstetter *et al*. 1973)	Richardson/Klabbers Eutrophication Model (Richardson and Klabbers 1974)	Tetra-Tech Water Water Quality Ecological Model (Chen *et al*. 1975)
Saginaw Bay Phytoplankton and Nutrient Cycling Model (Limno-Tech, Inc. 1978)	Mesolimnion Exchange Model (Burns and Ross 1972)	LAKE 1 (Thomann *et al* 1975; Thomann *et al* 1976)
Saginaw Bay Total Phosphorus Model (Canale and Squire 1976)		LAKE 1-A[1]
		LAKE 3[1]
		Lake Reactor Model
		Snodgrass/O'Melia Phosphorus Model (Snodgrass and O'Melia 1975)

TABLE 1 (CONTINUED)

Lake Huron/Saginaw Bay	Lake Erie	Lake Ontario
		Nutrient Accumulation Rate Model (Clark *et al*. 1976)
Management Model for Saginaw Bay (Limno-Tech, Inc. 1978)	AUTO-QUAL Estuary Model (Delos 1976)	LAKE 3[1]
FLUSH 02[1] BAY 16 (Richardson 1974; Richardson 1976)	Lake Erie Chloride Balance Model (Rumer, *et al*. 1974)	Rochester Embayment Model (Limno-Tech, 1976)

[1]Model developed at U.S. EPA's Large Lakes Research Station, Grosse Ile, Michigan. No published information currently available.

TABLE 2. SUMMARY OF CIRCULATION/TRANSPORT MODELS RELEVANT TO THE GREAT LAKES

Lake Superior	Lake Michigan
Lake Superior Circulation Model (Hoopes *et al*. 1973)	Estuary and Coastal Circulation Model (Lorenzen *et al*. 1974; Leendertse *et al*. 1973)
Lake Superior Transport Model (Diehl 1977)	Alternating-Direction-Implicit Model (Allender 1976)
	Katz-Kizlauskas Model (Allender 1976)
	Modified Simons Model (Allender 1976)
	Bennett Model (Allender 1976)
	Green Bay Diffusion Model (Ahrnsbrak and Ragotzkie 1970)
	Three-Dimensional, Variable Density, Rigid Lid Hydrodynamic and Heat Dispersion Model[1]
	Green Bay Hydrodynamic Model (Patterson *et al*. 1975)
	Nearshore Water Pollutant Fate Model for Lake Michigan (Wnek and Fochtman 1972)

Lake Huron/Saginaw Bay	Lake Erie	Lake Ontario
	Lake Erie Wind-Driven Current Model (Lorenzen *et al*. 1974)	Steady-State Circulation Model for Shallow Lakes (Lorenzen *et al*. 1974)
Alternating-Direction-Implicit Model (Allender 1976)	Partial Ice-Cover, Wind-Driven Current Model for Lake Erie (Lick 1976)	Three-Dimensional Lake Ontario Wind-Driven Current Model (Lorenzen *et al*. 1974)

TABLE 2 (CONTINUED)

Lake Huron/Saginaw Bay	Lake Erie	Lake Ontario
	Steady-State, Near-shore, Wind-Driven Current Model (Lick 1976)	Lake Ontario Winter Circulation Model (Paskausky 1971)
	Time-Dependent, Near-shore, Wind-Driven Current Model (Haq and Lick 1975; Lick 1976)	Bennett Model (Allender 1976)
Three-Dimensional, Variable Density, Rigid Lid Hydrodynamic and Heat Dispersion Model[1]	→	
	Simons Free-Surface Lake Circulation Model (Lick 1976)	→
	Constant-Depth, Finite Element Circulation Model (Lorenzen *et al*. 1974)	Lake Ontario Heat Transport Model (Simons 1975)
	Lake Erie Wind Tide Model (Lorenzen *et al*. 1974; Platzman 1963)	Lake Ontario Hydraulic Model (Rumer *et al*. 1974)
	Lam/Simons Chloride Transport Model (Lam and Simons 1976)	General Circulation Model for Lakes (Huang 1977)
	Lam/Jaquet Transport and Phosphorus Regeneration Model (Lam and Jaquet 1976)	
	Markov Process Circulation and Pollutant Distribution Model (Howell *et al*. 1970)	
	Great Lakes Diffusion Model (Boyce and Hamblin 1975)	
	Lake Erie Hydraulic Model[1]	

[1]No published information currently available.

TABLE 3. SUMMARY OF AVAILABLE HEAT DISPERSION, NONPOINT SOURCE, TOXIC SUBSTANCES AND MISCELLANEOUS MODELS RELEVANT TO THE GREAT LAKES

Heated-Effluent Dispersion Models	Nonpoint Source Models
Hoopes Heated Surface Jet-Steady Cross-Current Model (Policastro and Tokar 1972)	Universal Soil Loss Equation (Forest Service 1977; Forest Service 1977)
Motz/Benedict Heated Jet-Flowing Ambient Stream Model (Policastro and Tokar 1972)	Storm Water Management Model (Forest Service 1977; Forest Service 1977)
Stolzenbach/Harleman Heated Surface Jet Model (Policastro and Tokar 1972)	Hydrocomp Simulation Program (Forest Service 1977; Forest Service 1977)
Edinger-Polk Two-Dimensional Heated Effluent Model (Policastro and Tokar 1972)	Pesticide Transport and Runoff Model (Donigian and Crawford 1976)
Edinger-Polk Three-Dimensional Heated Effluent Model (Policastro and Tokar 1972	Unified Transport Model (Forest Service 1977; Forest Service 1977)
Csanady Offshore Outfall Model (Policastro and Tokar 1972)	Battelle Urban Wastewater Management Model (Branstetter et al 1973)
Csanady Surface-Discharge Model (Policastro and Tokar 1972)	Wisconsin Hydrologic Transport Model (Forest Service 1977; Forest Service 1977)
Kolesar/Sonnichsen Thermal Energy Transport Model (Policastro and Tokar 1972)	Storage, Treatment and Overflow Model (U.S. Army Corps of Engineers 1975)
Wnek Heat Dispersion Model (Policastro and Tokar 1972)	Agricultural Chemical Transport Model (Frere et al. 1975)
Pritchard Thermal Plume Model (Policastro and Tokar 1972)	Nonpoint Source Pollutant Loading Model (Donigian and Crawford 1976)
Sundaram Thermal Plume Model (Policastro and Tokar 1972)	Agricultural Runoff Management Model (Donigian and Davis 1978; Donigian and Crawford 1976)
Remote Sensing Thermal Plume Model (Cataldo et al. 1976)	Water-Sediment-Chemical Effluent Prediction Model (Bruce 1973)

TABLE 3 (CONTINUED)

Heated-Effluent Dispersion Models	Nonpoint Source Models
Wu/Gallagher Thermal Plume Model (Wu and Gallagher 1973)	LANDRUN (Konrad *et al*. 1978)
Longshore Thermal Plume Model (Palmer 1969)	Hydrological Land-Use Model (Bedient *et al*. 1977)
	Stormwater Overflow Pollution Stream Model (Smith and Eilers 1978)
	Stormwater Overflow Hydraulic Stream Model (Smith and Eilers 1978)

Toxic Substances Models	Miscellaneous Models
PCB Model for the Great Lakes (Whitmore 1977)	Water and Related Land Resources System Model (Haimes *et al*. 1973)
Great Lakes Radionuclide Model (Sullivan and Ellett 1976)	Phosphorus Mass Flow Program (Porcella and Bishop 1975)
Strontium 90 Concentration/Time Model (Lerman 1972)	Water Resource Allocation and Pricing Optimization Model (Narayanan *et al*. 1977)
Cadmium Food Chain Model for Lake Erie (Thomann 1974)	Spatial Pollution Analysis and Comparative Evaluation Model - SPACE (Heilberg 1976)
Aquatic Food Chain Model for Lake Ontario (Thomann 1978)	Lake Erie Integrated Policy Model (Mesarovic 1973)
Mercury Model (Miller 1978)	Hydrologic Models of the Great Lakes (Meredith 1975)
Vinyl Chloride Model (Miller 1978)	PLUARG Overview Model (Johnson *et al*. 1978)
Environmental Exposure Model (Miller 1978)	Lake Erie Phosphorus Discharge Simulation Model (Prober and Melnyk 1974)
Pesticide Transport and Runoff Model (Miller 1978)	REMOVE (Drynan 1978)
	CLEANER (Park *et al*. 1975)

TABLE 3 (CONTINUED)

Toxic Substances Models	Miscellaneous Models
	Imboden Phosphorus Model (Imboden 1974)
	Modified Imboden Phosphorus Model (Imboden and Gachter 1978)
	Oglesby/Schaffner Phosphorus Model (Oglesby 1977; Oglesby and Schaffner 1978)
	Dillon/Rigler Nutrient Loading Model (Dillon and Rigler 1974)
	Lorenzen Phosphorus Model (Lorenzen *et al*. 1976)

Lake Huron's Saginaw Bay, Lake Michigan's Green Bay, etc. The water quality variables most frequently simulated include phytoplankton, zooplankton, nutrient concentrations and dissolved oxygen concentrations. Several of these models have been used to evaluate the long-term response of receiving waters to hypothetical management scenarios. For example, eutrophication models have been applied to western Lake Erie for estimating reductions in nutrient concentrations and phytoplankton levels which may be expected from several alternative control strategies, including (1) 80 percent removal of all incoming phosphorus, (2) a detergent phosphate ban, and (3) a 50 percent decrease in the phosphorus load from agricultural runoff.

Circulation/Transport Models

Table 2 shows that several circulation models have been used to examine water movements in Lakes Michigan, Erie and Ontario. On the other hand, very little attention has been devoted to Lake Superior or Lake Huron. In the past, the majority of circulation models were limited to the study of average, two-dimensional (horizontal), central-lake current patterns for fixed wind directions and magnitude. However, the state-of-the-art in this area has advanced now to incorporate vertical variations in water movement, as well as time-dependent circulation in both the central lake and nearshore zones.

Hydrodynamic models have been used to identify dominant characteristics of lake water movement, and are often used in conjunction with water quality models to define the rates of water exchange among various segments of the lake system. They can also be applied to assess the effects of man-made structures on existing water movements in the nearshore zones of large lakes. This was exemplified in a study of expected modifications to coastal currents in the Cleveland area of Lake Erie as a result of constructing a jetport island approximately six miles offshore.

Heated Effluent Dispersion Models

Heat dispersion models are used to predict temperature distributions in waters receiving heated effluent discharges. They are designed for simulating conditions in the near field (the lake region at or near the point of discharge) and/or far field (the larger lake region where temperature effects of the thermal plume are still evident). Heat dispersion models have been developed to accomodate either surface or submerged discharges, and can be used to evaluate vertical as well as horizontal temperature distributions.

In reviewing several numerical models of heat dispersion in lakes (as listed in Table 3 and described in detail in Heidtke 1979), it was found that the state-of-the-art has progressed steadily over the past few years. Models have been developed which are capable of providing reasonable estimates of temperature fields in waters receiving heated effluents from steam-electric generation. Although no single model or technique is available for providing a comprehensive description of both near and far field temperature distributions, combinations of methods (e.g., physical models and field tests in conjunction with mathematical models) can be used to

generate reliable predictions under most conditions. A very informative discussion of this area can be found in a review of hydrothermal predictive techniques conducted by Jirka et al. (1976).

Nonpoint Source Models

Several models of land runoff quality and quantity have been developed and used to assess nonpoint source pollution loadings from rural and urban land. Their application to the Great Lakes has increased as recent studies, such as the U.S. and Canadian joint study on pollution to the Great Lakes from land drainage, have focused on the significance of nonpoint source pollution in the Great Lakes basin (Pollution From Land Use Activities Reference Group, 1978).

In generating output, mathematical models of land runoff rely upon detailed information concerning the physical and chemical characteristics of a given watershed. Input data generally includes predominant land use and soil types, topography, rainfall, snowmelt, temperature and land management practices. These models can be used to predict runoff quantity and quality at very short time intervals (every 15 minutes) or over relatively long period (average annual conditions). Several nonpoint source models incorporate a widely used relationship for estimating expected soil losses in the region of interest (Wischmeier and Smith).

Models of Toxic Chemicals

As might be expected, very few models are presently available for investigating the fate of low-level toxic chemicals in the aquatic environment. Of the small number of models which are available, only a few have been applied to study the effects of these contaminants in the Great Lakes basin (Table 3). One of the primary reasons for this is a lack of quantitative information on toxic chemical inputs to the lakes. A lack of empirical data for model calibration and verification further compounds the problem. There is an obvious need for increased research in developing modeling techniques and data acquisition systems to assist in broadening our understanding of the effects of toxic inputs to the Great Lakes.

Other Models

In view of the frequent need to consider Great Lakes problems other than those covered in the previous five categories, miscellaneous mathematical models potentially applicable to analysis of other factors (e.g., socioeconomic considerations, waste loadings, phosphorus removal efficiencies, etc.) were also reviewed. These models can be integrated with or used in parallel with more traditional models to yield a more comprehensive information base for decision-making. Because the general review revealed numerous models which fit this description, only models which have been previously used within the context of the lakes were considered in detail. These are listed in Table 3. A more complete description of each model is contained in Heidtke (1979).

The major emphasis in modeling the economic aspects of pollution control in the Great Lakes basin is in the area of "optimization". Optimization involves identifying an optimum policy under a given objective function (to maximize benefits or minimize costs) and set of constraints (e.g., an upper limit on costs, or a specification on the manner in which costs/benefits are distributed within a region).

Johnson et al. (1978) employed a general model of pollutant loadings (total phosphorus and suspended solids) to the Great Lakes to identify cost-effective strategies for achieving reduced phosphorus loads to the lakes. Drynan (1978) used a model of phosphorus removal processes in municipal sewage treatment plants to generate the costs of achieving specified effluent concentrations of total phosphorus. Each of these models can be used to complement other water quality models in order to obtain a better perspective for evaluating the desirability of alternative pollution control strategies.

MAJOR MODEL LIMITATIONS

Perhaps the most notable difficulty in attempting to model large bodies of water such as the Great Lakes is the problem of model verification. The relatively long response time of the lakes makes it difficult to test the ability of many models to accurately predict the long-term lake effects attributable to changes in different input variables (for example, reductions in existing pollutant loadings). An extensive historical data base is also necessary for quantifying the uncertainty associated with model projections. Consequently, a lack of appropriate verification data often limits the acceptance of model predictions by water resources planners and managers.

Tables 1 and 2 indicate that only a few water quality and circulation/transport models have been used to evaluate nearshore lake conditions. As is the case for many large lakes, water quality conditions in the nearshore zone of the Great Lakes is most critical from a human-use perspective. For this reason, predictive models are extremely valuable in helping to identify effective ways of managing this area. It is likely that the increased level of spatial and temporal refinement necessary for evaluating nearshore conditions can be readily accomodated using existing modeling techniques, although more extensive field data must be available for "fine-tuning" the models to localized lake conditions (shoreline features, bottom topography, nearshore currents, pollutant loads from local tributaries, etc.). Certainly there exist limitations as to the practicality of applying models for predicting water quality changes in nearshore areas. As finer and finer scales of time and space are introduced in the model application, the computer costs for simulating water quality profiles over a fixed period often increase significantly. Additionally, there are constraints on detail which are imposed by the numerical techniques often used in solving the quantitative expressions common to many of these models (this is particularly true for circulation/transport models shown in Table 2). Therefore, although water quality models have not been extensively applied for evaluating nearshore conditions, it appears that the technology is available if used within practical limits.

Although several heat dispersion models have been developed (Table 3), very few have as yet been applied to analyze thermal discharges to the Great Lakes. This is partially attributable to a lack of field data for calibration and verification. In order to better understand the limitations and appropriate uses of heat dispersion models, more extensive testing of model predictions against field measurements is required.

As noted in Table 3, several models are currently available to examine nonpoint source pollution in the Great Lakes basin. One of the more recent applications of a nonpoint source model within the context of the Great Lakes was carried out by Konrad et al. (1978). In this case, the model LANDRUN was used to estimate unit area loads of various contaminants from several areas of the Menomonee River basin located in the State of Wisconsin (tributary to Lake Michigan). However, because many models of land runoff often require a rather detailed data base on the aforementioned input variables, their application for assessing nonpoint source pollution from a large region such as the Great Lakes basin is limited. Several of the nonpoint source models listed in Table 3 are better suited for predicting runoff quality and quantity in small watersheds having well-documented physical and chemical characteristics.

PRACTICAL APPLICATION OF GREAT LAKES MODELS

While the many models developed to date have been extremely instructive from a large lakes research point of view, the true mark of achievement has been in the application of models in real planning situations. Back in the late 1960's, the Great Lakes Basin Commission, a U.S. planning organization with responsibility for the U.S. portion of the Great Lakes, began to view each of the Great Lakes and their basins as an integrated system.

It was apparent to the Great Lakes Basin Commission at that time that conventional planning techniques would not be sufficient for holistic evaluations of the Great Lakes. Consequently, after consulting extensively with scientific experts and other knowledgeable people from both the United States and Canada, the Basin Commission sponsored a feasibility study to demonstrate the application of system models to existing or hypothetical situations within the Great Lakes.

This feasibility study resulted in the comprehensive report entitled, "A Limnological Systems Analysis of the Great Lakes, Phase I" (Hydroscience 1973). This report documented the practicality and desirability of utilizing models in planning for the Great Lakes region, and made recommendations for specific modeling approaches which could be used in the near future.

This early pioneering effort stimulated additional modeling activities, further advancing the possibility of planning for the Great Lakes an an entire system. Some of the models proposed in Hydroscience (1973), such as a lakewide eutrophication model of Lake Erie and Lake Ontario, have already been developed and applied to some extent (Tables 1 and 2). These and other models have been used in several significant policy and resource management

decisions, e.g., the Lake Erie Wastewater Management Study (U.S. Army Corps of Engineers 1976) and the National Commission of Water Quality Regional Assessment Study (Rolan 1975).

One of the best examples of how mathematical models can be used in water resources decision-making was the formulation of desirable phosphorus loads or inputs to the Great Lakes. Given different alternative conditions of lake quality, a number of available models were used to determine the approximate total phosphorus loads necessary to achieve those conditions. Without the modeling work that has been conducted over the last several years, it would have been virtually impossible to determine the extent to which current loads must be reduced to achieve the desired trophic conditions.

One of the principal features of this particular application of models was that several independently developed models (at least three models were used in the analysis of a lake basin) were used to relate desired conditions to target loads. Results and projections of each model were then compared. The fact that different models, which varied in their complexity and spatial and temporal scale, predicted similar results provided an additional measure of confidence in the results. A detailed discussion of the models used, as well as the method by which the loads were determined, can be found in Bierman (1979) and Thomas et al. (1979).

FUTURE GREAT LAKES MODELING - WATER QUALITY, CIRCULATION/TRANSPORT AND NON-POINT SOURCES

To complement the recently completed review of past Great Lakes modeling capabilities, a separate study (Heidtke and Sonzogni 1979) was undertaken to provide some insight into ongoing or soon-to-begin modeling activities which have applicability or potential applicability to the Great Lakes. Information was obtained through a survey of several U.S. and Canadian agencies and academic institutions involved in modeling aquatic ecosystems.

According to the survey, continued emphasis will be placed on modeling the eutrophication process. Much of this work will be an extension and refinement of previous efforts to calibrate, verify and apply mathematical models to eutrophication problems in the Great Lakes, particularly the nearshore area of the lakes. Included in this work will be (a) refined spatial and temporal detail, (b) distinction among various species of phytoplankton and zooplankton present, (c) distinction among various forms of nutrients and their potential for influencing algal growth, and (d) consideration of the statistical reliability of model predictions. Additionally, water quality models which have been previously verified in Great Lakes applications will be used more extensively as aids in the decision-making process, i.e., in helping to identify and evaluate cost-effective strategies for managing the lakes.

Specific water quality problems and issues which will be addressed using mathematical modeling techniques include:

1. Phytoplankton/zooplankton production in Lake Ontario, as well as alternatives for achieving its control.

2. Statistical quantification of error bounds on output from eutrophication models, including identification of the major sources of error.

3. Development of wasteload allocations for conventional pollutants discharged to the Lower Fox River/Green Bay system of Lake Michigan.

4. Evaluation of the impact of changes in nutrient loadings on the growth and distribution of Cladophora in the Great Lakes.

Continued emphasis will be placed on the refinement and application of mathematical models for the study of Great Lakes hydrodynamics. It is anticipated that previous developments in the state-of-the-art will facilitate more practical applications and increased reliability in model predictions. Although research will still be directed at improving the predictive capabilities of circulation/transport models by revising and updating input data and/or various model assumptions, an increased effort will be made to take advantage of existing technology for planning and management purposes.

Specific developments in modeling the dynamics of water movements in the Great Lakes will include:

1. Modification and application of previously verified three-dimensional circulation models as tools for simulating pollutant transport in the lakes.

2. Critical comparison of circulation models through tests of model predictions against observed field data.

3. Assessment of modeling techniques for simulating wave heights and directions in Lake Michigan, Lake Superior and Lake Erie.

4. Design of methods for computing winds and associated surface stress on the basis of weather observations and output from large-scale weather prediction models.

5. Further integration of hydrodynamic models to provide more comprehensive evaluations of lake conditions.

6. Combined remote sensing and mathematical modeling for the study of sediment transport and thermal structure in Lake Erie.

It would appear that modeling of nonpoint source pollution will receive major emphasis over the next few years. Much of this work will be devoted to refinement and application of previously developed nonpoint source

models. A few of the anticipated activities in this area are briefly discussed below.

1. Previous applications of nonpoint source models have been limited to analysis of runoff quality and quantity from relatively small watersheds, which represents a serious constraint on their utility for generating basinwide estimates of nonpoint source pollutant inputs to the lakes; therefore, an attempt will be made to assess the predictive capabilities of such models when applied to larger watersheds of varying physiographic characteristics.

2. In recognition of the need to consider Great Lakes water quality/quantity problems and their possible solutions from a systems perspective, nonpoint source models will be linked with water quality models in an attempt to evaluate the impact of various land management practices on downstream receiving waters.

3. Similar to work being carried out in the area of water quality modeling, continued testing of certain nonpoint source models will be conducted in order to (1) quantify the errors in model predictions and (2) identify the source of those errors and how they may be modified to improve model predictions.

4. One of the major obstacles to more widespread use of models as planning and management tools is their failure to adequately consider the social, economic and administrative factors involved in many decision problems; to alleviate this shortcoming, research is ongoing which should provide valuable information in the aforementioned areas.

FUTURE GREAT LAKES MODELING - CHEMICAL TOXIC SUBSTANCES

Until recently, toxic chemicals have received very little attention in terms of attempts to quantify their pathways through, and effects on, the aquatic environment. However, increased awareness and concern over the potential health risks posed by these materials has now stimulated numerous research activities designed to advance the state-of-the-art in toxic substances modeling (Heidtke and Sonzogni 1979).

Toxic substances modeling of the Great Lakes is particularly important since the Great Lakes appear to be especially vulnerable to toxic contamination. Factors which may contribute to the sensitivity of the Great Lakes to toxics, as suggested at a recent workshop sponsored by the Great Lakes Basin Commission, include:

1. The Great Lakes are close to and often downwind of major sources of pollution.

2. Substances entering the Great Lakes are often subject to comparatively long retention times, resulting in high accumulation of even low level inputs.

3. Atmospheric inputs to the Great Lakes are large and are not "filtered" by soils.

4. The Great Lakes contain extensive oligotrophic areas with particularly sensitive biota.

5. Particulate material in the deep Great Lakes is deposited at a relatively slow rate, allowing more time for bioaccumulation of toxics.

6. The relatively unproductive nature of the lakes (except Lake Erie) may decrease the rate of removal of toxic substances from the water column, thus increasing the amount taken up by fish.

7. The low suspended sediment load per unit volume to each of the Great Lakes (except Lake Erie) may contribute to their sensitivity; higher volumetric sediment loads may provide more opportunity for sorption of toxics and their subsequent settling out of the water column (higher solids loads may also serve to "dilute" toxic concentrations in bottom sediments).

8. The active circulation and mixing which are characteristic of the Great Lakes helps to rapidly distribute toxics throughout the lakes.

These factors, which are also likely to be relevant to many other large lakes of the world, need to be given special consideration in the development of toxic substances models.

Included among the several toxic substances modeling studies which will be directed at the Great Lakes in the future are:

1. A model of the accumulation of PCBs in Lake Michigan sediments, as well as their subsequent uptake by pelagic fishes.

2. Development of a model to predict fluxes of toxic chemicals to and from sediments in Saginaw Bay, Lake Huron.

3. Continuation of efforts to formulate a modeling framework for the fate and effects of hazardous substances in the aquatic food chains of the Great Lakes.

At present it is difficult to assess how successful each of these modeling efforts will be in terms of increasing our understanding of the interactions and effects of toxic materials on the Great Lakes ecosystem. However, these activities likely represent only the beginning in terms of toxics modeling developments within the next few years. As more becomes known

about the behavior of toxic materials in the environment, priorities for research may be expected to shift. For example, various studies will be using models which have been previously applied in the analysis of other water quality/quantity phenomena (eutrophication, nonpoint source runoff, etc.). This work may reveal that the modeling technology already exists for evaluating the effects of toxic inputs to the Great Lakes. On the other hand, it may be necessary to pursue new and unique modeling avenues in order to effectively characterize the problem and answer critical management questions. In either case, modeling research is progressing in this area and should continue to do so over the next few years.

As a final note, perhaps one of the most critical needs for advancing the state-of-the-art in toxics modeling is a carefully designed field sampling program. This program must be coordinated with the spatial and temporal detail required for reliable model calibration/verification. The resulting historical data base should be regulary updated, easily accessible, and maintained in a format which promotes its effective use for evaluating models of toxic substances.

SUMMARY

During the past 15 years, over 100 mathematical models have been developed to assist in increasing our understanding of the Great Lakes system. Many of these models have been successful in terms of the information they have provided for making management and planning decisions, as well as the insight they have provided for future research. Water quality models have probably been given the most attention, with the majority designed to investigate conditions in the lower Great Lakes -- Erie and Ontario. However, recent modeling developments have more frequently looked at the Great Lakes as an integrated system, an approach that is fundamental for comprehensive resource management.

Perhaps the greatest constraint on the use of Great Lakes models is the inherent difficulty associated with model verification. This difficulty is due, at least in part, to the large size of the Great Lakes and their relatively long water and chemical residence times. However, a measure of confidence in model predictions has been achieved when different models, varying in complexity and temporal and spatial scale, have generated similar results.

Future Great Lakes modeling efforts should be directed toward toxic chemicals. Contamination by toxic chemicals is currently the most pressing problem affecting the Great Lakes. Modeling efforts should also concentrate on the nearshore area, which is the most critical sector from a human use perspective.

As a final comment, it should not be assumed that increased model complexity is always a prerequisite for improving their utility as decision-making tools. In the future it may be more effective, at least in terms of long-range planning objectives, to place greater emphasis on models which can be practically used to arrive at management decisions rather than on

models which incorporate maximum detail for all system parameters and variables. Similarly, if models are forced to meet extremely rigid calibration/verification tests as the criteria for judging their acceptability, much of their potential may go unrealized. This notwithstanding, the role of models in managing the lakes is now becoming better defined and their limitations more clearly understood. Hopefully, this will generate added confidence in mathematical models as a necessary and valuable asset in developing effective management plans for the Great Lakes and other large lakes throughout the world.

ACKNOWLEDGEMENTS

This paper is a contribution of the Great Lakes Environmental Planning Study. The assistance of Ms. Ann Davis in preparing the manuscript is gratefully acknowledged.

REFERENCES

Ahrnsbrak, W.F. and R.A. Ragotzkie. 1970. Mixing processes in Green Bay. Marine Studies Center, University of Wisconsin, Madison, Wisconsin. Sea Grant Prog. Reprint WIS-SG-71-312.

Allender, J.H. 1976. Water Resources Research Program: Review and appraisal of numerical circulation models for Lake Michigan. Argonne National Laboratory, Great Lakes Project, Argonne, Illinois. Prepared for U.S. Energy Research and Development Administration.

Bedient, P.B., W.C. Huber and J.P. Heaney. 1977. Environmental model of Kissimmee River Basin. J. Water Res. Plan. Mgt., ASCE, 103, WR2, pp. 241-256.

Bierman, V.J. and D.M. Dolan. 1976. Mathematical modeling of phytoplankton dynamics in Saginaw Bay, Lake Huron. In Proceedings of the Conference on Environmental Modeling and Simulation, U.S. Environmental Protection Agency, EPA Report No. EPA-600/9-76-016, pp. 773-779.

Bierman, V.J., Jr. 1979. A comparison of models developed for phosphorus management in the Great Lakes. Prepared for Conference on Phosphorus Management Strategies for the Great Lakes, Rochester, New York.

Boyce, F.M. and P.F. Hamblin. 1975. A simple diffusion model of the mean field distribution of soluble materials in the Great Lakes. Limnol. Oceanogr., 20(4), pp. 511-517.

Brandstetter, A., R.L. Engel and D.B. Cearlock. 1973. A mathematical model for optimum design and control of metropolitan wastewater management systems. Water Resour. Bull, 9(6), pp. 1188-1200.

Bruce, R.R. 1973. Water-sediment-chemical effluent prediction (WA-S-CH Model). Southern Peidmont Conservation Research Center, Agricultural Research Service, Department of Agriculture, Watkinsville, Georgia.

Burns, N.M. and C. Ross. 1972. Project Hypo -- An intensive study of the Lake Erie central basin hypolimnion and related surface water phenomena. Canada Centre for Inland Waters, Paper No. 6, U.S. Environmental Protection Agency, Technical Report, TS-05-71-208-24.

Canale, R.P., S. Nachiappan, D.J. Hineman and H.E. Allen. 1973. A dynamic model for phytoplankton production in Grand Traverse Bay. Proc. 16th Conf. on Great Lakes Res., Internat. Assoc. for Great Lakes Res., pp. 21-33.

Canale, R.P., R.L. Patterson, J.J. Gannon and W.F. Powers. 1973. Water quality models for total coliform. J. Water Pol. Control. Fed., 45(2), pp. 325-335.

Canale, R.P. and J. Squire. 1976. A model for total phosphorus in Saginaw Bay. J. Great Lakes Res., Internat. Assoc. Great Lakes Res., 2(2), pp. 364-373.

Canale, R.P., L.M. DePalma and A.H. Vogel. 1976. A plankton-based food web model for Lake Michigan. In Modeling Biochemical Processes in Aquatic Ecosystems. R.P. Canale (Ed.), Ann Arbor Science Publ., Inc., Ann Arbor, Michigan, pp. 33-73.

Cataldo, J.C., R.R. Zavesky and A.S. Goodman. 1976. Correlation of mathematical models for water temperature with aerial infrared water temperature surveys. Polytechnic Institute of New York. Brooklyn, New York, State Energy Research and Development Authority.

Chapra, S.C. 1977. Total phosphorus model for the Great Lakes, Env. Engr. Div., ASCE, 103, EE2, pp. 147-161.

Chen, C.W., M. Lorenzen and D.J. Smith. 1975. A comprehensive water quality-ecological model for Lake Ontario. Prepared for Great Lakes Environmental Research Laboratory, National Oceanic and Atmospheric Administration, by Tetra Tech., Inc.

Clark, P.A.A., J.P. Sandwick, D.J. Casey and A. Solpietro. 1976. An empirical model for nutrient accumulation rates in Lake Ontario. In Proceedings of the Conference on Environmental Modeling and Simulation, U.S. Environmental Protection Agency, EPA Report No. EPA-600/9-76-016, pp. 176-181.

Delos, C.G. 1976. Mathematical model of a Great Lakes estuary. In Proceedings of the Conference on Environmental Modeling and Simulation, U.S. Environmental Protection Agency, EPA Report No. EPA-600/9-76-016, pp. 115-119.

Diehl, S., W. Maanum and T. Jordon. 1977. Transport in Lake Superior. J. Geophy. Res., 82(6), pp. 977-978.

Dillon, D.J. and F.H. Rigler. 1974. A test of a simple nutrient budget model predicting the phosphorus concentration in lake water. J. Fish. Res. Board Can., 31, pp. 1771-1778.

Donigian, A.S., Jr. and N.H. Crawford. 1976. Modeling pesticides and nutrients on agricultural lands. U.S. Environmental Protection Agency, EPA Report No. EPA-600/2-76-043.

Donigian, A.S., Jr. and N.H. Crawford. 1976. Modeling nonpoint pollution from the land surface. U.S. Environmental Protection Agency, EPA Report No. EPA-600/3-76-083.

Donigian, A.S., Jr. and H.H. Davis, Jr. 1978. User's manual for agricultural runoff management (ARM) model. U.S. Environmental Protection Agency, EPA Report No. EPA-600/3-78-080.

Drynan, W.R. 1978. Relative costs of achieving various levels of phosphorus control of municipal wastewater treatment plants in the Great Lakes basin. Technical Report to the International Reference Group on Great Lakes Pollution from Land Use Activities, International Joint Commission, Windsor, Ontario.

Fee, F.J. 1973. A numerical model for determining integral primary production and its application to Lake Michigan. J. Fish. Res. Board Can., 30, pp. 1447-1468.

Forest Service, U.S. Department of Agriculture. 1977. Nonpoint water quality modeling in wildland management, a state-of-the-art assessment (Volume I - Text), U.S. Environmental Protection Agency, EPA Report No. EPA-600/3-77-036.

Forest Service, U.S. Department of Agriculture. 1977. Nonpoint water quality modeling in wildland management, a state-of-the-art assessment (Volume II - Appendixes). U.S. Environmental Protection Agency, EPA Report No. EPA-600/3-77-078.

Frere, M.H., C.A. Onstad and H.N. Holtan. 1975. ACTMO - An agricultural chemical transport model. Agricultural Research Service, Department of Agriculture, Hyattsville, Maryland, Report No. ARS-H-3.

Haimes, Y.Y., P. Das, K. Sung and K.S. Lee. 1973. Modeling and management of water and related land resources for phosphorus control and ecolibrium. Dept. of Systems Engineering, Case Western Reserve University, Cleveland, Ohio.

Haq, A. and W. Lick. On the time-dependent flow in a lake. J. Geophy. Res. 80(3), pp. 431-437.

Heidtke, T.M. 1979. Modeling the Great Lakes system: Update of existing models. Great Lakes Environmental Planning Study Report, Great Lakes Basin Commission, Ann Arbor, Michigan, 79 p.

Heidtke, T.M. and W.C. Sonzogni. 1979. Modelino the Great Lakes system: Ongoing and planned modeling activities. Great Lakes Environmental Planning Study Report, Great Lakes Basin Commission, Ann Arbor, Michigan.

Heilberg, E. 1976. SPACE: A closer look at the impact of environmental policy. U.S. Environmental Protection Agency, EPA Report No. EPA-600/9-76-016.

Hoopes, J.A., R.A. Ragotzkie, S.L. Lien and N.P. Smith. 1973. Circulation patterns in Lake Superior. Wisconsin Water Resources Center, Madison, Wisconsin.

Howell, J.A., K.M. Kiser and R.R. Rumer, Jr. 1970. Circulation patterns and a predictive model for pollutant distribution in Lake Erie. Proc. 18th Conf. on Great Lakes Res., Part 1, Internat. Assoc. Great Lakes Res., pp. 434-443.

Huang, J.C.K. 1977. A general circulation model for lakes. Great Lakes Environmental Research Laboratory, National Oceanic and Atmospheric Administration, Technical Memorandum ERL GLERL-16.

Hydroscience, Inc. 1973. Limnological systems analysis of the Great Lakes, Phase I. Prepared for the Great Lakes Basin Commission, Ann Arbor, Michigan, 474 p.

Imboden, D.M. 1974. Phosphorus model of lake eutrophication. Limnol. Oceanogr., 19(2), pp. 297-304.

Imboden, D.M. and R. Gachter. 1978. A dynamic lake model for trophic state prediction. J. Ecol. Modelling, 4, pp. 77-98.

Jirka, G.H., G. Abraham and D.R.F. Harleman. 1976. An assessment of techniques for hydrothermal prediction. Prepared for U.S. Nuclear Regulatory Commission, Report No. NUREG-0044.

Johnson, M.G., J.C. Comeau, T.M. Heidtke, W.C. Sonzogni. 1978. Management information base and overview modelling. Technical Report to the International Reference Group on Pollution from Land Use Activities, International Joint Commission, Windsor, Ontario.

Konrad, J.G. G. Chesters and K.W. Bauer. 1978. Summary pilot watershed report: Menomonee River Basin, Wisconsin. Technical Report to the International Reference Group on Pollution from Land Use Activities, International Joint Commission, Windsor, Ontario.

Lam, D.C.L. and J.M. Jaquet. 1976. Computations of physical transport and regeneration of phosphorus in Lake Erie, Fall 1970. J. Fish. Res. Board Canada, 33(3), pp. 550-563.

Lam, D.C.L. and T.J. Simons. 1976. Numerical computations of advective and diffusive transports of chloride in Lake Erie, 1970. J. Fish. Res. Board Canada, 33(3), pp. 537-549.

Leendertse, J.J., R.C. Alexander and S.K. Liu. 1973. A three-dimensional model for estuaries and coastal seas: Volume I: Principals of computations. Rand Corporation, Report No. R-1417-OWRR.

Lerman, A. 1972. Strontium-90 in the Great Lakes: Concentration-time model. J. Geophy. Res., 77(18), pp. 3256-3264.

Lick, W. 1976. Numerical models of lake currents. U.S. Environmental Protection Agency, EPA Report No. EPA-600/3-76-020.

Limno-Tech, Inc. 1976. Genesee River and Rochester embayment quality models and evaluations. Prepared for O'Brien and Gere Engineers, Syracuse, New York.

Limno-Tech, Inc. 1978. Projections of critical water quality conditions in Saginaw River and Bay. Prepared for East Central Michigan Planning and Development Regional Commission, Saginaw, Michigan.

Lorenzen, M.W., C.W. Chen, E.K. Noda and L.S. Hwang. 1974. Final report - Lake Erie wastewater management study. Prepared for U.S. Army Corps of Engineers, Buffalo District, by Tetra Tech, Inc., Tetra Tech Report No. TC-413.

Lorenzen, M.W., D.J. Smith and L.V. Kimmel. 1976. A long-term phosphorus model for lakes: Application to Lake Washington. In Modeling Biochemical Processes in Aquatic Ecosystems, R.P. Canale (Ed.), Ann Arbor Science Publishers, Inc., Ann Arbor, Michigan.

Maier, W.J. and W.R. Swain. 1978. Lake Superior organic carbon budget. Water Research, 12(6), pp. 403-412.

Meredith, D.D. 1975. Predictive models for Great Lakes hydrology. Water Res. Bull., 11(3), pp. 526-535.

Mesarovic, M. (Ed.). 1973. Multilevel systems model for interactive mode policy analysis in pollution control - 1: Interim report. Complex Systems Institute and Systems Research Center, Case Institute of Technology, Case Western Reserve University, Cleveland, Ohio.

Miller, C. 1978. Exposure assessment modeling: A state-of-the-art review. U.S. Environmental Protection Agency, EPA Report No. EPA-600/3-78-065.

Narayanan, R., B.C. Jensen and A.B. Bishop. 1977. An optimization model for efficient management of urban water resources. Water Res. Bull., 13(4), pp. 691-708.

O'Connor, D.J. and J.A. Mueller. 1970. Water quality model of chlorides in Great Lakes. J. San. Engr. Div., ASCE, 96, SA4, pp. 955-975.

O'Connor, D.J., D.M. DiToro and R.V. Thomann. 1975. Phytoplankton models and eutrophication problems. In Ecological Modeling in a Resource Management Framework, C.S. Russell (Ed.), Resources for the Future, Inc., Washington, D.C., pp. 149-209.

Oglesby, R.T. 1977. Phytoplankton summer standing crop and annual productivity as functions of phosphorus loading and various physical factors. J. Fish. Res. Board Can., 34, pp. 2255-2270.

Oglesby, R.T. and W.R. Schaffner. 1978. Phosphorus loadings to lakes and some of their responses. Part 2. Regression models of summer phytoplankton stand crops, winter total P, and transparency of New York lakes with known phosphorus loadings, Limnol. Oceangr., 23(1), pp. 135-145.

Palmer, M.D. 1969. Simulated thermal effluents into Lake Ontario. Proc. 12th Conf. on Great Lakes Res., Internat. Assoc. Great Lakes Res., pp. 674-685.

Park, R.A., D. Scavia and N.L. Clesceri. 1975. CLEANER: The Lake George model. In Ecological Modeling in a Resource Management Framework, C.S. Russell (Ed.), Resources for the Future, Inc., Washington, D.C., pp. 49-81.

Paskausky, D.F. 1971. Winter circulation in Lake Ontario. Proc. 14th Conf. on Great Lakes Res., Internat. Assoc. Great Lakes Res., pp. 593-606.

Patterson, D.J., E. Epstein and J. McEvoy. 1975. Water pollution investigation: Lower Great Bay and lower Fox River. U.S. Environmental Protection Agency, EPA Report No. EPA-905/9-74-017.

Platzman, G.W. 1963. The dynamic prediction of wind tides on Lake Erie. Meteorological Monographs, American Meteorological Society, 4(26), pp. 1-44.

Policastro, A.J. and J.V. Tokar. 1972. Heated-effluent dispersion in large lakes: State-of-the-art analytical modeling. Part 1. Critique of modeling formulations. Argonne National Laboratory, Argonne, Illinois, Report No. ANL/ES-11.

Pollution from Land Use Activities Reference Group. 1978. Environmental management strategy for the Great Lakes system. Final Report to the International Joint Commission, Windsor, Ontario, Canada, 115 p.

Porcella, D.B. and A.B. Bishop. 1975. Comprehensive management of phosphorus water pollution, Ann Arbor, Science Publ., Inc., Ann Arbor, Michigan.

Prober, R. and D.B. Melnyk. 1974. A simulation model for phosphorus water discharges in the Lake Erie basin. Proc. 17th Conf. on Great Lakes Research, Part 1, Internat. Assoc. Great Lakes Res., pp. 514-519.

Richardson, J.M., Jr. and J.G. Klabbers. 1974. A policy oriented model of the eutrophication problem in the Lake Erie ecosystem. Systems Research Center, Case Western Reserve University, Cleveland, Ohio, Report No. SRC 74-1.

Richardson, W.L. 1974. Modeling chloride distributions in Saginaw Bay. Proc. 17th Conf. on Great Lakes Res., Part 1, Internat. Assoc. Great Lakes Res., pp. 462-470.

Richardson, W.L. 1976. An evaluation of the transport characteristics of Saginw Bay using a mathematical model of chloride. In Modeling Biochemical Processes in Aquatic Ecosystems, R.P. Canale (Ed.), Ann Arbor Science Publishers, Inc., Ann Arbor, Michigan.

Richardson, W.L. and V.J. Bierman, Jr. 1976. A mathematical model of pollutant cause and effect in Saginaw Bay, Lake Huron. Water Quality Criteria Research of the U.S. EPA, U.S. Environmental Protection Agency, EPA Report No. EPA-600/3-76-079, pp. 138-158.

Rolan, R.G. 1975. Lake Erie regional assessment study. Prepared for the U.S. National Commission on Water Quality. Dalton, Dalton, Little, and Newport. Cleveland, Ohio.

Rumer, R.R., Jr., K. Kiser and C.Y. Li. 1974. Lake Ontario hydraulic model study (Preliminary results). National Oceanic and Atmospheric Administration Sea Grant 2-35281.

Rumer, R.R., Jr., D.D. Meredith and C.C. Chien. 1974. Chloride build-up and control in Lake Erie. Proc. 17th Conf. on Great Lakes Res., Part 1, Internat. Assoc. Great Lakes Res., pp. 520-534.

Scavia, D., B.J. Eadie and A. Robertson. 1976. An ecological model for Lake Ontario: Model formulation, calibration, and preliminary evaluation. National Oceanic and Atmospheric Administration Tech. Report No. ERL 371-GLERL 12.

Simons, T.J. 1975. Verification of numerical models of Lake Ontario II: Stratified circulations and temperature changes. J. Phys. Oceanogr., 5(1), pp. 98-110.

Smith, R. and R.G. Eilers. 1978. Stream models for calculating pollutional effects of stormwater runoff. U.S. Environmental Protection Agency, EPA Report No. EPA-600/2-78-148.

Snodgrass, W.J. and C.R. O'Melia. 1975. Predictive model for phosphorus in lakes. Env. Sci. Tech., 9(10), pp. 937-944.

Sonzogni, W.C., P.C. Uttormark and G.F. Lee. 1976. A phosphorus residence time model: Theory and application. Water Research, 10(5), pp. 429-435.

Sullivan, R.E. and W.H. Ellett. 1976. Radionuclide transport in the Great Lakes. In Proceedings of the Conference on Environmental Modeling and Simulation, U.S. Environmental Protection Agency, EPA Report No. EPA-600/9-76-016.

Tetra Tech, Inc. 1974. Report to Lake Erie Wastewater Management Study on Water Quality Models. Tetra Tech Report No. TC-413, Pasadena, California.

Thomann, R.V. 1974. A food chain model of cadmium in western Lake Erie. Water Research, 8, pp. 841-849.

Thomann, R.V., D.M. DiToro, R.P. Winfield and D.J. O'Connor. 1975. Mathematical modeling of phytoplankton in Lake Ontario. Part 1. Model development and verification. U.S. Environmental Protection Agency, EPA Report No. EPA-660/3-75-005.

Thomann, R.V., R.P. Winfield, D.M. DiToro and D.J. O'Connor. 1976. Mathematical modeling of phytoplankton in Lake Ontario. Part 2. Simulation using Lake 1 model. U.S. Environmental Protection Agency, EPA Report No. EPA-600/3-76-065.

Thomann, R.V. 1978. Size dependent model of hazardous substances in aquatic food chains. U.S. Environmental Protection Agency, EPA Report No. EPA-600/3-78-036.

Thomas, N., A. Robertson and W. Sonzogni. 1979. Review of control objectives, new target loads and input controls. Preprint of paper to be included in: Proceedings of the Conference on Phosphorus Management. Rochester, New York. (Preprint available from Great Lakes Basin Commission, Ann Arbor, Michigan).

U.S. Army Corps of Engineers. 1975. Lake Erie Wastewater Management Study preliminary feasibility report. Buffalo District Army Corps of Engineers, Buffalo, New York.

U.S. Army Corps of Engineers. 1975. Urban storm water runoff - STORM. The Hydrologic Engineering Center, Davis, California, Computer Program 723-SB-L2520.

Vollenweider, R.A. 1968. Scientific fundamentals of the eutrophication of lakes and flowing waters, with particular reference to nitrogen and phosphorus as factors in eutrophication. Organ. Econ. Coop. Dev., Paris, Technical Report No. DAS/CSI/68.27.

Vollenweider, R.A. and P.J. Dillon. 1974. The application of the phosphorus loading concept to eutrophication research. NRC Report No. 13690, Natural Resources Council of Canada, Ottawa, Canada.

Vollenweider, R.A. 1976. Advances in defining critical loading levels for phosphorus in lake eutrophication. Mem. Ist. Ital. Idrobio., 33, pp. 53-83.

Whitmore, F.C. 1977. A first order mass balance model for the sources, distribution and fate of PCB's in the environment. U.S. Environmental Protection Agency, EPA Report No. EPA-460/6-77-006.

Wischmeier, W.H. and D.D. Smith. 1965. Predicting rainfall - erosion losses for cropland east of the Rocky Mountains. Agricultural Handbook 282, U.S. Department of Agriculture, Agriculture Research.

Witten, A.J. and J.H. Thomas. 1976. Steady wind-driven currents in a large lake with depth-dependent eddy viscosity. J. Phys. Oceanogr., 6(1), pp. 85-92.

Wnek, W.J. and E.G. Fochtman. 1975. Mathematical models for the fate of pollutants in near-shore waters. Env. Sci. Tech. 6(4), pp. 331-337.

Wu, D.S. and B.J. Gallagher. 1973. Development of a complete mathematical model for describing the Point Beach Nuclear Power Plant thermal plume. Proc. of the First World Congress on Water Resources (4 Vol.), International Water Resources Association, Champaign, Illinois, pp. 319-336.

SECTION 3

DATA MANAGEMENT REQUIREMENTS FOR GREAT LAKES WATER QUALITY MODELING

William L. Richardson[1]

INTRODUCTION

An important but often neglected aspect of water quality research and management is data management. The time has past when individual investigators, biologists, chemists, limnologists and geologists working cooperatively with other investigators and agencies on large, complex and interacting systems such as the Great Lakes can record, process, and interpret data without the benefit of digital computers and computerized data bases. Data are being produced by numerous agencies and scientists for different purposes and components of the eco-water system using analytical instruments that produce analog and digital output at phenominal rates. These data must be recorded, transformed, verified, reduced, stored, retrieved, and statistically analyzed, before they become useful. This paper discusses the data management requirements for Great Lakes water quality research, management and mathematical modeling from a modeling perspective.

GREAT LAKES WATER QUALITY DATA

The need for data is perceived in various ways depending on one's viewpoint. The planner requires information to develop plans for future development of remedial programs while the regulator requires an assessment of which water quality standards are being violated and the cause. The public health administrator wants to know if the water is safe for drinking and swimming and whether the fish are safe to eat. The waste water treatment plant operator wants to know how much more effluent can be discharged without violating standards and the water supply manager wants to know the characteristic of the water so the plant can be operated in the most efficient manner. The scientist (ecologist and limnologist) desires an understanding of how and why the system behaves and the modeler quantifies hypotheses describing this behavior.

[1]U.S. Environmental Protection Agency, Large Lakes Research Station, Grosse Ile, Michigan 48138.

committee and will not be discussed in detail here. However, any water quality data base must provide for notation and qualification of the precession and accuracy of the data.

If data are to be transferred from one institution's computer to another, however, certain basic criteria must be followed. To facilitate efficient and accurate exchange of data the following guidelines should be followed (International Joint Commission, in preparation):

a. That data be stored at a minimum resolution of "raw data" i.e., at the spacial and temporal resolution at which an individaul sample or observation was collected.

b. That data be spacially referenced and stored according to either latitude-longtitude or Universal Transverse Mercater - 6 UTM grid coordinate.

c. That measurements be directly or indirectly referenced to a uniform table of nomenclature for parameters in accepted units preferably SI Units.

d. That individual data elements be stored in reference to time and date.

e. That the time of data turn-around from the field sample to storage be reduced to as short a time as possible with a goal of less than 90 calendar days.

f. That an index or catalog of data collected by participating agencies be maintained as an on-line computerized query system.

g. That the participants accept the responsibility for comprehensive verification of all data stored in their respective systems.

h. That the agencies maintain their data files indefintely.

i. That agencies process data requests from investigators as quickly as possible.

DATA NEEDS FOR MODELING

The role of modeling in the water quality management process can be perceived using Figure 1. Mathematical models provide the focus for the synthesis of the surveillance data and experimental research. Model results are used to translate data and tested theories into terms managers can use for decision making. Decisions usually result which either alter the quantities of residual materials allowed to enter the system or which alter the environmental goals. Data provide the basis for this process and the efficient, accurate, and timely management of these data is mandatory.

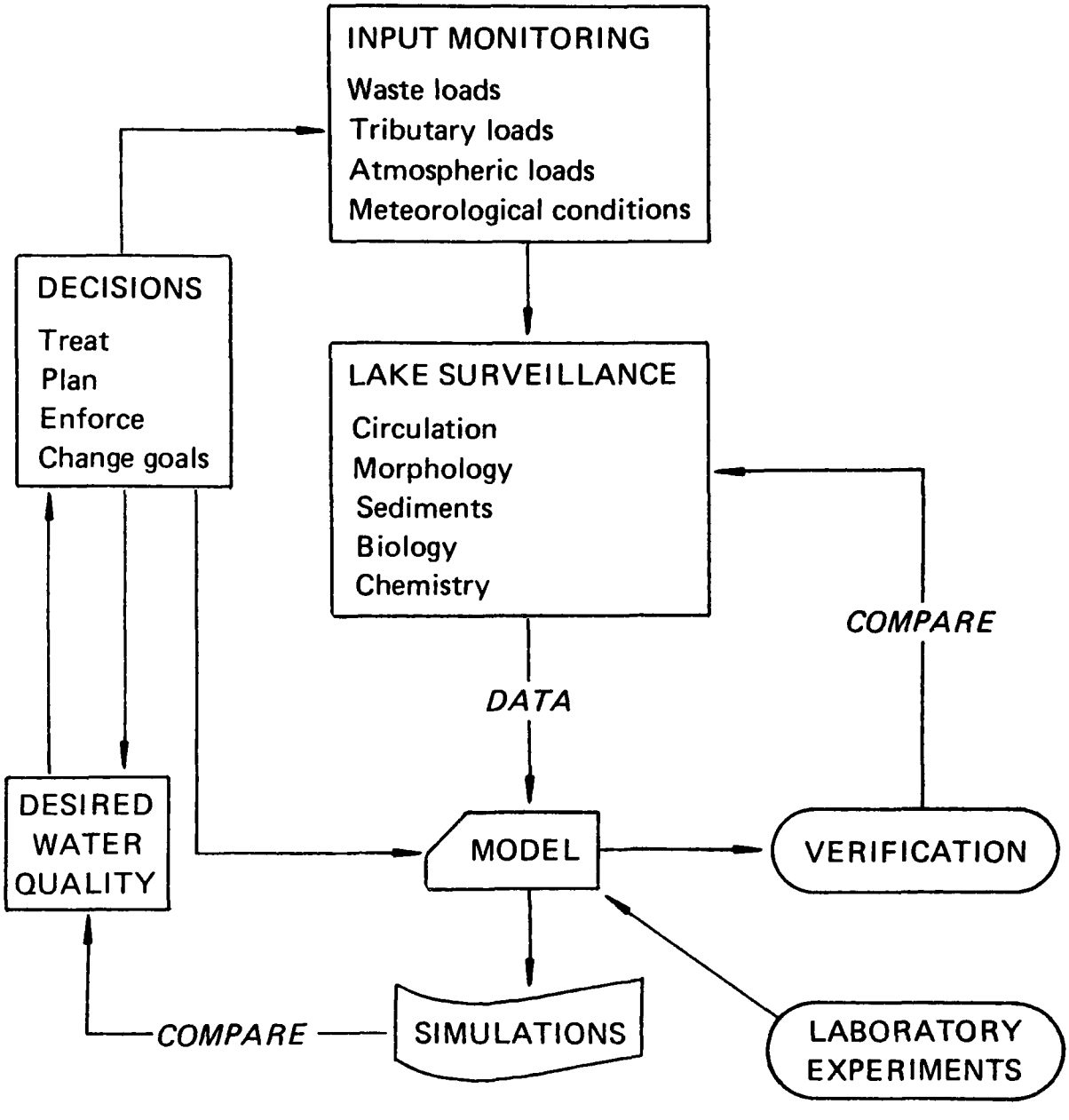

Figure 1. Great Lakes modeling-management process.

Therefore, data originate from surveys to determine the temporal and spatial characteristics of physical, chemical, and biological properties for a multitude of purposes. For the Great Lakes, Canadian and U.S. Agencies and laboratories are spending over $10 million per year on this effort, coordinated through the International Great Lakes Surveillance Plan required under the 1978 Water Quality Agreement (GLWQA 1978).

The general objectives of this plan include (International Joint Commission 1978):

1. To search for, monitor, and quantify violations of the existing Agreement objectives (general and specific), the IJC recommended objectives, and jurisdictional standards criteria and objectives.

2. To monitor local and whole lake response to abatement measures and to identify emerging problems.

3. To provide data for determining the cause-effect relationship between water quality and material inputs in order to develop the appropriate remedial/preventative actions and predictions of the rate and extent of local/whole lake response to alternate abatement proposals.

BASIC REQUIREMENTS

The component of the International Great Lakes Surveillance Plan which provides the primary means of data coordination is data management and interpretation. A work group of the International Joint Commission (IJC)[1] Surveillance Subcommittee has been established to develop a data management plan and to provide general guidelines for data interpretation. Some basic requirements of this plan include:

1. Accuracy and Timeliness: Timeliness is an essential factor in water quality research and management. Delays in processing results to the manager can result in inaccurate, erroneous decision-making and inefficiencies. However, accuracy should not be sacrificed for expediency. Accuracy must be assurred through careful transcription, keying, and verification. Accountability by the persons involved assures a higher degree of accuracy.

2. Compatibility: Because Great Lakes data are collected by a multitude of agencies and laboratories by various disciplines in two countries, one province and eight states, data base compatibility is a necessity. Comparable data first require uniform sampling and laboratory methodology and intercomparison studies and quality control must be incorporated into the surveillance program. For the Great Lakes International Surveillance Plan this is being coordinated by the Data Quality Work Group of the Surveillance Sub-

[1]A binational body which is responsible for the implementation of the U.S.-Canada Great Lakes Agreement

Generally, the data requirements for model calibration and verification are different than those for detecting and quantifying objective violations and water quality trends. The intensity of sampling depends on the time and space scale for water quality variables to which the model is being developed and applied. Table 1 includes a list of eutrophication models that were recently employed to establish the target phosphorus loadings for the renegotiated Great Lakes Agreement with Canada (Bierman 1979). These models are similar in that they relate loadings of phosphorus to phosphorus and phytoplankton biomass (represented by dry weight or chlorophyll a). They are different in that each represents a unique hypothesis of cause and effect. Each is an attempt to describe the eutrophication process for the subject lake (or lakes) to a different level of complexity in terms of time and space and biological and chemical resolution.

Input Requirements

Inputs represent the "knowns" in the mathematical expressions which represent the model. All of the models require basic morphometric data. Information on depth, volume, hydraulic detention time are normally available for U.S. lakes because of extensive work done in the past for other purposes such as navigation charts, flood control, and fish management and this information remains almost constant in time relative to other inputs.

External Loads

The mass loads of the primary model variables represent the "forcing functions" of the model equations. Loads are estimated by the product of water inflow and concentration. Extensive work has been done to develop loadings for the Great Lakes models (Corps of Engineers 1975; International Joint Commission 1976) and an extensive and unique data base is required for this purpose. The U.S. Geological Survey (USGS) measures flows of most of the major Great Lakes tributaries and these data are available through both USGS and EPA data bases. State and Provincial governments maintain monthly or bi-monthly water quality monitoring sites near mouths of most significant tributaries as required by the U.S.-Canadian Agreement and these data are stored in computerized data bases.

The resolution and accuracy to which loads must be measured depends on the system and the model. Vollenweider and Chapra's whole lake models need loads for just phosphorus estimated on an annual average basis. Thomann and DiToro's 2-layer models for Lakes Ontario (Thomann et al. 1975) and Huron (DiToro and Matystik 1979) also operate with annual loadings because of the long hydraulic detention times of these lakes, 23 and 8 years, respectively. DiToro's model (DiToro and Connolly 1979) of Lake Erie includes three horizontal segments with three layers with hydraulic detention times on the order of three months for the Western Basin to about 1-1/2 years for the central basin and seasonal loadings are needed for this finer resolution. Bierman's five segment model of Saginaw Bay (Bierman et al 1979) requires loadings resolved to the same degree as the daily hydrograph of Saginaw River because of the short detention time of the smallest segment.

TABLE 1. SUMMARY OF PRINCIPAL MODEL CHARACTERISTICS (Bierman 1979)

Characteristic	Vollenweider[1] (All Basins)	Chapra[2] (All Basins)	Thomann/[3] DiToro[4] (Lakes Ontario & Huron)	DiToro[5] (Lake Erie)	Bierman[6] (Saginaw Bay)
Time Dependence					
Dynamic		X	X	X	X
Steady-State	X				
Spatial Segmentation					
None	X				X
Horizontal		X	X	X	
Vertical			X	X	
Input Requirements					
External loads for primary variables	X	X	X	X	X
Depth	X	X	X	X	X
Volume	X	X	X	X	X
Hydraulic detention time	X	X			
Temperature			X	X	X
Light			X	X	X
Water circulation rates			X	X	X
Sediment nutrient release rates				X	
Primary Variables					
Phosphorus	X	X	X	X	X
Nitrogen			X	X	X
Silicon				X	X
Total forms only	X	X			
Available and unavailable forms			X	X	X
Secondary Variables					
Chlorophyll	X	X	X		
Diatom/Non-diatom chlorophyll				X	
Multi-class biomass					X
Zooplankton			X	X	X
Dissolved Oxygen	X	X		X	
Direct Calculations			X	X	X
Empirical correlation	X	X			

[1]From Vollenweider 1975.
[2]From Chapra 1977.
[3]From Thomann *et al*. 1975.
[4]From DiToro and Matystik 1979.
[5]From DiToro and Connolly 1979.
[6]From Bierman *et al*. 1979.

Primary and Secondary Variables

The models calculate concentrations of primary and secondary variables as shown in Table 1. The simulations are compared to actual data during calibration and model coefficents adjusted within acceptable ranges until the simulated concentrations describe the data to a satisfactory degree. Thomann (Thomann et al 1979) has developed a rigorous statistical approach to reduce arbitrary and qualitative judgement involved in this process.

To resolve seasonal variation in nutrient and biomass concentrations enough data are required to estimate a mean and standard error for each of the model segments at a sampling frequency sufficient to resolve important fluctuations. Rigorous approaches for sampling design are lacking but in general for each of the Great Lakes ten to twelve sampling cruises are required at a station density of one station per 100 square miles for Erie and Ontario and three stations per 1000 square miles for Michigan, Huron, and Superior. Vertical sampling density is related to defining the thermocline and associated chemoclines but generally the Great Lakes surveillance plan specifies depth samples at 1 meter, mid epilimnion, lower epilimnion, upper hypolimnion, 1 meter above bottom (International Joint Commission, 1978).

Uniformity

An implied data requirement of a modeling project is that all data should be obtained concurrently. Each lake and input sample must be analyzed for all model variables. For example, one cannot use ammonia data from a previous study and combine it with nitrate data for the current study and hope to model the nitrogen cycle. Also, one cannot use phosphorus loadings from one time period and combine it with concentration data from another and hope to get reliable results. Therefore, this requirement necessitates large, coordinated surveillance programs for the Great Lakes involving many agencies and laboratories. A uniformity of methods must be maintained along with a common approach to data management.

In summary, enough data must be available to obtain statistically significant estimates of mass loads and average concentrations for each variable in each segment and each time period (cruise). The dynamic, multicompartment, multi-segment (high resolution models) require more data than the steady state, single segment (whole-lake) single compartment (one variable) models. It is not the purpose of this discussion to judge the merits of each of the models or model types. The point is that modeling projects whose purpose is to obtain understanding of limnological processes at high resolution require significantly more data and, therefore, data management becomes much more critical.

GREAT LAKES DATA BASES

One means to effect data base uniformity is to require the surveillance and research organizations to use the same computer and data base system. This possibility was considered by the Data Management Work Group of the IJC

Surveillance Subcommittee but it was determined to be too complex to implement between two countries. Rather it was decided to recommend maintenance of existing data base systems with separate agreements between parties to exchange data as needed. In the U.S., however, it has become EPA policy to require all data collected by organizations under contracts, grants or interagency agreements to be stored into its data base system, STORET (International Joint Commission, in preparation).

STORET (STOrage-RETrieval) is a national, on-line data base system developed by EPA (and predecessor agencies) for the archiving of water quality data. Because of its utility, ease of use, and efficiencies, STORET is used by most all U.S. State and Federal agencies involved with collection of water quality information. The STORET water quality file contains about 60 million observations which are accessible on-line via a telecommunication network.

For the Great Lakes, STORET is viewed by many as an essential tool for meeting the mandates of federal laws and the Great Lakes Water Quality Agreement. Not only does it provide for long-term storage of data but it also provides for exchange of data as well as a means to statistically analyze data. Because the data base resides on on-line disks, access can be made by any user at their convenience via a telephone communications network. This eliminates much of the bureaucracy that has traditionally been associated with accessing data from other agencies.

Although STORET and the computer system on which it resides provide for some statistical application, many users would rather obtain copies of data sets and transfer these to their own computer where they may have available more specialized analysis programs. At the EPA, LLRS a system is being developed whereby subsets of the STORET are retrieved and telecommunicated to an in-house PDP 11/45 minicomputer. This "Mini-STORET" system will have various options which the user may specify. A schematic of this is shown in Figure 2. The user will have the choice of various output formats, hard copy listings, files for use by model programs, graphical output, or files for statistical programs.

The key objective is to make data manipulation as efficient as possible and easily accessible by non-computer personnel for interpretation. For example using manual techniques it may take a man-year just to get the data in the proper formats for modeling purposes. Using the Mini-STORET system it is expected that this will be reduced by at least 75%.

EXISTING GREAT LAKES DATA IN STORET

The Great Lakes data base in STORET consists of data collected by the U.S. participants in the Great Lakes Surveillance Plan and their grantees and contractors. Also, all the open lake data collected by the Canadian Center for Inland Waters (CCIW) has been stored through an agreement between CCIW and EPA, LLRS. In exchange for these data, CCIW has been provided with a STORET account for direct access to all U.S. data. Historical data has

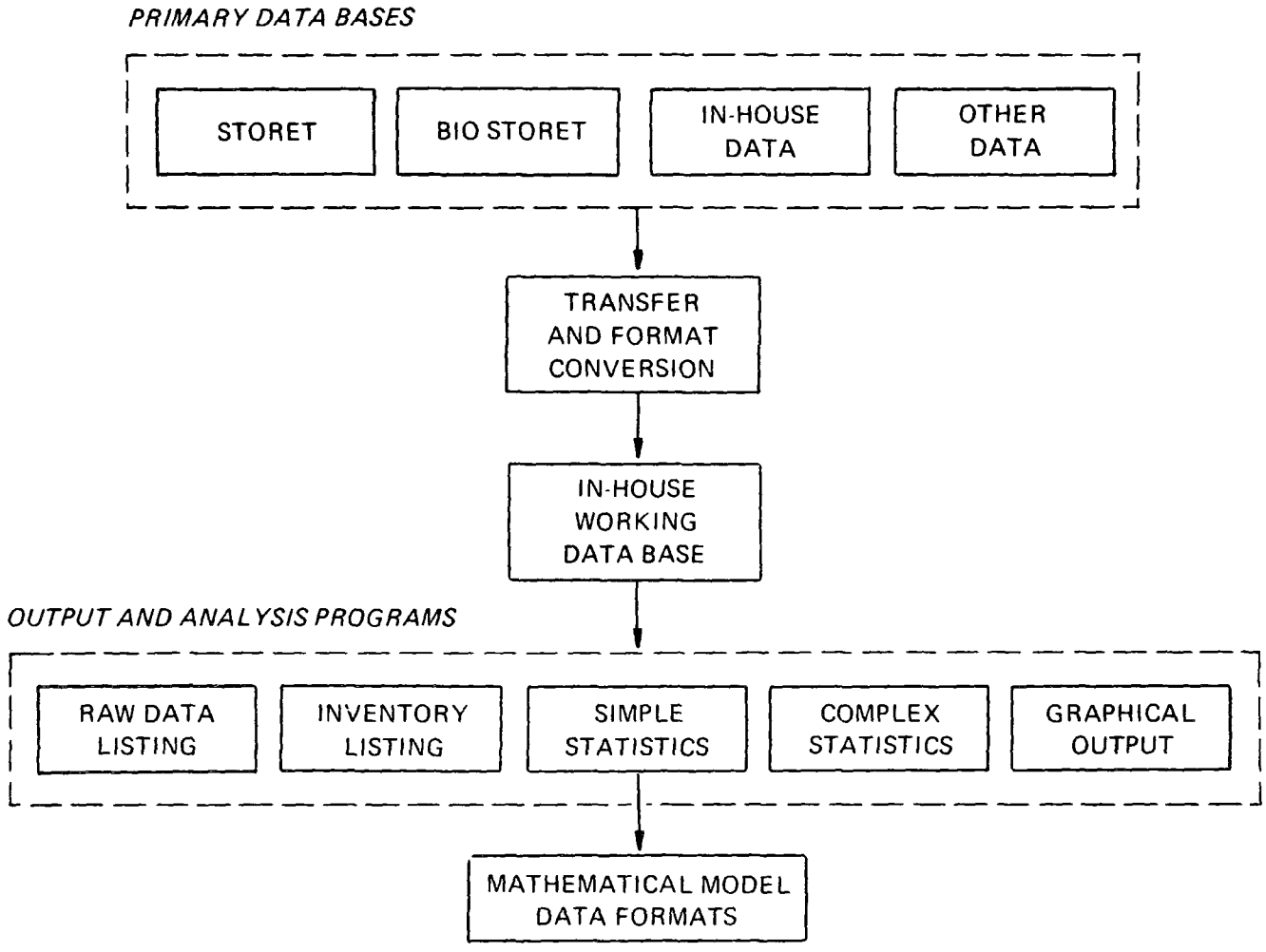

Figure 2. Large Lakes Research Station mini-storet system.

been stored where it has been available, but this is a very tedious and expensive task.

A complete inventory of all Great Lakes Data stored in STORET is contained in Appendix A. A summary of this inventory is given in Table 2. As this table indicates there are over 3 million observations for the Great Lakes stored in STORET or about 5% of the U.S. water quality file. This is not a significant proportion considering that the Great Lakes represents about 95% of the surface freshwater in the U.S. Figures 3 through 8 show the time distribution of data availability for each lake. Several interesting observations can be made from these graphs that reveal the history of Great Lakes surveillance. First it appears that prior to 1960 most data collection efforts were done on the connecting channels. The period 1962 through 1966 represent the first Federal surveillance effort for the open lakes. For Lake Ontario the peak in 1972 represents the data collected for the International Field Year on the Great Lakes. The 1975 peaks represent the surveillance effort of the IJC Upper Lakes Reference Study. Lake Erie was the subject of intensive sampling from 1967 to 1975 by both U.S. and Canadian agencies and the decline in 1976-1977 was due to the implementation of the IJC Surveillance plan which diverted most of the U.S. effort for that period to Lake Michigan and a new effort for Erie in 1978 and 1979.

The number of observations does not necessarily reflect the utility of these data for modeling purposes, however; but Table 3 might give some indication of this for eutrophication models. Ideally, each sample collected should have been analyzed for the basic state variables listed in Table 1. It can be seen that Chlorophyll a data are generally lacking. For all the lakes except Michigan Kjeldahl nitrogen data appears to be deficient. On the other hand there appears to be an over abundance of silica data. For Lake Michigan there is a higher proportion of phosphorus to nitrogen data. Since this table includes the entire period of record, it may not represent the more recent attempts by the Surveillance Subcommittee to obtain data for modeling purposes. To determine exactly whether existing data in STORET are suitable for modeling purposes, the interested reader is encouraged to review "raw" data in detail. Appendix B presents examples of STORET retrieval procedures.

BIOSTORET

Biological data have always presented difficulties for data management. There exists such a variety of samples, components and characteristics, that STORET has not been able to deal with the parameter code requirements. This is particularly the case for toxonomic data. In response to the need for a biological data base, EPA has developed a specialized system, BIOSTORET. The system is similar to STORET in that it is user oriented and references samples to sample location, depth, time, and concentration but extends the capability to deal with toxonomic information as well as other descriptive data. This system and data base are in a pilot stage and some of the Great Lakes data are being used to test the system. Appendix C contains an example BIOSTORET retrieval, command file, and output.

TABLE 2. SUMMARY OF GREAT LAKES DATA IN STORET
(As of June 1979)

Lake	Number of Stations	Number of Observations	Number of Samples
Superior	414	115,621	8,944
Michigan	2,249	663,144	70,463
Huron	1,089	306,717	26,582
Erie	2,426	1,050,639	128,445
Ontario	1,653	592,294	78,610
Total Lakes	7,831	2,728,415	313,044
Connecting Channel			
St. Mary's River	162	51,795	4,653
St. Clair River	159	46,863	5,532
Lake St. Clair	275	31,472	2,973
Detroit River	335	144,017	21,376
Niagara River	66	45,260	4,246
Total Conn. Channels	997	319,407	38,780
Total	8,828	3,047,822	351,824

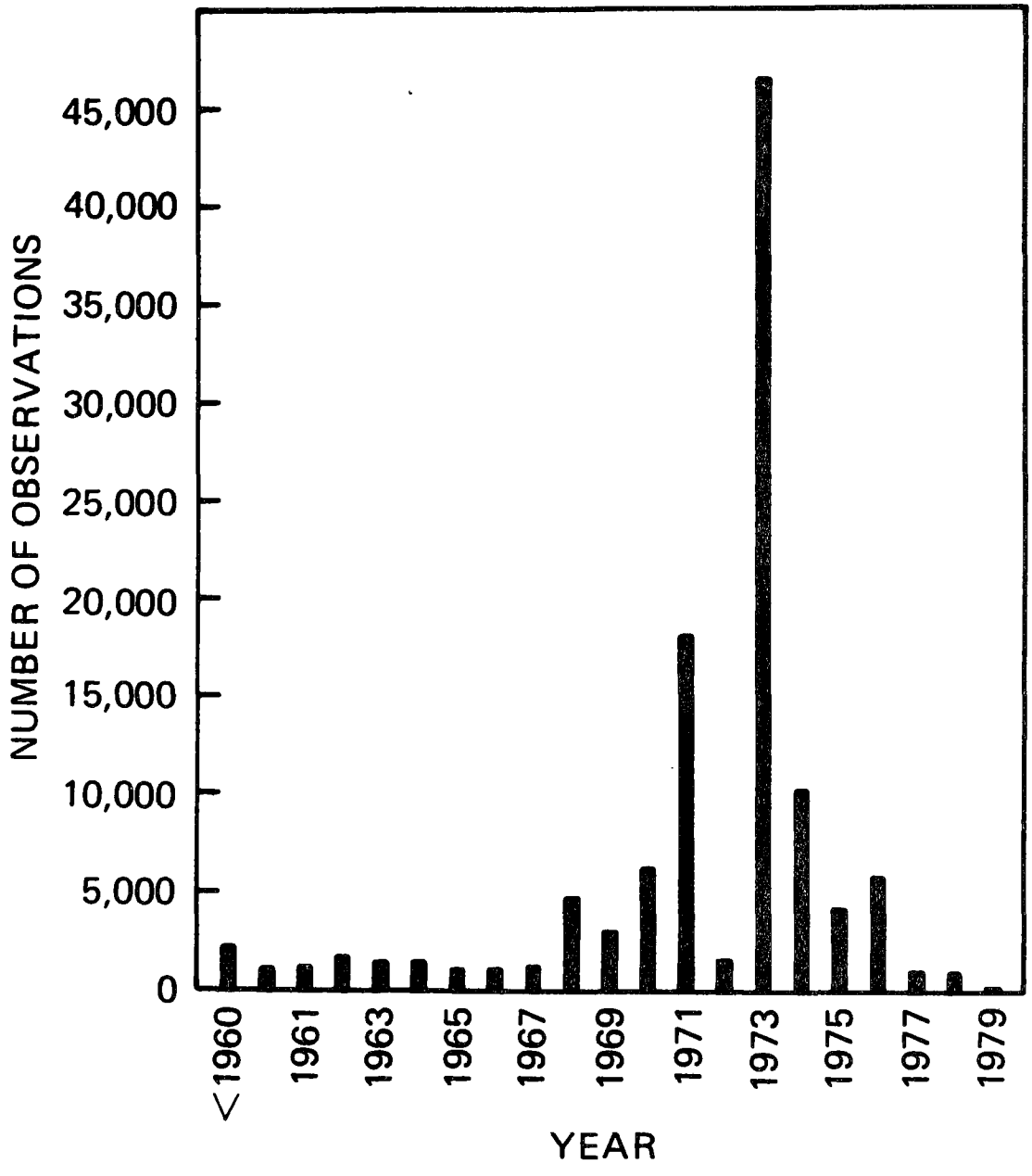

Figure 3. Summary of Lake Superior data from Storet water quality file.

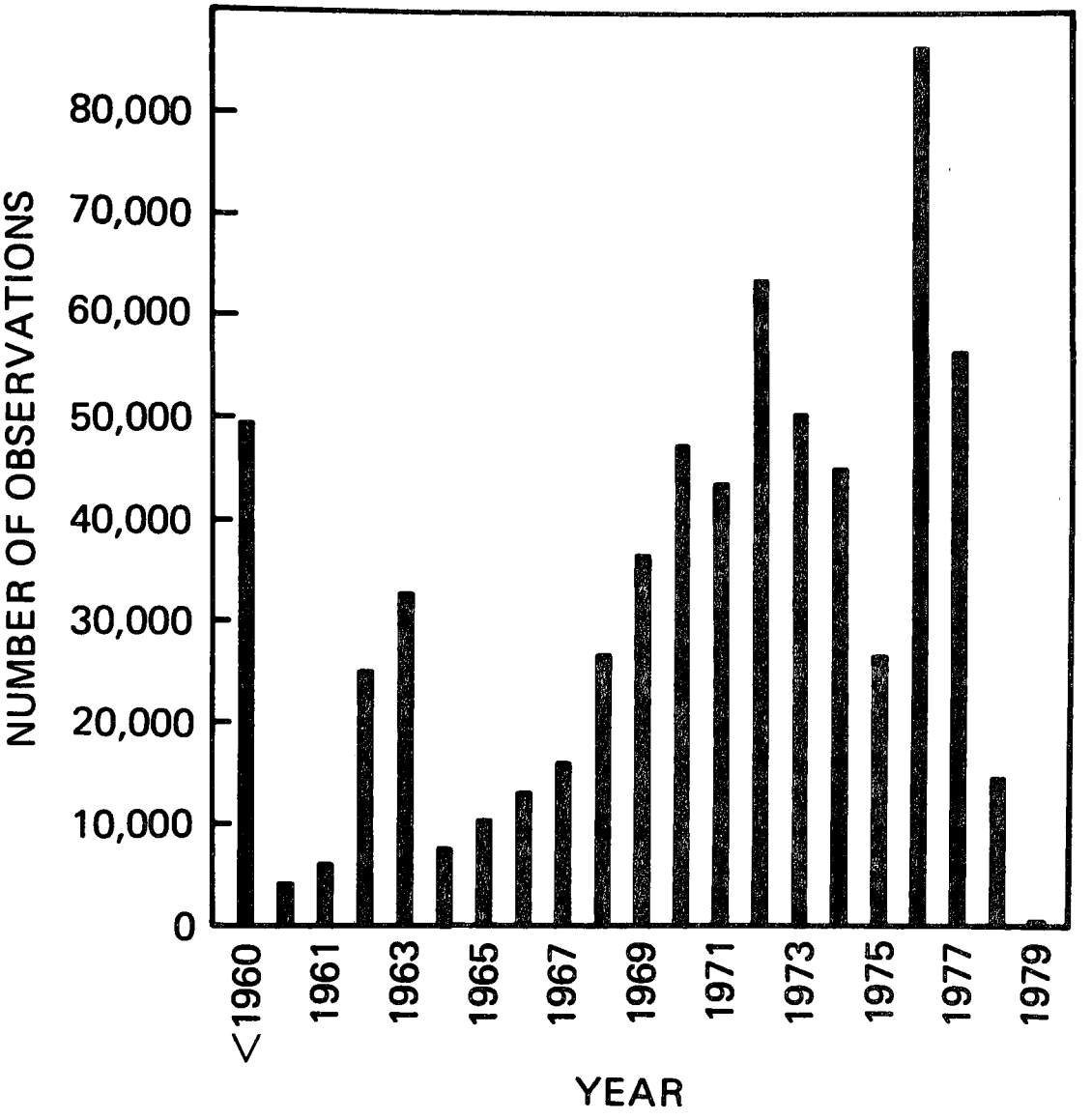

Figure 4. Summary of Lake Michigan data from Storet water quality file.

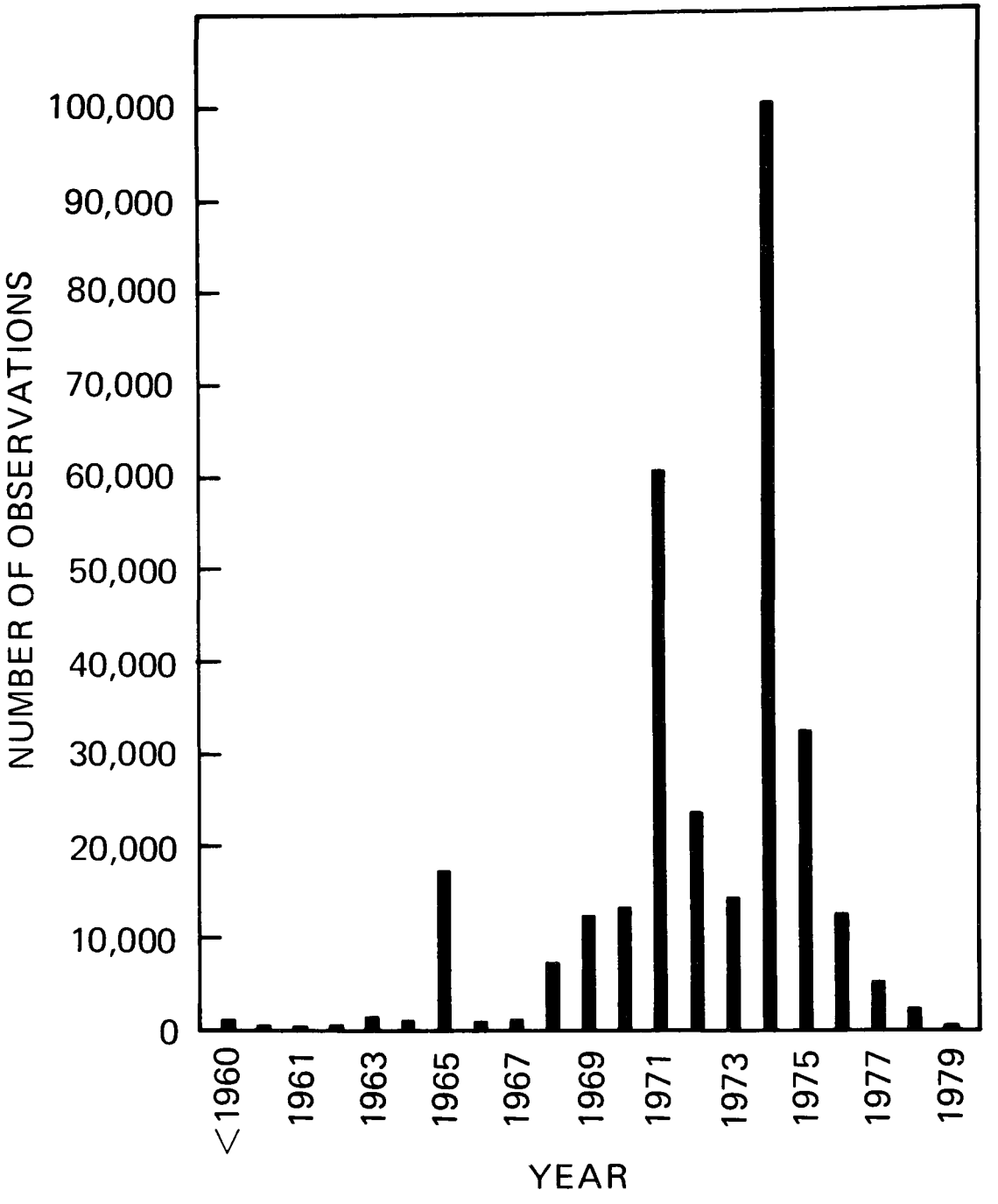

Figure 5. Summary of Lake Huron data from Storet water quality file.

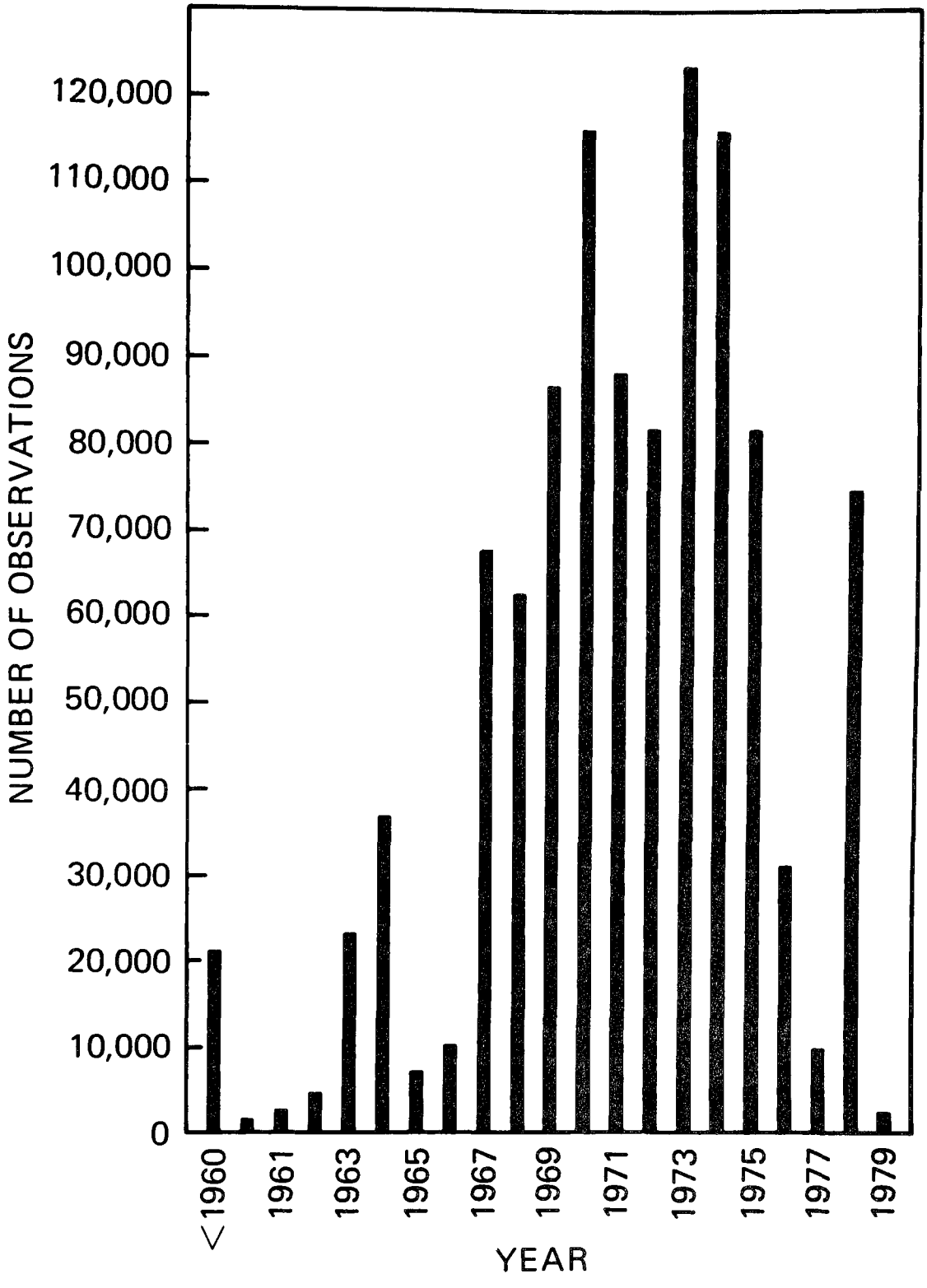

Figure 6. Summary of Lake Erie data from Storet water quality file.

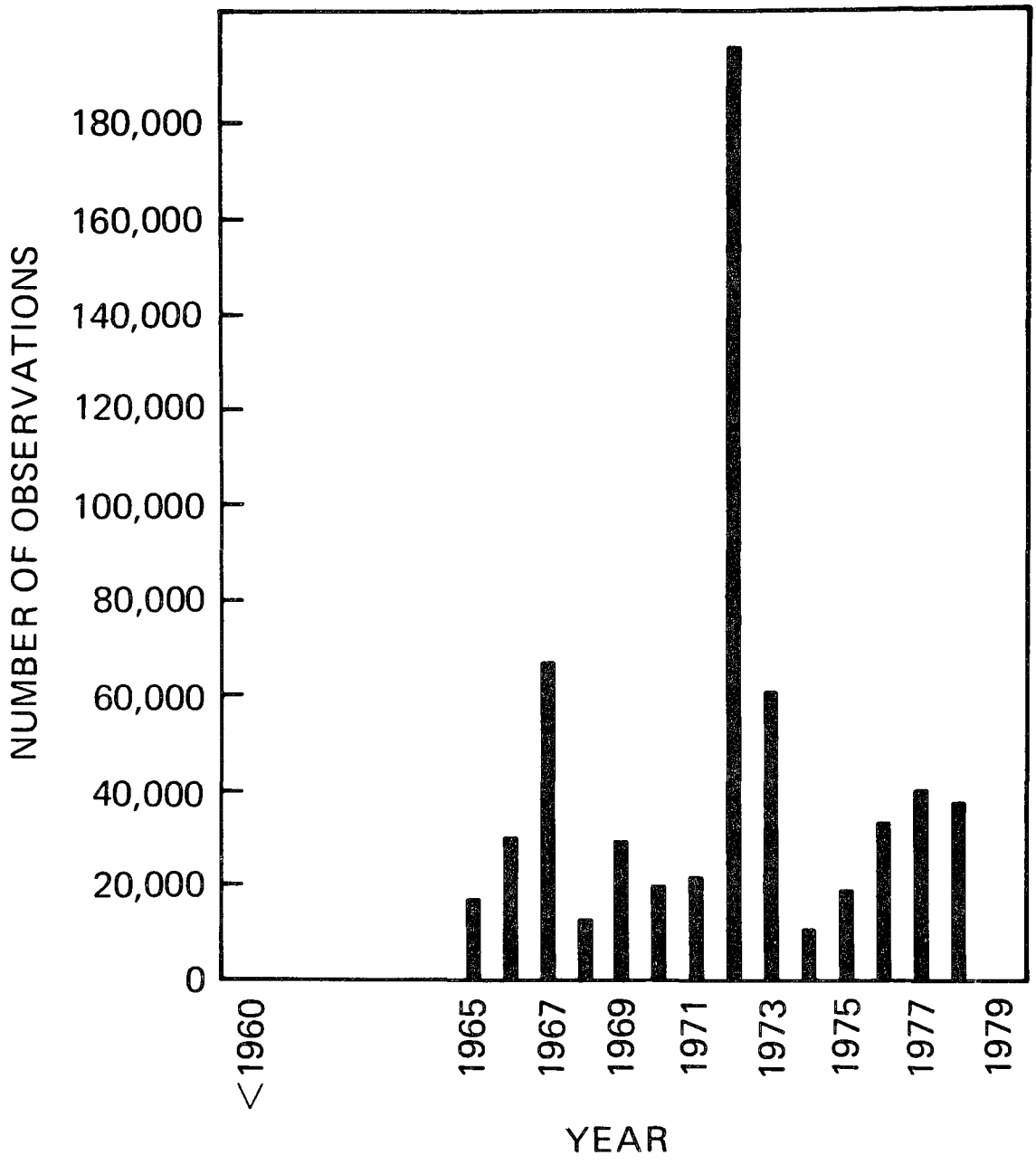

Figure 7. Summary of Lake Ontario data from Storet water quality file.

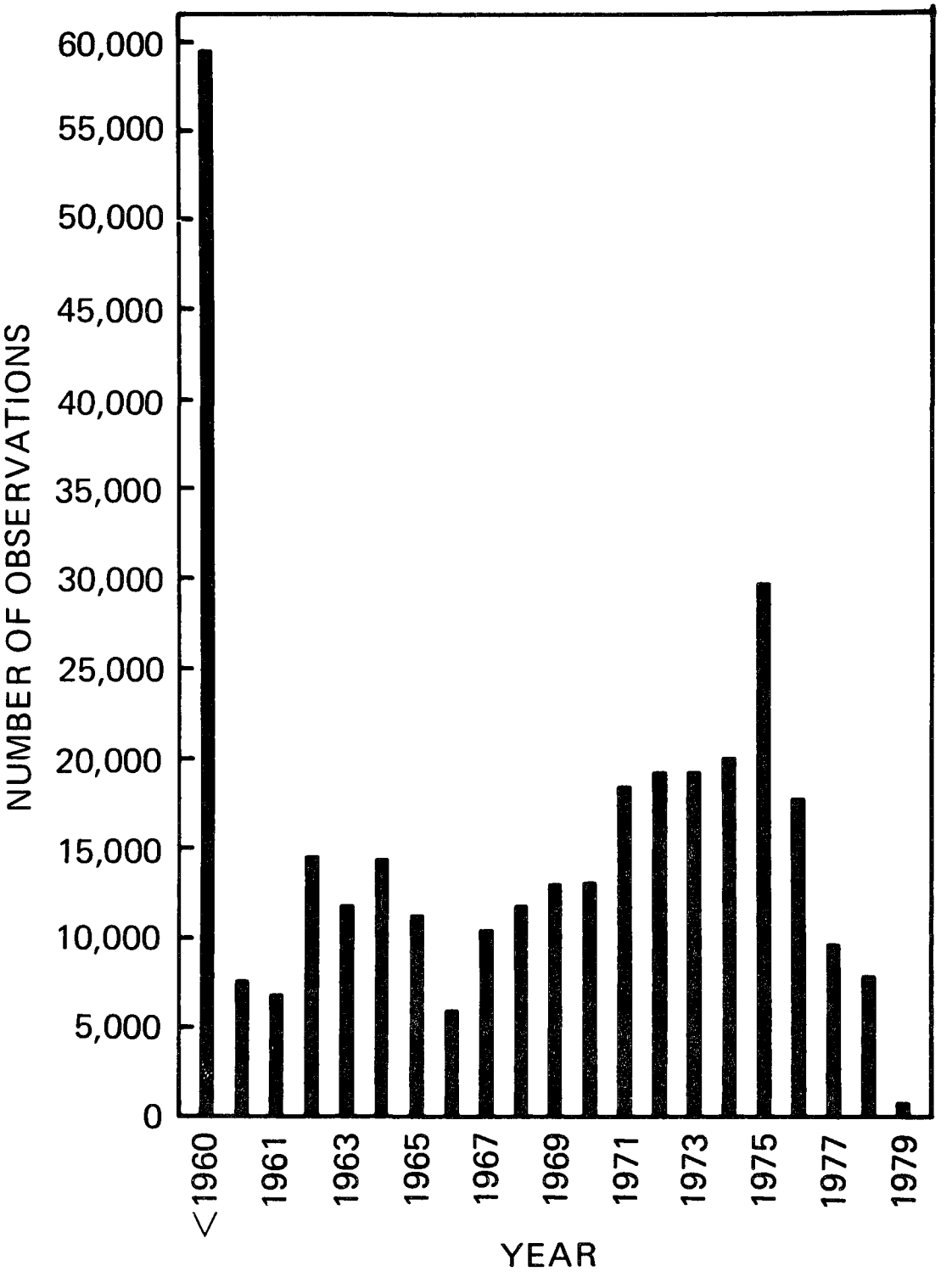

Figure 8. Summary of Connecting Channels data from Storet water quality file.

TABLE 3. STORET WATER QUALITY FILE SUMMARY OF GREAT LAKES EUTROPHICATION DATA (As of June 1979)

	Number of Observations					
	Superior	Michigan	Huron	Erie	Ontario	Connecting Channels
Total Phosphorus	3,483	13,805	11,867	16,702	23,342	6,389
Phosphorus Dissolved Ortho	3,729	6,531	8,638	13,064	19,427	331
Phosphorus Dissolved	2,610	5,891	10,531	11,889	16,272	1,761
Total Kjeldahl Nitrogen	275	3,969	3,282	5,003	7,380	2,499
NO_2 + NO_3 Dissolved	3,793	2,680	11,799	9,761	20,534	275
NH_3-N Dissolved	3,639	3,592	9,868	8,957	22,937	261
Silica Dissolved	3,853	6,717	12,404	16,508	24,787	1,004
Chlorophyll 'A' (Corrected)	-	388	3,168	6,830	9,200	5
Temperature	7,236	27,675	19,942	96,559	56,979	23,613

RESOURCE REQUIREMENTS

Data handling is often done as an afterthought. As a result, deadlines have been missed, scientific personnel have been misused, data have been lost, more errors have been made, and project effectiveness reduced. To remedy this managers must allocate adequate resources for data management. Resources include a budget, trained personnel, and adequate computer hardware and software.

The EPA, Large Lakes Research Station eutrophication studies on Saginaw Bay devoted about 10% of total resources to data management. This covered all effort required to get results from bench sheets to a data base.

Data base costs (STORET) include initial storage charges (computer time) of about $.01 per observation and storage changes of about $.005 per observation per year. Based on these unit costs Great Lakes data base costs about $15,000. per year to maintain on disk. (The entire STORET water quality file costs about $300,000. per year to maintain). Another 10 to 15 percent of total surveillance resources are required for statistical analysis and modeling.

CONCLUSIONS

Efficient data management is essential to water quality management and research programs. Program managers must recognize the role of data management and make adequate staffing and budget provisions for its implementation. This is the case for whatever purpose to which the data are being applied; however, it is an absolute requirement for timely development of mathematical models.

Models require complete sets of data for all state variables for the time and space resolution desired. Although the most critical need for modeling is proper surveillance design in the first place, accurate and timely data processing plays a key role in the modeling process. As models become more complex the quantity and complexity of data increases and automated, computerized data base and data analysis tools become more important. As a rule of thumb about 10% of total project costs should be devoted to data management.

REFERENCES

Bierman, Victor J., Jr. 1979. A comparison of models developed for phosphorus management in the Great Lakes. Prepared for Conference on Phosphorus Management Strategies for the Great Lakes, Rochester, N.Y. April 17-19, 1979 (in press).

Bierman, V.J., Jr., D.M. Dolan, E.F. Stoermer, J.E. Gannon and V.E. Smith. 1979. The development and calibration of a multi-class, internal pool, phytoplankton model for Saginaw Bay, Lake Huron. In press, EPA Ecological Research Series.

Chapra, S.C. 1977. Total Phosphorus model for the Great Lakes. Journal of the Environmental Engineering Division, American Society of Civil Engineers. 103 (EE2):147-161.

Corps of Engineers, Department of Army, Buffalo District. Lake Erie Wastewater Management Study, Preliminary Feasibility Study, Volume 1 and 2, December 1975.

DiToro, D.M. and W. Matystik, Jr. 1979. Mathematical models of water quality in large lakes, Part I: Lake Huron and Saginaw Bay model development, verification, and simulations. EPA Ecological Research In Preparation, EPA Ecological Research Series.

DiToro, D.M. and J.F. Connolly. 1979. Mathematical models of water quality in large lakes, Part II: Lake Erie. In preparation, EPA, Ecological Research Series.

Great Lakes Water Quality Agreement of 1978 Agreement with annexes and terms of reference between the United States of America and Canada, signed at Ottawa, November 22, 1978.

International Joint Commission. In preparation. Data Management and Interpretation component of the Lake Erie Surveillance Plan prepared by the Data Management and Interpretation Work Group for the Surveillance Subcommittee, Great Lakes Water Quality Board, June 1979.

International Joint Commission. 1976. Water Quality Board. Great Lakes Water Quality 1975, Appendix B, Surveillance Subcommittee Report. July 1976.

International Joint Commission. 1978. Lake Erie Surveillance Plan prepared by the Lake Erie Work Group for the Surveillance Subcommittee, Great Lakes Water Quality Board, Revised March 1978.

Thomann, R.V., D.M. DiToro, R.P. Winfield and D.I. O'Connor. 1975. Mathematical modeling of phytoplankton in Lake Ontario, I. Model development and verification, U.S. Environmental Protection Agency Ecological Research Series. EPA-600/3-76-065.

Thomann, R.V., R.P. Winfield, J.I. Segma. 1979. Verification Analysis of Lake Ontario and Rochester Embayment Three Dimensional Eutrophication Model. In press, EPA Ecological Research Series.

Vollenweider, R.A. 1975. Input-output models with spatial reference to the phosphorus loading concept in limnology. Schweigresche Zeitschrift fur Hydrologie. 37:53-84.

APPENDIX A

INVENTORY OF WATER QUALITY DATA FOR THE GREAT LAKES CONTAINED ON THE STORET WATER QUALITY FILE

Available upon request from:

William L. Richardson
EPA, Large Lakes Research Station
9311 Groh Road
Grosse Ile, Michigan 48138

APPENDIX B

EXAMPLES OF STORET RETRIEVAL PROCEDURES

Available upon request from:

William L. Richardson
U.S. Environmental Protection Agency
Large Lakes Research Station
9311 Groh Road
Grosse Ile, Michigan 48138

APPENDIX C

EXAMPLES OF BIOSTORET RETRIEVALS AND PROCEDURES

Available upon request from:

William L. Richardson
U.S. Environmental Protection Agency
Large Lakes Research Station
9311 Groh Road
Grosse Ile, Michigan 48138

SECTION 4

OPTIMAL SAMPLING FOR LONG TERM TRENDS IN LAKE HURON

David M. Dolan[1]

INTRODUCTION

A major goal of the International Surveillance Program for the Great Lakes is to detect long-term changes in the concentrations of various parameters in each of the lakes. With this in mind, the Lake Huron Work Group of the Surveillance Subcommittee of the International Joint Commission has designed a Lake Huron Surveillance Plan. The plan calls for intensive sampling of the main lake in 1980, and sampling of all the major tributaries each year. The intensive main lake effort will be repeated in 1989, and again in 1998. After each intensive sampling, the data will be examined and trends evaluated.

In order for the Surveillance Program to be successful, data must be provided of sufficient quality so that trends may be accurately assessed. The required accuracy for trend detection can be expressed conveniently in probablistic terms (DePalma 1977). For example, if it is desired to detect changes in the lakewide average concentration of chloride of 1 mg/ℓ or greater with 90% probability, it can be shown that the standard error of chloride measurements must not exceed 0.158 mg/ℓ. Since the measurement procedure for chloride is well established, the usual way to decrease the standard error is to increase the number of observations. However, each additional sample collected results in higher surveillance costs. Thus, there is a trade-off between accuracy and funds required. A method is needed to optimize the sampling program to obtain the required accuracy at minimum cost.

If a reliable mathematical model was available for the parameter of interest for Lake Huron, sampling costs could be reduced drastically. It would only be necessary to update the information on model forcing functions, such as loading rates and water movements, to accurately identify trends. Unfortunately, models of Lake Huron, even for the simplest conservative substances, are imperfect because of inaccurate model parameters. It is intuitively obvious that a procedure which would combine the best infor-

[1]U.S. Environmental Protection Agency, Large Lakes Research Station, Grosse Ile, Michigan 48138.

mation available from a model with the information from sampling a lake would be highly desirable and could result in significant cost savings. Such a procedure is available using the Kalman filtering technique.

The Kalman filter (Kalman 1960; Kalman and Bucy 1961) is an information processing technique that has had much use in aerospace engineering. It combines model calculations and sampling results to estimate a parameter of interest. The estimate is, ideally, better than one obtained from either a model or a series of measurements alone. The basic function of the Kalman filter is the calculation of the Kalman gain. This gain provides the relative weighting of model and measurements to obtain a estimate at a desired time. If the model is inaccurate compared to the data, the data will receive most of the weight. If the data is "noisy" compared to the model, the model estimate will be given the most weight. The advantage of the linearized Kalman filter for lake concentration sample optimization is that the estimation errors at future times can be calculated independently of the actual concentration estimates. Thus, as a model increases in accuracy as more data becomes available, the model output will receive higher weight in the estimate, and fewer measurements will be necessary to meet accuracy requirements.

The Kalman filtering technique has been applied to lake concentration estimation for the case of Lake Michigan (DePalma et al. 1979). This paper is an application of the procedure to Lake Huron.

THE LAKE HURON SYSTEM

The Lake Huron system has been described in detail elsewhere (Upper Lakes Reference Group 1977). The system, the third largest of the Great Lakes by volume, is composed of four interconnected water bodies: the main lake, Saginaw Bay, North Channel and Georgian Bay (Figure 1). It is connected to Lake Michigan at the Straits of Mackinac, to Lake Superior by the St. Mary's River and to Lake St. Clair by the St. Clair River (Table 1). In

TABLE 1. LAKE HURON MAJOR INFLOWS AND OUTFLOWS

Lake	Route	Annual Average Flow
Michigan	Straits of Mackinac	1920 m^3/sec
Superior	St. Mary's River	2110 m^3/sec
St. Clair	St. Clair River	5050 m^3/sec

general, water entering in the northern part of the lake flows south along the Michigan coast. There are also strong northern currents along the Ontario coast (Figure 1).

At present, main Lake Huron is considered to be an oligotrophic lake, as is indicated by a number of chemical and biological parameters (Table 2).

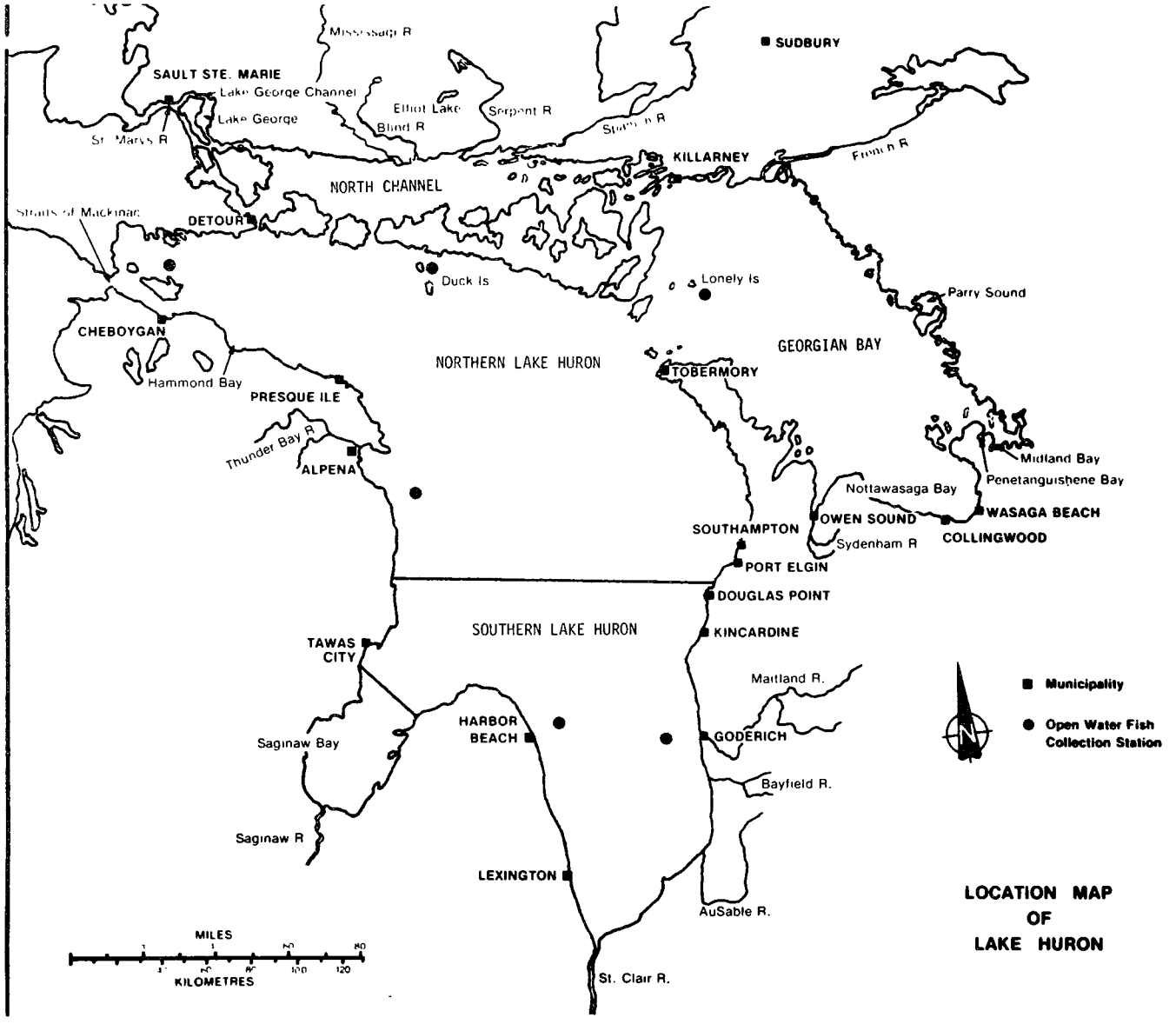

Figure 1. The Lake Huron system.

TABLE 2. CHEMICAL AND BIOLOGICAL INDICATORS OF TROPHIC STATUS - MAIN LAKE HURON

Nutrients	Spring Average Concentration
Total Phosphorus	5.4 μg/ℓ
Total Dissolved Phosphorus	3.2 μg/ℓ
Dissolved Reactive Phosphate	0.9 μg/ℓ
Dissolved Nitrate & Nitrite	282.4 μg/ℓ
Dissolved Ammonia	6.1 μg/ℓ
Dissolved Reactive Silicate	1.46 mg/ℓ
Dissolved Oxygen	13.2 mg/ℓ
Biology	
Chlorophyll a	1.4 μg/ℓ
Phytoplankton Biomass	1000 mg/m^3 (10% blue-green)
Zooplankton Biomass	60 mg/m^3 (60% calanoid copepods)

Georgian Bay is also classed as oligotrophic, and North Channel is considered mesotrophic. However, Saginaw Bay is highly enriched and is classed as eutrophic. This bay receives wastes from the highly populated Saginaw River Basin. These wastes include both industrial discharges and agricultural runoff. The influence of this bay on trends in the main lake is substantial as will be shown.

As a result of the influence of Saginaw Bay, the assumption of a homogenous main lake cannot be made in the case of Lake Huron. In the previous application of Kalman filtering to Lake Michigan, the open lake was treated as one, well-mixed segment. Also, unlike Lake Michigan, Lake Huron receives substantial net input of water from two other Great Lakes. Thus, the application of this procedure to Lake Huron has some unique and interesting aspects.

Loadings of nutrients to Lake Huron are expected to increase in the next three decades due to industrial and urban growth. Even slight increases in the present levels of phosphorus and nitrogen concentrations threaten the oligotrophic status of the main lake. The International Joint Commission has set a goal of non-degradation for this lake. Therefore, any increase in nutrient levels would not be in accordance with this goal. It is for this reason, that the optimal sampling design procedure has been applied to the nutrient parameters total phosphorus and nitrate-nitrite nitrogen.

MASS BALANCE MODEL

The model to be used with the Kalman filter to provide estimates of lake concentration for trend detection is a dynamic mass balance model (Figure 2). The basic equation for each substance is:

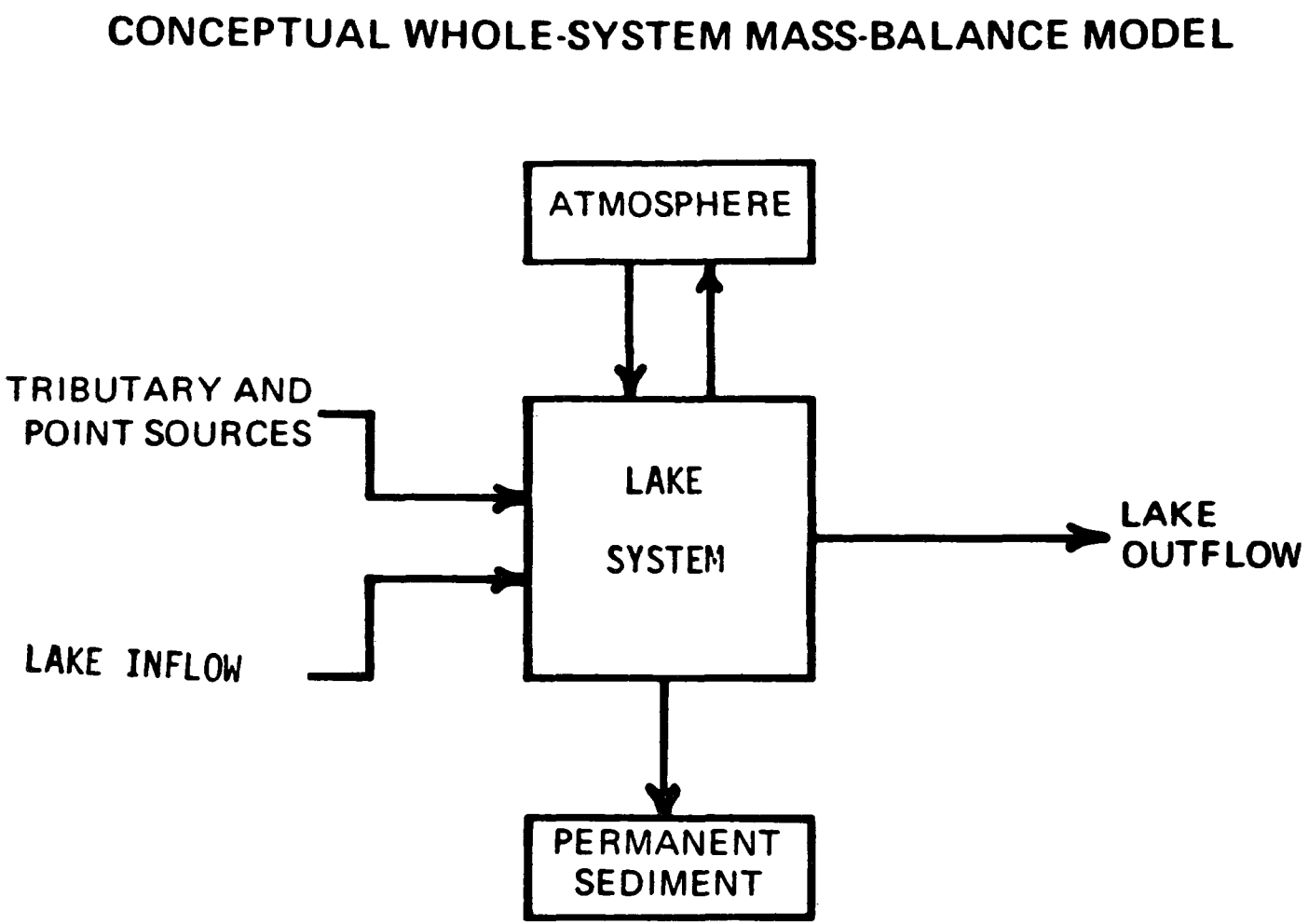

Figure 2. Simplified mass balance model.

$$V \frac{dc}{dt} = W + \Sigma\ QIN_i{*}CIN_i - \Sigma\ QOUT_j{*}c - k{*}c{*}V \qquad (1)$$

where: V is the volume of the body of water

$\frac{dc}{dt}$ is the rate of change in concentration with time.

W is the loading rate.

QIN_i is the flow rate of the ith input

CIN_i is the concentration of the ith input

$QOUT_j$ is the flow rate of the ith output

c is the concentration in the water body.

k is the first order removal coefficient which may be an apparent settling rate or a degradation constant.

Included in the W term are atmospheric loading, direct loadings and small tributary loadings. QIN and QOUT refer to major water bodies that interact with the one of interest. An equation similar to (1) is written for each body of water that can be considered well-mixed. In the case of main Lake Huron, 2 segments must be formed, Northern Lake Huron and Southern Lake Huron. The division of the lake follows that used by DiToro (in press). A separate mass balance equation is written for each segment and the two are coupled:

$$V_1 \frac{dc_1}{dt} = W_1 + \sum_{i=1}^{2} QIN_i\ CIN_i - QNS\ c_1 - k\ c_1 V_1 \qquad (2)$$

$$V_2 \frac{dc_2}{dt} = W_2 + QNS\ c_1 - QOUT\ c_2 - k\ c_2\ V_2 \qquad (3)$$

where: QNS is the net flow between northern and southern Lake Huron.

Since c_1 appears in both equations, they are considered to be coupled. These equations are then linearized about nominal values, $CNOM_1$ and $CNOM_2$ for use in the Kalman filter procedure.

Note that in (2) the QIN_i's refer to flows from Lake Michigan and Lake Superior. The CIN_i's are concentrations of these lakes which are subject to dynamics different from Lake Huron. To avoid including added complexity in the model, these concentrations are treated as inputs. In other words, the boundary concentrations for the lake are modeled separately and then stored for later use with this model.

MEASUREMENTS

There are three types of measurements that can be made on the Lake Huron system that will improve the estimate of lakewide concentrations. The first type is the actual sampling of the open lake. A second type puts the principal of mass balance to use: tributary and point source sampling. Here the assumption is that if inputs are changing, then lake concentrations must, as a consequence, change. The third type is actually a miscellaneous category and includes all field and laboratory measurements that improve the accuracy of the mass balance model, and thus improve the estimate. Such measurements include apparent settling velocity, boundary flow rates, atmospheric loading rates, and intersegmental exchange rates for the case of more than one segment. Each of these types of measurements can improve the accuracy of concentration estimates for trend detection with the use of a Kalman filter.

The actual sampling of the open lake is the most direct way to determine the lakewide average concentration of a substance. If unlimited funds were available, a model would not be necessary. However, open lake sampling cruises are expensive and represent a major surveillance effort. Lake Huron is to be sampled intensively only every nine years. This is, in part, a reflection of the enormous costs of such a project. However, if enough samples are taken, open lake concentrations can be determined quite accurately.

Tributary sampling is also extremely expensive. In this case each individual tributary must be sampled. There are 23 major tributaries to Lake Huron. Since loading is often a seasonal phenomemon, accurate time histories for each tributary are necessary. Fortunately, there are estimation methods for those tributaries with complete flow records so that daily sampling is not necessary (Dolan et al. in preparation; U.S. Army Corps of Engineers 1975). Even if the tributary loads are known accurately, however, the resultant concentration estimate for the lake is still influenced by the accuracy of the model, including parameters and other forcing functions.

These various model parameters and forcing functions can be determined to a considerable degree of accurancy by the proper experiments in both field and laboratory. Many investigators have devised ways to estimate apparent settling velocity. Atmospheric deposition of pollutants is the subject of much current research (Murphy and Doskey 1975; Murphy 1975; Delumyea and Petel 1979). There are several methods available for estimating boundary flows and intersegmental exchanges (Quinn 1977; Chapra 1979; Upper Lakes Reference Group 1977; Dolan et al. in preparation). If one of these components is particularly limiting with regard to accuracy of concentration estimates, specific research aimed at improving the knowledge of the component can be initiated.

Obviously, there are costs and benefits associated with each of the three types. The techniques described in this paper can choose the optimal conbinations of these measurements to meet the accuracy constraints at minimum costs.

OPTIMAL SAMPLING STRATEGY

For purposes of comparison, the proposed Lake Huron work group surveillance plan will be evaluated for trend detection in each of the two segments of main Lake Huron. The optimal strategy will then be presented. It should be noted that the surveillance plan includes sampling for many other parameters besides nitrate-nitrite and total phosphorus and thus, it is not likely to be optimal with regard to these two parameters.

As stated previously, any increase in nutrient levels in Lake Huron would not be in accordance with IJC goals for this lake. Therefore, the criteria for trend detection is the following: The sampling plan must detect changes of 1 μg/ℓ of total phosphorus and 50 μg/ℓ of nitrate-nitrite with 90% certainty every 9 years. This criterion is met with ease in the northern Lake Huron segment (Table 3). In the south, only the nitrate-

TABLE 3. LAKE HURON SURVEILLANCE PLAN TREND DETECTION CAPABILITIES

	Northern Lake		Southern Lake	
	w/o filter	w filter	w/o filter	w filter
Parameter				
Nitrate Nitrite				
1980	18 μg/ℓ	18 μg/ℓ	37 μg/ℓ	36 μg/ℓ
1989	18 μg/ℓ	18 μg/ℓ	37 μg/ℓ	35 μg/ℓ
1998	18 μg/ℓ	18 μg/ℓ	37 μg/ℓ	35 μg/ℓ
Total Phosphorus				
1980	.60 μg/ℓ	.60 μg/ℓ	1.83 μg/ℓ	1.67 μg/ℓ
1989	.60 μg/ℓ	.59 μg/ℓ	1.83 μg/ℓ	1.64 μg/ℓ
1998	.60 μg/ℓ	.54 μg/ℓ	1.83 μg/ℓ	1.63 μg/ℓ

nitrite criterion is met. The use of the Kalman filter does improve the accuracy of the estimate slightly, but the plan as it is presently conceived, cannot detect changes in total phosphorus of 1 μg/ℓ in southern Lake Huron.

In order to meet this criterion, it can be shown that 65 stations must be added to the open lake sampling plan in the southern segment of the lake. This results in a total of 138 stations for the total main lake effort. If the optimization procedure developed for Lake Michigan (DePalma 1977) is utilized it can be shown that accuracy criteria in both lake segments can be met with 105 stations if the only goal of sampling is trend detection. This assumes that accuracy requirements are met exactly and that the Kalman filter is used in conjunction with a mass balance model to improve the estimates where possible. This comparison emphasizes that uniform spatial coverage of the open lake is not desirable for trend detection. Rather, it is more important to locate extra stations in areas of high spatial variability.

SENSITIVITY ANALYSIS

It can be seen from Table 3 that the use of the filter in conjunction with the mass balance model previously described, only marginally improves the accuracy of the concentration estimates. This is an indication that the model itself is inaccurate, probably because some or all of the model parameters and forcing functions are imperfectly characterized. If some of these quantities can be better determined, the model accuracy will improve, the trend detection capability will increase and the associated sampling costs will decrease.

The Kalman filtering technique has been used to estimate improvements in trend detection accuracy attributable to research and experimentation in each of five areas:

1. Atmospheric Loading - Of all the input to lakes of pollutants, this component is usually the least accurately known. Research is presently being conducted to improve measurement accuracy of atmospheric loading (Murphy 1975; Delumyea and Petel 1979). Also, it is possible to model atmospheric fallout, greatly improving estimates of loading in areas where no sampling occurs (Sydor in press; Kabel 1975; Acres Consulting Services 1975).

2. Intralake Exchange - This is defined to be the net effect of advection and diffusion at the assumed interface between northern and southern Lake Huron. Estimates of this quantity can be greatly improved using existing models. The Lake Huron surveillance Plan includes a design for estimation of this parameter.

3. Interlake Exchange - This is defined to be the net effect of advection and diffusion at interfaces with Lake Michigan, the St. Mary's River, and the St. Clair River. The effects of diffusion at the river interfaces is nil so that these two components can be easily improved by measuring flow rates. Much work has already been done on the Straits of Mackinac (Quinn 1977), and these results with other measurements can greatly improve the accuracy of this component.

4. Initial Settling Velocity Uncertainty - At present, the procedure assumes that very little is known about the settling rate of nutrients, and that knowledge improves as measurements are taken. In reality, much is already known, and more work is ongoing in this area (Chapra in press).

5. Tributary Load Estimation Error - This is always a large source of error in any lake model. However, not only are methods of sampling improving for tributaries, but also methods of calculation to obtain better estimates with sparse data are becoming available (Dolan in preparation). In addition, 24% of the tributary nutrient loads to Lake Huron come from the Saginaw River alone. This tributary could be monitored intensively to reduce estimation errors.

The increases in accuracy with improvements in each of these five areas are compared to a base case which is the optimal strategy with no improvements (Table 4). The results are expressed in terms of standard errors of

TABLE 4. SENSITIVITY ANALYSIS FOR STANDARD ERROR (μg/ℓ) IN SOUTHERN LAKE HURON FOR TOTAL PHOSPHORUS

Run Description	Year 1980	1989	1998
Present Optimum	.1571	.1575	.1569
Improve Atmospheric Estimates	.1569	.1572	.1566
Improve Intralake Exchange Estimates	.1570	.1573	.1568
Improve All Exchange Estimates	.1562	.1559	.1551
Improve Initial Settling Rate Accuracy	.1556	.1570	.1567
Improve Tributary Load Estimate	.1535	.1541	.1536
Improve All of the Above	.1467	.1465	.1456
Improve All of the Above Plus Initial Condition Estimates	.1429	.1440	.1440
Improve Open Lake Measurements	.0161	.0162	.0162

the estimates for total phosphorus in southern Lake Huron for each year in which a determination of trends is desired. These estimates are most sensitive to improvements in tributary load estimation accuracy. If all five areas are improved, the accuracy of the estimates would increase by 7 percent by 1998. If, in addition, the initial concentration of total phosphorus had been better estimated, further gains in accuracy would be realized. For comparison purposes, the effect of a 10-fold increase in the accuracy of open lake measurements for total phosphorus has been included. Naturally, the total phosphorus estimates are much more sensitive to this kind of improvement; however, such increases in accuracy would probably be impossible to achieve in practice.

DISCUSSION

Trend detection is an important part of any lake sampling plan. In the case of oligotrophic lakes such as Lake Huron, the early observation of trends towards mesotrophy is critical. Given this reasoning, the confidence level of 90% used in this analysis may be too low. If high confidence is required, the use of a model becomes even more important.

Each of the five areas for improvement mentioned in the preceding section are interesing for reasons beyond mass balance modeling and thus may be the subject of limnological research in the future. If the optimal strategy for trend detection is recomputed assuming significant improvement in all these areas, substantial reductions in the number of stations necessary for sampling would be realized (Table 5). Also, the model's capabilities would increase as measurements are made.

TABLE 5. COMPARISON OF STATIONS REQUIRED BY DIFFERENT STRATEGIES

Strategy	Year 1980	1989	1998
Lake Huron Work Group Plan	138	138	138
Optimal Strategy	105	104	104
Optimal Strategy with Research on Model Parameters	85	83	79

Another advantage would be that trends for other, less variable, parameters; such as chloride could be detected with the help of the model and the tributary load estimates even during years when no lakewide measurements were taken.

CONCLUSION

The techniques discussed in this paper are extremely useful for designing and/or evaluating a plan for trend detection. Even if the model associated with the Kalman filter is inaccurate, the procedure leads to orderly acquisition and evaluation of data pertaining to trend detection. If the model can be improved, significant increases in accuracy can be realized or, alternatively, sampling costs can be decreased. In either case, these techniques provide a systematic way of evaluating a proposed measurement strategy as well as determining if another strategy could give substantial gains in accuracy.

In the case of Lake Huron, application of this procedure has shown that for nutrients, the northern segment of the lake is over-sampled, while the southern segment is under-sampled. This situation can be improved by increasing the number of stations in the southern segment, or by improving the model to be used with the Kalman filter to obtain estimates of trends. These results are probably generalizable to other parameters that could be described well by a simple mass balance, such as conservative substances, radionuclides, some heavy metals and suspended solids. Biological parameters and certain organic contaminants would require a more sophisticated approach (Canale et al. in press; Chiu 1978).

REFERENCES

Acres Consulting Services - Earth Science Consultants. 1975. Atmospheric Loadings of the Upper Great Lakes. Phase Two Report. Canada Centre for Inland Waters.

Canale, R.P., L.M. DePalma and W.F. Powers. In press. Sampling Strategies for Water Quality in the Great Lakes. EPA Ecological Research Series. U.S Environmental Protection Agency, Duluth, Minnesota. 102 pp.

Chapra, S.C. 1979. Applying Phosphorus Loading Models to Embayments. Limnology and Oceanography, 24(1): 163-168.

Chapra, S.C. In press. Simulation of Recent and Projected Total Phosphorus Trends in Lake Ontario. J. Great Lakes Research.

Chiu, C. (Ed.). 1978. Applications of Kalman Filtering to Hydrology, Hydraulics, and Water Resources. Department of Civil Engineering, University of Pittsburgh, Pennsylvania. 783 pp.

Delumyea, R. and R.L. Petel. 1979. Deposition Velocity of Phosphorus-Containing Particles Over Southern Lake Huron, April-October, 1975. Atmospheric Environment, 13: 287-294.

DePalma, L.M. 1977. A Class of Measurement Strategy Optimization Problems-With an Application to Lake Michigan Surveillance. Ph.D. Thesis, The University of Michigan, Ann Arbor, Michigan. 122 pp.

DePalma, L.M., R.P. Canale and W.F. Powers. 1979. A Minimum-Cost Surveillance Plan for Water Quality Trend Detection in Lake Michigan. In Perspectives on Lake Ecosystem Modeling, eds. D. Scavia and A. Robertson, Ann Arbor: Ann Arbor Science. pp. 223-246.

DiToro, D.M. and W.F. Matystik, Jr. In press. Mathematical Models of Water Quality in Large Lakes. Part I: Lake Huron and Saginaw Bay, Model Development, Verification and Simulations. EPA Ecological Research Series. U.S. Environmental Protection Agency, Duluth, Minnesota.

Dolan, D.M., A.K. Yui and R.D. Geist. In preparation. Evaluation of River Load Estimation Methods for Total Phosphorus. U.S. Environmental Protection Agency, Large Lakes Research Station, Grosse Ile, Michigan.

Dolan, D.M., R.D. Geist and K. Salisbury. In preparation. Applications of a Dynamic Mass Balance to Water Quality Problems in the Great Lakes. U.S. Environmental Protection Agency, Large Lakes Research Station, Grosse Ile, Michigan.

Kabel, R.L. 1975. Atmospheric Impact on Nutrient Budgets. In: Proceedings of the First Specialty Symposium on Atmospheric Contribution to the Chemistry of Lake Waters. Internat. Assoc. Great Lakes Res. pp. 114-126.

Kalman, R.E. 1960. A New Approach to Linear Filtering and Prediction Problems. Trans. ASMF, J. Basic Engr. 82B: 34-35.

Kalman, R.E. and R. Bucy. 1961. New Results in Linear Filtering and Prediction Theory. Trans. ASMF, J. Basic Engr. 83D: 95-108.

Murphy, T.J. and P.V. Doskey. 1975. Inputs of Phosphorus from Precipitation to Lake Michigan. EPA-600/3-75-005, U.S. Environmental Protection Agency, Duluth, Minnesota. 27 pp.

Murphy, T.J. 1975. Concentrations of Phosphorus in Precipitation in the Lake Michigan Basin. In: Proceedings of the First Specialty Symposium on Atmospheric Contribution to the Chemistry of Lake Waters, Internat. Assoc. Great Lakes Res. pp. 127-131.

Quinn, F.H. 1977. Annual and Seasonal Flow Variations through the Straits of Mackinac. Water Resources Research, 13: 137-144.

Sydor, M. Particle Transport in Duluth-Superior Harbor. EPA Ecological Research Series. U.S. Environmental Protection Agency, Duluth, Minnesota.

Upper Lakes Reference Group. 1977. The Waters of Lake Huron and Lake Superior, V. 2. International Joint Commission, Windsor, Ontario. 743 pp.

U.S. Army Corps of Engineers. 1975. Lake Erie Wastewater Management Study Preliminary Feasibility Report. Buffalo District Army. Corps of Engineers, Buffalo, New York.

Verhoff, F.H., S.M. Yaksich and D.A. Melfi. In press. Estimation of Nutrient Transport in Rivers. J. Environmental Eng. Div. Amer. Soc. Civil Engr.

SECTION 5

A MODEL APPROACH TO ESTIMATING THE EFFECTS OF ANTHROPOGENIC INFLUENCES ON THE ECOSYSTEM OF LAKE BAIKAL

A.B. Gorstko[1], Yu.A. Dombrovskiy[1], V.V. Selyutin[1], F.A. Surkov[1], A.M. Nikanorov[2] and A.A. Matveev[2]

Lake Baikal is located in the southern portion of eastern Siberia between 51°29' and 55°46'N (Figure 1). Ranking eighth in area and first in depth among all continental bodies of water of the planet, it contains about 20 percent of the world reserves of fresh surface water. The basic morphometric characteristics of the lake are presented in Table 1.

TABLE 1. MORPHOMETRIC CHARACTERISTICS OF LAKE BAIKAL

Number	Characteristic	Value
1	Length	
	a) of lake	636 km
	b) of shoreline	2000 km
2	Width	
	a) mean	48 km
	b) maximum	79 km
	c) minimum	26 km
3	Area	
	a) total	31.5 $10^3 \cdot km^2$
	b) of zone less than 50 m deep	2.5 $10^3 \cdot km^2$
	c) of zone less than 250 m deep	6 $10^3 \cdot km^2$
4	Depth	
	a) mean	730 m
	b) maximum	1620 m
5	Volume	23.6 $10^3 \cdot km^3$
6	Altitude Above Sea Level	456 m
7	Area of Watershed Basin	557 $10^3 \cdot km^2$

[1]Institute for Mechanics and Applied Mathematics, Rostov State University, 192/2 Stachky Prospect, 344090 Rostov-on-Don, USSR.

[2]Hydrochemical Institute, 192/3 Stachky Prospect, 344090 Rostov-on-Don, USSR.

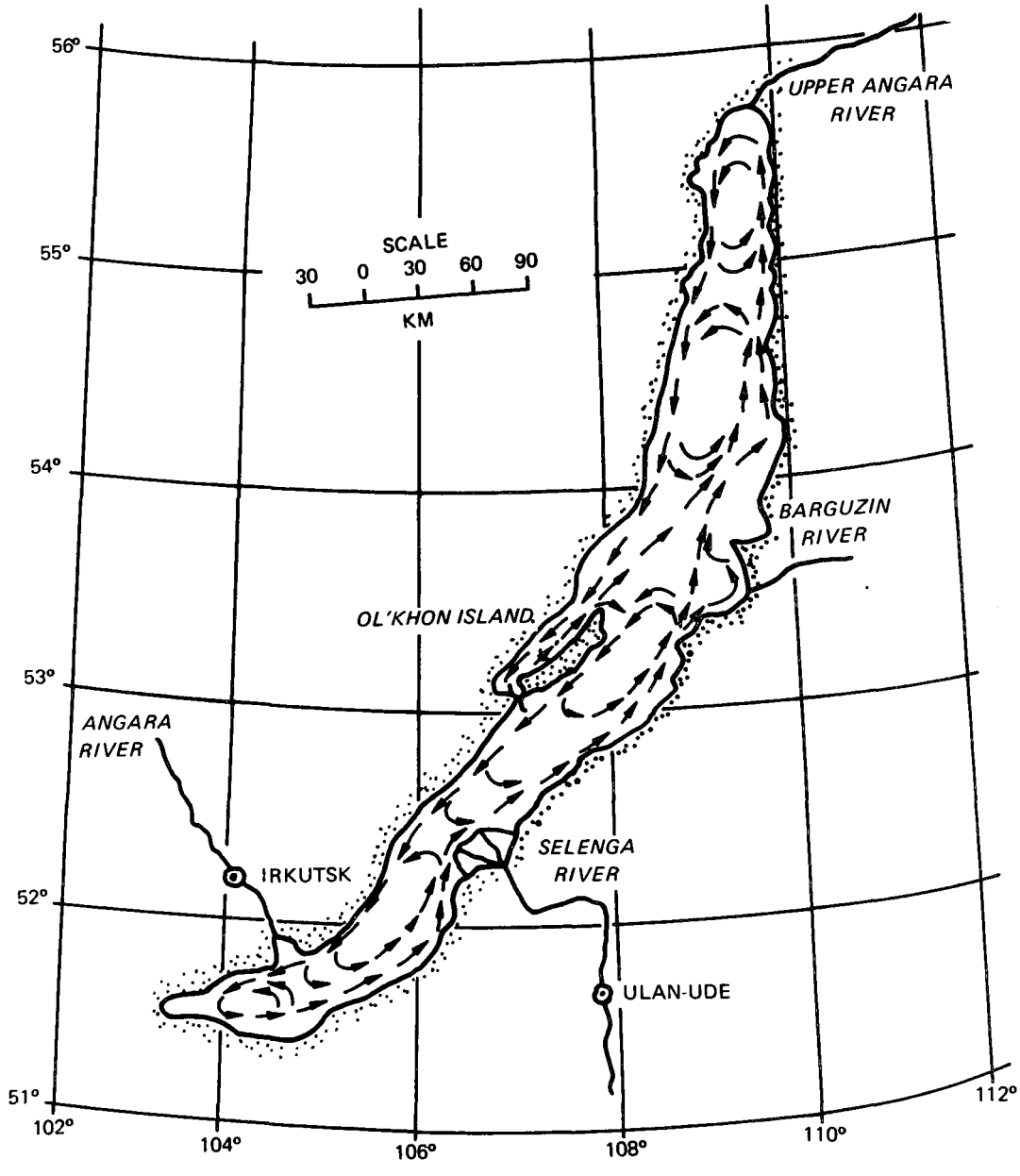

Figure 1. Diagram of surface currents in Baikal during the ice-free season.

The annual surface runoff into the lake is about 59 km^3, of which one-half is provided by the Selenga River, while the annual outflow of the Angara River is 61 km^3.

The most important characteristic of Lake Baikal is the exceptionally high quality of its water. It is distinguished by its low mineral content (many ions in concentrations of less than 100 mg/liter), high transparency (Secchi depth measurements of up to 40 m), an abundance of dissolved oxygen (at least 9.5 mg/ℓ, even at depths of 1300-1400 m), and low temperature (mean annual surface temperature 4.5°C).

Given these conditions, a unique ecologic system exists in the lake, the most important peculiarity of which is the existence of an endemic complex of aquatic organisms populating the open regions of Baikal. The richness and variety of the flora and fauna of the lake, numbering 2400 species and subspecies, of which approximately three-fourths are endemic species; the extensive branching of the trophic chain, ending in the Baikal seal; and the nature and scale of the dynamic processes in the water enable Baikal to be considered as a world ocean in minature. A large quantity of information on Baikal has been systematized (Kozhov 1972), and the results of later studies can be found in the works of the Limnologic Institute, Siberian Branch, Acad. Sci. USSR (1977, 1978).

While it represents tremendous ecologic and scientific value, Lake Baikal is also an important national economic resource. The economic utilization of Baikal consists of three basic uses:

a) water consumption,
b) culture and harvesting of fish, and
c) recreational uses.

The floating of timber and the construction of large industrial enterprises which might act as sources of pollution are forbidden in the immediate vicinity of the lake, and navigation is limited. However, it is impossible to completely eliminate the entry of various impurities into the lake. The most important sources are surface runoff and atmospheric precipitation. Preliminary analysis shows that currently it is difficult to see any evidence of changes in the ecosystem of the lake as a result of human activity. On the one hand, this is a result of timely preventive measures taken as a result of the resolution of the Central Committee and USSR Council of Ministers of 16 June 1971, in which it was stated that lake protection should contain, "additional measures to assure rational utilization and conservation of the natural riches in the basin of Lake Baikal"; while on the other hand, it also results from the great self-purifying capacity of the lake. Thus, it is of great importance to obtain well-founded long-term predictions concerning the possibility of future effects of human activity. The model approach to the prediction of the status of this ecosystem is intended to provide the most objective estimate of such effects in the Baikal region and provide an effective solution to the problem of its preservation and efficient use. This paper considers some trends in the realization of the model approach.

LAKE DYNAMICS

Information on currents in the lake at various periods of time, represented in the form of a field of velocities or flows between various volume elements of the lake, is necessary for modeling of the hydrochemical regime and the dynamics of the plankton population. There are two possibilities in this case: 1) to perform numerical hydrodynamic calculations, or 2) to use the data from natural observations of speeds and directions of currents. Both methods were used in the present work.

The starting point used was a diagram of convective-gradient currents (Figure 1) obtained by processing observed data on water temperature by the dynamic method (Krotova 1970). The surface of the lake was divided into 14 regions (Figure 2), and 4 depth layers were distinguished: 0-25 m, 25-50 m, 50-250 m and 250 m to the bottom. The extensive material obtained in field observations, summarized in the collective monograph Techeniya v Baikale (Currents in Baikal) (1977), allowed an estimation of movements through the boundary regions selected for various seasons of the year.

In addition, a UNIVAC 1100/40 computer, utilizing a program developed by J. Paul, was used to calculate the velocity fields corresponding to various wind situations. These calculations yielded results similar to those obtained by means of a baroclinic model (Tsvetova 1977).

WATER QUALITY

The basis of the models for the dynamics of the concentrations of substances entering the lake is the equation of turbulent diffusion of a nonconservative impurity:

$$\frac{\partial c}{\partial t} = \text{div}\ (D\ \text{grad}\ c) + v\ \text{grad}\ c - kc + f \qquad (1)$$

$$\text{grad}\ c/S = 0 \qquad (2)$$

where: $c(t; x, y, z)$ is the concentration of the substance;
$D(t; z)$ is the coefficient of turbulent diffusion;
$v(t; x, y, z)$ is the velocity vector;
$k(t)$ is the decay rate;
$f(t; x, y, z)$ is the loading of the substance into the lake;
$S(x, y, z)$ is the boundary surface.

In the calculations, Equation (1) was replaced by a finite-difference system corresponding to the regionalization used in the model. The time-series plots of concentrations of an arbitrary substance in the various regions of the lake are shown in Figure 2. The basic sources are assumed to be the Selenga River (Region 4), and the Baikal Cellulose-Paper Combine (BCPC, Region 2).

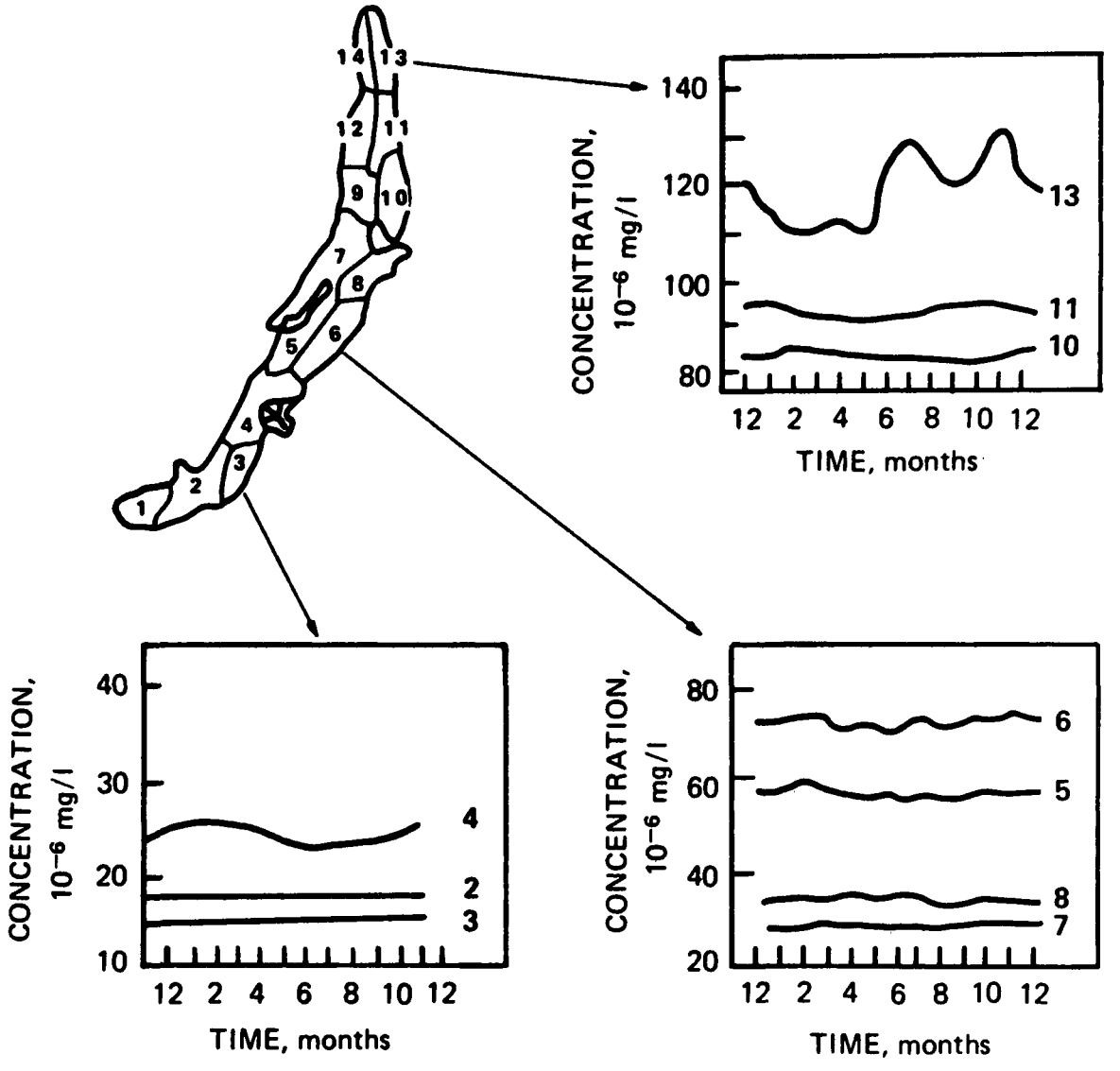

Figure 2. Time-series plots of concentrations of an arbitrary pollutant in the various regions of Lake Baikal.

The concentration fields in the vicinities of "local" pollution sources were calculated with a significantly smaller grid (0.5 km horizontally; 0.02 km in depth), again using Equation (1). Concentration of an arbitrary substance in the upper (0-20 m) layer near the BCPC is shown in Figure 3. Data on flow velocities were taken from field observations. Measurements of velocities during 1977 were conducted by V.M. Sleptsova of the Baikal Weather Observatory, using an especially detailed plan of observations incorporating the requirements of the mathematical model. The experiments showed that the propagation of a patch of material in the lake depends essentially on the velocity field, and changes significantly from season to season. At the same time, concentrations were found to be relatively insensitive to variations in diffusion coefficients. The mean area of calculated patch of material was small, 4-5 km^2.

BIOTIC CYCLE

The biotic cycle, i.e., the chain of transformation of living and dead organic matter, binds together all of the biologic, biochemical, physical and other processes occurring in the ecosystem. The most important index of the biotic cycle is the biotic balance, reflecting the relationship between the system of productive and destructive processes at all trophic levels. The mean annual biotic balance of Baikal, calculated on the basis of results of studies of the Limnologic Institute, Siberian Branch, USSR Acad. Sci., for 1964-1970, is presented in Table 2.

However, the practical usefulness of this balance is limited, due to its static nature. For completeness, nonliving organic matter, which acts as a nutrient medium for bacteria, and nutrients limiting primary production should also be included.

The pelagic ecosystem of the lake, encompassing 80 percent of its area, occupies the most important position in the cycle of organic matter in Baikal. A simplified plan of the cycle of matter and energy in the pelagic zone is presented in Figure 4.

Differentiation of dissolved organic matter (DOM) into easily oxidizable (OOM) and non-oxidizable aquatic humus (IOM) is necessary to provide an accurate estimate of the bacterial production. This differentiation was performed arbitrarily, based on the relationships of permanganate and bichromate oxidizability, and the ratio of organic carbon (C_{org}) to organic nitrogen (N_{org}). In particular, analysis of the vertical distribution of $\lambda = C_{org}/N_{org}$, reflecting the relative increase in the fraction of aquatic humus in the DOM with depth, showed that for the complex of matter forming the IOM, $\lambda = 6$ can be assumed, while for the IOM, $\lambda = 22$. Then the fraction of C_{org} represented by IOM (x_c) can be calculated by the equation:

$$x_c = 1.38 \left(1 - \frac{6}{\lambda}\right) . \qquad (3)$$

The ratio of mineral nitrogen to mineral phosphorus in the waters of Baikal lies between 7 and 10 (Votintsev et al. 1975), approximately corre-

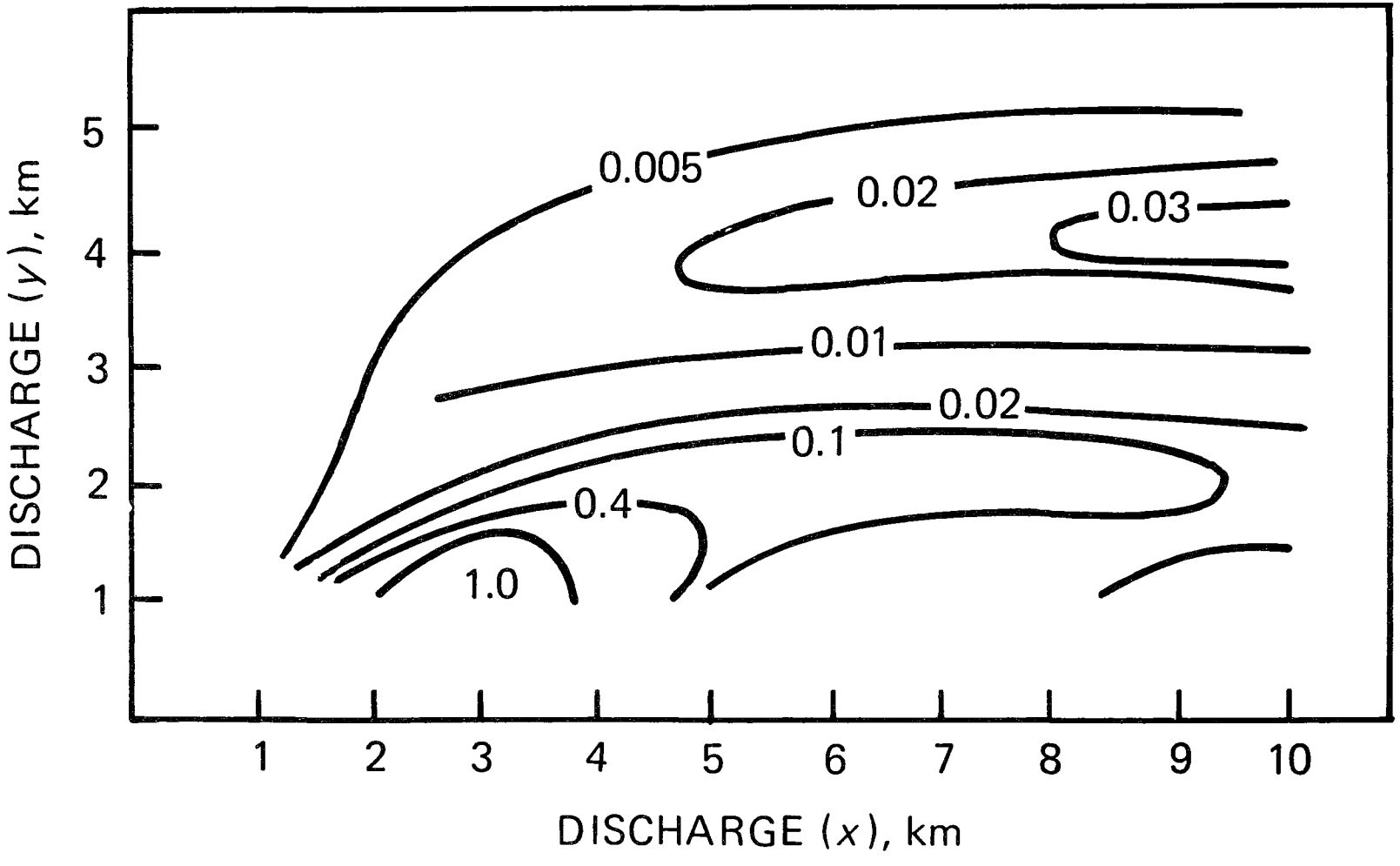

Figure 3. Concentration field (mg/liter) of a pollutant in the 0-20 m layer near BCPC. $D = 10^4$ cm^2/s; K - 0.086 day^{-1}.

TABLE 2. BIOTIC BALANCE OF THE PELAGIC ECOSYSTEM OF LAKE BAIKAL kcal/m^2/year (from Botintsev *et al*. 1975)

Component	B	P	P/B	K	T	T/B	A	R
Phytoplankton	3.0	875	290	0.9	97	32	972	-
Bacterioplankton	9.4	315	34	0.5	262	28	602	602
Epischura (*Epischura baicalensis*)	6.0	80.5	13.5	0.25	245	41	326	407
Cyclops (*Cyclops colensis*)	0.3	3.4	11.3	0.27	9.2	30.6	12.6	15.7
Macrohectopus (*Macrohectopus branizkii*)	3.1	4.7	1.5	0.26	13.3	4.3	18.0	22.5
Omul (*Coregonus autumnolis migration*)	1.9	0.38	0.2	0.33	0.76	0.4	1.14	1.4
Large and Small Gblomyanka (*Comephorus baicalensis comephorus dybowskii*	3.69	2.95	0.8	0.45	3.52	0.9	6.47	8.1
Bullhead sac-fry and fingerlings (*Cottocomephorus grewingki cotto-comephorus inermis*)	0.23	0.23	1.0	0.21	0.84	3.7	1.07	1.34
Nerpa (seals) (*phoca sybirica*)	1.26	0.22	0.18	0.17	1.08	0.8	1.30	1.6

B = biomass
A = assimilation of food
P = production
T = destruction (loss to metabolism)
R = ration
A = 0.8 R; P = A - T; K_2 = P/A

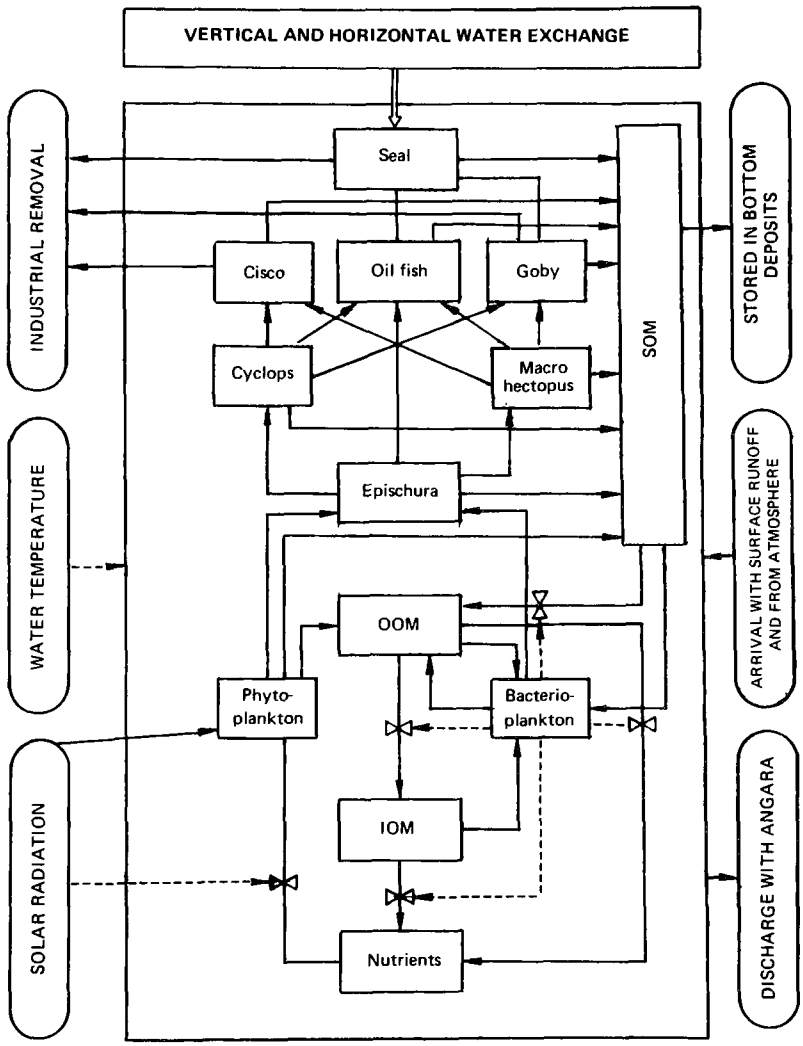

Figure 4. Diagram of cycle of matter and energy in pelagic Lake Baikal. SOM = suspended organic matter (PM), detritus; OOM - oxidizable fraction of dissolved OM; IOM = nonoxidizable fraction of dissolved OM, aquatic humus. a) Direction of solid lines coincide with direction of flow of matter and energy; b) Oriented dotted lines symbolize participation of initial component in process indicated.

sponding to their proportions upon photosynthesis. However, the more rapid regeneration of phosphorus, relative to nitrogen, causes a decrease in this ratio, frequently dropping to 0, during periods of maximum development of phytoplankton. Since nitrite and ammonia nitrogen are practically absent in the waters of Baikal (Votintsev 1961), the limiting biogenic element, completing the biotic cycle, is nitrate nitrogen.

To estimate the changes in the status of the lake's ecosystem considering the excess input of biogenic substances and other impurities, and anthropogenic action, distinct from natural background fluctuations, one can use a model based on the dynamic balance method (Gorstko et al. 1977). The algorithm for this method is presented in the following section.

DYNAMIC BALANCE METHOD

Two groups of equations are used to describe the ecosystem. The first group reflects the productive nature of the system, i.e., the fact that matter in some components is produced by the consumption of others:

$$P(\tau) = A(\tau)[X^t + P(\tau) + U(\tau)] \tag{4}$$

where: $X = (X_1, X_2, \ldots, X_n)$ is the state vector of the ecosystem, the coordinates of which represent the instantaneous values of biomass or concentration of the components;

$P(\tau) = (P_1(\tau), P_2(\tau), \ldots, P_n(\tau))$ is the production vector of the ecosystem in period τ;

$U(\tau) = (U_1(\tau), U_2(\tau), \ldots, U_n(\tau))$ is the control vector, characterizing the arrival (or removal) of individual components during period τ;

$A(\tau) = [a_{ij}(\tau)]$ is the production matrix of the ecosystem;

$a_{ij}(\tau)$ is the fraction of the matter of the jth component consumed by the ith component in period τ.

The superscript t represents discrete time. The other grouping reflects the dynamic nature of the system. It is as follows:

$$X^{t+\tau} = B(\tau)\ [X^t + P(\tau) + U(\tau)] \tag{5}$$

where: $B(\tau) = \mathrm{diag}(B_1(\tau), B_2(\tau), \ldots, B_n(\tau))$ is a diagonal matrix, and $B_i(\tau)$ is the fraction of the i component which remains at the end of period $(t, t + \tau)$.

The elements of matrices A and B are defined through the rates of mutual consumption or transformation of components f_{ij} (the flux of matter or energy is directed from the jth component toward the ith component):

$$B_j = \frac{1}{1 + \tau \sum_{k \varepsilon Q_j} \gamma_{kj} f_{kj}} \tag{6}$$

$$a_{ij} = \frac{f_{ij} \gamma_{ij}}{1 + \tau \sum_{k \varepsilon Q_j} \gamma_{kj} f_{kj}} \tag{7}$$

where: f_{kj} is the rate of decrease of the jth component as a result of consumption by the kth component;

γ_{kj} is the conversion coefficient between the units of measurement of the corresponding components;

Q_j is the set of consumers of the jth component.

If all components of the model are expressed in units of one chemical element (for Baikal, as noted, nitrogen can serve as such an element), obviously, the system is balanced:

$$\sum_{i=1}^{N} X_i^{t+\tau} = \sum_{i=1}^{N} X_i^t + \sum_{i=1}^{N} U_i \ . \tag{8}$$

Equation (8) can be easily obtained by adding (4) and (5) term by term and keeping in mind that

$$\sum_{i=1}^{N} a_{ij} + B_j = 1, \quad \forall j \ . \tag{9}$$

To consider the flow of matter from the lake p_0, which depends on internal processes, the fictitious component X_0 is introduced such that $f_{i,0} = 0$, $\forall i$. Then $X_0^{t+\tau_0} = X_0^t + p_0$ and

$$\sum_{i=0}^{N} X_i^{t+\tau} = \sum_{i=0}^{N} X_i^t + \sum_{i=0}^{N} U_i \rightarrow \sum_{i=1}^{N} X_i^{t+\tau} = \sum_{i=1}^{N} X_i^t + \sum_{i=1}^{N} U_i - p_0 \ . \tag{10}$$

In particular, we can distinguish two such components in the model of Baikal, reflecting irrecoverable losses from the lake: 1) the discharge of organic, mineral substances, and plankton with the waters of the Angara, and 2) the partial sedimentation of QOM onto the deposits on the lake floor.

Since $\sum_{i=1}^{N} a_{ij} < i \ \forall j, \ \tau > 0,$

then equation (4) always has a positive solution (Bellman, 1969):

$$P = (I - A)^{-1} A(X^t + U) \tag{11}$$

where I is a unit maxtrix.

Consequently, this system is noncontradictory. The basic task of simulation of the ecosystem is reduced to identification of the matrix $F = [f_{ij}]$ as a function of the values of the state variables, and the environmental factors (illumination, temperature, secondary impurities, etc.), with subsequent allowance for various input perturbations and control actions.

Consideration of the three-dimensional structure of the ecosystem in the model can be achieved by using the same approach in two modifications:

1. Combined Model. This model involves an increase in the dimensionality of the state vectors of production and control, the coordinates of which are grouped according to the number of spatial units distinguished. In the same manner, the dimensionality of matrices A and B increase, as they are converted to block matrices, their elements decreasing due to addition of the speeds of flow or migration of components between neighboring cells in the denominator:

$$B_j^k = \frac{1}{1 + \tau\left(\sum\limits_{r \in Q_j} f_{rj}^{(k)} \gamma_{rj} + \sum\limits_{s \in Q_k} g_{sk}^{(j)}\right)} \tag{12}$$

$$a_{ij}^{k\ell} = \begin{cases} \dfrac{\tau g_k^{(i)}}{1 + \tau\left(\sum\limits_{r \in Q_j} f_{rj}^{(\ell)} \gamma_{rj} + \sum\limits_{s \in Q_\ell} g_{s\ell}^{(i)}\right)} & i = j \wedge k = \ell \\[2ex] \dfrac{\tau f_{ij}^{(k)} \gamma_{ij}}{1 + \tau\left(\sum\limits_{r \in Q_j} f_{rj}^{(\ell)} \gamma_{rj} + \sum\limits_{s \in Q_\ell} g_{s\ell}^{(i)}\right)} & i \neq j \wedge k = \ell \\[2ex] 0 & i \neq j \wedge k = \ell \end{cases} \tag{13}$$

where the subscripts i, j, r indicate the numbers of the components,

k, ℓ, s are the cell numbers;

$g_{sk}^{(i)}$ is the rate of outflow (migration) from the kth cell into the sth cell by the ith component;

$f_{ij}^{(k)}$ is the rate of loss of the jth component due to consumption by the ith component in cell k.

This modification allows simultaneous description of the biotic cycle and transfer (migration) of components; however, the increase (proportional to the square of the number of cells M) in dimensionality of matrix A, which must be repeatedly transformed, places a limit on its use.

2. Method of Splitting. Sequential operation of two models is used: 1) a model of the dynamics of the water (migration of components), and 2) a model of the biotic cycle.

If x_k is that portion of the state vector which relates to cell k:
x_i is that portion of the state vector which relates to component i:
R_k is the model operator of the biotic cycle in cell k:
G_i is the model operator of water exchange (migration of the ith component, then:

$$\bar{x}_k = R_k\ (x_k^t) \qquad k = 1,2,\ldots M$$

$$\bar{x}_i^{t+\tau} = G_i\ (\bar{x}_i) \qquad i = 1,2,\ldots N$$

where: $\bar{x}$ is the intermediate vector;
M is the number of cells;
N is the number of components.

CONCLUSION

At present, anthropogenic effects on the ecosystem of Lake Baikal are at a minimum. Therefore, we can judge their possible effects only if we have adequate models for long-term prediction. One such possible model is a rather complete dynamic model of the biotic cycle. In addition to its primary function as a predictive instrument, this model can act as a connecting link between various branches of limnologic study of Lake Baikal, helping to provide mutual testing of the materials produced, and indicating the direction for studies necessary for elimination of restrictions in information support.

REFERENCES

Bellman, R. 1969. Vvedeniye v teoriy matrits (Introduction to matrix theory), Moscow, Nauka Press, 367 pp.

Biologic productivity of the pelagic area of Baikal and its variability. 1977. Trudy LIN SO AN SSSR, Vol. 19(39), Novosibirsk, Nauka Press, 254 pp.

Botintsev, K.K., A.M. Meshcheryakova and G.I. Popovskaya. 1975. Krugovorot organicheskogo veshchestva v ozere Baikal (The cycle of organic matter in Lake Baikal), Novosibirsk, Nauka Press, 189 pp.

Botintsev, K.K. 1961. Gidrokhimiya ozera Baikal (The hydrochemistry of Lake Baikal), Moscow, Acad. Sci. USSR Press, 311 pp.

Gorstko, A.B., Yu.A Dombrovskiy and V.V. Selyutin. 1977. Application of the dynamic balance method to modeling of the biotic cycle under conditions of anthropogenic eutrophication. Antropogennoye evtrofirovaniye prirodnykh vod (Anthropogenic eutrification of natural waters), Part I, Chernogolovka, pp. 75-79.

Kozhov, M.M. 1972. Ocherki po baykalovedeniyu (Essays on the science of Baikal), Irkutsk, Vost.-Cib. kn. izd-vo press, 254 pp.

Krotova, V.A. 1970. Geostrophic circulation of the waters of Baikal during the period of direct thermal stratification. Trudy LIN SO AN SSSR, Vol. 14(34), pp. 11-44.

Problems of Baikal. 1978. Trudy LIM SO AN SSSR, Vol. 16(36), Novosibirsk, Nauka Press, 295 pp.

Techeniya v Baikal (Currents in Baikal). 1977. Novosibirsk, Nauka Press, 160 pp.

Tsvetova, Ye.A. 1977. Mathematical modeling of the circulation of the water of a lake. Ibid., pp. 63-81.

SECTION 6

SPECIES DEPENDENT MASS TRANSPORT AND CHEMICAL EQUILIBRIA: APPLICATION TO CHESAPEAKE BAY SEDIMENTS

Dominic M. Di Toro[1]

INTRODUCTION

The analysis of the interactions between sediments and the interstitial waters is a problem of substantial difficulty. The complex chemical and biochemical reactions which affect the concentrations of the substances of interest are coupled to each other and to the gas and solid phases of the sediment. In addition, fluxes exchange mass across the sediment-water interface and redistribute it within the sediment via interstitial water diffusion and physical and biological mixing in the surface layer. Clearly a comprehensive analysis is necessary in order to understand these interrelationships and to establish the primary controlling factors.

The calculation presented below is based on the mass balance models of observed increases or decreases in interstitial water concentrations of various substances (Goldberg and Koide 1963; Lerman and Taniguchi 1972; Berner 1974). Typically these models are applied to a single constituent of interest, e.g., ammonia. For multiple constituents a conceptual simplification is available if the reactions are being driven by the decay of organic matter of a fixed stoichiometry (Richards 1965). A further simplification occurs if it is assumed that certain species are at chemical equilibrium. For certain inorganic dissolved species and certain redox reactions this is a well known approximation that has been tested by a number of investigators (e.g., Garrells and Christ 1965; Kramer 1964; Thorstenson 1970). While it has often been pointed out that overall and complete thermodynamic equilibrium is never attained for all species in all settings it is also clear that certain reactions occur so quickly that they are virtually in equilibrium over the time scale of the analysis. Thus while not as universally applicable as the principle of mass balance it is nonetheless a useful approximation in certain contexts. For the calculation of sediment behavior presented below, the equations of mass balance and chemical equilibrium are combined into a single structure for the analysis of sediment interstitial water and gas phase concentrations.

---

[1]Environmental and Engineering and Science Program, Manhattan College, Bronx, New York 10471.

COMPUTATIONAL FRAMEWORK

The equations of mass conservation provide the starting point for the analysis of the distribution of dissolved and particulate materials in sediments. For a steady state one dimensional analysis let D_i be the diffusion coefficient porosity product of species A_i and let w_i be the corrected (Imboden 1975) advective velocity of A_i, the velocity induced by the sedimentation of mass relative to a coordinate system fixed with respect to the sediment surface corrected for compaction, and assume they are constants in depth. The one dimension mass transport equations for the N_S species, A_i, are:

$$- D_i \frac{d^2[A_i]}{dz^2} + w_i \frac{d[A_i]}{dz} = f_i\ ([A_i],\cdots,[A_{N_S}]) \qquad i=1,\cdots,N_S \qquad (1)$$

where $f_i([A_i],\ldots,[A_{N_S}])$ is the sum of all sources and sinks for species A_i. For rapid chemical reactions such as acid-base reactions these equations are very difficult to solve using straight-forward numerical methods (DiToro 1976).

The method developed for this situation depends on separating the fast and slow reactions and requiring that the fast reactions be at equilibrium. Consider the species (the fast reactants) that are involved in at least one fast reaction and number them $i=1,\cdots,N_{fs}$. For example HCO_3^- would be in this category. The remaining species (the slow reactants) are numbered $i=N_{fs}+1,\ldots,N_S$. Particulate organic matter would be in this latter category. For this division the mass balance equations can be written:

$$- D_i \frac{d^2[A_i]}{dz^2} + w_i \frac{d[A_i]}{dz} = S_i + \sum_{j=1}^{N_{fr}} \nu_{ji} R_j \qquad i=1,\cdots,N_{fs} \qquad (2)$$

$$- D_i \frac{d^2[A_i]}{dz^2} + w_i \frac{d[A_i]}{dz} = S_i \qquad i=N_{fs}+1,\cdots,N_S \qquad (3)$$

where the rate at which A_i is produced by fast reaction j is $\nu_{ji}R_j$. R_j is the reaction rate of the jth of N_{fr} fast reactions and ν_{ji} is the reaction stoichiometric coefficient. S_i is the net source of A_i due to the slow reactions. This separation of the equations simplifies the solution procedure since equations (2) for the fast reactants can be transformed into a smaller set of equations for the N_C components, B_j, that form the fast reactants. Using the stoichiometric coefficients, a_{ij}, of the species in terms of the components equation (2) becomes (DiToro 1976):

$$\sum_{i=1}^{N_{fs}} \left(-D_i \frac{d^2}{dz^2} + w_i \frac{d}{dz}\right) a_{ik}[A_i] = \sum_{i=1}^{N_{fs}} a_{ik} S_i \qquad k=1,\ldots,N_C \qquad (4)$$

Although the species concentrations, A_i, are nonlinear functions of the N_c components B_k via the equilibrium relationships, the equations (3) and (4) can be solved more directly than the species equations themselves. In terms of number of equations, for example, the twenty-three fast reactants considered in the application below would each require an equation in each segment whereas seven component equations in each segment suffice. The solution procedure for equation (4) is detailed in the Appendix.

CLASSIFICATION OF THE REACTIONS

The initial choice for an application of these methods is the species to be considered and whether they are fast reactants. For the calculations presented below it appeared reasonable to restrict the computations to the distributions of the species with components: carbon, nitrogen, sulfur, hydrogen, oxygen, and, because of its availability in the data to be analyzed, argon. The species and their relevant properties are listed in Table 1.

Consider, first, the species involved in purely aqueous reactions. The acid-base reactions are clearly rapid and at equilibrium over the time scale of sediment diffusion. However it is not clear that the redox reactions are either as rapid or at chemical equilibria. The principal aqueous redox reactions for the species in Table 1 are the reduction of sulfate and the production and consumption of methane. Since bacterially mediated kinetics are responsible for these redox reactions, it might seem at first glance that the notion of chemical equilibrium is of little value in this context. However it has been pointed out that the thermodynamically predicted sequence of oxidation-reductions is commonly observed in nature as oxidation of organic material occurs (Stumm 1966) so that this appears to be a reasonable simplification of the complex reaction kinetics actually taking place if they are, in fact, rapid. The assumption is also quite convenient since equilibrium calculations are independent of the reaction pathways and no detailed specification of the kinetics are necessary; only the thermodynamic constants of the species of interest are required. One of the interesting results of the application discussed below is that it appears reasonable to assume that the reactions involving sulfate and methane are indeed rapid, relative to other reactions and the transport, and at equilibrium.

For the redox reactions involving nitrogen, although it may be reasonable to assume they are rapid, the equilibrium that is calculated from thermodynamics is unreasonable. For example, the thermodynamically favored oxidation of ammonia to nitrogen gas within the zone of sulfate reduction does not appear to occur, nor does the oxidation of nitrogen gas to nitrate in oxic environments. As a consequence the only nitrogen species considered in the fast reactant set is gaseous and dissolved N_2. Ammonia is assigned to the slow reactants; nitrite and nitrate are not considered as their concentrations are quite small in the application considered below.

Consider, next, the aqueous-gas phase reactions. As methane is produced it is possible that a gas phase (bubbles) will form. Whether the gas phase is in equilibrium with the interstitial water at that location depends on

TABLE 1. CHEMICAL FAST REACTANTS STRUCTURE AND AQUEOUS DIFFUSION COEFFICIENTS

Phase	pK[1]	Relative Diffusion Coefficient[2]	Phase	pK[1]
Aqueous			Gas	
H^+	0.0[3]	4.582	H_2O	-1.56
OH^-	-14.5	2.597	O_2	-86.0
H_2O	0.0[3]	1.0	CO_2	0.0[3]
O_2	-89.0	0.989	CH_4	24.31
CO_2	-0.77	0.842	N_2	0.0[3]
HCO_3^-	-7.07	0.583	H_2S	0.0[3]
$CO_3^=$	-17.6	0.488	Ar	0.0[3]
CH_4	22.18	0.733		
N_2	-2.57	0.984	pH	
H_2S	-1.12	0.748		
HS^-	-8.36	0.852	H^+	7.42
$S^=$	-22.74	0.406		
$SO_4^=$	-43.55	0.524	pS	
Ar	-2.23	0.990		
			H_2S	4.6

SLOW REACTANTS

Phase	Relative Diffusion Coefficient[2]	Reaction Source(+) Sink(-)
Aqueous		
NH_4^+	0.963	$S = + K\gamma\ [CH_\beta O_2(NH_3)_\gamma]$
Organic Sediment		
$CH_\beta O_2(NH_3)_\gamma$	0.0	$S = - K\gamma[CH_\beta O_2(NH_3)_\gamma]$

[1] Aqueous phase concentrations in mole/ℓ, Gas phase concentrations in mole fractions. pK for the reaction with ths species concentration on the left hand side and the component concentrations on the right hand side, e.g., $[HCO_3^-] = 1.0\ [CO_2(g)] + 1.0\ [H_2O(aq)] - 1.0\ [H^+(aq)]$. For T = 15°C and gas phase total pressure of 4 atm. Aqueous CO_2 equilibria adjusted for Cℓ = 10%. (Wagman, et al., 1968; Stumm and Morgan, 1970; Atkinson and Richards, 1967; Yamamoto et al., 1976; Harvey, 1966; Weiss, 1970).

[2] $D_{species}/D_{C\ell^-}$ with $D_{C\ell^-} = 2.032 \cdot 10^{-5} cm^2/sec$ @ 25°C (Robinson and Stokes, 1959; Himmelblau, 1964; Chapman, 1967; Li and Gregory, 1974; Reid et al., 1977).

[3] Indicates a component as well as a species. e^- is the remaining component.

the rapidity of the mass transfer across the liquid-gas interface. For stationary or slowly moving bubbles, equilibrium is obviously reasonable. For rapid bubble motion with mass transport across the interface, however, the assumption is incorrect. Therefore assigning the aqueous-gas phase reactions to the fast set precludes the analysis of non-equilibrium mass transfer within this framework.

The aqueous-sediment reactions are not mechanistically included in this calculation. Rather the reactions controlling pH and pS are adjusted such that the pH and pS are at their observed values. The relevant sediment buffering and precipitation reactions are simulated rather than explicitly included. In addition, it appears that ammonia adsorption can be neglected based on the magnitudes of the transport and reaction parameters as shown below, although its inclusion would not materially complicate the calculation.

The principal slow aqueous-sediment reaction considered is the decay of sedimentary organic material. In fact the rate of this decay and the diffusion and advective transport set the time scale within which the other reactions must be rapid. The structure of the calculation which results from these concentrations is shown in Table 1.

The aqueous diffusion coefficients are species dependent as shown and these differences are included in the calculation. However, the coupling of the diffusion fluxes due to the electrical potential generated by the differing diffusion coefficients appears to have only a small effect at sea water concentrations (Ben-Yaakov 1972) and is neglected although its inclusion presents no real difficulty.

SPECIES INDEPENDENT TRANSPORT

As can be seen in Table 1, the assumption that aqueous species diffuse at the same rate is in error by a factor of two and, if H^+ and OH^- are considered, by a factor of twenty. The situation becomes more implausible if the gas and stationary phases are considered to be diffusing as well. The assumption of species independent transport also requires that the species are advecting with the same velocity. This is reasonable for the aqueous and solid phases in the absence of groundwater intrusion, but it is certainly possible that the gas phase is advecting at a different velocity and in a different direction relative to the aqueous and solid phases.

Nevertheless the solution of the relevant differential equations are so simplified by this assumption that it is useful to pursue the result. For the decay of sedimentary organic material, with a sedimentation velocity, w, a first order decay with rate constant, K, and zero diffusion the solution to equation (3) is an exponentially decreasing concentration of sediment organic material in depth: $c_0 \exp(-Kz/w)$, with surface boundary concentration c_0. The spatial distribution of the source due to this slow reaction is: $S_\ell = Kc_0 \exp(-Kz/w)$, where ℓ is the species index of sediment organic matter.

For the case of species-independent transport equations (4) each become an equation in a component since $\sum_i a_{ik}[A_i] = [B_k]$. The source term is just the quantity of that component being produced by the decay of sedimentary organic matter since $a_{\ell k}$ is its component stoichiometry. Further the equations are not coupled to each other and they can be solved separately. The result is:

$$[B_k](z) = [B_k]_o + \frac{a_{\ell k} c_o}{1+KD/w^2}(1 - e^{-Kz/w}) \qquad k=1,\ldots,N_c \qquad (5)$$

where $[B_k]_o$ are the component boundary concentration at z = 0, the sediment-water interface. For components that are not part of the stoichiometry of the sedimentary organic matter, i.e., the B_k's such that $a_{\ell k} = 0$, their concentrations are constant in depth.

Perhaps the most useful way of picturing the calculation implied by equation (5) is to interpret $\xi = 1 - \exp(-Kz/w)$ as a variable that reflects the extent of a titration of sedimentary organic matter into the chemical system defined by the boundary concentrations of the components. As depth increases, ξ increases and more sedimentary organic material is titrated into the chemical system where it reacts with the boundary-defined component composition to produce a new composition of species. Thus with species-independent transport, the depth distribution in the sediment is simply the result of an exponential titration of organic matter into the chemical system defined by the surface boundary composition of the sediment.

It is interesting to note that the chemical equilibrium investigations of reducing sediments by Thornstenson (1970) and Gardner (1973) are conceived as titrations of organic matter into chemical systems comprised of entirely dissolved species or with solid phases present. The above analysis indicates that for species-independent transport the depth distribution of species indeed reflects a simple titration and the results of such calculations are directly relevant.

It is useful to realize that this solution satisfies the conditions of the mass balance equations with species-independent transport coefficients so that, in fact it is a plausible solution for situations wherein that assumption is reasonable. Conversely for species-dependent transport due to gas phase motions, stationary solid phases, and the differing molecular diffusion coefficients of aqueous species, the requirements of mass balance are more complex and the distributions of components can no longer be calculated from equation (5).

CHESAPEAKE BAY SEDIMENT PARAMETERS

In order to investigate the feasibility and utility of these computations for species dependent transport an initial application has been made to observed distributions of carbon, nitrogen, sulfate and dissolved gases in Chesapeake Bay sediments. The species chosen (Table 1) are dictated pri-

marily by the available data. The other major cations and anions are not considered as they were not consistently reported.

Ideally, the relevant sediment parameters: the diffusion and advection coefficients, sedimentary organic matter stoichiometry, and its reaction rate should be determined together with the observations of interstitial water concentrations. While this is not the case for the historical data considered in this application, a reasonably complete set of estimates can be made from other investigations. These are listed in Table 2. The ratio of sediment organic carbon to organic nitrogen is reasonably constant over the 30 cm. of interest and both decay exponentially as shown in Figure 1 (Schubel et al. 1977). The boundary condition for sediment organic carbon ranges between 2 and 3% (Biggs 1967). The sedimentation velocity has been determined by Pb^{210} dating and other methods and ranges between 0.1 and 0.28 cm/yr. It is, therefore, possible to estimate the first order decay rate constant, and knowing the water content and surface sediment concentrations, the rates of organic carbon and nitrogen sources resulting from this slow reaction. Essentially a three-fold uncertainty exists for both these sources as shown. An independent estimate of the chloride diffusion coefficient is available, based on an analysis of the time variable chloride profiles in the sediment (Holdren et al. 1975).

The parameter values in Table 2 can be used to assess the importance of ammonia adsorption and the need to include a solid phase ammonia species. It has been shown (Berner 1977) that if $DK/w^2 >> 1+K^*$, where K^* is the linear adsorption coefficient, $K^* = [ads.NH_4]/[NH_4(aq)]$, the adsorption can be neglected in the computation of the interstitial water ammonia concentration. For the parameter ranges in Table 2, DK/w^2 ranges from 5 to 130. Although no ammonia adsorption coefficient is available for Chesapeake Bay sediments, the value of 1.6 has been reported for a Long Island Sound sediment (Rosenfeld and Berner 1976). Thus it is probable that ammonia adsorption can be neglected in this calculation.

There is only one remaining uncertainty: the hydrogen (actually the electron) stoichiometry of the sediment. Although it is conventional to assume that Redfield's ratio (CH_2O) applies to sedimentary organic material it is possible that other ratios might be appropriate. For the components used in this calculation the required stoichiometry is

$$CH_{\beta+2}\,O_{2+\delta}(NH_3)_\gamma = CO_2 + \beta H^+ + \beta e^- + \gamma NH_3 + \delta H_2O \qquad (6)$$

It is intersting to note that the oxygen stoichiometry is essentially irrelevant once the carbon and hydrogen stoichiometry are established since it is related to the H_2O content of the organic matter. The quantity of H_2O introduced by the organic material decay is negligible relative to the concentration present and the convenient choice is $\delta = 0$ corresponding to the "dry" stoichiometry of the organic material, i.e., $(CO_2)H_\beta(NH_3)_\gamma$. Any additional water added to this material does not alter the results and is therefore irrelevant for this computation. For this convention the Redfield stoichiometry is CH_4O_2 corresponding to the electron to carbon stoichiometric ratio of glucose.

TABLE 2. CHESAPEAKE BAY SEDIMENT PARAMETERS

Description	Symbol	Value	Units	Station[1]	Reference
Ratio of Sediment Org C to Org N	$\frac{[\text{Org C}]}{[\text{Org N}]}$	10.9 ± 1.1	mole/mole	842D	Schubel *et al.* (1977)
Sediment Org C at z = 0	$[\text{Org C}]_o$	2.7	% dry wt.	842D	Schubel *et al.* (1977)
		2.0 - 3.0	% dry wt.	820	Biggs (1967)
Sedimentation Velocity	w	0.09 - 0.12	cm/yr	842D	Schubel *et al.* (1977)
		0.1	cm/yr	-	Carpenter (1975)
		0.28	cm/yr	-	Powers (1954)
Sediment First Order Decay Coefficient	K	0.005 - 0.0067	yr^{-1}	842D	Figure (1)
Water Content	p	0.5 - 0.6	% wet wt.	820	Biggs (1967)
Organic Carbon	$S_{Org-C}(0)$	15.2 - 45.9	μM/ℓ/day	-	Computed[2]
Chloride Diffusion Coefficient	$D_{C\ell^-}$	0.22 - 0.44	cm^2/day	856C	Holdren *et al.* (1975)
Sediment Sulfide Concentration	FeS(s)	1.0 - 1.3	% dry wt.	61	Biggs (1963)
	FeS(s)	0.7 - 0.8	% dry wt.	61	Biggs (1963)
Gas Phase Volume	V_{gas}	0.1 - 1.0	% volume	Pier 22	Schubel (1974)
		∿0.1		Pier 31	Schubel (1974)

[1] See Bricker *et al.* (1977) for the relationship to latitude and longitude.

[2] $S_{Org-C}(0) = K[\text{Org C}]_o(1-p)/p$.

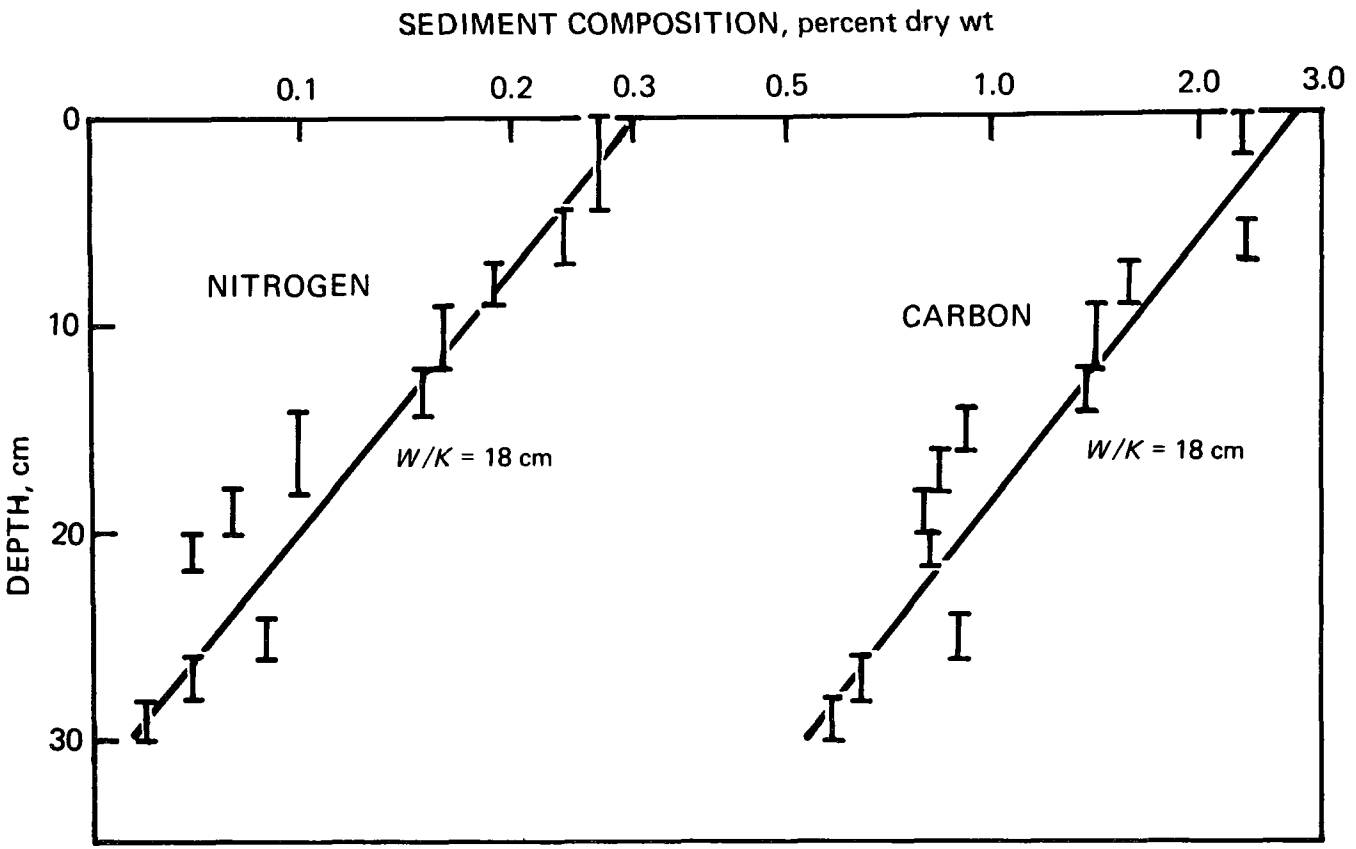

Figure 1. The vertical distribution of sediment organic carbon and nitrogen as percent dry weight. Chesapeake Bay Station 842D (Schubel et al., 1977). The solid lines represent exponential decays: exp (-Kz/w), with w/K = 18 cm and a molar carbon to nitrogen ratio of 10.9.

A few representative examples for other sediments and their organic fractions are shown in Table 3. The electron to carbon ratio, β, which is computed from the reported elemental analysis (C,H,O,N) after conversion to dry stoichiometry, ranges from 3.8 for fulvic acids to 5.3 for bitumen from recent Bering Sea sediment. Thus the fraction of the sediment organic carbon that is decaying is likely to have an electron to carbon ratio in the lower end of this range since the resistant fractions (bitumen and kerogen) have the higher stoichiometries and the initially deposited material is probably close to the Redfield ratio of 4.0. The nitrogen to carbon ratio is also listed which, except for bitumen, spans a range from 0.05 to 0.1.

CHESAPEAKE BAY STATION 856: CARBON AND AMMONIA

The parameter values in Table 2 set the probable ranges for Chesapeake Bay sediments. For an application to any particular set of data it is likely that the specific values for the parameters will differ somewhat, however the ranges are known.

An extensive set of interstitial water chemistry data for Chesapeake Bay sediments is available (Bricker et al. 1977) that can be analyzed within the context presented above. A composite data set has been examined from the winter of 1971-1972. All stations with the designation 856, that is at the latitude 38°56' and for which measurements of pH, SO_4, alkalinity, and NH_4 are available simultaneously, have been grouped. The average and standard deviation of both the midpoint sampling depth and the concentrations have been calculated for the overlying water, and for the midpoint depth intervals: 0-5 cm., 5-10 cm., 10-25 cm., 45-85 cm., and 85-100 cm. In the plots that follow the data are represented by the means $\pm$ the standard deviation of both the concentration and the midpoint sampling depths. If no error bars appear they are smaller than the plotting symbol. The depth intervals are chosen to minimize the overlap between the actual sampling intervals used in the surveys. The total carbon dioxide concentration is calculated from the reported pH and alkalinity data with the equilibrium constants adjusted for the reported chloride concentration (Stumm and Morgan 1970).

The boundary condition concentrations are established from the overlying water data except for the initial ammonia concentration which is chosen to reproduce the total carbon dioxide to ammonia ratio at 5 cm. This refinement affects only the computed carbon to ammonia ratio at the sediment-water interface and is made in order to better reflect the initial ammonia concentration just below the interface. These concentrations are listed in Table 4 together with the parameters chosen for the transport and sediment organic matter stoichiometry. The diffusion, advection, and reaction rate coefficients are those reported (Table 2). The sediment organic carbon decay rate and the electron and nitrogen to carbon ratios are adjusted within the reported range to produce an acceptable fit. The resulting parameters are listed in Table 4. The organic carbon decay rate is at lower limit of the probable range as is the chloride diffusion coefficient. Since only the ratio of these parameters affects the computed profiles the values chosen appear to be quite reasonable. The electron to carbon ratio of 3.33 is sub-

TABLE 3. SEDIMENT ELECTRON[1] AND NITROGEN STOICHIOMETRY
$CH_{\beta}O_2(NH_3)_{\gamma}$

	β	γ	Reference
Fulvic Acid	3.80 ± 0.36	0.0912 ± 0.0247	Rashid & King (1970)
Humic Acid	4.24 ± 0.19	0.0766 ± 0.0129	Rashid & King (1970)
Marine Sediment	4.04 - 4.23	0.089 - 0.091	Kemp (1973)
Marine Sediment	4.64	0.098	Trask (1938)
Lithified Marine Sediment	4.99	0.054	Trask (1938)
Kerogen	4.64	0.062	Philip & Calvin (1976)
Bitumen	5.29 - 5.33	0.01 - 0.012	Bordovskiy (1965)

[1] $\beta = 4 + \frac{[H]}{[C]} - 2\frac{[O]}{[C]} - 3\frac{[N]}{[C]}$.

TABLE 4. STATION SEDIMENT PARAMETERS

Parameter	Units	Station 856	Station 858-C
Sampling Dates	-	1 Oct 71 to 31 Jan. 73	22-XI-66, 5- I-67
γ^{-1} = [Org C]/[Org N]	mole/mole	9.0	10.6
β = [Org H]/[Org C]	mole/mole	3.33	2.67 - 3.0
K	yr^{-1}	0.005	0.005
w	cm/yr	0.1	0.1
$S_{Org-C}(0)$	μM/ℓ/day	13.5[1]	30.0
$D_{C\ell^-}$	cm^2/day	0.25[1]	0.25
$[SO_4]_o$	g/ℓ	1.24[2]	1.45[3]
$[NH_4]_o$	mgN/ℓ	1.55[4]	-
$[\Sigma CO_2]_o$	mgC/ℓ	21.2[2]	18.4[2]
$[A\ell k]_o$	g $CaCo_3$/ℓ	0.073[2]	-
$[N_2]_o$	mgN/ℓ	-	7.0[5]
pH	-	7.4	7.4
pS	-	12.5	12.5

[1] Any value in the ranges in Table 2 will produce the same result so long as $S_{Org-C}(0)/D_{C\ell^-}$ = 13.5/0.25 = 27.0/0.50.

[2] Average of overlying water data.

[3] Computed from reported Cℓ concentration 10.4°/₀₀.

[4] Estimated from C/NH_3-N ratio at 5 cm. Overlying water conc. = 0.3 mgN/ℓ.

[5] Estimated from 0-15 cm data.

stantially lower than what would be expected (Table 3). Evidently the reductions of iron and manganese, which are not considered in this calculation, are responsible for this difference. Those reactions are presumably utilizing the electrons corresponding to the difference between $\beta = 3.33$ required for sulfate reduction and methane production and the expected ratio of $\beta \sim 4$.

Figure (2) presents the comparisons to the observed ammonia and total inorganic carbon data as well as their ratio. Solutions for both the species dependent and the species independent diffusion coefficients cases are presented with the latter using the diffusion coefficient of chloride ion for all species. No gas phase is computed to form in either case so that its transport coefficients are not involved. For both cases the ammonia profile is essentially the same since the ammonia diffusion coefficient is almost equal to that for chloride, but not for the total carbon dioxide profile due to the substantially smaller bicarbonate diffusion coefficient.

The effect of species dependent diffusion is most markedly apparent in the computed total carbon dioxide to ammonia ratio as shown in Figure (2). The sediment organic matter carbon to nitrogen molar ratio is estimated to be 9.0 whereas the interstitial water molar ratio is observed to be 16.0 near the sediment water interface and decreases to 12.5 at 100 cm. The species independent case calculation begins at the specified molar ratio of the boundary conditions and rapidly declines to the sediment organic matter ratio. The behavior of the species dependent calculation is more complex. The molar ratio declines to a plateau of 14.4 until a depth of 30 cm. after which it abruptly declines to 13.5 at 40 cm. and further decreases to 12.5 at 100 cm.

The initial plateau value can be understood in terms of the differing diffusion coefficients. The ammonia profile follows equation (5) since it is a conservative slow reactant. Until the onset of methane production, total carbon dioxide can also be described by a similar equation with a diffusion coefficient adjusted for the fraction of total CO_2 that is $CO_2(aq)$, $\sim$10%; HCO_3^-, $\sim$90%; and $CO_3^=$ (negligible). The boundary concentrations are quickly overwhelmed by the source due to the sediment decay and the ratio approaches:

$$\frac{[\Sigma CO_2]}{[NH_4]} \rightarrow \frac{[\text{Org C}]_\circ}{[\text{Org N}]_\circ} \frac{1 + D_{NH_4} K/w^2}{1 + D_{\Sigma CO_2} K/w^2} \tag{7}$$

Since the total CO_2 diffusion coefficient is substantially smaller than the ammonia diffusion coefficient, and for the transport and reaction parameters for this station: $D_{NH_4}K/w^2 = 44$, the observed interstitial water ratio is larger than the sediment organic matter ratio by the factor: $D_{NH_4}/D_{\Sigma CO_2} = 1.6$. The importance of this species dependent transport effect for ammonia, sulfate, and phosphorus concentrations has been pointed out (Berner 1977).

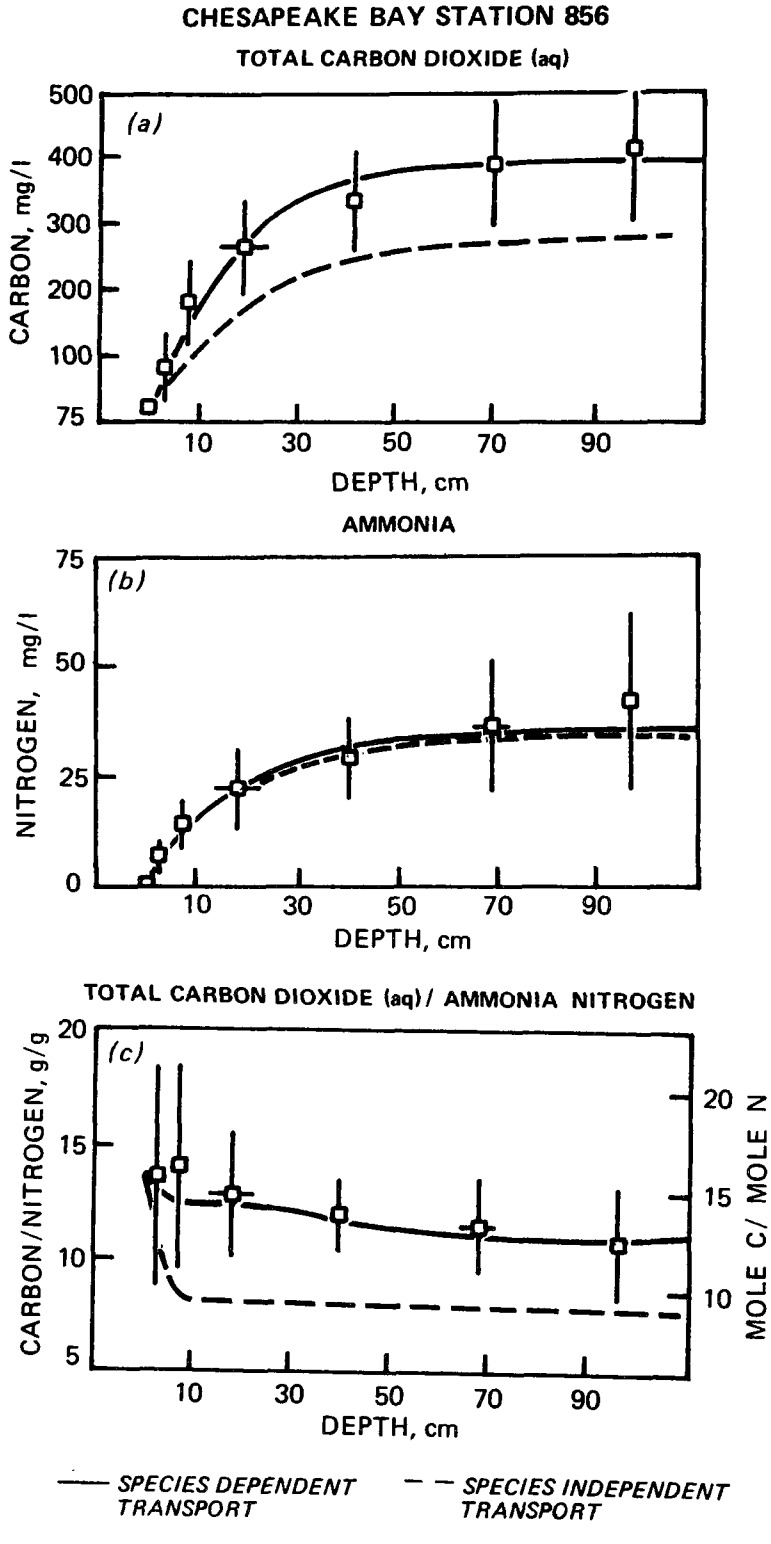

Figure 2. Chesapeake Bay Station 856: Observed (symbols) and computed (lines) vertical distribution of (a) total aqueous carbon dioxide; (b) aqueous ammonia nitrogen and (c) their ratio. The computation for both the species dependent transport case (solid line), and the species independent transport case (dashed line) with all diffusion coefficients set at the value for chloride ion for these sediments (Table 2). The symbols represent the mean + the standard deviation of the observations and the midpoints depths of the sampled sediment sections.

The further decline of the total CO_2 to ammonia ratio after a depth of 30 cm is due to the onset of methane production. Since a fraction of sediment carbon is now being reduced to methane, the production of total CO_2 declines somewhat while the production of ammonia continues. Thus the ratio is calculated to decline as do the observations.

SULFATE, ALKALINITY, AND NET ALKALINITY

The increase of alkalinity and the decrease of sulfate are major features of the interstitial water chemistry of sediments. The computed alkalinity and sulfate profiles are compared to observations in Figure 3a and 3b. With all aqueous diffusion coefficients set to that of chloride (species independent transport), a twofold increase in the sulfate diffusing in and the bicarbonate diffusing out reduces the alkalinity and increases the sulfate profiles as shown. If all aqueous diffusion coefficients are set at the value for sulfate, the computed profiles are close to the species dependent case.

The accumulated precipitated sulfide in the pS phase provides a check of the calculation. The estimated quantity present in certain Chesapeake Bay sediments is on the order of 0.07 - 0.23 mol/l (Table 2) in comparison to the calculated range of 0.08 - 0.37 mol/l for station 856 sediments. As pointed out by Berner (1974), this provides support for the values of the sedimentation velocity used in the calculation.

The relationship between alkalinity, sulfate, ammonia, and the other major cations in anoxic sediments has been investigated (Berner et al. 1970) and applied to Chesapeake Bay interstitial waters for which the relevant data were available (Bray 1973). The idea is to balance the charges of the protolytic and nonprotolytic ions (Ben-Yaakov 1973). This charge balance equation must be satisfied. The equivalent sum of the protolytic ions is very nearly titration alkalinity (corrections for uncharged ions that consume acidity should be made, e.g., $NH_3(aq)$ which is normally small at the pH of interstitial water). As a consequence, the behavior of alkalinity can be deduced from the behavior of the nonprotolytic ions in the charge balance equation.

Following this reasoning the alkalinity is given by the relationship:

$$[Alk] \stackrel{\Delta}{=} [HCO_3^-] + 2[CO_3^=] + [HS^-] + 2[S^=] + [OH^-] - [H^+]$$

$$= [Cl^-] \left\{ \frac{Alk}{Cl} + 2\frac{SO_4}{Cl} - \frac{NH_4}{Cl} - 2\frac{Ca}{Cl} - 2\frac{Mg}{Cl} - \ldots \right\} \qquad (8)$$

$$- 2[SO_4^=] + [NH_4^+] + 2[Ca^{++}] + 2[Mg^{++}] + \ldots$$

where the ratios: Alk/Cl, SO_4/Cl etc. are the sea water ratios, and the term multipled by $[Cl^-]$ expresses the contribution of the original sea water. The remaining terms account for the effects of the interstitial

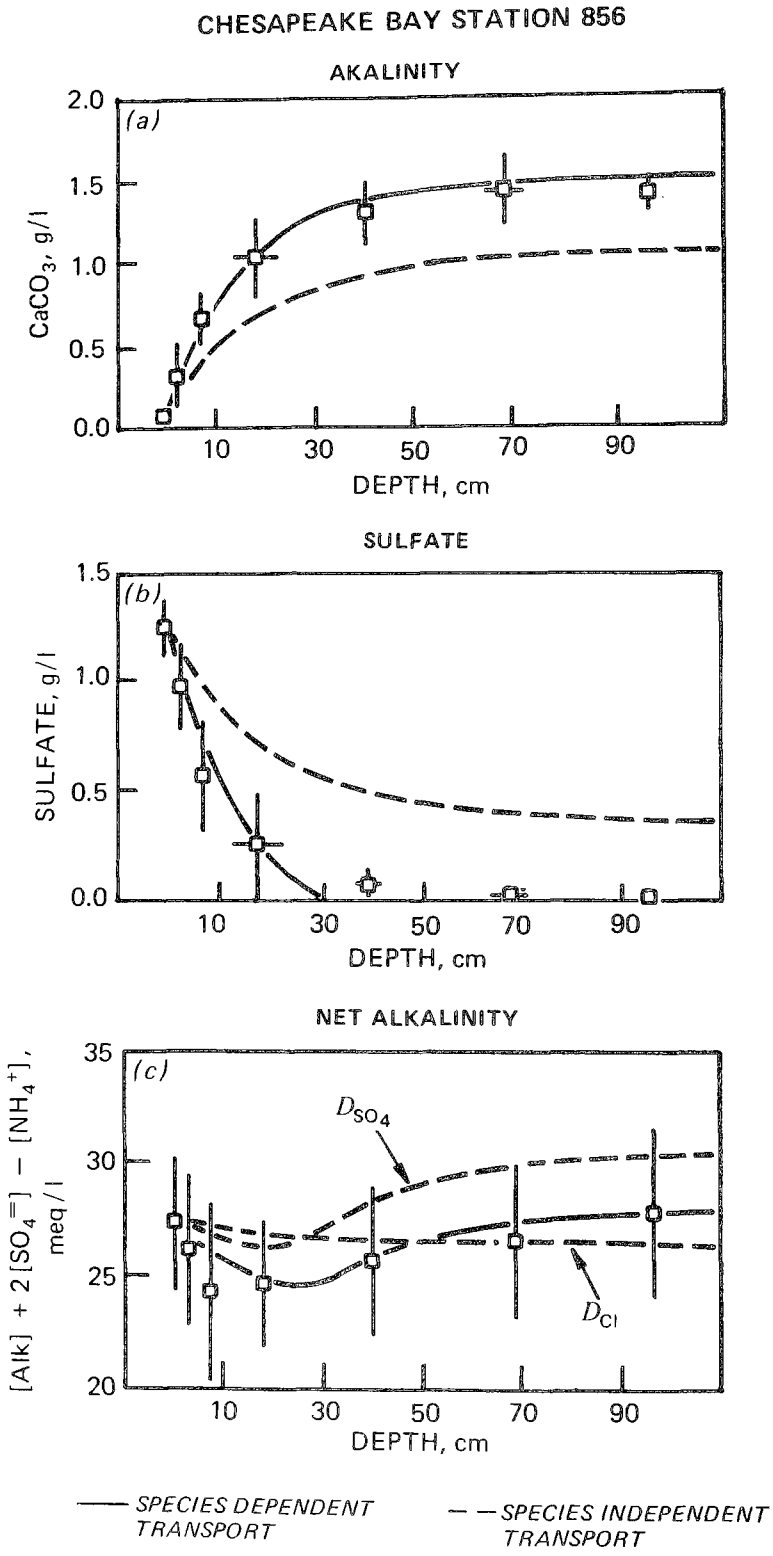

Figure 3. Chesapeake Bay Station 856: Observed (symbols) and computed (lines) vertical distribution of interstitial water: (a) titration alkalinity, gm/l of $CaCO_3$ equivalents; (b) sulfate, gm SO_4/l; (c) net alkalinity, milliequivalents/l. The pH and pS are fixed at their observed values (Table 4). The solid line is the species dependent transport computation. The dashed lines in (a) and (b) are the species independent case at the diffusion coefficient of chloride ion. The species independent transport case for (a) and (b) at the diffusion coefficient of sulfate ion are nearly indistinguishable from the solid lines. However for net alkalinity (c) the two cases are distinguishable as indicated.

water and sediment reactions on the major cations and anions. Note that if all the cations and anions were included in this formula as implied by the dots in the equation, then the sea water term would be zero (it is electrically neutral) and the only relevant terms are the sediment interstitial water concentrations themselves. Since the major variations occur for sulfate and ammonia, consider a quantity which might be termed net alkalinity:

$$[\text{Net Alk}] = [\text{Alk}] + 2[SO_4^{=}] - [NH_4^{+}] = 2[Ca^{++}] + 2[Mg^{++}] + \ldots \qquad (9)$$

which is the equivalent sum of the sediment-derived cations and anions due to precipitations, dissolutions, and cation exchanges. Strictly speaking, the definition of net alkalinity should include nitrite and nitrate concentrations since their reduction to nitrogen gas increases alkalinity. However in anoxic marine sediments their effects are usually small relative to other cations and anions. Net alkalinity should be more sensitive to changes in solid phase-interstitial water reactions since the masking effects of the large sulfate and ammonia changes have been removed. In fact net alkalinity is clearly independent of the aqueous reactions associated with the decay of sediment organic matter (unlike alkalinity itself) and responds only to solid phase interactions and, as shown subsequently, species dependent transport effects.

It is clear from this discussion that the calculation of alkalinity, and certainly net alkalinity, requires a knowledge of the behavior of the sediment solid phases and the major cations. It is possible to simulate their behavior by introducing two artificial phases, called the pH and pS phases in Table 1, which keep the aqueous concentration of H^+ and $S^=$ at specified values. The pH phase behavior is analogous to a reservoir of available strong acid or base which is titrated into the aqueous phase as required.

The operation of the pS phase is based on the precipitation of ferrous sulfides (Berner 1970). The net effect of this reaction on the species considered in this calculation is to remove H_2S (Ben-Yaakov 1973) to the extent determined by the activity of $S^=$.

The computed net alkalinity, (Figure 3c) is quite interesting. For species dependent transport the net alkalinity first decreases and then increases, as do the observations. The species independent cases also show decreases and then increases. Therefore both the species dependent transport and simulated solid phase interactions are responsible for the shape of the net alkalinity profile.

In order to understand the solid phase role consider the species independent case. The sources and sinks that affect net alkalinity must come from the solid phase-aqueous phase interactions. The production of carbon dioxide by the sediment organic matter oxidation does not influence alkalinity since it is uncharged. The same is true for the removal of H_2S. However both reactions affect pH. Therefore with the pH phase present the removal of H_2S tends to increase the pH and the pH phase responds by removing alkalinity. This is the cause of the initial drop in net alkalinity. Once sulfate reduction is over the pH tends to drop as CO_2 production con-

tinues. The pH phase responds by adding alkalinity. This is the cause of the rise in net alkalinity after a depth of 30 cm.

For the species independent case with all species at the smaller sulfate diffusion coefficient these variations in net alkalinity are intensified since more CO_2 and H_2S are retained within the sediment, relative to the species independent case with all species at the chloride diffusion coefficient. Of course these changes are occurring in the alkalinity profile itself but they are masked by the large increase due to sulfate reduction. The net alkalinity response is much more sensitive to these variations.

A more detailed investigation of the behavior of net alkalinity is given in Figure 4. The first case (Figure 4a) considers the behavior with no sulfide precipitation (pS free) but with a fixed pH. The only significant effect is that due to carbon dioxide production at a fixed pH, which increases net alkalinity. With all diffusion coefficients at the value of sulfate the increase is larger than the chloride diffusion case due to the increased retention of carbon dioxide within the sediment interstitial waters.

In order to understand the species dependent transport calculations consider the principle ions that form net alkalinity in this calculation and their diffusion coefficients:

$$\begin{array}{lcccccc} [\text{Net Alk}] & \simeq & [HCO_3^-] & + & 2[SO_4^=] & + & [HS^-] & - & [NH_4^+] \\ \text{Diffusion Coefficients} & & (0.583) & & (0.524) & & (0.852) & & (0.963) \end{array} \qquad (10)$$

As net alkalinity is produced or destroyed within the sediment by the solid phases it tends to diffuse either out to or in from the boundary, since it is driven by the gradient of net alkalinity. If the diffusion coefficients of the species that make up net alkalinity are all lowered, more net alkalinity remains in the sediment as can be seen from the two species independent cases in Figure 4a. The species dependent profile can be understood by comparing it to the species independent profile at the diffusion coefficient of sulfate. The differences are a slightly increased bicarbonate diffusion coefficient relative to sulfate, equation (10), an increased bisulfide diffusion coefficient and an almost twofold increase in ammonia diffusion. The effect on the diffusion of net alkalinity toward the boundary is in proportion to the quantity of each ion and the change in diffusion coefficients. Computations show that the largest effect is due to the excess bicarbonate diffusion, which causes a decline in the profile, followed by the bisulfide diffusion, which is most effective in the region of sulfate reduction and causes the initial drop in the profile.

The direction of the change to be expected from the excess diffusion relative to sulfate can be understood in terms of the profiles of the individual species that make up net alkalinity. Bicarbonate is increasing with respect to depth so that the transport will therefore lower the net alkalinity profile. The same is true for bisulfide. For ammonia, the diffusion is also toward the boundary so that increased diffusion will lower the ammonia profile. But this increases the net alkalinity since ammonia enters

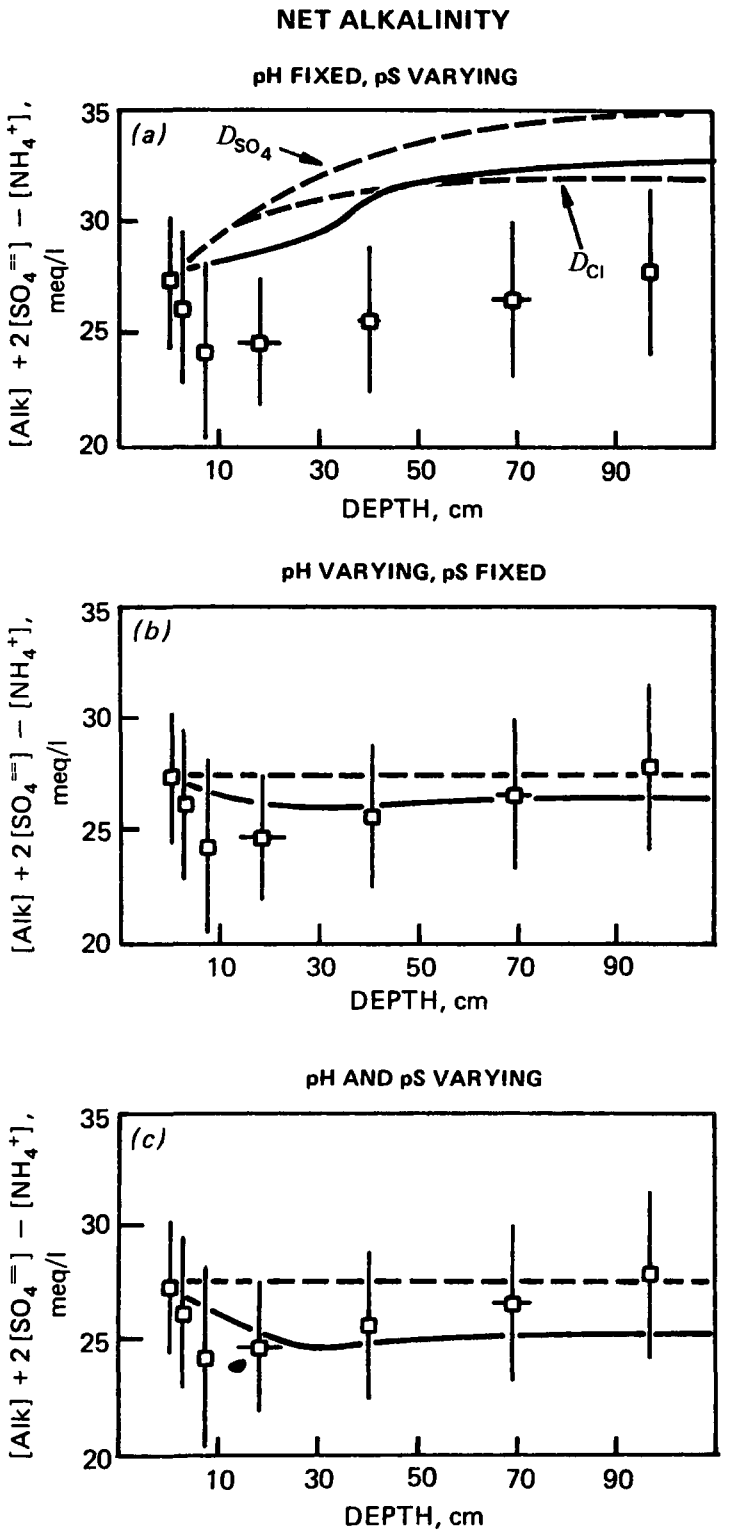

Figure 4. The effects of species dependent transport and solid phase reactions on net alkalinity. Chesapeake Bay Station 856 data included for visual reference. Solid lines are the species dependent transport cases, dashed lines are the species independent transport cases. (a) The pH is fixed at the observed value but the pS is allowed to vary. The results for the species independent transport cases at the diffusion coefficient for chloride ion, D_{Cl} and at the diffusion coefficient for sulfate ion, D_{SO_4}, are as indicated. (b) The pH is allowed to vary (no solid phase buffering reactions) but the pS is fixed at the observed value. Both species independent transport cases give identical results (dashed line). (c) Both the pH and the pS are allowed to vary. Both species independent transport cases give identical results.

the definition of net alkalinity with a minus sign, Equation (10). Thus the decreases due to the excess bicarbonate and bisulfide diffusion are compensated for to some extent by the excess ammonia diffusion. It is these excess diffusion effects that cause the species dependent profile in Figure 3c, the calculation with both pH and pS phases fixed, to be lower than the species independent profile at the diffusion coefficient of sulfate.

These effects are even more apparent in Figures 4b and 4c which are calculated without the pH phase present. Since the pH is now free to respond to additions of carbon dioxide and the removal of H_2S (Figure 4b) no net alkalinity is generated and for the species independent transport case the net alkalinity is constant. The decrease in the species dependent case is due to the bicarbonate excess diffusion which is compensated for to some extent by the ammonia excess diffusion. With the pS also free in Figure 4c, the only difference is the presence of HS^- as a component of net alkalinity and its excess diffusion further lowers the profile.

To summarize, the net alkalinity can initially decrease for two reasons: either as a purely species dependent transport effect (Figure 4c), or in response to the precipitation of ferrous sulfide at constant pH (Figure 3c), where the decrease in this case is enhanced by species dependent effects. The subsequent increase is in response to the production of carbon dioxide at constant pH (Figures 3c and 4a) and is again modified by species dependent transport effects.

An interesting question arises if one inquires into the generality of these results. Since they depend so directly on the assumption of constant pH controlled by a pH phase and since the pH of interstitial waters is seldom constant, although for station 856 data it is very nearly constant: pH = 7.40 $\pm$ 0.18, it might appear that their applicability to other situations is restricted. However consider the following: The calculated responses of net alkalinity to the CO_2 source and the H_2S sink are the result of the requirement of a constant pH, that is, an infinitely well-buffered system. Suppose that in most sediments there are solid phase-aqueous phase reactions which serve as buffers and tend to resist the pH changes induced by the CO_2 source and H_2S sink. These reactions would titrate net alkalinity into or out of the aqueous phase, much as the hypothetical pH phase does, but without its infinite buffer capacity. Thus the pH would change somewhat in response to the sources and sinks, but so also would the net alkalinity. As a consequence one would expect to see profiles of net alkalinity that only increase, if no sulfide precipitation occurs, or initially decrease and then increase after sulfate depletion, or only decrease if sulfate is not depleted.

A selection of net alkalinity profiles are shown in Figure 5. They have been chosen to display the characteristic shapes that are calculated in Figures 3 and 4. Figure 5a shows an increase due, presumably, to the CO_2 source but with sulfate present and approximately constant, indicating that another electron acceptor was involved. Figure 5b from a station in the upstream reach of Chesapeake Bay (Cl < 1°/₀₀) exhibits the expected increase. The small quantity of available sulfate is depleted in the top five cm, after which the net alkalinity increases in response to the CO_2 source. Fi-

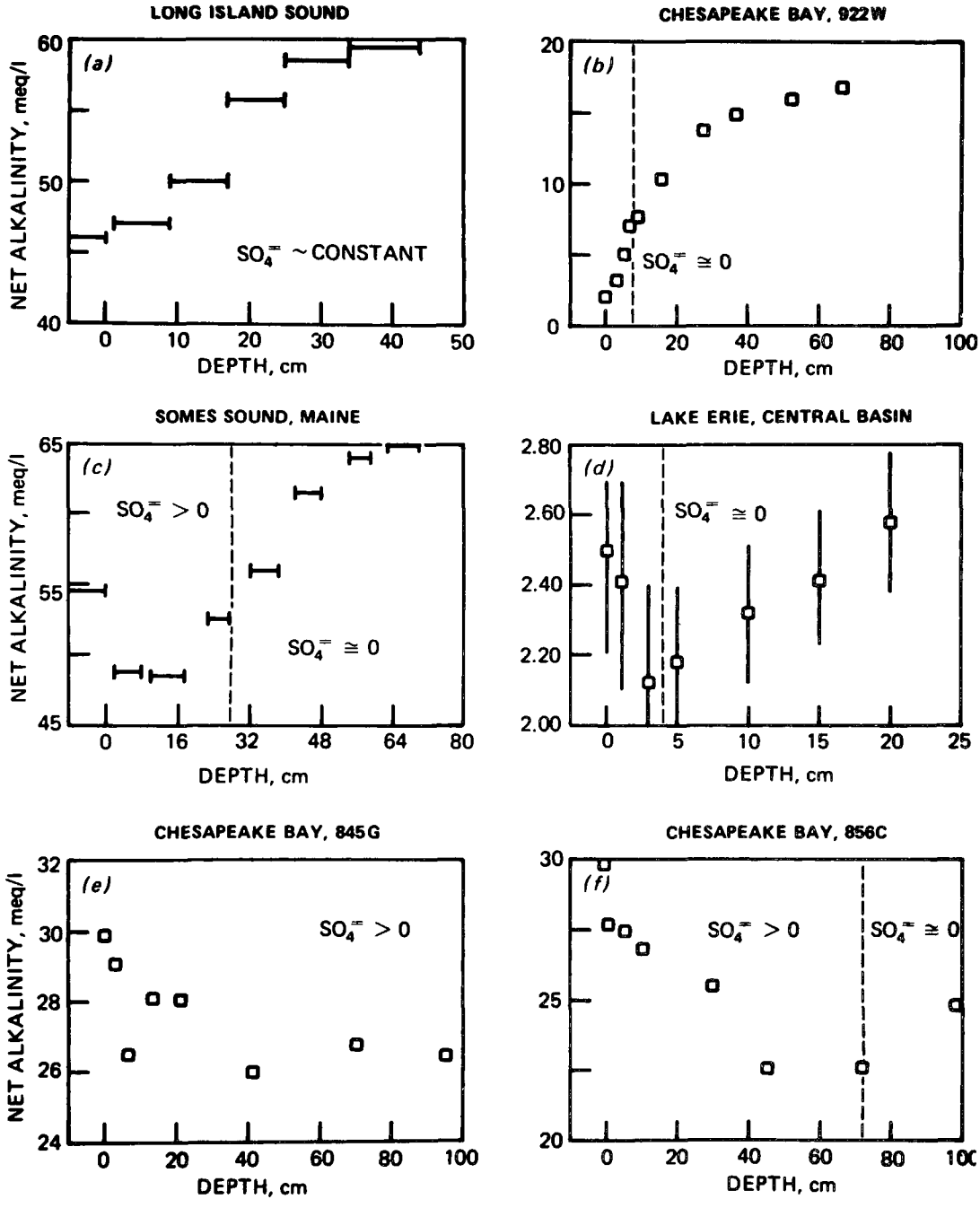

Figure 5. Characteristic shapes for net alkalinity. The vertical dashed line marks the depth of sulfate depletion. Increasing net alkalinity: (a) Intertidal zone, Long Island Sound, Clinton, Conn. (Berner et al., 1970); (b) Chesapeake Bay Station 922W, 18/XII/73 (Bricker et al., 1977). Net alkalinity decreasing then increasing after sulfate depletion; (c) Somes Sound, Maine (Berner et al., 1970). (d) Lake Erie, Central Basin. Mean ± standard deviation of three stations: 41°49'03", 42°00'00", 42°27'14", sampled every month from May through August, 1971 (Weiller, 1972). Net alkalinity decreasing; (e) Chesapeake Bay Station 845G, 21/VIII/72 (Bricker et al., 1977). (f) Chesapeake Bay Station 856C, 30/VI/71 (Bricker et al., 1977). Note the increase after the depletion of sulfate.

gures 5c and 5d illustrate the initial decline due to sulfide precipitation and the subsequent increase after the depth at which the sulfate is depleted. The location is indicated on the figure. The example from Lake Erie is included because of its similar behavior in all respects except that the magnitudes of the changes in net alkalinity are an order of magnitude smaller than the brackish and sea water examples. Figures 5e and 5f from Chesapeake Bay stations with higher salinity (Cl $\simeq$ 10°/$_{oo}$) have more extensive regions of declining net alkalinity. In both cases the decline is within the region of sulfate reduction as indicated. The majority of other profiles examined from Chesapeake Bay sediments exhibit the decreasing and increasing pattern in the saline regions, with the increase starting after sulfate is depleted, and a purely increasing pattern in the fresher water regions, as illustrated in Figure 5.

Similar patterns are present in the Santa Barbara Basin data of Sholkovitz (1973). Two cores (B and G1) exhibit a continual decline in net alkalinity in the presence of decreasing sulfate concentration. For the third core (G2), the net alkalinity profile is essentially constant to 30 cm with an increase at the last measured depth (33 cm). The sulfate is essentially constant as in the case of the Long Island Sound example (Figure 4a).

These observations tend to indicate that the results of the detailed calculations of net alkalinity (Figures 3 and 4) and the interpretation of the changes have a certain generality. The net alkalinity changes are due to the solid phase buffering reactions only and not aqueous phase reactions. The buffereing reactions are responding to the precipitation of sulfide by decreasing alkalinity and to the production of carbon dioxide by increasing alkalinity after the depletion of sulfate. It is expected that the decline is accentuated and the increase is somewhat mitigated by species dependent transport effects.

DISSOLVED GASES AND GAS PHASE TRANSPORT

After the depletion of sulfate, methane forms and if the sum of the partial pressures of the dissolved gases exceed the total static pressure at that depth bubbles will form (Reeburgh 1969). The calculation presented below is designed to reproduce this behavior and to examine the consequences of various gas phase transport mechanisms on the distribution of dissolved nitrogen, argon, and methane.

As in the case of sulfate reduction the processes by which methane is formed are bacterial. The basic features of the reaction in sediments is that methane is produced only if sulfate is essentially absent and it is consumed within the zone of sulfate reduction (Martens and Berner 1977; Reeburgh and Heggie 1977). This is precisely the behavior predicted by thermodynamic equilibria calculations. In order to assign these reactions to the fast reaction set it is necessary that the kinetics be rapid relative to the principal slow reaction: the decomposition of sediment organic matter ($K = 0.005\ yr^{-1}$) and the mass transport time scale ($z^2/2D$ = 200 - 1250 days for z = 10 - 25 cm). No direct evidence exists that the kinetics have the

required time scale so that the results of these calculations and their comparison to observations are indirect evidence.

The observations for Chesapeake Bay sediments come from station 858-C which is at a sounding depth of 30 m (Reeburgh 1967, 1969) for the winter of 1967. The dissolved nitrogen, argon, and methane concentrations are reported for two cores, the total carbon dioxide for one core. The reported chloride concentration and temperature are used to set the solubility of the dissolved gases at a pressure of four atmospheres (Table 1), and the boundary concentration of sulfate. The nitrogen and argon boundary conditions are set at the average of the reported 0-15 cm values in order to mitigate the time variable effects of the seasonal variation of the overlying water concentrations (Martens and Berner 1977). The depth of penetration for seasonal time variable effects in on the order of $\sqrt{2D/\omega}$ = 5.5 cm ($\omega = 2\pi/365$ radians/day) so that the effect should not extend below 10 or 15 cm. Bioturbation effects are probably limited to this depth as well (Martens and Berner 1977).

The purpose of this calculation is to investigate the effects of gas phase transport. Consider the simpliest assumption: that the gas phase is stationary relative to the solid phase and that it is not diffusing. Since in these examples the location of gas phase formation is below 30 cm bioturbation need not be considered in the mixing of the gas phase. The results are shown in Figure (6). The total CO_2 is higher than station 856 which implies a larger decomposition rate. The remaining parameters are as before (Table 4). Increasing the electron to carbon stoichiometry increases the concentration of methane and decreases the concentration of total CO_2 as more of the carbon in being reduced to methane. The availability of more methane causes a larger gas phase which forms closer to the sediment water interface. The dissolved methane profile flattens as the dissolved gas equilibrates with its gas phase partial pressure. The calculated quantity of gas is discussed below.

The computed dissolved nitrogen, argon, and their molar ratio, together with the observations, are shown in Figure 7. The sharper decline of the dissolved nitrogen relative to argon is due to its relative insolubility (Reeburgh 1969). As gases equilibrate with the gas phase, nitrogen preferentially migrates to that phase. An electron to carbon stoichiometry of $\beta = 3$ appears to be consistent with these data. The gas phase is computed to be 85 - 88% CH_4 which seems quite reasonable (Martens 1976).

The most interesting and initially unexpected feature of these profiles is that they are linearly decreasing even within the zone of sulfate reduction where no gas phase is computed to exist. This is a direct consequence of the mass balance requirements and the hypothesized gas phase transport. The stationary gas phase is advecting at the sedimentation velocity which causes a downward flux of nitrogen and argon. This downward flux must be supplied from the sediment-water interface and in the presence of substantail diffusion of the dissolved species a linear gradient is required. Since relatively more nitrogen is advecting with the gas phase its gradient is steeper than that for argon. The nitrogen to argon ratio reflects this effect.

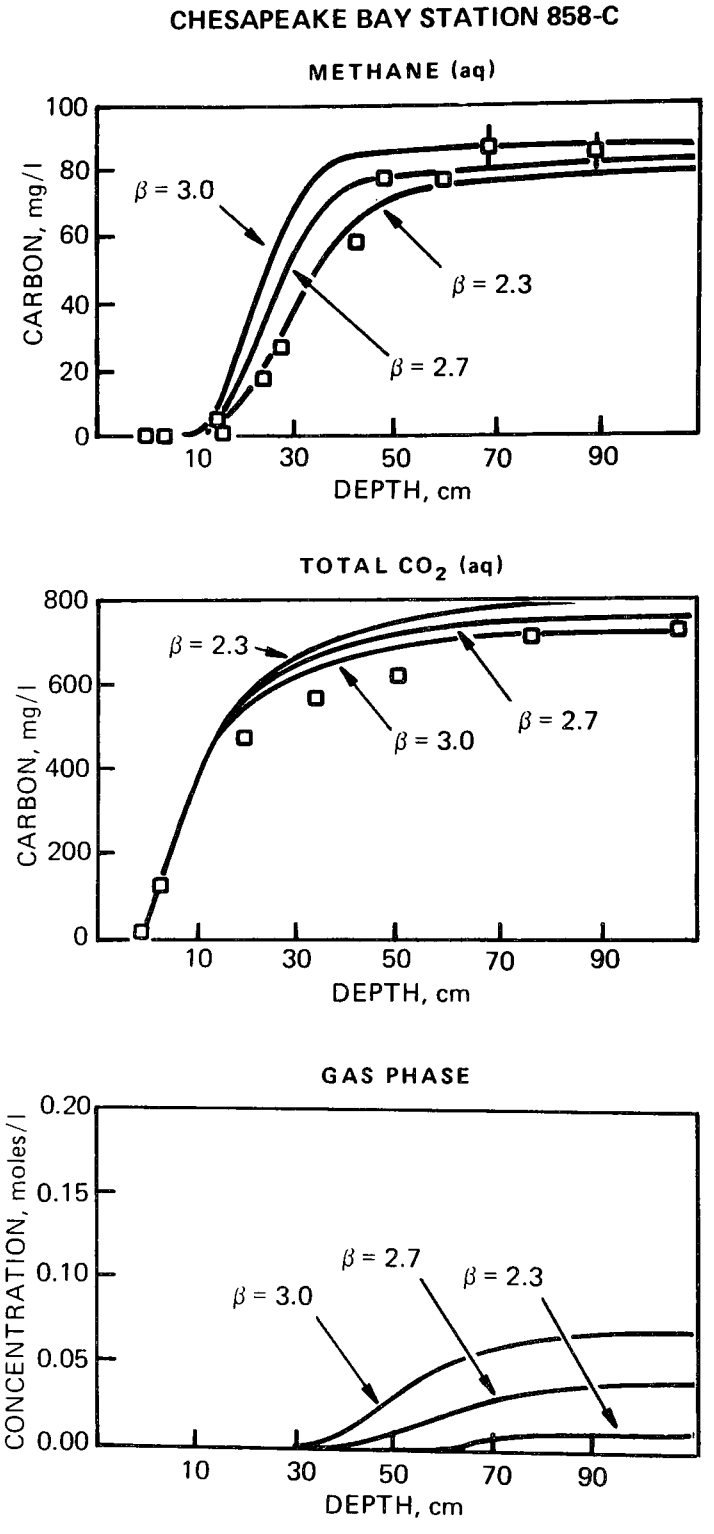

Figure 6. Chesapeake Bay Station 858C: Observed (symbols) and computed (lines) vertical distributions of (a) dissolved methane, mg carbon/l; total aqueous carbon dioxide, mg carbon/l; and total gas phase concentration, moles of gas/l of gas plus aqueous phase volume. Species dependent transport is used for all calculations. The gas phase is assumed to be stationary with respect to the sediment solds and not diffusing. The three cases presented are for increasing β: the carbon to hydrogen ratio of organic sediment matter consumed by the aqueous phase reduction reactions.

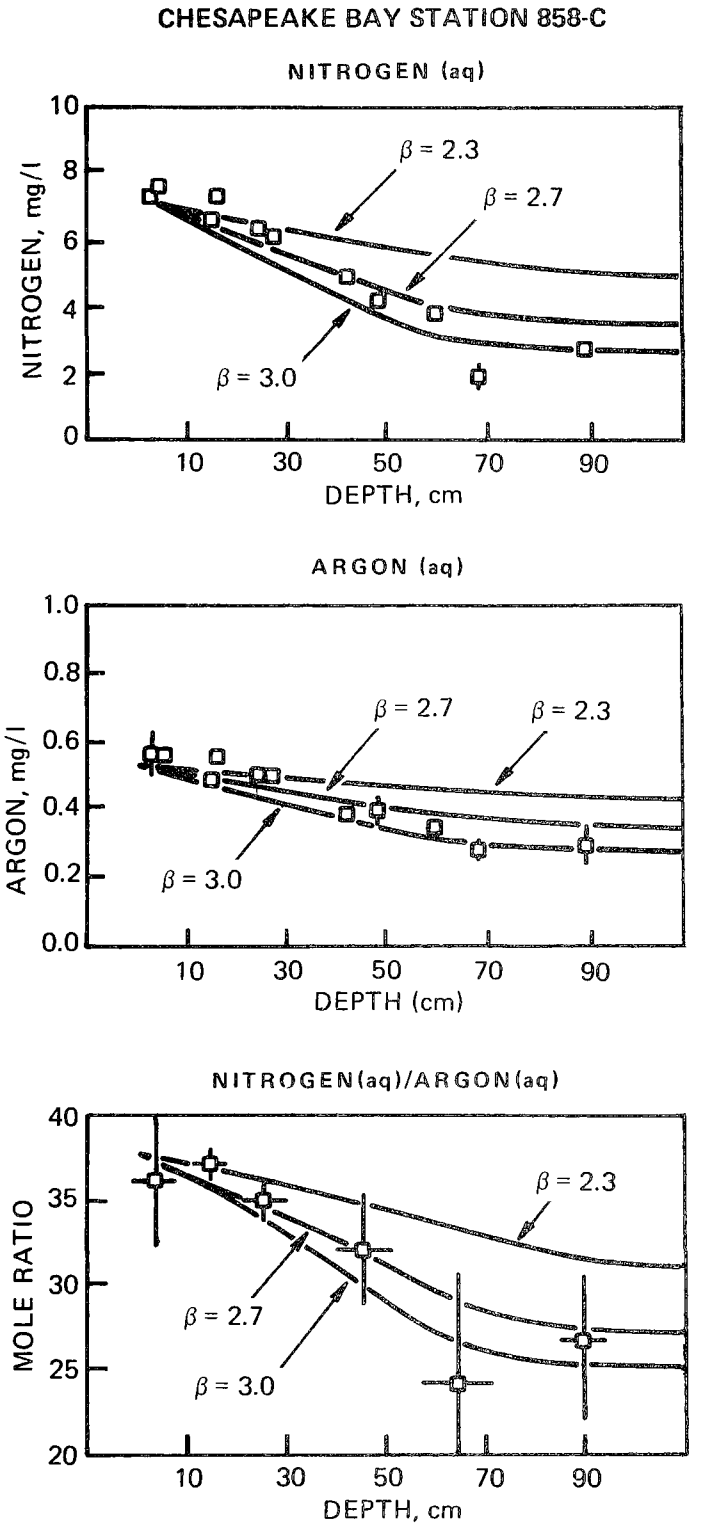

Figure 7. Chesapeake Bay Station 858C: Observed (symbols) and computed (lines) vertical distributions of: (a) Dissolved nitrogen gas, mg nitrogen/l; (b) Dissolved argon, mg argon/l; (c) Their mole ratio. The conditions are as in Figure 6.

The quantity of total gas formed is calculated to range from 10 - 70 mM or 5 - 30% of the total volume at 4 atm. Although gas phase volume was not measured for these sediments, observations by Schubel (1974) suggest that it is on the order of 0.1 to 1.0% of the total volume when it is observed (Table 2). A possibility is that the gas phase migrates to the sediment-water interface via "bubble tubes" as observed by Martens (1977) without any appreciable interaction with the pore waters. This would correspond to a loss of the gas phase that is essentially independent of the transport mechanisms considered in these calculations. The sole effect of the bubble tube transport mechanism would be to decrease the size of the gas phase but not the mole fractions since the removal would be proportional to the gas phase composition. Therefore the computed profiles of the dissolved species would remain unchanged.

A second possibility is that the gas phase has an upward velocity relative to the solid phases and that this velocity is low enough so that the aqueous gas phase equilibria is maintained everywhere. Figure 8 illustrates the computed results for upward velocities of 0.5 and 5.0 cm/yr. As expected (Barnes et al. 1975) there is a peak of nitrogen, argon, and their ratio at the location of the gas phase dissolution. As a consequence there is an increasing gradient from the sediment-water interface to the location of gas phase formation. The mass fluxes of nitrogen and argon associated with this gradient are upward; that is, nitrogen and argon are being supplied to the overlying water. Their source, in this calculation, is the lower boundary of the sediment, which is set at the computed concentrations of the previous stationary gas phase calculations. It is necessary to specify the boundary concentrations at the lower boundary of the sediment only if there is transport from this boundary into the sediment segments within the calculation. For an upward gas phase velocity this situation occurs, but for all previous calculations this boundary is irrelevant. It is evident that the situation depicted in Figure 8 cannot persist indefinitely since eventually the nitrogen and argon at the bottom boundary of the sediment will be depleted. As a consequence, although these peaks in nitrogen, argon, and their ratio are consistent with mass balance, they must be a temporary effect.

Eventually, for a constant upward gas phase velocity, the bottom boundary concentrations will be zero and the computed profiles for this situation are shown in Figure (9) for total CO_2, methane and the gas phase concentration; and in Figure (10) for nitrogen, argon, and their ratio. The upward gas phase velocity is chosen to be 5 cm/yr, which results in gas phase volumes within the reported range (Schubel 1974). The gas phase concentration is highest at the point of formation since the upward gas phase velocity is transporting gas that has been generated by the methane formation to this location. The transport of nitrogen and argon below the depth of gas phase formation is downward via diffusion of the dissolved gases and upward via the gas phase velocity. The net result is essentially a zero gradient of concentration above the depth of gas phase formation.

The consequences of this transport regime is that no flux of gas is computed at the sediment-water interface. If such fluxes are known to occur, this would indicate that the results of the stationary gas phase with rapid

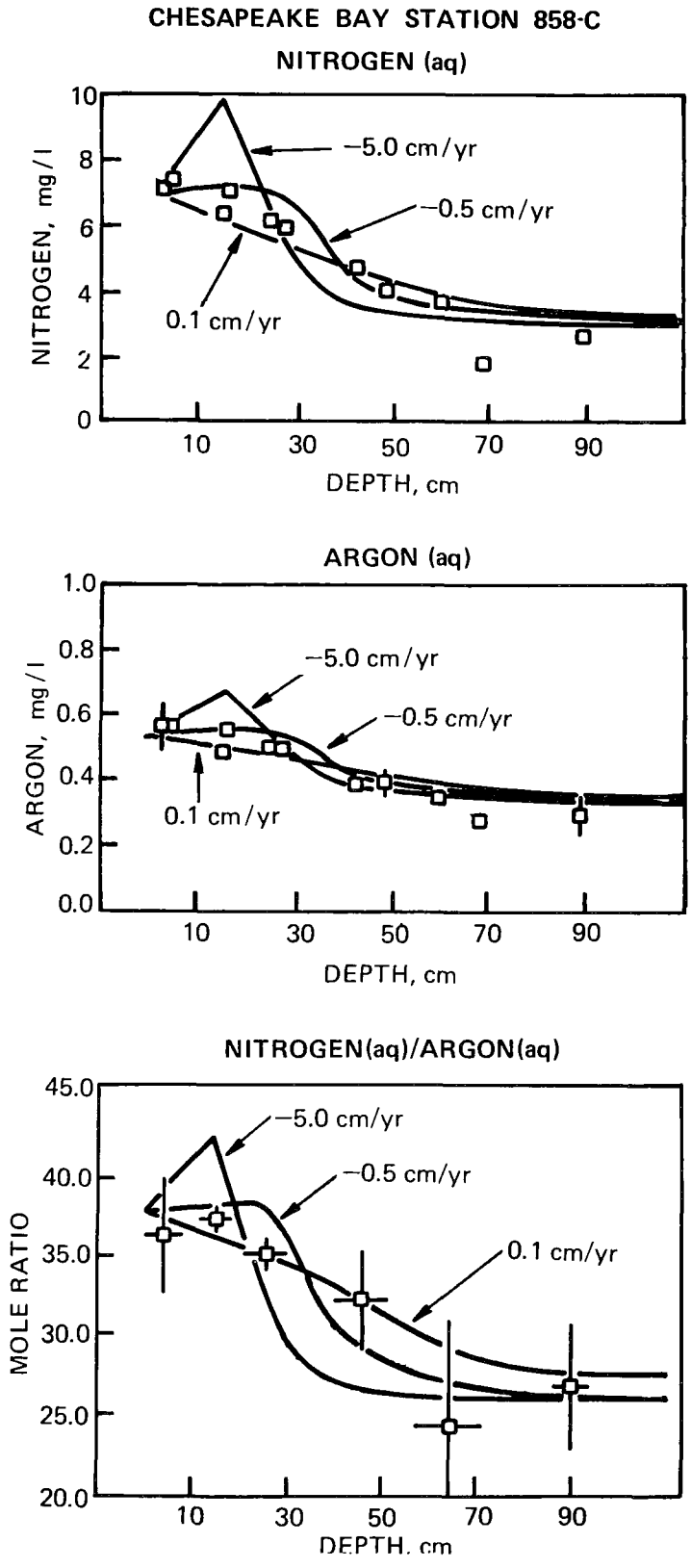

Figure 8. The effect of an upward gas phase velocity. Species dependent transport, no gas phase diffusion, and $\beta = 2.7$ are used in the calculation. The three cases are for a stationary gas phase relative to the sediment solids ($w_{gas} = 0.1$ cm/yr) and two upward gas phase velocities ($w_{gas} = -0.5$ cm/yr and $w_{gas} = -5.0$ cm/yr). All gas phase species have the same velocity. The boundary conditions at the sediment bottom are set to the concentrations computed for the stationary gas phase case in the last computational segment.

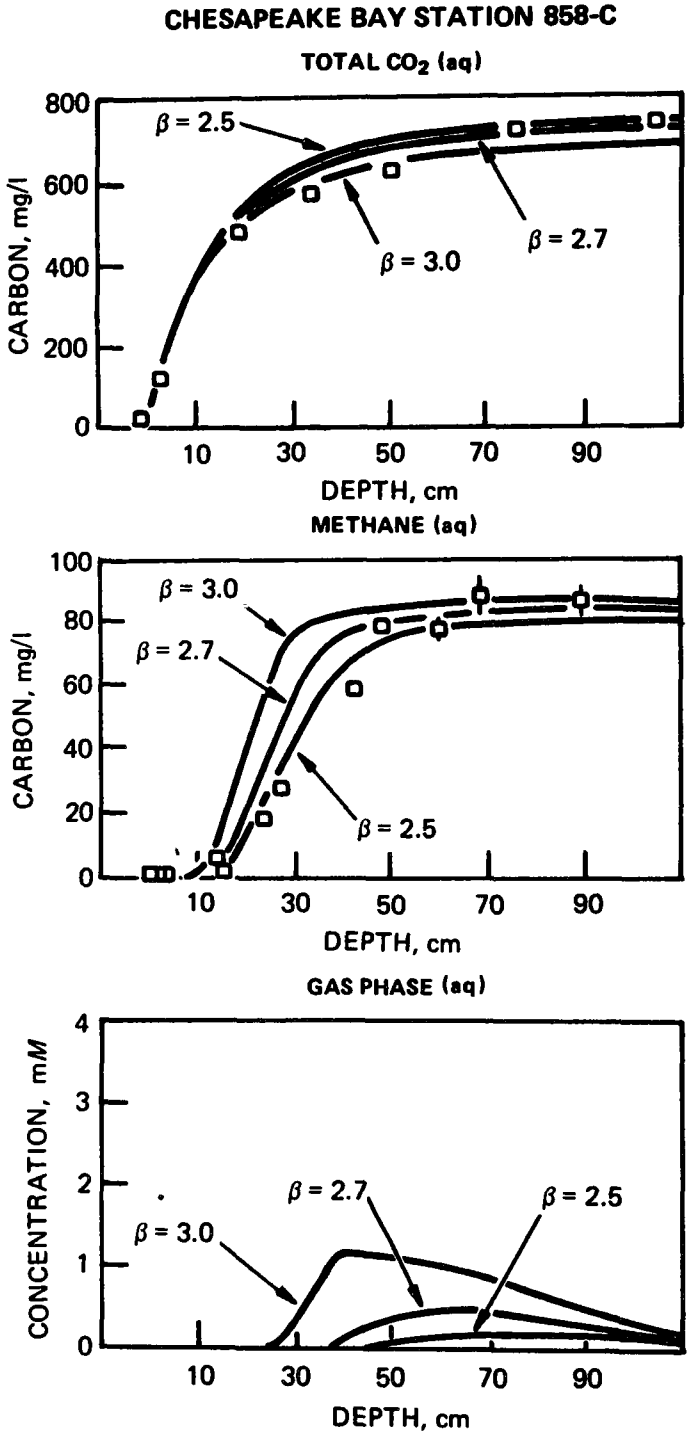

Figure 9. The effect of an upward gas phase velocity with zero lower boundary conditions. Species dependent transport, no gas phase diffusion, and w_{gas} = - 5.0 cm/yr used in the computation. The vertical distribution of observed (symbols) and computed lines: (a) total aqueous carbon dioxide, mg carbon/l; (b) dissolved methane, mg carbon/l; and total total gas phase concentration, millimoles gas/l of gas plus aqueous phase volume. The The three cases correspond to those in Figure 6.

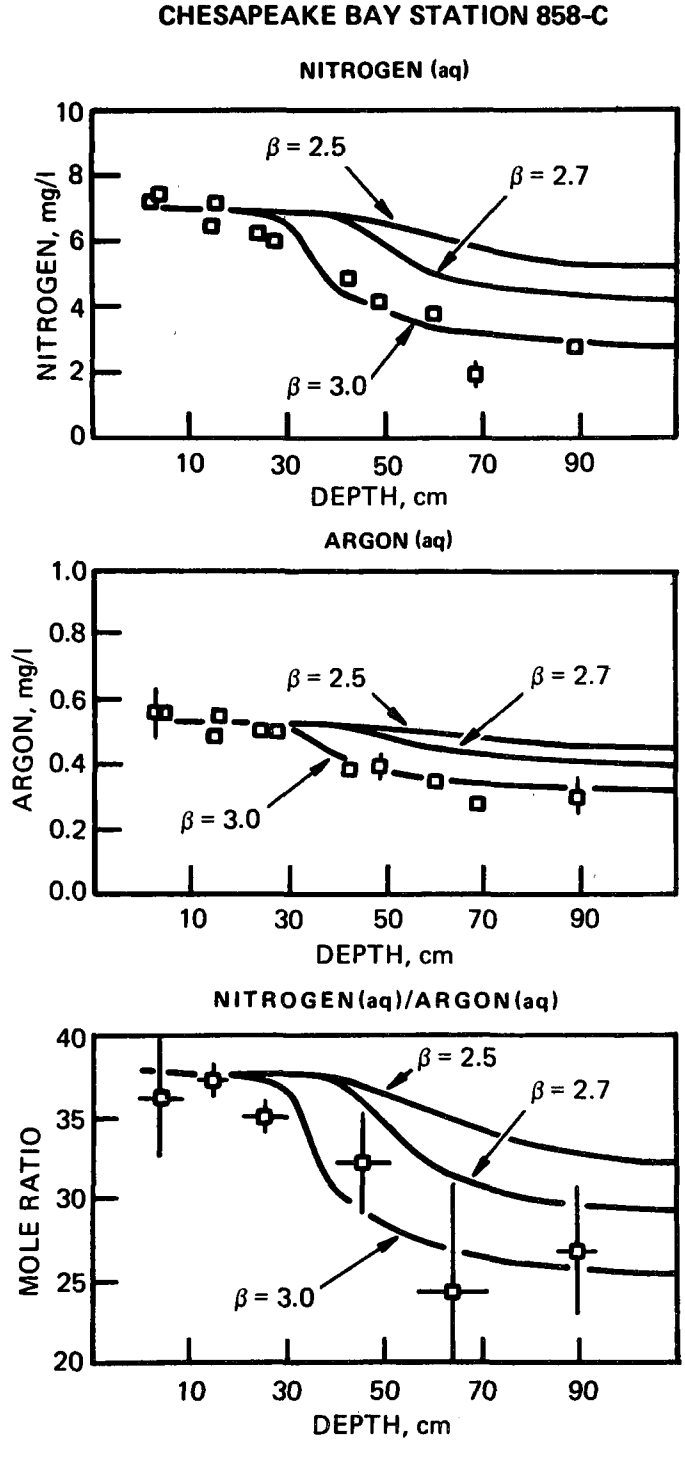

Figure 10. The effect of an upward gas phase velocity with zero lower boundary conditions. Otherwise the computation is as in Figure 9 and the three cases are as in Figure 7.

bubbling would be more realistic. However without seasonal measurements of the gas flux as well as complete interstitial and gas phase measurements, it is not possible to decide if upward velocities with gas phase dissolution does or does not occur at certain periods. The observations of Barnes et al. (1975) suggest that it can occur. But the interstitial water measurements themselves cannot be used to distinguish between the regimes of gas phase transport discussed above.

CONCLUSIONS

The mass balance equations for species dependent transport and fast reactants at equilibrium can be solved using the methods presented above. It appears to be a reasonable approximation to compute the distribution of the species with components C,H,O, and S using the requirements of chemical equilibrium, but not the nitrogen species. The gas phase - aqueous phase reactions at equilibrium correspond to the case of slow gas phase motion.

For species dependent transport the computations reproduce the major features of the observed data as well as the more detailed variations of the carbon to nitrogen ration and the net alkalinity. The use of net alkalinity as a variable that reflects only the effects of the solid phase - aqueous phase reactions and species dependent transport simplifies the interpretation of observed alkalinity variations. The initial decline appears to be due to sulfide precipitation if it is occurring, and the subsequent increase is due to CO_2 production. The net alkalinity change is due to the response of the sediment solid phase - aqueous phase buffering reactions. The computational framework provides the means for examining the relative impact of the various mechanisms that affect net alkalinity and the other species.

The distribution of the dissolved gases is affected by the transport of the resulting gas phase. For the Chesapeake Bay station analyzed, a stationary gas phase is consistent with the dissolved gas observations but not the gas phase volume, which is larger than that observed at other stations. It is possible that the excess gas is vented sporadically via bubble tubes. Alternately a slow upward motion of the gas phase is consistent with the dissolved gas data and the probable gas phase volume but would not account for observations of gas escaping from the sediment-water interface. It is not possible to distinguish between these gas phase transport regimes without simultaneous measurements of dissolved gas concentrations, gas flux and sediment gas volume. For a complete analysis, seasonal data and a time variable computation are necessary.

A completely comprehensive analysis would include the solid phase - aqueous phase reactions explicitly; in particular, the reductions of iron and manganese and the relevant sediment buffering reactions. It is clear from this analysis that a very comprehensive data set is required that includes not only the complete interstitial water chemistry but also a detailed analysis of the sediment solid phases. Both the organic material and the inorganic phases must be characterized. The sediment buffering reactions are central to a detailed understanding of the net alkalinity and

their nature, e.g., precipitation or dissolution of calcium carbonate, clay cation exchanges, authigenic mineral formations, etc., would have to be considered. An analysis within the framework presented above would then clarify their relative importance.

REFERENCES

Atkinson, L.P. and F.A. Richards. 1967. The occurrence and distribution of methane in the marine environment. Deep-Sea Res., 14. pp. 673-684.

Barnes, R.O., K.K. Bertine, and E.D. Goldberg. 1975. N_2: Ar nitrification and denitrification in Southern California borderland basin sediments. Limnol. and Oceanogr. 20. pp. 962-970.

Ben-Yaakov, S. 1972. Diffusion of sea water ions. I. Diffusion of sea water into a dilute solution. Geochim. et. Cosmochim. Acta. 36 p. 1395- 1406.

Ben-Yaakov, S. 1973. Buffering of pore water of recent anoxic marine sediment. Limnol. and Oceanogr. 18(1). pp. 86-94.

Berner, R.A. 1970. Sedimentary pyrite formation. Am. J. Sci. 268. pp. 1-23.

Berner, R.A. 1974. Kinetic models for the early diagenesis of nitrogen, sulfur, phosphorus and silicon in anoxic marine sediments. In The Sea, Vol. 5, E.D. Goldberg (Ed.). J. Wiley and Sons, N.Y. pp. 427-450.

Berner, R.A. 1977. Stoichiometric models for nutrient regeneration in anoxic sediments. Limnol. and Oceanogr. 22(5). pp. 781-786.

Berner, R.A., M.R. Scott and C. Thomlison. 1970. Carbonate alkalinity in the pore water of anoxic marine sediments. Limnol. and Oceanogr. 15. pp. 544-549.

Biggs, R.B. 1963. Deposition and early diagenesis of modern Chesapeake Bay muds. Ph.D. Thesis. Lehigh University, Pa.

Biggs, R.B. 1967. The sediments of Chesapeake Bay. In Estuaries. G.H. Lauff (Ed.). Publ. No. 83. Am. Assoc. Adv. Sci., Washington, D.C. pp. 239-260.

Bordovskiy, O.K. 1965. Accumulation and transformation of organic substances in marine sediments. Mar. Geol. 3. pp. 33-82.

Bray, J. 1973. The behavior of phosphate in the interstitial waters of Chesapeake Bay sediments. Ph.D. Thesis. Johns Hopkins University, Baltimore, MD. pp. 1-149.

Bricker, O.P., G. Matisoff, and G.R. Holdren, Jr. 1977. Interstitial water chemistry of Chesapeake Bay sediments. Dept. of Natural Resources. Maryland Geological Survey. Basic Data Report No. 9. pp. 1-67.

Carpenter, J.H. 1957. A study of some major cations in natural waters. Chesapeake Bay Institute of the Johns Hopkins Univ., Tech. Report XV, 80 p. Quoted by Biggs (1963).

Chapman, T.W. 1967. The transport properties of concentrated electroltic solutions. Ph.D. Thesis. Univ. of Calif., Berkeley (UCRL-17768).

DiToro, D.M. 1976. Combining chemical equilibrium and phytoplankton models - a general methodology. In Modeling Biochemical Processes in Aquatic Ecosystems. R. Canale (Ed.). Ann Arbor Science Press, Ann Arbor, Mich. pp. 233-256.

Gardner, L.R. 1973. Chemical models for sulfate reduction in closed anaerobic marine environments. Geochim. et. Cosmochim. Acta 37.

Garrells, R.M. and C.L. Christ. 1965. Solutions, minerals and equilibrium. Harper, N.Y. 450 p.

Goldberg, E.D. and M. Koide. 1963. Rates of sediment accumulation in the Indian Ocean. In Earth Science and Meteoritics. J. Geiss and E.D. Goldberg (Eds.). North-Holland Pub. Co., Amsterdam. pp. 90-102.

Harvey, H.W. 1966. The chemistry and fertility of sea waters (2nd edition), Cambridge Univ. Press, London. p. 168.

Himmelbau, D. 1964. Diffusion of dissolved gases. Chem. Rev.

Holdren, G.R., Jr., O.P. Bricker, III, and G. Matisoff. 1975. A model for the control of dissolved manganese in the interstitial waters of Chesapeake Bay. In Marine Chemistry in the Coastal Environment. T.M. Church (Ed.). ACS Sym. Ser. 18, Am. Chem. Soc., Washington, D.C. pp. 364-381.

Imoboden, D.M. 1975. Interstitial transport of solutes in non-steady state accumulations and compacting sediments. Earth . Planet . Sci. Letters 27. pp. 221-228, 1975.

Kemp, A.L.W. 1973. Preliminary information on the nature of organic matter in the surface sediments of Lakes Huron, Erie and Ontario. Proc. Symp. on Hydrogeochemistry and Biogerchemistry. E. Ingerson (Ed.). The Clarke Co., Washington, D.C. Vol. II., pp. 40-48.

Kramer, J.R. 1964. Theoretical model of the chemical composition of fresh water with application to the Great Lakes. Pub. No. 11, Great Lakes Research Division, Univ. of Mich. p. 147.

Lerman, A. and H. Taniguchi. 1972. Strontium 90 - diffusional transport in sediments of the Great Lakes. J. Geophic. Res. 77(3). p. 474.

Li Y-H, Gregroy, S. 1974. Diffusion of ions in sea water and deep-sea sediments. Geochim. et Cosmochim. Acta 38. pp. 703-714.

Martens, C.S. 1976. Control of methane sediment-water bubble transport by macroinfaunal irrigation in Cape Lookout Bight, North Carolina. Science 192. pp. 998-1000.

Martens, C.S. and R.A. Berner. 1977. Interstitial water chemistry of anoxic Long Island Sound sediments. I. Dissolved gases. Limnol. and Oceanogr. 22(1). pp. 10-25.

Philp, R.P. and M. Calvin. 1976. Kerogen structures in recently deposited algal mats at Laguna Mormona, Baja, California: A model system for the determination of kerogen structures in ancient sediments. In Environmental Biogeochemistry, vol. 1. J.O. Nriagu (Ed.). Ann Arbor Science, Ann Arbor, Mich. pp. 131-148.

Powers, M.C. 1954. Clay diagenesis in the Chesapeake Bay area: Clays and Clay minerals. Natl. Conf. 2nd Natl. Acad. Sci. Natl. Res. Council Pub. 327. pp. 68-80. Quoted by Biggs, 1963.

Rashid, M.A. and L.H. King. 1970. Major oxygen-containing functional groups present in humic and fulvic acids fractions isolated from contrasting marine environments. Geochim. et. Cosmochim. Acta. 34. pp. 193-201.

Reeburgh, W.S. 1967. Measurements of gases in sediments. Ph.D. Thesis. Johns Hopkins Univ., Baltimore, MD.

Reeburgh, W.S. 1969. Observations of gases in Chesapeake Bay sediments. Limnol. and Oceanogr. p. 368.

Reid, R.C., J.M. Prausnitz and T.K. Sherwood. 1977. The properties of gases and liquids. McGraw Hill, N.Y. p. 576.

Robinson, R.A. and R.H. Stokes. 1959. Electrolyte solutions. Butterworths, London. p. 463.

Rosenfeld, J.K. and R.A. Berner. 1976. Ammonia adsorption in nearshore anoxic sediments. Abstr. Geol. Soc. Am. Annu. Meeting (Denver). p. 1076. Quoted by Berner, 1977.

Schubel, J.R. 1974. Gases bubbles and the acoustically imperetrable of turbid character of some estuarine sediments. In Natural Gases in Marine Sediments. I.R. Kaplan (Ed.). Plenum Press, N.Y. pp. 275-298.

Schubel, J.R. and D.J. Hirschberg. 1977. Pb^{210} - determined sedimentation rate and accumulation of metals in sediments at a station in Chesapeake Bay. Ches. Sci. 18(4), pp. 379-382.

Sholkovitz, E. 1973. Interstitial water chemistry of the Santa Barbara Basin sediments. Geochim. et. Cosmochim. Acta. Vol. 37. pp. 2043-2073.

Stumm, W. 1966. Redox potential as an environmental paramter: Conceptual significance and operational limitation. 3rd Intl. Conf. on Water Pollut. Res. Munich, Germany, Paper No. 13. pp. 283-308.

Stumm, W. and J.J. Morgan. 1970. Aquatic chemistry. J. Wiley, N.Y.

Thorstenson, D.C. 1970. Equilibrium distribution of small organic molecules in natural waters. Geochim. et. Cosmochim. Acta. 34. pp. 745-770.

Trask, P.D. 1939. Organic content of recent marine sediments. In Recent Marine Sediments. P.D. Trask (Ed.). Dover Publications, N.Y., 1968. pp. 428-453.

Wagman, D.D., W.H. Evans, V.B. Parker, I. Halow, Bailey, and R.H. Schumann. 1968. Selected values of chemical thermodynamic properties. NBS Tech. Note 270-3. National Bureau of Standards, Washington, D.C.

Weiller, R.R. 1972. The composition of the interstitial water of sediments in the Central Basin of Lake Erie. Unpublished report. Canada Centre for Inland Waters, Burlington, Ontario, Canada.

Weiss, R.F. 1970. The solubility of nitrogen, oxygen and argon in water and seawater. Deep Sea Research 17. pp. 721-735.

Yamamoto, S., J.B. Alcauskas and T.E. Crozier. 1976. Solubility of methane in distilled water and seawater. J. Chem. Engr. Data 21(1). pp. 78-80.

APPENDIX A

FINITE DIFFERENCE EQUATIONS AND SOLUTION METHOD

Mass Transport Equation:

$$\frac{d}{dz}\left\{\sum_{i=1}^{N_{fs}} w_i\, a_{ik}\, A_i - \sum_{i=1}^{N_{fs}} E_i\, a_{ik}\, \frac{dA_i}{dz}\right\} = \sum_{i=1}^{N_{fs}} a_{ik}\, S_i \qquad k=1,\ldots,N_c \qquad \text{(A1)}$$

where: A_i = i^{th} fast reactant species concentration, $i=1,\ldots,N_{fs}$

S_i = i^{th} species source due to the slow reactants

a_{ik} = stoichiometric coefficient of kth component, B_k, in the ith species

w_i = i^{th} species sedimentation velocity

E_i = i^{th} species diffusion coefficient

z = depth, positive downward.

Finite Difference Equation: For modes located at $z^1, z^2,\ldots,z^{N+2}$ with spacing $h^n = z^{n+1} - z^n$:

$$\sum_{i=1}^{N_{fs}} \left\{ a_{ik}\, c_i^{n+1}\, A_i^{n+1} + a_{ik}\, d_i^n\, A_i^n + a_{ik}\, e_i^{n-1}\, A_i^{n-1} \right\} - s_k^n = 0 \qquad \text{(A2)}$$

$$k = 1,\ldots,N_c$$

$$n = 2,\ldots,N+1$$

where: $c_i^{n+1} = \beta^{n+\frac{1}{2}}\, w_i^{n+\frac{1}{2}} + E^{n+\frac{1}{2}}/h^n$

$$d_i^n = \frac{E_i^{n+\frac{1}{2}}}{h^n} + \frac{E_i^{n-\frac{1}{2}}}{h^{n-1}} + \alpha_i^{n+\frac{1}{2}}\, w_i^{n+\frac{1}{2}} - \beta_i^{n-\frac{1}{2}}\, w_i^{n-\frac{1}{2}}$$

$$e_i^{n-1} = -\alpha_i^{n-\frac{1}{2}} w_i^{n-\frac{1}{2}} - E_i^{n-\frac{1}{2}}/h^{n-1}$$

$$s_k^n = \sum_{i=1}^{N_{fs}} a_{ik} S_i^n (h^{n-1} + h^n)/2$$

$\alpha_i^{n+\frac{1}{2}} = 1 - \beta_i^{n+\frac{1}{2}}$, the finite difference weights for the velocity

$w_i^{n+\frac{1}{2}}$, $E_i^{n+\frac{1}{2}}$, the velocity and diffusion evaluated at the midpoint between z^n and z^{n+1}.

<u>Perturbation Equation</u>: For estimates B_j^n, $j=1,\cdots,N_c$; $n=2,\cdots,N+1$, at the N interior nodes and the boundary conditions at n=1 and n=N+2, evaluate equation (A2) yielding the errors ε_k^n. To compute correction δB_j^n, to the estimates B_j^n, solve:

$$\sum_{j=1}^{N_c} \left\{ \delta B_j^{n+1} \sum_{i=1}^{N_{fs}} a_{ik}\, c_i^{n+1}\, J_{ij}^{n+1} + \delta B_j \sum_{i=1}^{N_{fs}} a_{ik}\, d_i^n\, J_{ij}^n + \delta B_j^{n-1} \sum_{i=1}^{N_{fs}} a_{ik}\, e_i^{n-1}\, J_{ij}^{n-1} \right\} = \varepsilon_k^n \qquad \begin{matrix} k=1,\ldots,N_c \\ n=2,\ldots,N+1 \end{matrix} \tag{A3}$$

where the Jacobian is:

$$J_{ij}^n = \frac{\partial A_i^n}{\partial B_j^n} \tag{A4}$$

<u>Initial Estimate</u>: Let $B_j^n = 0$, $j=1, \quad ,N_c$; $n=2,\ldots,N+1$. Then assuming species independent transport ($c_i^n = c^n$, $d_i^n = d^n$, $e_i^n = e^n$) and using the fact that:

$$\sum_{i=1}^{N_{fs}} a_{ik} J_{ij}^{n} \begin{cases} = 0 & k \neq j \\ = 1 & k = j \end{cases} \tag{A5}$$

solve equation (A3) for $B_j^n = - \delta B_j^n$ as the initial estimate.

<u>Newton-Raphson Iteration</u>: Using $B_j^n(\ell)$ as the ℓth approximation, and a_n chemical equilibria calculation to obtain A_i^n implied by the $B_j^n(\ell)$, the residual errors are evaluated using equation (A2). Equation (A3) is solved, using the appropriate Jacobians, to obtain δB_j^n, the corrections. These are used to produce the $(\ell+1)^{th}$ approximation:

$$B_j^n(\ell+1) = B_j^n(\ell) - \rho \delta B_j^n(\ell) \qquad \begin{matrix} j=1,\ldots,N_c \\ n=2,\ldots,N+1 \end{matrix} \tag{A6}$$

where $0 < \rho < 1$ is the relaxation parameter which is chosen small enough to insure convergence and non-negative $B_j^n(\ell)$ for the appropriate components. Convergence achieved when:

$$|\delta B_j^n(\ell)/B_j^n(\ell)| < 10^{-4} \tag{A7}$$

for approximately 0.01% error.

SECTION 7

SIMULATION OF THE DISTRIBUTION OF POLLUTED WATER IN RESERVOIRS FROM CONCENTRATED EMISSIONS

A.V. Karaushev and V.V. Romanovskiy[1]

Perceptible currents may be absent during certain periods of time in areas of lakes and large reservoirs where waste waters have been emitted, thus allowing pollutants to accumulate in the region of the emissions. As a result of turbulence, the polluted water is moved by the surrounding waters. Movement of patches (clouds) of the pollutant occurs both as a result of emissions of new portions of waste waters and due to turbulent diffusion.

The process of diffusion of pollutants can be simulated on the basis of an equation for turbulent diffusion in cylindrical coordinates (Karaushev, 1969). In essence, this equation is written for the case of a concentrated emission, but it can also be used for dispersive emissions of relatively small length scales as a first approximation, especially in the case of an emission into a large, deep reservoir. It is arbitrarily assumed that emission of the entire discharge of waste waters takes place through one central opening located in the center of the coordinates. The equation describes the process of diffusion of a dissolved substance in the plane of the surface of the reservoir; the concentration is assumed to be invariant with respect to angular position.

The method of calculating the diffusion in reservoirs, developed in the State Hydrological Institute (SHI) based on an equation for diffusion in cylindrical coordinates, is reported as a first approach (Karaushev, 1969), and as a more refined approach (Karaushev, 1979). The case of an emission of a non-conservative substance into a reservoir, whose decomposition takes place according to a first order reaction, is considered in the new, refined approach.

The differential equation for turbulent diffusion in cylindrical coordinates for a non-conservative substance is written as follows:

$$D \frac{\partial^2 c}{\partial r^2} + \frac{\beta}{r} \frac{\partial c}{\partial r} + k_H c = \frac{\partial c}{\partial t} . \qquad (1)$$

[1]State Hydrological Institute, Vtoraya liniya, dom 23, 199053 Leningrad, USSR.

Here, as previously, c is the concentration of the pollutant in the water (kg/m^3); t is the time (s); D is the turbulent diffusion coefficient (m^2/s); r denotes the distance from the center (from the source of pollution); alternatively, this is the radius (m) of a circle or sector of pollution limited by an arc coinciding with the isopleth of concentration c; k_H is a coefficient (1/s) which accounts for the non-conservation of the substance; it is assumed that on decomposition of the substance $k_H < 0$, and when the amount of the substance increases due to internal processes in the reservoir, $k_H > 0$. For conserved substance, $k_H=0$, and the third term in the left part of the equation is thus eliminated.

Parameter β is expressed by the equality:

$$\beta = D - \frac{R_{cm}}{\phi H}, \tag{2}$$

where R_{cm} is the discharge of waste waters (m^3/s); H is the mean depth of the reservoir (m) in the area of the discharge and diffusion of the waste waters; ϕ is the angle of distribution of the waste waters from the focal source expressed in radians: $\phi = \pi$ for emission at the shore; $\phi = 2\pi$ for emission at a significant distance from the shore.

The method of finite differences is one of the simplest approaches for applying equation (1) for practical calculations. This method is examined below.

In calculating turbulent diffusion, radius r is transformed into calculated elements (rings or semi-rings) Δr. The ordinal number of element Δr, calculated from the center of the coordinates, is designated by n. The values of Δr, n and r are related by the correlation:

$$r = (n - \tfrac{1}{2})\,\Delta r. \tag{3}$$

Adjacent to the center, the element (where r = 0) has the number n = 1.

Figure 1 shows the calculated grid in sector of the pollutant diffusion zone. The values for the concentration of the pollutant in each section of the grid at a given instant in time $t = t_i$ and at the following instant $t = t_{i+1} = t_i + \Delta t$ are indicated in the figure. For a given instant in time, we have the following values of the concentrations: $C_{i,n-1}$ (in section n-1), $C_{i,n+1}$ (in section n+1). For the following (calculated) interval of time in calculated section n, we have the concentration $C_{i+1,n}$ (see Figure 1).

The calculated equation is written as:

$$C_{i+1,\,n} = \eta\, C_{i,n} + \nu_n\, C_{i,n-1} + M_n\, C_{i,n+1}\,. \tag{4}$$

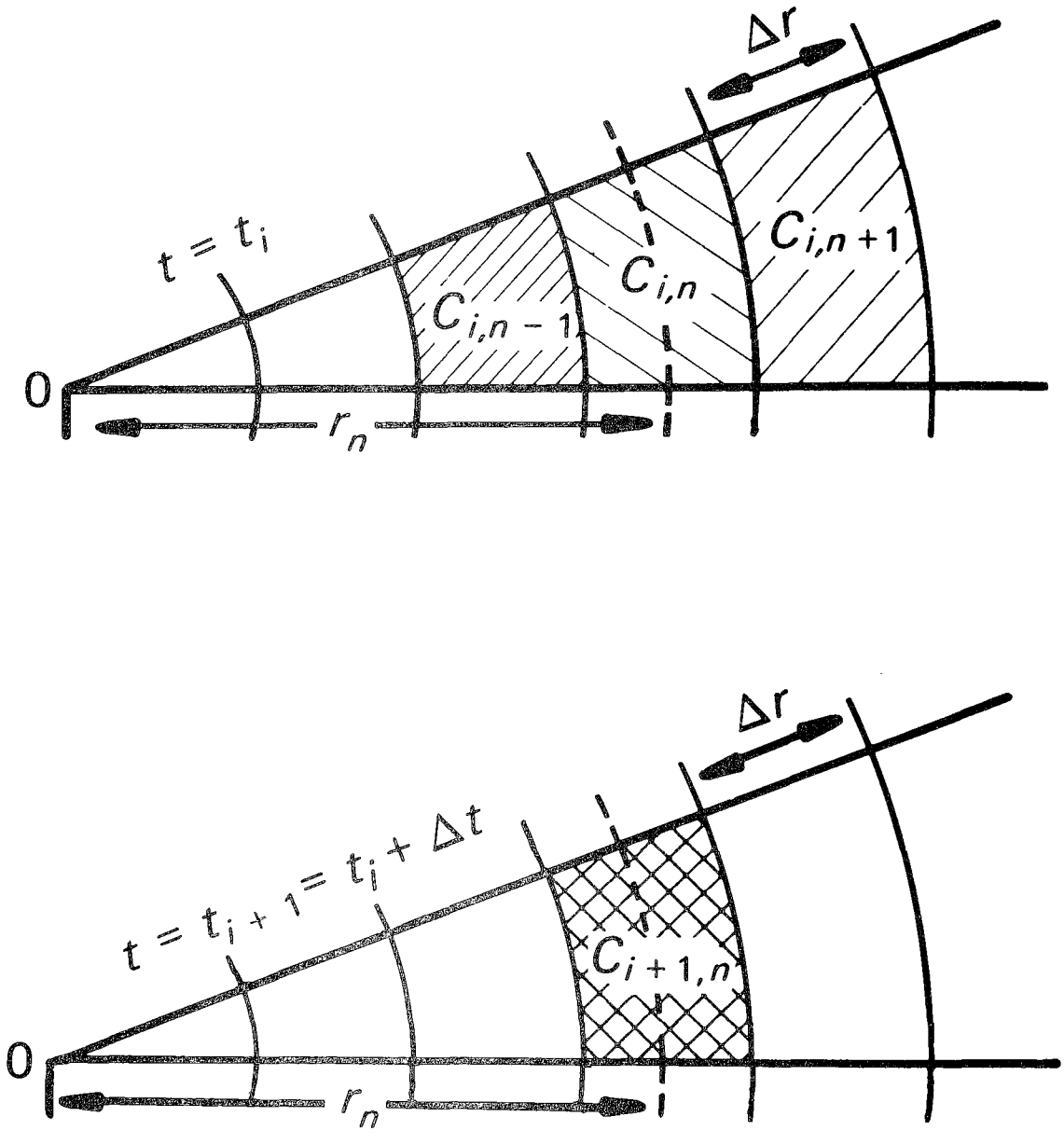

Figure 1. Diagram for calculating the diffusion of pollutants in an aquatic ecosystem.

Coefficients η, ν_n and M_n are first calculated according to the formulas shown below. The first one is a constant, and the other two vary with the length of radius r with respect to the increase in the section number n.

$$\eta = 1 - 2D \frac{\Delta t}{\Delta r^2} + k_H \Delta t, \tag{5}$$

$$\nu_n = (D - \frac{\beta}{2n-1}) \frac{\Delta t}{\Delta r^2}, \tag{6}$$

$$M_n = (D + \frac{\beta}{2n-1}) \frac{\Delta t}{\Delta r^2}, \tag{7}$$

Equation (1) describes a non-stationary process of diffusion, developing in time t. The dilution is calculated according to formula (4) with respect to the boundary and initial conditions. The absence of pollution within the limits of the entire calculated area, or some constant for the range of the concentration of the pollutant, e.g., corresponding to the natural (basal) concentration, is used as the initial condition.

It is convenient to express the concentration in excess over the natural concentration level in calculating the pollution. The boundary condition is written for the first section of the calculated grid (i.e., for the first element adjacent to the center) in the form of the following material balance equation:

$$\frac{R_{cm}}{\phi H} (C_{cm} - C_r) = \frac{\Delta r^2}{2} \frac{\partial C}{\partial t} - D(\frac{\partial c}{\partial r})_r \Delta r - \frac{k_H}{2} \Delta r^2 C_1 \tag{8}$$

where C_r and $(\frac{\partial c}{\partial r})_r$ are respectively the values of the concentration and the derivative at distance r from the center of the coordinates; C_1 is the mean concentration in the first calculated section.

The concentration in the first section for each interval of time Δt calculated, including the initial one, is calculated according to the following formula derived from Equation (8):

$$C_{i+1,1} = aC_{cm} + bC_{i,1} + dc_{1,2}, \tag{9}$$

where $C_{i,1}$ and $C_{i,2}$ are respectively the mean values of the concentration in the first and second sections in the interval of time preceding the calculated interval.

The coefficients contained in formula (9) are calculated as follows:

$$a = \frac{2R_{cm}}{\phi H} \frac{\Delta t}{r^2}, \tag{10}$$

$$b = 1 - \frac{R_{cm}}{\phi H} \frac{\Delta t}{\Delta r^2} - 2D \frac{\Delta t}{\Delta r^2} + k_H \Delta t, \tag{11}$$

$$d = 2D \frac{\Delta t}{\Delta r^2} - \frac{R_{cm}}{\phi H} \frac{\Delta t}{\Delta r^2}. \tag{12}$$

Note that as the material decomposes, k_H becomes negative; for this reason, the term containing k_H in formulas (5) and (11) is also negative. When k_H is positive, this term is also positive.

The calculation begins with the fact that the area of possible diffusion of pollutants from the source, which is set at the center of this area, is estimated based on general considerations. Depth H is based on the data from measurements, and the mean coefficient for the turbulent diffusion D for the entire area is calculated. D is calculated according to a formula which best fits the conditions in the reservoir considered. The arguments contained in the formulas for diffusion coefficient D are assumed to be average for the entire area of diffusion of pollutants. The size of the calculated segment of radius Δr is indicated in consideration of the condition:

$$H \leq \Delta r = \frac{1}{m} R_{3,ex}, \tag{13}$$

where m = 20 + 30, and $R_{3,ex}$ is the expected value of the radius of the area of diffusion of polluted water in the reservoir.

The method of calculation examined here has limited applications; it can only be used for those cases where $D \geq -\beta$, which is equivalent to the inequality:

$$R_{cm} \leq 2\phi HD. \tag{14}$$

The calculated time interval is selected according to the condition:

$$\Delta t \quad \frac{\Delta r^2}{2D + \frac{R_{cm}}{\phi H} - k_H \Delta r^2}. \tag{15}$$

All coefficients for the formulas (a, b, d, η, ν_n, M_n) are calculated by assigning fixed values to Δr and Δt, and then forming a table of

these values. Correct calculation of the coefficients is verified according to the conditions:

$$\eta + \nu_n + M_n - k_H \Delta t = 1, \tag{16}$$

$$a + b + d - k_H \Delta t = 1. \tag{17}$$

All coefficients should be calculated with high precision so that the deviations from unity in control formulas (16) and (17) do not exceed 0.001. Condition (16) should be fulfilled for each element n.

The sequence of calculating the field of the concentration is as follows: the concentration in the 1st section is first calculated according to formula (9), then the concentration in the 2nd, 3rd, etc. sections is calculated according to formula (4) up to the end of the area of diffusion of the pollutants obtained by calculation, i.e., up to the section where the calculation will produce C = 0. The next calculated interval is then considered, and the calculations are done in the same order. The area of diffusion of pollutants is increased by one step of Δr for each interval of time. The calculations for the case of diffusion of a conservative substance in the reservoir are done by the same method, taking into consideration the fact that in this case, $k_H = 0$.

The calculation for a conservative substance must be verified based on the substance balance. The mass of the substance, $\pi_{pol,j}$ entering the reservoir through the emission considered for the entire period calculated, $t_j = \sum_{j=1}^{i} \Delta t$, is first calculated.

Calculation of the diffusion allows obtaining the values of the concentration in each nth section. After calculating the volume of each section and multiplying it by the corresponding concentration, the mass of the substance in the elements is found.

In adding the mass of the substance in all elements, the total mass in the zone of diffusion of the substance is determined. It is obvious that the total mass of the substance at time t_j should be equal to $\pi_{pol,j}$.

If the sums do not coincide and errors are found, then the values of the concentration obtained are correspondingly equal to the value of the error. After the appropriate correction is made, the calculation can be continued in the normal order. Monitoring and corrections can be performed repeatedly.

Note that the composition of these values in calculations for non-conservative substances should produce an inequality which expresses the natural processes of the decomposition of the substance due to the physiological or biological processes which take place in the reservoir. In this case, the calculation is not verified by the method examined above.

The calculations are made for the entire period when there are no unidirectional currents capable of carrying the polluted water beyond the limits of the area affected by the emissions, i.e., for periods of calm, or a period of stable ice on the surface water.

REFERENCES

Karaushev, A.V. 1969. River hydraulics. Gidrometeoizdat, Leningrad. 416 p.

Karaushev, A.V. 1979. A model and a calculated solution to the problem of diffusion in reservoirs. Proc. of the VI All-Union Symposium on Contemporary Problems in Self-Purification of Reservoirs and Water Quality Control. Tallin. p. 45-47.

SECTION 8

RESULTS OF A JOINT USA/USSR HYDRODYNAMIC MODELING PROJECT FOR LAKE BAIKAL

John F. Paul[1], Alexandr B. Gorstko[2] and Anton A. Matveyev[3]

INTRODUCTION

The United States of America (U.S.A.) and Union of Soviet Socialist Republic (U.S.S.R.) are confronted with many environmental problems which can affect the health and welfare of their respective societies. Expanding populations and industries, and increasing urbanization and farming have resulted in alterations to the hydrosphere and to changes in loads of waste materials which effect the quality of the environment. The mutual concern for the environment provided the impetus for the U.S.A./U.S.S.R. Agreement on Cooperation in the Field of Environmental Protection signed in 1972.

As part of the Agreement, Project 02.02-12, Protection and Management of Water Quality in Lakes and Estuaries, was initiated. Although the two nations share no common boundaries on any lake or estuary, they do share a common concern for water quality preservation, and the need to understand the physical, chemical, and biological processes that effect and determine water quality. To share scientific knowledge on limnological processes, a joint modeling project was initiated during the exchange visit by Soviet representatives to the U.S.A. in 1976.

In June 1977, Dr. Tudor T. Davies from U.S. Environmental Protection Agency (EPA), Environmental Research Laboratory, Gulf Breeze, Florida, and Dr. John F. Paul and Mr. William L. Richardson from EPA, Large Lakes Research Station, Grosse Ile, Michigan, visited the Institute of Mechanics and Applied Mathematics, Rostov State University, Rostov-on-Don, U.S.S.R. They met with Drs. A.A. Zenin, A.A. Matveyev, A.B. Gorstko and F.A. Surkov. During this visit, the details of the joint modeling project were arranged, and a project report outline prepared. As a first step, it was agreed to

[1]U.S. Environmental Protection Agency, Large Lakes Research Station, Grosse Ile, Michigan 48138, USA.
[2]Institute of Mechanics and Applied Mathematics, Rostov State University, 192/2 Stachky Prospect, 344090 Rostov-on-Don, USSR.
[3]Hydrochemical Institute, 192/3 Stachky Prospect, 344090 Rostov-on-Don, USSR.

compare formulations and results of hydrodynamic and transport models developed by the two groups. The objective was to provide a basis for further verification of lakewide and nearshore hydrodynamic and transport models.

This paper describes the application of a hydrodynamic model, previously developed for and applied to areas of the Great Lakes, to Lake Baikal in the U.S.S.R. The model results are compared to available field and remotely sensed data.

BACKGROUND ON LAKE BAIKAL

The basin of Lake Baikal is located almost centrally in Asia, in a very rugged mountain province in south Siberia, the Baikal Region. The characteristic geomorphological features of the region include medium and high mountain ranges extending over 1500 km in the southwest to northeast direction, and an alternation of ridges and trenches, the largest of which is filled with waters of the lake.

Lake Baikal is the oldest and deepest intracontinental body of water in the world. The formation of the Baikal trench began about 30 million years ago. The watershed area of the lake is 0.54 million km^2, and the area of the lake itself is 31.5 thousand km^2. The length of the lake is 636 km; maximum width, 79 km; minimum width, 25 km; maximum depth, 1620 m; and volume of the water mass, about 23 thousand km^3. The topography of the lake is shown in Figure 1. The trench of Lake Baikal is divided into three basins, of which the middle one is the deepest. It is separated from the southern basin by the Selenga shallows, a delta formed by the lake's largest tributary, the Selenga River. The contribution of the Selenga amounts to about 50% of the total runoff into the lake. Table 1 provides an annual average water balance for the lake (Vikulina and Kashinova 1973).

TABLE 1. ANNUAL AVERAGE WATER BALANCE FOR LAKE BAIKAL DURING THE PERIOD 1901-1970 (km^3/year)

Inflow		Outflow	
Precipitation	9.29	Runoff to Angara River	60.39
Condensation on lake surface	.82	Evaporation	10.77
River inflow	58.75		
Groundwater inflow	2.30		
Total	71.16	Total	71.16

Lake Baikal contains approximately 4/5 of the total surface water reserves of the U.S.S.R. However, the importance of the lake does not end there. During the past approximately 1 million years, when this body of water was formed in its present boundaries, special characteristics were developed: low solute content, high transparency, low temperature, and high saturation with dissolved oxygen.

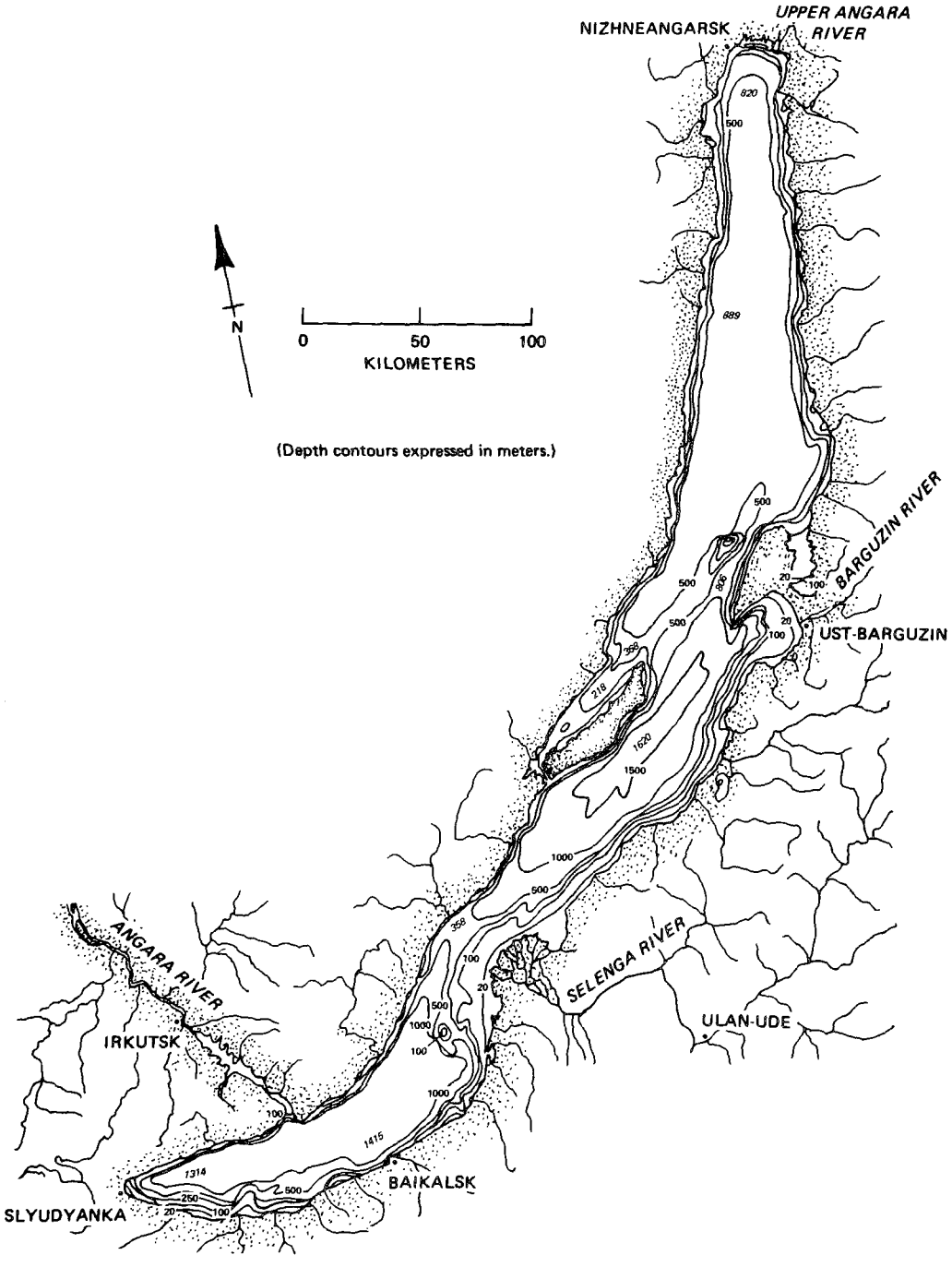

Figure 1. Lake Baikal.

Lake Baikal's ecosystem is distinct and closely balanced. In the course of its evolution, its organisms have adapted to conditions varying little with time, and have reacted very sensitively to changes in these conditions. Indicative of this sensitivity is the fact that organisms of the open deep-water parts of the lake do not dwell in the shallow regions near the Selenga delta, which are subjected to the action of the river runoff.

HYDRODYNAMIC MODEL

This model is composed of two components: the basic hydrodynamic calculation and the transport of dissolved and/or suspended material. Each component will be discussed separately.

Summary of Hydrodynamic Component

The equations for the hydrodynamic component are derived from the time-dependent, three-dimensional equations for conservation of mass, momentum and energy. The principal assumptions used are:

(a) The pressure is assumed to vary hydrostatically.

(b) The rigid-lid approximation is made, i.e., the vertical velocity at the undisturbed water surface is assumed to be zero. This approximation is used to eliminate surface gravity waves and their associated small time scales, greatly increasing the maximum allowable time step in the numerical computations.

(c) Eddy coefficients are used to account for the turbulent diffusion effects. The horizontal coefficients are assumed to be constant, but the vertical coefficients are assumed to be some function of the local dependent variables.

The resulting equations are:

$$\frac{\partial u}{\partial x} + \frac{\partial v}{\partial y} + \frac{\partial w}{\partial z} = 0, \tag{1}$$

$$\frac{\partial u}{\partial t} + \frac{\partial u^2}{\partial x} + \frac{\partial uv}{\partial y} + \frac{\partial uw}{\partial z} + f_o v = -\frac{1}{\rho_o}\frac{\partial P}{\partial x} + \frac{\partial}{\partial x}\left(A_H \frac{\partial u}{\partial x}\right)$$

$$+ \frac{\partial}{\partial y}\left(A_H \frac{\partial u}{\partial y}\right) + \frac{\partial}{\partial z}\left(A_V \frac{\partial u}{\partial z}\right) \tag{2}$$

$$\frac{\partial v}{\partial t} + \frac{\partial uv}{\partial x} + \frac{\partial v^2}{\partial y} + \frac{\partial vw}{\partial z} - f_o u = -\frac{1}{\rho_o}\frac{\partial P}{\partial y} + \frac{\partial}{\partial x}\left(A_H \frac{\partial v}{\partial x}\right)$$

$$+ \frac{\partial}{\partial y} \left(A_H \frac{\partial v}{\partial y}\right) + \frac{\partial}{\partial z} \left(A_V \frac{\partial v}{\partial z}\right) \tag{3}$$

$$\frac{\partial T}{\partial t} + \frac{\partial uT}{\partial x} + \frac{\partial vT}{\partial y} + \frac{\partial wT}{\partial z} = \frac{\partial}{\partial x} \left(B_H \frac{\partial T}{\partial x}\right) + \frac{\partial}{\partial y} \left(B_H \frac{\partial T}{\partial y}\right)$$

$$+ \frac{\partial}{\partial z} \left(B_V \frac{\partial T}{\partial z}\right) \tag{4}$$

$$\frac{1}{\rho} \frac{\partial P}{\partial z} = g \tag{5}$$

$$\rho = f(T), \tag{6}$$

where

x,y	=	horizontal coordinates,
z	=	vertical coordinate,
u,v	=	fluid velocities in x and y directions,
w	=	fluid velocity in z-direction,
t	=	time,
P	=	pressure,
T	=	temperature,
ρ	=	density,
f_0	=	Coriolis parameter,
A_H	=	horizontal eddy viscosity,
A_V	=	vertical eddy viscosity,
ρ_0	=	density at reference conditions,
B_H	=	horizontal eddy conductivity,
B_V	=	vertical eddy conductivity,
g	=	gravitational acceleration, and
$f(T)$	=	equation-of-state.

Before the above equations are put into appropriate finite-difference form, they are transormed by a stretching of the vertical coordinate. With such a transformation, the same number of vertical grid points can be present in the shallow as in the deeper parts of the water body. This ensures that in the shallow areas there is no loss of accuracy in the computations due to lack of vertical resolution. The transformation is:

$$x \leftrightarrow x,$$
$$y \leftrightarrow y,$$
$$\sigma \leftrightarrow z/h(x,y).$$

The boundary conditions used with the equations are the following: the bottom and shore are taken as no-slip, impermeable, no-flux surfaces; inflows or outflows along with appropriate fluxes of heat are specified at rivers; at the water surface, a wind-dependent stress and a specified heat flux are specified. The initial conditions used are either some simple

specification for the variables (e.g., zero) or specification of all variables from some previous calculation.

The equations are put into finite-difference form in both space and time. The spatial discretizing is accomplished by integration of the differential equations about appropriate grid cells. The finite-difference equations are explicit in time, except with respect to the Coriolis terms and the vertical diffusion terms which are written implicitly. This is done to eliminate the small vertical diffusion time step restriction and the instability associated with explicit form of the Coriolis terms.

The equations as written can not be solved directly if the rigid-lid condition is to be satisfied. To develop a solution scheme, an additional equation is derived directly from the other equations and the rigid-lid condition. This equation is derived by vertically summing the two finite-difference equations for the horizontal velocities, then taking the finite-difference analog of the divergence. The rigid-lid condition is used along with the vertically summed continuity and hydrostatic pressure equations. The result is a Poisson-type finite-difference equation in the surface pressure. The surface pressure is the "integration constant" resulting from the vertical summation of the hydrostatic pressure equation. The surface pressure is a function of the horizontal coordinates. This procedure for deriving the Poisson-type equation for the surface pressure, a modification of the SMAC procedure by Amsden and Harlow (1970), is different than previous models which first derived the pressure equation from the differential equation, then discretized it (Paul and Lick 1974, Paul 1976). The distinction between these two procedures is that with the use of the latter, the finite-difference equation that results for the pressure will not necessarily be directly deriveable from the finite-difference forms of the horizontal momentum equations. This is strictly a numerical error associated with approximating the differential equations; however, this error reflects in the inability of the numerical solution to satisfy the rigid-lid condition to an acceptable degree. Even if direct methods are used to solve the finite-difference pressure equation or if an iterative procedure is used with stringent convergence criteria, errors are manifested in the vertical velocity at the rigid lid. These errors are not always small, especially in problems where there is significant differences in depths between the shallow and deep areas of the water body. These errors might not appear to be of much significance in some calculations, but they do create appreciable errors when the resultant velocities are used to calculate dispersion of substances in the body of water. Also, if advantage is taken of the time implicit nature of the vertical diffusion terms (i.e., time steps are large with respect to the explicit vertical diffusion time limit), these errors become large and ultimately make the solutions meaningless. Complete details of this numerical procedure appear in the report by Paul and Lick (1980).

Summary of Dispersion Component

The transport and dispersion of material in the turbulent flow will be described in a manner similar to that used for the transport and turbulent dispersion of heat and momentum. Refer to Sheng (1975) for a summary of this procedure. The concentrations of the material to be dispersed are

treated as continuous on the length scales considered. The concentrations are sufficiently small so that they do not significantly alter the density of the water (the momentum equations can be solved independently), and they function as completely conservative substances in the water column convected with the local fluid velocities. The only exception to the latter condition will be when gravitational settling is important for the material considered. In this situation, the vertical convection of the material is enhanced by a settling velocity. The basic equation used to predict the dispersion of the material is:

$$\frac{\partial C}{\partial t} + \frac{\partial (Cu)}{\partial x} + \frac{\partial (Cv)}{\partial y} + \frac{\partial (Cw)}{\partial z} = \frac{\partial}{\partial x}\left(D_H \frac{\partial C}{\partial x}\right)$$

$$+ \frac{\partial}{\partial y}\left(D_H \frac{\partial C}{\partial y}\right) + \frac{\partial}{\partial z}\left(D_V \frac{\partial C}{\partial z}\right), \qquad (8)$$

C = concentration of material per unit volume,
x,y = horizontal coordinates,
z = vertical coordinate,
t = time,
u,v = particle (or fluid) velocities in the x and y directions,
w = particle velocity (the sum of the fluid velocity and the settling velocity, w_s, of the substance relative to the fluid) in the z direction,
D_H = horizontal eddy diffusivity, and
D_V = vertical eddy diffusivity.

The boundary conditions used are that all surfaces have zero net flux of the material through them except at rivers. In this latter situation, the net flux is either into or out of the water, depending on the flow of the river. The magnitude of the flux depends on the local concentration of the material. The same transformation of the vertical coordinate that is used for the hydrodynamic component is used here. The finite-difference analysis of the equation is similar to that used for the hydrodynamic component. Paul and Patterson (1977) have used this basic dispersion component to calculate the transport of larval fishes in the western basin of Lake Erie.

RESULTS

The parameters used for the application of the hydrodynamic model to Lake Baikal are listed in Table 2. The vertical diffusion is dependent on the local depth, resulting in larger mixing in the deeper sections of the lake. Constant-density calculations were performed for the four main wind directions on the lake; these are listed as Cases 1 through 4 in Table 2. These main wind directions are the same as indicated in the Baikal Atlas (Anonymous 1969). Figure 2, taken from the Baikal Atlas, indicates the relative frequency of the four wind directions during the summer and autumn periods. The water current data with which the calculations are compared is only of a general nature since lakewide currents for specific episodes in

TABLE 2. PARAMETERS FOR LAKE BAIKAL HYDRODYNAMIC MODEL

Grid spacings	15 km y-direction 7.8 km x-direction
Horizontal extents	600 km y-direction 150 km x-direction
Number of grid points	41 y-direction 21 x-direction 8 z-direction
Minimum depth	10 m
Maximum depth	1620 m
Coriolis parameter (53° N)	1.16×10^{-4}/sec
Horizontal eddy viscosity	10^7 cm^2/sec
Vertical eddy viscosity	$3.85\ (1 + 258.7\ \frac{h}{h_o})$ cm^2/sec
Surface wind stress	1 dyne/cm^2
Wind directions:	
Case 1	Southwest
Case 2	Northeast
Case 3	Northwest
Case 4	Southeast
River flows:	
Selenga	9.64×10^8 cm^3/sec
Barguzin	4.10×10^8 cm^3/sec
Upper Angara	5.78×10^8 cm^3/sec
Angara	19.52×10^3 cm^3/sec
Horizontal eddy diffusivity	10^6 cm^2/sec
Vertical eddy diffusivity	$.385\ (1 + 258.7\ \frac{h}{h_o})$ cm^3/sec
Particle settling velocity	10 m/day

where:

h = local depth
h_o = reference depth

FREQUENCY OF FALL WINDS (PERCENT):

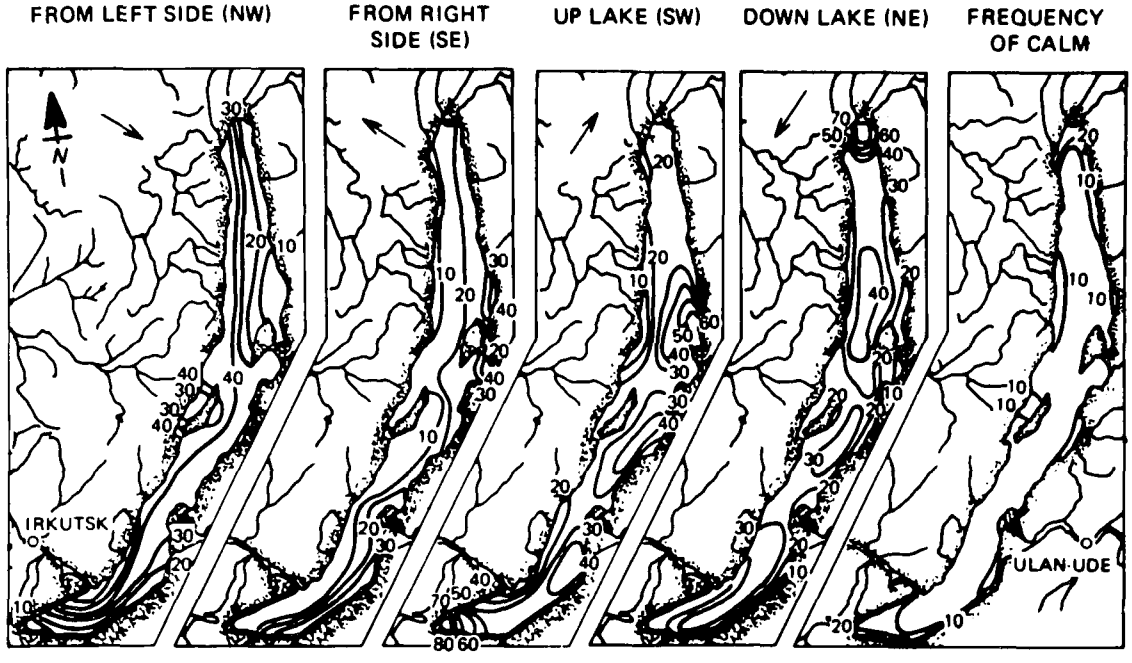

FREQUENCY OF SUMMER WINDS (PERCENT):

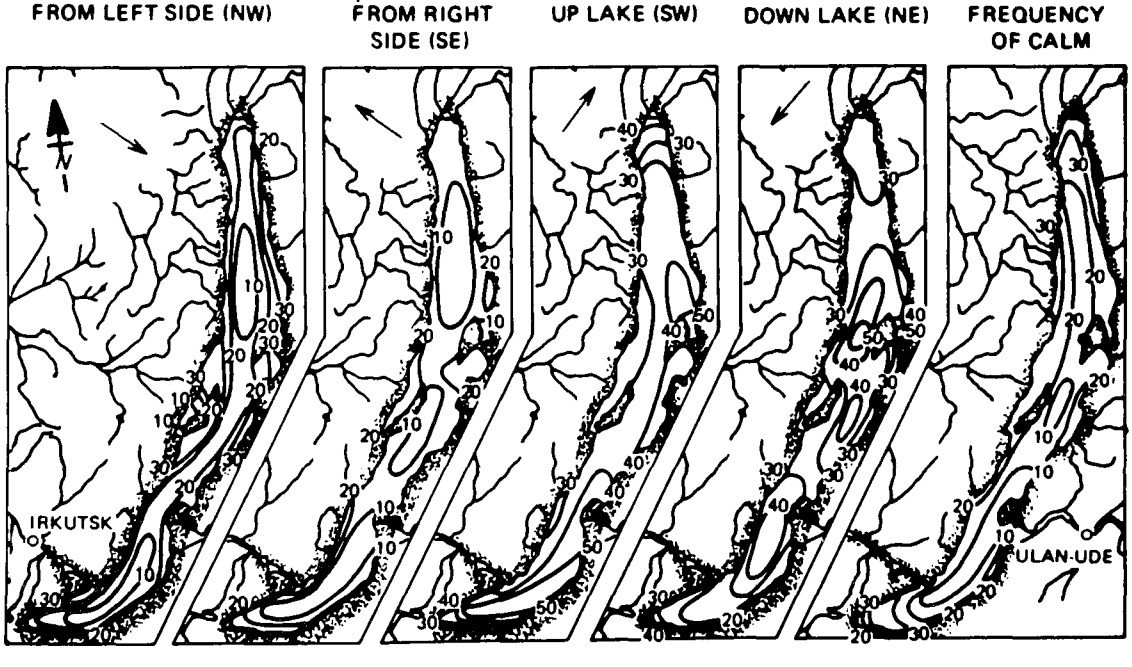

Figure 2. Frequency of winds over Lake Baikal in the summer and autumn.

time were not obtainable during the course of this study. Since an insufficient amount of data was available on the thermal regime for the entire lake, the calculations were performed assuming this aspect to be negligible. The wind direction for Case 1, from the southwest, was also used in a calculation with the northern basin of the lake ice covered. This type of calculation is of interest to assess the significance of the ice cover on the central and southern basins. The northern basin is generally ice covered through the middle of May, and occasionally until the beginning of June (Anonymous 1969).

Detailed results of the hydrodynamic calculations are presented in Paul, Richardson, Gorstko, and Matveyev (1979). Representative results will be discussed here. All of the calculations were performed for 12 days of real time, after which essentially steady-state conditions were obtained. Figures 3 and 4 show the surface velocities and vertically integrated velocities for the southwest wind (Case 1) and the northwest wind (Case 3). For all of the calculations, the results are typical of what might be expected from the simple theory of motion which balances Coriolis force, vertical friction, and horizontal pressure gradients. The deep areas of the lake are generally characterized by geostrophic motion, while the shallower areas are markedly influenced by vertical friction. The magnitude and directions of the surface currents indicate the different balances in the motion as one goes from shallow to deep waters. The general circulation of the lake is composed of the basic circulation in the three basins. Because the northern and southern basins are relatively flat in their long dimension compared with the central basin, the magnitude of the vertically integrated velocities for the southwest wind are smaller in these basins compared to the central basin. This is in agreement with the steady-state solutions obtained for simple basins by Gedney (1971). He solved the equations which balance Coriolis force, pressure gradients, and vertical friction. For constant depth basins, the steady-state vertically integrated velocities are everywhere equal to zero, while for parabolic shaped basins, the vertically integrated velocities form two rotating gyres, with the magnitudes dependent on the degree of the bottom slopes. Thus, the gyres in the calculations for the vertically integrated velocities are functions of the local topography. Differences are apparent for the different wind direction calculations, but this is because the basins are elongated and the topography is highly variable.

Data on surface currents in the Selenga region are shown in Figure 5. Three cases are shown: prevailing southwesterly winds, prevailing northwesterly winds, and steady-lasting northwesterly winds. The first two are separated by only a day, and it is apparent that the currents on the second day show the effects of the previous day's winds. This can be seen by comparing the second and third plot. The currents in the third plot compare quite well with the surface current calculation for the northwesterly wind (Figure 4). The first plot compares reasonably well with the calculation for the southwesterly wind (Figure 3), but discrepancies do exist, apparently a function of the transitory behavior of the currents. The second plot appears to be some combination of the two calculations, as would be expected.

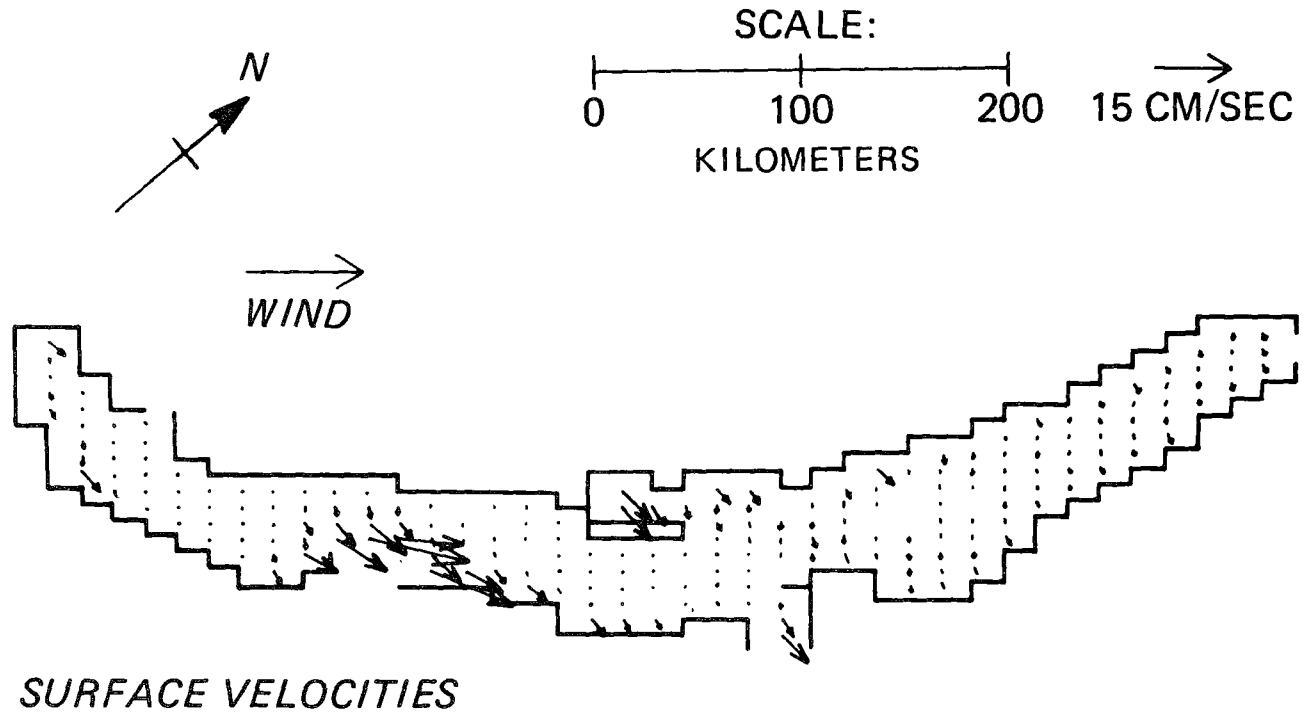

Figure 3a. Hydrodynamic model calculation for Lake Baikal with southwest wind.

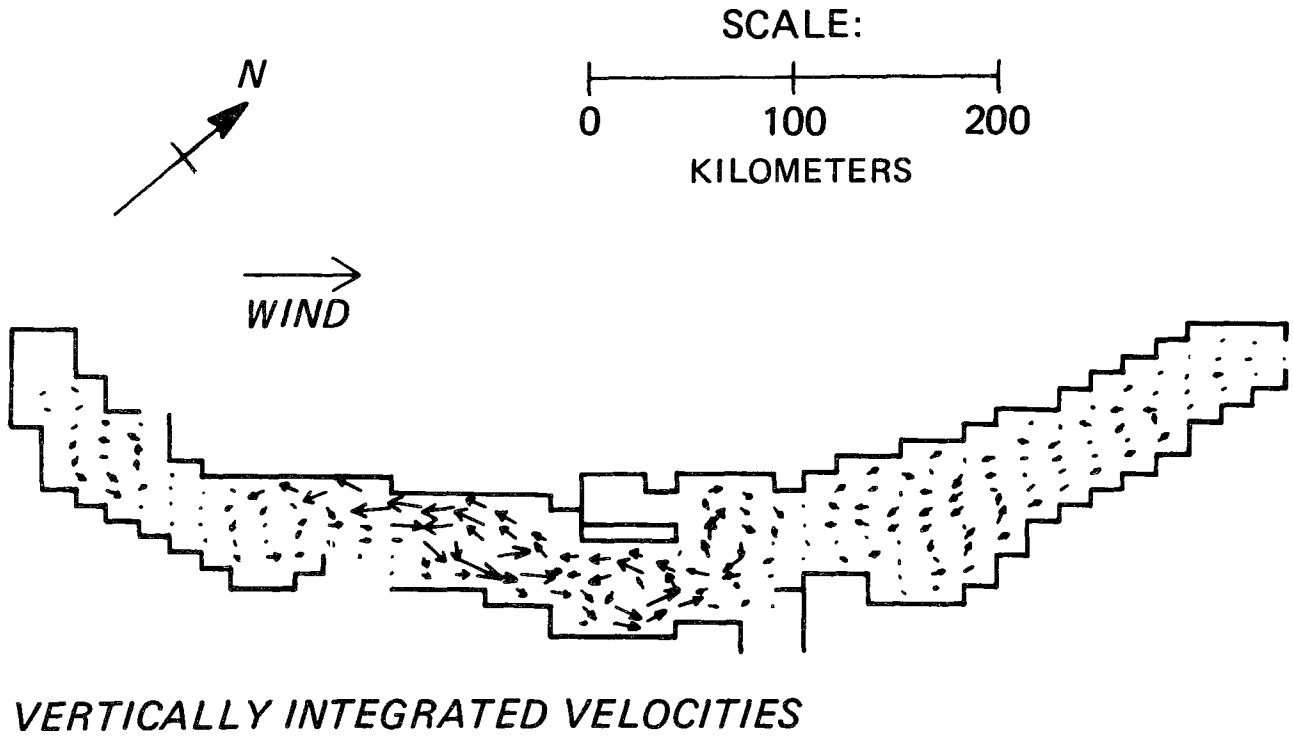

Figure 3b. Hydrodynamic model calucation for Lake Baikal with southwest wind.

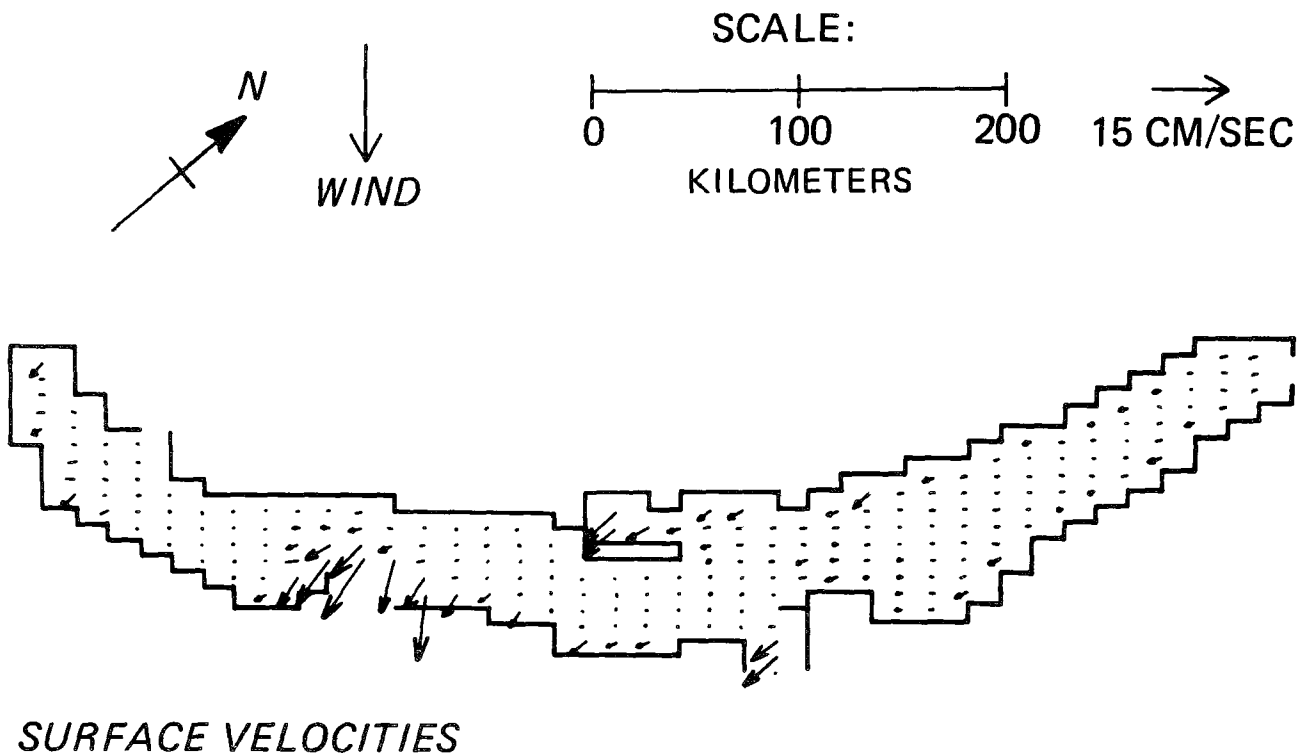

Figure 4a. Hydrodynamic model calculation for Lake Baikal with northwest wind.

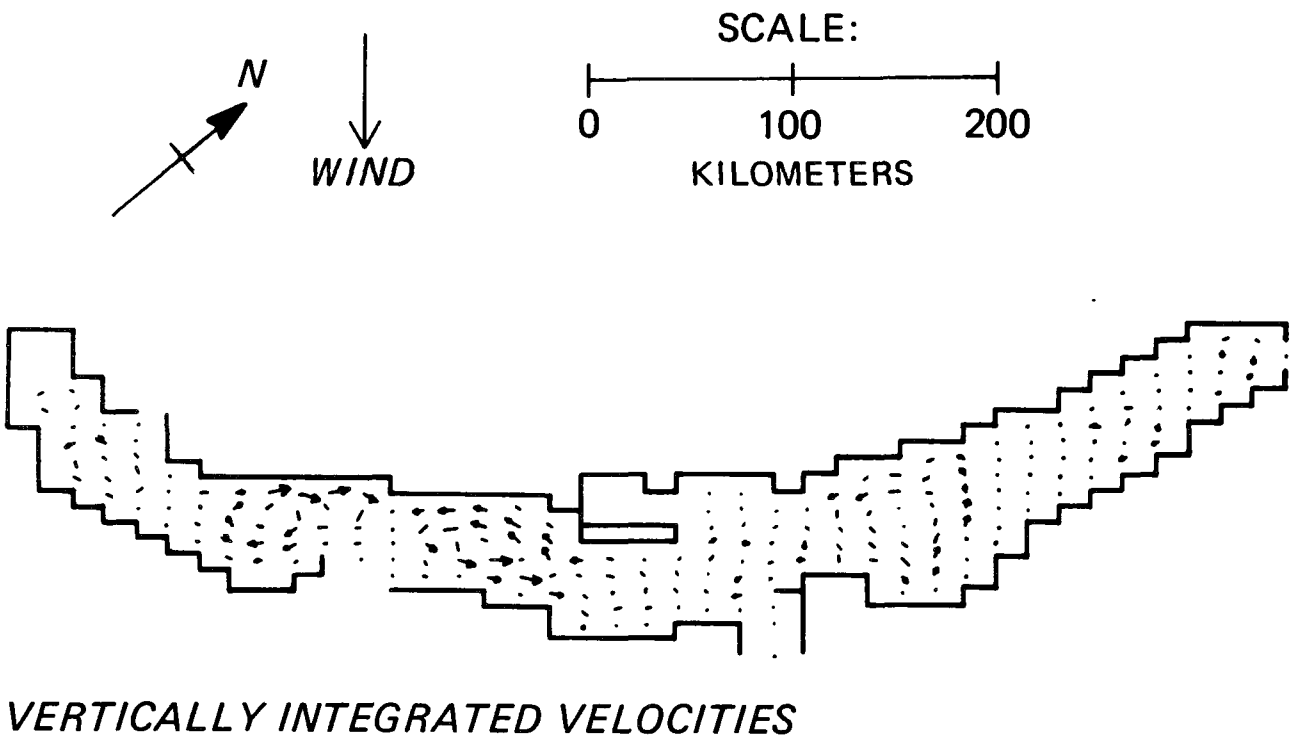

Figure 4b. Hydrodynamic model calculation for Lake Baikal with northwest wind.

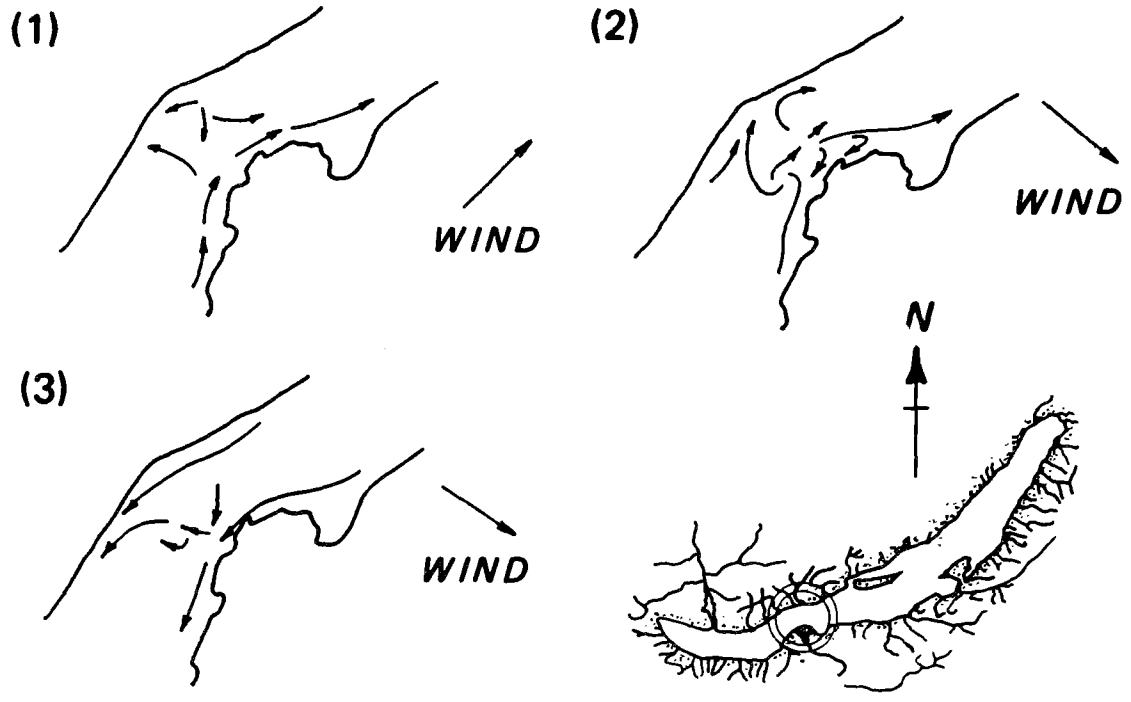

(1) Prevailing southwesterly wind (30 Aug 1972).
(2) Prevailing northwesterly wind (31 Aug 1972).
(3) Steady lasting northwesterly wind (8 Sep 1972).

Figure 5. Observed surface currents in the Selenga River Region of Lake Baikal.

The only data for lake-wide currents is a plot which appears in the Baikal Atlas (Figure 6). This is depicted as representative of the typical currents that exist in the lake. With reference to the wind frequency plot for the lake (Figure 2), it can be seen that for the most part, the winds from the southwest are the most typical. A comparison of the data plot (Figure 6) with the vertically integrated velocities calculated for a southwest wind (Figure 3) indicates a very good agreement. The observed gyres are replicated quite well in the calculation. The data plot does not indicate magnitude of the currents so no comparisons can be made on this aspect.

Using the steady-state currents that were calculated, the transport and dispersion of material in the lake were calculated. A series of 8 calculations were performed: for each of the four main wind directions, for material which is neutrally buoyant and for material which has a gravitational settling velocity of 10 meters per day. This settling velocity corresponds with the mean Stokes settling velocity for the predominant particle sizes observed in the suspended material in the Selenga River runoff. The two calculations for each current pattern indicate the difference in distributions that can be achieved when one considers dissolved material (neutrally buoyant) and suspended material (positive settling velocity). The parameters used for the calculations are listed in Table 2. The calculations were performed for 28 days of real time for each circumstance. Material was entered continuously during the calculation through the Selenga, Barguzin and Upper Angara Rivers. The material concentration in each river was set equal to 1.0. Since the transport equations are linear in the material concentration, the actual concentration level is not important in the calculation. The results for all the calculations are presented in Paul, Richardson, Gorstko, and Matveyev (1979). Representative results will be discussed here. Figure 7 indicates surface and bottom concentrations with a southwest wind for both neutrally buoyant and suspended material. The effect of the settling velocity on the concentration distributions is important. The main reason for this is that the currents over the water column are, in general, going in different directions. If the material remains essentially uniform over the water column (i.e., for the neutrally buoyant material), then the material is primarily transported by the currents over the upper portion of the water column. These are the currents which have the larger magnitude. When gravitational settling is introduced, the material tends to concentrate near the bottom, and thus, is transported horizontally by the currents that are near the bottom. Since these currents are in generally in a different direction than the near surface currents, the concentration distribution appears different.

The data that is available for comparison with the calculations are shown in Figure 8. These data are taken from the Hydromet cruise in the Selenga River Region of the lake on 28-29 May 1976. The plots are for PO_4^{-3} (a dissolved substance) and total suspended solids. The winds over the region were highly variable during the cruise, ranging from southwest to southeast during the first part of the cruise, and to northeast during the final part of the cruise. A reasonable comparison can be made with the calculations for the southwest wind (Figure 7). The currents in the vicinity of the Selenga delta are easterly near the surface and over the most of the vertical column near the river area of the lake. As one goes away from the

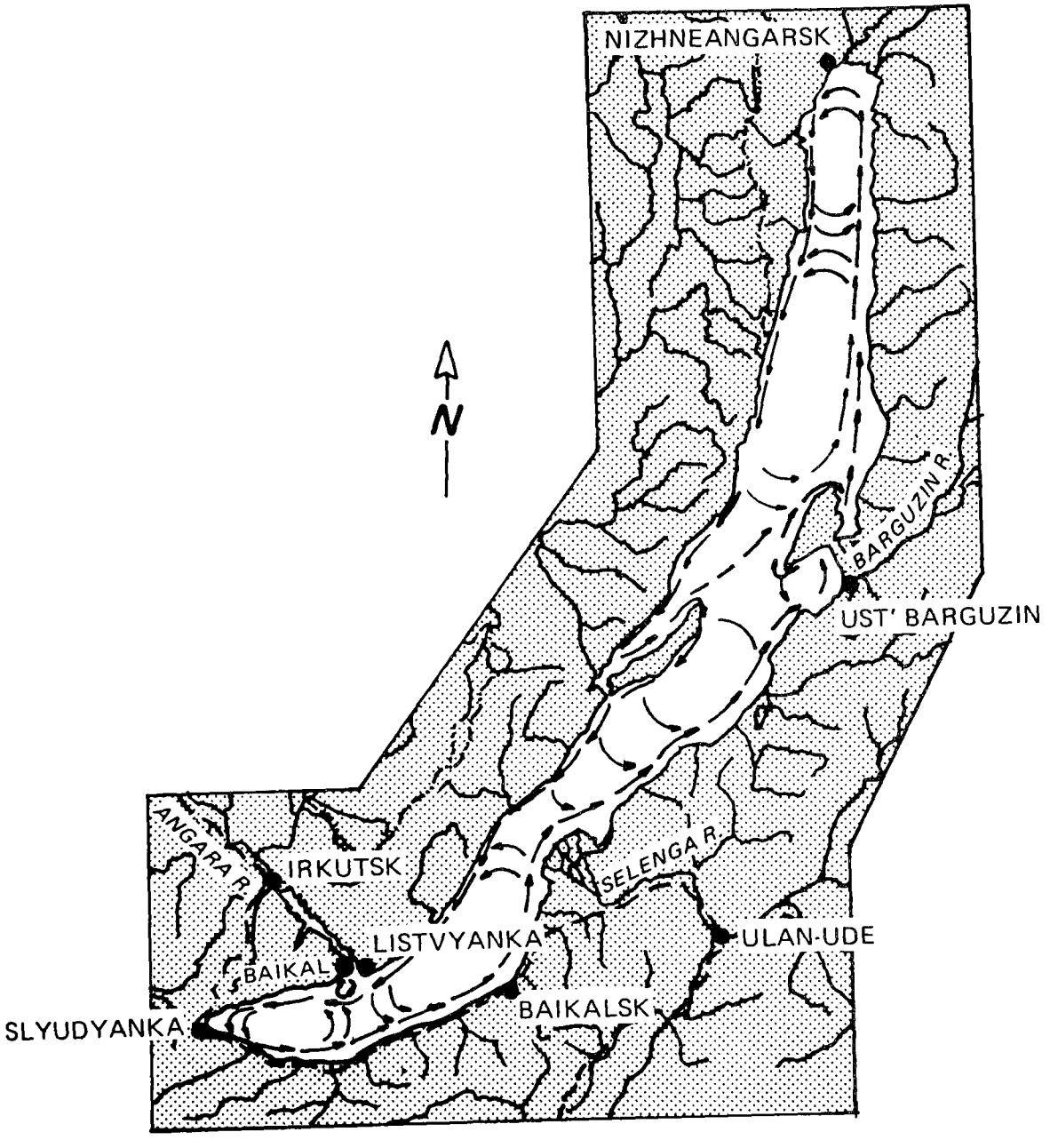

Figure 6. Lake Baikal whole lake dominant currents.

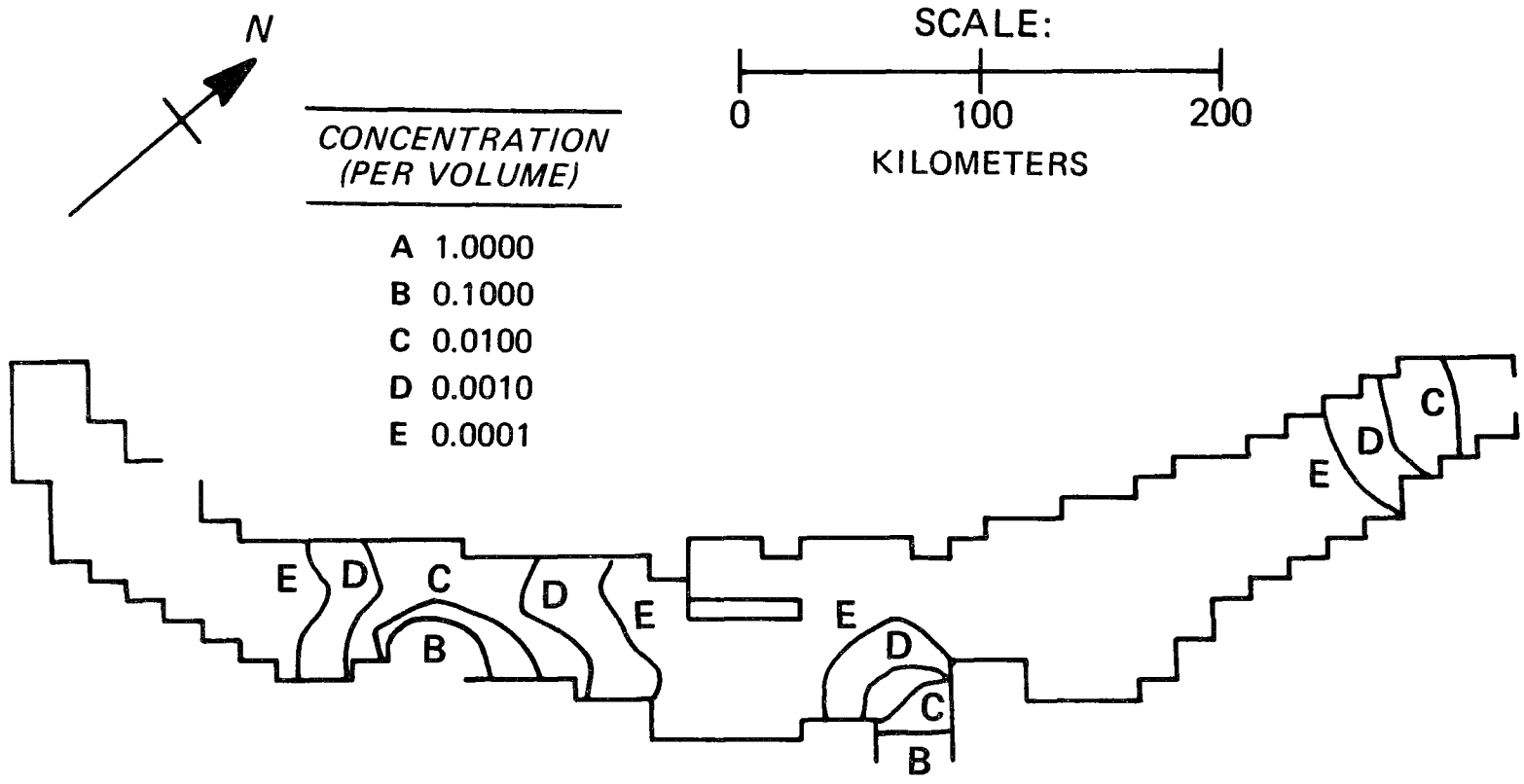

Figure 7a. Dispersion model calculation for Lake Baikal with southwest wind.

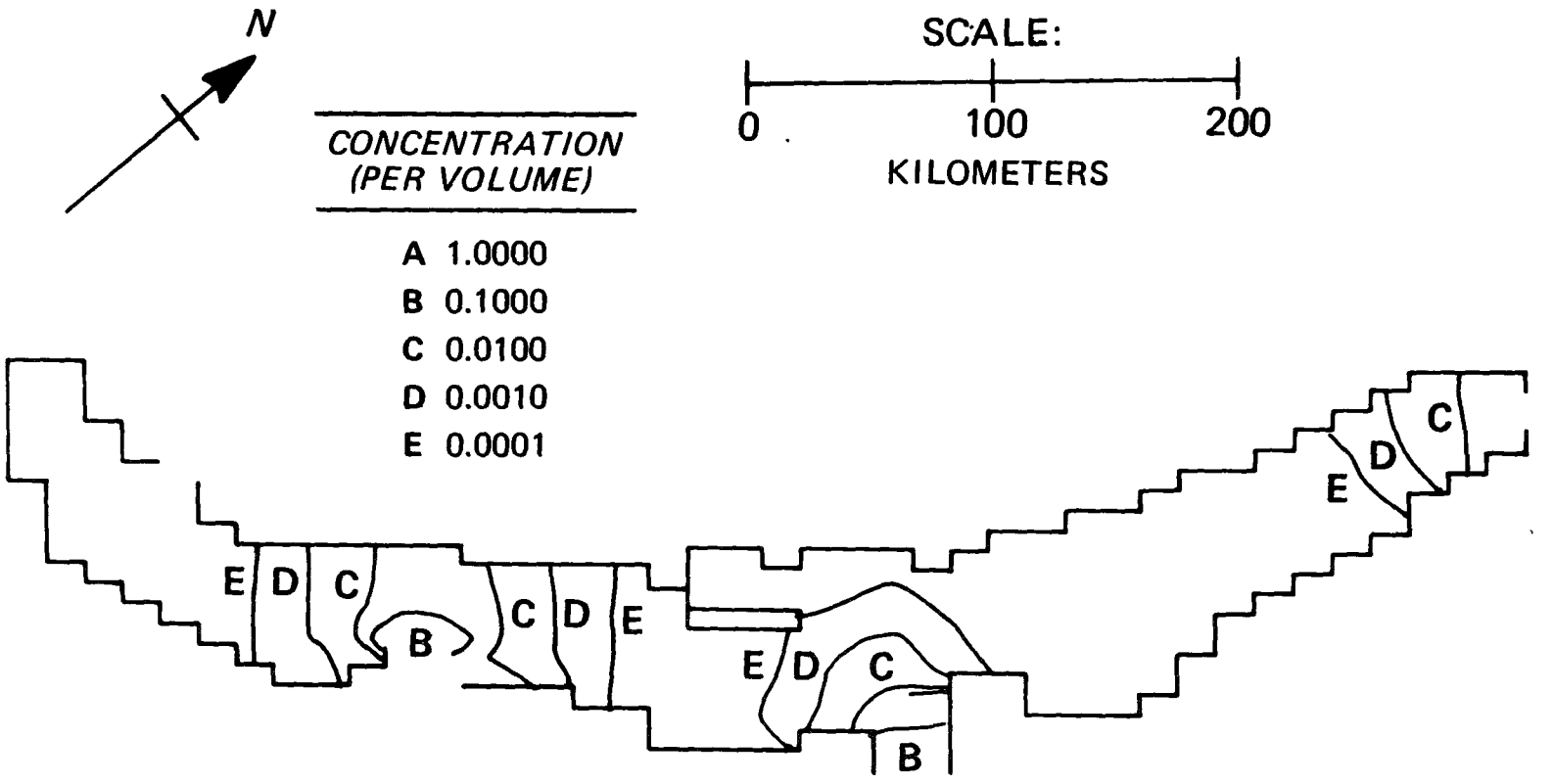

BOTTOM CONCENTRATIONS (NO SETTLING VELOCITY)

Figure 7b. Dispersion model calculation for Lake Baikal with southwest wind.

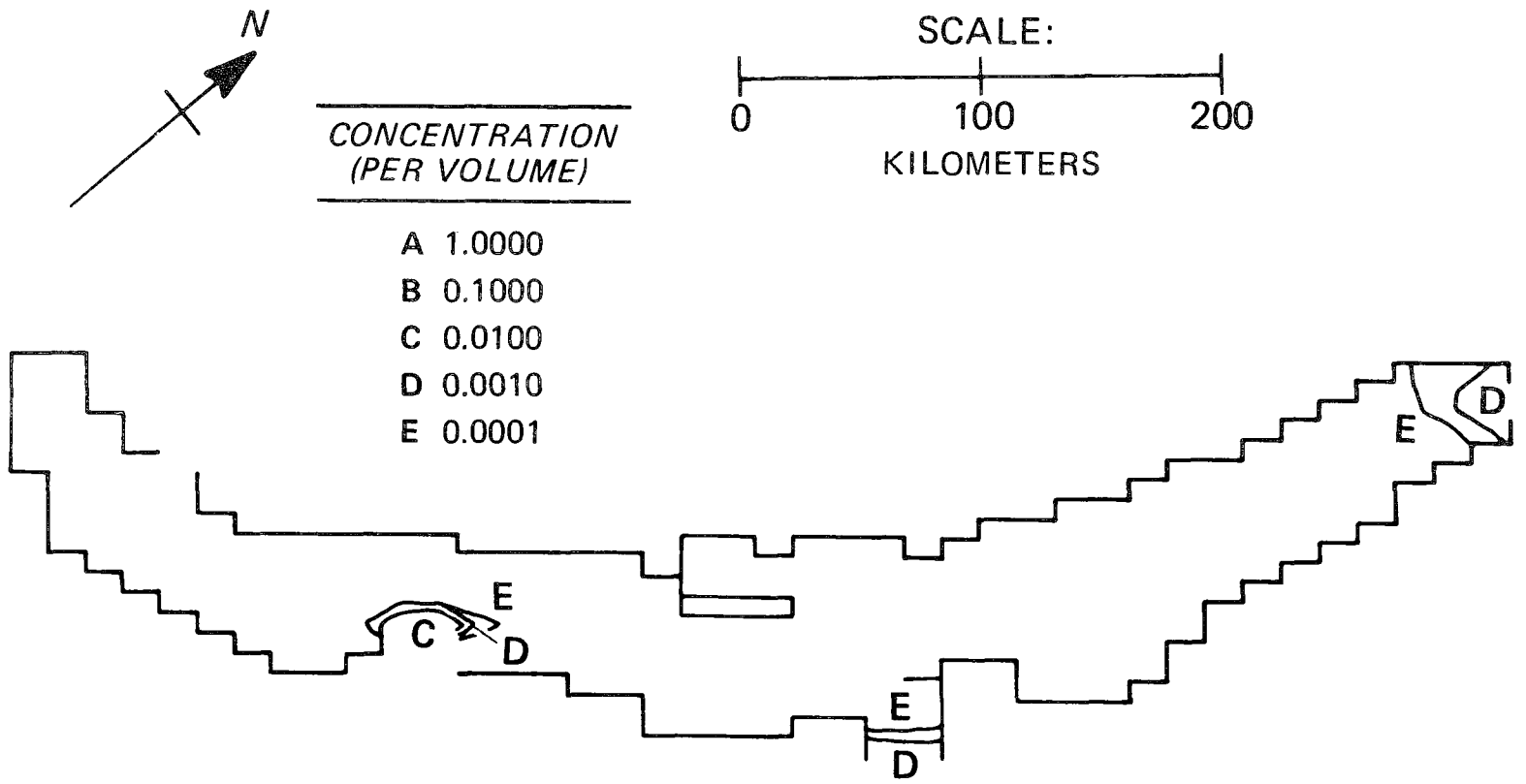

SURFACE CONCENTRATIONS (SETTLING VELOCITY, 10 m/day)

Figure 7c. Dispersion model calculation for Lake Baikal with southwest wind.

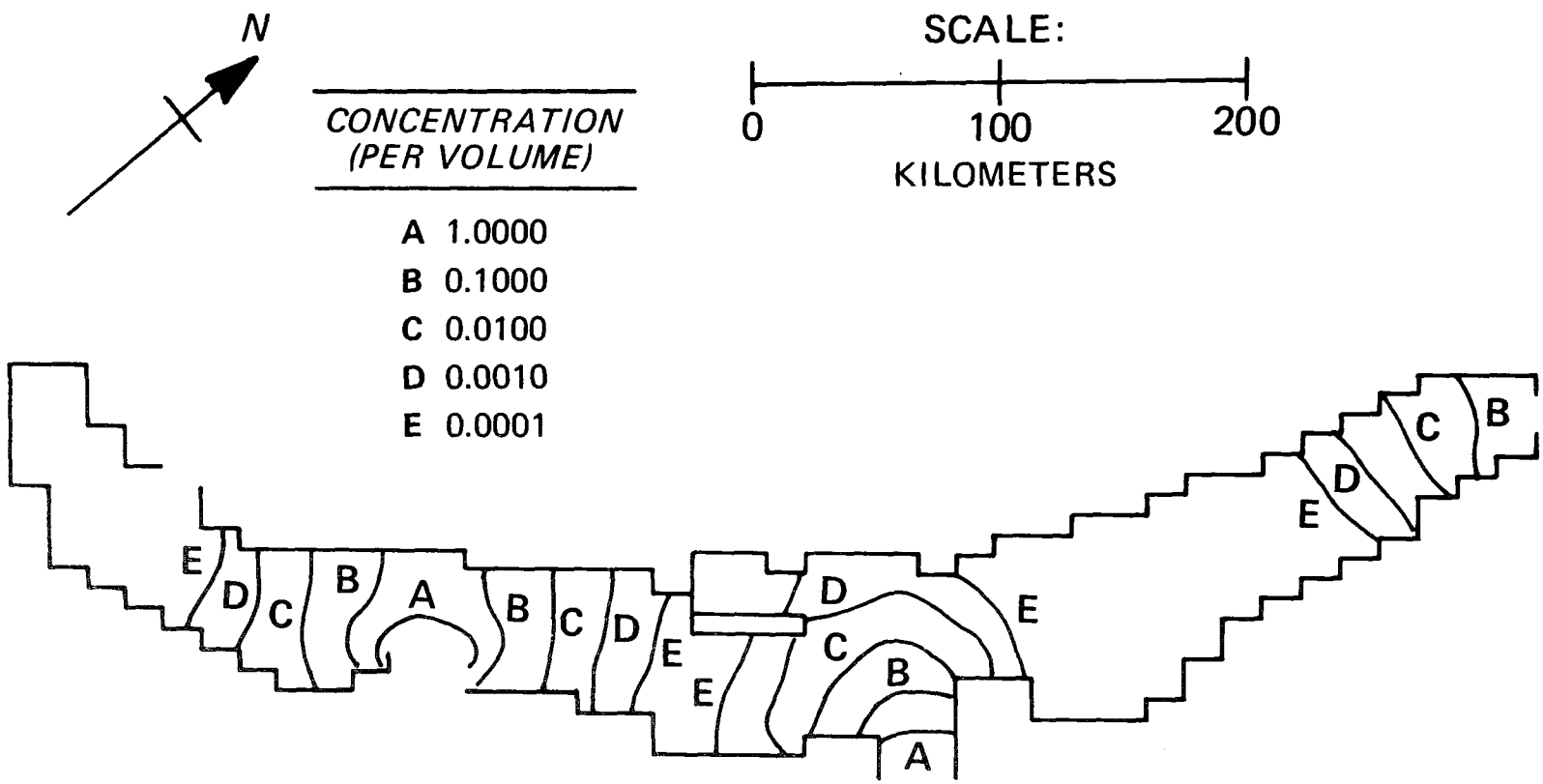

Figure 7d. Dispersion model calculation for Lake Baikal with southwest wind.

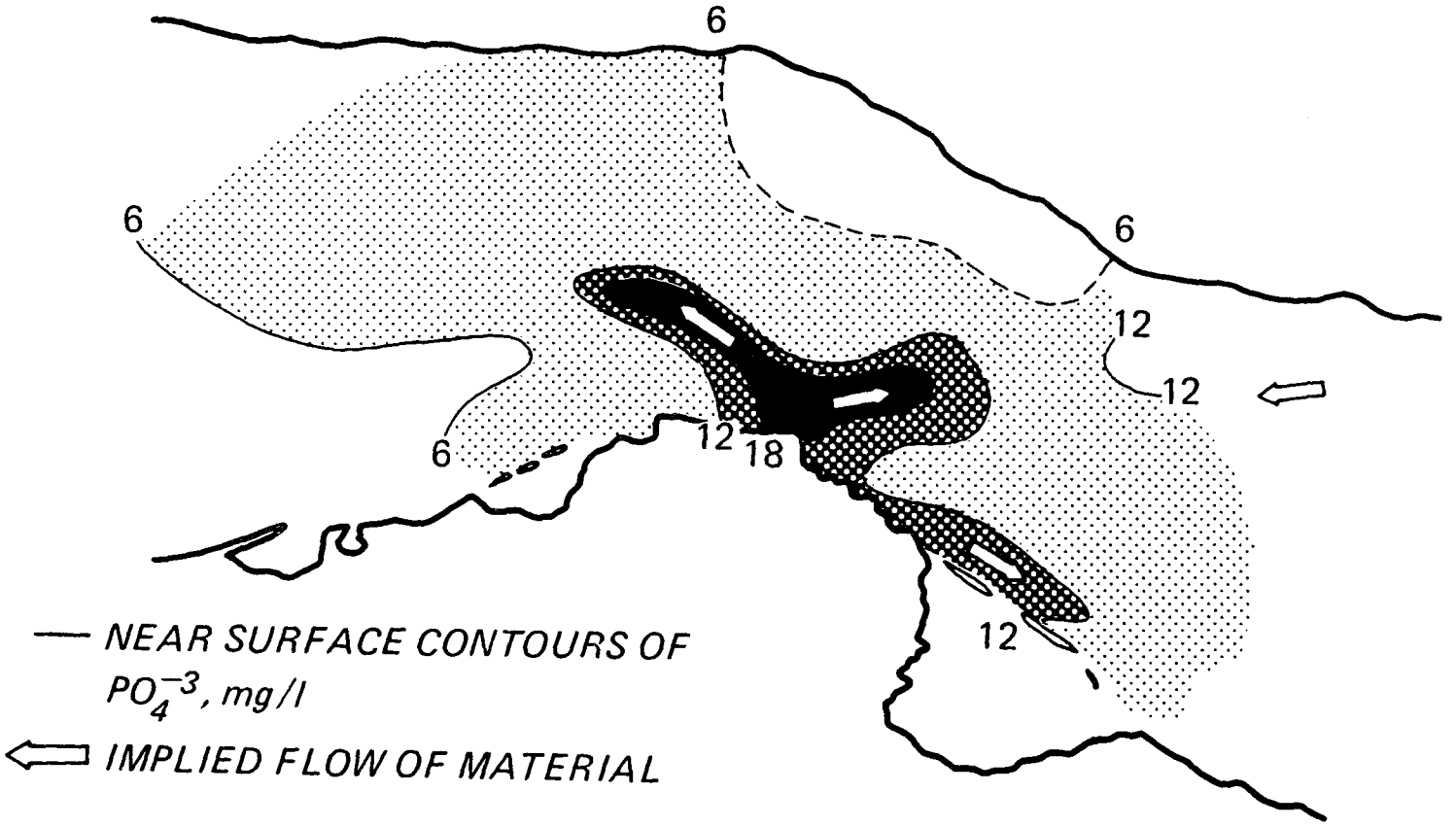

Figure 8a. Sample results from Hydromet cruise in Selenga Shallows on 28-29 May 1976.

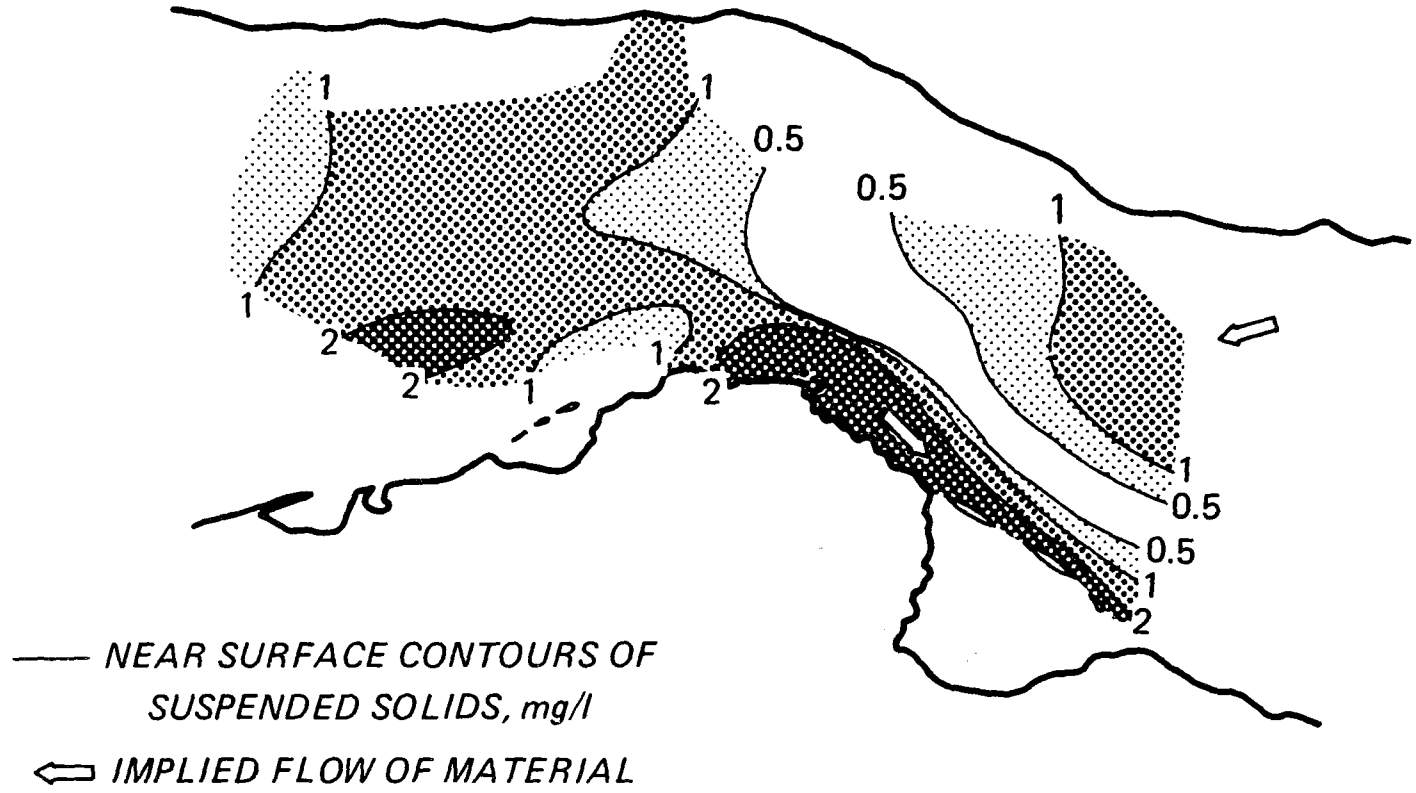

Figure 8b. Sample results from Hydromet cruise in Selenga Shallows on 28-29 May 1976.

river area, the subsurface currents are generally southwesterly. The suspended solids settle out as they enter the lake and are transported by the near-bottom currents. The dissolved material remains nearly uniform vertically, and is transported out into the lake by the subsurface currents. The data generally agree with the calculated distributions.

Additional data available for the Selenga region is the Landsat satellite image shown in Figure 9. This image records observations of 9 July 1975. Unfortunately, no wind information was available for this date. The image does indicate the same sort of suspended solids pattern as was observed during the 28-29 May 1976 Hydromet cruise (Figure 8).

DISCUSSION AND RECOMMENDATION

The work summarized in this paper represents just a preliminary step in a possible comprehensive joint modeling and field study by scientists from our two countries. It is hoped that the work discussed here will continue and that this continued work will enable scientists from both countries to expand their knowledge of the physical process in lakes.

It is recommended that a comprehensive joint USA/USSR modeling and field survey program be initiated for a lake such as Lake Baikal. This program would be used to both verify the models and increase the understanding of the processes at work in the lake. Modeling work already underway, along with information available from previous field surveys, would be used to plan an extensive one year field survey. The information that would be available from satellites (for example, LANDSAT and NIMBUS) would be utilized. The usefulness of the satellite imagery to characterize suspended solids in lakes, in conjunction with field data and modeling results, has been demonstrated by Sydor and Oman (1977); Sydor, Stortz, and Swain (1978); and Paul, Mielnik, and Shute (1979). The satellite provides synoptic information on a whole lake basin, while the survey ships provide information at different depths in the lake and can provide ground-truth for the satellite information. Such a program would cover a period of three years: the first year for preparation, the second year for the field surveys, and the third year for the analysis.

ACKNOWLEDGEMENTS

This work could not have been undertaken without the sponsorship of the former coordinators for the Lakes and Estuaries Project, Drs. T.T. Davies and A.A. Zenin.

Dr. Michael Sydor, University of Minnesota-Duluth, provided the Landsat satellite image.

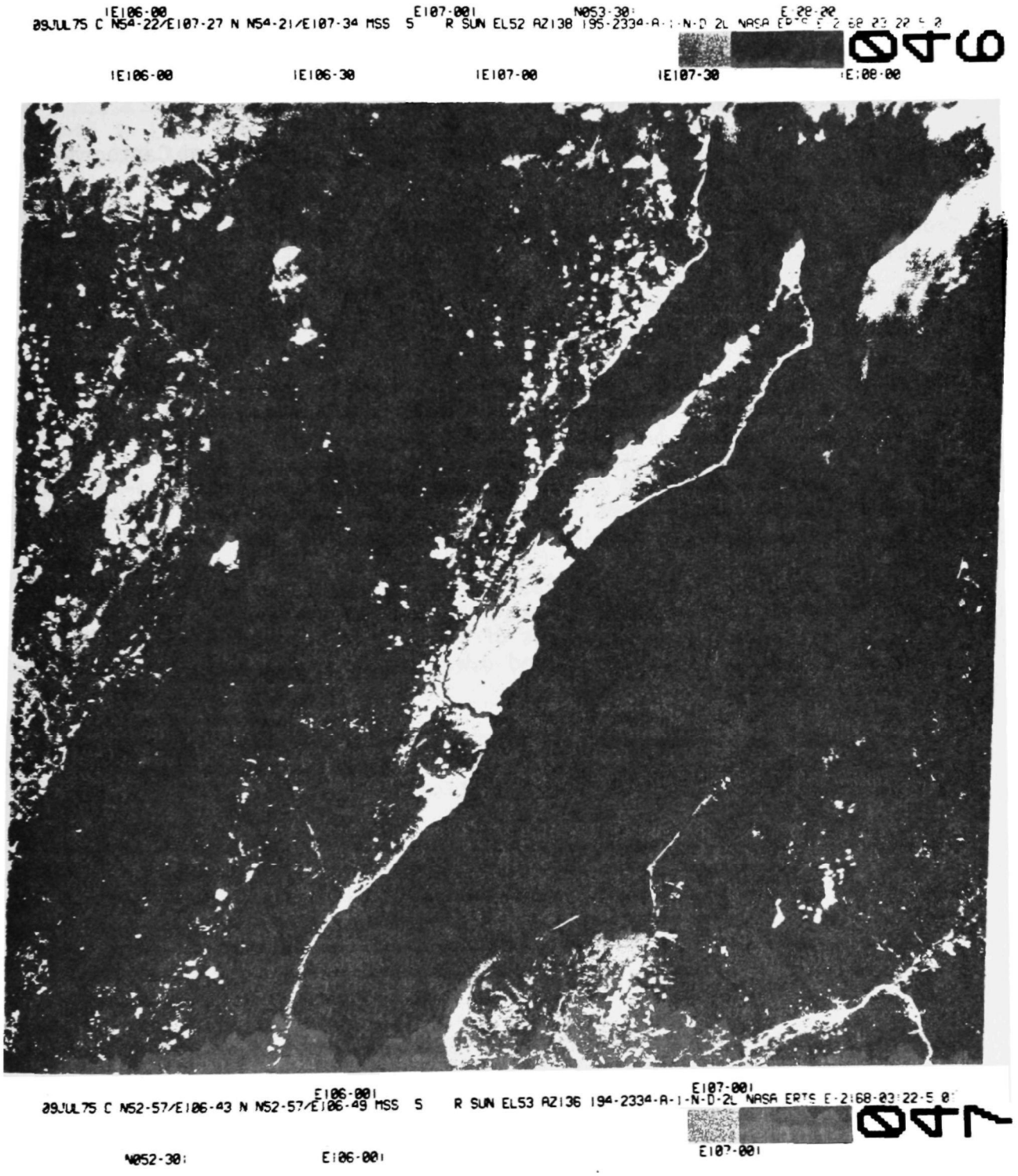

Figure 9. LANDSAT satellite image of Lake Baikal.

REFERENCES

Amsden, A.A. and F.H. Harlow. 1970. The SMAC method: A numerical technique for calculating incompressible fluid flows. Los Alamos Scientific Laboratory, Report No. LA-4370, Los Alamos, New Mexico.

Anonymous. 1969. Atlas of Baikal. Govt. Dept. Geodosy and Cartography. Irkutsk and Moscow.

Crowley, W.P. 1968. A global numerical ocean model: Part 1. J. Computational Physics, 3: 111-147.

Gedney, R.T. 1971. Numerical calculations of the wind-driven currents in Lake Erie. NASA TM X-52985.

Paul, J.F. and W.J. Lick. 1974. A numerical model for thermal plumes and river discharges. Proc. 17th Conf. Great Lakes Res., I.A.G.L.R., pp. 445-455.

Paul, J.F. 1976. Modeling the hydrodynamic effects of large man-made modifications to lakes. Proc. of the EPA Conf. on Environmental Modeling and Simulation (W.R. Ott, ed.), EPA-600/9-76-016, pp. 171-175.

Paul, J.F. and R.L. Patterson. 1977. Hydrodynamic simulation of movement of larval fishes in western Lake Erie and their vulnerability to power plant entrainment. Proceedings of the 1977 Winter Simulation Conference (H.J. Highland, R.G. Sargent and J.W. Schmidt, ed.), WSC Executive Committee, pp. 305-316.

Paul, J.F. and W.J. Lick. 1980. Numerical model for three-dimensional variable-density, rigid-lid hydrodynamic flows: Vol. 1, details of the numerical model. Report in preparation.

Paul, J.F., R.A. Mielnik, and P.A. Shute. 1979. Use of LANDSAT imagery to characterize the suspended solids in Lake Baikal. Project report for Remote Sensing of Earth Resources, Eastern Michigan University.

Paul, J.F., W.L. Richardson, A.B. Gorstko, and A.A. Matveyev. 1979. Results of a joint U.S.A./U.S.S.R. hydrodynamic and transport modeling project. EPA-600/3-79-015.

Semenov, A.E., ed. 1972. Hydrometeorological investigations of the southern seas and Atlanta Ocean. Collected Works of the Laboratory of the Southern Seas, Volume 11. Moscow.

Sheng, Y.-Y. P. 1975. The wind-driven currents and contaminant dispersion in the near-shore of large lakes. Lake Erie International Jetport Model Feasibility Investigation Report 17-5, Contract Report H-75-1, U.S. Army Engineer Waterways Experiment Station, Vicksburg, Miss.

Sydor, M. and G.J. Oman. 1977. Effects on Nemadji runoff on Lake Superior, effects of river inputs on the Great Lakes. Dept. of Physics, Univ. of Minn., Duluth.

Sydor, M., K.R. Stortz, and W.R. Swain. 1978. Identification of contaminants in Lake Superior through LANDSAT 1 data. J. Great Lakes Res., 4(2): 142-148.

Vikulina, Z.A. and T.D. Kashinova. 1973. Water balance of Lake Baikal.. Trudy GGI, Issue 203, pg. 268. Gidrometeoizdat, Leningrad.

SECTION 9

THE STRUCTURE OF HYDROCHEMICAL FIELDS AND SHORT-TERM PREDICTION

A.M. Nikanorov, B.M. Vladimirskiy, V.L. Pavelko, Ye.V. Melnikov and K.L. Botsenyuk[1]

INTRODUCTION

The concept of the field presumes the existence of coordinated indices located in some predictable manner in space, and characterized by a set of parameters which jointly fix the observed structure.

> "Thus, ... the system of a field refers to a system having the following properties. It is a spatial unity, at least with respect to certain of its properties. It is also a unity based on its interactions in the sense that it can be deformed only as a unit and that in relationship to certain significant ... peculiarities, a change in one portion of the field has a significant influence on changes of other parts. It is an organized whole with definite integral manifestations and should be studied as a whole, not as the summary result of the combination of its parts and their activities" (Huxley 1935, cited by Waddington 1948).

The concept of the field structure of phenomena is supplemented with its specific content in actual experiments, including observations and measurements. Based on these data, models of the phenomena are constructed which then serve as the basis for development of corresponding theories by the method of trail and error. The predictive capabilities of models created on the basis of accepted theories are obvious. The accuracy of predictions using these models increases as the corresponding theories are refined and expanded. The desire, frequently the need, to predict phenomena which do not have corresponding theoretical interpretation or, consequently, models based on them, makes it necessary to use empirical models for predictive purposes.

---

[1]Hydrochemical Institute, 192/3 Stachky Prospect, 344090 Rostov-on-Don, USSR.

The construction of empirical models, reflecting information concerning the actual, real aspects of phenomena in a form convenient for use, is also inseparable from observations and experiments. Thus, analysis of the structure of hydrochemical fields and resulting empirical descriptions are inseparably related both to the points of measurement selected, and to the mathematical apparatus used. Naturally, the mathematical model incorporates certain subjective and contradictory aspects, related to the selection of the specific model, to the particular goal of modeling, and to the set of models with which the same result can be achieved. It is this contradiction which must be resolved as a result of introduction of the concept of the field in the creation of empirical models. Thus, the concept of the field in the analysis of hydrochemical information is used not as a causal principal, but rather as a method of analysis.

HYPOTHESES CONCERNING THE STRUCTURE OF HYDROCHEMICAL FIELDS

The results of factor and regression analysis presented in this section are based on earlier published data (Zenin 1961). From these results evolve a number of statements which are of basic significance in both modeling the structure of hydrochemical fields, and in empirical prediction.

The data used represent the results of many years of measurement of a number of hydrochemical indices in reservoirs along the Volga River and its tributaries. In all, some 30,000 measurements were used in the analysis. The results of factor analysis are presented in Tables 1-7. Analysis of the results demonstrate several facts. Both for the reservoirs and for the tributaries, the factor solutions can be characterized by virtually the same set of factors. Thus, it may be assumed that the same mechanisms lie at the basis of formation of the assigned set of indices. It should be noted that the significance of individual factors (see the rows of "all factors" in Tables 1-7) changes, with one exception. The significance of this change is identical for all factors without exception. Obviously, the remaining factors reflect the specific characteristics of the hydrochemical situation in the reservoirs studied. It is important for the modeling of the structure of a hydrochemical field based on the vectors of mean and covariation matrices that the factor mapping remain constant, or that the internal factors of the covariance matrices and the variability of weights of the factors, the eigenvalues of the covariation matrices, remain constant.

The initial material used for analysis of the capabilities for empirical prediction was made up of series of hydrochemical indices from three hydraulic projects over a period extending from 1951 through 1973. It should be noted that the frequency of all data available was rather arbitrary. Examples of the time series of indices used for analysis are presented in Figure 1. The results of factor analysis for these data are presented in Tables 8 and 9, and enable confirmation of the hypothesis developed earlier in our analysis of data on the Volga reservoirs.

Regression models were constructed in which the computational procedure used was step-by-step regression. A linear model for 6 and 13 indices analyzed produced a high degree of agreement (see Figure 2). Furthermore,

TABLE 1. FACTOR SOLUTION FOR THE RESULTS OF CHEMICAL ANALYSIS OF WATER SAMPLES OF THE GORKY RESERVOIR IN 1954-1958

1	Factor Mapping Coefficient				
	2	3	4	5	6
Level	-0.05	0.01	0.00	0.12	0.08
Cl^-	0.70	0.68	0.02	-0.03	0.10
SO_4^{2-}	0.79	0.16	0.15	-0.07	-0.53
HCO_3^- mg/liter	0.95	-0.03	-0.06	-0.12	0.24
Ca^{2+}	0.93	-0.06	-0.25	-0.08	0.18
Mg^{2+}	0.89	0.02	-0.12	-0.41	0.10
$Na^+ + K^+$	0.23	-0.01	0.82	0.38	-0.24
Σi	0.99	-0.03	-0.02	-0.10	0.12
Cl^-	-0.07	-0.99	-0.06	-0.01	-0.08
SO_4^{2-}	-0.25	0.17	0.33	-0.12	-0.78
HCO_3^- % eq.	0.29	0.28	-0.27	0.02	0.84
Ca^{2+}	0.16	-0.06	-0.95	0.10	0.19
Mg^{2+}	0.22	0.02	-0.31	-0.90	0.00
$Na^+ + K^+$	-0.26	0.04	0.86	0.38	-0.17
Weight of factor[1]	2.24	1.26	1.64	1.16	1.36

[1]The weight of the factor is calculated as the root mean square of the coefficient by columns.

TABLE 2. FACTOR SOLUTION FOR RESULTS OF CHEMICAL ANALYSIS OF WATER SAMPLES OF TRIBUTARIES OF THE GORKY RESERVOIR, 1954-1958

1	Factor Mapping Coefficient				
	2	3	4	5	6
Level	-0.00	0.00	-0.00	+0.00	0.00
Cl^-	0.24	0.15	0.10	0.74	0.49
SO_4^{2-}	0.19	-0.37	0.01	0.83	-0.20
HCO_3^- mg/liter	0.17	0.26	0.12	0.94	-0.08
Ca^{2+}	0.04	0.20	-0.07	0.94	-0.18
Mg^{2+}	0.10	0.13	0.15	0.92	-0.20
$Na^+ + K^+$	0.60	0.01	-0.02	0.74	0.11
Σi	0.19	0.17	0.08	0.96	-0.09
Cl^-	0.04	-0.21	-0.02	0.34	0.91
SO_4^{2-}	-0.06	-0.99	-0.02	-0.09	-0.04
HCO_3^- % eq.	0.04	0.93	0.02	0.21	-0.26
Ca^{2+}	-0.75	-0.08	-0.54	-0.37	-0.07
Mg^{2+}	-0.15	0.06	0.92	0.35	0.10
$Na^+ + K^+$	0.98	0.05	0.02	0.18	0.01
Weight of factor	1.44	1.49	1.10	2.40	1.14

TABLE 3. FACTOR SOLUTION FOR RESULTS OF CHEMICAL ANALYSIS OF WATER SAMPLES FROM KUYBYSHEV RESERVOIR, 1954-1961

1	Factor Mapping Coefficient				
	2	3	4	5	6
Level	-0.05	-0.01	-0.03	-0.10	-0.03
Cl^-	0.45	0.29	0.82	0.07	0.13
SO_4^{2-}	0.79	0.05	0.21	0.19	0.52
HCO_3^- mg/liter	0.96	0.17	-0.06	0.16	-0.01
Ca^{2+}	0.92	-0.06	0.22	0.13	0.28
Mg^{2+}	0.80	0.01	0.12	0.55	0.20
$Na^+ + K^+$	0.45	0.77	0.35	-0.21	0.07
Σi	0.92	0.18	0.21	0.16	0.22
Cl^-	-0.04	0.26	0.93	-0.00	-0.07
SO_4^{2-}	0.37	-0.18	0.05	0.21	0.82
HCO_3^- % eq.	-0.19	-0.08	-0.57	-0.06	-0.44
Ca^{2+}	-0.07	-0.73	-0.13	-0.12	0.07
Mg^{2+}	0.19	-0.32	-0.12	0.87	0.07
$Na^+ + K^+$	-0.05	0.89	0.19	-0.38	-0.08
Weight of factor	2.12	1.51	1.48	1.19	1.16

TABLE 4. FACTOR SOLUTION FOR RESULTS OF CHEMICAL ANALYSIS OF WATER SAMPLES FROM KUYBYSHEV RESERVOIR TAKEN NEAR VYAZOVYYE (VOLGA RIVER) AND SOKOLI GORY (KAMA RIVER) AND NEAR KOMSOMOLSKIY (TAILWATER), 1958-1959

1	Factor Mapping Coefficient				
	2	3	4	5	6
Level	-0.02	0.18	-0.01	-0.00	0.07
Cl^-	0.84	0.05	-0.12	-0.08	-0.51
SO_4^{2-}	0.45	-0.10	0.42	0.06	-0.76
HCO_3^- mg/liter	0.14	-0.14	0.10	0.13	-0.95
Ca^{2+}	0.36	-0.09	0.08	-0.04	-0.89
Mg^{2+}	0.23	-0.54	0.05	0.07	-0.77
$Na^+ + K^+$	-0.01	0.02	0.03	-0.01	-0.08
Σi	0.49	-0.06	0.03	0.06	-0.86
Cl^-	0.96	-0.01	-0.23	-0.02	-0.17
SO_4^{2-}	-0.10	-0.07	0.98	-0.02	-0.04
HCO_3^- % eq.	-0.93	0.05	-0.30	0.03	0.20
Ca^{2+}	-0.72	0.11	0.03	-0.46	0.43
Mg^{2+}	-0.58	-0.78	-0.12	-0.05	0.10
$Na^+ + K^+$	0.80	0.26	-0.08	0.37	-0.37
Weight of factor	2.16	1.03	1.16	0.62	2.06

TABLE 5. FACTOR SOLUTION FOR RESULTS OF CHEMICAL ANALYSIS OF WATER SAMPLES OF TRIBUTARIES OF THE VOLGA RIVER AND KUYBYSHEV RESERVOIR, 1954-1961

1	Factor Mapping Coefficient				
	2	3	4	5	6
Level	-0.04	-0.08	-0.20	0.05	-0.03
Cl^-	0.28	0.33	-0.86	-0.02	-0.10
SO_4^{2-}	0.92	-0.13	-0.08	0.27	-0.07
HCO_3^- mg/liter	0.97	-0.04	0.13	-0.02	-0.06
Ca^{2+}	0.97	-0.14	-0.06	0.12	-0.12
Mg^{2+}	0.96	-0.04	-0.03	0.08	0.18
$Na^+ + K^+$	0.45	0.59	-0.47	0.03	-0.26
Σi	0.99	-0.02	-0.09	0.08	-0.09
Cl^-	-0.15	0.27	-0.94	-0.03	-0.09
SO_4^{2-}	0.62	-0.26	-0.20	0.67	-0.20
HCO_3^- % eq.	-0.44	0.03	0.69	-0.52	0.20
Ca^{2+}	0.24	-0.90	0.02	0.13	0.32
Mg^{2+}	-0.05	-0.05	0.24	-0.10	0.89
$Na^+ + K^+$	-0.21	0.89	-0.13	-0.05	-0.28
Weight of factor	2.37	1.50	1.58	0.92	1.10

TABLE 6. FACTOR SOLUTION FOR RESULTS OF CHEMICAL ANALYSIS OF WATER SAMPLES FROM VOLGOGRAD RESERVOIR, 1954-1961

1	Factor Mapping Coefficient				
	2	3	4	5	6
Level	-0.09	0.14	0.15	-0.05	-0.07
Cl^-	0.68	0.71	-0.04	-0.02	0.18
SO_4^{2-}	0.84	0.18	-0.09	-0.47	0.13
HCO_3^- mg/liter	0.95	-0.04	-0.13	-0.06	0.23
Ca^{2+}	0.94	0.22	-0.00	-0.21	-0.06
Mg^{2+}	0.06	0.08	-0.04	-0.03	0.02
$Na^+ + K^+$	0.61	0.16	0.12	-0.08	0.75
Σi	0.92	0.19	-0.09	-0.20	0.21
Cl^-	0.01	0.98	0.05	0.15	0.07
SO_4^{2-}	0.42	0.08	-0.05	-0.86	-0.05
HCO_3^- % eq.	-0.17	-0.46	0.00	0.24	0.04
Ca^{2+}	-0.11	-0.05	0.35	0.00	-0.88
Mg^{2+}	0.03	0.08	-0.98	-0.09	-0.11
$Na^+ + K^+$	0.04	-0.00	0.20	0.05	0.72
Weight of factor	2.10	1.36	1.08	1.07	1.43

TABLE 7. FACTOR SOLUTION FOR RESULTS OF CHEMICAL ANALYSIS OF WATER SAMPLES FROM TRIBUTARIES OF VOLGA RIVER BELOW KUYBYSHEV RESERVOIR, 1954-1961

1	Factor Mapping Coefficient				
	2	3	4	5	6
Level	-0.26	0.06	0.07	-0.02	0.02
Cl^-	0.04	0.31	0.10	0.93	0.08
SO_4^{2-}	0.97	-0.03	-0.08	-0.19	-0.06
HCO_3^- mg/liter	0.77	0.29	-0.30	-0.20	0.40
Ca^{2+}	0.97	-0.13	-0.05	-0.00	0.09
Mg^{2+}	0.89	0.05	-0.43	0.05	0.04
$Na^+ + K^+$	0.31	0.82	0.16	0.27	0.16
Σi	0.97	0.17	-0.10	0.02	0.14
Cl	-0.31	0.26	0.14	0.89	-0.12
SO_4^{2-}	0.85	-0.11	-0.16	-0.46	-0.09
HCO_3^- % eq.	-0.75	-0.16	-0.05	-0.55	0.23
Ca^{2+}	0.04	-0.97	0.19	-0.16	0.02
Mg^{2+}	0.34	0.14	-0.91	-0.20	0.02
$Na^+ + K^+$	-0.21	0.90	0.29	0.25	-0.04
Weight of factor	2.44	1.66	1.15	1.57	0.56

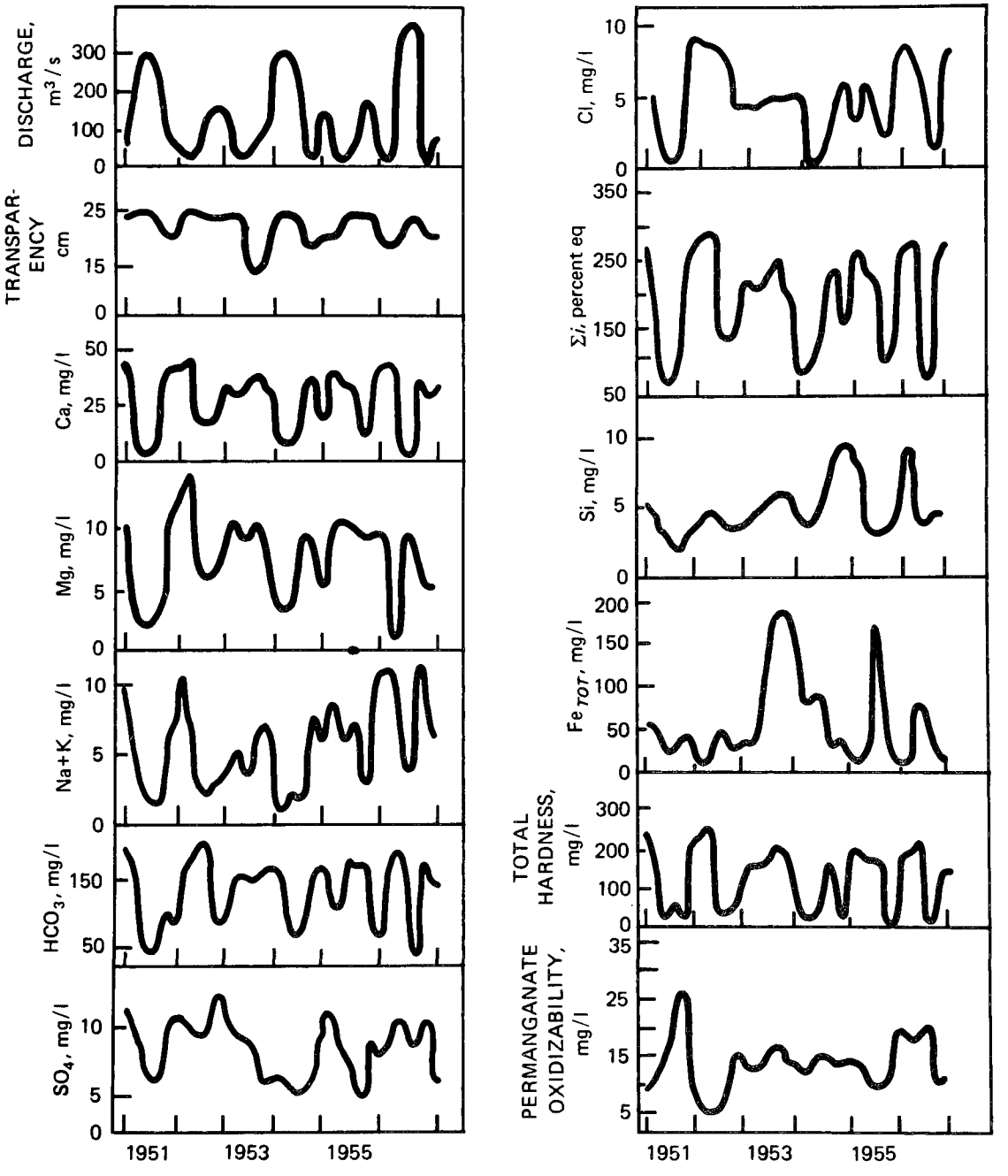

Figure 1. Berezina River at Gorval, 1951-1956.

TABLE 8. FACTOR SOLUTION FOR RESULTS OF ANALYSIS OF WATER SAMPLES OF GORVAL TRIBUTARY, BEREZINA RIVER, 1951-1956

1	Factor Mapping Coefficient				
	2	3	4	5	6
Discharge, m^3	-0.35	-0.07	0.40	0.40	
Ca^{2+}, mg/liter	0.69	-0.28	-0.24	0.11	
Mg^{2+}	0.56	0.08	-0.08	0.00	
$Na^+ + K^+$	-0.10	0.92	-0.34	-0.12	
HCO_3^-	0.79	-0.42	-0.39	0.22	
SO_4^{2-}	0.87	-0.02	0.17	-0.01	
Cl^-	0.66	0.32	-0.03	-0.01	
Hardness	-0.12	-0.18	-0.04	-0.42	
Σi % Eq.	0.88	0.05	-0.46	0.10	
Si	0.02	0.02	-0.16	-0.02	
Fe	0.03	-0.17	-0.02	-0.08	
Hardness	0.09	-0.16	-0.42	-0.83	
Perman. oxide	0.00	0.09	0.06	-0.35	

TABLE 9. FACTOR SOLUTION FOR RESULTS OF ANALYSIS OF WATER SAMPLES FROM BOBRUSK TRIBUTARY OF BEREZINA RIVER, 1957-1973

1	Factor Mapping Coefficient				
	2	3	4	5	6
Discharge, m^3	-0.22	-0.20	0.09	0.08	0.35
Ca^{2+}, mg/liter	0.84	0.12	0.03	-0.11	-0.21
Mg^{2+}	0.58	0.16	-0.14	0.31	-0.36
$Na^+ + K^+$	-0.05	0.16	-0.87	0.03	-0.14
HCO_3^-	0.88	0.11	0.08	-0.02	-0.40
SO_4^{2-}	0.75	0.35	-0.07	0.36	0.10
Cl^-	0.19	0.92	-0.11	0.04	-0.07
Hardness	0.87	0.19	-0.29	0.07	-0.34
Σi % Eq.	0.06	0.00	-0.05	0.02	-0.31
Si	-0.18	0.02	0.18	-0.00	0.08
Fe	0.33	-0.02	-0.21	0.00	0.32

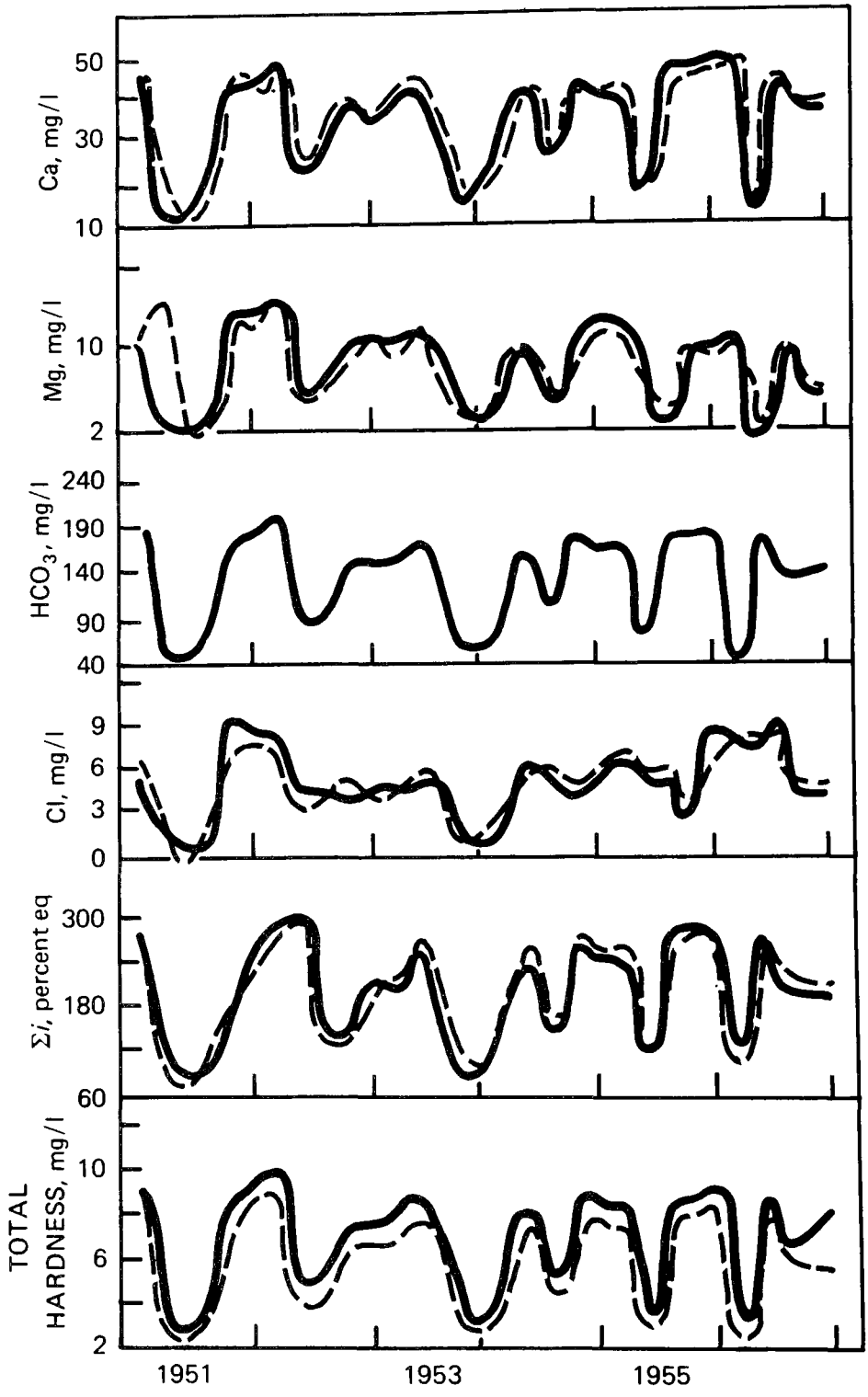

Figure 2. Berezina River at Gorval, 1951-1956.

analysis of the regression equations indicates that by selecting the corresponding concentrations of Ca^{2+} and HCO_3^- ions as basic variables, one can reliably predict four other variables, i.e., Mg^{2+}, Cl^-, the sum of ions, and total hardness. In Figure 2, the broken line shows the predicted values for these variables.

Attempts were made to use models generated for one of the points and the interrelated variables utilizing linear regression for prediction of the behavior of variables at other points. As before, the values of the concentration of Ca^{2+} and HCO_3^- were used as the base variables. The results of this prediction are shown in Figure 3 and 4. The high degree of accuracy achieved remains constant throughout a 10-year period. Additional analysis of these data has shown that the concept of multidimensional samples lacking a natural mean, or a natural average of eigenvalues of the covariation matrix is not suitable for statistical interpretation of series of hydrochemical indices. Correlation was found between measurements of the vector of means, and the vector of eigenvalues in the time scale of reading. The introduction of these hypotheses relative to the structure of the hydrochemical fields enables a modeling approach from the point of view outlined below.

SELECTION OF PARAMETERS OF THE MODELING SYSTEM FOR DETERMINATION OF THE SPATIAL STRUCTURE OF HYDROCHEMICAL FIELDS

Based on the above general considerations concerning the unity of all indices forming the structure of a hydrochemical field, a method of placement of a system of observations for determining the spatial organization of the field naturally follows. The essence of this method is that parameters of the empirical models are determined which can be used to make the transition from integral field characteristics to particular characteristics for a predetermined point. The network of initial observations can be adjusted in order to select empirical dependence adequate to the existing structure of the hydrochemical field, considering the limited nature of the number of measurements.

Sequential analysis of the structure of the hydrochemical field can be represented by the placement of r measurements on a grid of $k \cdot \ell$ possible measurements ($r \ll k \cdot \ell$). In this case, p and q are the ordinal numbers of the points at which information is obtained, corresponding to the coordinates Z_p and X_p; $p = 1,\ldots, k$; $q = 1,\ldots \ell$. The introduction of the vector $\beta_{pq} = \beta_{pq}(Z_p, X_q)$, of dimensionality n, characterizes a corresponding cell of the field, obtained by the results of measurement of a list of n indices.

In each cell of the field, m_{pq} measurements of the index $y_{pq}(s)$; $s = 1,\ldots,n$ are performed, and the vector of mean values $\overline{y}_{pq}$ is calculated. Since in the initial stage of analysis, $m_{pq} \approx s$, and the reliable matrices R_{pq} of the indices cannot be calculated, we can represent the field as follows:

$$\overline{y} = \frac{1}{k} \sum_{p=1}^{k} \frac{1}{\ell} \sum_{q=1}^{\ell} \overline{y}_{pq}; \quad \overline{y}_{pq} = \frac{1}{m_{pq}} \sum_{i=1}^{m_{pq}} y_{pq}(i);$$

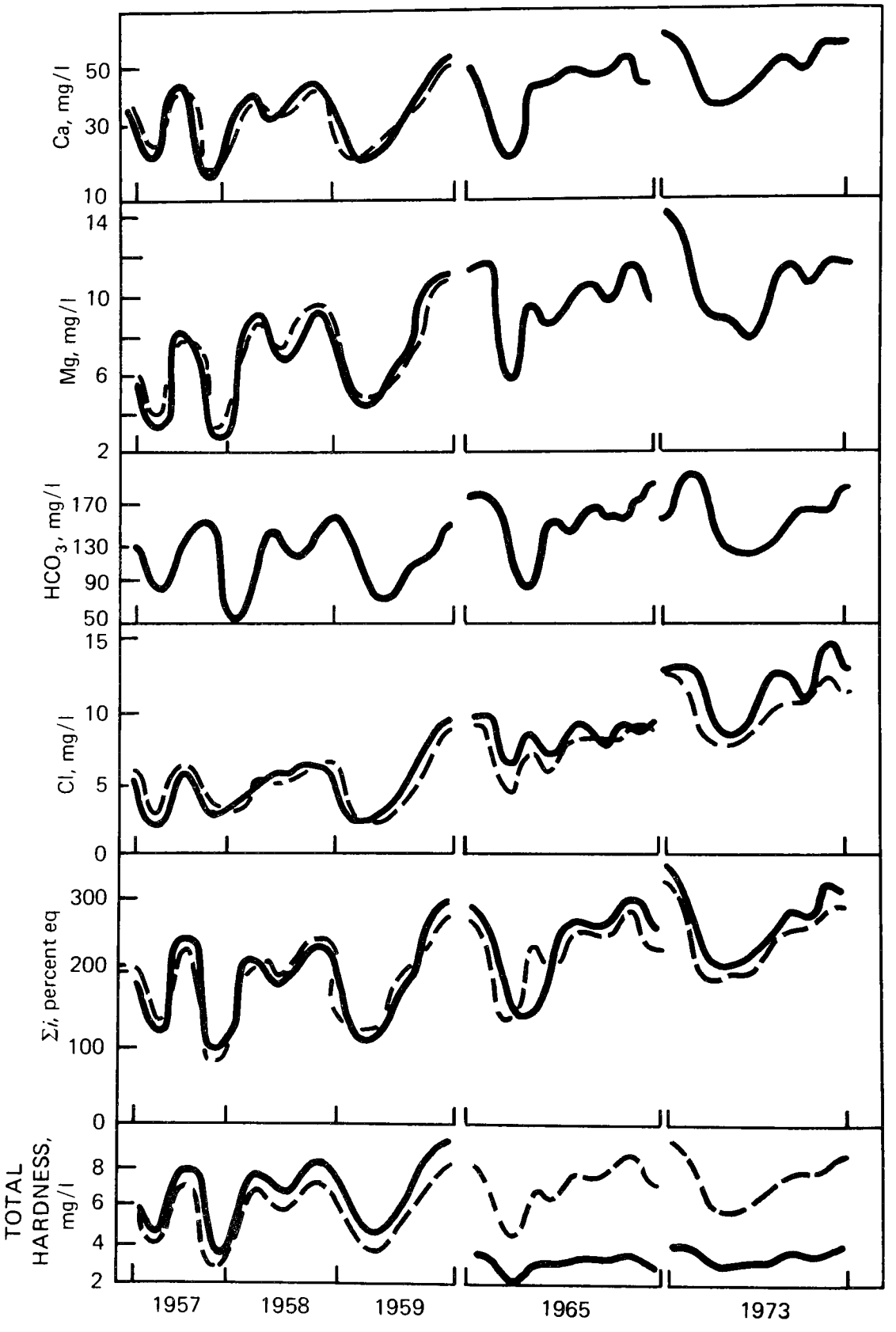

Figure 3. Berezina River at Bobruysk.

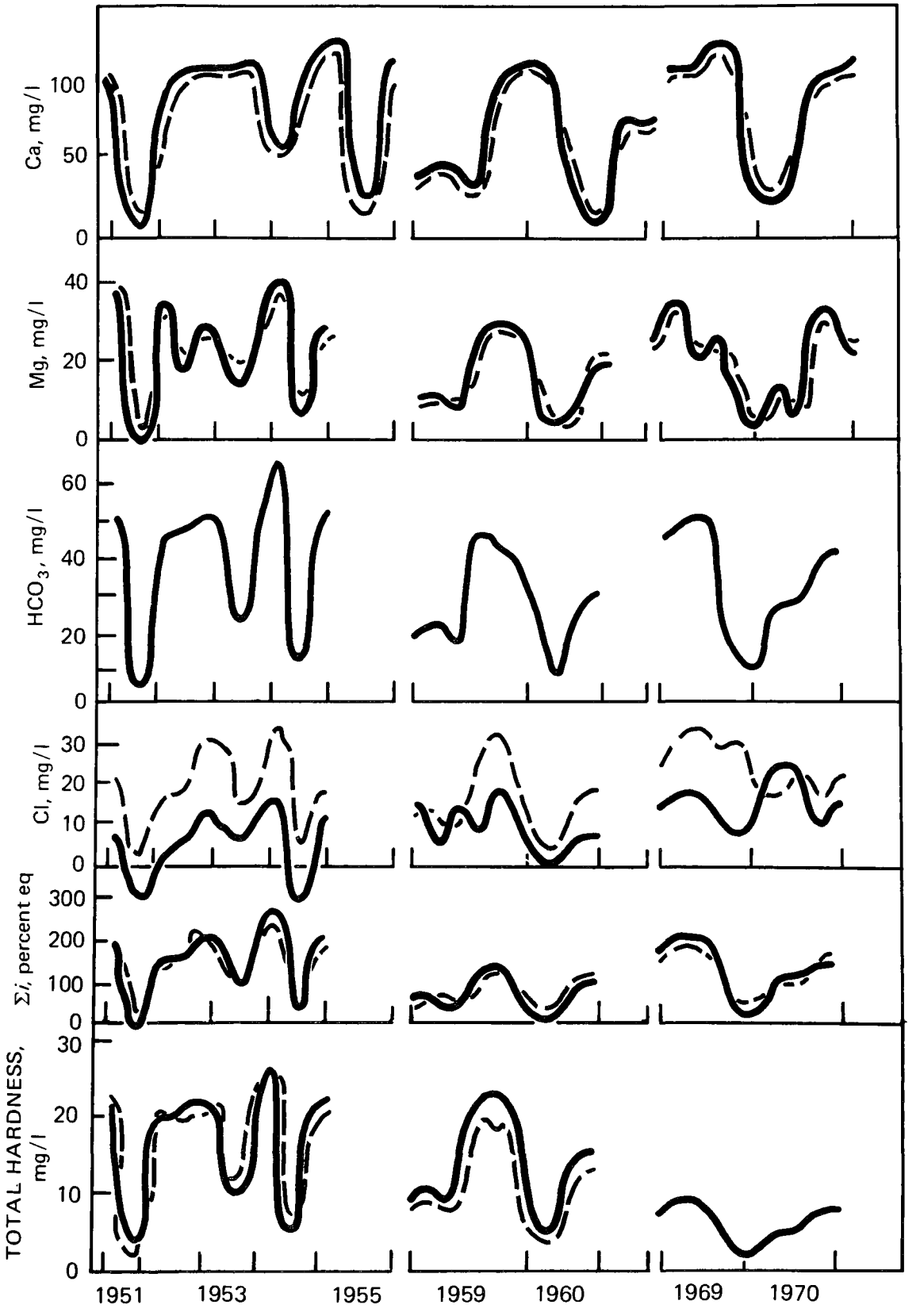

Figure 4. Sula River at Zelenkova.

$$R(i,j) = \frac{1}{\ell k-s} \sum_{p=1}^{k} \sum_{q=1}^{\ell} (\bar{y}_{pq}(i) - \bar{y}(i)) (\bar{y}_{pq}(i) - \bar{y}(j)). \quad (1)$$

Suppose the mean value of the vector of observed indices, and the corresponding covariance matrix at this point in the field can be restored by means of a linear transform of the vector of mean values and covariance matrix, characterizing the entire field as a whole, i.e.,

$$\bar{y}_{pq} = L_{pq}\bar{y};$$

$$R_{pq} = L_{pq}RL_{pq}^{T}; \quad (2)$$

where L_{pq} is an $n \cdot n$ matrix of coefficients.

Suppose

$$R_{pq} = H\alpha_{pq}H^{-1}; \; R = H\alpha H^{-1};$$

$$L_{pq} = L_{pq}^{T} = H\beta_{pq}H^{-1};$$

where α, α_{pq} and β_{pq} are the diagonals of an n n matrix of eigenvalues; while H is an $n \cdot n$ matrix of eigenvectors.

In this case, the simplifications

$$\begin{cases} \bar{y}_{pq} = H\beta_{pq}H^{-1}\bar{y}; \\ H\alpha_{pq}H^{-1} = H\beta_{pq}H^{-1}H\alpha H^{-1}H\beta_{pq}H^{-1}; \end{cases}$$

$$\begin{cases} H^{-1}\bar{y}_{pq} = \beta_{pq}H^{-1}\bar{y}; \\ \alpha_{pq} = \beta_{pq}\alpha\beta_{pq}; \end{cases} \quad (4)$$

can be applied.

The procedure of calculation of β_{pq} at each instant in time after a group r of measurements includes the following sequence of operations:

1. Refinement of vector $\overline{y}_{pq}$ if measurements have been performed at a given point in the field.

2. Refinement of the vector $\overline{y}$.

3. Refinement of the matrices R, H^{-1}, α.

4. Calculation according to (4) for each point in the field β_{pq}, α_{pq}.

In this case, the vector β_{pq} represents each cell of the field as independent of all previous measurements in any of the cells of the field. The expediency of this very procedure is demonstrated by the following considerations.

The recursive nature of the estimation of parameters of a point in the field, even with non-optimal placement of points of information measurement, guarantees

$$\lim_{t \to \infty} \beta_{pq}(t) \to \beta_{pq}; \tag{5}$$

where t is the next measurement time.

If the number of experiments is sufficient to guarantee (5), this plan of estimation allows an explicit prediction to be given for an arbitrary point in the network. The error of prediction in this case depends not on the random errors of measurement at arbitrary points on the network, but rather on the number of experiments performed and the resolution of the network as a whole.

Adaptive estimation of parameters β_{pq} is possible, and is accomplished by the introduction of the strategy of effective "omission". For example, in the exponential form $\varepsilon = \exp\{\gamma(t_i - t)\}$, where t is the current instant in time of the measurement; t_i is the instant in time of the previous measurement, then γ is the "omission" factor. This strategy accomplishes experimental planning with respect to possible instabilities.

Finally, each cell of the network is characterized by the actual vector of means and covariance matrix, which allows testing of rather complex multidimensional statistical hypotheses concerning the network as a whole. This, in turn, allows a tranformation of the network, increasing its resolving capacity.

Determination of optimal values of the frequencies of performance of observations , based on the spatial heterogeneity of the field of measured statistical indexes , may be made. The regression equation for $\beta_{pq}(s)$, where s = 1,...,n (the number of measured characteristics at a point in the field), in the case of two-dimensional extrapolation (Fedorov 1971; Krug et al. 1977) can be represented as follows:

$$\hat{\zeta}(Z_p,x_q) = E[\beta_{pq}(s)] = \sum_{\substack{i=1\\p\neq i}}^{k} \sum_{\substack{j=1\\q\neq j}}^{\ell} L_i(Z_p)L_j(x_q)\beta_{ij}(s);$$

$$L_i(Z_p) = \frac{(Z_p-Z_1)\ldots(Z_p-Z_{p-1})\ (Z_p-Z_{p+1})\ldots(Z_p-Z_k)}{(Z_i-Z_1)\ldots(Z_i-Z_{i-1})\ (Z_i-Z_{i+1})\ldots(Z_i-Z_k)}, \tag{6}$$

where $L_j\ (x_q)$ is an analogous expression.

The dispersion of this estimate is

$$d[\hat{\zeta}(Z_p,x_q)] = \sigma^2 \sum_{\substack{i=1\\p=1}}^{k} \sum_{\substack{j=1\\q=j}}^{\ell} L_i^2(Z_p)L_j^2(x_q)\ \frac{1}{\phi_{ij}}; \tag{7}$$

where ϕ_{ij} are the optimal values of the frequency of observation

$$\phi_{ij} = \frac{|L_i(Z_p)L_j(x_q)|}{\sum_{\substack{i=1\\p\neq 1}}^{k} \sum_{\substack{j=1\\q\neq j}}^{\ell} |L_i(Z_p)L_j(x_p)|}; \tag{8}$$

is obtained from the condition of the minimum of (7).

The dispersion of the prediction is represented as

$$d[\hat{\zeta}(Z_p,x_q)] = \sigma^2 [\sum_{\substack{p=1\\p\neq i}}^{k} |L_i(Z_p)|]^2\ [\sum_{\substack{j=1\\q\neq j}}^{\ell} |L_j(x_q)|]^2 . \tag{9}$$

This enables the development of the following algorithm for calculation of the frequency of observations in each cell of the field:

1. Select the field with their known characteristics.
2. Calculate $\hat{\beta}_{pq}(s)$ according to (6).
3. Calculate $\sigma^2 = [\hat{\beta}_{pq}(s) - \beta_{pq}(s)]^2$.
4. Calculate the dispersion of the prediction according to (9).

5. Discard in sequence one of the cells of the field and perform calculations in (2), (3) and (4).

6. Discard that field cell from analysis which by elimination produces the greatest change in (9).

7. The procedure terminates with a transition to step 9 if the discarding of any point leads to an increase in the value of (9).

8. Return to step 1.

9. Calculate ϕ_{ij} according to (8).

10. Recalculate the frequencies of measurements at the point

$$r_{pq}(s) = \sum_{i=1}^{k} \sum_{j=1}^{\ell} r\ \phi_{ij}(s). \tag{10}$$

The calculations should be performed for all values of $s = 1,\ldots,n$; $p = 1,\ldots,k$; $q = 1,\ldots,\ell$ ($k \cdot \ell \cdot n$ plans in all). As a result of the calculations performed, for each point the summary necessary number of measurements which can be perfomed given the arbitrary distribution of measurement frequencies at this point is obtained. This is converted to the assigned number of measurements. Naturally, when the arbitrary distribution is achieved, priority recommendations (cost or any other consideration) can be made for the conduct of measurements. This is achieved by modifying (6) and (9).

The requirements of (5) assured consistency of estimate , but the results of two-dimensional extrapolation, namely the calculation of the dispersion of the prediction for a number of points relative to the remaining points, may differ significantly from the desired value. The heterogeneity of the calculated statistical indexes β_{pq} results from the lack of homogeneity of the measured field. In this case, based on the information accumulated, and by testing of the corresponding statistical hypotheses (Kulbak 1967), the entire space of observations is divided into the corresponding subspaces.

CLASSIFICATION OF STRUCTURES OF HYDROCHEMICAL FIELDS

Sequential analysis of the structures of hydrochemical fields, which forms the basis of solution of the extreme problem of placement of the network of observations, utilizes the concept of smoothness of distribution of the observed field parameters.

The lack of homogeneity of observed or calculated indices is interpreted by the researcher as a lack of homogeneity in the observed field. This conclusion is correct within the framework of the conceptual or empirical model selected. In this case, the model of the field description toward which the researcher was oriented should be changed. Since the model uses not only

the mathematical apparatus of empirical field description, but also the selected configuration of the observation network, additional empirical information on the field is required.

The planning of measurements at new points on the field or the introduction of new indices is necessary, but the uncertainty of this planning is great. In this case, the problem of classification arises, the solution to which provides the necessary information for planning of new experiments. The conceptual model of the field in this case is fixed by preceding stages of research, and, within the framework of this model, the empirical material must be classified so that the heterogeneous field is approximated by classes of homogeneous fields. It is necessary to realize which of the two tasks is being performed by the researcher: typization or separation (Ayvazyan et al. 1974). The task of typization (representation), the solution of which always exists, assumes separation of the set of observed indices (in this case, vectors β_{pq}) into a comparatively small number of grouping areas. The grouping areas are analogs of the grouping intervals used in processing of one dimensional observations, which defines the nature of the requirements: uniform coverage of the entire set of experimental data by nonintersecting classes of samples, and assurance of the minimum possible distance between these areas. The task of separation, whose solution may yield a negative result if the entire sample belongs to one cluster, assumes natural stratification of the initial observations into a clearly expressed cluster (in this case, vectors y_{pk}).

Before indicating the relationship between the performance of the tasks of typization and separation in the reconstruction of a model of the structure of hydrochemical fields, it is necessary to indicate the specific characteristics of the use of the methods of pattern recognition in hydrochemisty. As we perform the task of recognition, the most interesting characteristics are those for which the difference between the mean values of classes is great in comparison with the standard deviations within classes, and not those for which the standard deviations are great (Duda and Hart 1976).

The introduction of measures of difference between classes in the form of Euclidian distances, transformation by means of the main components, or factor mapping of the initial matrix of data on a standardized matrix (with the introduction of Euclidian distances) presumes that the space of characteristics is isotropic, i.e., the groups defined by these distances will be invariant with respect to shifts, rotations, or dilations (Ayvazyan et al. 1974; Duda and Hart 1976). However, as studies have shown, the assumption that the fields of hydrochemical indices are isotropic is not valid. The absence of isotropicity can be clearly seen from the tables of factor solutions presented above. In addition to the constantly acting factors, and practically constant dispersions of indices from object to object, the variable parameters are the weights of the factors participating in the description of the dispersion of the measured indices.

A natural invariant for each of the measured vectors $y_{pq}(s)$ of the field is represented by the calculated indices β_{pq}, where p, q are, as before, the number of the measured point, while s is an ordinal number with respect to

time. Actually, when the task of typization is performed for statistical parameters (the number of vectors to be analyzed is only $k \cdot \ell$, significantly less than the number of all experiments in the network for measurement of vectors $y_{pq}(s)$), we obtain nontrivial information on the structure of the hydrochemical field. The presence of $\beta(r)$, where r is the class number, enables a fixed description for the entire set of characteristic measurement points in the form of statistical characteristics, namely the covariance matrices

$$R(r) = H\beta(r)\alpha\beta(r)H^{-1}; \tag{11}$$

and the vectors of means

$$m(r) = H\ (r)H^{-1}\bar{y}; \tag{12}$$

where H, α and $\bar{y}$ are defined and calculated according to (3), (4), while N is, as before, the number of classes, r = 1,...,N.

The information measure of difference for classes i, j (Kulbak 1967) in this case, if the hypothesis of mixed multidimensional normal distributions is accepted, is as follows:

$$\partial(i,j) = \frac{1}{2}\ \mathrm{tr}\ \{[R(i) - R(j)]\ [R^{-1}(j) - R^{-1}(i)] +$$

$$\frac{1}{2}\ [m(i) - m(j)]^T\ [R^{-1}(i) + R^{-1}(j)]\ \ m(i) - m(j)]\}$$

$$= \frac{1}{2} \sum_{a=1}^{n} \{[\beta(i,a)\alpha(a)\beta(i,a) - \beta(j,a)\alpha(a)\infty(j,a)]\ x$$

$$[(\beta(j,a)\alpha(a)\beta(j,a))^{-1} - (\beta(i,a)\alpha(a)\beta(i,a))^{-1}\} +$$

$$\frac{1}{2}\ \bar{y}^T\ H\alpha H^{-1}\bar{y}; \tag{13}$$

where a = 1,...,n is the ordinal number of the index

$$\alpha(a) = [\beta(i,a) - \beta(j,a)]\ [\frac{1}{\beta^2(j,a)\ \alpha(a)} + \frac{1}{\beta^2(i,a)\alpha(a)}]\ x$$

$$[\beta(i,a) - \beta(j,a)] = \frac{[\beta(i,a) - \beta(j,a)]^2\ [\beta^2(i,a) + \beta^2(j,a)]}{\beta^2(j,a)\ \alpha(a)\ \beta^2(i,a)}. \tag{14}$$

Using the expression

$$\bar{y}^T H\alpha H^{-1}\bar{y} = \mathrm{tr}\ \{H^{-1}\bar{y}\,\bar{y}^T H\}\ ; \tag{15}$$

we can write

$$\partial(i,j) = \frac{1}{2}\sum_{a=1}^{n}\left[\frac{\beta^2(i,a) - \beta^2(j,a)}{\beta(i,a)\ \beta(j,a)}\right]^2 + \frac{1}{2}\,\mathrm{tr}\ \{\alpha H^{-1}\bar{y}\,\bar{y}^T H\}\,. \tag{16}$$

Analysis of the expressions (14), (16) indicates that both of the components contain the terms

$$\frac{[\beta(i,a) - \beta(j,a)]}{\beta(i,a)\cdot\beta(j,a)}\ .$$

If the entire sample is normalized with respect to the mean, i.e., $\bar{y} = 0$, then (16) becomes

$$\partial(i,j) = \frac{1}{2}\sum_{a=1}^{n}\left[\frac{\beta^2(i,a) - \beta^2(j,a)}{\beta(i,a)\cdot\beta(j,a)}\right]^2\ . \tag{17}$$

It is seen from (17) that the Euclidian distance providing isotropicity of the space of characteristic on the assumption of nonisotropicity of the space of characteristics y has been achieved. This, in turn, opens the possibility of using factorial analysis for the solution of the problem of dimensionality of the space of characteristics β_{pq}, which enables simplification of the task of typization objects of observation.

However, the question of the minimum number of classes into which the space of characteristics should be divided remains open. Following the common recommendations (Ayvazyan et al. 1974; Duda and Hart 1976), it can be indicated that the approach of directed decision-making functions here. The classification procedure leads to a decrease in (9), which is equivalent to a contradiction between the statistical classification and spatial homogeneity of classes.

Thus, the methods of analysis suggested do not contradict the concept of the field used in hydrochemistry, and can be used in the prediction of space-time characteristics of hydrochemical indices, providing optimization of the network, with respect to spatial parameters and with respect to time.

REFERENCES

Ayvazyan, S.A., Z.I. Bezhayeva, and O.V. Staroverov. 1974. Classification of multidimensional observations, Moscow, Statistika Press, 240 pp.

Duda, R. and P. Hart. 1976. Pattern recognition and cost analysis, Moscow, Mir Press, 511 pp.

Fedorov, V.V. 1971. Optimal experiment theory. Moscow, Nauka Press, 312 pp.

Krug, G.K. et al. 1977. Experimental planning in problems of identification and extrapolation. Nauka Press, Moscow, 208 pp.

Kulbak, S. 1967. Information theory and statistics. Nauka Press, Moscow, 408 pp.

Waddington, K.H. 1948. Organizers and genes. Foreign Literature Press, Moscow, 206 pp.

Zenin, A.A. 1961. Results of hydrochemical studies of the Volga reservoirs in 1954-1961. Rostov-na-Donu, 209 pp.

SECTION 10

TRANSPORT OF MINING WASTE IN LAKE SUPERIOR

M. Sydor, G.E. Glass[1] and W.R. Swain[2]

INTRODUCTION

The western arm of Lake Superior has a 100 km trough which extends along the Minnesota shoreline from Knife River, Minnesota where the trough is 180 m deep past Silver Bay, Minnesota, where depths range around 250 m (Figure 1). An average of 67,000 tons of fine iron ore tailings are discharged at Silver Bay into the lake every day. The discharge is the largest source of particulates along the Minnesota shore. Transport of tailings in western Lake Superior have been the subject of considerable local interest (Cook 1974) and general interest regarding dispersion of contaminants in the Great Lakes. The transport of particulates can be investigated through use of remote sensing and numerical modeling. Fine particulates in lakes are identifiable through use of Landsat data (Sydor, Stortz, and Swain 1978; Sydor 1978). Their remote sensing signatures provide valuable information for studies of the dispersal processes and verification of numerical models (Diehl et al. 1977). We consider here measurements and remote sensing data which suggest transport of tailings by means of an upwelling. Two wind episodes are discussed in detail. In one instance transports and dispersal of a plume is simulated numerically for the actual wind and pressure conditions over the lake. The model results are subsequently compared with measurements of suspended solids and the remote sensing data for the plume. The results show that the direct transport of tailings cannot readily account for the episodes of high concentration of tailings at the Duluth water intake. In the instance chosen as our second example, Landsat images for two consecutive days show discrete high concentration patches of tailings which appear to have upwelled during westerly winds. The successive images and current measurements at two stations show that tailings patches are transported in accordance with the results from numerical models. The patches appear to have originated from an upwelling near the Duluth water intake. The data for the intake show that the concentration of tailings in the

---

[1]U.S. Environmental Protection Agency, Environmental Research Laboratory, Duluth, Minnesota 55804.
[2]U.S. Environmental Protection Agency, Large Lakes Research Station, Grosse Ile, Michigan 48138.

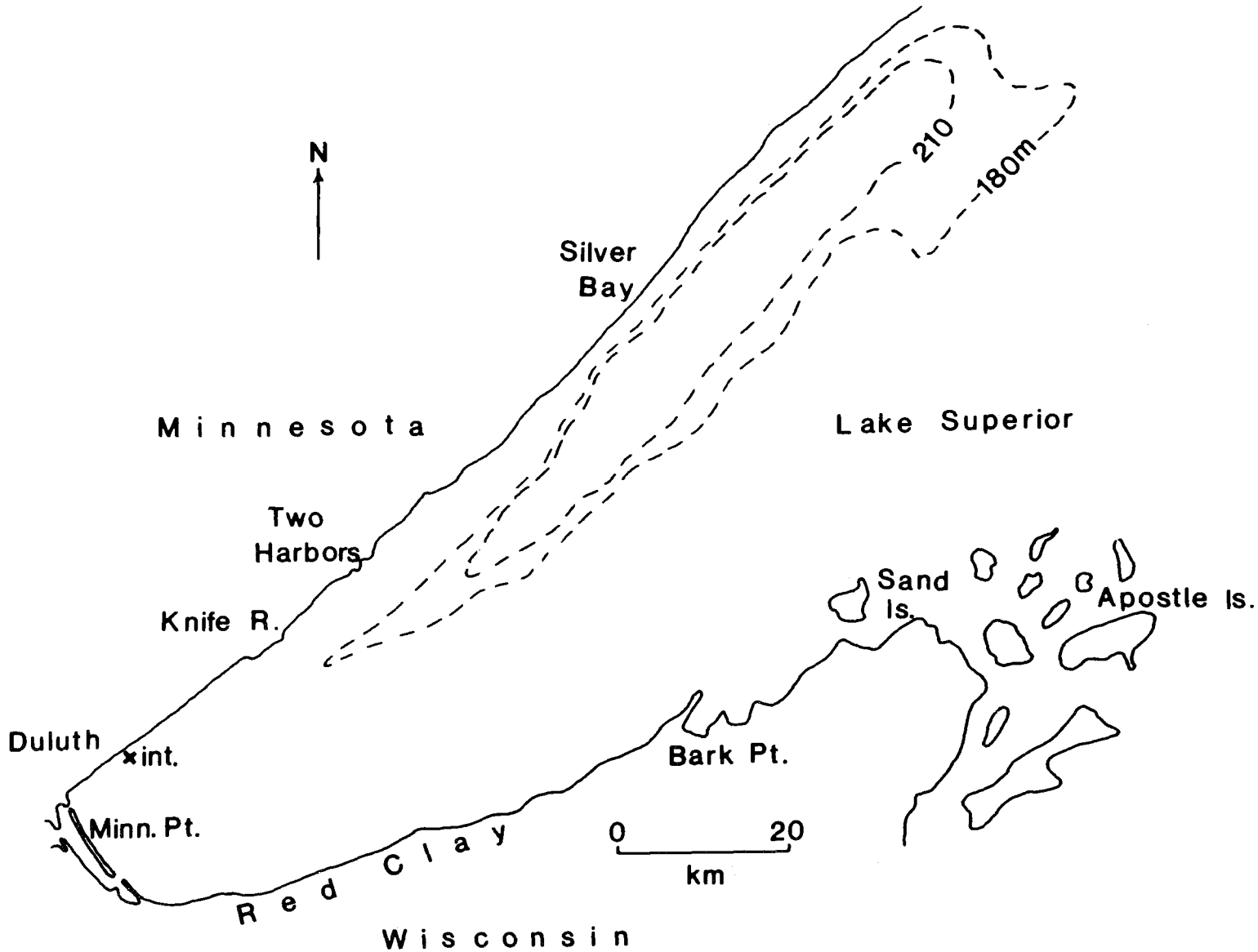

Figure 1. Study area showing the outline of a deep trough where tailings are discharged and the discharge source location at Silver Bay.

patches exceeded 3 mg/ℓ, a level which is an order of magnitude higher than the concentrations produced by the direct transport of turbidity to Duluth.

DISCUSSION

Information regarding direct transport of tailings in the form of a surface turbidity plume along the Minnesota shore from Silver Bay to Duluth can be obtained by using remote sensing data for a specific storm event. During November 9-14, 1975, a severe storm produced an extensive turbidity plume off Silver Bay. Remote sensing data for the event provides information on the extent of the plume at one instant of time. To determine the dispersal of turbidity throughout the event we can simulate the plume numerically for the entire period and compare the results of the model with the remote sensing data for November 14, 1975 at the instant of time when the image was taken.

It was first necessary to calculate the transports in the lake throughout the event. This was done using a depth integrated model for Lake Superior performed on a 6 x 6 km grid, using quadratic bottom friction and employing a numerical scheme due to Leendertse (1967). The results of the model for a generalized steady wind function have been discussed in detail by Diehl et al. (1977). However, for the case here a numerical method of handling the actual pressure distribution term and the wind function which occurred on November 9-14, 1975 was needed. The function and the pressure term for the storm were devised from approximation of the actual winds measured at weather stations around Lake Superior (Maanum 1977). Weather records from nine Coast Guard stations around the lake provided information on wind speed, wind direction, and the atmospheric pressure gradients every 2 hours. The problem of finding pressure gradients at every grid point was handled by devising a fit to the atmospheric pressure data for a low pressure cell which moved in the proximity of the lake during the storm.

The formula used to fit the atmospheric pressure data was

$$p_a = f(a,r)\ (b+cx+dy)$$

where p_a is the atmospheric pressure,

(x,y) is the position in cartesian coordinates relative to the center of the storm,

r is the distance from the storm center,

a,b,c,d are empirical coefficients, and

f(a,r) is some function of r and a.

The coefficients b, c, and d were treated as quadratic functions of time:

$$p_a = f(a,r)\,[(b_o + b_1 t + b_2 t^2) + (c_o + c_1 t + c_2 t^2)x + (d_o + d_1 t + d_2 t^2)y]$$

The function f was taken as $f(a,r) = r^2 + ar^3$, which provided a good fit to the radial dependence of the pressure term. The value of a was varied while the other 9 coefficients were found by the method of least squares until the sum of the squared differences between the calculated and measured pressures was minimized.

Atmospheric pressures calculated by this model agreed well with the measured pressures both in time and space. Once the coefficients were found, the pressure gradients were also known by taking spatial derivatives of the empirical formula. Subsequently, wind directions were obtained by rotating the direction of the pressure gradient field 125° counterclockwise. A form similar to the one used to fit pressures was fitted to the measured winds to obtain wind speeds everywhere.

Wind speeds were given by

$$W = f'(a',r)\ (b' + c'x + d'y)$$

where W is the wind speed, the coefficients b', c', and d' were treated as 4th-order functions of time, and $f'(a',r) = r/(r^2 + a'^2)$. Figure 2 shows the fit to the wind data at Duluth. The calculated and measured water levels are shown in Figure 3. Spectral analysis of the calculated water levels produce free surface modes given by Mortimer and Fee (1976). To check the direction and speed of the vertically averaged currents at Silver Bay we considered measurements of currents for several wind episodes reported by Baumgartner et al. (1973). The comparison was made for the well-mixed isothermal conditions in March, April, October, and November and is shown in Tables 1 and 2. The calculated transports agree reasonably well with the expected currents. The transport pattern for the entire area is shown in Figures 4 and 5. Generally, the patterns in Figures 4 and 5 show typical results for westerly and easterly winds (Ruschmeyer 1956; Diehl et al. 1977). The transports for both winds move down the Minnesota shore from Silver Bay towards Duluth. For westerly winds, Figure 4, the pattern shows a broad turn around between Knife River and Duluth. Thus, the surface contaminants from Silver Bay would be normally transported away from the shore in this region of the lake. Westerly winds produce a counterclockwise circultion cell in the extreme western Lake Superior west of a line from Sand Island to Silver Bay (Ruschmeyer 1956). The transport pattern for easterly winds, Figure 5, is quite different. For easterly winds the cell-like structure disappears. Figure 5 shows transports following the Minnesota shore all the way from Silver Bay to Duluth. For easterly winds the magnitude of currents along Minnesota shore ranges from 6 - 30 cm/sec, averaging at 10 cm/sec. One would thus anticipate for the event modeled here, that the tailings caught in the turbulence at the onset of the high winds on November 10 would be transported from Silver Bay for a distance of about 30 km to the vicinity of Two Harbors by the time of the satellite overpass on November 14. This was indeed the case, Figure 6.

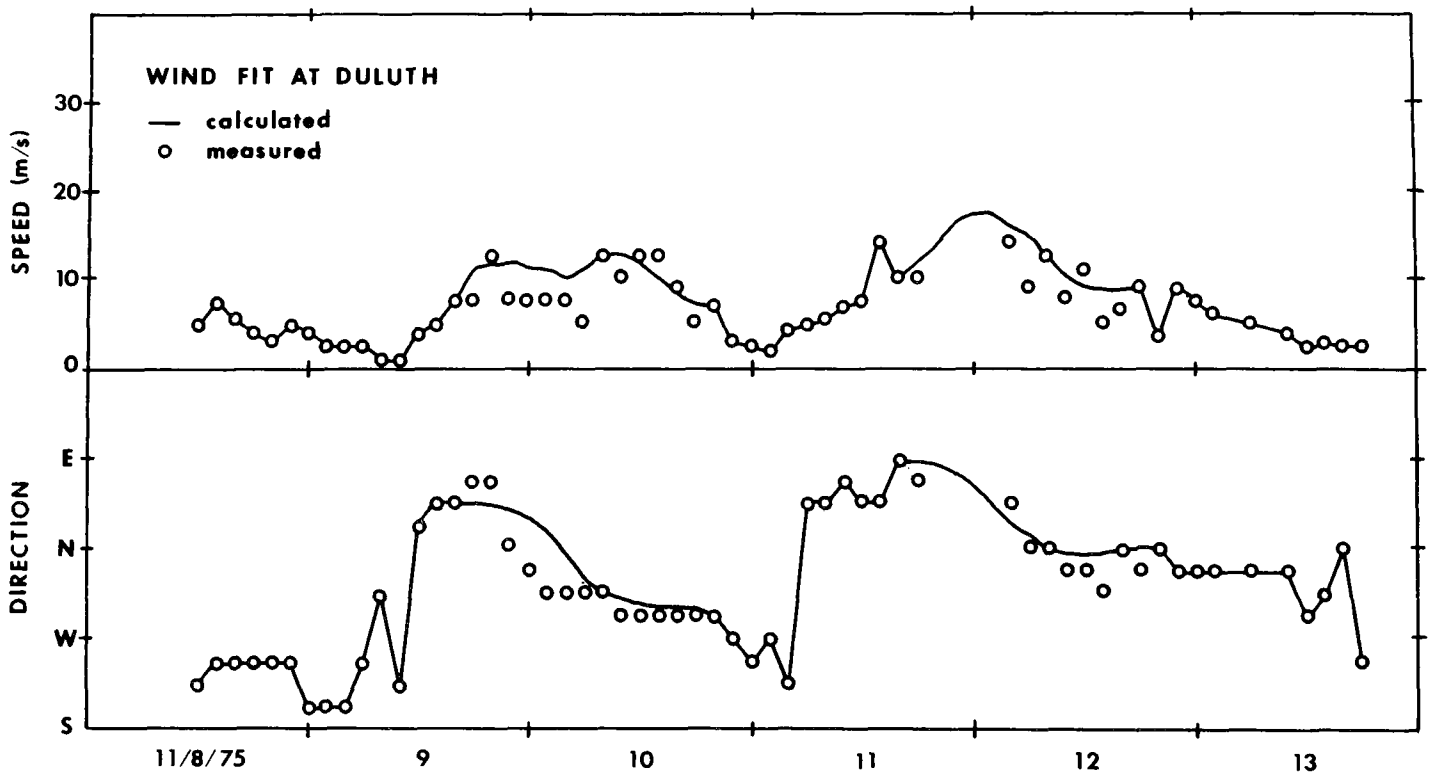

Figure 2. Comparison at Duluth of the measured winds and wind function used for modeling of Lake Superior for the November 1975 storm.

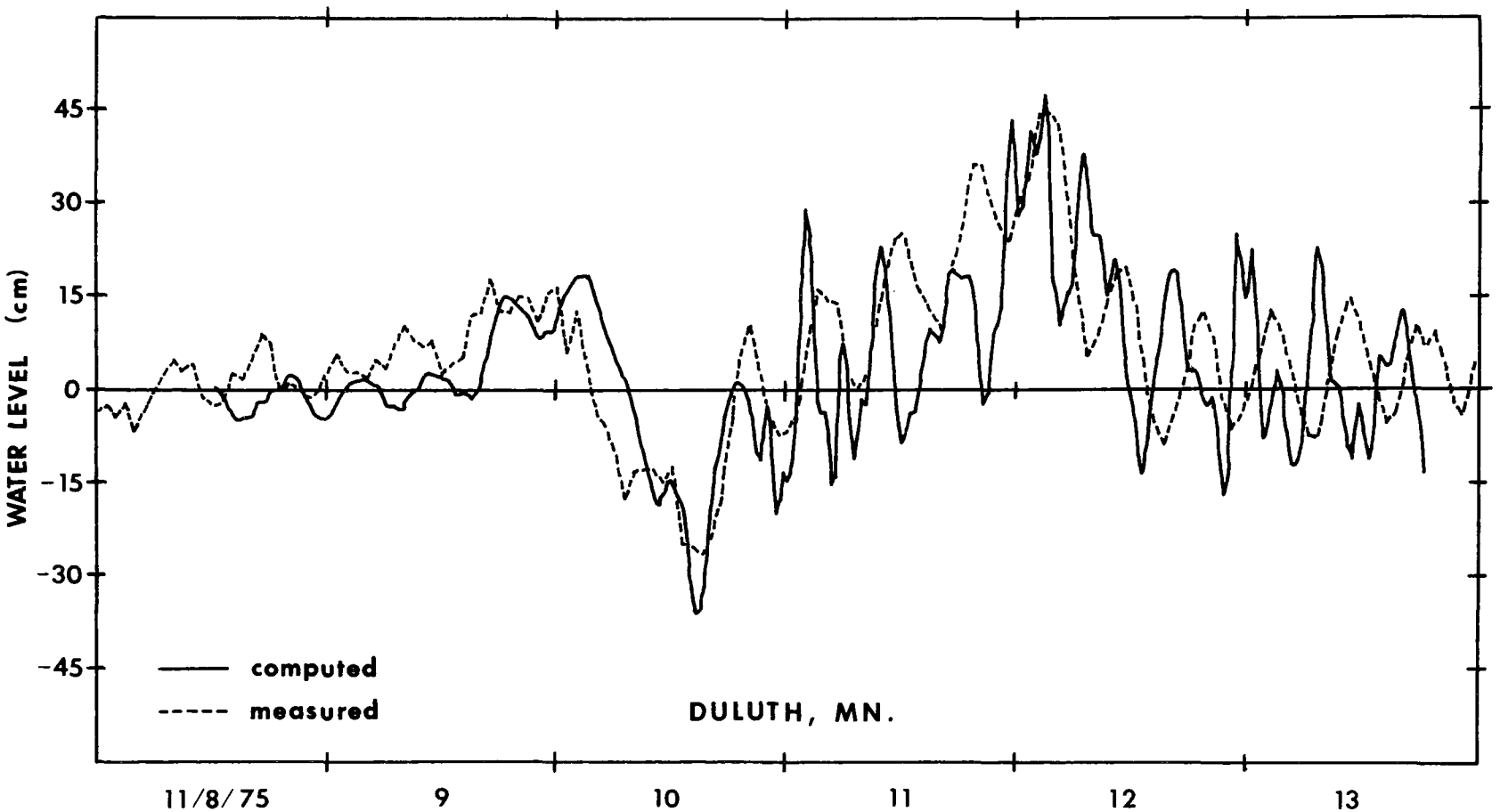

Figure 3. Comparison at Duluth of the measured water level fluctuations with the fluctuations derived from the numerical model of Lake Superior for the November 1975 storm wind.

TABLE 1. COMPARISON OF CURRENTS NEAR DULUTH

Conditions	Wind Speed M/S	Wind Dir.	Currents Speed CM/S	Currents Dir.	Date	Time
Simulated North-easterly	12	NE	13.2	224°	11/10/75	0400
	10-11.5	NE	13.6	226°	4/3/76	1600
	17	NE	20.2	230°	11/13/75	0200
	15	NE	19.2	221°	Composite	
Measured North-easterly	10-11.5	NE	21.1	243°	10/24/73	0800
	13	NE	17.5	225°	11/13/73	0400
Simulated Westerly	13	WNW	1.5	50°	Composite	
	13	NW	2.7	49°	11/11/75	0600
Measured Westerly	13	WNW	3.1	30°	10/26/73	0000

Measured currents at 18 m depth at Duluth intake in Lake Superior.

Calculated current at grid 3 average depth 24 m at grid center 3 km from Duluth intake.

TABLE 2. COMPARISON OF CURRENTS NEAR SILVER BAY

Conditions	Wind Speed M/S	Wind Dir.	Currents Speed CM/S	Currents Dir.	Date	Time
Simulated North-easterly	15	NE	5	243°	Composite	40 hrs
	17.5	NE	9.7	236°	11/13/75	0200
Measured North-easterly	10	NE	5.3	210°	9/18/72	30 hrs
			4-7.4	160-255°	October	
Simulated Westerly	13	NW	3.6	234°	11/11/75	1800
	8	NW	1.6	226°	3/31/76	0200
Measured Westerly	11	WNW	7.8	243°	10/8/72	1400
	11	WNW	8	229°	10/14/72	1600

Measured currents 8 km from Silver Bay every 1/2 hour at 3 depths (15 m, 46 m, 191 m) time averaged over 4 hours were used to determine the depth integrated flow speed.

Calculated current 12 km southwest from Silver Bay at grid center 14 average depth 175 m.

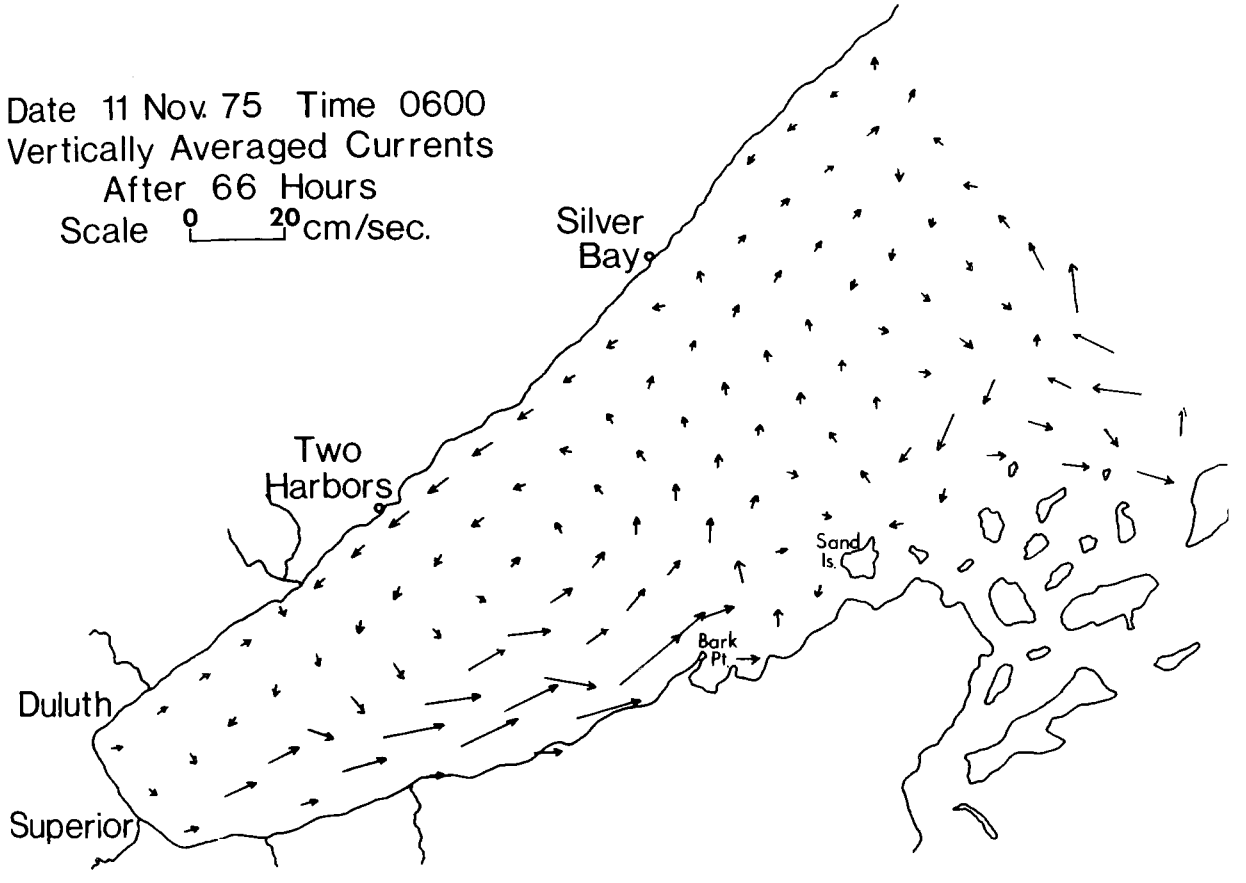

Figure 4. Water transports due to westerly wind stress. A circulation cell which forms for the westerly winds is responsible for entrapment of pollutants and subsequent increased biological productivity in this region of the lake.

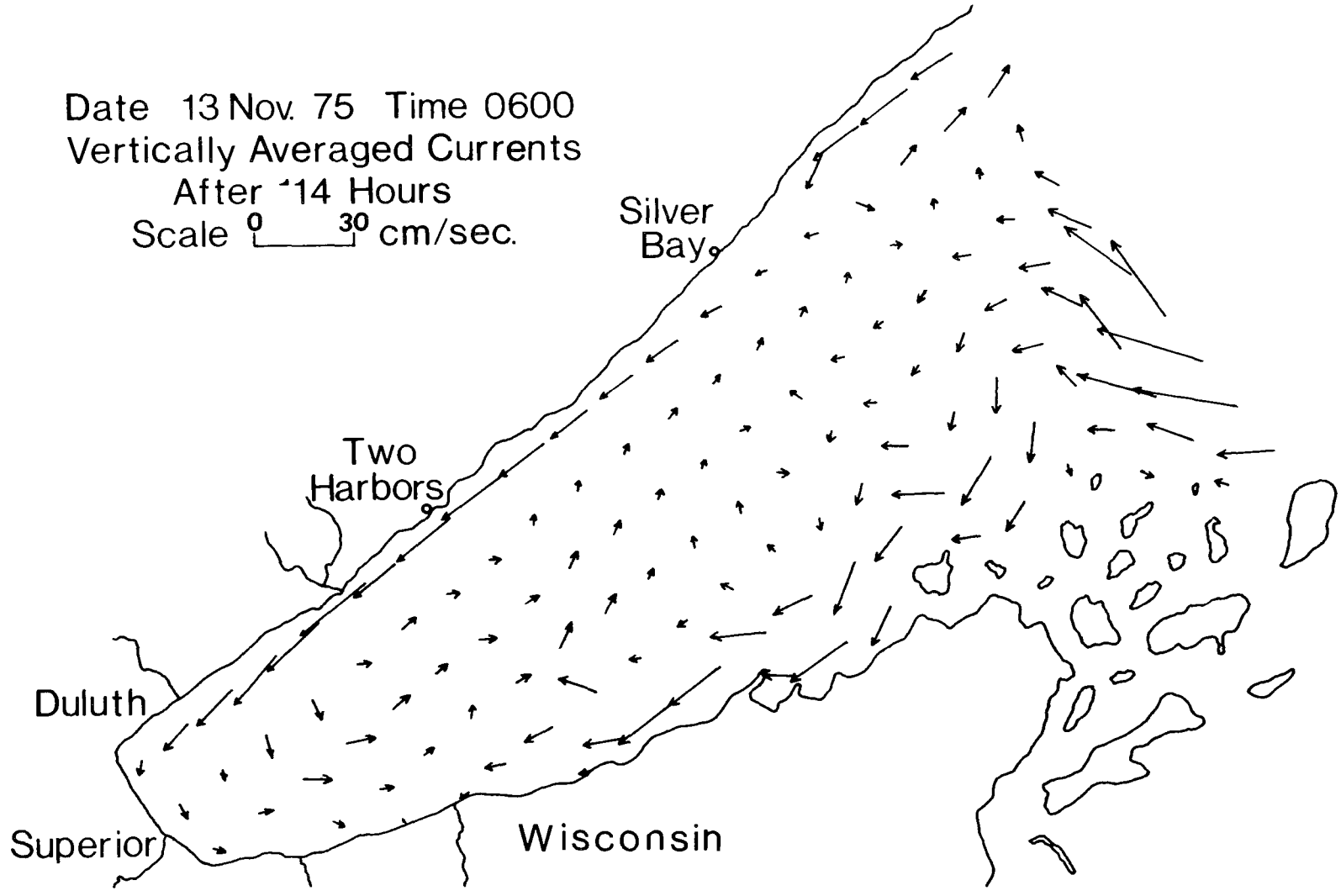

Figure 5. Calculated transports for November 13, 1975 showing water movement for high fetch northeasterly winds. For northeasterly winds tailings discharged at Silver Bay are transported directly to Duluth. Note that for easterly winds the transports along the Wisconsin shore also bring turbidity to the Duluth area. (See the corresponding pattern for distribution of suspended solids in Figure 8).

To compare the dimensions and the concentrations of the observed plume with predicted transport of tailings, the turbidity plume itself was modeled. The discharge of tailings is a slurry which takes most of the tailings down in a density current to the bottom of the lake. However, some tailings are stripped off from the density current to form a turbidity plume. To simulate the dispersal of the turbidity plume, transports had to be approximated on much finer grid scale. The grid size used in the calculation of transports had to be subdivided to the dimensions compatible with representation of the mixing processes (Csanady 1973, Galloway 1977). The original 6 x 6 kilometer grid used in calculation of transport was thus subdivided in the dispersion model into 0.6 x 1 km subgrids, a size comparable to transport lengths per half hour integration time step used in the turbidity dispersion model. The currents at the subgrids were obtained by interpolation of currents found in the transport model. Near the shore the tangential currents were held constant and the normal currents were terminated linearly to zero.

In each subgrid of the dispersion model the residual suspended load brought in by the currents and diffusion was completely mixed every half hour. A diffusivity of 1 m^2/sec was used (Orlob 1959). Since the currents were largely responsible for the transport of the suspended load, the differential scheme for turbidity dispersion was essentially first order in the temporal and spatial coordinates and no problems with convergence or stability occurred. Numerical mixing method accentuates the diffusion of the source, and introduces distortion due to preferential spreading of the leading edge of the plume. Thus, the calculated plume overestimated the actual plume length. To minimize this problem and to assure stability the upstream suspended solids concentration gradients were used for calculation of new concentrations at each grid, however, even with optimum time step slight skewing of the concentrations was expected in the calculated plume. The center of mass of the simulated plume was, however, transported properly. The advantage of using the finite difference method for calculation of dispersal of turbidity comes from the ease of calculation and low machine time cost.

In simulation of the November 14 plume at Silver Bay, the source of the fine particulates was approximated by taking 3% of the 67,000 tons/day discharge as the fraction of fines which would escape the density current under storm conditions (Glass 1973). This approximation appeared reasonable upon comparison of the actual and the simulated concentrations of the suspended solids within the plume. An equilibrium concentration of tailings amounting to 10,000 tons of fines distributed uniformly over a .6 km^2 grid located at the source was taken as the initial boundary condition. The resulting simulated plume, Figure 6, compares well with the turbidities found from sampling measurements near Two Harbors, Figure 7, and the distribution of turbidity, Figure 8, derived from the relationship shown in Figure 7 and Landsat data for November 14, 1975. Many plumes observed in Landsat imagery for Silver Bay show similar characteristics. The remote sensing data generally verify the transport patterns exhibited by the numerical model and agree with the distribution of suspended particulates predicted by the dispersion model over a period of several days. One can thus expect the numerical methods to yield reasonable results for longer term dispersal, say over a

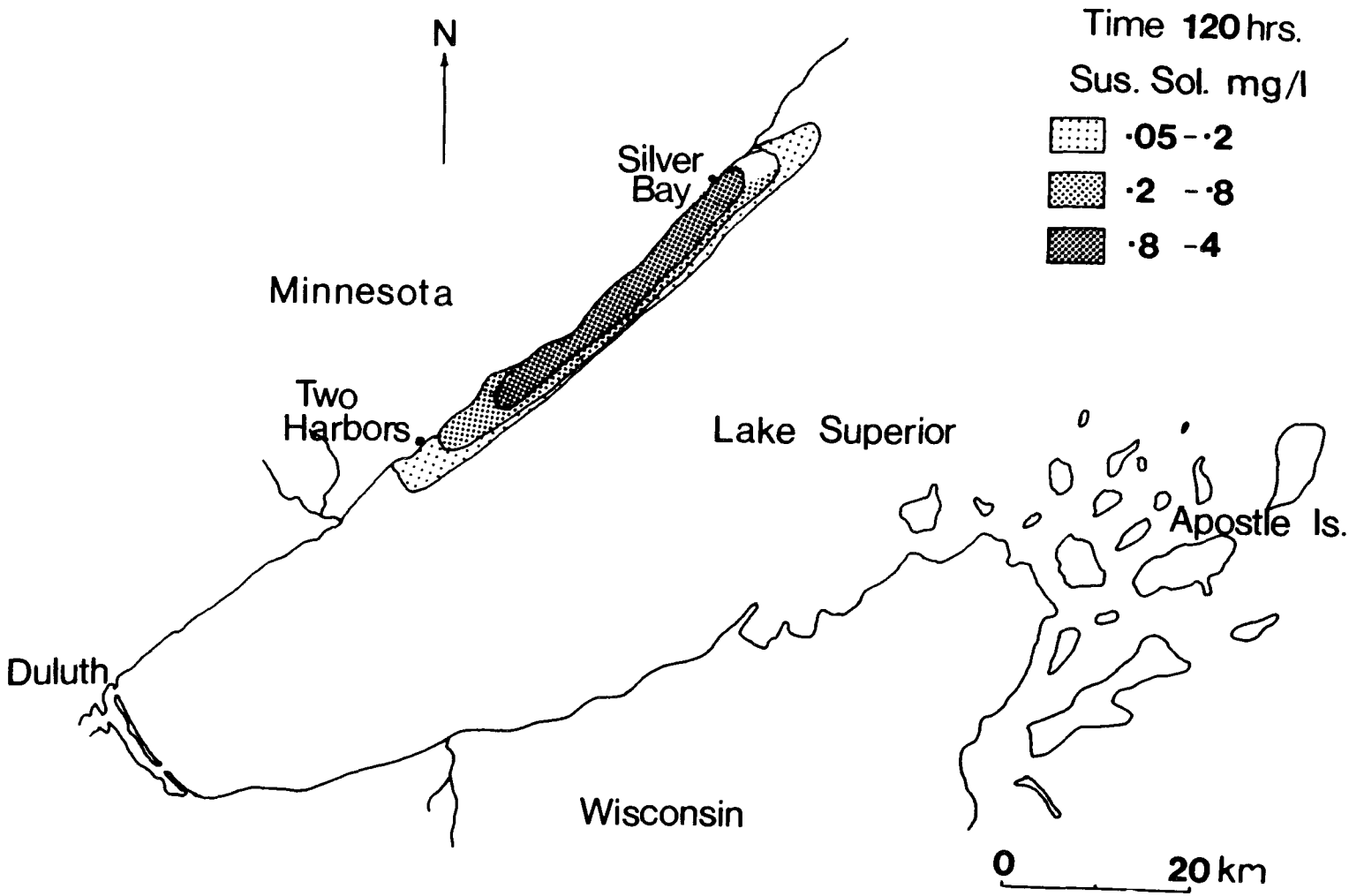

Figure 6. Numerical simulation of the plume of mining waste from point source at Silver Bay, Minnesota. The plume represents the dispersal of 3% of suspended solids stripped off from the discharge slurry.

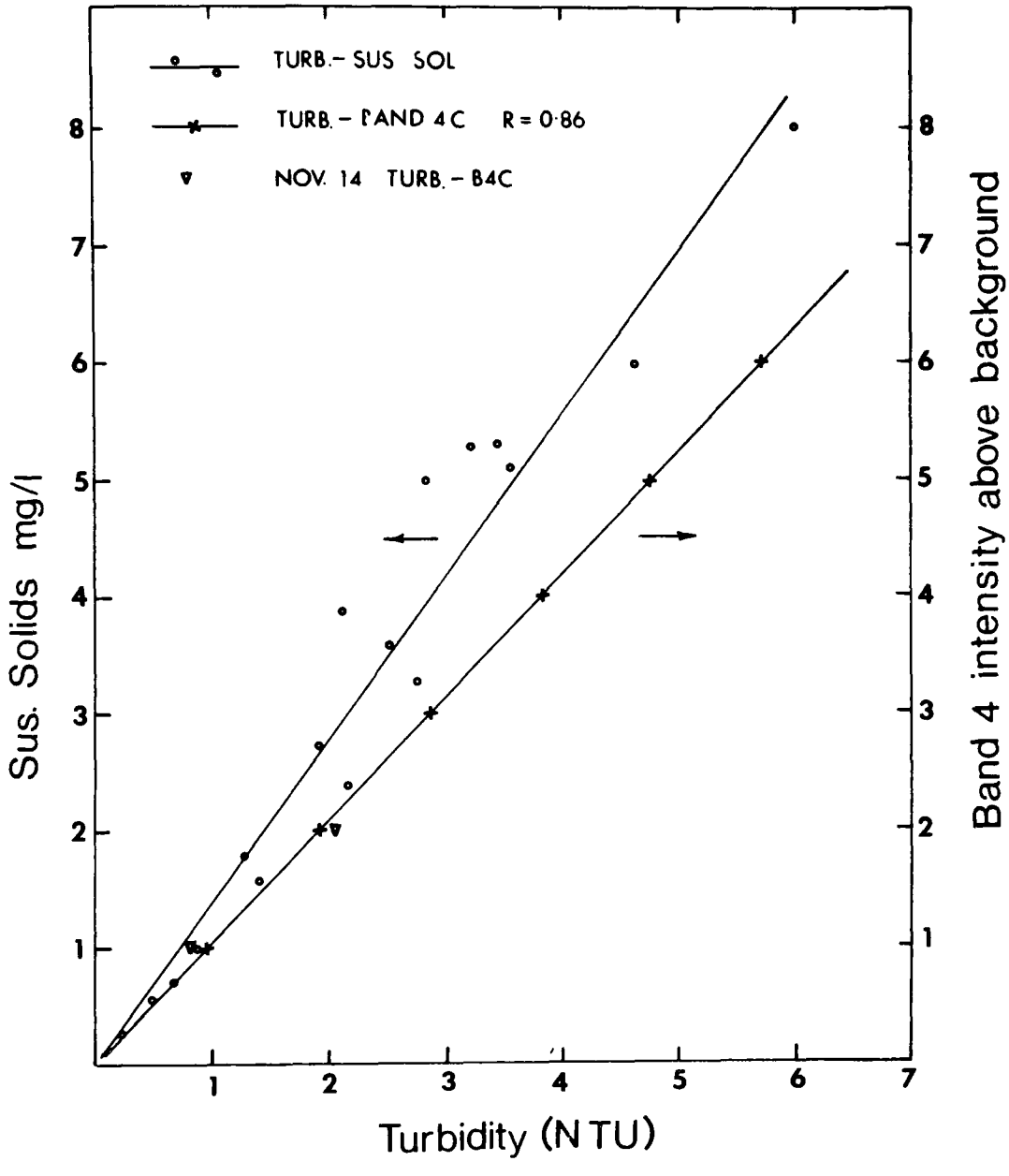

Figure 7. Turbidity vs. Landsat Band 4 intensity above background. Measured values of suspended solids for November 14 near Two Harbors are indicated by the open triangles. This relationship used in conjunction with Landsat data allows for derivation of the distribution of surface concentrations of suspended solids in Lake Superior.

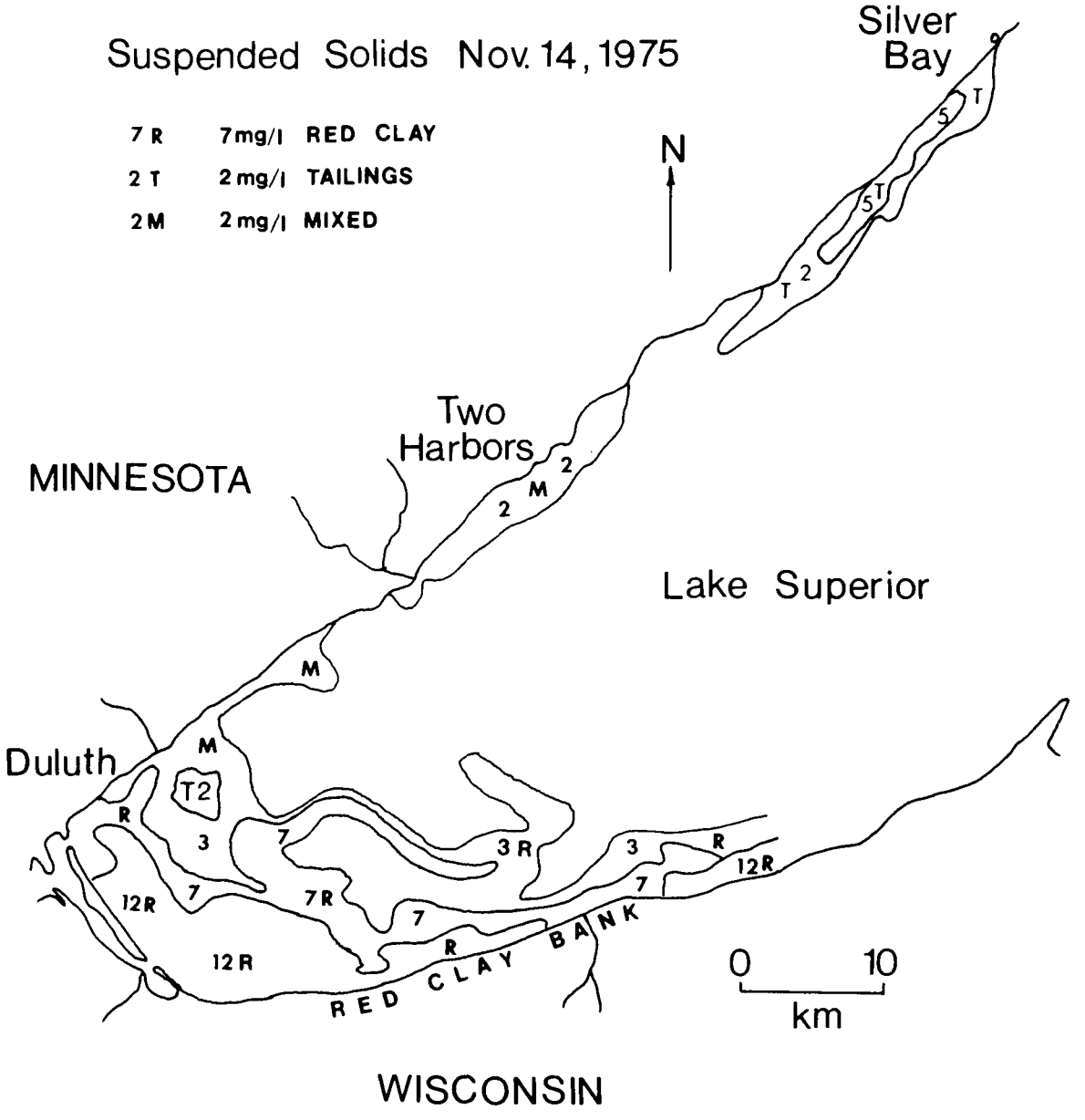

Figure 8. Turbidity plume derived from Landsat data for November 14, 1975. Particulate concentrations and type are marked by numbers, (mg/ℓ) and letters respectively; where R - red clay, T - tailings, M - mixed red clay tailings. Note the red clay originating from erosion along the Wisconsin shore is transported towards Duluth, and is subsequently taken out in a narrow plume along the center axis of the lake. (See reference 4).

couple of weeks. Starting with the turbidity distribution observed on November 14, 1975 as the initial condition, plume dispersal calculation was extended over a period of two weeks, a time sufficient for the transport of the center of mass of the plume to Duluth. After two weeks of simulation time the model produced concentrations of tailings near Duluth ranging around 0.2 mg/ℓ, a background concentration typically found at the Duluth water intake. It is therefore unlikely that direct transport of large tailings plumes from Silver Bay to Duluth could produce concentrations of tailings near Duluth in excess of 1 mg/ℓ, a value necessary to explain high momentary concentrations of amphibole fibers at the Duluth intake shortly after a passage of high easterly winds (Cook 1974).

As mentioned before, satellite data can be used to identify the type of particulates in the lake based on the spectral dependence of the volume reflectance of suspended solids (Sydor 1978). Using the signature given in Table 3 for tailings and red clay, we obtain a classification of the tur-

TABLE 3. BAND COMBINATIONS FOR SIGNATURE CLASSIFICATION OF CONTAMINANTS

Contaminant		Band Combinations	
Red Clay	(Landsat 1)	$(B_4-B_5) < 0$ $(B_4-B_6)/(B_5-B_6) < 1$	$(B_5-B_6) > 1$
	(Landsat 2)	$(B_4-B_5) < 1$ $(B_4-B_6)/(B_5-B_6) \leq 1\ 2$	$(B_5-B_6) > 1$
Tailings		$(B_4-B_5) > 0$ $(B_4-B_5)/(B_5-B_6) \geq 1{\cdot}5$	$(B_4/B_5) \geq 1{\cdot}5$
Tannin		$(B_4-B_5) \leq -2$ $(B_4/B_5) \leq 0{\cdot}6$	$(B_4-B_6) \leq -2$

B_4 - Band 4 signal intensity above the clear water background.

bidities observed in the November 14, 1975 image. The results are shown in Figure 8. It can be seen that the turbidity plume at Silver Bay and a turbidity patch near Duluth are identified as tailings. The origin of the plume has been already discussed. The area of tailings near Duluth appears to have resulted from an upwelling produced by onset of westerly winds on November 10 and 11. Unfortunately the ground truth data at Duluth intake does not show a pronounced peak for tailings. This could be largely due to the presence of high turbidity background due to intrusion of red clay.

To consider a clear possibility of upwelling of tailing we examine data for June 26 - July 3, 1973 when high concentration of tailings was observed in the Duluth area, but when winds were predominately northwesterly and no turbidity plume was evident near Silver Bay. Suspended solids and currents were monitored for those dates. Landsat images for July 2 and 3, 1973 show that red clay turbidity was confined to the Wisconsin shore so that the

identification of suspended solids would be largely confined to turbidity due to single contaminant type rather than a mixture of contaminants as was the case for November 14, 1975 when ambiguities in identification in ground truth and satellite data could arise for the mixtures of suspended solids. The July images, Figure 9, show distinct patches of tailings with concentrations of 3 mg/ℓ. The patches are well down stream from the Silver Bay discharge source. The patches occurred after prolonged westerly-northwesterly winds on June 26-30, 1973. Easterly winds over the lake were observed on July 1, 1973, and the currents along Minnesota shore were directed on July 1 towards Duluth (Keillor 1976). The easterly winds on July 1 were insufficient to produce large plumes at Silver Bay. On July 2 and 3 the winds returned to westerly directions. The background concentration of suspended solids along the Minnesota coast was 0.9 mg/ℓ. The records at the Duluth water intake (Cook et al. 1974) showed a pulse of tailings in excess of 3 mg/ℓ, confirming the tailing patch detected in the satellite data. Comparison of the successive positions of the discrete tailings patches for the consecutive July 2 and 3 images verify the circulating transports for westerly winds. The currents observed for July 1-3, 1973 (Keillor 1976) also support the transport patterns predicted by the numerical model.

Thus high concentration of tailings found at the Duluth water intake appear to arise from discrete patches of tailings upwelled from lake bottom during the westerly winds. The material taken down with the discharge slurry at Silver Bay remains unconsolidated at the bottom of the lake trough and extends over a long stretch of the valley from Silver Bay to Two Harbors. This unconsolidated material forms at the rising slope of the trough a secondary source of tailings close to the Duluth water intake. At times of turbulence the material is readily resuspended and upwells with passage of westerly winds. A following spell of easterly wind transports the material to the Duluth water intake. The direct turbidity plume at densities in excess of 1 mg/ℓ appear confined to the vicinity of Silver Bay. The plumes generally disperse below 0.2 mg/ℓ level by the time they reach Duluth.

REFERENCES

Baumgartner, D.J., W.F. Rittall, G.R. Ditsworth, and A.M. Teeter. 1973. Investigation of pollution in western Lake Superior due to discharge of mine tailings, Data Report 1971. Pacific Northwest Environmental Research Laboratory Working Paper No. 10. In Studies Regarding the Effect of the Reserve Mining Company Discharge on Lake Superior. USEPA, Washington, D.C. p. 423.

Csanady, G.T. 1973. Turbulent Diffusion in the Environment. Boston: D. Reidel.

Cook, P.M., G.E. Glass, and J.H. Tucker. 1974. Asbestiform amphibole minerals: Detection and measurement of high concentrations in municipal water supplies, Science, 185, 853.

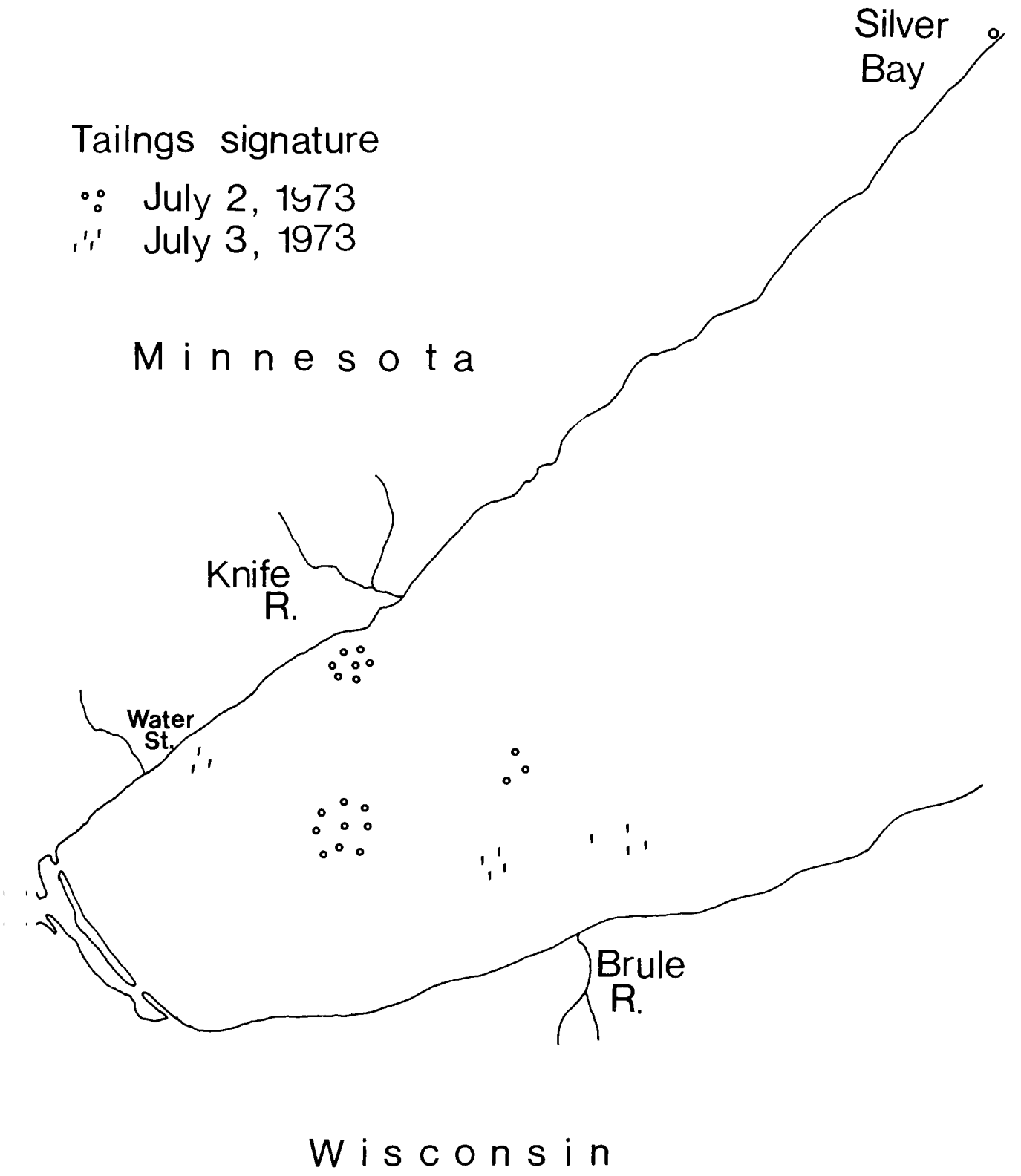

Figure 9. Discrete patches of upwelled tailings observed in Landsat data for July 2 and 3, 1973. The material upwelled during westerly winds was responsible for a high influx of tailings to the Duluth water supply. The influx usually occurs when the winds shift from westerly to easterly directions causing the transport of the upwelled tailings to Duluth.

Diehl, S.R., W.E. Maanum, T.F. Jordan, and M. Sydor. 1977. Transports in Lake Superior. J. Geophys. Res. 82(6): 977-79.

Galloway, F.M., Jr. and S.J. Vakil. 1977. Criteria for the use of vertical averaging in Great Lakes dispersion models. J. Great Lakes Res. 3(1-2): 20-28.

Glass, G.E. 1973. A study of western Lake Superior: Surface sediments, interstitial water and exchange of dissolved components across the water-sediment interface. In Studies Regarding the Effect of the Reserve Mining Company Discharge on Lake Superior. USEPA, Washington, D.C. p. 1034.

Keillor, J.P., J. Young, and R.A. Ragotzkie. 1976. An assessment of the environmental effects of dredged material disposal in Lake Superior, Marine Studies Center, Univ. of Wisconsin, Madison Publication, 4, 79, 91.

Leendertse, J.J. 1967. Aspects of a computational model for long period water wave propagation, Memo R.M. 5294-PR, Rand Corp., Santa Monica, California.

Maanum, W.E. 1977. Numerical prediction of currents and transport in western Lake Superior, Thesis, Univ. of Minnesota.

Mortimer, C.H. and E.J. Fee. 1976. Free surface oscillations and tides of Lake Michigan and Superior. Phil. Trans. R. Soc., London A., 281, 1-61.

Orlob, G.T. 1959. Eddy diffusion in homogenous turbulence. J. of Hydraulics Division, ASEC 1149. pp. 75-101.

Ruschmeyer, O.R. and T.A. Olson. 1958. Water movements and temperatures of western Lake Superior. Univ. of Minnesota School of Public Health, Minneapolis Publication.

Sydor, M., K.R. Stortz, and W.R. Swain. 1978. Identification of contaminant in Lake Superior through Landsat I data. J. Great Lakes Res. 4(2): 142-148.

Sydor, M. 1978. Analysis of suspended solids in lakes through use of Landsat data. J. Canadian Spectroscopy. 2(3): 91.

SECTION 11

PRINCIPLE OF ORGANIZATION OF AN AUTOMATED INFORMATION SYSTEM

V.L. Pavelko[1]

The tasks of control of environmental quality are both local and global in nature. They range from the study of individual objects or even parts of objects to planetary tasks, from evaluation of states in a narrow time section to historical scale, from an individual process at some single trophic level to an ecologic environmental system. This directly requires that large volumes of both basic and supplementary information be processed, and that large amounts of combinations of various data be processed. All of this requires the use of computers. A step beyond this level is the construction and study of ecologic mathematical models which is in and of itself a very cumbersome procedure, impossible without computers.

Therefore, a major problem of testing and control of the status of the environment is the creation of an automated information system for water quality (AIS) as a section of a more general ecologic information system.

The flow of information determines the external conditions of existence of the processes which we are studying. These, in turn, define the function of the source of a pollutant and are a response to the condition of water objects, and will be referred to as accompanying flows. These flows of information are related to hydrochemical subjects as follows:

1. "External conditions" - hydrologic flow (discharge, speed and direction of currents, water temperature); meteorology (precipitation, solar radiation, direction and speed of the wind); hydrobiologic data (the self-purifying capability of rivers), etc.;

2. "Source function" - data on waste waters, pollution of the atmosphere and soil, hydrogeologic data, data on intentional and natural sedimentation, burial of pollutants (in cases of secondary chemical pollution), hydrobiologic characteristics (in connection with eutrophication, oxygen starvation, etc.);

[1]Hydrochemical Institute, 192/3 Stachky Prospect, 344090 Rostov-on-Don, USSR.

3. "Response" - sanitary-hygienic data, hydrobiologic, ichthyologic data, data on industrial water use, marine hydrochemistry, etc.

Many of these flows were used in AIS which had been created before the hydrochemistry AIS. Therefore, the results were analyzed and compilation of the best achievements were made, in order to minimize the time required to translate the data banks created from one system of coding and indexing to another for purposes of merging the streams of information in various research programs.

This is equally true of the realization of various programs based on the hydrochemical branch in question. For example, in the USSR, the stream of hydrochemical information includes a subsystem in the nationwide service of observation and testing of the level of pollution (OGSNK), the State Water Cadastre (GVK), the State Water Report (GUB) and the Global Monitoring System (GSMOS).

The principles which were used in the creation of AIS-hydrochemistry system are summarized below. Included are some of the results obtained, which are recommended as principles for the creation of a global monitoring AIS, which it is expected will ultimately include all nations, including, the USSR and the USA.

1. According to estimates, there are 2-5 million polluting substances in the water, of which over 500 are toxic. (Maximum allowable concentration values having been established for them). It is estimated that polluting substances increase annually by about 20,000 compounds. Approximately 100 of these are determined by manual methods. However, the annual increase in analytical capabilities for these substances is only 4-10.

   Some 10-15 components are able to be automatically determined, and the annual increase in the number of such determinations is about one. Therefore, as information is collected, for the immediate future, GSMOS should be oriented to 100-300 water quality components, determined basically in stationary and mobile laboratories.

   Result: 1.1 Hydrochemical codes containing the names of components, regardless of taxonomy, should have a capacity of up to 300 units (V.V. Tarasov 1971, 1974).

   Result: 1.2 Forms must be developed for recording of information obtained primarily manually. The forms should be adapted to manual and automatic punching.

2. Manual punching is a labor-consuming stage of automated data processing systems, the source of various errors, and the reason for a severe decrease in the timeliness of automated information systems. Therefore, the volume of punching should be greatly minimized without reducing the information content of the data entered in the computer.

Information is universally suitable for the solution of various estimates, predictions and other tasks, if the initially processed data and the results of analysis are stored in a computer. The storage of more generalized characteristics prevents the performance of a number of tasks. Minimization of the volumes of information to be punched and stored should be achieved by classification and formal methods of reduction.

3. The classes used might be: results of analysis $[x_i]$ and the corresponding characteristics $[d_{ij}]$. The results of analysis x_i can be divided into groups: principal ions, gas composition, heavy metals, oil and petroleum products, fertilizers, toxic substances, etc. Preliminary subdivision into nondegradable and degradable (self-purifying) substances may also be made. There are other classifications--as to type of effect (organoleptic, persistent, toxic, etc.); type of biota on which the substance acts, etc. However, these classifications are not of particular interest for the planning of the AIS, since it is desirable to store all results of analysis of an individual sample together. Combining storage, search, and processing, though it increases the cumbersomeness of the machine procedure involved, greatly increases the information content (both formal and inductive) of estimates of the status (effect of completeness of results analyzed).

   The characteristics $[d_{ij}]$ should be divided into constant and variable. The corresponding class characteristics can be noted in service labels. Permanent characteristics include the name of the body of water, region, nearby town, etc. Variable characteristics include the list of observed components, date and depth of sampling, etc. Permanent characteristics should be recorded in computer memory once in the form of a catalogue of permanent characteristics (CPC), significantly minimizing the amount of punching which must be done.

   Variable characteristics should be coded in the form of numbers and stored together with the numerical results of analysis. The composition and taxonomy of the characteristic depend on the type of task to be performed which required their determination in the first place. For example, if the output result from GSMOS is a prediction of the pollution of water through the atmosphere locally (within the limits of a region) in a time cross section, the characteristics used include only the names of chemical substances subject to atmospheric transfer and the accompanying meteorologic characteristics. If the purpose of the model of atmospheric transfer is the spatial distribution of pollutants, we must also know the geographic coordinates of the points.

   If the self-purifying capability of a body of water in a preserve is studied, we must know the names of virtually all of the hydrochemical and hydrobiologic characteristics, and such secondary characteristics as water temperature, speed of current, etc. The characteristics in the CPC might include landscape zones, characteristics of the climate, underlying soils and rocks, altitude above sea level and other characteristics which depend on the task to be performed using the data collected.

4. Characteristics have various weights (Gaussian distribution). An error in storage or recording of one characteristic leads to an error in the interpretation of an individual word or small group of words, while an error in another characteristic might result in the introduction of errors to a large data file. For example, an error in the code "petroleum products" might cause a given concentration for a given date to be omitted not only from petroleum products, but also from all other headings. An error in the entry indicating the year of observation would cause the loss of all observations for the entire year (they could not be retrieved according to the characteristic of the year). Therefore, the data storage unit must include a code protection system, the reliability of which should be directly dependent on the weight of each characteristic.

5. Various hydrochemical components have different precision in terms of methods of analysis and natural variability. Therefore, the same frequency of observations leads to different errors in reflection of natural trends from the observations (a space-time resolution of an observation system which is uniform with respect to all observed components becomes nonuniform). This requires that as the observation system is planned, various data reading intervals be assigned, leading to observations of equal accuracy. This step simplifies their processing and assures the highest reliability of output materials with the minimum cost of observation. However, the varying frequencies of observations of different components leads to the situation that each sampling date generates a different list of observed components. This does not allow a rigid model to be used to record the results of observations.

   For diffusion systems, it is more economical to record the results of observations $[x_i]$ together with the variable characteristics $[d_{ij}]$ in the form of a polynomial:

$$T = d_1 d_2 d_3 \ldots x_1 + d_1' d_2' d_3' \ldots x_2 + d_1'' d_2'' d_3'' \ldots x_3 + \ldots,$$

   which can be subjected to various convolutions.

6. The first convolution is that the characteristics $[d_{ij}]$ are removed from the brackets, e.g., as follows:

$$T = d_2^k (d_3^\ell (d_1 x_1 + d_1' x_2 + \ldots) + d^{\ell+1} (d_1^m x_1' + d^{m+1} x_2' + \ldots) \ldots).$$

   This means in practice that for a given sampling data (d_1), it is possible to record all the results of analysis of samples taken on this date, without repeating the date next to each determination. The set of data for a certain observation year ($[x_i]$) may have a single notation d_3 in the observation file header for the year. The file of data for the entire period of observation for a given biologic observation station may have a single header--the station code d_2, etc. Obviously, each information branch and each observation program should have its own code.

These convolutions may not achieve the global minimum of the volume of data stored, since one criterion used in data reduction is convenience of retrieval of the data necessary for performance of the main tasks.

Result: 6.1 To optimize decision making in the creation of a monitoring AIS, technical requirements must be placed on the GSMOS materials in terms of reliability, completeness, timeliness, need, etc.

7. In reduction of characteristics, the names of hydrochemical components require that a semi-rigid entry standard is used. The form carries the results of analysis of not one, but a large number of samples; the names of the components determined are entered into the head of the form so that each form has a rigidly defined list of components, but the heads of two different forms are nearly always different. This allows the entry of one row of characteristics d, d', d", ..., for the entire matrix (n x N) of data, where n is the number of components in a sample, and N is the number of samples. Secondly, binary coding is used to index the names of the components defined (Tarasov 1971). The essence of binary coding is that a list of names of hydrochemical components is developed. They are assigned codes in the following sequence.

1, 2, 4, 10, 20, 40, 100, 200, 400, 1000, 2000, 4000...

The results of analysis are entered into the forms in accordance with this list, while the codes are summed and a so-called code row is thus developed.

Example. Lists of components and their codes

Oxygen	1
BOD_5	2
Petroleum products	4
Phenols	10
Surfactants	20
NH_4	40
NO_3	100
NO_2	200
DDT	400
HCCH	1000
Cl	2000
Cu	4000
Zn	10000
Ni	20000

If the form contains:

				Sample				
	O_2	BOD_5	Phen	NH_4	NO_3	NO_2	DDT	Cl
1	x	x	-	x	x	x	x	-
2	x	x	x	x	x	x	-	x
3	-	x	x	x	x	x	-	x
. . .	. . .	. . .	. . .	. . .	. . .	. . .	. . .	. . .
	-	x	x	-	-	-	x	x

the code row of the form consists of these names.

O_2	1
BOD_5	2
Phenols	10
NH_4	40
NO_3	100
NO_2	200
DDT	400
Cl	4000
	4753

which, after addition, yields the code 4753. This value unambiguously decodes the names of the elements in the matrix.

This coding method allows all combinations of 8 x 37 = 296 different hydrochemical components to be stored in eight 37-bit memory locations. These eight words of the code line relate to virtually 100 elements of the matrix. Therefore, where n = 30 and N = 30, the amount of memory expended in recording of variable characteristics (names of components) is a fraction of 1 percent of the volume of useful information, and thus reduces the volume of punching to less than half.

8. Since modern computer central processers operate very rapidly, while peripheral information input-output devices operate comparatively slowly, it is desirable to record only the initial quantities, producing the intermediate values in the computer by computation.

   Taken together, all of these suggestions allow the volume of information punched and stored in the computer to be reduced by approximately a factor of 12, without loss of information contents. This greatly decreases the cumbersomeness of manual operations, input-output functions, data search and retrieval operations.

9. Preparation of data for punching, the punching operation, review and correction of data may require one or two orders of magnitude more time than the actual machine processing. This requires a cautious attitude toward the organization of operations. It is suggested that the initial data be punched onto paper tape, allowing the use of a non-rigid form for recording of the initial data, and allowing transmission of data through communications channels. Since operator fatigue depends on the time of continuous work (Figure 1), it is suggested that operations be

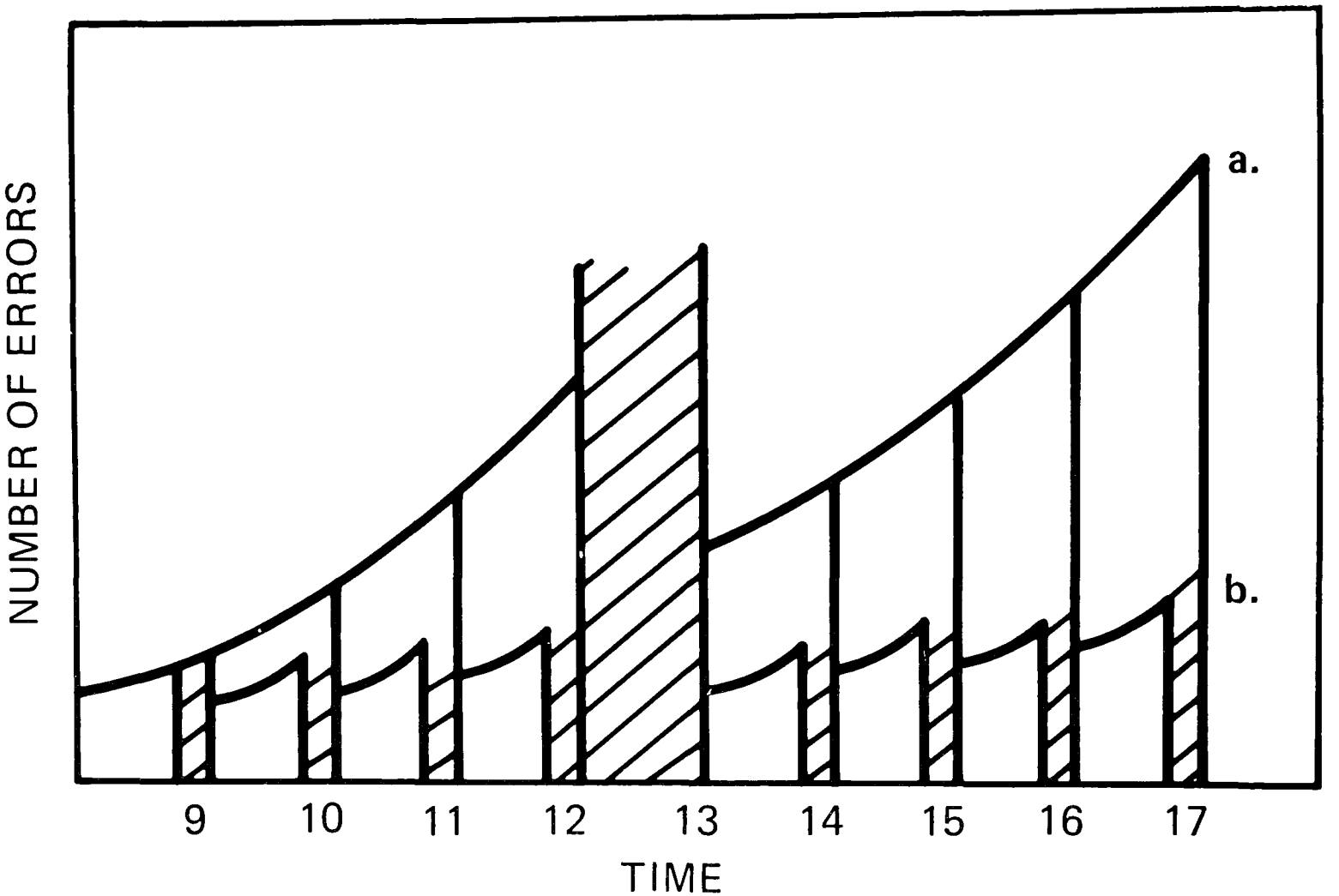

Figure 1. Variation in number of errors v with time of continuous work t. a) Work with one large break; b) Work with numerous shorter breaks.

organized according to plan "B" which reduces the number of errors significantly, and generally increases the productivity of labor.

10. Since visual testing of the results of punching using a control tape or computer printout requires intensive attention, and the reading of large numbers of correct entries unavoidably reduces attention, it is suggested that double punching be used (by two operators independently), with the punch tapes checked by the computer. If the relative number of errors for individual punching is $p = 0.5$ percent, the probability of simultaneous appearance of an error on two punched tapes in the same location is $p_1 \times p_2 = 0.000025$, while the probability of appearance of an error in the same digit of a given word and the probability that the error in this word will be identical is negligible.

    After machine verification of the two punched tapes for agreement, the technician checks only the words which disagree and gives the keypunch operator instructions for corrections of both punched tapes, after which they are tested once more.

11. Manual entry of information produced on forms, punching, and recording from the temporary information form to computer memory should be performed without preliminary sorting of data, as the results of analysis come in. This freedom levels the work load on testers, and allows the process of systematization to be automated. The short period of time between receipt of data and entry and testing of the data in the computer allows some of the erroneous results of analysis to be corrected.

12. Machine testing of information recorded in a form should include the performance of logic and calculation procedures. Logical testing checks such relationships as the number of hours (not over 24) recorded, such as the time of taking a sample, the depth of the body of water (no less than the sampling depth), equality of the sum of anions and cations, etc.

    Calculation procedures presume 1) that the results of analysis will fall within certain tolerance limits determined by retrospective examination of information, 2) that relationships between certain components will be maintained in multidimensional statistical models, and 3) that deviations from the approximating surface will be statistically heterogeneous, etc. As a result of machine testing, data are classified as false or doubtful. The flagged machine results can be conveniently printed in a form identical to the input form. A final decision as to whether data flagged by the computer are bad or good, as well as correction of some of the bad data, are the job of a hydrochemical specialist, in combination with the analytic technician who performed the analysis.

13. If nonsystematic punching of tapes is used (contents of forms), a temporary catalogue (TC) should be made, containing the label "sample" and the address of the location of the sample in peripheral storage. The TC has been used for rapid retrieval of the necessary information for

systematization of the data (according to dates, depths and sampling locations). The identifying code used to mate the information recorded and the data of the TC (and, subsequently, with the CPC) could be the sampling location, e.g., the geographic coordinates of the station, the point of a vertical line unambiguously defining the location of the point where the information was read.

14. The sampling location may have various types of tie-ins depending on the type of task being performed. For example, the geographic coordinates, the distance from the mouth of a river, the distance from local landmarks (bridge, cliff, waterfall, dock, etc.) may be used. The form should contain one type of tie-in which can be numerically expressed, e.g., geographic coordinates. The other types should be stored in the CPC (the TC and CPC should be included in the identifying code).

15. Systematization of data before long-term storage or before use can be performed by various systems. The selection of a plan for systematization depends on the type of tasks performed, which should also be included in the technical assignment for the AIS.

    The first (or main) systematization should provide for convenient performance of priority tasks. It is possible to store initial data using several models (systems), each of which is convenient for its own range of tasks. The expediency of storage using several models can be easily established by technical and economic calculations.

16. In addition to the storage of initial data, it is also possible to store summary results, if they are used for systematic performance of certain tasks. The desirability of storing files of summary data must also be determined by engineering-economic calculations.

17. To solve each class of problems, retrieval files (RF) of characteristics are formed from the CPC. Each class of tasks should correspond to its own RF. The RF also includes the necessary list of characteristics based on the model, which is oriented to the performance of a given range of tasks. All of this facilitates retrieval and processing of the necessary information.

18. Systematized data for long-term storage are standardized, equipped with service labels and stored in the form of magnetic or binary microfilm, and standardized by means of a special data description language. Models are developed using information compression techniques, leading to significant savings of machine time.

19. Processing algorithms may include:

    - estimates of states based on various lists of components (independently for each component), made up for fixed periods of observation;
    - combined estimates of states based on the entire list of observed components;
    - comparative estimates of states at various observation points;
    - determination of trends at various frequency levels of variability;

- determination of local time anomalies;
- prediction of hydrochemical states;
- a combined estimate of states for all media to be controlled;
- transfer between media;
- identification of anomalies with sources of pollution;
- combined prediction for all media tested;
- warnings of increasing pollution and the possibility of unfavorable after-effects.

These algorithms, presumed to be the purpose of organization of monitoring, are in various stages of development in the USSR.

20. The creation of the monitoring AIS requires the selection of intelligent proportions for standardization of codes, the organization of data bases, internal and external software, the class of computers used and algorithmic languages. This will determine both the success of individual units of specific subsystems of the AIS, and the effectiveness of functioning of these subsystems. Therefore, their performance is of primary significance in the task of mass production of mathematical models (both particular hydrochemical models and general ecologic models), which is the technical and theoretical basis of the problem of storage and effective utilization of the resources of the biosphere.

REFERENCES

Tarasov, V.V. 1971. One method of information storage. Tr. NIIAK, No. 77, Moscow.

Tarasov, V.V., V.V. Pugolovkin and V.L. Pavelko. 1974. Coding of information for computer storage. Ekspress-informatsiya, Obninsk, No. 4(24).

SECTION 12

A MULTI-LAYERED NESTED GRID MODEL OF LAKE SUPERIOR

G.J. Oman and M. Sydor[1]

INTRODUCTION

Lake Superior is the largest, cleanest, deepest, and coldest of the Great Lakes. The size and complex bathymetry of Lake Superior pose serious obstacles when attemping to understand lake dynamics. Numerical modeling and remote sensing provide relatively easy means of studying large bodies of water. The art of numerical modeling has developed to the point where it has been able to correctly predict large scale circulation patterns in the Great Lakes. An understanding of the physical processes occurring in Lake Superior will probably best be achieved by means of numerical modeling in conjunction with remote sensing data and direct measurements made on the lake.

A variety of numerical techniques exist for modeling large bodies of water. Several authors have attempted to assess the state of the art in numerical modeling of the Great Lakes (Lick 1976; Katz and Schwab 1976; Cheng et al. 1976). In addition, techniques used in atmospheric and oceanographic models have potential applications to the Great Lakes (Paul and Lick 1979). A review of existing three-dimensional Great Lakes models is undertaken to find an appropriate model for Lake Superior. The decision was made to first develop and verify an isothermal model before dealing with the much more difficult task of simulating stratified flows.

GREAT LAKES MODELS

Simons (1973) developed a free surface model which he used to simulate storm surges on Lake Ontario (Simons 1974, 1975, 1976) and in the Baltic Sea (Simons 1978). Katz and Schwab (1976, 1978) also used Simons' model to predict currents in Lake Michigan. The model employs grid A+B shown in Figure 1, which consists of two independent grids staggered in space and time. This grid permits use of centered differences in space and time for terms in the equations of motion which govern seiche oscillations. Since both components of velocity are defined at the same point, terms for the Coriolis force can be evaluated using centered semi-implicit time differences which

[1]Department of Physics, University of Minnesota, Duluth, Minnesota 55812.

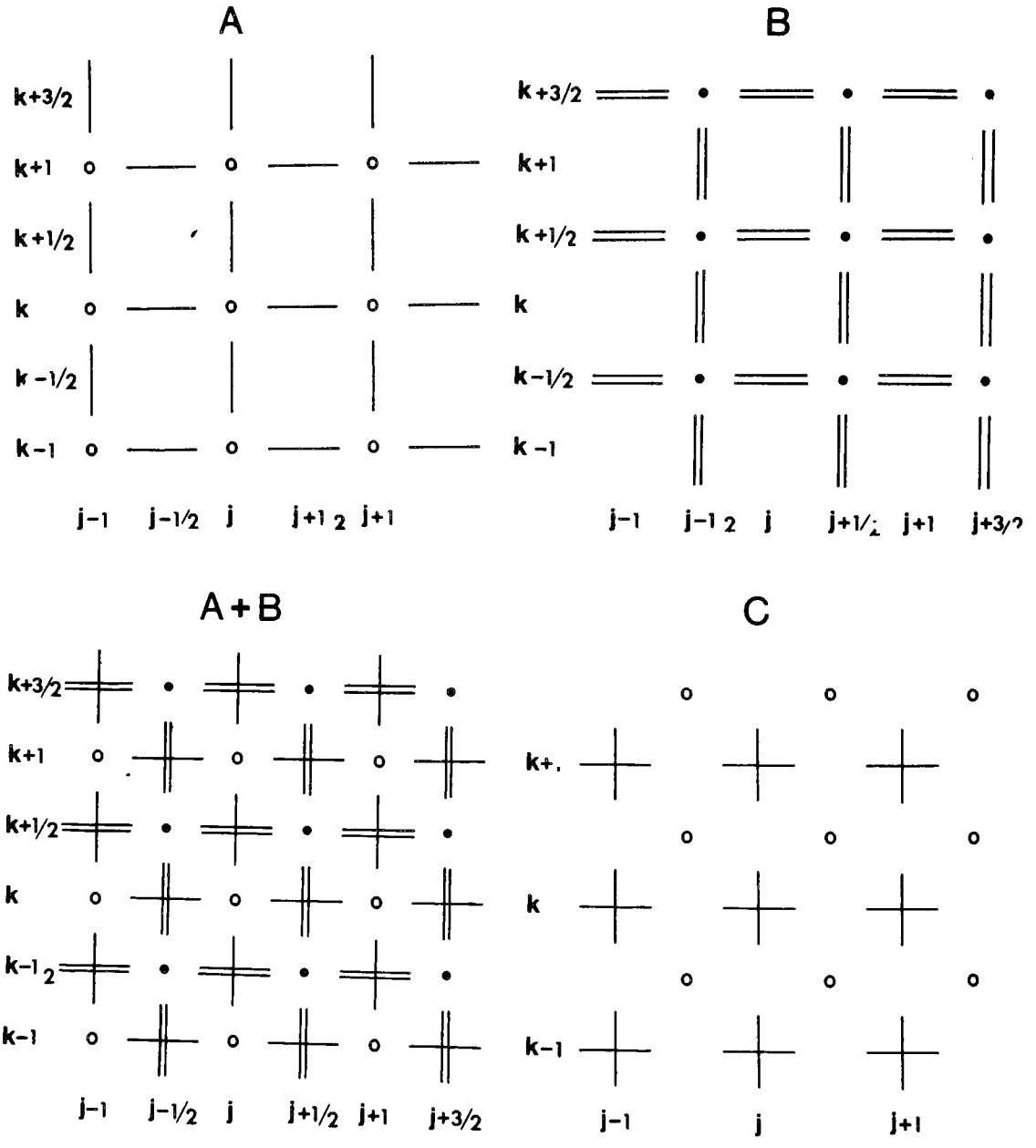

Figure 1. Grids used in various models.

assure both numerical accuracy and computational stability. Forward time differences are used for diffusion. This model permits any number of fixed permeable layers of variable thickness and may be altered to employ moveable impermeable layers.

Free surface models require very short time steps because they take into consideration fast-moving gravity waves. In Simons' model, the computation time is reduced by separating internal and external modes of oscillation. This separation is accomplished by first summing the equations of motion over the vertical axis to separate out the external gravity waves. Then, appropriate differences between layers are taken to filter out fast moving gravity waves. In this way, external gravity waves are integrated using a short time step, while internal waves which determine vertical current profiles are integrated using a much longer time step.

This model treats both inertial and seiche modes of oscillation well. Its main drawback is grid dispersion. The two solutions on subgrids A and B of Figure 1 are only weakly coupled. Because the two subgrids are staggered in space, the two nearly independent solutions provided by them may begin to differ appreciably as time progresses. This possibility appears particularly ominous for complex bathymetry.

Lick and his associates at Case Western Reserve University have developed a number of different models of lake currents (Lick 1976). Included are steady state models (Gedney and Lick 1970, 1971, 1972; Gedney et al. 1973), free surface constant density models (Sheng and Lick 1975, Sheng 1975), and rigid lid models (Paul and Prahl 1971; Paul and Lick 1973, 1974, 1975). Sheng et al. (1978) later developed an improved free surface model.

The earlier free surface model used a single horizontal grid like grid A in Figure 1. Centered space differences were used for all terms. A forward backward time differencing scheme was used in which all terms in the momentum equations were stepped forward in time and water levels were calculated using the new transports. Internal and external modes were not separated and advection of momentum was ignored. The more recent free surface model uses grid C, shown in Figure 1. Internal and external modes are separated and advection of momentum is included. This later model represents inertial and fundamental seiche oscillations well. Two point averaging is needed to calculate terms describing gravity waves. This averaging reduces the effective spatial resolution of the model and could give rise to false two grid space gravity waves. The four point averaging needed to calculate vertical velocities might also poorly represent vertical advection over complex bottom topography.

The rigid lid variable density model also employs grid C shown in Figure 1. The rigid lid condition sets the vertical velocity at the surface to zero. Although evaluation of the surface is not permitted, surface pressure is defined. Surface pressure is obtained by solving a Poisson's equation derived from cross differentiating the momentum equations and applying the rigid lid condition. Surface pressure corresponds to water level oscillations in free surface models, except that gravity waves are eliminated. The rigid lid condition, in effect, filters out gravity waves. Thus, rigid

lid models may use much longer time steps and require considerably less computation time. Sheng et al. (1978) have shown for both constant and variable winds that currents from rigid lid and free surface models display very similar long term trends.

Both the free surface and rigid lid models developed at Case Western Reserve employ the stretched coordinate system (Freeman et al. 1972). The vertical coordinate z is transformed to the sigma coordinate σ by dividing by depth. At each grid point currents are given at specified values of σ. In the transformed coordinate system, each grid point have the same depth and the same number of layers. This greatly reduces programming complexities and assures adequate vertical resolution of currents at all points. The main problems are poor resolution of surface layers in deep water and in shallow water excessively thin layers which require implicit integration of vertical diffusion.

Another rigid lid model was developed by Bennett (1977). Bennett's model employs a single grid lattice like grid A in Figure 1. The momentum equations are cross-differentiated using the rigid lid condition giving an equation for the stream function. The momentum equations are stepped forward in time, ignoring surface pressure. The new approximate currents are used to calculate a new stream function. The currents are then corrected for the neglection of surface pressure by using the new stream function. In this way, only one array is needed for the stream function and each velocity component. Since the two components of current are not defined at the same point in Bennett's grid, four point averaging was necessary to calculate the Coriolis force. This averaging gave rise to spurious inertial modes which had to be controlled using excessively high horizontal diffusion.

Kizlauskas and Katz (1974) developed a two layer model of Lake Michigan. The two layers which represent the epilimnion and hypolimnion are separated by a moveable impermeable surface. This model would only be applicable after lake stratification.

In addition to the models mentioned above, numerical techniques developed in simulating flows in estuaries, oceans, and atmospheres have potential application in the Great Lakes. In particular, semi-implicit time integration techniques (Madala and Piacsek 1977; Kwizak and Robert 1971) show promise for the Great Lakes (Paul and Lick 1979). Semi-implicit schemes are much more complicated but allow much longer time steps and produce much smoother results. With a few modifications, a three-dimensional estuary model developed by Leendertse (Leendertse et al. 1973, 1975a, 1975b) would also be applicable to the Great Lakes. This model employs two grids like grid A in Figure 1 staggered in time. A pressure gradient averaging technique used in meteorological models (Schoenstadt and Williams 1976; Brown and Campana 1978) could also be used to almost double the maximum allowable time step used in explicit, centered time integrations.

THE MODEL

In developing a numerical model of Lake Superior, a number of points had to be taken into consideration. Since model verification would be based largely upon recorded water levels and remote sensing observations of major and minor storms, a free surface model seemed more appropriate. Rigid lid models are more useful for modeling extended periods of time, i.e., several weeks or more. At the present time, such an effort would be hard to verify. The complex bathymetry and highly variable thermal structure of Lake Superior can be handled more conveniently with layers of fixed depth, letting only the bottom layer vary in thickness. When using layers of fixed depth, the surface layer also corresponds more closely to the layer seen by remote sensing. Implicit and explicit time differencing should be considered. At the present stage of development, only explicit techniques have been considered. Finally, in order to assure adequate spatial solution in regions of interest, either a variable grid or a nested grid model should be used. The latter is used in the present model.

A number of explicit numerical integration techniques exist for solving the equations of motion for geophysical fluids. A number of authors have analyzed these various methods (Fischer 1965; Grammeltvedt 1969; Matsuno 1966). These various techniques have desirable smoothing properties, but none of them are more accurate or more efficient than centered time differencing. Computational modes may develop with centered time differencing, but these can be controlled using half time step starting procedures and periodic explicit smoothing operators. In addition, a pressure gradient averaging technique proposed by Shuman nearly doubles the maximum allowable step for centered differences.

A lattice like grid A in Figure 1 permits centered differences in both space and time for terms associated with gravity waves. If a single grid is used, centered differences for the Coriolis force are not possible. Forward differencing of this term can lead to computational instability (Fischer 1959). A second identical lattice staggered in time is often used to solve this problem. In Simon's model, this second lattice was also staggered in space. This method raises the possibility of grid dispersion. In the present model, the second grid is staggered in time but not in space. This is the grid structure used by Leendertse (1973). Simons also used this structure in modeling the Baltic Sea (Simons 1978). As Simons pointed out, the main problem with this grid is the development of spurious inertial modes associated with four point averaging used in calculating the Coriolis terms. This can be controlled by increasing horizontal diffusion. Another possibility would be to use grid C of Figure 1 which would permit centered semi-implicit evaluation of the Coriolis terms. However, centered time differences for gravity waves seem to lead to computational difficulties on this grid (Sheng, personal communication).

The Lake Superior model is similar to Leendertse's estuary model (Leendertse et al. 1973, 1975a, 1975b). It ignores vertical accelerations and assumes pressure varies hydrostatically. It has a free surface and uses constant eddy coefficients to represent vertical and horizontal diffusion. Horizontal and vertical advection of momentum are represented using an

energy conserving formulation. Centered space differences are used for all terms. Centered time differences are used for all terms except horizontal and vertical diffusion which are approximated using forward differences. A quadratic bottom friction is used.

The equations are given by Leendertse and are listed in Appendix A. Five important modifications were made to Leendertse's model. First, the model was made isothermal. Leendertse's complex formulations for vertical momentum exchange was replaced by simple vertical diffusion with constant diffusivity. Second, the depth of the bottom layer was allowed to vary. Following Simons (1973), the equations of motion were integrated from either the bottom of the lake or the depth of a given layer to either the surface or the bottom of the next layer. Third, a pressure gradient averaging technique originally proposed by Shuman was added. Fourth, internal and external modes of oscillations were separated. Fifth, provisions were made for saving model parameters along open boundaries to be used later on nested subgrids.

Shuman pressure gradient averaging is a very simple technique capable of nearly doubling the maximum allowable time step for centered time differencing of barotropic waves (Schoenstadt and Williams 1976; Brown and Campana 1978). In the equations of motion, time centered pressure gradient terms associated with water level oscillations are replaced by a simple average over three consecutive time steps. For example, at the nth time step the pressure gradient in the x-direction P_x is normally given by Equation (1) in which ζ is water level and g the acceleration of gravity.

$$P_x^n = g\left(\frac{\partial \zeta}{\partial x}\right)^n \tag{1}$$

This is simply replaced by Equation (2) below, where α is a constant which may vary between 0 and .25 the case of no advection of momentum

$$P_x^n = g\left[\left(1-2.\ x\ \alpha\right)\left(\frac{\partial \zeta}{\partial x}\right)^n + \alpha\left(\left(\frac{\partial \zeta}{\partial x}\right)^{n-1} + \left(\frac{\partial \zeta}{\partial x}\right)^{n+1}\right)\right] \tag{2}$$

The term $\left(\frac{\partial \zeta}{\partial x}\right)^{n+1}$ is available at time step n because in centered time differencing water levels at step n+1 are derived from vertical velocities at step n and water levels at step n-1.

The separation of internal and external modes was accomplished as follows. First, the equations of motion were integrated from bottom to surface in order to get an equation which included the effects of gravity waves. This external oscillation mode was integrated using a very short time step. Next, equations of motion at consecutive layers were subtracted to eliminate the external gravity wave. For example, consider the x components of velocity U_k and U_{k+1} at the k and k+1 layers. The equation of motion can be written

$$\frac{\partial h_k U_k}{\partial t} = R_k + h_k g \cdot \frac{\partial \zeta}{\partial x} \tag{3}$$

$$\frac{\partial h_{k+1} U_{k+1}}{\partial t} = R_{k+1} + h_{k+1}\, g\, \frac{\partial \zeta}{x} \tag{4}$$

where t represents time, h layer thickness, g acceleration of gravity, ζ water level, and R the remaining terms. Multiplying (3) by h_{k+1} and (4) by h_k and subtracting eliminates the pressure gradient term and hence the gravity wave. Replacing the time derivatives by finite differences gives

$$(U_k)^{n+1} - (U_{k+1})^{n+1} = S_k^{\,n} \tag{5}$$

where n refers to the time step. The form of $S_k^{\,n}$ depends on the kind of time differences used for the internal wave. In any case, it is evaluated using values at time step n and earlier. If there are M layers, this procedure gives M-1 equations in M unknowns. The equations used to derive the velocity shears are stepped forward once using an internal time step which is an integral number N times the time step used for the external depth-integrated model. The external mode is then stepped forward N times to give the total transport T at the next internal time n+1. The provides an M<u>th</u> equation in U_k^{n+1}, namely.

$$\Sigma h_k U_k^{\,n+1} = T \tag{6}$$

Equations (5) and (6) can be readily solved by elimination for U_k. Bottom friction is then calculated at the new internal time step and used in calculating the external mode. In this manner internal and external modes are treated separately and efficiently while still being allowed to interact with one another.

The addition of open water boundaries and nested subgrids introduces a completely new set of problems and modeling decisions. Upon reaching the boundary between coarse and fine grid, waves can reflect and generate false computational modes or false gravity waves. Proper formulation of open water boundary condition can prevent this. Grids of differing size can be coupled using either one-way or two-way interaction schemes. In one-way interaction schemes (Chen and Miyakoda 1974; Miyakoda and Rosati 1977) the entire lake is first modeled on a coarse grid ano model parameters on the boundary between grids are saved. The saved parameters are interpolated in space and time and used as open boundary values in the fine grid. In this method, information is allowed to pass from the coarse grid to the fine grid but not vice versa. In two-way interactions (Harrison and Elsberry 1972; Browning <u>et al</u>. 1973) both fine and coarse grid models are integrated simultaneously. <u>At</u> the boundary between grids, information needed by the coarse grid from the fine grid is obtained using values from the fine grid and vice versa. In this way, full interaction between grids is possible.

In order to reduce computer memory requirements, the one-way interaction scheme is used in the Lake Superior model. Two-way interaction schemes are necessary only when processes occurring in the nested subgrid have profound

influences on large scale circulation, as for instance in hurricane modeling. In the program the location of any number of open boundaries are read and model parameters along these boundaries are saved for latter fine grid calculations. These stored model parameters are then interpolated in time using a four-point formula given by Wang and Halpern (1970). Space interpolation is achieved using a method which approximates linear interpolation of currents but assures that the total normal and tangential transport and the total surface elevation along the boundary is the same in both grids. A local boundary smoothing procedure proposed by Chen and Miyakoda (1974) can be used if necessary.

EXAMPLE: RESULTS FOR LAKE SUPERIOR

For purposes of illustration the model was run for a 24 hour periods for easterly and westerly winds on Lake Superior, Figure 2. A 10 km square grid and time steps of 12 minutes for the internal mode and 90 seconds for the external mode were used. Vertical and horizontal diffusivities were .01 m^2/s and 10 m^2/s respectively. A constant wind stress of .675 nt/m^2 and a constant Chezy coefficient of 50 $(m/s^2)^{-1/2}$ were used. In these runs, four layers were used with interfaces at depths of 20 m, 50 m, 110 m.

Figures 3-6 show surface currents for easterly winds after 3, 9, 15, and 24 hours respectively. The currents in the central regions of the lake are clearly rotating in a manner attributable to interaction of wind stress and Coriolis force. As expected, currents in the lower layers show a similar rotation in the opposite direction. Figures 7-9 show currents in the subsurface layers after 24 hours. Return currents are clearly evident in deep trenches parallel to the wind. The results for westerly winds were similar except current directions were reversed. Downwelling and upwelling for easterly and westerly winds are shown in Figures 10 and 11 respectively. Comparing Figures 8 and 9 with Figure 10 provides evidence that for constant easterly winds, taconite tailings dumped into the lake at Silver Bay would be downwelled and carried along the bottom toward the south shore where they would be upwelled. Isolated patches of tailings have been detected in this region using Landsat data (Oman and Sydor 1977).

The model was also run on a 2.5 kilometer nested subgrid in extreme western Lake Superior. Surface and second layer currents for easterly winds after 24 hours are shown in Figures 12 and 13 and for westerly winds in Figures 14 and 15. For both winds, surface currents in the extreme western reach of the lake seem to form circulation cells. These cells seemed to reach steady state quickly and are consistent with observations by Ruschmeyer et al. (1961) which indicated that nutrients from the Duluth-Superior Harbor often remain trapped within 15 to 30 km of the harbor for extended periods of time. The return current in layer 2 for easterly winds, Figure 13, corresponds exactly with resuspension plumes observed in Landsat images. The hooking return current in layer 2 for westerly winds is also consistent with Landsat observations of westerly wind events.

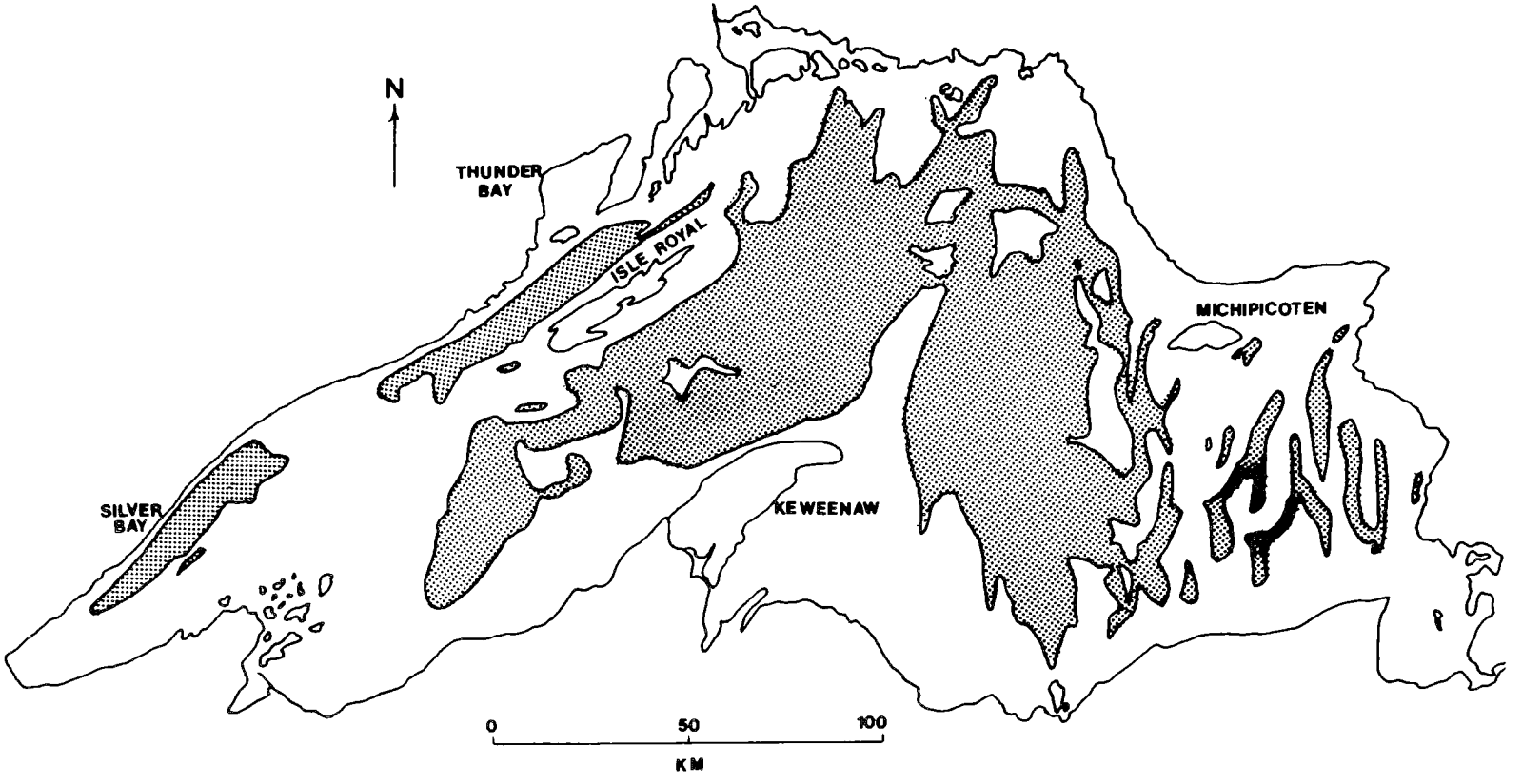

Figure 2. Map of Lake Superior showing regions deeper than 200 m.

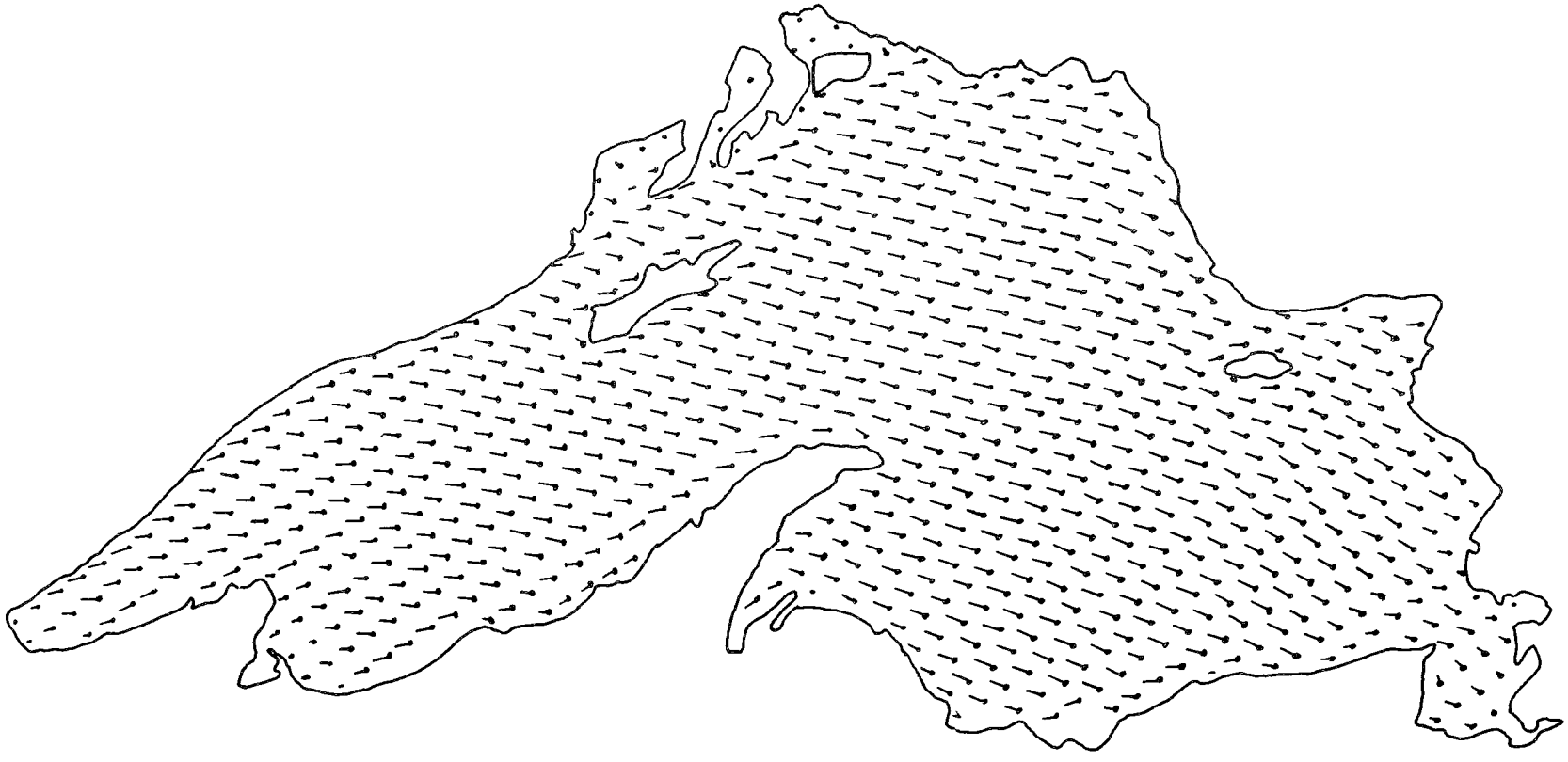

East Wind

Currents

One Grid Space = 50.0 cm/sec

Layer 1, 0 to 20.0 meters

Time = 0/0300:00

Figure 3. Surface currents after 3 hours of constant easterly winds.

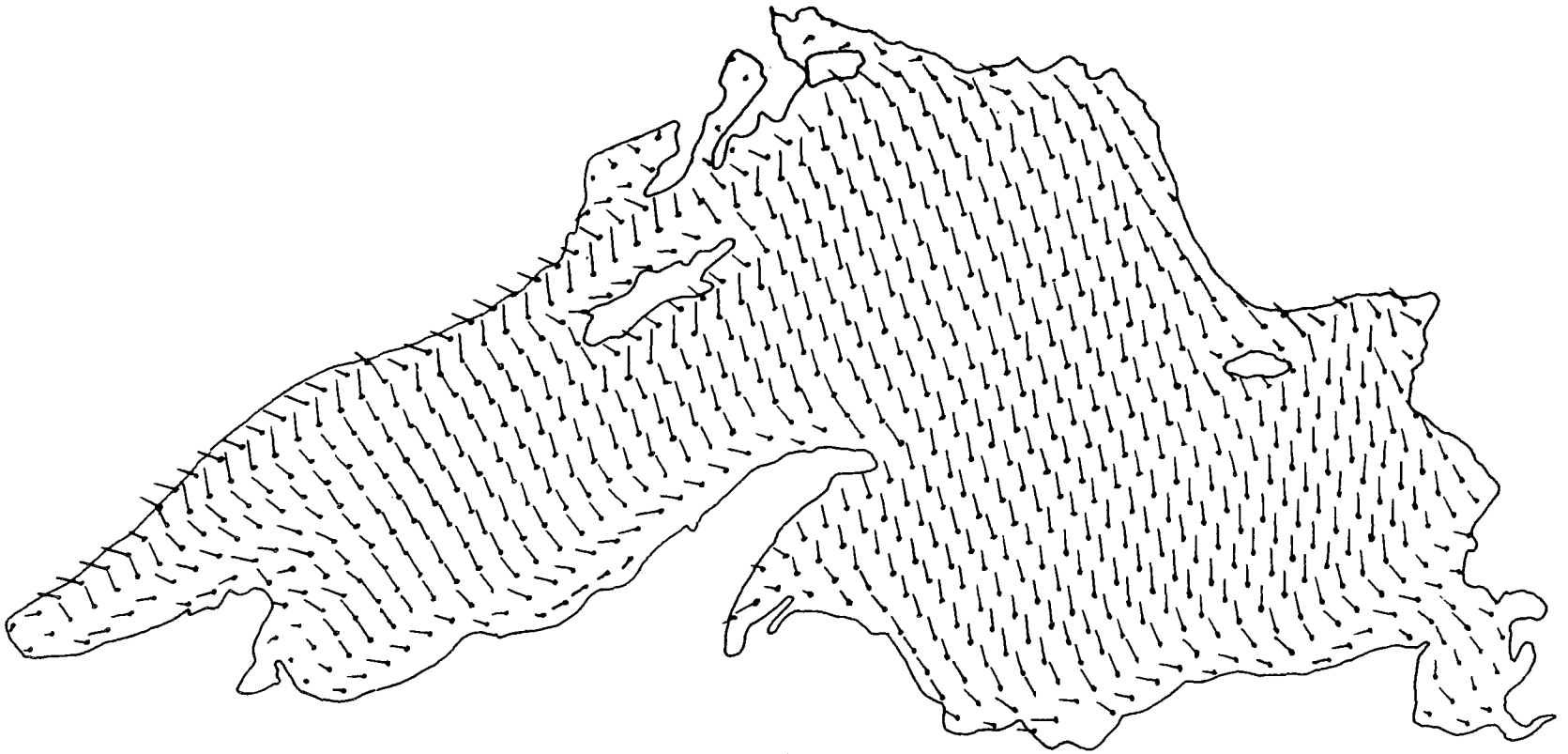

East Wind
Currents
One Grid Space = 50.0 cm/sec
Layer 1, 0 to 20.0 meters
Time = 0/0900:00

Figure 4. Surface currents after 9 hours of constant easterly winds.

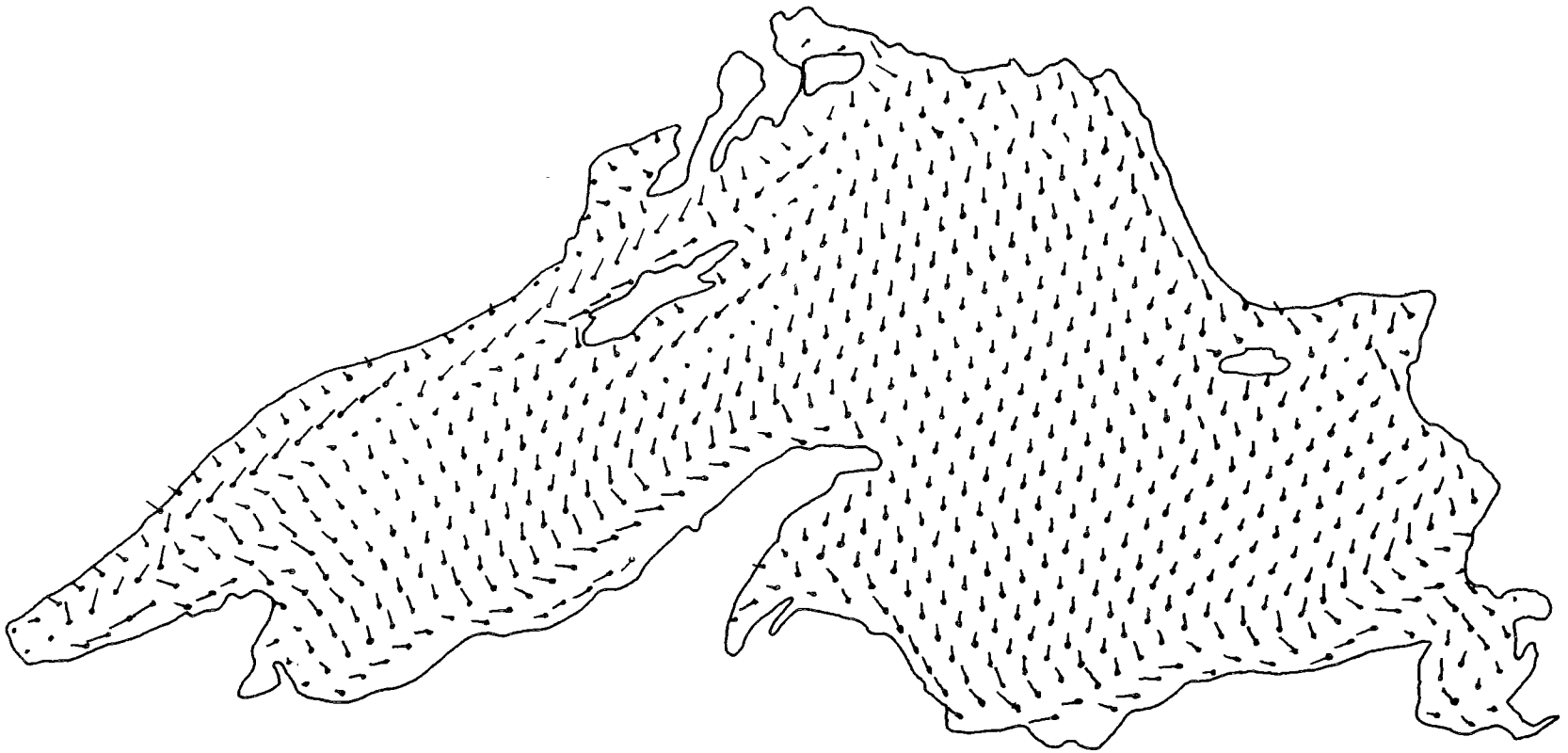

East Wind
Currents
One Grid Space = 50·0 cm/sec
Layer 1, 0 to 20·0 meters
Time = 0/1500:00

Figure 5. Surface currents after 15 hours of constant easterly winds.

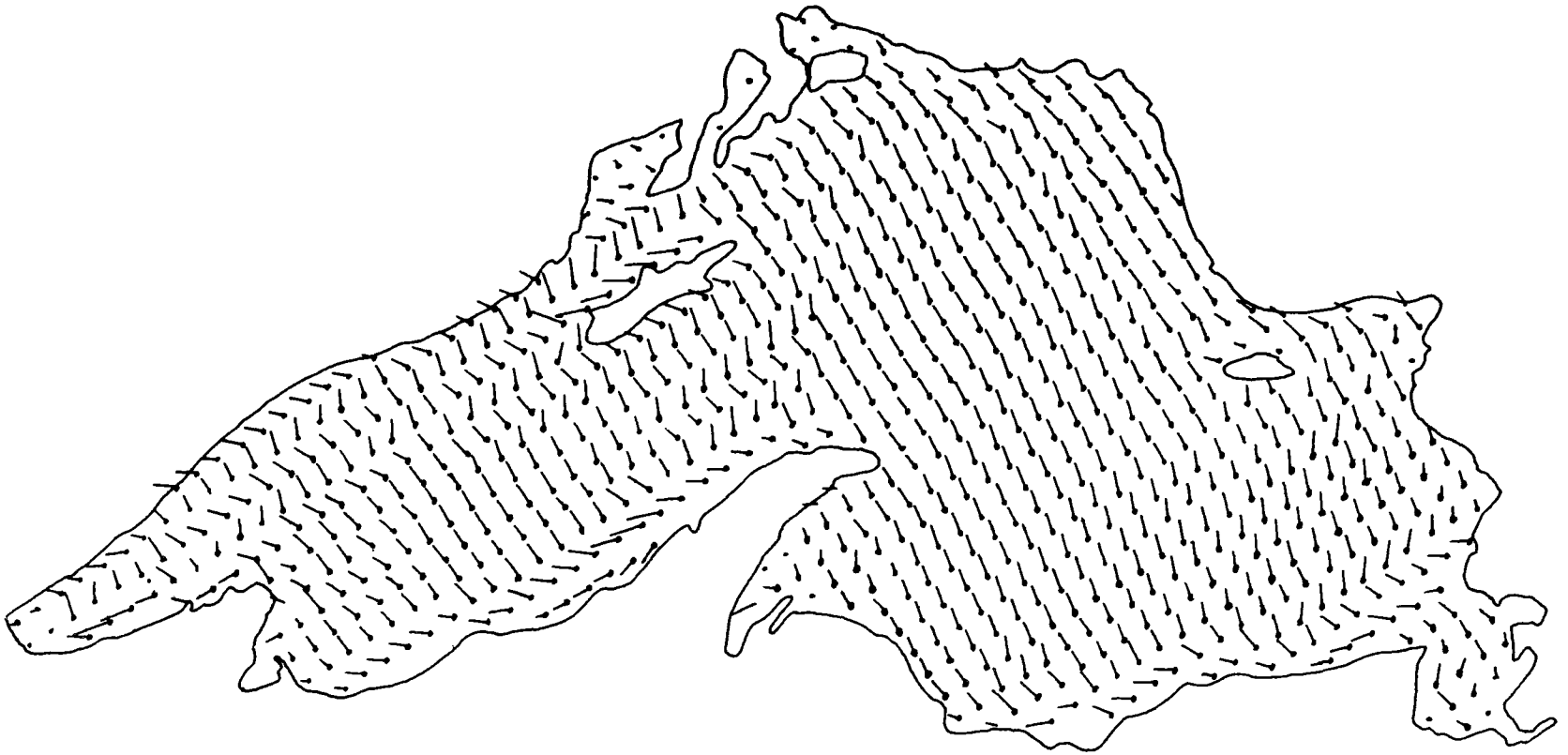

East Wind
Currents
One Grid Space = 50·0 cm/sec
Layer 1, 0 to 20·0 meters
Time = 1/0000:0

Figure 6. Surface currents after 24 hours of constant easterly winds.

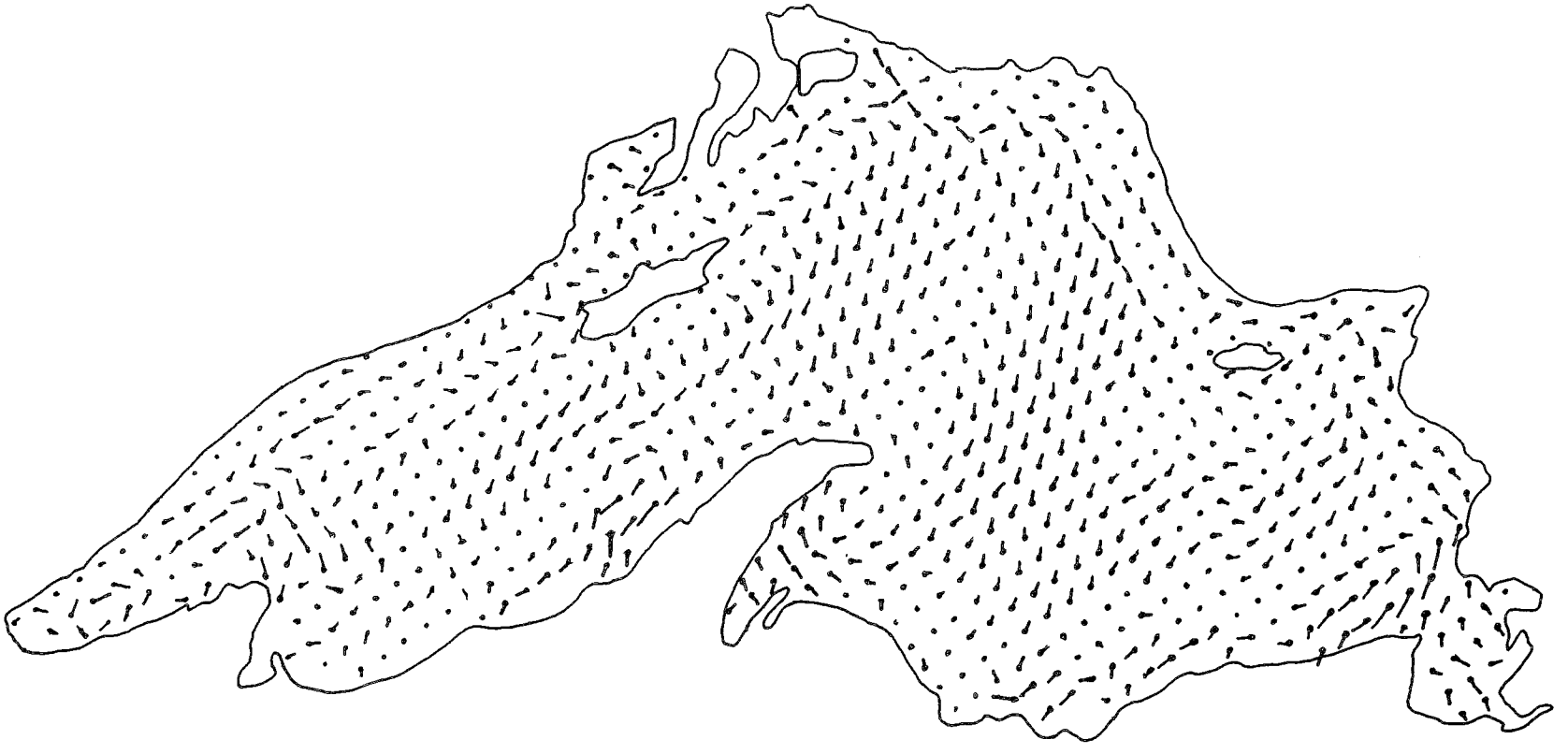

East Wind
Currents
One Grid Space = 25.0 cm/sec
Layer 2, 20·0 to 50·0 meters
Time = 1/0000:00

Figure 7. Currents in layer 2 after 24 hours of constant easterly winds.

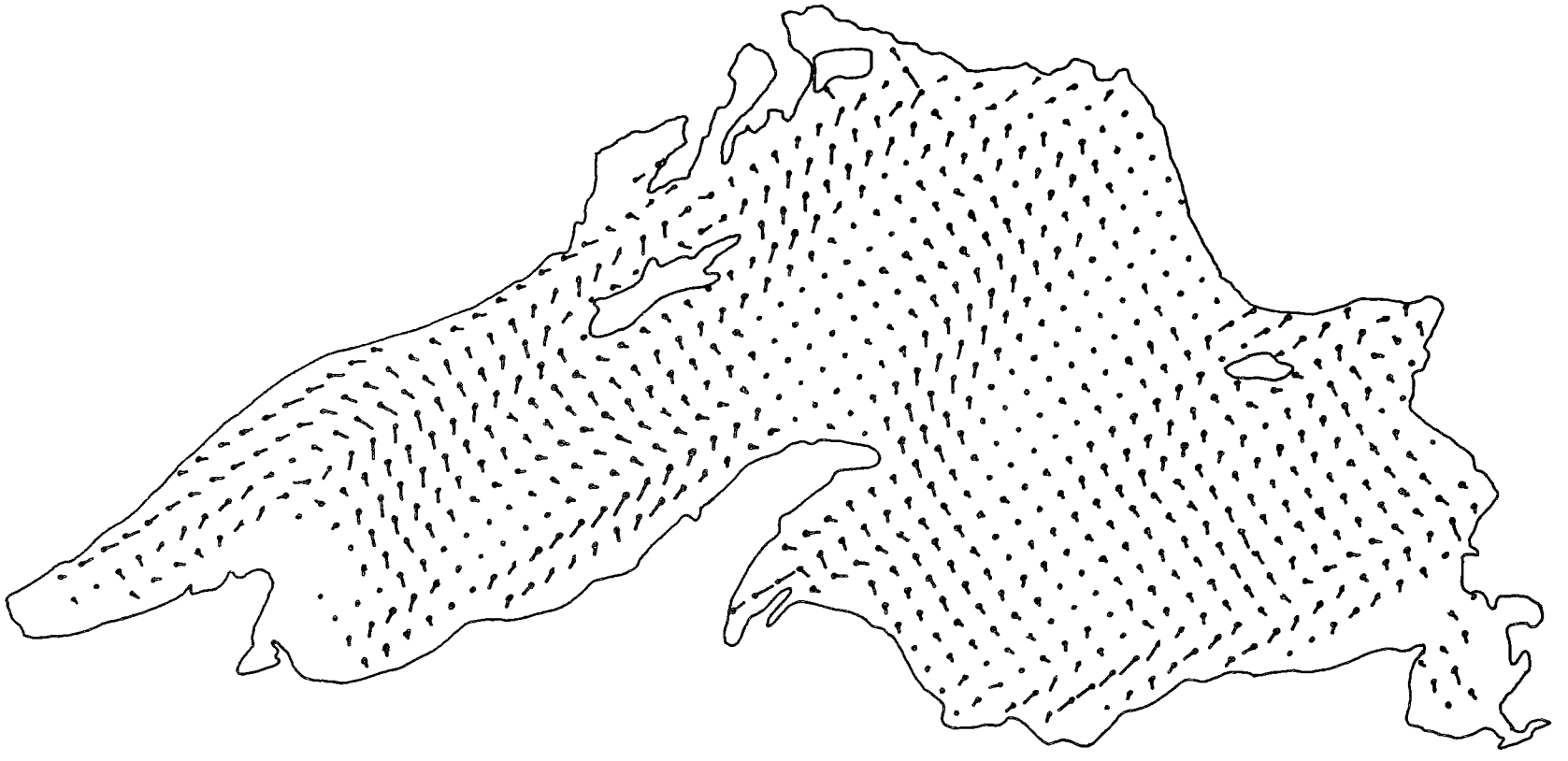

East Wind
Currents
One Grid Space = 25·0 cm/sec
Layer 3, 50 to 110·0 meters
Time = 1/0000:0

Figure 8. Currents in layer 3 after 24 hours of constant easterly winds.

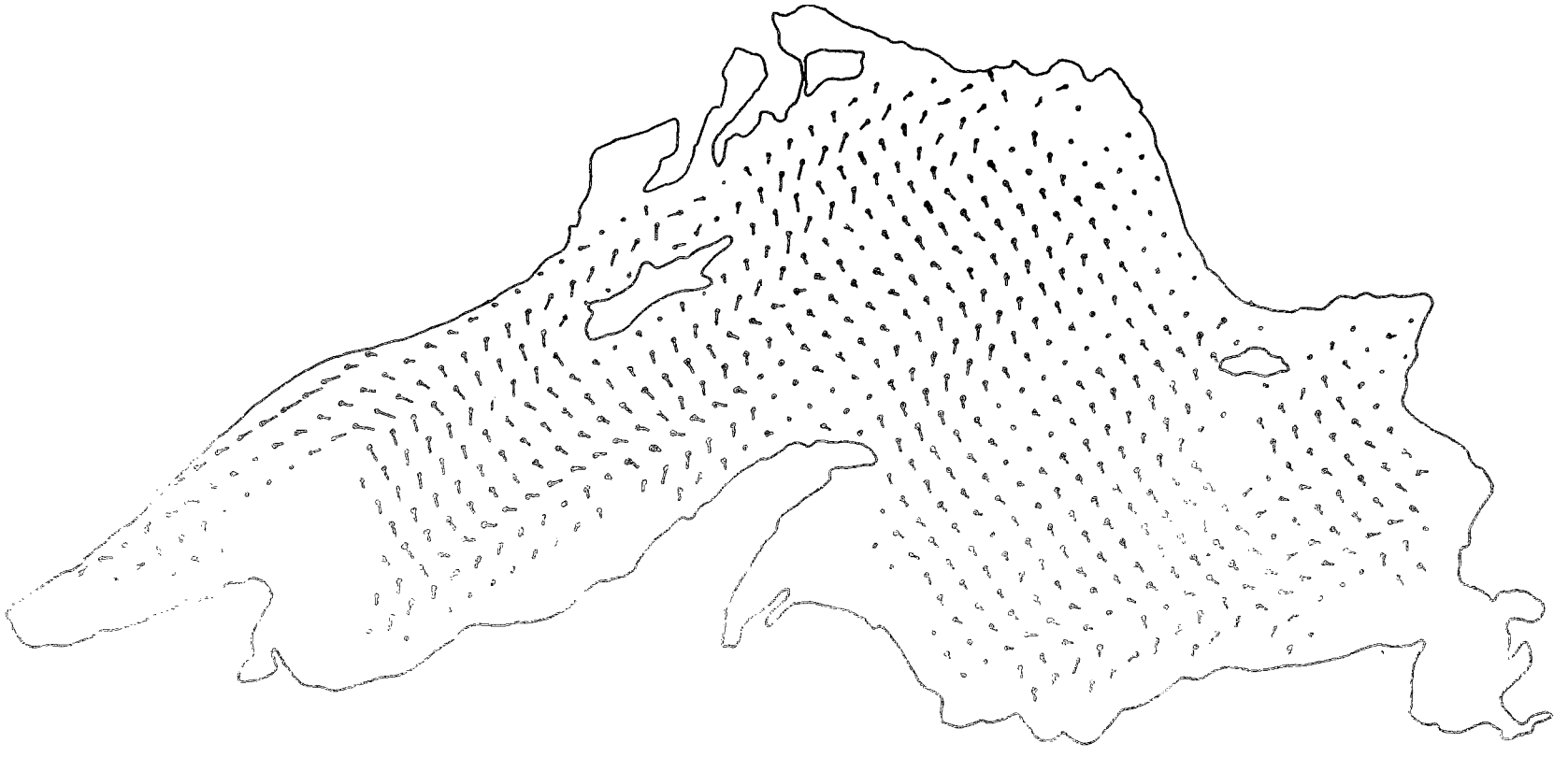

Figure 9. Currents in layer 4 after 24 hours of constant easterly winds.

Figure 10. Layer 2 downdwelling in western Lake Superior after 24 hours of constant easterly winds. One grid space corresponds to 1 mm/sec.

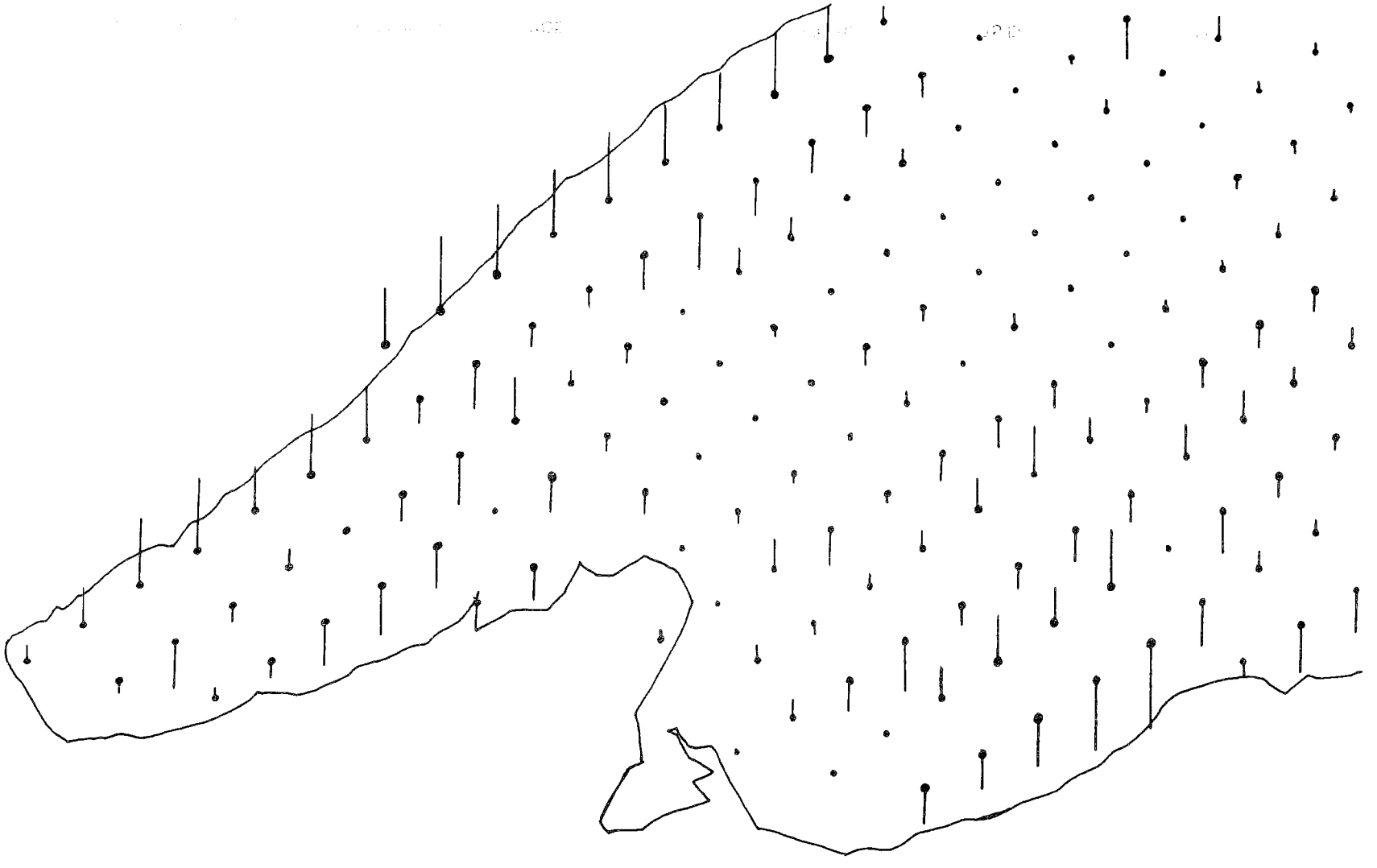

Figure 11. Layer 2 upwelling in western Lake Superior after 24 hours of constant easterly winds. One grid space corresponds to 1 mm/sec.

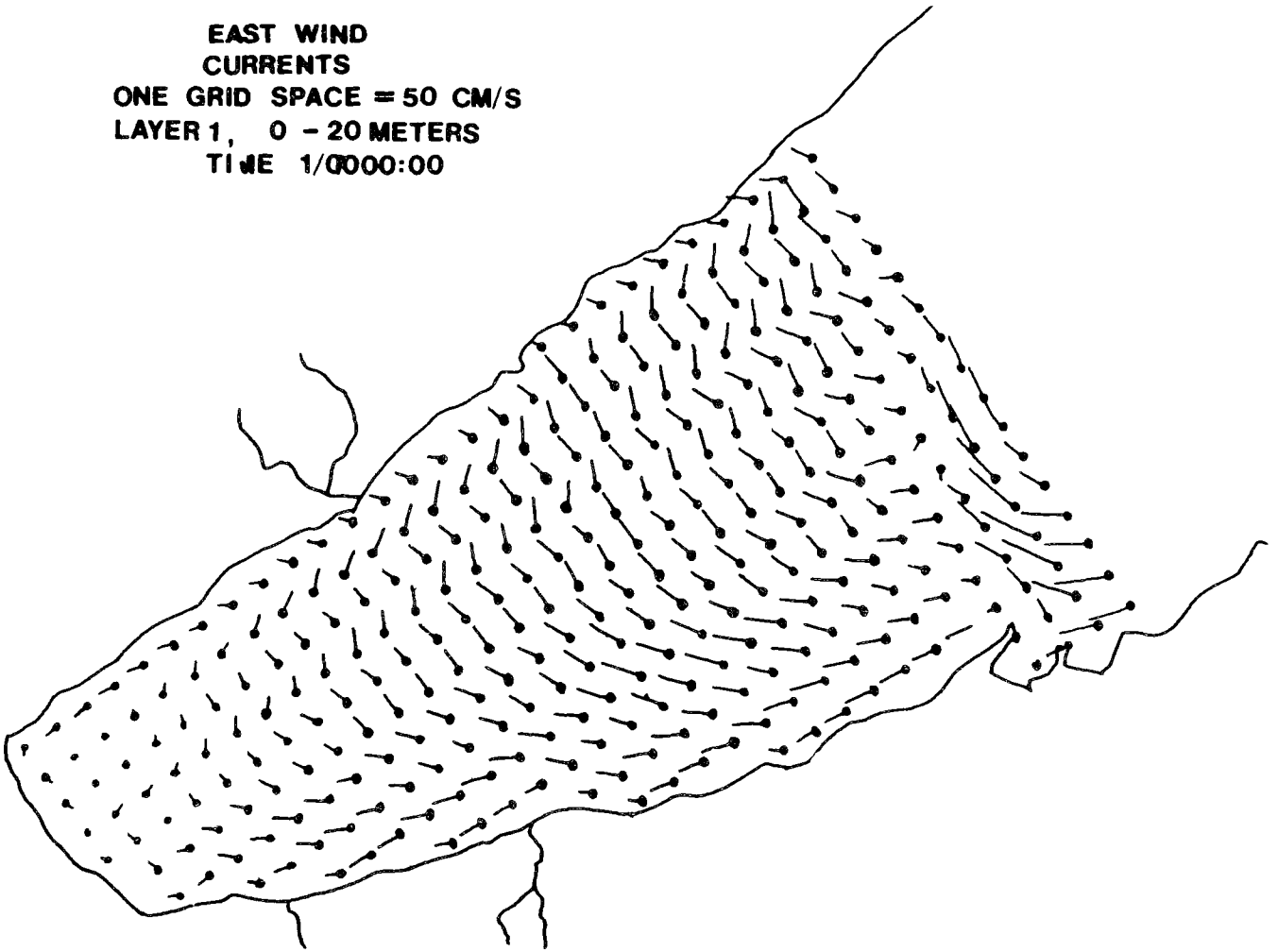

Figure 12. Surface currents in nested subgrid after 24 hours of constant easterly winds.

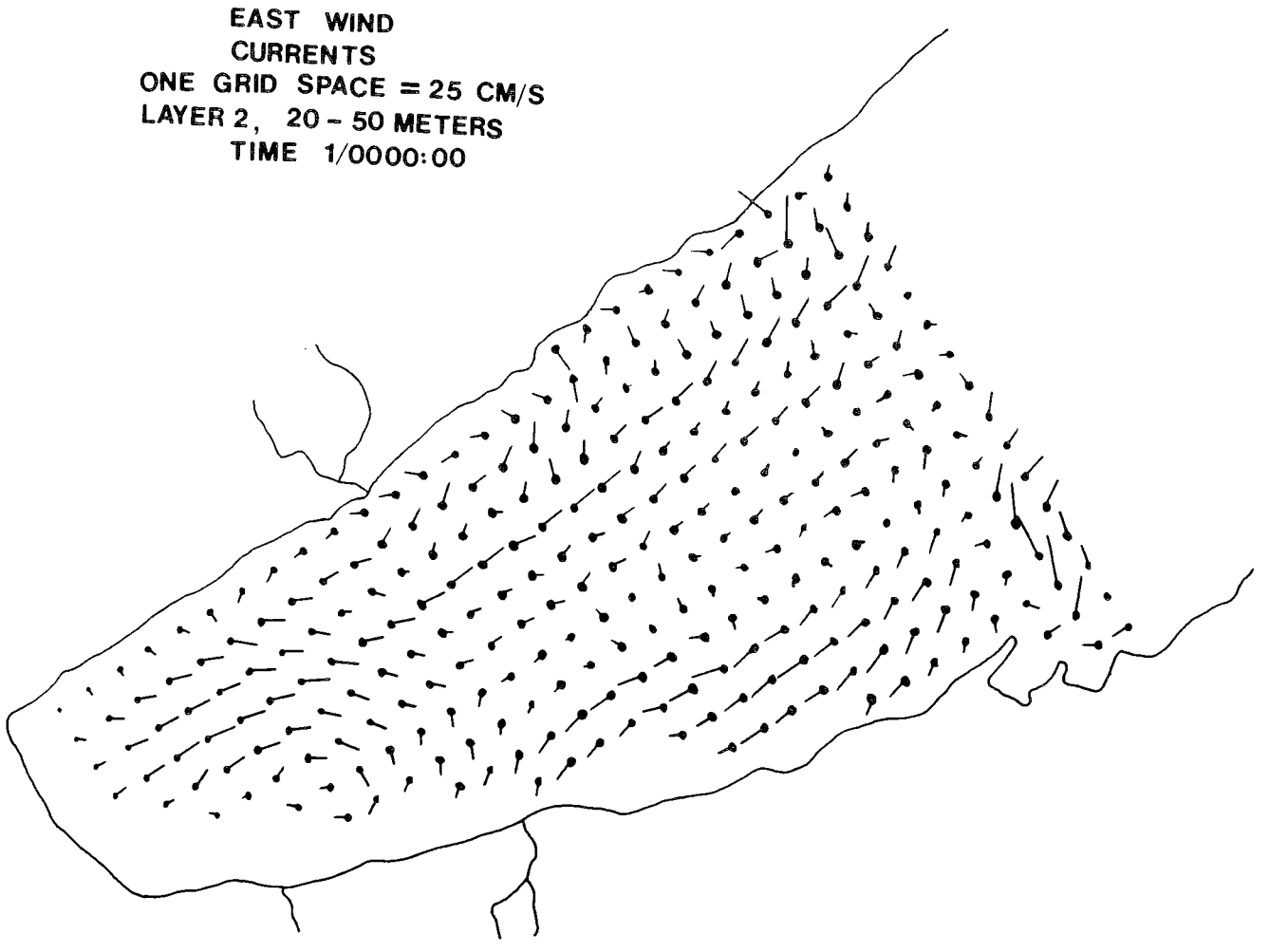

Figure 13. Layer 2 currents in nested subgrid after 24 hours of constant easterly winds.

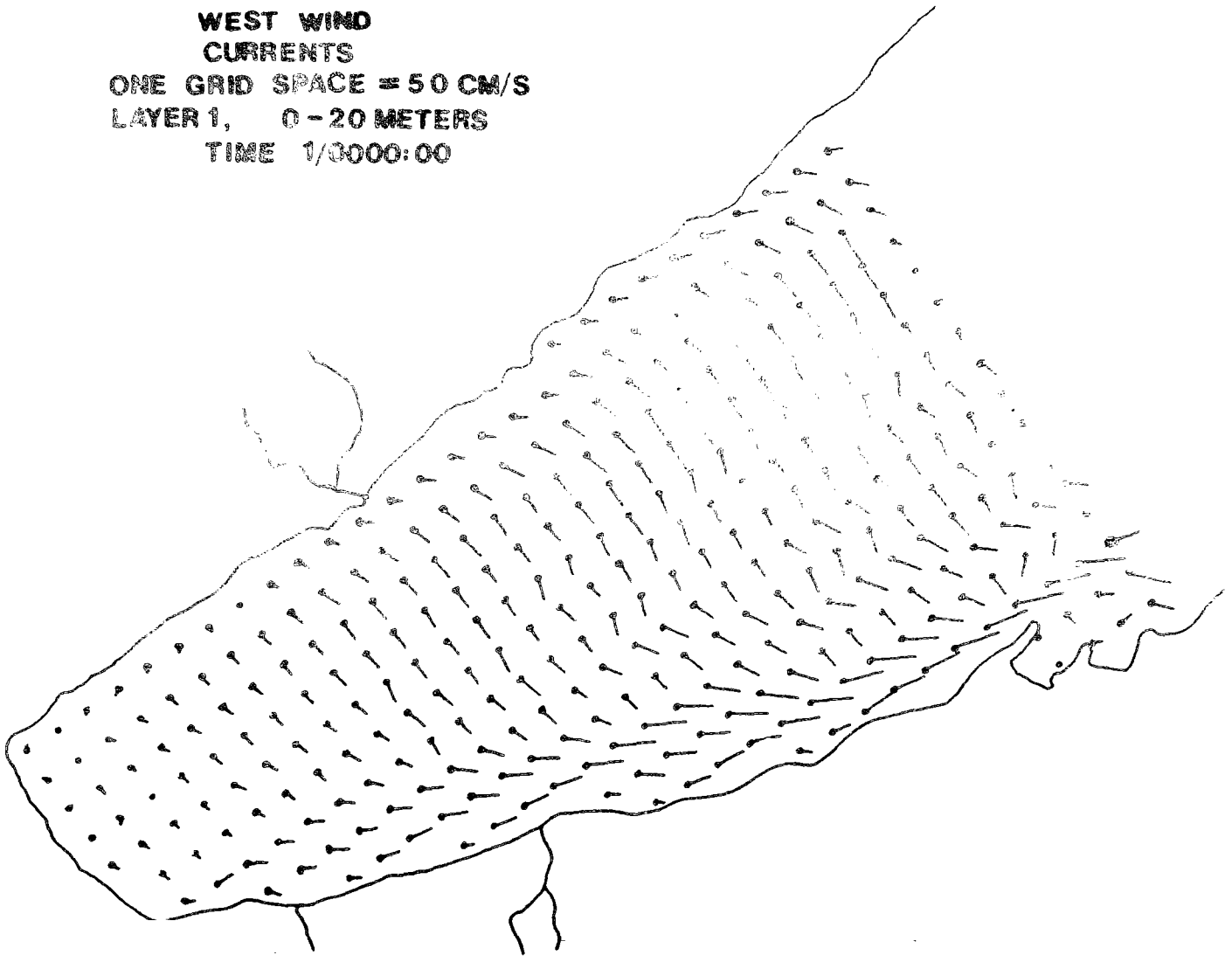

Figure 14. Surface currents in nested subgrid after 24 hours of constant westerly winds.

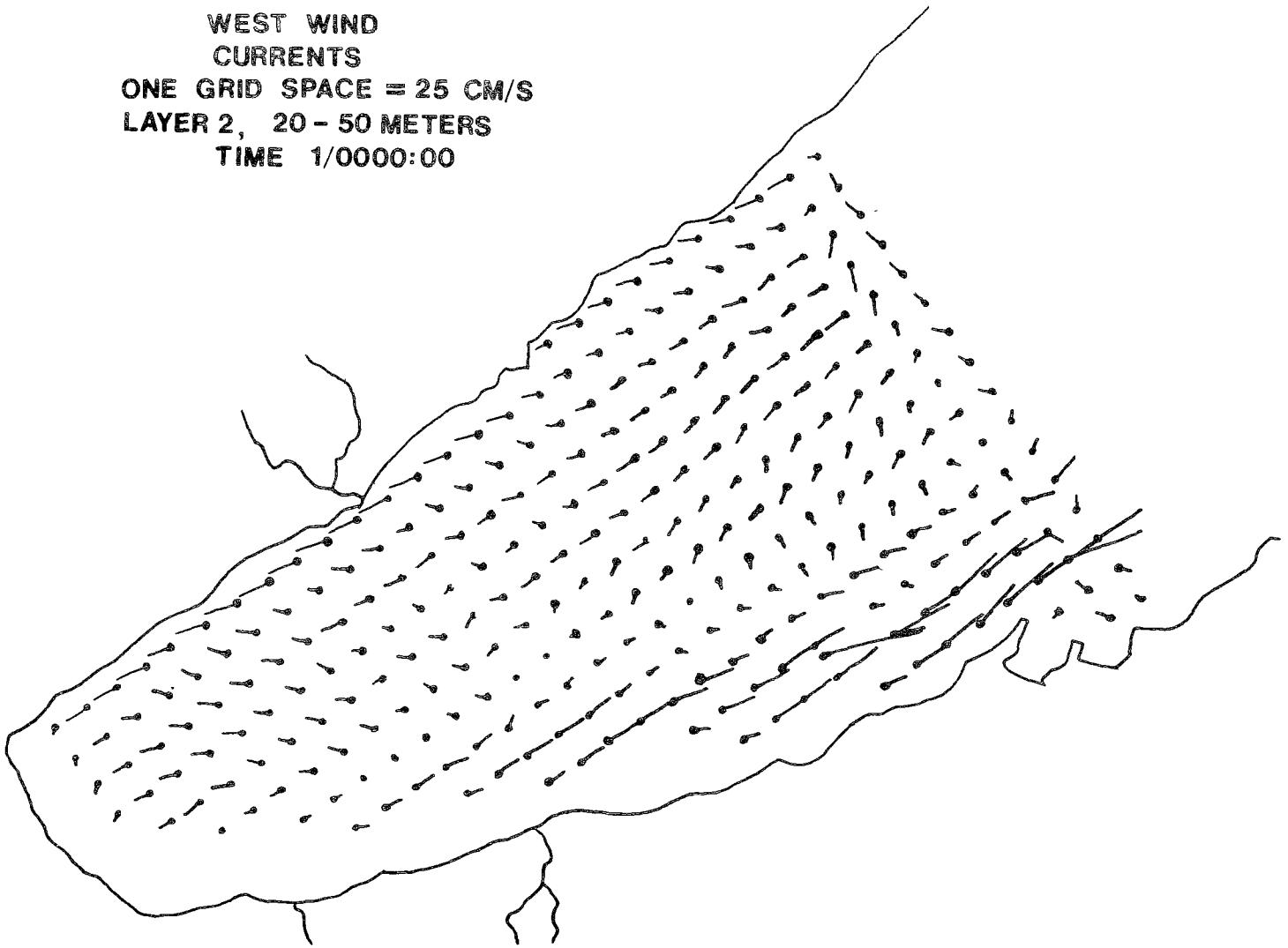

Figure 15. Layer 2 currents in nested subgrid after 24 hours of constant westerly winds.

REFERENCES

Bennett, J.R. 1977. A three dimensional model of Lake Ontario's summer circulation. I. Comparison with observations. J. Phys. Oceanogr. 7: 591-601.

Brown, J.A. and K. Campana. 1978. An economical fine differencing system for numerical weather prediction. Mon. Weather Rev. 106: 1125-1136.

Browning, G., H.O. Kreiss, and J. Oliger. 1973. Mesh refinement. Math. Comp. 27: 29-39.

Chen, J.H. and K. Miyakoda. 1974. A nested grid computation for the barotropic free surface atmosphere. Mon. Weather Rev. 102: 181-190.

Cheng, R.T., T.M. Powell and T.M. Dillon. 1976. Numerical models of wind driven circulation in lakes. Appl. Math. Modeling. 1: 141-159.

Fischer, G. 1959. Ein numerisches verfahren zun errechnung von windstau und gezeiten in randmeeren. Tellus. 11: 60-76.

Fishcer, G. 1965. A survey of finite-difference approximations to the primitive equations. Mon. Weather Rev. 93: 1-10.

Freeman, N.G., A.M. Hale, and M.B. Danard. 1972. A modified sigma equations' approach to the numerical modeling of Great Lakes hydrodynamics. J. Geophys Res. 77: 1050-1060.

Gedney, R.T. and W. Lick. 1970. Numerical calculations of the steady-state wind-driven currents in Lake Erie. Proc. 13th Conf. Great Lakes Res. pp. 829-838.

Gedney, R.T. and W. Lick. 1971. Numerical calculations of the wind driven current in Lake Erie and comparison with measurements. Proc. 14th Conf. Great Lakes Res. pp. 454-466.

Gedney, R.T. and W. Lick. 1972. Wind-driven current in Lake Erie. Proc. 15th Conf. Great Lakes Res. pp. 2714-2723.

Gedney, R.T., T.B. Molls, and W. Lick. 1973. A simplified stratified lake model for determining effects of wind variation and eddy diffusivity. Proc. 15th Conf. Great Lakes Res. pp. 710-722.

Grammeltvedt, A. 1969. A survey of finite-difference schemes for the primitive equations for a barotrophic fluid. Mon. Weather Rev. 97: 384-404.

Harrison, E.J. and R.S. Elseberry. 1972. A method for incorporating nested finite grids in the solution of systems of geophysical equations. J. Atmos. Science. 29: 1235-1245.

Katz, P.L. and G.M. Schwab. 1976. Currents and pollutant dispersion in Lake Michigan modeled with emphasis on the Calumet Region. Department of Information Engineering, University of Illinois at Chicago Circle.

Kizlauskas, A.G. and P.L. Katz. 1973. A two layer finite difference model for flow in thermally stratified Lake Michigan. Proc. 16th Conf. Great Lakes Res. pp. 743-753.

Kwizak, M. and A.J. Robert. 1971. A semi-implicit scheme for grid point atmospheric models of the primitive equations. Mon. Weather Rev. 99: 32-36.

Leendertse, J.J. R.C. Alexander and S.K. Liu. 1973. A three-dimensional model for estuaries and coastal seas: Volume I, Principals of computation. The Rand Corporation. R-1417-OURR.

Leendertse, J.J. and S.K. Liu. 1975a. A three-dimensional model for estuaries and coastal seas: Volume II, Aspects of computation. The Rand Corporation. R-1764-OWRT.

Leendertse, J.J., S.K. Liu and A.B. Nelson. 1975b. A three-dimensional model for estuaries and coastal seas: Volume III, The interim program. The Rand Corporation. R-1884-OWRT.

Lick, W. 1976. Numerical models of lake currents. Ecological Research Series Report EPA-600/3-76-020.

Madala, R.V. and S.A. Piacsek. 1977. A semi-implicit numerical model for baroclinic oceans. J. Computer Phys. 23: 167-178.

Matsuno, T. 1966. Numerical integrations of the primitive equations by a simulated backward difference method. J. Meteorol. Soc. Japan. 44: 76-84.

Miyakoda, K. and A. Rosati. 1977. One-way nested grid models: The interface conditions and the numerical accuracy. Mon. Weather Rev. 105: 1092-1107.

Paul, J.F. and J. Prahl. 1971. Experimental and numerical investigations of rectangular jet. Proc. 14th Conf. Great Lakes Res. pp. 607-617.

Paul, J.F. and W.J. Lick. 1973. A numerical model for a three-dimensional variable-density jet. Proc. 16th Conf. Great Lakes Res. pp. 818-830.

Paul, J.F. and W.J. Lick. 1974. A numerical model for thermal plumes and river discharges. Proc. 17th Conf. Great Lakes Res. pp. 445-455.

Paul, J.F. and W.J. Lick. 1976. Lake Erie international jet port model feasibility investigation, Report 17-6, Application of three-dimensional hydrodynamic model to study effects of proposed jetport island on thermocline structure of Lake Erie. Department of Earth Sciences, Case Western Reserve University, Cleveland, Ohio.

Paul, J.F. and W.J. Lick. 1979. An efficient, implicit method for calculating time dependent, free-surface hydrodynamic flows. Proc. 22nd Conf. Great Lakes Res., held at Rochester, New York, May 1979.

Ruschmeyer, O.R., T.A. Olson and H.M. Bosch. 1961. Lake Superior studies, 1956-1961. School of Public Health, University of Minnesota, Minneapolis.

Schoenstadt, A.L. and R.T. Williams. 1976. The computational stability properties of the Shuman pressure gradient averaging technique. J. Computer Phys. 21: 166-177.

Schwab, G.M. and P.L. Katz. 1978. Multiple-grid numerical simulation of transient near shore current in southwestern Lake Michigan: Comparison with observations. Proc. 21st Conf. Great Lakes Res., held at University of Windsor, Ontario, May 9-11, 1978.

Sheng, Y.P. 1975. Lake Erie international jetport model feasibility investigation, Report 17-5, The wind driven currents and contaminant dispersion in the near shore of large lakes. Department of Earth Sciences, Case Western Reserve University, Cleveland, Ohio.

Sheng, Y.P. and W.J. Lick. 1976. Currents and contaminant dispersion in the nearshore region and modification by a jetport. J. Great Lakes Res. 2: 402-414.

Sheng, Y.P., W.J. Lick, R.T. Gedney and F.B. Molls. 1978. Numerical computation of three-dimensional circulation in Lake Erie: A comparison of a free-surface model and a rigid-lid model. J. Phys. Oceanogr. 8: 713-727.

Simons, T.J. 1973. Development of three-dimensional numerical models of the Great Lakes. Scientific Series No. 12, Inland Waters Directorate, Canada Centre for Inland Waters, Burlington, Ontario, 1973.

Simons, T.J. 1974. Verification of numerical models of Lake Ontario. Part I: Circulation in spring and early summer. J. Phys. Oceanogr. 4: 507-523.

Simons, T.J. 1975. Verification of numerical models of Lake Ontario. Part II: Stratified circulations and temperature changes. J. Phys. Oceanogr. 5: 98-110.

Simons, T.J. 1976. Verification of numerical models of Lake Ontario. Part III: Long term heat transports. J. Phys. Oceanogr. 6: 372-378.

Simons, T.J. 1978. Wind driven circulations in the southwest Baltic. Tellus. 30: 272-283.

Sydor, M. and G. Oman. 1977. Effects of nemadji runoff on Lake Superior. Final Report, U.S. EPA Grant No. R-005286-01, Department of Physics, University of Minnesota, Duluth.

Wang, H.H. and P. Halpern. 1970. Experiments with a regional fine mesh prediction model. J. Appl. Meteorol. 9: 545-553.

APPENDIX A

THE FINITE DIFFERENCE EQUATIONS

The finite difference equations listed in this Appendix are based largely upon the work of Leendertse (1973, 1975). The equations of motion for an incompressible fluid are given in Equations (A-1)-(A-4). In these equations, vertical accelerations have been ignored and the hydrostatic assumption imposed; Equation (A-3). The Coriolis parameter is also assumed constant. As Simons (1973) points out, these equations can be integrated over the kth layer to give Equations (A-5)-(A-7).

If layer thickness varies, terms involving products of the horizontal velocity and partial derivatives of layer thickness are absorbed into the vertical velocity term w. In these equations, the horizontal stress terms are approximated by simple diffusion of layer transport. The vertical stress term at the surface is given by a quadratic function of wind, Equation (A-8), and at the bottom by a quadratic function of current, Equations (A-9)-(A-10). Stresses between layers are approximated by simple diffusion.

Before giving the finite difference equations, the finite difference operators listed in Equations (A-11)-(A-15) must be defined. First, all model parameters must be defined on a grid lattice as in Equation (A-11). In the present model, a spatially staggered grid is used which is ideally suited for solving the continuity equation. In this grid only normal components of velocity are defined at the six sides of a rectangular box which constitute a grid cell. Thus, the u, v and w components of velocity are defined at half integral values of i, j and k respectively. Averaging and finite differencing operators in the x-direction are given in Equations (A-12) and (A-13). Similar operators are defined in the Y and Z directions and in time. Future and past values are signified as shown in Equations (A-14) and (A-15).

The finite difference equations which form the basis of the model are listed in Equations (A-16)-(A-19). Stress terms between layers are given by Equations (A-20) and (A-21). These equations were then modified as described by the main text.

$$\frac{\partial u}{\partial t} + \frac{\partial(uu)}{\partial x} + \frac{\partial(uv)}{\partial y} + \frac{\partial(uw)}{\partial z} - fv + \frac{1}{\rho}\frac{\partial p}{\partial x} - \frac{1}{\rho}\left(\frac{\partial \tau_{xx}}{\partial x} + \frac{\partial \tau_{xy}}{\partial y} + \frac{\partial \tau_{xz}}{\partial z}\right) = 0 \qquad \text{(A-1)}$$

$$\frac{\partial v}{\partial t} + \frac{\partial(uv)}{\partial x} + \frac{\partial(vv)}{\partial y} + \frac{\partial(vw)}{\partial z} + fu + \frac{1}{\rho}\frac{\partial p}{\partial y} - \frac{1}{\rho}\left(\frac{\partial \tau_{yx}}{\partial x} + \frac{\partial \tau_{yy}}{\partial y} + \frac{\partial \tau_{yz}}{\partial z}\right) = 0 \qquad \text{(A-2)}$$

$$\frac{\partial p}{\partial z} + \rho g = 0 \qquad \text{(A-3)}$$

$$\frac{\partial u}{\partial x} + \frac{\partial v}{\partial y} + \frac{\partial w}{\partial z} = 0 \qquad \text{(A-4)}$$

Where: t is time
x, y are coordinates in the horizontal plane
z is the vertical coordinate, positive upwards
u, v, w are velocity components in the x, y, z directions
f is the Coriolis parameter
ρ is the density of the fluid
p is pressure
τ represents the stress tensor
g is the acceleration of gravity.

$$\frac{\partial(hu)}{\partial t} + \frac{\partial(huu)}{\partial x} + \frac{\partial(hvu)}{\partial y} + (wu)_{k-\frac{1}{2}} - (wu)_{k+\frac{1}{2}} + fhv + \frac{h}{\rho}\frac{\partial p}{\partial x}$$

$$+ \left(\frac{1}{\rho}\tau^{xz}\right)_{k+\frac{1}{2}} - \left(\frac{1}{\rho}\tau^{xz}\right)_{k+\frac{1}{2}} - \frac{1}{\rho}\frac{\partial\left(hA_x \frac{\partial u}{\partial x}\right)}{\partial x} - \frac{1}{\rho}\frac{\partial\left(hA_y \frac{\partial u}{\partial y}\right)}{\partial y} = 0 \qquad \text{(A-5)}$$

$$\frac{\partial(hv)}{\partial t} + \frac{\partial(hvu)}{\partial x} + \frac{\partial(hvv)}{\partial y} + (wv)_{k-\frac{1}{2}} - (wv)_{k+\frac{1}{2}} + fhu + \frac{h}{\rho}\frac{\partial p}{\partial y}$$

$$+ \left(\frac{1}{\rho}\tau^{yz}\right)_{k+\frac{1}{2}} - \left(\frac{1}{\rho}\tau^{yz}\right)_{k-\frac{1}{2}} - \frac{1}{\rho}\frac{\partial\left(hA_x \frac{\partial v}{\partial x}\right)}{\partial x} - \frac{1}{\rho}\frac{\partial\left(hA_y \frac{\partial v}{\partial y}\right)}{\partial y} = 0 \qquad \text{(A-6)}$$

$$\frac{\partial}{\partial x}(hu) + \frac{\partial}{\partial y}(hv) + (w)_{k-\frac{1}{2}} - (w)_{k+\frac{1}{2}} = 0 \qquad \text{(A-7)}$$

where h is layer thickness, A_x, A_y are horizontal diffusion coefficients.

$$\tau_0 = \rho \overline{Cu}|\overline{u}| \qquad \text{(A-8)}$$

Where: ρ is the density of the moving fluid,
$\overline{u}$ is the mean wind speed, and
C is a drag coefficient.

$$\tau_x^b = \rho g \frac{u\sqrt{u^2 + v^2}}{C^2} \tag{A-9}$$

$$\tau_x^b = \rho g \frac{v\sqrt{u^2 + v^2}}{C^2} \tag{A-10}$$

$$F_{ij}^n = F(i\Delta x,\ j\Delta y,\ h_k,\ n\Delta t) \tag{A-11}$$

$$\overline{F}^x = \tfrac{1}{2}\,(F_{i+\frac{1}{2}jk} + F_{i-\frac{1}{2}jk}) \text{ at } (i,j,k) \tag{A-12}$$

$$\delta_x F = \frac{1}{\Delta x}\,(F_{i+\frac{1}{2}jk} - F_{i-\frac{1}{2}jk}) \text{ at } (i,j,k) \tag{A-13}$$

$$F_+ = F_{ijk}^{n+1} \tag{A-14}$$

$$F_- = F_{ijk}^{n-1} \tag{A-15}$$

$$\overline{\delta_t \zeta}^t = -\sum_k \quad \delta_x(\overline{h}^x u) + \delta_y(\overline{h}^y v) \qquad \text{at } i,\ j,\ n \tag{A-16}$$

$$\overline{\delta_t(\overline{h}^x u)}^t = -\delta_x(\overline{\overline{h}^x u\,\overline{u}^x}) - \delta_y(\overline{\overline{h}^y v\,\overline{u}^y}) - \overline{h}^x \delta_z(\overline{u}^z \overline{w}^x)$$

$$+ f\overline{h}^x \overline{v}^{xy} - g\,\overline{h}^x \delta_x \zeta - (\frac{1}{\rho}\,\underline{\tau}^{xz})_{k+\frac{1}{2}} + (\frac{1}{\rho}\,\underline{\tau}^{xz})_{k-\frac{1}{2}}$$

$$+ \frac{1}{\rho}\,\delta_x A_x \delta_x \overline{h}^x u + \frac{1}{\rho}\,\delta_y A_y \delta_y \overline{h}^x u \qquad \text{at } i + \tfrac{1}{2},\ j,\ k,\ n \tag{A-17}$$

$$\overline{\delta_t(\overline{h}^y v)}^t = -\delta_x(\overline{\overline{h}^x u\,\overline{v}^x}) - \delta_y(\overline{\overline{h}^y v\,\overline{v}^y}) - \overline{h}^y{}_z(\overline{v}^z \overline{w}^y)$$

$$- f\overline{h}^y \overline{u}^{xy} - g\,\overline{h}^y\,\delta_y \zeta - (\frac{1}{\rho}\,\underline{\tau}^{yz})_{k+\frac{1}{2}} + (\frac{1}{\rho}\,\underline{\tau}^{yz})_{k+\frac{1}{2}}$$

$$+ \frac{1}{\rho} \delta_x A_x \delta_x \overline{h}^y v + \frac{1}{\rho} \delta_y A_y \delta_y \overline{h}^y v \qquad \text{at } i,\ j + \tfrac{1}{2},\ k,\ n \qquad \text{(A-18)}$$

$$\delta_z w = - \delta_x(\overline{h}^x u) - \delta_y(\overline{h}^y v) \qquad \text{at } i,\ j,\ k,\ n + 1 \qquad \text{(A-19)}$$

$$\frac{1}{\rho} \cdot (\tau^{xz})_{k+\frac{1}{2}} = A_z \frac{(U_k - U_{k+1})}{\frac{1}{2}(\overline{h}^x_k + \overline{h}^x_{k+1})} \quad \text{at } i+\tfrac{1}{2}\ j \qquad \text{(A-20)}$$

$$\frac{1}{\rho} \cdot (\tau^{yz})_{k+\frac{1}{2}} = A_z \frac{(V_k - V_{k+1})}{\frac{1}{2}(\overline{h}^y_k + \overline{h}^y_{k+1})} \quad \text{at } i\ j+\tfrac{1}{2} \qquad \text{(A-21)}$$

SECTION 13

A REVIEW OF SOME METHODS AND PARAMETERS USED IN ASSESSING EFFECTS OF WATER INTAKES ON FISH POPULATIONS

Richard L. Patterson[1]

INTRODUCTION

It may be difficult to imagine that a water intake could have any effect whatsoever upon the status of a fish population. Unlike fishermen who move from place to place to improve their catch wherever it may be found, or unlike low temperatures or low dissolved oxygen concentrations which exert their effects over wide areas on survival of all eggs and larvae, a water intake remains in a fixed position and has the single function of removing water from the river, lake, reservoir, or estuary. It does not pollute the waters around it and the only organisms that are affected in any direct way are those which happen to find themselves so close to the mouth of the intake that they are sucked into the intake canal. It would therefore appear that the only possible direct effect of a water intake upon a population might be measured in terms of total numbers of organisms removed by the intake or in terms of percentages of populations removed by the intake in a given year. However, direct effects upon sections of the aquatic habitat may conceivably be triggered by withdrawal of excessive quantities of water which, in turn, may effect recruitment or survival of the species inhabiting the area. If a water intake exhibits size or species selectively in its cropping of individuals the possibility of imbalance in food chains might be considered as an indirect effect. The losses in new recruits in subsequent years due to cropping of individuals in the present year is another type of indirect effect that may be important for a given population. Consequently, the question of impact of a water intake upon fish populations becomes a matter for investigation. Reviewed below are some population parameters and methods which are used to assess direct and indirect effects of water intakes on fish populations. Certain of the techniques are not widely known due to the recent emphasis in assessing point sources of losses of fishes from their habitats. Although the natural assumption may be that impacts of water intakes are "bad" there is nothing inherent in the methods or parameters reviewed below that requires possible impacts to be detrimental to the populations.

[1]School of Natural Resources, University of Michigan, Ann Arbor, Michigan.

NEED FOR HISTORICAL REVIEW

Aquatic populations of the Great Lakes have experienced the effects of man's activities for the past one hundred twenty years. Wells and McLain (1973) and Smith (1972) have described the historical trends in Great Lakes fish stocks depressed by (a) exploitation due to commercial fishermen, (b) introduction of exotic species, (c) accelerated eutrophication, and (d) other forms of pollution due to a variety of causes related in one way or another to industrialization and shoreland and shoreline development. When evaluating the impacts of a particular factor of fish mortality (such as power plant effects) on a fishery, this factor should be viewed within the context of the larger set of factors whose cumulative net effects produced the environmental conditions surrounding and mitigating the effect of the factor to be evaluated.

Applying the above to the evaluation of effects of water intakes as, for example, power plant cooling water intakes which cause entrainment and impingement of yellow perch populations of western Lake Erie, commercial catch data reported by Muth (1977) show the perch population to be in a depressed condition in 1977 with production having declined each year from 1973-1976. Moreover, analyses of catches showed that about 60 percent of the catch was less than the 8.5 inch minimum size recommended by the Lake Erie Technical Committee on Yellow Perch as a management strategy to protect the stocks. The Ohio Division of Wildlife (1977) also reported that the majority of the 1973 year class in the Western Basin (due to slower growth) was sublegal.

Except for increases in 1971 and 1972 yellow perch production in Lake Erie has declined steadily since 1968. Between 1952 and 1968 production fluctuated considerably but the overall trend was upward. Jobes (1952) reviewed yellow perch production in Lake Erie prior to 1952 and found it to be relatively low compared to the 1955-1968 period except for a few years of high production in the 1930's. The effects and implications of power plant induced entrainment and impingement mortality upon yellow perch in western Lake Erie beginning in the early 1970's should therefore be interpreted in light of a set of factors whose net effect produces a declining population (due most likely to a combination of overexploitation and adverse habitat conditions resulting in poor year classes in recent years). Such a trend suggests that the compensatory reserve of the population may be exhausted. That is, if an additional amount of the population is removed each year beginning in a given year, the population reaches a point at which it is unable to recover any part of this added loss. A declining population in which small sizes predominate in the catch suggests that compensation for additional removals of stocks whether by fishing, natural mortality, or entrainment and impingement may be slight at best. Additional losses to a declining population could project it into a prolonged or permanent state of depression unless stresses are relaxed. Yellow perch in the Great Lakes appear to be capable of recovering from severe stress conditions when those conditions are removed so that the possibility of its extinction is not seriously considered.

WATER INTAKES AS A FACTOR IN FISH POPULATION DYNAMICS

A box and arrow diagram, depicting flows of numbers or biomass of a fish population (Figure 1), is a convenient tool for showing the standing crops of subpopulations and their transfers which should be taken into account in order to conduct analyses of direct (same year) and long run (subsequent years) impacts of water-intake caused entrainment and impingement losses to a fish population and its associated fisheries. Direct effects of entrainment and impingement mortality refer to immediate (same year) losses sustained by age or size classes both separately and collectively including the egg state. Direct effects also include percentage loss of larval production and percent reduction of the young-of-year class caused by entrainment losses to the larval stage. An assessment of direct effects is complicated by (a) the need to obtain larval production and natural mortality estimates as well as estimates of standing crops of other size classes and (b) the differential impact that a particular water intake may exert if it selectively crops size classes and the implications of this differential cropping of size classes upon the percent reduction in the population.

Longer range or subsequent year-to-year effects are caused by losses of fishes in various size classes in earlier years. Such subsequent year effects may occur in the form of reduced numbers in different size classes, reduced yields, changes in production rate of larvae per individual adult, and changes in the natural mortality rate of larvae. Longer run effects may be termed indirect effects to emphasize their separation in time from immediate or direct effects. Long run predicted effects of water intake caused mortality may or may not be verifiable from direct measurements of standing crops in subsequent years, being a particularly difficult because of (a) the confounding of possible multiple causes of reduced population, and (b) the high statistical variability of estimates of standing crops. Methods of predicting long run impacts of water intake caused mortality require the application of numerical simulation models of a fish population of which there are a number of different types in use. They can be lumped into two groups depending upon whether they simulate the differences in a population (with and without the presence of water intake caused mortality) directly in which case they are called <u>equivalent adult</u> models or whether they simulate the fish population without the presence of water intake mortalities and again with additional losses caused by water intakes. The use of numerical simulation models requires assumptions concerning fish behavior and estimates of parameters such as female fecundity and compensatory reserve of the population. Therefore, the assessment of long run impacts of water intake caused mortality upon a fish population has all the problems of assessing direct effects plus the additional ones mentioned above.

REVIEW OF FACTORS NEEDED FOR ASSESSING DIRECT EFFECTS

Mortality Rates of Entrained Larvae

Physiological effects of chemical, thermal, abrasive, pressure and shear stresses encountered by individuals during passage through the power plant cooling cycle have been investigated and reported at various symposia.

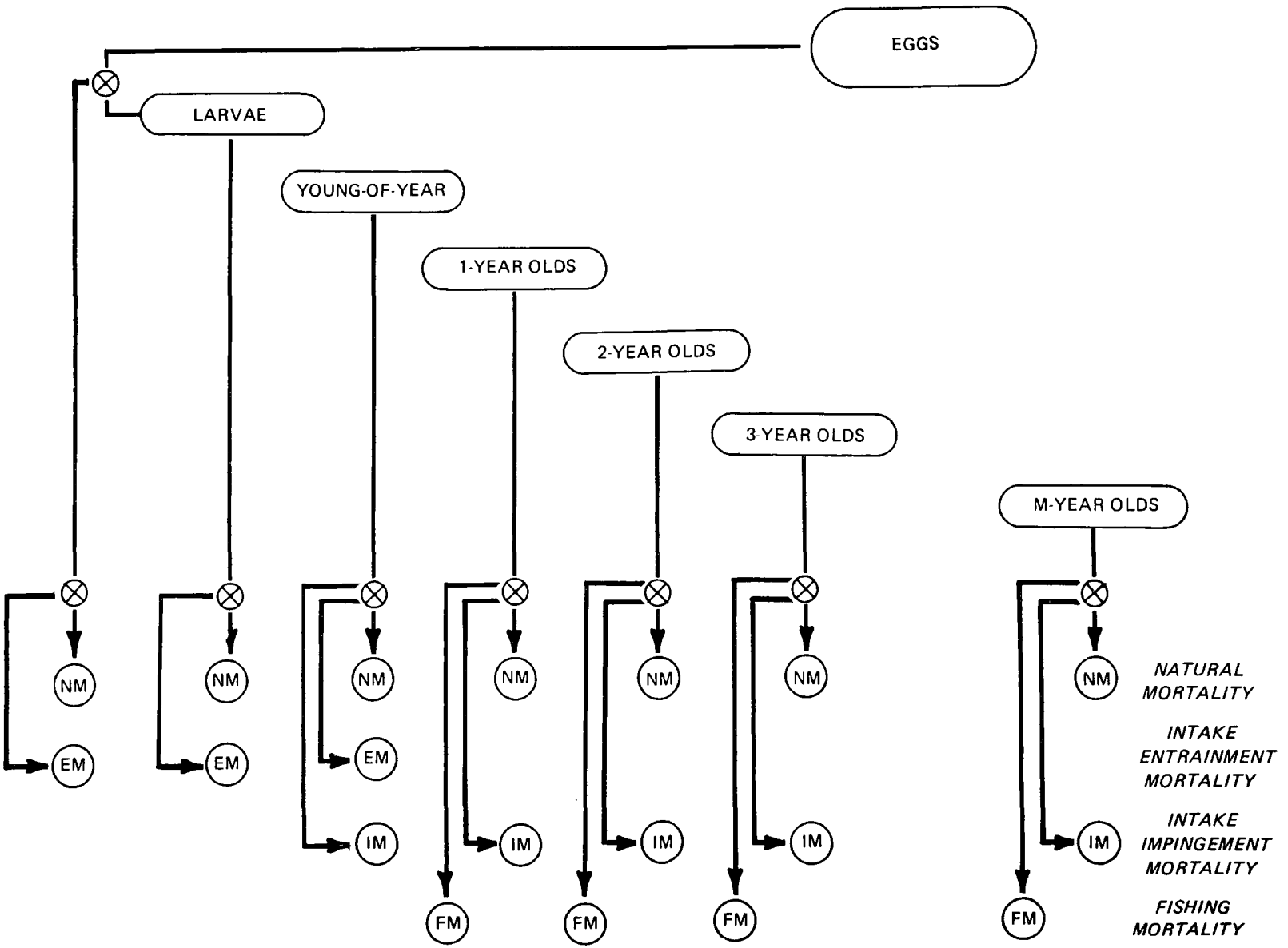

Figure 1. Box and arrow diagram summarizing transfers of fish biomass.

(Saila et al. 1975; Jensen et al. 1977). These studies provide understanding of causes of mortality of individuals and also provide a basis for estimating the mortality rates of eggs and fishes of various sizes which are entrained or impinged. Laboratory studies have shown that mortality rates can be highly variable, ranging from less than 20 percent to nearly 100 percent. The percents mortality of entrained and impinged individuals of various size classes become important when coupled with entrainment and impingement rates ranging into millions of individuals per year. Mortality rates due to entrainment and impingement must be studied on a plant by plant basis unless 100 percent mortality of all individuals is assumed. Mortality rates of entrained individuals can be estimated by a number of formulae, perhaps the most common being the difference between the percent alive at entry into and discharge from the cooling cycle:

$$\text{Percent mortality} = p_D - p_E \qquad (1)$$

Where: p_D = percent alive at discharge
p_E = percent alive at entry

For small sample sizes at either discharge or entry the standard error of the estimate of the difference of two fractions is large. Other problems arise in estimating p_D and p_E. Individuals are killed during capture and identification and Equation (1) assumes that this effect is cancelled out by virtue of the difference. Bias in the estimates of p_D or p_E or both can occur due to stratification of larvae either horizontally or vertically in the water column, by the use of sampling gear which tends to clog or operate only intermittently or by sampling infrequently during a day or week. Each of these possible causes of bias in the estimates of p_E and p_D create practical problems if they are to be eliminated. Laboratory experimental results are not a sufficient substitute for field sampling to establish entrainment mortality rates at an individual power plant intake.

Size Distribution of Entrained Larvae

Equation (1) classifies larvae of all lengths into a single category. That is, all individuals from approximately 5-35 mm are lumped into a single class called "larvae" for purposes of computing p_D and p_E. While this procedure may be acceptable due to the difficulty of obtaining samples of sufficient size, it is important to measure lengths of individual larvae in order to estimate the size distribution of entrained larvae. It is easily demonstrated mathematically (Patterson 1979) that if larger (older) larvae have a higher survival rate to the juvenile stage of development, their losses have stronger implications for the population as a whole than does the loss of newly hatched larvae. A second important reason for obtaining a size distribution of entrained larvae is to compare it to the size distribution of larvae in source waters, so that it can be determined whether selective cropping of larvae by the water intake is taking place. If it is concluded that selective cropping of larvae by size class is occurring then the sample of larvae used to estimate total numbers entrained will produce a biased estimate of the fraction of total larval production (or total standing crop) that is entrained.

Total Numbers of Entrained Larvae

The numbers, $E(t_1,t_2)$, of larvae entrained in a water intake is equal to

$$E(t_1,t_2) = \int_{t_1}^{t_2} C_p(t)\cdot Q_p(t)dt \qquad (2)$$

Where: $C_p(t)$ = concentration of larvae in water entering the intake at time t.

and $Q_p(t)$ = water flow through the intake at time t.

Records of $Q_p(t)$ are usually maintained and so this factor may be determined relatively precisely. Determination of $C_p(t)$ is another matter and for power plants with large intakes one may expect considerable error in estimating the mean concentration of larvae in the water column over even a short interval of time. Sources of error in the estimation of $C_p(t)$ directly are:

1. Stratification of larvae both vertically and horizontally in the intake canal the configuration of which may vary over time.

2. Random variation in larval densities within the water column.

3. Passage of large clumps of extremely dense larvae through the intake without being detected.

4. Clogged or inoperable sampling gear.

Direct estimation occurs by measuring larval densities at the point at which water enters or leaves the plant. Since water intakes can be very large indeed (10 m x 10 m cross sectional area) the impossibility of sampling more than a fraction of one percent of the water becomes obvious.

Indirect estimation of $C_p(t)$ occurs by measuring $C_v(t)$, larval densities in source waters (rivers, lakes, or estuaries) and assuming that

$$C_p(t) = f\cdot C_v(t) \qquad (3)$$

Where: f = ratio of mean concentration of larvae in intake water to mean concentration of larvae in source water.

The parameter f is important when concentrations in the water intake must be estimated using indirect methods and upon occasion has become the object of much debate (Oak Ridge National Laboratory Report 1977). When source waters are divided as, for example, in the case of the Monroe, Michigan power plant $C_v(t)$ is a weighted sum of mean concentrations in each source. Various methods have been used to estimate $C_v(t)$. Hubbell and Herdendorf (1977) used four methods for estimating $C_v(t)$ which differed in the way in which larval concentrations in depth zones of the source waters were averaged and

the lengths of time that larvae were assumed to be present. In each case they assumed a value of 1 for the ratio f so that $C_p(t) = C_v(t)$. Patterson (1979) estimated total numbers of yellow perch larvae entrained at the Monroe power plant in 1975 using three sets of data: (a) larval concentrations in the Raisin River channel downstream from the water intake, (b) larval concentrations at the point of discharge of cooling water from the plant, and (c) larval concentrations in lake waters near the mouth of the Raisin River. Applying Equations (2) and (3) using concentrations obtained from data sets (a), (b), and (c) Patterson obtained two estimates of f: 0.60 and 1.36. An average estimated value of 0.98 was thus obtained for f.

Total Number and Size Distribution of Impinged Individuals

Impingement occurs when individuals too large to filter through a screening device are caught and held against the device by the force of the incoming water. Impingement is estimated directly by counting the number of individuals accumulated in collecting pans or other collection hardware over a fixed time interval. As in the case of entrained larvae it is important to obtain the size distribution of impinged fishes for two reasons: (a) so that a determination of whether the impinged individuals are representative of the population as a whole, and (b) so that survival rates of fishes that are impinged and later returned to the source waters can be estimated by size class. The latter reason is particularly important because much effort is being devoted by power plant management to returning impinged fishes to source waters in a viable condition. Therefore if mortality occurs, for example, to selected size classes only, the end result amounts to selective mortality among adults induced by the power plant.

Since a complete census of impinged fishes is not taken problems of estimating total numbers impinged based upon sampling techniques arise. Statistical sampling designs for estimating total impingement have been discussed by Murarka and Kumar (Jensen 1977, Pages 267-289).

Percentage of Annual Larval Production Lost Through Entrainment

The percentage of larval production lost through entrainment mortality can be most directly and quickly estimated as:

$$\text{Percent lost in week } i = 100\left(\frac{E_i}{A_i}\right) \qquad (4)$$

Where: E_i = estimated number of larvae entrained in week i.
A_i = estimated abundance of larvae in source waters in week i.

If length data are not recorded on entrained and standing crops of larvae then both E_i and A_i are recorded in terms of total numbers only. A bias in the estimate of the percentage will then occur if the length distributions contained in E_i and A_i are significantly different. In addition, Equation (4) will overestimate percent of production lost due to entrainment because

abundance is less than production. This bias can be reduced or eliminated by replacing Equation (4) by Equation (5):

$$\text{Percent lost in week } i = 100 \frac{\Sigma E_i}{\text{Estimated annual production}} \quad (5)$$

Where: E_i = estimated number killed due to entrainment in week i. And estimated annual production is obtained by some method such as Patterson's or Polgar's.

Used as an indicator of water intake effect the percentage of annual larval production lost due to entrainment has the advantage of not requiring assumptions of any kind about the parent population and can be calculated from direct measurements obtained in the field. It has the disadvantages of susceptibility to bias and lack of interpretability in terms of implications to the adult population in source waters.

Percent Reduction in Number of Young-of-Year Recruits Due to Larval Entrainment Mortality

The percentage by which the number of young-of-year recruits is reduced due to entrainment of larval fishes is estimated as:

$$\text{Percent reduction in number of y-o-y recruits} = 100\ 1 - \left(\frac{R_1}{R_1 + R_2}\right) \quad (6)$$

Where: R_1 = number of young-of-year recruits in source waters in the presence of water intake operations.

And R_2 = number of larvae killed due to entrainment that would have otherwise survived to reach young-of-year age.

The estimate of R_1 is:

$$\hat{R}_1 = (\text{estimated number of larval produced but not entrained}) \times (e^{-D \cdot p}) \quad (7)$$

Where: D = number of days in larval stage

And p = mean daily instantaneous natural mortality rate of larvae.

An alternate estimate of R_1 can be obtained by estimating young-of-year standing crops directly and correcting for natural mortality of young-of-year to produce an estimate of number of y-o-y recruits.

The estimate of R_2 is:

$$\hat{R}_2 = \text{(estimated number of larval killed due to entrainment)} \times \int_0^D f(x) \cdot e^{-(D-x)p} dx \qquad (8)$$

Where: x = age of larvae at entrainment
$f(x)$ = relative frequency of larvae at age x when entrained.

If length data are not obtained on entrained larvae (from which ages can be estimated) than an average age $\bar{d}$ of larvae at entrainment must be used and Equation (8) becomes:

$$\hat{R}_2 = \text{(estimated number of larvae killed due to entrainment)} \times e^{(D-\bar{d}) \cdot p} \qquad (9)$$

In contrast to Equation (5) the use of Equation (6) as an indicator of water intake effect on the population projects larval mortality into a later stage of physical development. If survival rates in stages subsequent to the larval stage are known then it is theoretically possible to estimate percentages by which later life stages are reduced as a result of larval entrainment. However, the requirement of additional parameter estimates (survival fractions for life stages) renders all such estimates more and more unreliable. Equation (6) only accounts for a projected equivalent loss of young-of-year fishes due to entrainment. It does not consider number of young-of-year fishes entrained or impinged directly and consequently does not evaluate total loss to the young-of-year class. By projecting the number of larvae lost due to entrainment through several subsequent stages of physical development and applying survival factors at each stage to obtain estimates of equivalent projected losses at later stages (in later years) it is obvious that these estimates are no longer direct effects. Whether they can be considered estimates of population impacts depends upon whether they are projected to occur on a regular annual basis so that a long run change in the population and fishery can be projected.

Percent Reduction in Size or Age Classes Due to Entrainment and Impingement Losses

The number of individuals in each and every size or age class from young-of-year through adult stages killed as a result of entrainment and impingement can be estimated if the required data are obtained. Length distributions must be estimated together with total numbers impinged/entrained. If some methods is used to return impinged fishes to the source waters in a viable condition then impingement mortality must be adjusted. If estimates of standing stocks of the population are available by comparable length or age classes then estimates can be computed of percent reduction in standing stock by size class due to impingement mortality.

Vulnerability of Larval Population to Entrainment

The vulnerability of a larva to entrainment is the chance that it will be entrained during its life time (in the larval state). Larval vulner-

ability depends upon the geomorphometry of the basin of the source waters, advective and dispersive flow characteristics of the source waters, length of life of the larvae, and flow of water into the intake. Hydrodynamic models of river, lake, and estuary circulation have been used to estimate larval vulnerability to entrainment (Paul and Patterson 1977; Lawler et al. 1975) and seem to be particularly relevant in situations in which water circulation patterns (a) cause larvae to repeatedly pass near a water intake or (b) transport high concentrations of larvae long distances to the mouth of a water intake. Vulnerability is a difficult parameter to quantify because there are many environmental factors which should be taken into account quantitatively but which exhibit large variability (wind, water circulation, density of spawners, larval swimming patterns) and are difficult to measure. If a larval subpopulation occupies a certain location in source waters and is never vulnerable to entrainment it may be argued that the subpopulation sustains no direct impact but it does not necessarily follow that there is no long run impact to that subpopulation. Since it is probable the vulnerability to entrainment varies across the source water basin it is of importance to determine the degree of variation in vulnerability throughout a basin. In an extreme case it might be discovered that in only 25 percent of the basin is there a positive probability of larval entrainment while larvae which enter the remaining 75 percent of the basin become immune to entrainment. If such a condition prevailed it would be important not only for purposes of siting of future water intakes, but for purposes of managing flows into existing water intakes to know the location of the zone of high vulnerability. It may be possible to adjust intake flow regimes so as to reduce entrainment levels if a constant source of entrained larvae is identified. If larvae are differentially vulnerable to entrainment depending upon their location in the source water basin then the direct effect measured in terms of percent of the population entrained will vary across the basin.

The ratio of total numbers entrained to total numbers produced in the entire basin is simply an average percentage which may exhibit considerable variation if the ratio were calculated on a sub-basin basis.

ESTIMATING POPULATION PARAMETERS IN SOURCE WATERS

Total Annual Larval Production

Total production of larvae must be carefully defined with reference to the source waters as there can be numerous points of larval entry including spawning and hatching of eggs directly in source waters, transport of eggs and larvae into source waters by stream flow, and migration of larvae from adjacent connecting lakes, embayments, and back waters. An obvious definition of production is the number of eggs which hatch in the source waters. This definition eliminates confusion of production with migration at the theoretical level but does not eliminate the problem of separating production from immigration in the estimation process when the number of newly hatched eggs cannot be estimated directly (the usual case). A method used by Patterson (1979) to estimate production of larval yellow perch in western Lake Erie is based upon a differential equation of mass balance for larval abundance in the source waters:

$$\dot{N}(t) = h(t)-v(t)-r(t)-m(t)-L(t)-E(t) \quad (10)$$

Where:
- $h(t)$ = daily input rate of larvae to source waters
- $v(t)$ = daily emigration rate of larvae from source waters
- $r(t)$ = daily rate of larvae recruitment into first juvenile stage of development in reference volume
- $m(t)$ = daily rate of mortality of larvae in reference volume
- $L(t)$ = daily rate of withdrawl of larvae in reference volume by water intakes other than power plants
- $E(t)$ = daily rate of withdrawl of larvae in reference volume by power plants
- $\dot{N}(t)$ = net daily rate of change of larval abundance in reference volume.

By making assumptions about the forms of the various functions defined above and by experimentally estimating each function wherever possible the solved form of Equation (10) is fit to field based estimated of N(t) (larval abundance on day t) by least squares. The by-products of this exercise are estimates of total larval production and total natural mortality of larvae in source waters. Patterson assumed that net daily migration was zero and defined all larvae entering the reference volume to be part of production.

A second method which has been used to estimate larval production in source waters consists of (a) estimating total larval abundance on a periodic basis (weekly in the case of Lake Erie) throughout the entire period of larval abundance, and (b) summing the periodic estimates of abundance. The total sum is the estimate of production. This method has the advantage of requiring only estimates of abundance but requires the assumptions that (a) new crops of larvae are sampled each period, (b) all crops of larvae are sampled, and (c) natural mortality does not significantly depress each new crop prior to its being sampled.

A third method for estimating total larval production in source waters was developed by Polgar (1977) and applied to the estimation of striped bass larval production in the Potomac River. It is a refinement of the second method mentioned above and incorporates a mortality function so that the larval mortality rate is estimated together with production. In this respect it is comparable to Patterson's method.

All three methods have been applied in situations in which larval densities in source waters have been sampled at weekly intervals.

Natural Mortality Rate of Larvae

The natural mortality rate of larvae in source waters is difficult to estimate and may be the least precisely known of all population parameters. It is quite obviously an important factor in the determination of year class strength and hence of successful propagation of the population and fishery. The methods of Patterson and Polgar (preceding section) for estimating total larval production both incorporate mortality parameters and, upon assuming that mortality is proportional to abundance, yield (simultaneously with

estimates of production) estimates of the instantaneous natural mortality rate. Both estimates depend numerically upon periodic measurements of larval abundances in the source waters but differ in another respect. Patterson's method assumes a single instantaneous natural mortality rate which is constant throughout the entire length of the larval stage. The method of least squares is applied to fit the solution of Equation (10) to a time series of larval abundance data (over the entire period of larval abundance) over a two dimensional grid of mortality rate-production rate parameter combinations. Simultaneous pairs of production and mortality parameters are thus identified which minimize the mean square deviation of predicted abundance (from the solution to Equation 10) from estimated abundance based upon field measurements of larval densities. Polgar's method breaks the larval stage down into three sub-stages plus an additional stage representing eggs. Three recursive difference equations of the following form are solved:

$$\frac{A_i P_i e^{-p_i t_i}}{1-e^{-p_i t_i}} = \frac{A_{i+1} P_{i+1}}{1-e^{-p_i t_i}} \qquad (i=0,1,2,3) \tag{11}$$

Where: A_i = total estimated abundance of stage i larvae in source waters summed over all periods of observation.
p_i = mean instantaneous natural mortality rate of stage i larvae.
t_i = length of stage i development time interval.

One of the parameters p_i must be estimated independently in order to sequentially solve Equations (11).

A third method for estimting the natural mortality rate of larvae was presented by Hackney and Webb (1977). Total abundance of larvae for each 5 millimeter length class is estimated weekly based upon field sampling. Total abundance, N_i, for the entire season of each length class i is then estimated and a relationship between length class and age (days) of larvae is then established. Finally, total abundance of each successive length class i is plotted on semi-log paper against age for the respective length class, and the slope is the estimate of the mean instantaneous natural mortality rate p_i. The Hackney and Webb method is similar to Patterson's method to the extent that it uses a special case of Equation (10) which is then fit to abundance data. Instead of fitting a production function h(t) of known form to abundance data (Patterson's method), Hackney and Webb estimated a proportion of weekly production by measuring larval abundance (weekly) by 5 mm length class.

REVIEW OF FACTORS NEEDED FOR ASSESSING LONG RUN EFFECTS

Assessment of effects upon a fish population caused by water intake losses of previous years is difficult because of (a) large natural vari-

ability of the population standing crop or fishery yield from one year to the next, (b) confounding of effects of water intake caused losses with other causes of population reduction, and (c) variability of the direct effects of the water intakes from one year to the next. Consequently, it is very difficult to estimate the impact of a water intake by estimating differences in the population standing crop directly in the field from one year to the next. Special situations can be visualized such as a power plant cropping fishes of all ages from a reservoir with other environmental factors remaining fixed. If the fish population exhibits a downward trend over a period of years it may be not plausible to assume that the losses are due to the cumulative direct effects of the power plant. As plausible as this assumption might appear it remains to be tested because fish populations have been known to go into states of decline for no apparent reason. The accumulation of direct effects of annual entrainment and impingement losses are very frequently analyzed by numerical models which fall into one of two groups. A fish population is typically assumed to exist in a condition of statistical equilibrium implying that the full set of environmental conditions surrounding the population are constant. Under these conditions age distribution and fishery yields are constant. Let the population standing crop and fishery yields be denoted by N_1 and Y_1 respectively. A water intake caused loss is then introduced on a fixed annual basis. Let the new equilibrium levels of population standing crop and fishery yields be denoted by N_2 and Y_2 respectively. Then two long run impacts of the water intake are measured in terms of N_1-N_2 and Y_1-Y_2. One type of numerical model attempts to mimic the fish population before and after the introduction of the water intake and therefore estimates N_1 (or Y_1) and N_2 (or Y_2) separately, after which the difference N_1-N_2 (or Y_1-Y_2) is calculated as a measure of long term impact. Leslie-Matrix models and their modification (DeAngelis 1978) are examples of this type. A second type of model focuses upon the annual losses into an equilibrium estimate of the amount by which the population is reduced (N_1-N_2) or the amount by which the fishery yields are reduced (Y_1-Y_2). This type of model is called an "equivalent adult" model because it only is concerned with converting annual water intake caused losses into equivalent losses to standing crop or fisheries. In these models standing crops are never estimated because it is only the differences N_1-N_2 or Y_1-Y_2 that are of concern (Patterson 1978; Goodyear 1978). Each approach has advantages and disadvantages involving assumptions and parameter requirements, verifiability, and ease of development and application. It is the opinion of some that numerical models of impacts represent a "last resort" when analyzing effects of water intakes upon fish populations. In recent years, however, it appears that this method of last resort is invariably used as one means of evaluating power plant impacts upon fish populations. It is difficult to determine whether cropping caused by water intakes is sufficiently severe to project a population into an inferior competitive position within an aquatic community. If such were the case then it is an example of an ecological impact triggered by what would initially appear to be a completely unrelated cause of fish mortality. Long run ecological impacts of water intake cropping which go beyond a single population may exist and may even be significant in some cases but are even more difficult to assess.

REFERENCES

DeAngelis, D.L. et al. 1978. A generalized fish life-cycle population model and computer program. Environmental Sciences Division Publication No. 1128, Oak Ridge National Laboratory, Oak Ridge, Tenn.

Goodyear, C.P. 1978. Entrainment impact estimates using the equivalent adult approach. Power Plant Project, Biological Services Program, Fish and Wildlife Service, U.S. Department of the Interior.

Hackney, P.A. and J.C. Webb. 1977. A method for determining growth and mortality rates of ichthyoplankton. Fourth National Workshop on Entrainment and Impingement. EA Communications, A Division of Ecological Analysts, Inc., Melville, N.Y. pp. 115-124.

Hubbell, R.M. and C.E. Herdendorf. 1977. Entrainment estimates for yellow perch in western Lake Erie 1975-1976. CLEAR Technical Report No. 71, The Ohio State University Center for Lake Erie Area Research, Columbus, Ohio.

Jensen, L.D. 1977. Fourth National Workshop on Entrainment and Impingement. EA Communications, A Division of Ecological Analysts, Inc. Melville, N.Y.

Jobes, F.W. 1952. Age, growth, and production of yellow perch in Lake Erie. U.S. Department of the Interior, Fish and Wildlife Service. Fishery Bulletin 70.

Lawler, Matusky and Skelly, Engineers. 1975. Report on development of a real time, two dimensional model of the Hudson River striped bass population (1975). LMS Project No. 115-49, Tappan, New York.

Muth, K.M. 1977. Status of major species in Lake Erie, 1976 commercial catch statistics, current studies and future plans. U.S. Fish and Wildlife Service, Sandusky, Ohio.

Ohio Department of Natural Resources Division of Wildlife. 1977. Status of Ohio's Lake Erie fisheries.

Ohio Ridge National Laboratory. 1977. A selective analysis of power plant operation on the Hudson River with emphasis on the Bowline Point Generating Station. Oak Ridge National Laboratory Report No. TM-5877, Volume 2. pp. 5-78.

Patterson, R.L. 1979. Production, mortality, and power plant entrainment of larval yellow perch in western Lake Erie. U.S. Environmental Protection Agency Research and Development Report. EPA-600/3-79-087.

Paul, J.F. and R.L. Patterson. 1977. Hydrodynamic simulation of movement of larval fishes in western Lake Erie and their vulnerability to power plant entrainment. Proceedings of the 1977 Winter Simulation Conference. Vol. I. National Bureau of Standards. Gaitherburg, MD. pp. 305-316.

Polgar, T.T. 1977. Population dynamics of ichthyoplankton. Proceedings of the Conference on Assessing the Effects of Power Plant Induced Mortality on Fish Populations, Pergamon Press. pp. 115-120.

Saila, S.B. 1975. Fisheries and energy production, A Symposium. Lexington Books, D.C. Heath and Company, Lexington, Mass.

Smith, Stanford H. 1972. The future of salmonid communities in the Laurentian Great Lakes. J. Fish Res. Bd. Canada 29: 951-957.

Wells, LaRue and A.L. McLain. 1973. Lake Michigan, man's effects on native fish stocks and other biota. Great Lakes Fishery Commission Technical Report No. 20.

SECTION 14

CONTROL OF THE WATER RESOURCES OF THE AZOV SEA USING THE "AZOV PROBLEM" FAMILY OF SIMULATION SYSTEMS

A.B. Gorstko[1], F.A. Surkov[1], L.V. Epshteyn[1] and A.A. Matveyev[2]

A well-developed industrial and agrarian complex has grown up in the Azov Sea drainage basin. In a territory of 618,000 km^2, with a population of 33 million persons (13 percent of the entire population of the USSR), some 15 percent of the industrial and 21 percent of the gross agricultural products of the country are produced. Virtually the entire area of the region is utilized agriculturally, with crops covering 86 percent of the area of the drainage basin. Industrial utilization of the deposits of minerals in the area has reached a high level. Most of the deposits which have been discovered are being utilized to some extent. The entire water area of the Azov Sea (38,000 km^2) is utilized for fishing, and the use of the sea coast for recreation is growing. Thus, the most important natural resources of the region have been involved in the process of economic activity. This is referred to as the emerging regional natural-technical system (NTS) of the Azov Sea basin (Borovich et al. 1977).

The water resources represent an important structural element of the natural-technical system of the Azov Sea basin. Significant volumes of fresh water, which must be of high quality, are necessary for normal functioning and further development of industry, agriculture, power engineering, fishing, water transport, and for supporting normal living conditions of the population. However, the region is poor in fresh water resources. Whereas each resident in the European portion of the USSR has at his disposal some 6000 m^3 of fresh water per year, in this area, only 1700 m^3/yr per resident is available. Of all natural resources, it is water which presently limits the development of agricultural production in this area.

The possibility of deterioration in water quality, due to its shortages and the intensive agricultural utilization, plays a significant role in

[1]Institute of Mechanics and Applied Mathematics, Rostov State University, 192/2 Stachky Prospect, 344090 Rostov-on-Don, USSR.

[2]Hydrochemical Institute, 192/3 Stachky Prospect, 344090 Rostov-on-Don, USSR.

limiting the rate of growth of agricultural production. An increase of capital investment in agriculture and an increase in the sophistication of land use can provide an increase in the productivity of agriculture, but not rapidly enough and, more importantly, these measures cannot, in and of themselves, guarantee stability of agricultural production. The impossibility of broadening the agriculture base leaves the problem of intensification of agricultural production in a region with no alternative solutions.

The decisive factor in the intensification and stabilization of agricultural production in the region should be irrigated agriculture. The yield from irrigated land is not only significantly higher, but is is also less subject to fluctuations at the mercy of natural weather conditions than is the yield from nonirrigated land. Improvement in the sophistication of land use could also be greatly aided by irrigated agriculture.

However, construction of irrigation systems in the region would lead to a number of significant structural changes in the nature of transformation and consumption of the water reserves in the area. First of all, we must note the negative influence of the use of water for irrigation on the quality of water in rivers and streams, due to increased introduction of pollutants (particularly if mineral fertilizer is intensively used), and due to changes in the salt and nutrient composition of the runoff. Furthermore, an increase occurs in the consumptive use of water for agriculture, as a result of increased transpiration of water by plants in irrigated fields and the evaporation of water from the surfaces of reservoirs and from irrigation systems. Finally, regulation of runoff, in order to hold back flood waters for the needs of agriculture, results in seasonal leveling of the discharge of rivers and streams, which influence the hydrologic and water/salt regimes in the Azov Sea.

By 1976, the total amount of irrigated land had reached 13,300 km^2 in this area (double the area of 1971). In order for irrigated agriculture to become a truly decisive factor in the intensification and stabilization of agricultural production in the region, this surface area must clearly be increased. Plans for the development of irrigation call for continuation of the high rates of growth of irrigated land areas through the end of the century. By 1975, the total quantity of water diverted for irrigation was 9.22 km^3, the consumption use was 8.69 km^3 (Bronfman 1976).

The total consumption of water for industry, power engineering and by the population of cities and towns was 10.6 km^3 in 1975, including nonrecovered consumption on the order of 1 km^3. The volume of water diverted and consumed by these structural elements of the NTS is expected to grow slowly in the future, as planned steps are taken to develop recycling systems and introduce new technological systems which use less water.

The nature of the use of the water resources in the continental portion of the Azov Sea basin will also determine the functioning of such structural elements of the NTS as the ecosystem of the Azov Sea. This system is the most productive marine body of water, in terms of fishing, in the world. In the mid-1930's, the total catch in this sea reached 300,000 tons ($8\text{-}9 \cdot 10^3$

tons/km^2), while the potential of the sea is estimated as 850,000 tons (over $20 \cdot 10^3$ tons/km^2).

Since the Azov Sea is the final link in the chain of transformation of water resources in the region, it follows from general ecologic principles that the effects of anthropogenic action throughout the basin will be accumulated in the sea (Dyuvino and Tang 1973). Analysis of the results of observations of the status of the ecosystem confirms this belief (Vorovich et al. 1977). The present level of consumptive use of water and of discharge of pollutants, the seasonal leveling of the discharge of rivers and streams, the change in the biogenic and mineral runoff and other anthropogenic factors will cause a decrease in the biologic productivity of the sea.

Thus, the shortage of high-quality water will limit the rates of development (and in some cases, will set absolute limits of development) of the NTS of the region as a whole. To study this problem further, the region was divided into territories, the boundaries of which do not agree with any administrative-territorial boundaries. The selection of a region on the basis of geography (more precisely, hydrogeology) meets the needs of this regional study: analysis of water resources as a functional element in the natural-technical system, and the development of the scientific principles for the control of the water resources of the region.

The range of problems related to the use of water resources in the Azov Sea basin, conservation or conscientious reconstruction of the ecosystem of the Azov Sea, and the development of macroregional programs of supplementing the continental runoff in the basin will be referred to as the Azov problem. The Azov problem includes the problem of the Azov Sea in its entirety (Vorovich et al. 1977).

Solution of the Azov problem requires systematic development of a multitude of versions of regional ecologic policies and water management strategies in the Azov Sea basin, and evaluation of the probable effects of these versions in combination with macroregional projects. Tremendous human and material resources, planning, project and scientific organizations have been drawn into this process. The importance of the problem, unprecedented in terms of the scale of macroregional water management steps to be taken (Voropayev 1976; Dunin-Barkovskiy 1976), the complexity and nonintuitive nature of the behavior of the NTS (Forrester 1974), requires organization of the development and evaluation of plan versions designed to facilitate and accelerate both the generation and the evaluation of alternative plans. It seems that the basic principle of organization of all scientific plans and plan development on the Azov problem should be the idea of the man-machine system. This should include structural subsystems, decision making personnel (DMP) at various levels; experts on the Azov problem as a whole, and experts on its individual aspects; plan developers; families of "Azov problem" simulation systems (SS); an information bank; and persons who plan and conduct experiments with the SS.

The simulation system is a modular structure of significant complexity, allowing a broad range of experiments to be performed. The elements of the

structure, the modules, are essentially complete models of individual processes.

It is this representation of the SS as an element in a man-machine system which served as the basis for development of the "Azov problem" family of simulation systems. Work on the creation of the entire family is far from complete. However, the development and operation of SS should not be regarded as consisting of sequential stages. They are actually phases in a continuous process.

The "Azov problem" family of SS must include purely descriptive systems, systems with partial optimization, and the more standard, unified and detailed systems. At the present time, three simulation systems have been developed: 1) the "rough prediction" system (ISGP), 2) the "Azov Sea" system (ISAM), which is descriptive in nature, and 3) a detailed simulation system, "the land of the Azov basin" (DISSAB), a descriptive system with elements of optimization. The methodologic basis of the development of the model has been the method of simulation modeling (Gorstko 1977).

In addition to these systems, the "Azov problem" family should include the following SS, currently under development: 1) a "regional optimizer", a standard economic model, developing the structure of branches of the economy, to be optimal from the standpoint of criteria related to water resources; 2) "Aksakal", a simulation system which "allocates water" among branches and territorial systems in case of shortages, zonal economic models based on optimization of the utilization of water in agricultural production; 3) a "local optimizer", a standard economic model answering the same questions as the "regional optimizer", but developed for a significantly smaller territorial breakdown of the region; 4) "water purity", a standards SS, defining the necessary level of purification of water and the loss resulting from failure to meet purification standards. The general properties are shared by the SS of the family to various degrees.

In all SS, the object being modeled is considered to be divided into individual segments (regions). The status of each segment is described by a set of ingredients, combined in the description of the segment (status vector). The territory (or water area) of the segment is considered homogeneous in all ingredients. The union of the status vectors of all segments is called the status vector of the system as a whole.

The ingredients of the status vectors change discretely, the selection of the time step representing a complex, informal process which is conducted in combination with decomposition of the system into processes modeled by individual modules and separation of the objects into segments. The art and erudition of the creators of the SS, not only mathematicians, but also scientists studying the system from the standpoint of natural science and social-economic disciplines (hydrology, biochemistry, demography, etc.) must be employed here.

In the ISAM and DISSAB, the model is limited to a single time step (of 5 and 10 days, respectively). In the ISGP, two time steps are studied, a small step (1 month) to model rapid processes, and a larger step (1 year or

5 years, depending on the purposes of the specific simulation experiment). The latter is used to simulate long-term economic programs and versions of possible climate-determined changes which are important for the status of the water resources of the region.

The modular structure of the SS makes it possible to describe each process modeled using the mathematical apparatus which is most adequate to the nature of the process. Further, it allows independent identification of each unit before it is included in the composition on the SS.

In the "Azov Sea" simulation system, the status of each of the 7 segments, into which the water area is divided (Figure 1), is described by a

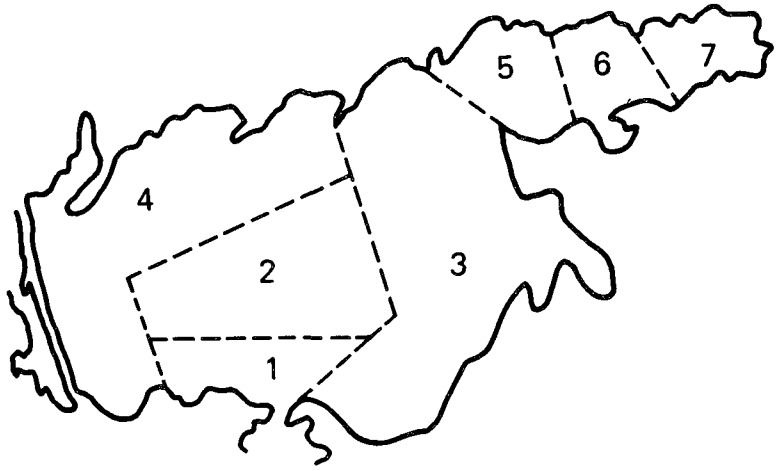

Figure 1. Diagram of regions of the Azov Sea.

status vector including 120 ingredients. The processes modeled in ISAM are distributed among 15 models (modules): WATER DYNAMICS, NUTRIENT ELEMENTS, OXYGEN, WATER QUALITY, PHYTOPLANKTON, ZOOPLANKTON, BENTHOS, GOBY, PIKE-PERCH, BREAM, ROACH, STURGEONS, HERRING, ANCHOVY, OTHER FISH. The module entitled WATER DYNAMICS includes the volume of water exchanged among regions of the sea during the five-day period in question. The module called NUTRIENT ELEMENTS describes the cycle in the SS of the compounds of nitrogen, phosphorus and silicon considering the processes of transfer, breakdown, consumption, erosion of the shore and other processes. The module termed OXYGEN models the enrichment of the water with oxygen during photosynthesis, and by atmospheric aeration; consumption of oxygen in biochemical processes, and distribution of dissolved oxygen between surface and bottom layers. The WATER QUALITY module, one of the most important in the system, models the dynamics of the concentration of pollutants considering their input and breakdown. The rate of self-purification of the bodies of water depends on the temperature of the water, type of pollutant and condition of the aquatic ecosystem.

The modules describing the dynamics of living organisms in the ecosystem consider the processes of grazing, respiration, breeding, migration and

death. Controlling influences such as removal of a fraction of the population and stocking of the sea with young fish are considered for the fish populations.

From the standpoint of program organization, the "Azov problem" simulation system is a hierarchical structure, the elements of which are standard program and information modules for this information system. The software modules consist of banks of programs (BP) on information carriers, while the information modules consist of banks of data (BD). The SS is a variable composition system, i.e., without changing the overall structure of the system, additional modules can be added to or removed from the BP and BD in the system. The modeling, control and service programs in the BP are not distinguished in the sense of rules of accessing them: Each module is assigned an arbitrary number, the first digit of which represents the hierarchical level of which the module belongs, while the second indicates its functional purpose (modeling program, control program, service program, service BD, etc.). Subsequently, several digits are provided for the class number, and several more for modifications. Addition or removal of modules in the BP includes a stage of updating the BP directory, which can be printed out by a special service program. The BP catalogue contains basic information on the module, the number, value, data of inclusion, a comment section and the number of the last simulation experiment in which the module of the BP and SS was used. The "Azov problem" family has from 3-5 hierarchical levels. Modules of higher levels hierarchy can be accessed only by programs of lower hierarchical levels.

The first hierarchical level of the entire SS contains the control programs, which call the basic control modules, check the correctness of a call and transfer control to it. The modules of the first hierarchical level operate once each time the system is initialized (STARTER class).

Modules of the second hierarchical level (REGIME class) are the main control programs. The functions of this group include actual organization of operation of the SS in accordance with its program, assigned by one or more information control files. These files are defined by the experimental planner. Their specific structure is dictated by the structure of each SS and differs greatly, e.g., between ISAM and DISSAB. We can say with sufficient generality that the control files consist of macroinstructions which are interpreted by REGIME.

The third hierarchical level of modules consists of the MODELS of various classes (e.g., in the "SEA" SS - the class WATER DYNAMICS, NUTRIENTS, etc.); the subordinate control programs (for ISAM - the classes REPLACEMENT, CHECK, ADJUST); the service programs (the classes PRINT RESULT, NORMAL OUTPUT, EMERGENCY OUTPUT); programs for generation of external factors (STOCHASTIC PREDICTION, REGRESSION ANALYSIS, EXOGENOUS FACTORS); and the basic programs for the systems servicing the BP and BD.

Modules of the fourth and fifth hierarchical levels include programs which run algorithms common for several blocks (e.g., the modules FEED, MIGRATION, CATCH, and ISAM), for all programs of the complexes which service the BP and BD, and which are accessed by the base modules of the third hier-

archical level. The program structure of one simulation system - ISAM - is shown schematically in Figure 2.

The data bank also has a hierarchical structure. All information modules have a standard format in accordance with one of the PROTOTYPES. The PROTOTYPES developed for each SS are divided into two classes - INITIAL PROTOTYPES and ANNUAL PROTOTYPES. INITIAL PROTOTYPES are designed for storage of information entering the SS from the external world, and are developed so that the information is easy and convenient to prepare. This SS is a system of variable composition with respect to INITIAL PROTOTYPES. ANNUAL PROTOTYPES describe the structure of the information modules used directly in the operation of the SS program modules. Their composition is rigidly defined, while the PROTOTYPES are developed either as unchanging, or as having an unchanging portion (e.g., prototypes of files with floating boundaries such as the prototype CHAMBER DESCRIPTION in the model LAND).

The system of modules servicing the BD is designed for input and recording of information modules with checking for the agreement of preparation of the initial data with the PROTOTYPES, adjustment of files using CORRECTING PROTOTYPES (a subclass of the class of INITIAL PROTOTYPES), sorting of information, elimination of modules, generation of new modules using FINISHED PROTOTYPES, work with the BD CATALOGUE, and output of information concerning the composition of the BD and printout of modules on the request of REGIME.

It should be noted that the FINISHED IS PROTOTYPE must include prototypes of all control modules, while the INITIAL PROTOTYPES must include prototypes of the correcting files, which can be used to generate a new control file from those already present in the BD. Thus, the BD contains a set of finished programs from the simulation experiments, and an experiment can be repeated by simply inputting a single item of data, its number. Furthermore, due to the ease of generation of new information control files in the BD, it is simple to perform new simulation experiments without preparing large files of initial data.

The most important systems functions, among those defining the difference of the simulation system from a simple large model, are performed by the modules which track the course of the simulation experiment and adjust the calculation trajectory of the system. They can be considered as a subsystem for automatic tuning of the SS in various functioning regimes during the course of an experiment, depending on the results of calculations already performed. For example, the modules of the CONTROL class in ISAM give the experimental planner the ability to see that the values of ingredients or certain simple functions (with ingredients taken as their arguments) do not go beyond established limits, or, if they do, to take certain actions.

In order to solve the Azov problem to the extent which is objectively required and possible, application of a combination of regional and macroregional, technical, economic and ecologic measures, using the "Azov problem" family of simulation systems as a tool for this purpose must be made.

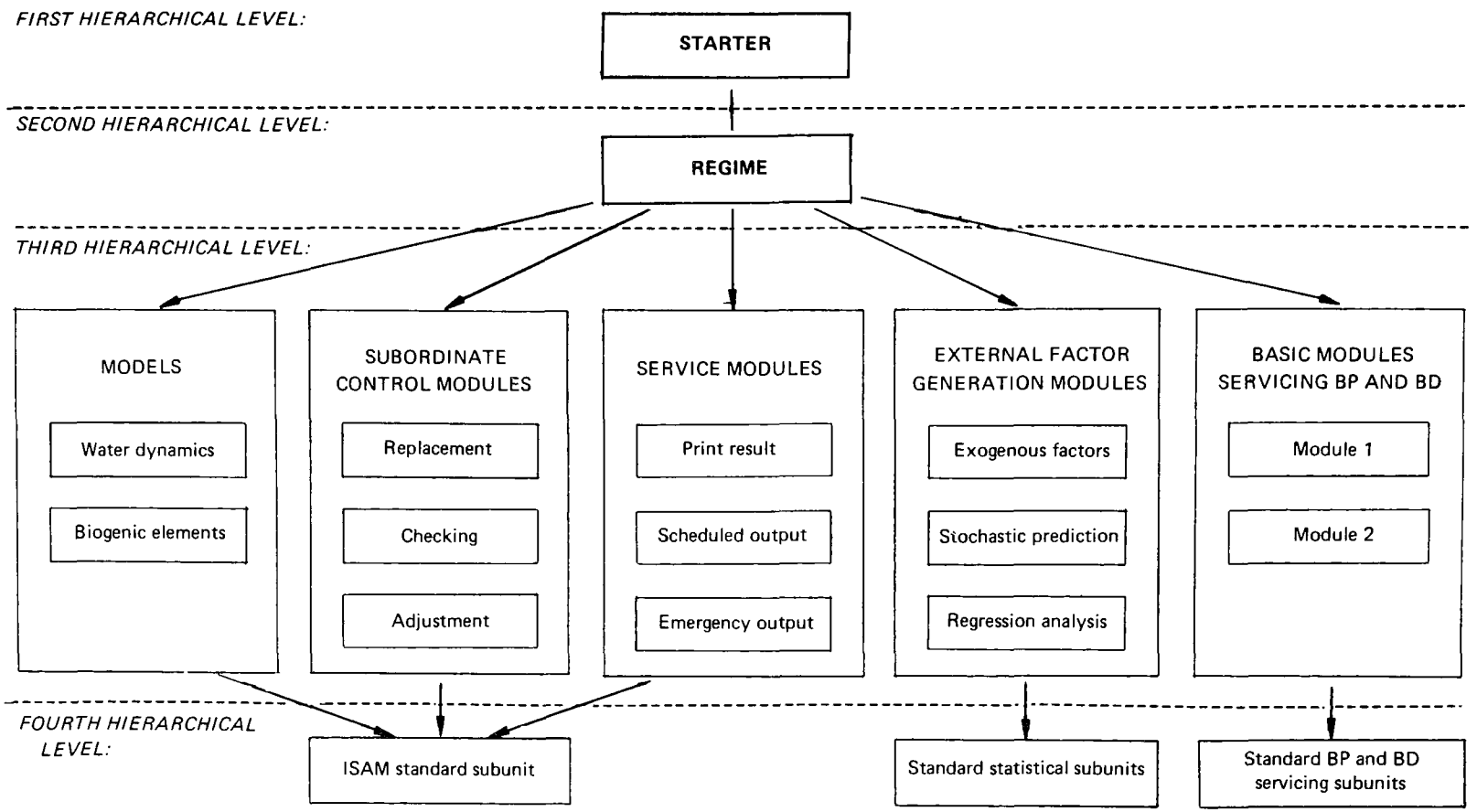

Figure 2. Program structure of the "Azov Sea" SS.

REFERENCES

Bronfman, A.N. 1976. Experience in study and solution of ecologic-geographic problems of the Azov Sea basin. Chelovek i sreda. Materials of the 23rd International Geographic Congress, Moscow, Nauka Press.

Dunin-Barkovskiy, L.V. and N.N. Moiseyev. 1976. A system of models of the redistribution of the river runoff of the USSR. Vodnyye resursy, No. 3.

Dyuvino, M. and T. Tang. 1973. Biosfera i mesto v ney cheloveka (The biosphere and man's place in it), Moscow, Mir Press.

Forrester, J. 1974. Dynamics of urban development. Translation edited by Yu. Ivanilov, Moscow, Progress Press.

Gorstko, A.B. 1977. Simulation modeling. Izvestiye SKNTs VSh, Estestv. nauki, No. 2.

Voropayev, G.V. 1976. Tasks and organization of scientific research in connection with the problem of redistribution of water resources. Vodnyye resursy, No. 3.

Vorovich, I.I., A.M. Bronfman, S.P. Volovik, and E.V. Makarov. 1977. The Azov Sea problem. IZvestiya SKNTs VSh, Estestv. nauki, No. 2.

SECTION 15

THE TRANSPORT OF CONTAMINANTS IN LAKE ERIE

Wilbert Lick[1]

INTRODUCTION

The general purpose of our research is to understand more thoroughly and be able to predict the transport and fate of contaminants in lakes. This transport and fate is a complex matter which involves physical, chemical, and biological processes, all of which need to be considered before the fate of contaminants can be predicted. In the present paper, only the physical processes of transport are discussed in detail.

Much of our work has been concerned with contaminants in Lake Erie (see Figure 1) and that work will be emphasized here. Lake Erie is a large shallow lake approximately 386 km long and 80 km wide with an average depth of 20 m. Topographically, it can be separated into three basins: (1) a shallow Western Basin with an average depth of 7 m, (2) a large, relatively flat Central Basin with an average depth of 18 m, and (3) a deeper, cone-shaped Eastern Basin with an average depth of 24 m. The Western and Central Basins are separated by a rocky chain of islands.

In the following section, a general discussion of the processes affecting the transport of contaminants is given. The results of analyses of two specific problems of contaminant transport are then presented. These are (1) the resuspension, transport, and deposition of sediments in the Western Basin of Lake Erie, and (2) the temperatures, currents, and the transport of contaminants in the Central Basin of Lake Erie during summer stratification.

FACTORS AFFECTING THE TRANSPORT OF CONTAMINANTS IN LARGE LAKES

A brief discussion of the factors affecting the transport of contaminants in lakes is given here. The transport of sediments is discussed first. Sediments are significant contaminants in themselves, since they increase the turbidity of the water and, when heavy sedimentation occurs, may require that large amounts of dredging be done. However, most importantly

[1]Department of Mechanical and Environmental Engineering, University of California at Santa Barbara, Santa Barbara, California 93106.

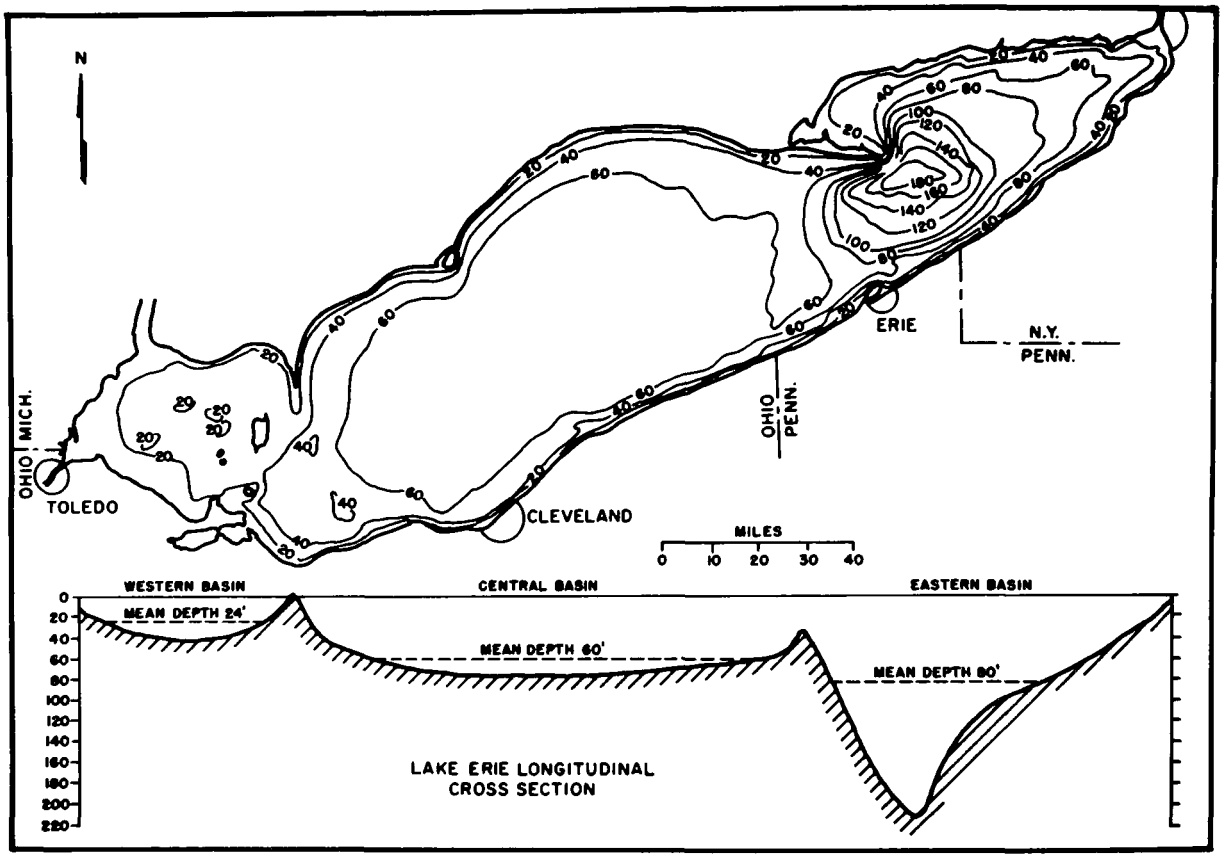

Figure 1. Lake Erie bottom topography.

in the present context, sediments (especially the fine-grained, clay-sized fraction) readily adsorb many other contaminants such as phosphates, heavy metals, and toxic hydrocarbons. Hence, if we understand the transport of sediments, we can then more readily understand the transport and fate of other contaminants.

After this brief review of sediment transport, a few comments are made on the transport and fate of other contaminants, specifically radioactive materials, nutrients, and chlorinated hydrocarbons. The discussion is meant to apply to large lakes in general. However, when specific values of parameters are needed for illustration, parameters appropriate to Lake Erie have been chosen.

Sediment Transport

The primary sources of sediments in lakes are river inflows and shore erosion while the primary sinks are river outflows and the deposition and ultimate consolidation of sediments into the permanent sedimentary bottom of the lake.

The process of the transport of sediments from the primary sources to ultimate sinks occurs by frequent cycles of resuspension, transport, and deposition. This cycle occurs on the order of a few days while the time from input to final deposition and consolidation probably occurs on the scale of months to years, perhaps tens of years. Transport may occur as suspended load (for the finer sediments) or as bed load (for the coarser sediments). The emphasis here is on the fine-grained sediments, and therefore suspended load, since the fine-grained sediments are responsible (because of their large surface area and hence adsorptive capacities) for the greater flux of contaminants.

Mass Balance Equation--

Preliminary attempts have been made to develop predictive numerical models of the transport of fine-grained sediments in large lakes (Lick *et al*. 1976; Sheng and Lick 1979). These models are predicated on the solution of the following mass balance equation,

$$\frac{\partial C}{\partial t} + \frac{\partial (uC)}{\partial x} + \frac{\partial (vC)}{\partial y} + \frac{\partial [(w + w_s)C]}{\partial z} = \frac{\partial}{\partial x}\left(D_H \frac{\partial C}{\partial x}\right) + \frac{\partial}{\partial y}\left(D_H \frac{\partial C}{\partial y}\right) + \frac{\partial}{\partial z}\left(D_V \frac{\partial C}{\partial y}\right) \quad (1)$$

where C is the concentration of the sediment, t is time, u, v, and w are fluid velocities in the x, y, z directions respectively, w_s is the settling speed of the sediment, D_H is the horizontal eddy diffusivity, and D_V is the vertical eddy diffusivity.

In order to obtain solutions to this equation and hence to determine sediment transport, various quantities such as the fluid velocities, the settling velocities, the eddy diffusivities, and of course the entrainment and deposition rates at the sediment-water interface must be known or calculated. The determination of these quantities is discussed below.

Settling Velocities--

It is known that settling velocities depend on the mineralogy and grain size of the sediments, on the ionization strength of the water, and on the sediment concentration (Owen 1978; Terwindt 1977; Fukuda 1978). Little work has been done to characterize the settling velocities of fresh water sediments and much more needs to be done. The distribution of settling velocities for a sediment from the Western Basin of Lake Erie is presented in Figure 2. Shown is the percent of suspended sediment within various settling velocity intervals. It is quite evident that the settling velocities range over four orders of magnitude, a range that must be considered in any quantitative description of sediment transport.

Entrainment and Deposition--

The net flux of sediment q_s at the sediment-water interface is the difference between the entrainment rate E and the deposition rate D, or

$$q_s = E - D \tag{2}$$

As a first approximation, it can be assumed that the deposition is proportional to concentration, and hence

$$q_s = E - \beta C \tag{3}$$

where β is the coefficient of proportionality, is known as the reflectivity parameter, and has the units of velocity. It is convenient to rewrite the above equation as

$$q_s = \beta(C \quad - C) \tag{4}$$

where $C_{eq} = E/\beta$ and represents a steady-state, or dynamic equilibrium, concentration.

The above relations are strictly only valid for sediments of uniform grain size. They are only approximations for naturally occurring sediments which have effective grain sizes varying over several orders of magnitude (indicated by the variation in settling velocities shown in Figure 2), but nevertheless are useful for organizing experimental data. It is becoming evident from our previous modeling attempts and from our experimental work that this range of effective grain sizes must be considered in any quantitative description of sediment transport.

The processes that govern the behavior of the parameters E, β, and C_{eq} are not well understood (especially for fine-grained sediments in fresh water). It is known that these parameters depend on the shear stress applied at the sediment-water interface, on the bulk sediment water content, on the mineralogy of the solid sediment, and probably on the activity of the benthic organisms present in the sediment. Experiments have been made (Fukuda 1978; Fukuda and Lick 1979; Lee 1979) and are being made to quantify these phenomena.

In experiments thus far, only the top few millimeters of sediment have been entrained. Since properties of the sediment such as water content and

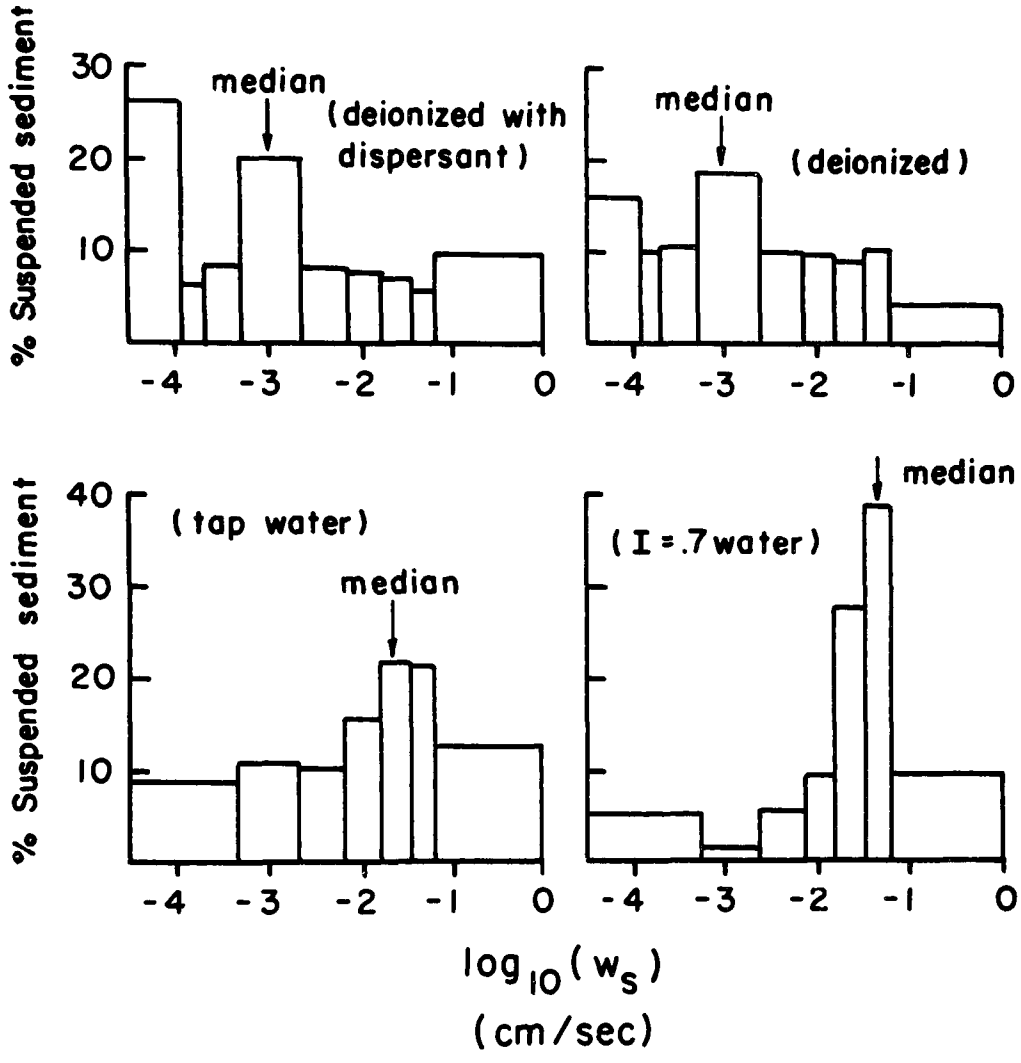

Figure 2. Settling velocity versus percent of suspended sediment for the Western Basin sediment.

grain size change rapidly with depth, it is expected that entrainment rates will also change rapidly with depth. Experiments are now being made to understand and quantify this variation, a variation that is essential to accurately predict sediment transport.

It is also becoming evident (e.g., see Thomas et al. 1972, 1976; Sly 1978; Sheng and Lick 1979) that sediment properties vary greatly throughout a lake and even throughout portions of a lake such as basins or bays. For example, entrainment rates vary by at least two orders of magnitude for sediments throughout the Western Basin of Lake Erie (Lee 1979). If this variation is not considered, accurate predictions of sediment transport can not be made.

A major influence on sediment properties that has not been quantitatively investigated as yet is the effect of benthic organisms on entrainment and deposition rates. Benthic organisms are plentiful in lakes, especially in the near-shore areas. They influence sediment properties by (1) reworking the sediments (Fisher et al. 1979; Fisher and Lick 1979) i.e., by burrowing, passing particulate matter through their guts, and egesting fecal pellets of different shape, size, and content than the original sedimentary material, and (2) excreting mucus on the surface and on burrow walls which may assist in binding the sediments. Preliminary work has been done on this problem but adequate information on the effect of benthic organisms on entrainment and deposition rates is not available.

Wave Generation and Bottom Stress--

Our sediment flux experiments give the entrainment and deposition rates as a function of the applied shear stress. In lakes, this stress is due to wave action and currents, with wave action dominating in shallow water.

In order to predict this wave action, a wave generation analysis is needed. In our computations (Kang et al. 1979), the standard SMB procedure modified for shallow water (CERC 1973; Pore 1979) has been used and is believed to give satisfactory results. This procedure gives wave height and period and water velocities throughout the water column as a function of the wind velocity and fetch.

Additional theoretical work (Kajiura 1968) is then necessary to determine the bottom stress. Recent work has attempted to extend the analysis to the case where waves and currents are considered simultaneously in their effect on bottom stress (Grant and Madsen 1979). However, no substantive field work has been done to verify these analyses and this needs to be done.

Currents--

Of course, to solve Equation (1), one must also know the currents in the lake. These may readily be obtained from present three-dimensional time-dependent numerical analyses. For a non-stratified lake, this procedure is relatively well understood, at least in principle, even though the practical application of this knowledge leaves much to be desired. In contrast, the temperatures, currents, and the dispersion of contaminants in a stratified lake are not well understood, not even in principle, although progress is being made in this respect.

Thermal stratification significantly affects the dispersion of contaminants in a lake but the effects are not quantitatively understood. For example, it is necessary to know how contaminants are transported from the hypolimnion to the epilimnion. That is, after contaminants are released in the hypolimnion, do they mainly diffuse vertically or are they convected horizontally to a near-shore area and then diffused and convected vertically into the epilimnion? Also, due to thermal stratification, strong internal waves and hypolimnetic currents may be present in sufficient strength to cause entrainment of bottom sediments. These processes are presently being investigated by means of a two-dimensional model of a stratified lake (Heinrich et al. 1979).

Characteristic Times--

Particulate matter is transported vertically through the water column to the sediment-water interface by a combination of convection, settling, and turbulent diffusion. Vertical convection is generally only significant where strong upwelling and downwelling occur, e.g., in near-shore regions, while settling and turbulent diffusion are ubiquitous phenomena. A characteristic time for settling is $t_s = h/w_s$ while a characteristic time for turbulent diffusion is $t_{diff} = h^2/2D_V$, where h is the depth of the water column. These times are equal when $h = 2D_V/w_s$. For shallow waters where $h \leq 2D_V/w_s$, turbulent diffusion dominates and settling can be neglected to a first approximation. As an example, for the Western Basin of Lake Erie, h = 7m, $D_V = 25\ cm^2/sec$, and $w_s = 2.5 \times 10^{-2}$ cm/sec. Hence, $t_s = 3 \times 10^4$ sec while $t_{diff} = 10^4$ sec and settling can be neglected compared to turbulent diffusion.

These are characteristic times for transport through the water column. The rate at which particulate matter is taken out of the water column is determined by the deposition rate $D = \beta C$. A characteristic time for deposition can be determined to be $t_{dep} = h/\beta$. From experiments, β is approximately 8×10^{-3} cm/sec. For the Western Basin, t_{dep} is then 10^5 sec and much greater than t_s or t_{diff} and is therefore the rate controlling step.

These characteristic times are only meant to give some indication of the relative importance of the different processes. No account has been taken of variations in β or the range in effective sizes and settling velocities of the particles of sediment.

Verification--

The times between storm or strong wind events in the Great Lakes area is approximately three to seven days. This is longer than or at most comparable with the time scales associated with the sediment transport processes. This leads to the conclusion that the sediment concentrations in the water column during a strong wind event are primarily dependent on conditions during that event and are not dependent on conditions much before that event. Therefore, for adequate verification of the resuspension, transport, and deposition processes, the output from the numerical models must be compared with sets of observations taken no more than a few days apart. For these purposes, satellite and aircraft (which give synoptic surface concentration data) coupled with surface ships (which give vertical profiles of concentration at a relatively few points throughout the area) are excellent.

Although the above procedure will serve to verify the short-term resuspension, transport, and deposition processes, the major question is the ultimate fate of contaminants and this involves time scales of months and years. Once the short-term processes are understood and verified, it is then necessary to do a long-term calculation and verification. By a long-term calculation, I mean either a one-year calculation under actual conditions or a set of short-term calculations statistically-averaged over a year. The latter may be more efficient and also statistically correct considering the short time scales associated with the resuspension-deposition cycle as compared to a year or the long time scales for deposition and ultimate consolidation. This long-term verification must be made by comparison of model output with sediment accumulation rates and/or accumulation in the sediments of other easily measured and easily modeled substances such as radioactive materials.

Other Contaminants

Sediments are a relatively simple contaminant to model since no biochemical transformations are involved. In attempting to predict the ultimate fate of other contaminants, quite complex chemical and biological transformations must be considered as well as the physical processes discussed above. These transformations occur not only in the water column but also in the bottom sediments and in aquatic organisms.

The basic mass balance equation for any substance is simply Equation (1) with the addition of a source-sink term S which describes these biochemical transformations. For radioactive materials, the next easiest contaminant to model after sediments, this source-sink term is given by $S = -\lambda C$, where $1/\lambda$ is the radioactive decay time. Because of the simplicity of this reaction and because of the observational data available (e.g., Robbins 1979; Robbins and Edgington 1979a,b) it is possible to develop and verify a model of transport of radioactive materials relatively simply compared to other contaminants. With radioactive materials and with other contaminants as well, processes occurring in the sediments such as benthic activity, chemical transformations and diffusion, and resuspension and deposition processes are especially important and must be considered in the interpretation of vertical sediment concentration profiles.

Nutrients are another important class of contaminants and their ultimate disposition is an important problem. Water quality models (which describe the interactions between nutrients, phytoplankton, and zooplankton) are available (Bierman 1979; Thomann *et al.* 1976; DiToro 1979) and are constantly being improved. These models are presently being coupled with hydrodynamic models, at least in a crude sense. It is becoming more evident that transfer of nutrients to and from the bottom sediments, particularly when the lake is stratified, is a significant factor in the overall nutrient mass balance equation. Experimental and theoretical work has been done (Mortimer 1941, 1942, 1971; DiToro 1979) and is being done to understand this process better. Detailed analyses coupling this sediment work and hydrodynamic models with water quality models needs to be done.

Probably the most important class of contaminants in lakes at the present are the toxic chlorinated hydrocarbons. Although the physical processes by which they are transported are generally understood, their biochemical transformations are not generally quantitatively known. A description of their ultimate fate depends on obtaining this information.

With many hazardous substances, it is also imperative to consider the accumulation of these substances throughout the aquatic food chain. A discussion of this problem and the appropriate equations for dispersal in the aquatic system and accumulation in the aquatic food chain is given by Thomann (1979).

THE RESUSPENSION, TRANSPORT, AND DEPOSITION OF SEDIMENTS IN THE WESTERN BASIN OF LAKE ERIE

The Western Basin of Lake Erie is quite wide, with an average width of approximately 50 km, but is extremely shallow, with an average depth of only 7 m. Because of this and because of large inputs of sediments from the Maumee and Detroit Rivers and from shore erosion, large sediment concentrations and especially large variations in sediment concentration are present in the Western Basin.

These large variations in sediment concentration make the Western Basin particularly amenable to sediment transport analyses. In addition, an excellent surface sediment concentration data base is available. This data base consists of synoptic maps every few days of surface sediment concentrations in March and April 1976 and was made by means of aircraft overflights. For these reasons, it was decided to model the sediment transport in the Western Basin of Lake Erie.

In order to have a valid, predictive analysis of sediment transport, it is necessary to know (1) the resuspension and deposition rates as a function of the applied stress for sediments throughout the area being investigated, (2) the bottom stress as caused by the combined action of waves and currents, and (3) the currents as determined by winds, throughflow, and any possible stratification. These components must then be coupled with the sediment mass balance equation, Equation (1), to give the sediment concentration as a function of position and time. A summary of our work on these problems for the Western Basin of Lake Erie follows.

Resuspension and Deposition Rates

Experimental work has been done by us to determine the resuspension and deposition rates for sediments from the Western Basin (Fukuda 1978; Fukuda and Lick 1979; Lee 1979). The experiments were done in a circular flume (see Figure 3) with an outer radius of 66 cm and an inner radius of 51 cm for a channel width of 15 cm. The top rotates and produces a shear flow which in turn exerts a shear stress on the sediment-water interface. Velocity profiles were carefully measured and were used to determine this shear stress as a function of ring rotation rate.

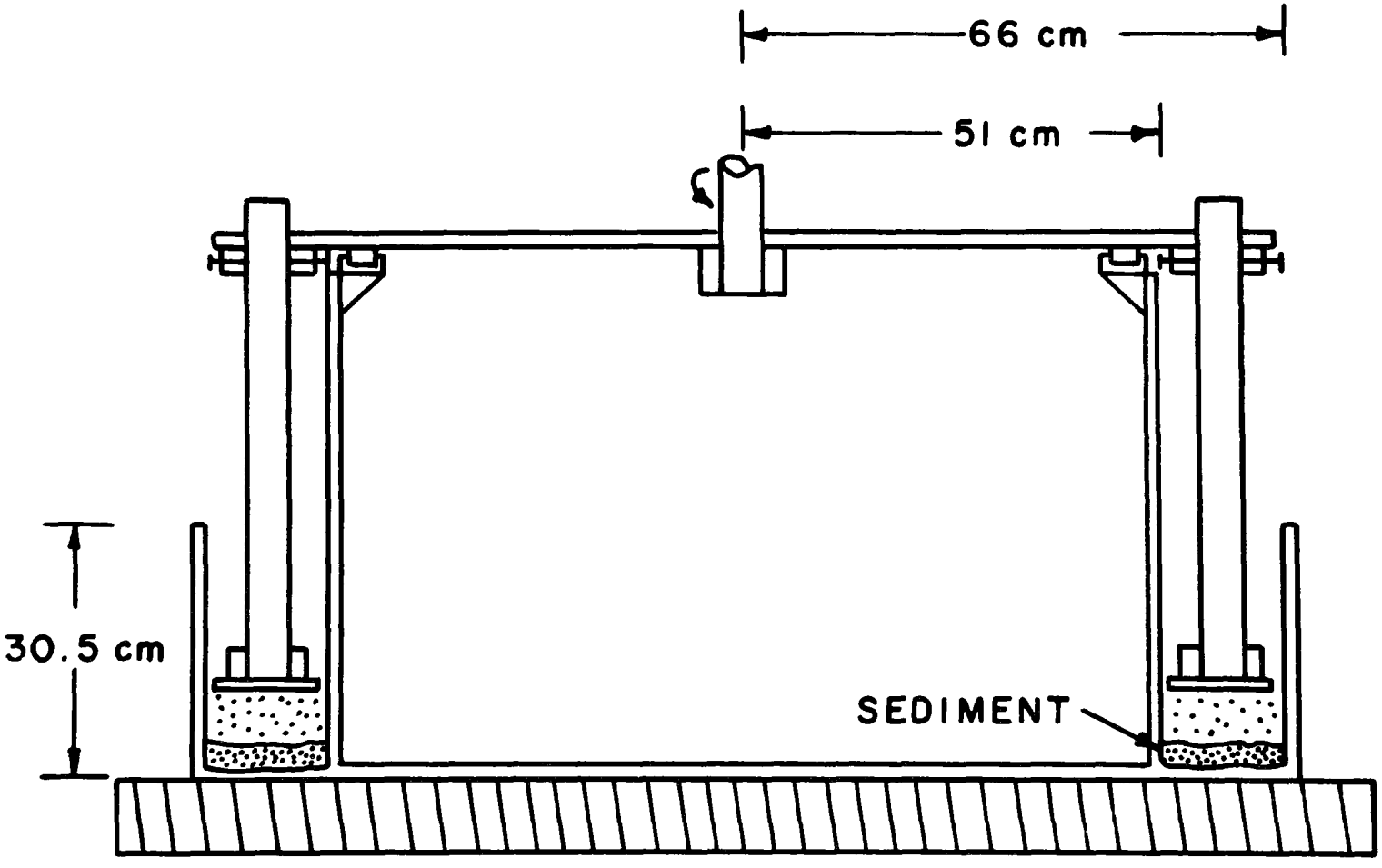

Figure 3. Side view of the flume.

The sediments were placed in the flume and allowed to settle for periods of one to ten days until the desired water content was reached. The top was then rotated at a prescribed rate corresponding to the desired shear stress. Due to this stress, the suspended sediment concentration increased with time until a steady state was reached.

A typical variation of concentration with time is shown in Figure 4. The entrainment parameters (E, C_{eq}, and β) were obtained from data of this type, i.e., C_{eq} is steady state concentration, E can be determined from the initial slope of the concentration versus time curve, and β can then be calculated from $\beta = E/C_{eq}$.

Typical results for the entrainment rate for three different types of sediments (a shale-based sediment with a high clay content of 68%, a sediment from the Western Basin with a clay content of 38%, and a sediment from the near-shore of the Central Basin with a clay content of 34%) are shown in Figure 5. It is quite clear that the entrainment rate varies rapidly with the applied shear stress and bulk sediment water content and also depends strongly on the sediment type. Results for C_{eq} show similar variations. The entrainment rates on a linear scale for the Western Basin sediments are shown in Figure 6. It can be seen that E increases rapidly near a critical stress but then increases less rapidly at higher stresses. More work is being done at these higher stresses to better delineate these parameter variations.

The variation of the reflectivity parameter β with applied shear stress is shown in Figure 7. It can be seen that the variation of β is rather small compared to the variations in E and C_{eq}. The average value of β for all three sediments is 8.4×10^{-3} cm/sec with a standard deviation of $\pm$ 5.9×10^{-3} cm/sec.

Additional work has been done on other sediments from the Western Basin (Lee 1979). From these latter experiments, it can be shown that, although the general functional dependences of E, C_{eq}, and β on shear stress and water content are similar for all sediments tested, the values of these parameters change from one sediment to another by as much as two orders of magnitude. This obviously has a significant effect on sediment concentrations and sediment transport.

Wave Action and Bottom Stress

Surface waves are generated by the winds through energy transfer from the winds to the waves. Although recent theoretical developments are useful in understanding the wind-wave energy transfer mechanisms, the most useful procedures for predicting wave parameters are the semi-empirical methods such as the PNJ method developed by Pierson, Neumann, and James (1955) and the SMB method developed by Sverdrup, Munk, and Bretschneider (Sverdrup and Munk 1947; Bretschneider 1958).

The SMB method as modified for shallow water (Bretschneider 1958; CERC 1973) has been used in our calculations. These relations give the significant wave height H and significant wave period T as a function of wind speed

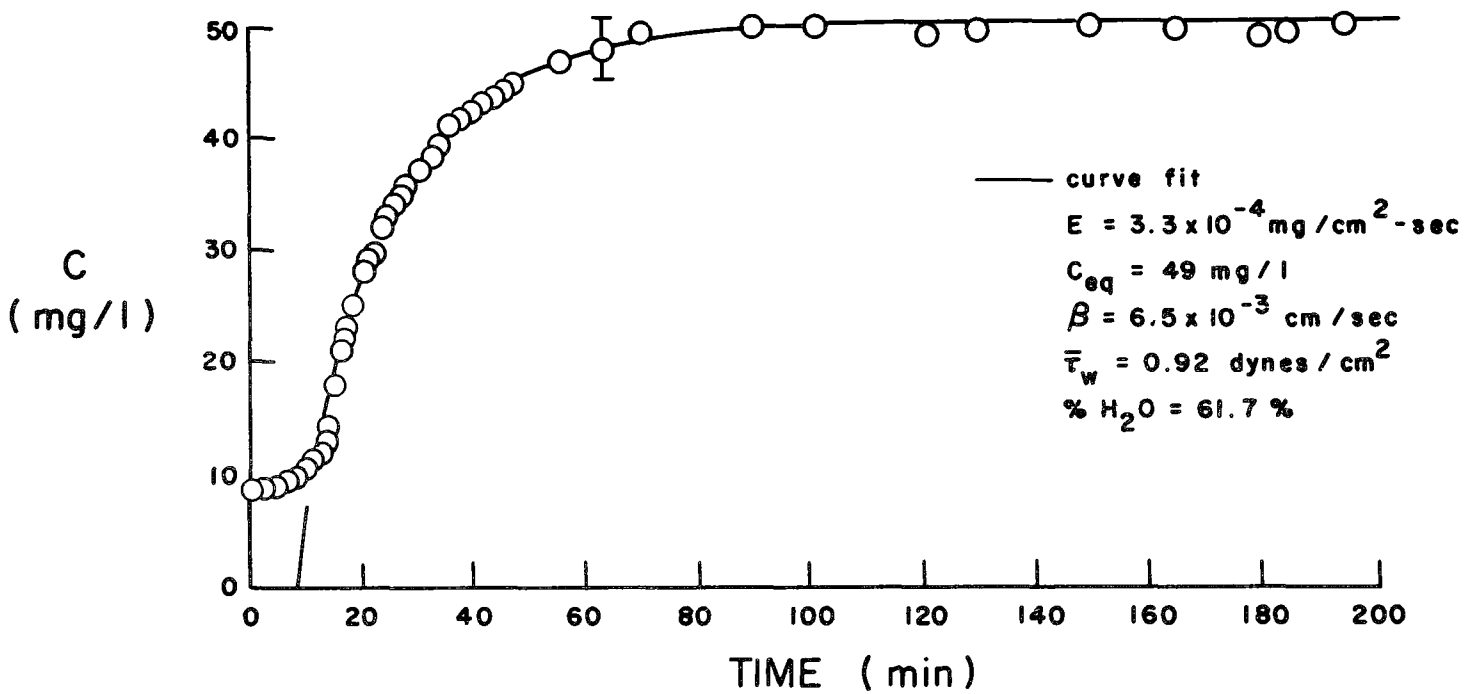

Figure 4. Example of the concentration time history data for the shallow-based sediment with τ_W = 0.92 dynes/cm^2 and a water content of 6.7%.

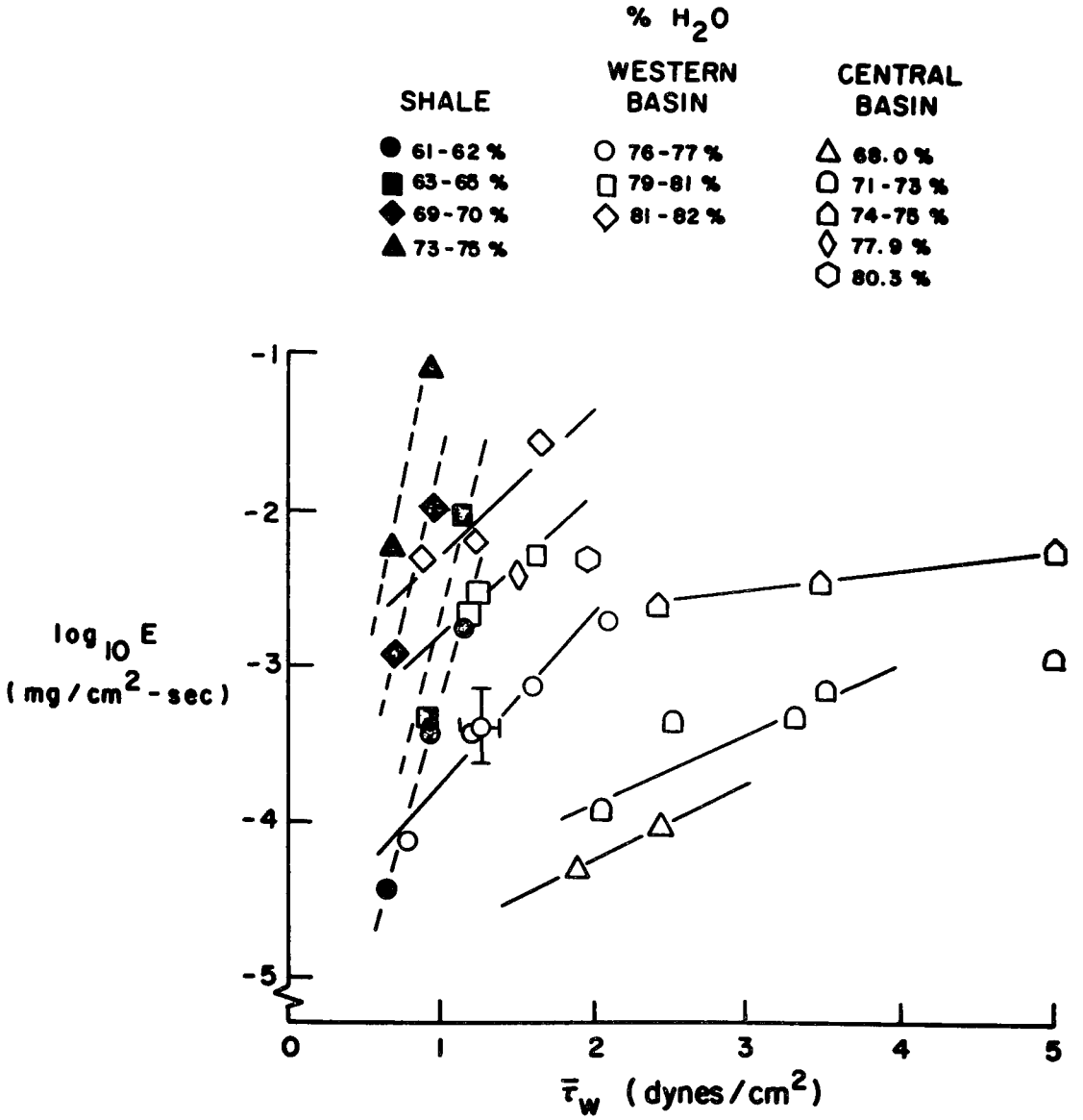

Figure 5. The entrainment rate as a function of the average boundary shear stress for the shale-based, Western Basin, and Central Basin sediments.

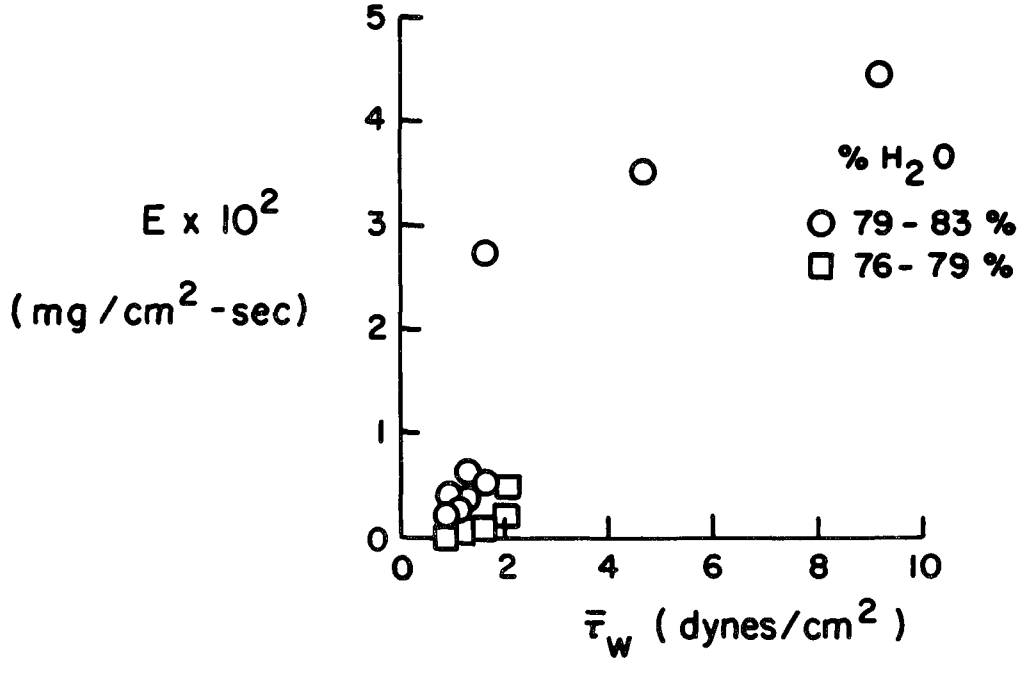

Figure 6. The entrainment rate as a function of shear stress on a linear scale for the Western Basin sediment.

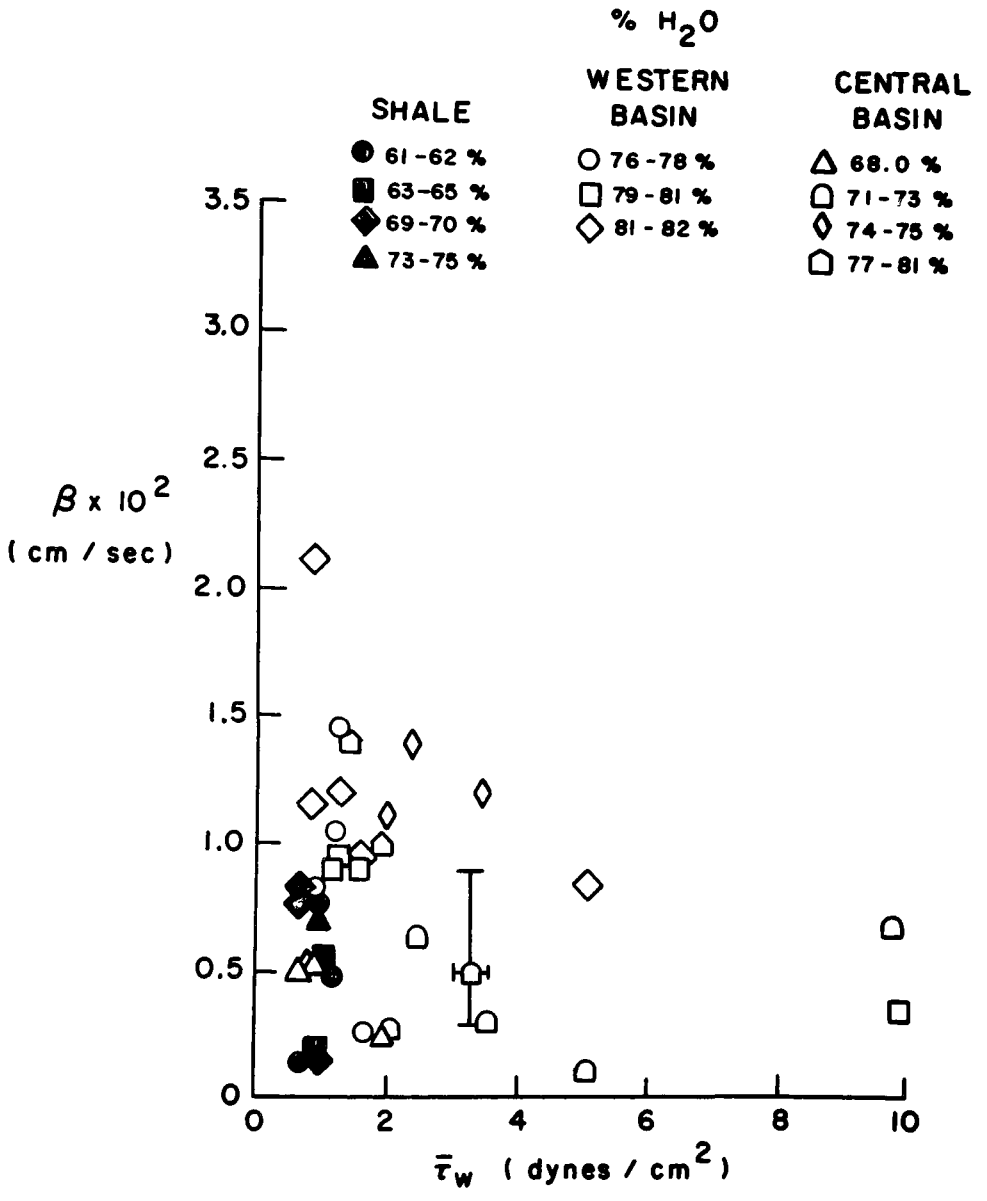

Figure 7. The reflectivity parameter as a function of shear stress for the shale-based, Western Basin, and Central Basin sediments.

U, fetch length F, and mean depth D. From these relations and assuming inviscid flow, the horizontal periodic flow at the sediment-water interface can be determined. Near this interface, of course, a turbulent boundary layer occurs and produces a shear stress on the sediment-water interface.

In general, this maximum shear stress τ_w can be written as

$$\tau_w = C_{fw}\rho\,\overline{U}^2 \tag{5}$$

where ρ is the water density, $\overline{U}$ is the maximum velocity just outside the boundary layer, and C_{fw} is a bottom friction coefficient which depends on both surface roughness and flow characteristics in the wave boundary layer. Kajiura (1968) has analyzed this problem and developed a relationship between C_f and R where $R = \overline{U}/(\sigma\nu)^{1/2}$, ν is the kinematic viscosity, and σ is the wave frequency. This relationship is shown in Figure 8.

By use of the above equations and parameters, we have developed a numerical routine to give wave amplitude, period, bottom velocity, and bottom stress as a function of wind speed for any location on Lake Erie (Kang et al. 1979). Typical results are shown in Figures 9a, b, and c for the Western Basin and for a South-West wind at a speed of 11.2 m/sec (25 mi/hr). Of most interest for the present purposes is Figure 9c which shows the bottom stress. It can be seen that in much of the Western Basin the bottom stress is greater than one dyne/cm^2 and therefore at least the fine surficial sediments can be readily resuspended. Along the northern shore, bottom stresses of 5 to 10 dynes/cm^2 are present leading to entrainment of all but the coarsest particles. As can be seen in Figures 9a, b, c, a difficulty with the present analysis is that it does not include effects of wave diffraction and refraction, effects which are obviously important in the lee of the islands.

Currents

The wind-driven currents were calculated by means of a two-mode, time-dependent, free-surface model (Sheng and Lick 1979). Basic assumptions of the model were that the pressure varied hydrostatically, eddy coefficients were used to account for turbulent diffusion in both the horizontal and vertical directions, and the density was constant. Vertically stretched coordinates were used.

At the free surface, the wind stress was specified. At the sediment-water interface, the shear stress τ_c due to currents was given by

$$\tau_c = \rho C_{fc} u_B \,|u_B| \tag{6}$$

where C_{fc} = .004 and is a dimensionless skin friction coefficient (Sternberg 1972) and $|u_B|$ is the magnitude of the bottom flow velocity u_B.

An Analysis of a Specific Event

The above investigations of sediment resuspension and deposition, wave action, and currents were coupled with the sediment mass balance equation,

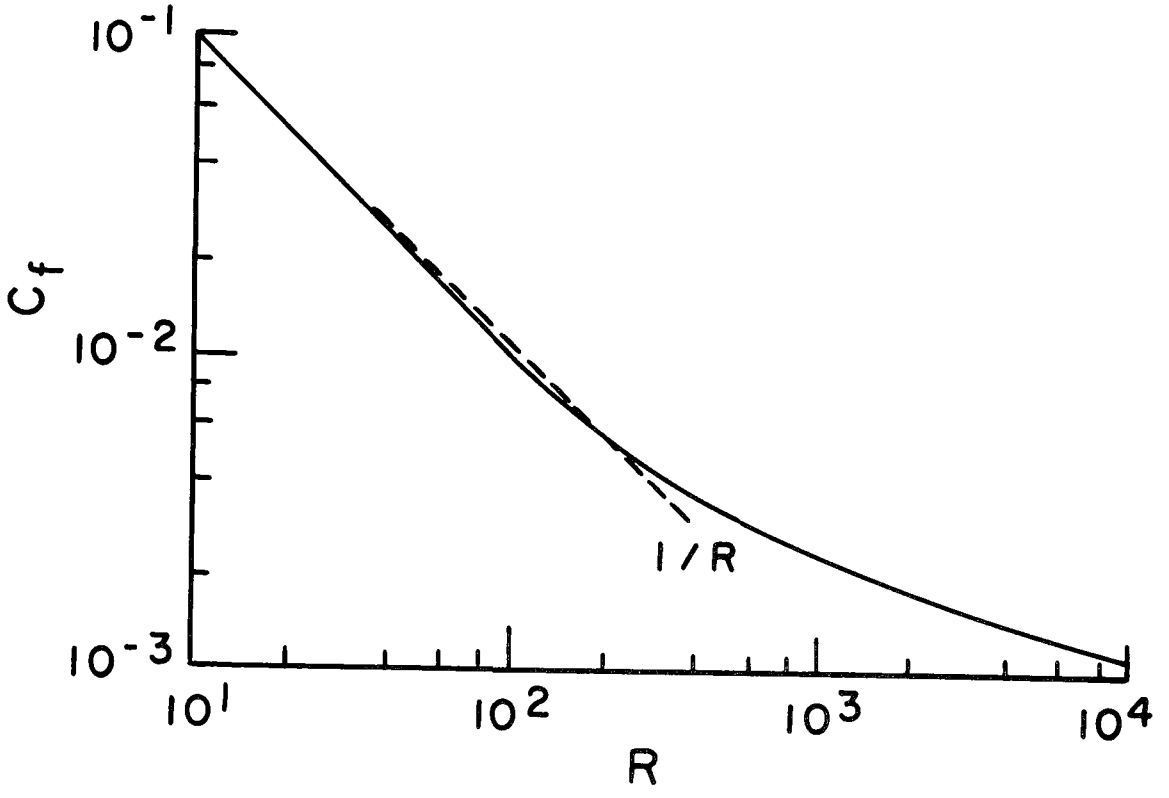

Figure 8. Friction coefficient as a function of Reynolds number for an oscillatory flow over a smooth bottom.

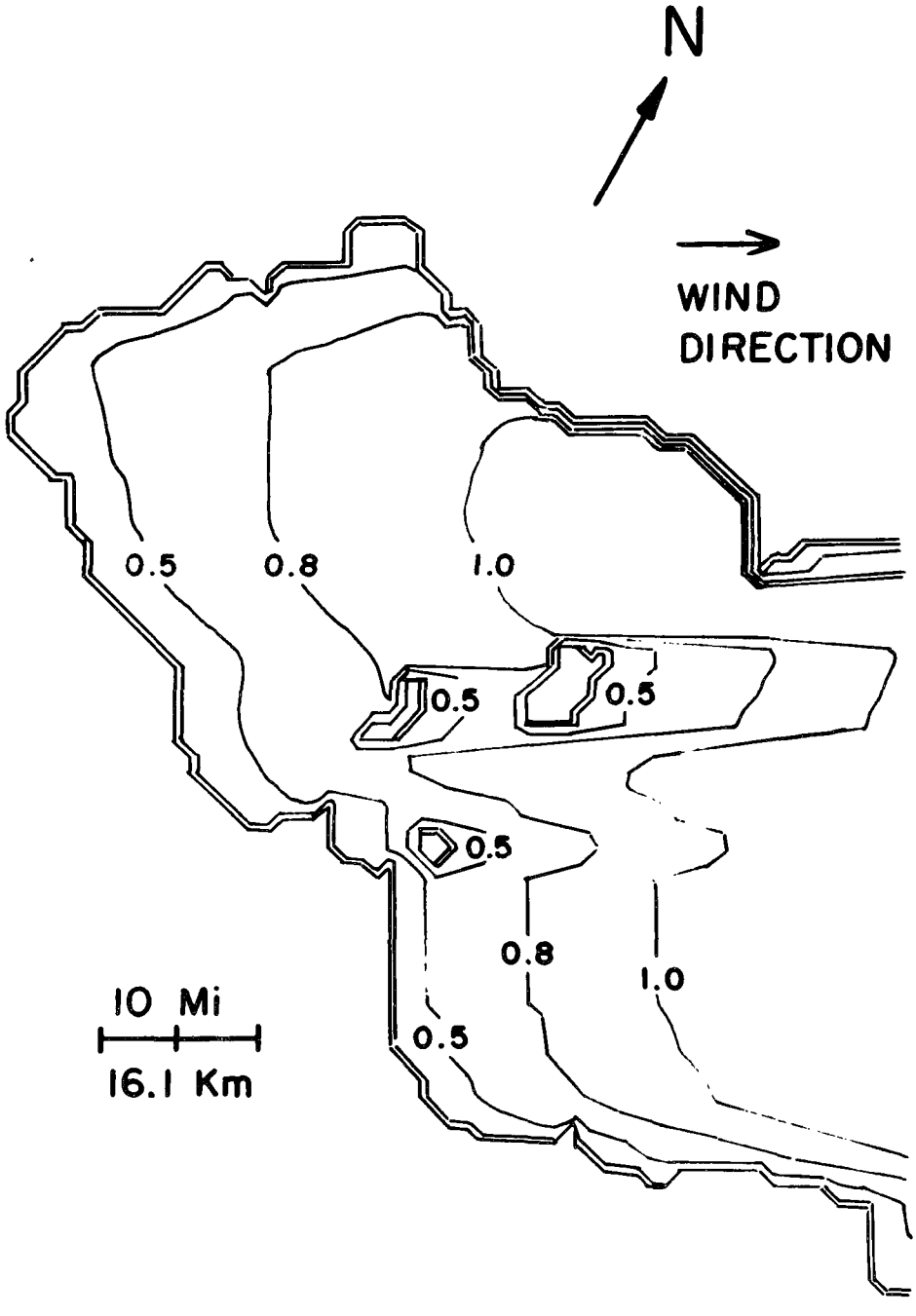

Figure 9a. Significant wave height in meters for a winds speed of 11.2 m/sec (25 mi/hr) and a southwest wind.

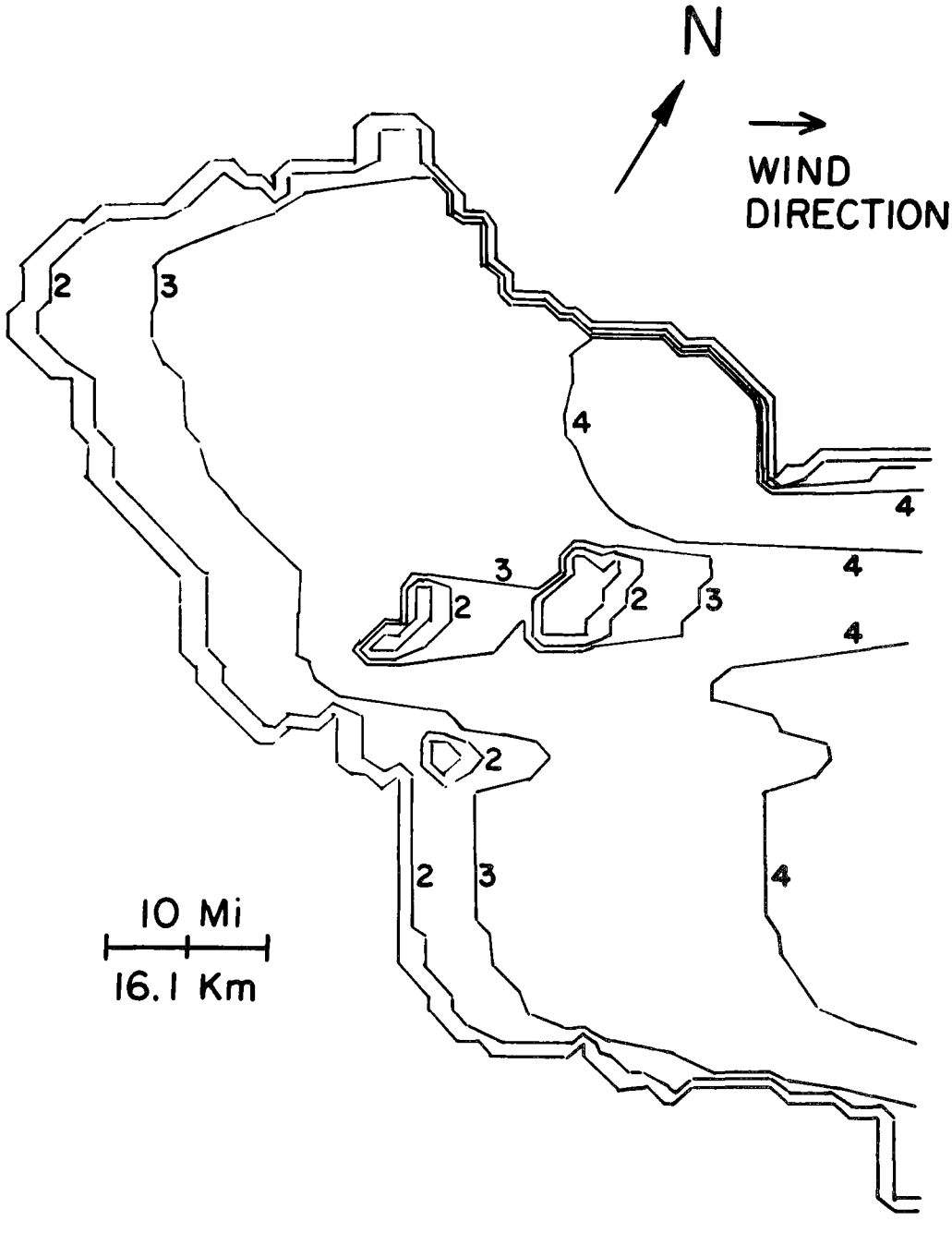

Figure 9b. Significant wave period in seconds for a winds speed of 11.2 m/sec (25 mi/hr) and a southwest wind.

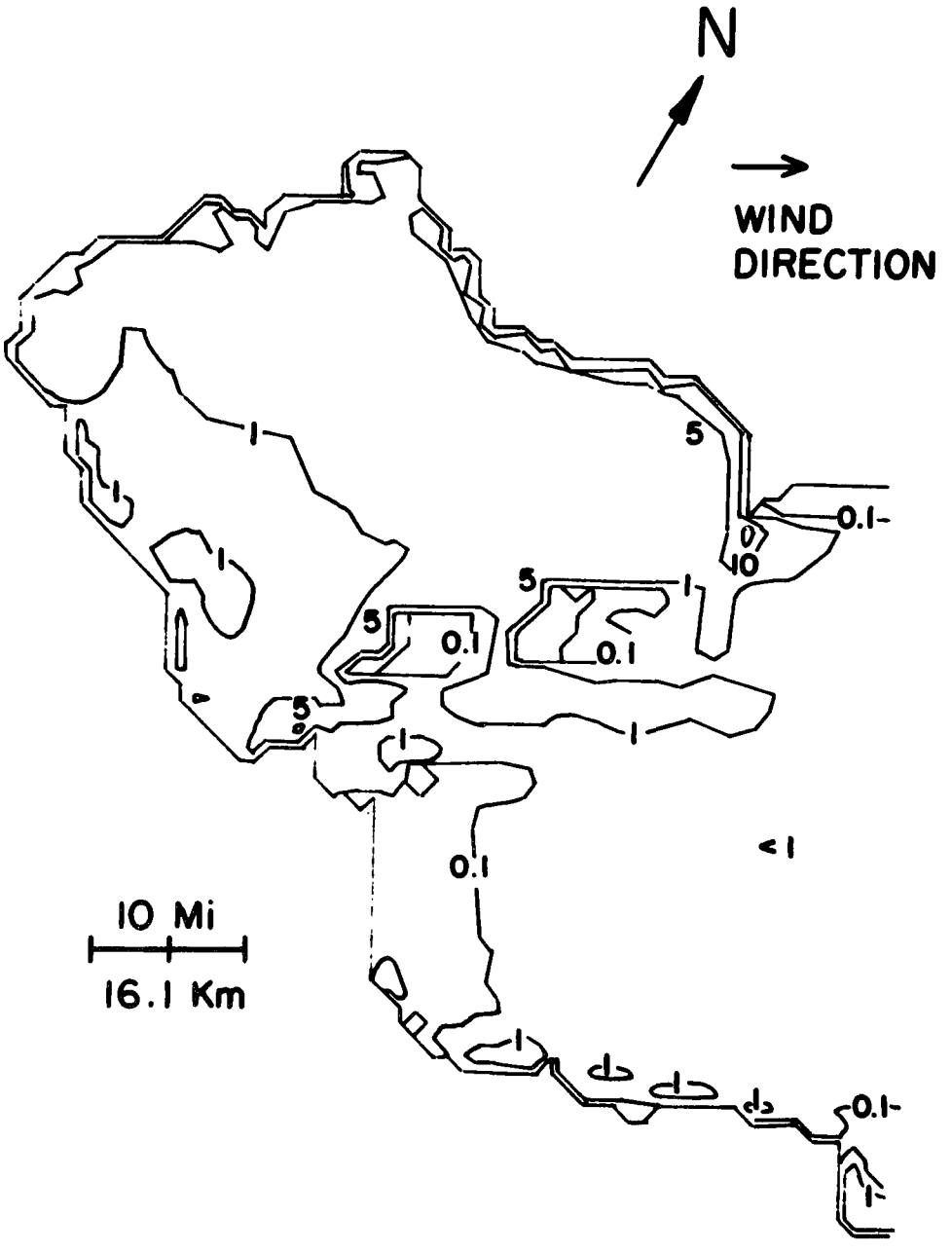

Figure 9c. Bottom stress in dynes/cm^2 for a wind speed of 11.2 m/sec (25 mi/hr) and a southwest wind.

Equation (1), and used to calculate the sediment concentrations during a specific, short-term event from 8 March to 11 March, 1976 in the Western Basin (Sheng and Lick 1979).

In the numerical calculations, a one-mile grid was used in the Western Basin and was coupled with an eight-mile grid throughout the rest of the lake. Seven points in the vertical were used. Wind data at hourly intervals from nine weather stations were used to generate the wind field over the lake. A settling speed for the sediments of 0.05 cm/sec was assumed. The results are not sensitive to the value of this parameter. To estimate the bottom shear stresses due to the combined action of waves and currents, it was assumed that the time-averaged shear stress τ_B was given by

$$\tau_B = \frac{1}{T} \int_0^T |\tau_W + \tau_C| \, d\tau \tag{7}$$

where τ_W and τ_C are given by Equations (5) and (6) respectively and T is the wave period.

The sediment concentration data at noon, 8 March, 1976 (obtained from aircraft imagery and surface ships) were taken as initial data to the sediment transport model and are shown in Figure 10. The calculation was continued until noon, 11 March. The observations and the computed results at this time are shown in Figures 11 and 12.

It can be seen that near the southern shore there is reasonable agreement between the observations and the calculations. In other areas, significant discrepancies exist. It is believed that the major reason for this is an inadequate knowledge of the sediment resuspension and deposition rates throughout the Basin. Recent work (Lee 1979) has indicated that significant variations in sediment entrainment rates occur throughout the Basin. In particular, near the mouth of the Detroit River, the entrainment rate has been found to be less than the rate used in the calculation above by approximately a factor of ten. Other areas also showed much lower entrainment rates than the one used above.

In addition, in the calculations, since no data was available, no account was taken of the change of entrainment rate with depth, a variation that surely must be significant. It is also believed that the bottom stresses are not adequately specified. More work is needed to analyze properly and especially to verify the stresses due to the combined actions of waves and currents.

TRANSPORT IN THE CENTRAL BASIN OF LAKE ERIE DURING SUMMER STRATIFICATION: A TWO-DIMENSIONAL MODEL

The Central Basin of Lake Erie is wide, flat, and shallow (see Figure 1). The Basin stratifies during the summer with a thermocline generally at a depth of 16 to 20 m and only a few meters from the bottom. The epilimnion temperatures in late summer are near 20°C while the hypolimnion temperatures

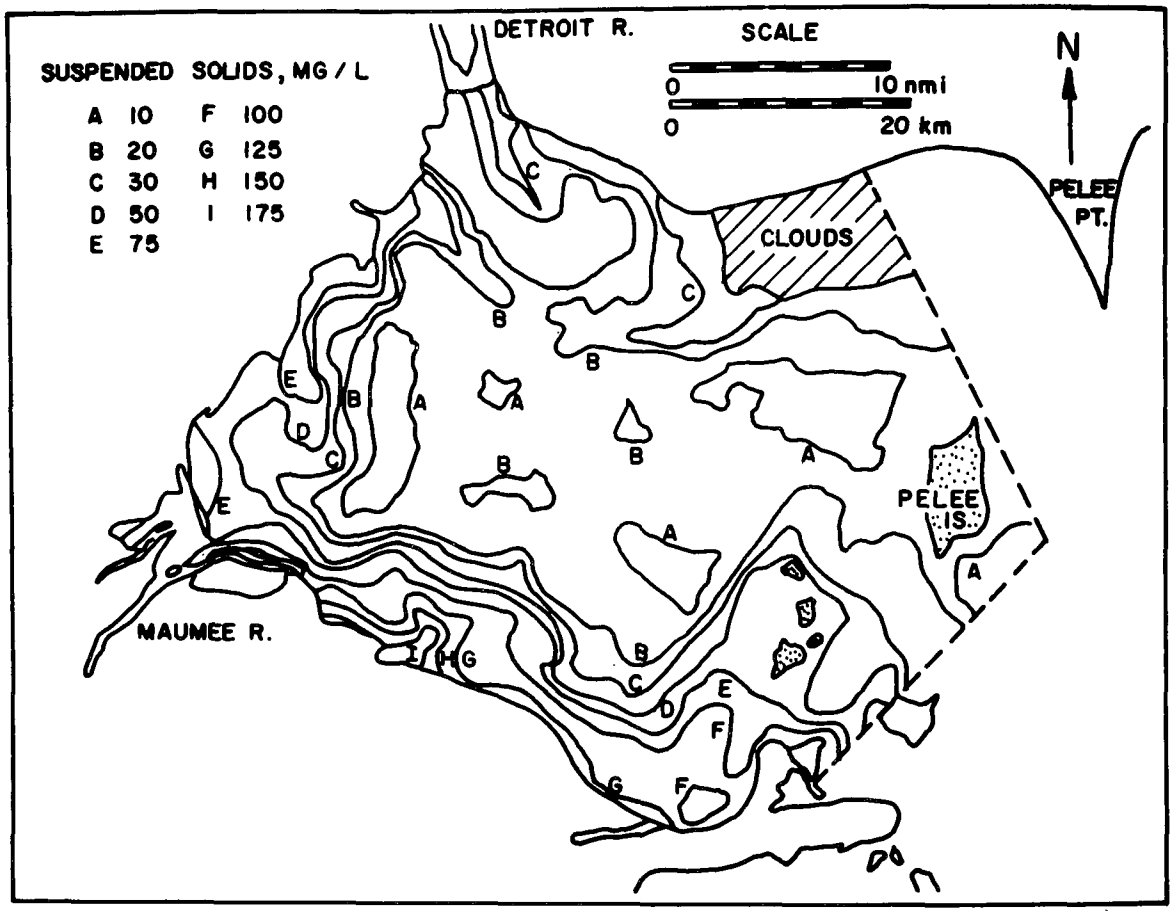

Figure 10. Near-surface total suspended solids map for the Western Basin of Lake Erie on March 8, 1976.

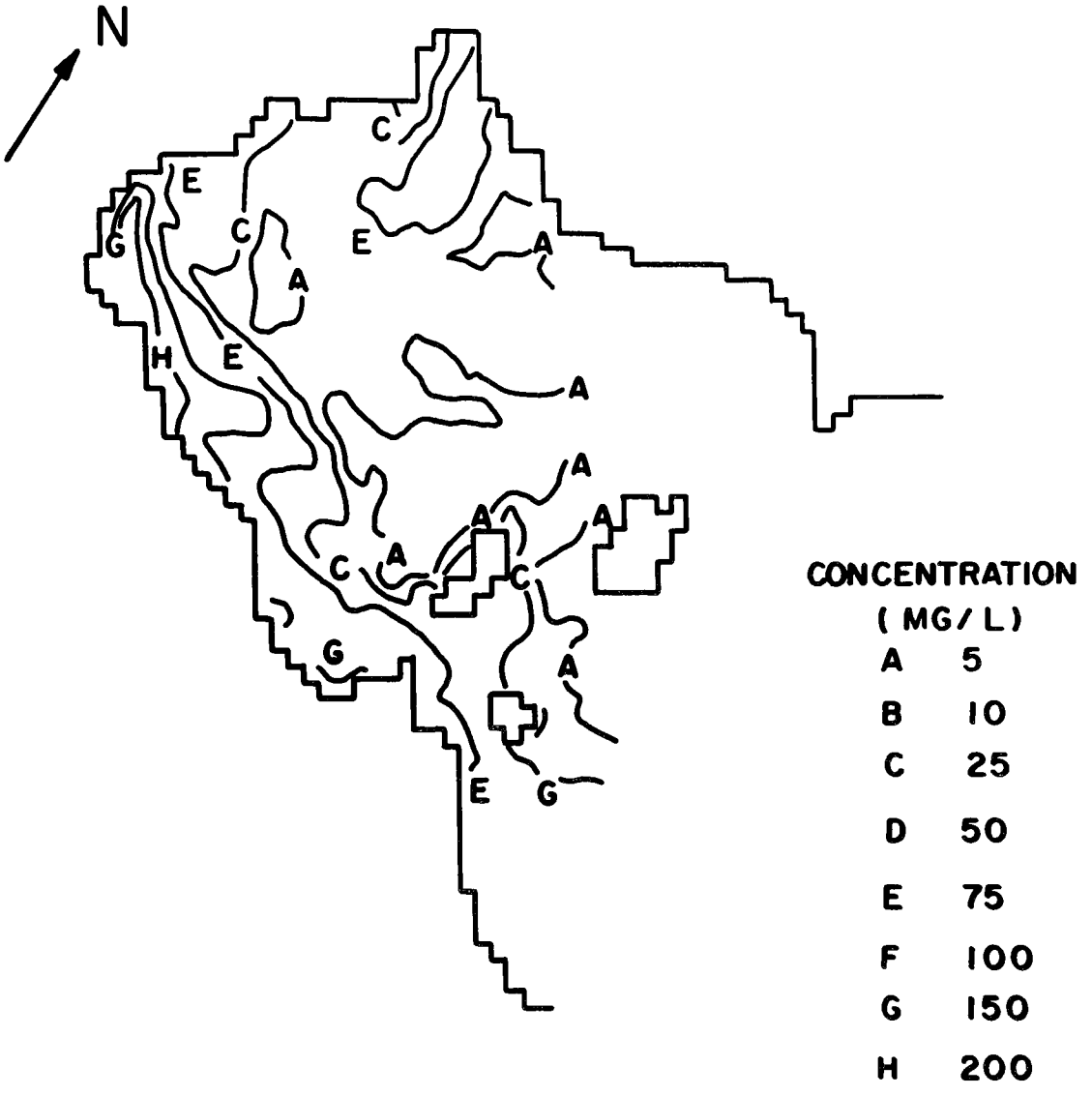

Figure 11. Observed surface sediment concentrations for the Western Basin of Lake Erie on March 11, 1976.

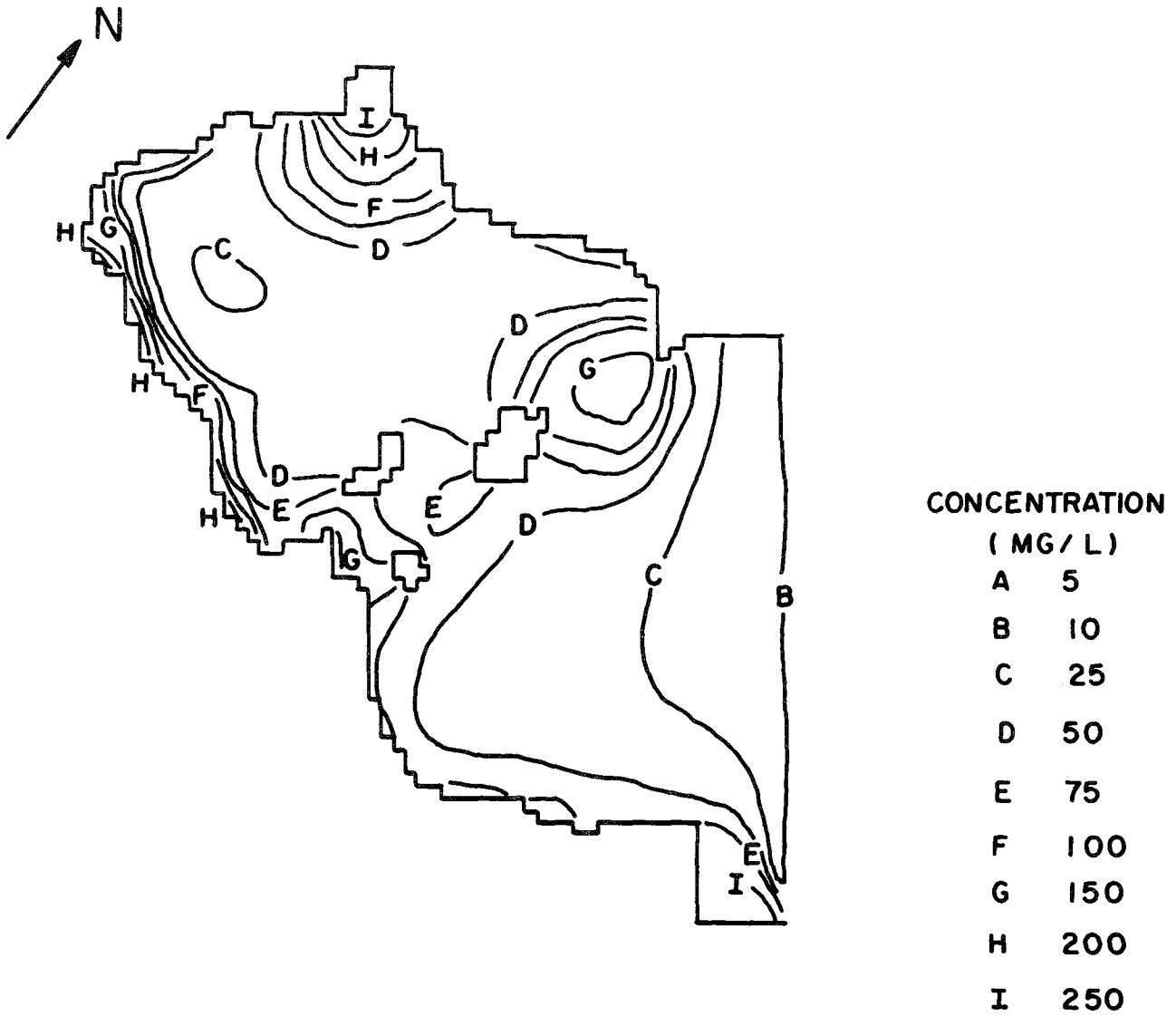

Figure 12. Calculated surface sediment concentrations on the Western Basin of Lake Erie on March 11, 1976.

are near 10°C to 12°C. The stratification and the oxygen demand of the sediments generally leads to anoxic conditions in the hypolimnion of the Central Basin in late summer. This has a significant effect on water quality and motivated our present work on stratified flow.

Flow in a stratified lake and the change with time of this stratification are not well understood and much field work and numerical experiments need to be done in order to understand and model the effects of different parameters on this stratification and the associated currents. Three-dimensional, time-dependent models of lake circulation including the effects of thermal stratification have been developed and preliminary calculations of stratified flow have been made. However, these three-dimensional models are relatively difficult to use and consume considerable amounts of computer time.

In order to do the numerical experiments efficiently and therefore be able to investigate the effects of various parameters more readily, we have developed a two-dimensional, time-dependent model of a stratified lake (Heinrich, Lick and Paul 1979). In this model, a cross-section of an infinitely long lake is considered. It is assumed that properties of the flow vary only in the vertical direction z and one horizontal direction x but not in the other horizontal direction y. Coriolis forces are included. A pressure gradient in the y-direction is assumed such that the net flux in the y-direction at any time is zero.

The horizontal eddy diffusivity and conductivity have been assumed constant. The vertical eddy conductivity K_V has been assumed to have the general form

$$K_V = \frac{K_S\,(C_1 + C_2 e^{-z/D})}{\left(1 + \sigma_2 \frac{\rho g \alpha}{|\tau_W|} D^2 e^{2z/D} \frac{\partial T}{\partial z}\right)^{3/2}} \tag{8}$$

where K_S is a function of the wind stress τ_W and the depth h, where C_1, C_2, σ_2, and D are empirical constants, g is the gravitational acceleration, and α is the thermal expansion coefficient given by

$$\alpha = 1.5 \times 10^{-5}\,(T-4) - 2.0 \times 10^{-7}\,(T-4)^2 \tag{9}$$

where the temperature T is in degrees Centigrade. An analogous form for the vertical eddy diffusivity is

$$A_V = \frac{A_S\,(C_1 + C_2 e^{-z/D})}{\left(1 + \sigma_1 \frac{\rho g \alpha}{|\tau_W|} D^2 e^{2z/D} \frac{\partial T}{\partial z}\right)^{1/2}} \tag{10}$$

where A_S is a function of the wind stress and depth and σ_1 is an empirical constant.

Only representative calculations from this model are presented here. A more complete set of calculations and a discussion of the model are given in the report by Heinrich, Lick and Paul (1979).

Constant Depth Basin

To investigate the effects of various parameters without the complications due to a complex geometry, a series of calculations was made for a constant depth basin 100 km wide and 25 m deep, dimensions which approximate the Central Basin of Lake Erie. In one such calculation, the following was assumed: an initial, spatially uniform temperature of 6°C, a zero initial velocity, a constant heat flux of 0.003 cal/cm^2-sec, a wind stress of 1.0 dynes/cm^2, $C_1 = C_2 = 1.0$, $\sigma_2 = .0045$, $\sigma_1 = 3\sigma_2 = .0135$, D = 2000 cm, $A_S = K_S = 15.0$ cm^2/sec, and $A_H = K_H = 10^6$ cm^2/sec.

In the calculations, after an initial transient, a quasi-steady state results in which the velocities and temperatures are changing relatively slowly. At 30 days, only a mild stratification is present as can be seen in Figure 13a. The associated velocities are shown in Figures 13b and 13c.

At later times, the thermocline develops much more strongly and inhibits the flow. At 90 days, the results for the temperature and velocity fields are as shown in Figures 14a, b, and c. It can be seen that a strong thermocline has formed at 15 to 16 m, the epilimnion temperatures are 15°C to 18°C while the hypolimnion temperatures are 12°C to 14°C. The flow is largely restricted to the epilimnion with a strong return flow near the top of the thermocline.

Additional calculations were made to investigate the effects of varying the heat flux, the level of turbulence, and the depth of the basin. Increasing the heat flux causes the thermocline to form higher and earlier, the hypolimnion temperatures to be lower, the epilimnion temperatures to be higher, and the convection to penetrate less deeply. A change in heat flux from 0.003 cal/cm^2-sec to 0.004 cal/cm^2-sec caused a decrease in the thermocline depth of 2 to 3 m, a significant variation when this change is compared with an average hypolimnion thickness of only 5 m. Decreasing the level of turbulence, i.e., decreasing the magnitude of the eddy coefficients K and A for example from 15 cm^2/sec to 10 cm^2/sec, caused the depth of the thermocline to decrease by 2 to 3 m, an effect similar to increasing the heat flux.

Increasing the depth of the basin to 30 m, 35 m, or 40 m caused the thermocline to form deeper. The thermocline was also more diffuse. Increasing the basin depth even further caused little further change in the thermocline depth. Decreasing the basin depth below 25 m decreased the depth of the thermocline and delayed its formation. From these calculations, it was quite evident that, for depths comparable to those found in the Central Basin of Lake Erie, the basin depth significantly influenced the thermocline depth and structure.

An interesting result which appeared in many of our calculations was the formation of a second thermocline above the first thermocline some time

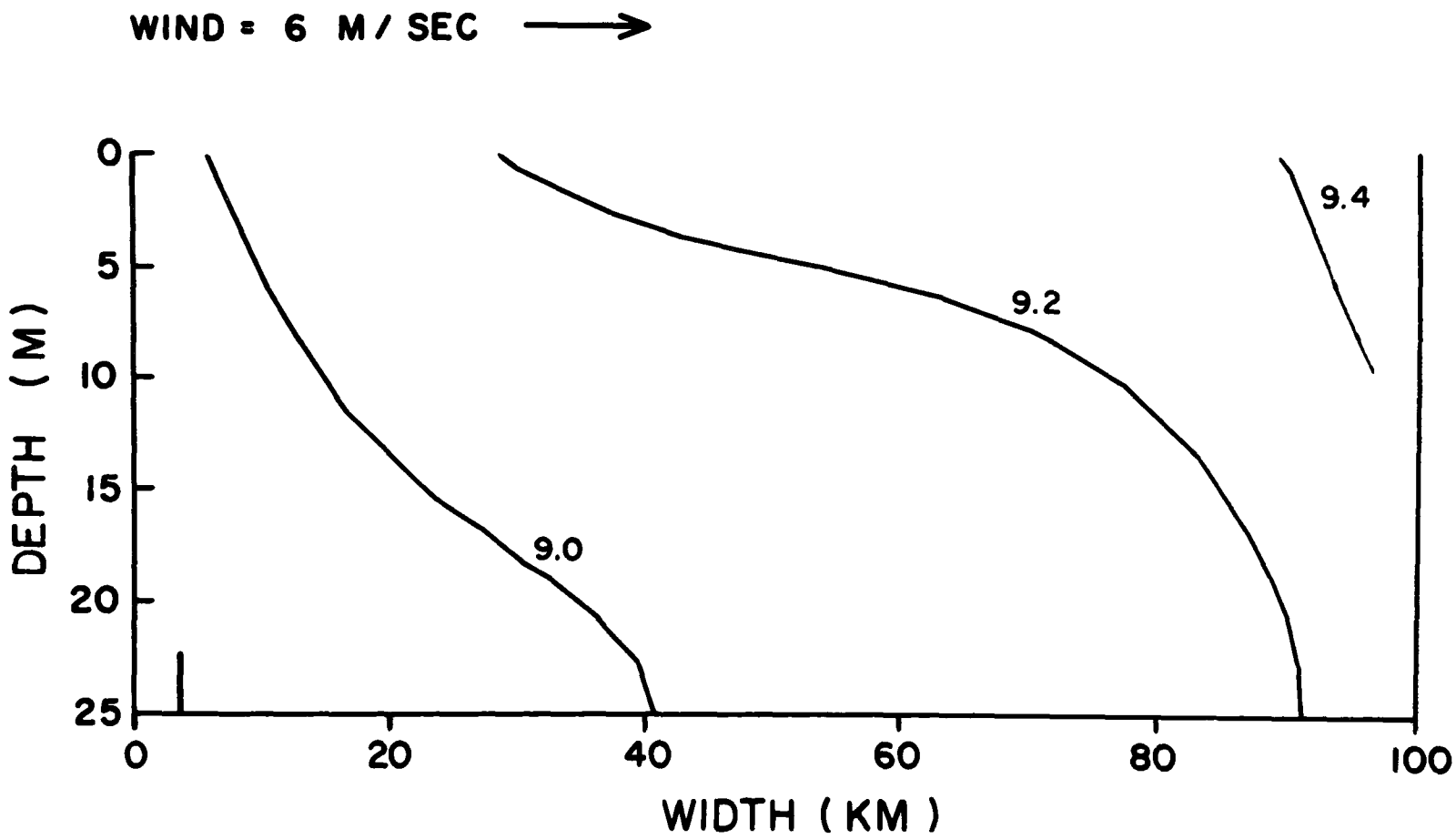

Figure 13a. Temperature distribution at 30 days for constant depth basin.

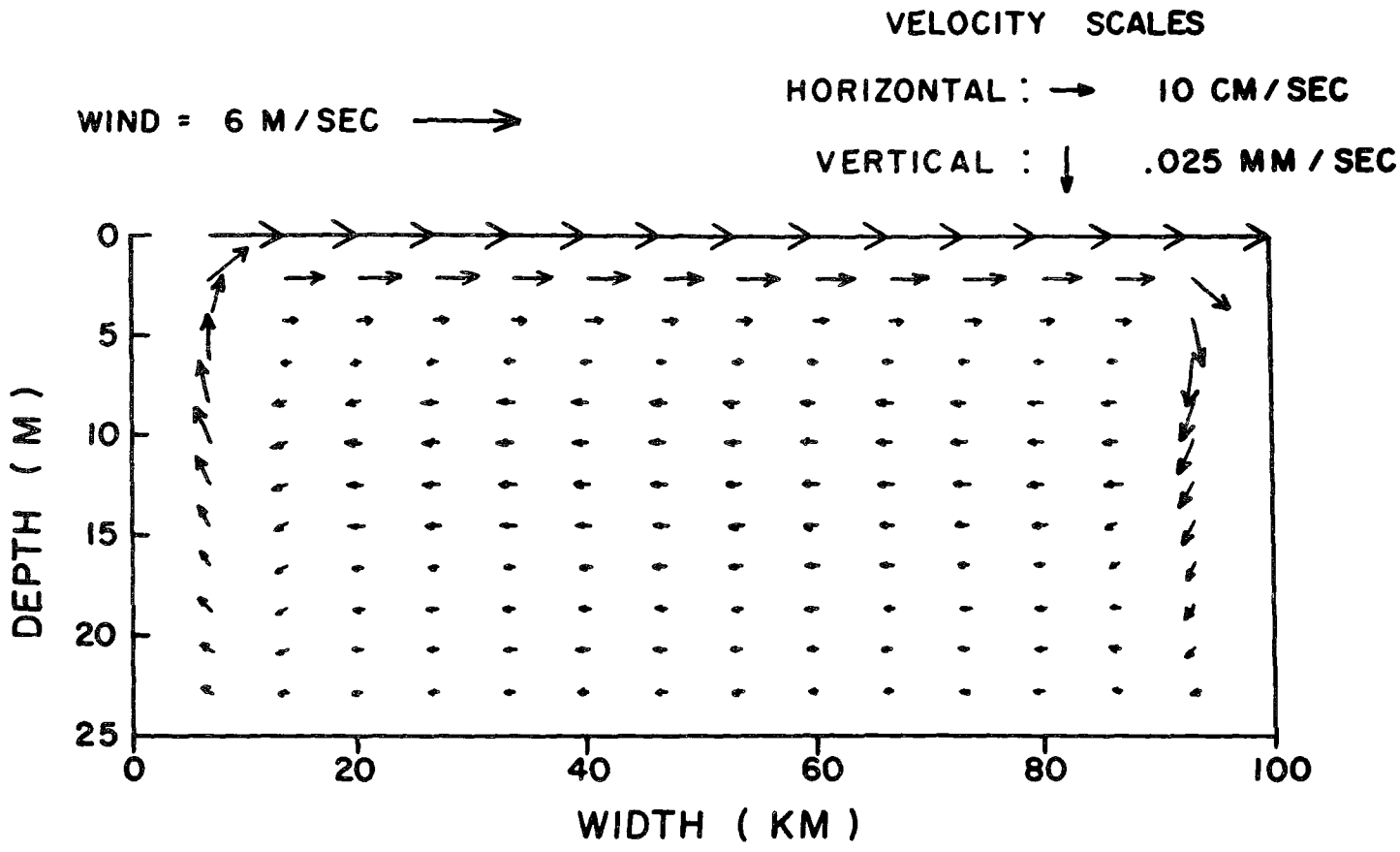

Figure 13b. Velocities (u and w) at 30 days for constant depth basin.

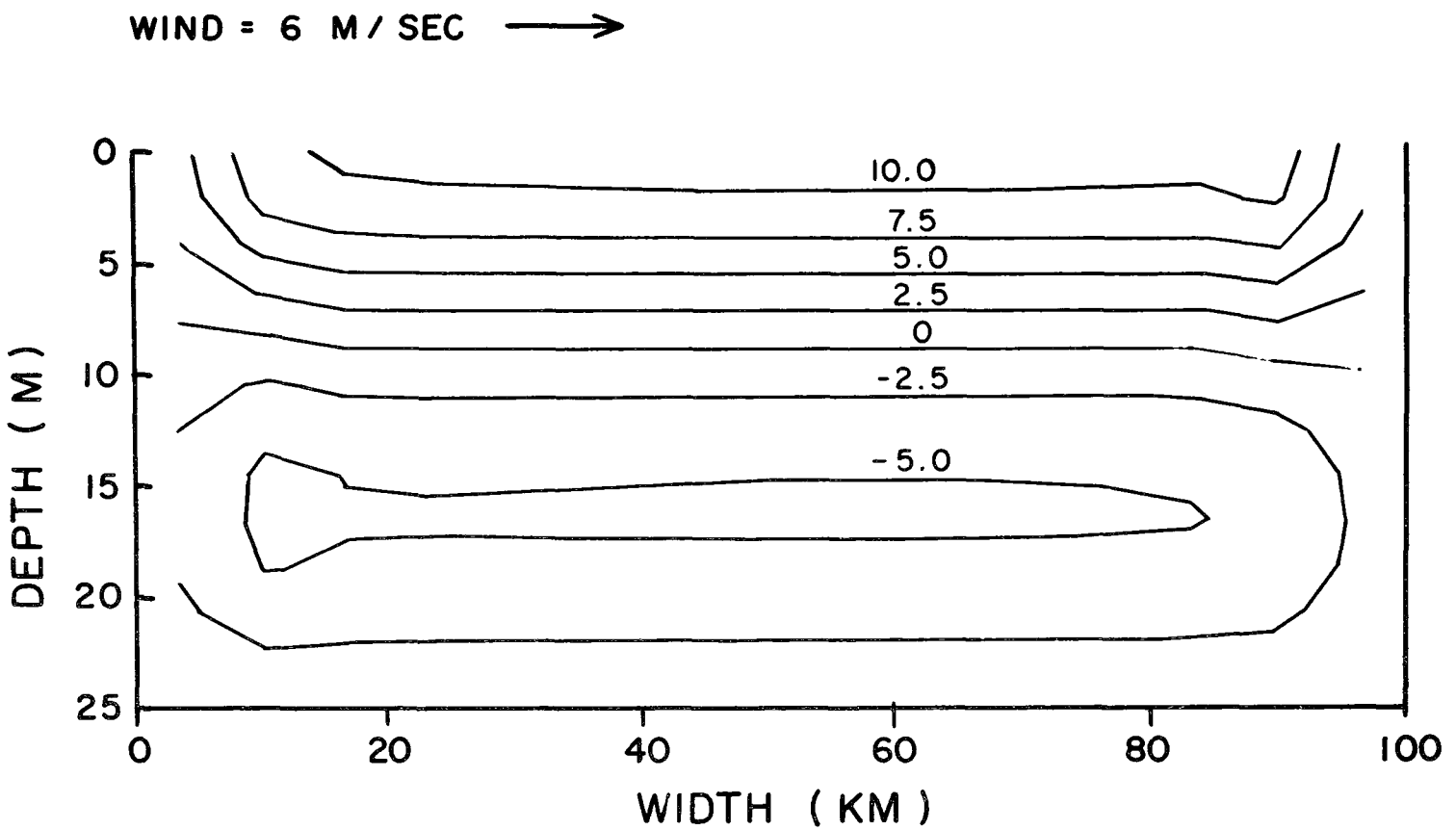

Figure 13c. Velocities perpendicular to cross-section at 30 days for constant depth basin.

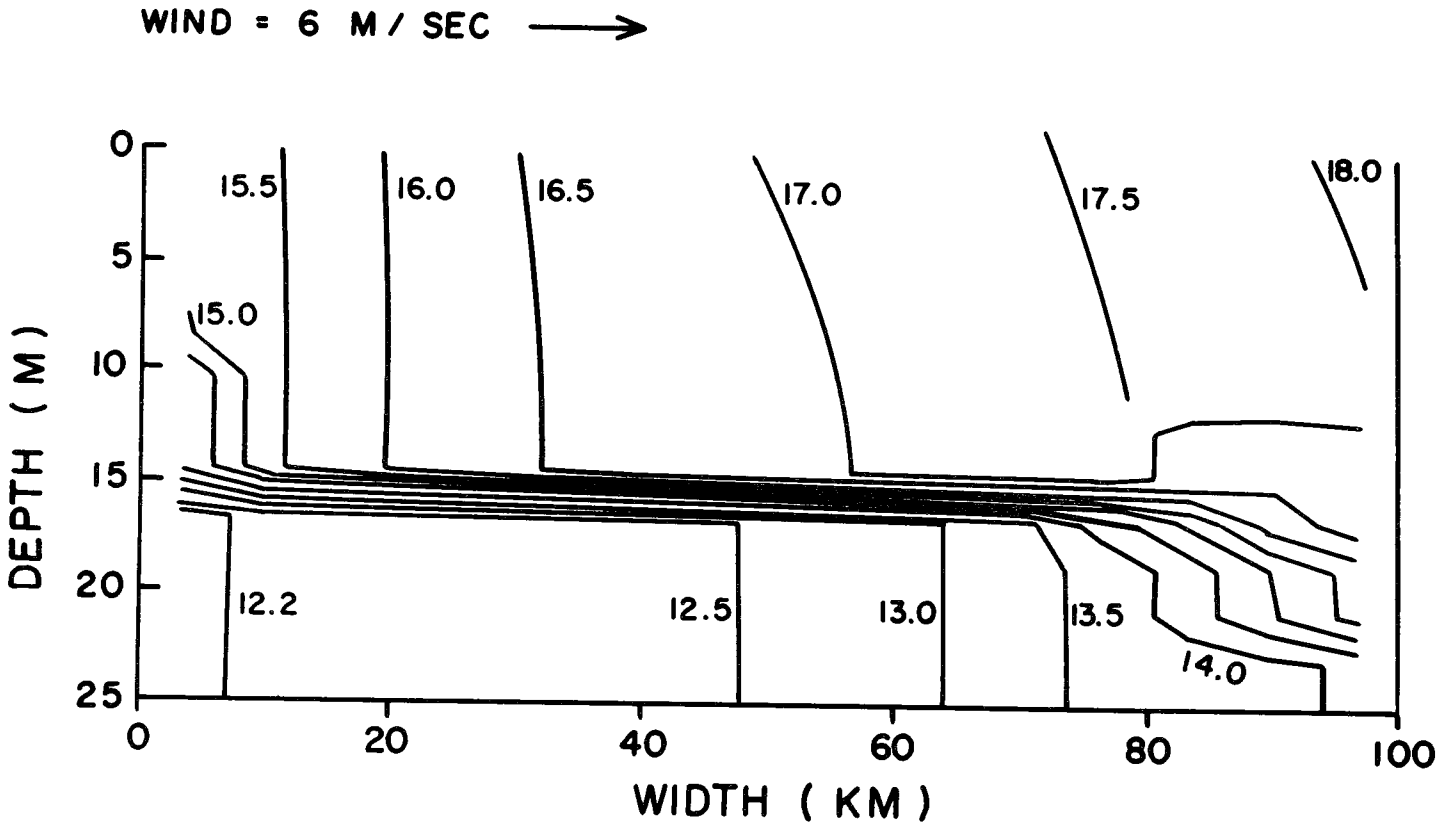

Figure 14a. Temperature distribution at 90 days for constant depth basin.

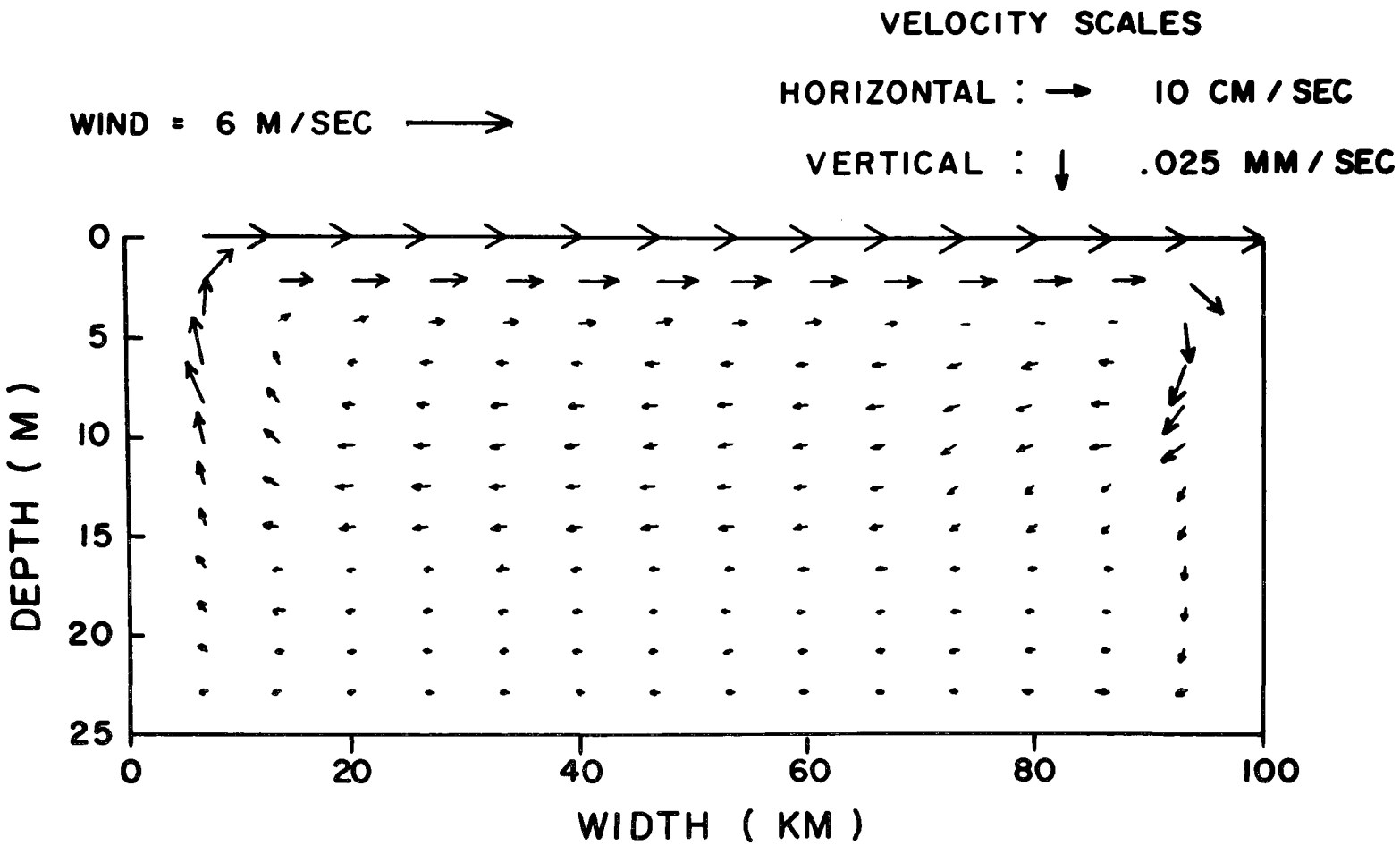

Figure 14b. Velocities (u and w) at 90 days for constant depth basin.

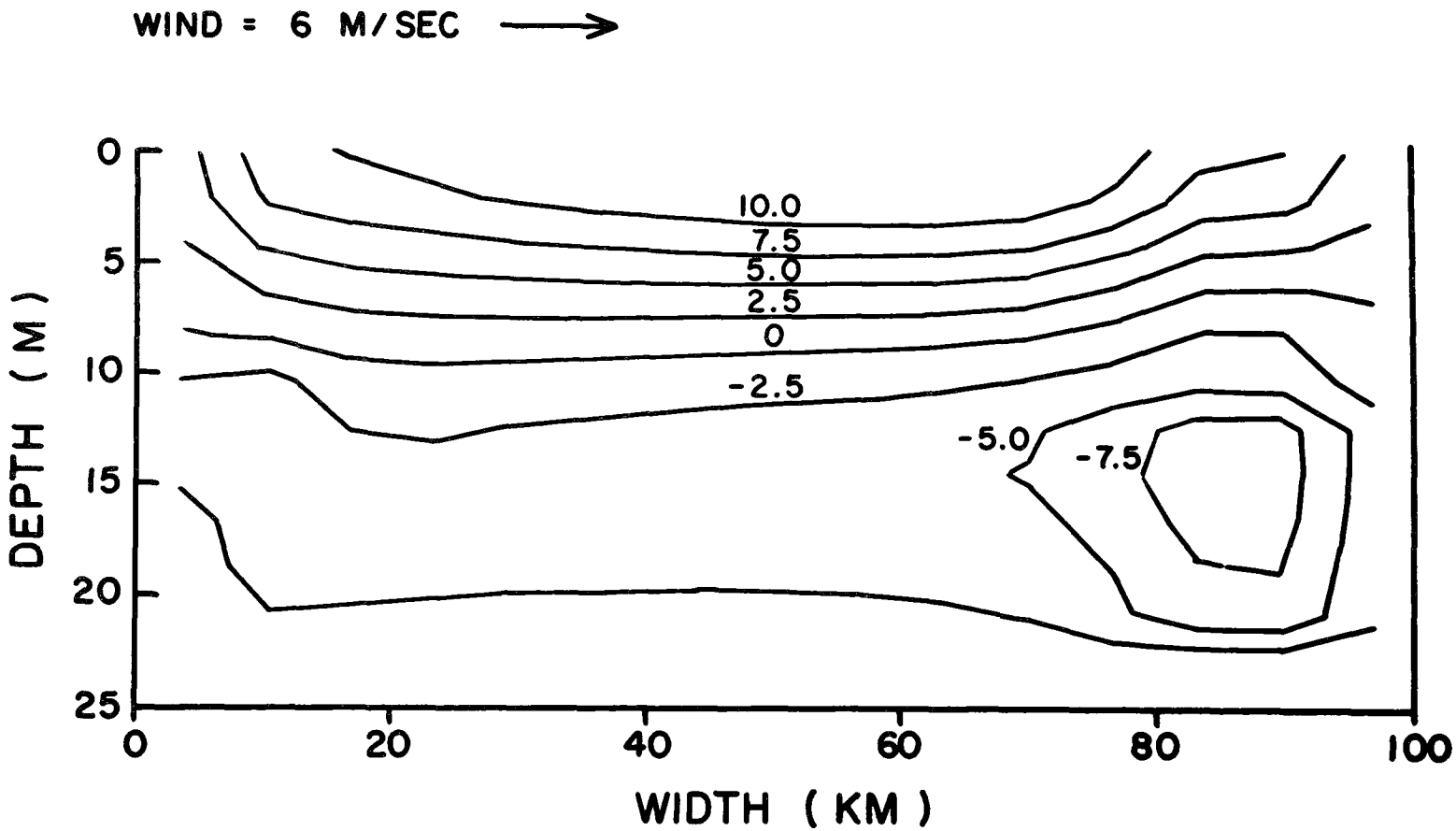

Figure 14c. Velocities perpendicular to cross-section at 90 days for constant depth basin.

after the formation of the first thermocline. This phenomena is mainly due to the temperature dependence of the thermal expansion coefficient α. Multiple thermoclines have been observed in lakes and it is interesting to speculate whether the above mechanism may be partly responsible for the observed phenomena.

Variable Depth Basin

A series of calculations was also made for a more realistic geometry corresponding to a section across the Central Basin of Lake Erie from Ashtabula, Ohio to Port Stanley, Ontario (see Figure 1). Only one set of calculations, chosen to illustrate the formation, maintenance, and decay of the thermocline, is presented here. Assumed values of the parameters are: $C_1 = 0.5$, $C_2 = 1.5$, $\sigma_1 = \sigma_2 = .001875$, $D = 900$ cm$_2$, $A_S = K_S = 15$ cm^2/sec, $A_H = 10^6$cm^2/sec, and $K_H = 3 \times 10^5$cm^2/sec.

For the first 50 days, it was assumed that the heat flux was 0.003 cal/cm^2-sec and the wind stress was 0.75 dynes/cm^2 with the wind directed from left to right. At 50 days, the temperature and velocity fields were as shown in Figures 15a, b, and c. A thermocline has formed at approximately 16 m depth with the hypolimnion temperatures from 10°C to 12°C. Both of these results are in agreement with observations.

Starting at 50 days, the heat flux was reduced in a linear manner such that the heat flux was zero at 120 days and negative thereafter. At 50 days, the wind direction was reversed for a period of 25 days at which time it was returned to its original direction, from left to right. The effect of the wind reversal was to eliminate a second thermocline which tended to form when the wind was not reversed. Little effect of this reversal on the temperature structure other than this was noted.

The temperature fields after 80, 120, 150, and 180 days are shown in Figures 16, 17, 18, and 19. At 120 days, the heat flux has decreased to zero, the epilimnion temperatures are 18°C to 19°C while the hypolimnion temperatures are 12°C to 14°C. At 180 days, the heat flux is negative and the lake is rapidly cooling, the thermocline has disappeared and the temperatures throughout are between 13°C to 15°C.

These calculations are in reasonable agreement with observations. Additional improvements can be made to the model and the parameters can be refined further so as to more closely approximate actual conditions. However, at this point, three-dimensional effects tend to become important and further improvements need to be made in conjunction with numerical results from three-dimensional calculations.

Stratification obviously has a significant effect on the transport of contaminants. Calculations are presently being made to investigate this further. Results of two preliminary calculations are presented here. In these calculations, a steady state flow field as assumed corresponding approximately to that shown in Figure 16 (80 days).

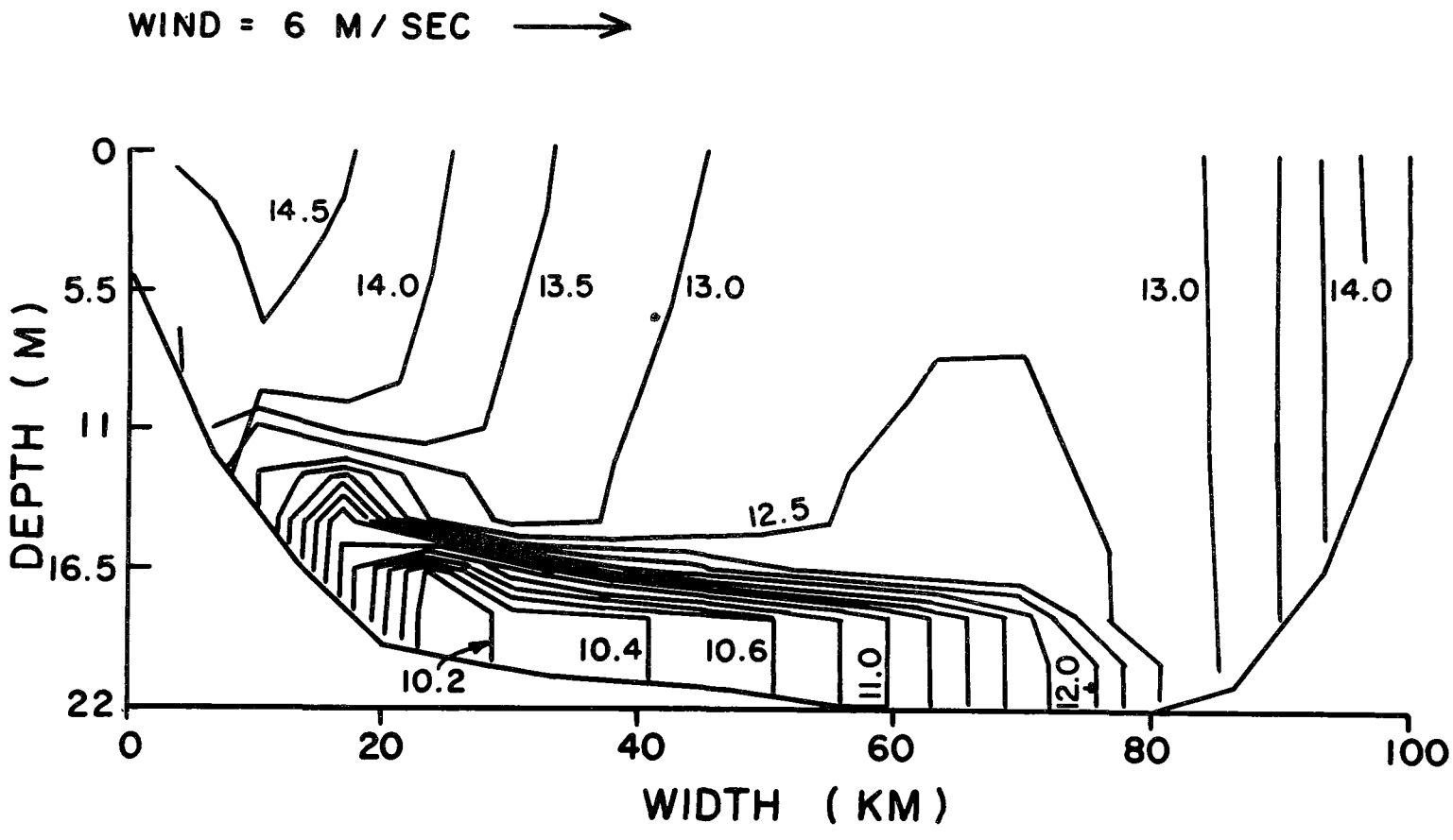

Figure 15a. Temperature distribution at 50 days for variable depth basin.

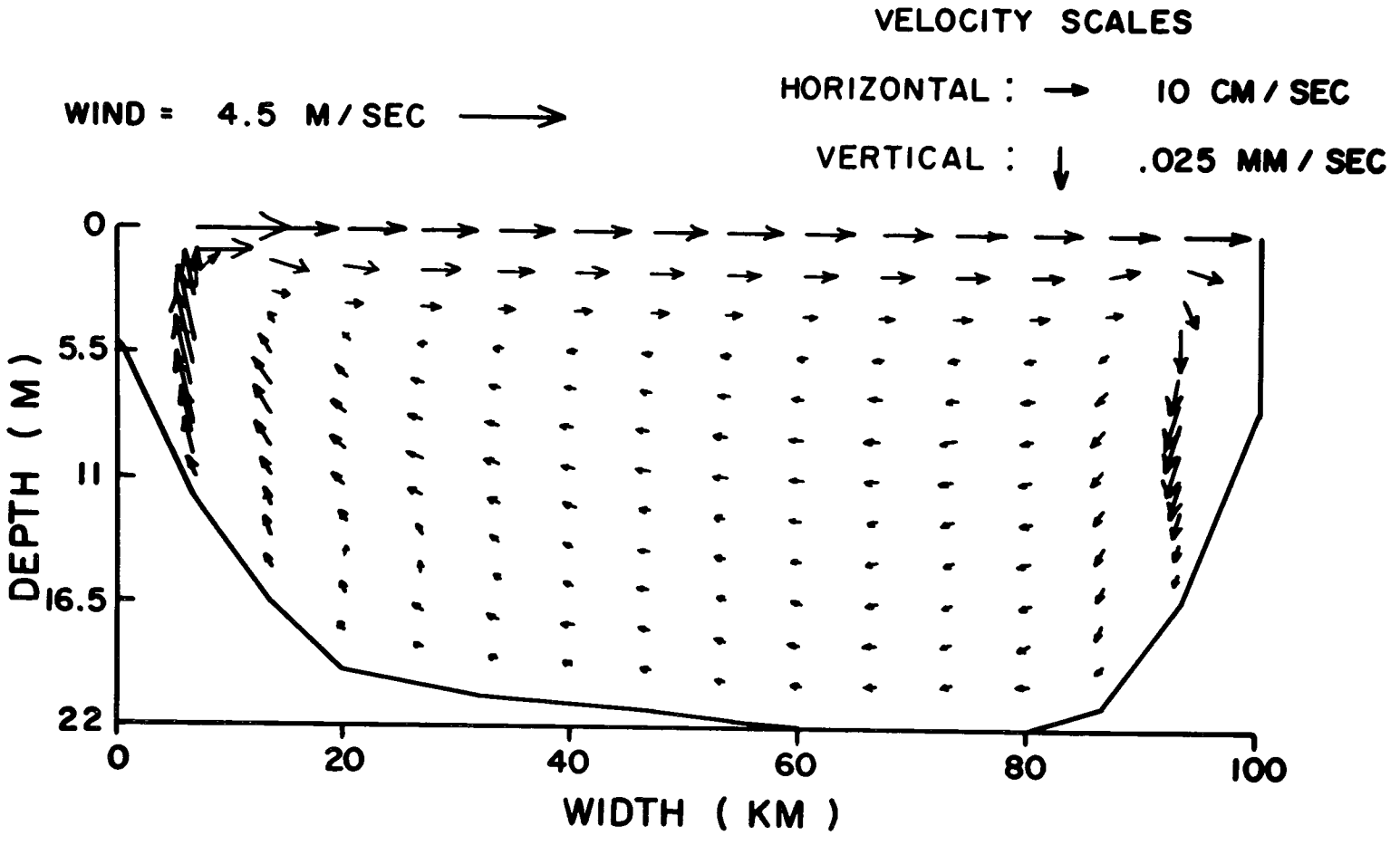

Figure 15b. Velocities (u and w) at 50 days for variable depth basin.

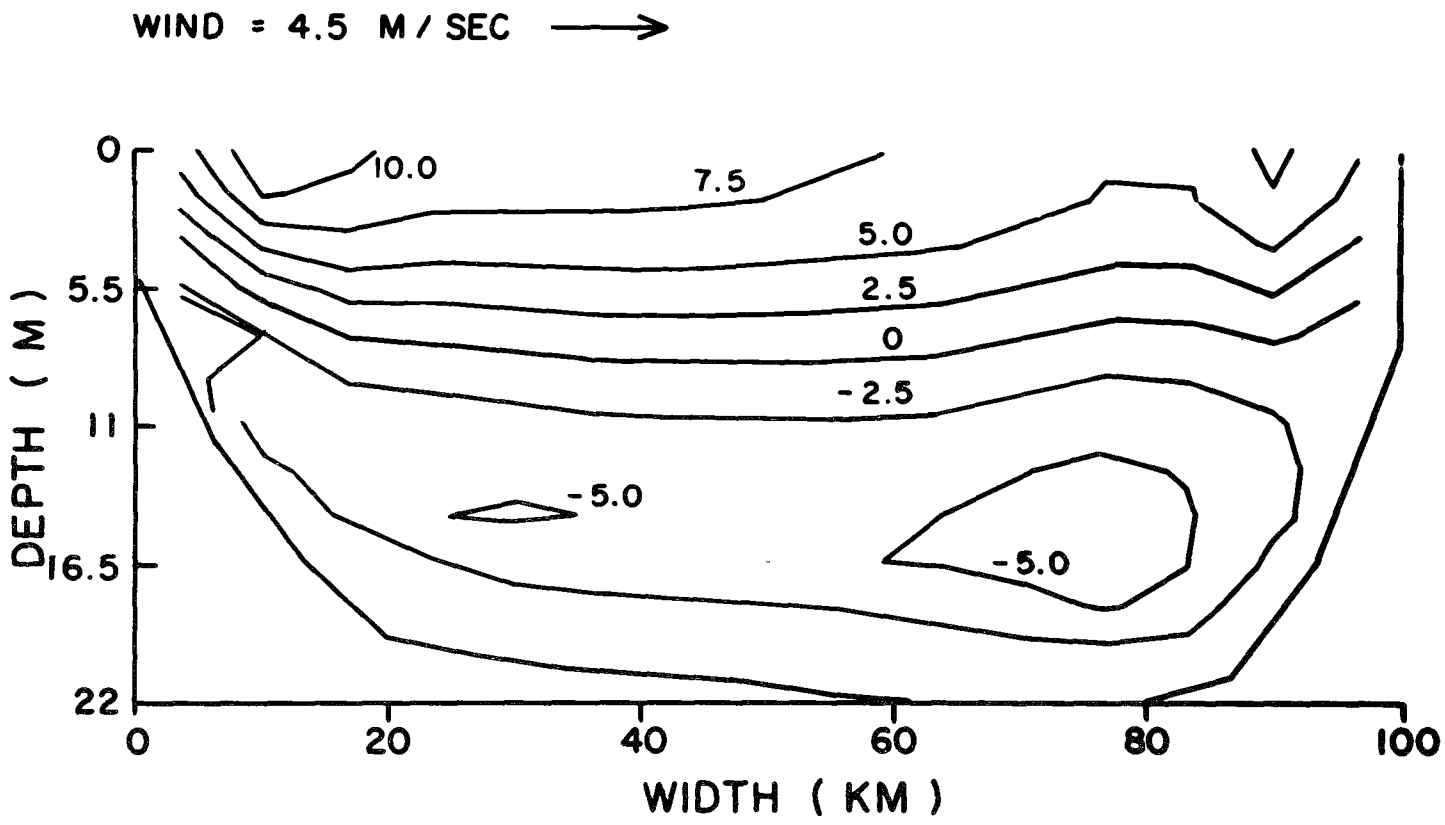

Figure 15c. Velocities perpendicular to cross-section at 50 days for variable depth basin.

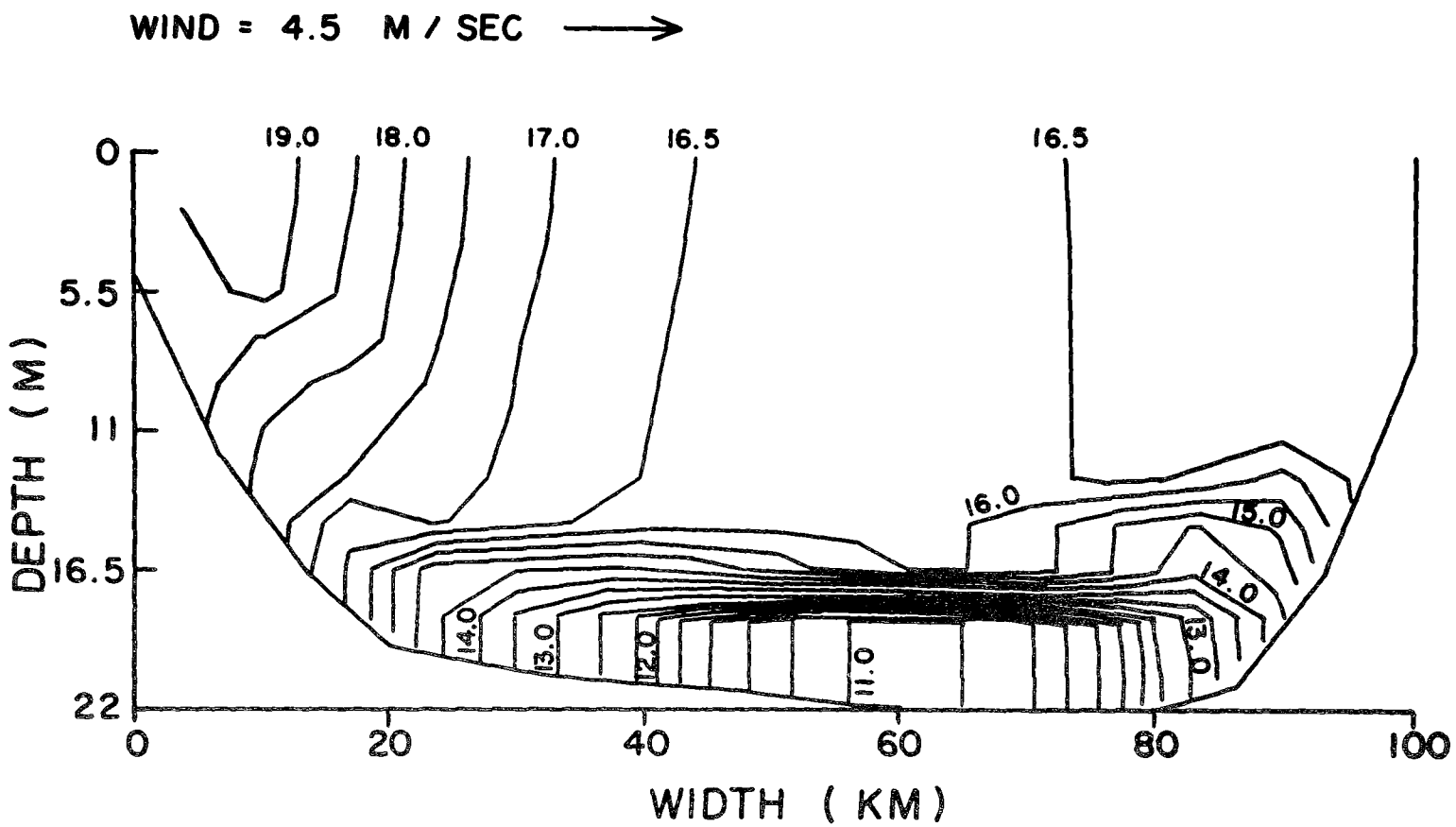

Figure 16. Temperature distribution at 80 days for variable depth basin.

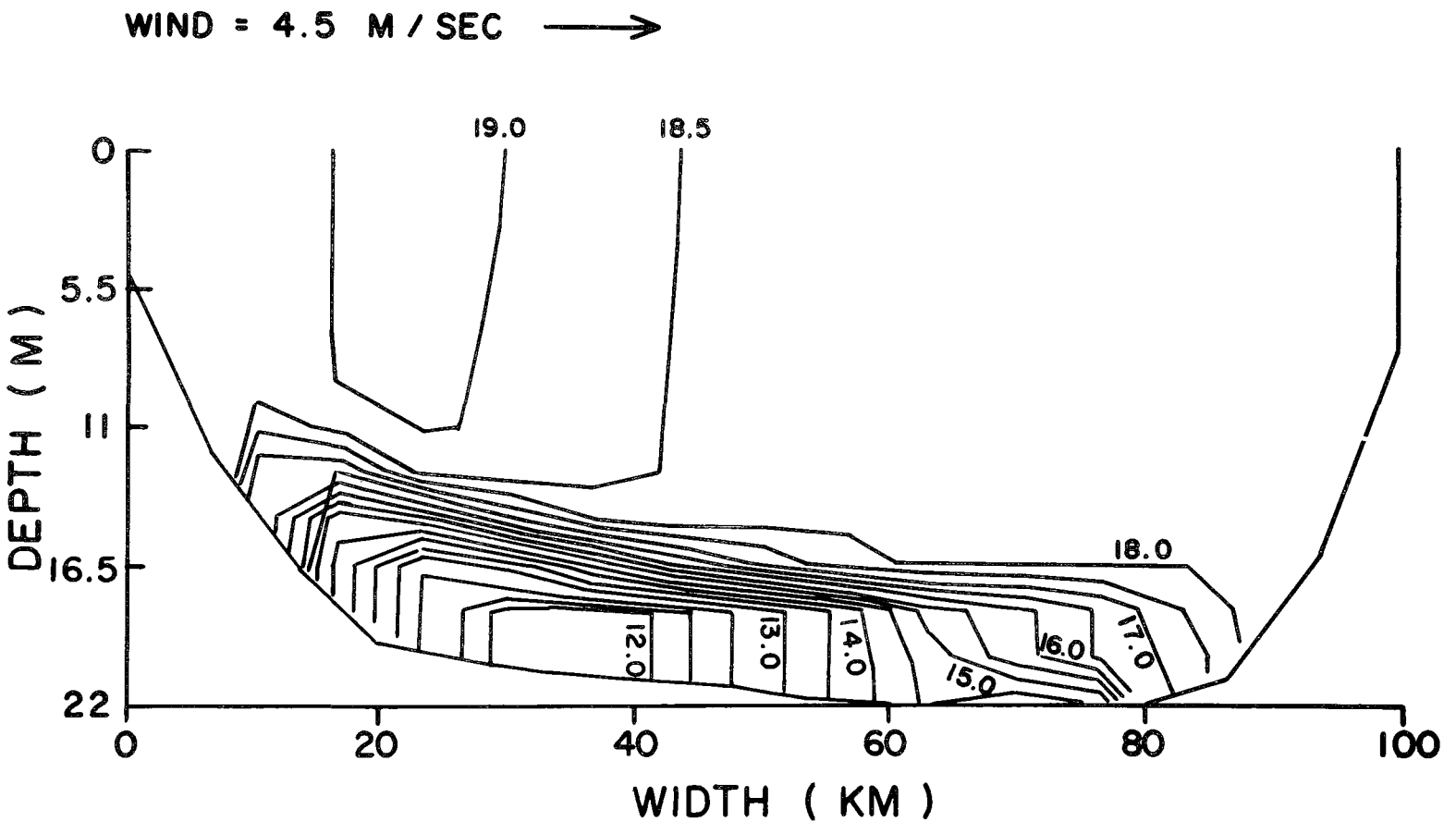

Figure 17. Temperature distribution at 120 days for variable depth basin.

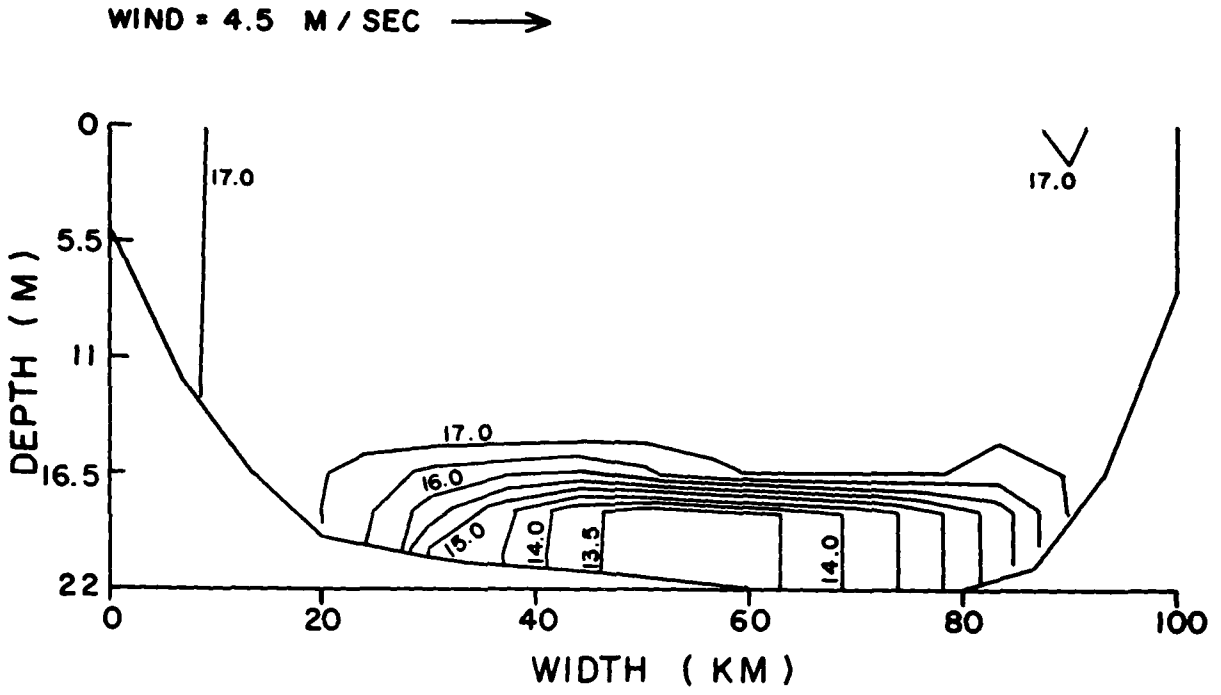

Figure 18. Temperature distribution at 150 days for variable depth basin.

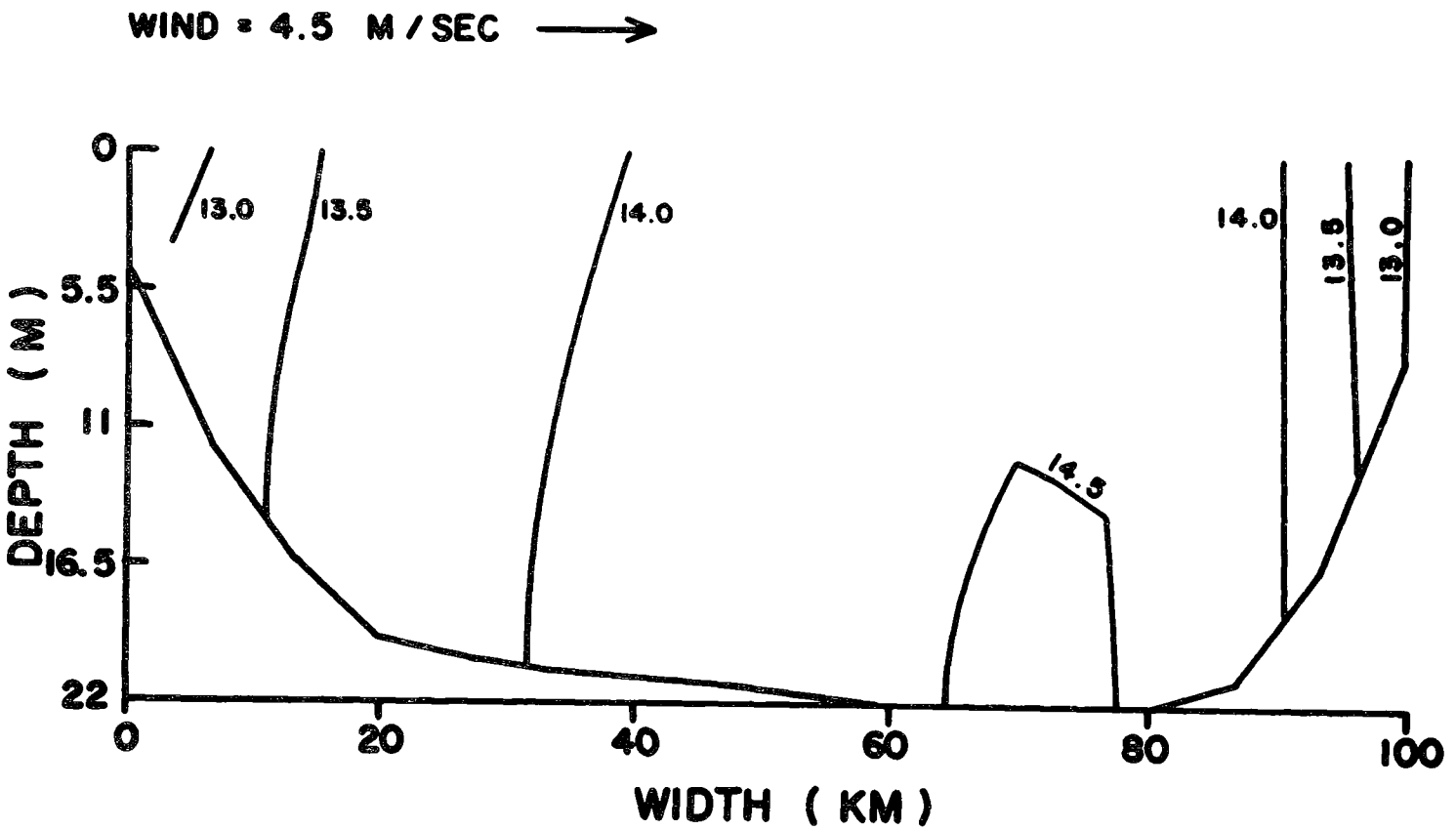

Figure 19. Temperature distribution at 180 days for variable depth basin.

In the first calculation, it was assumed that a contaminant was instantaneously released at time zero at the surface approximately in the middle of the lake (actually at a point 53 km from the left side). The amount released was 6.11×10^3 gm/cm (corresponding to an initial concentration in one cell volume of 100×10^{-6} gm/cm^3). At 30 days, the concentrations are shown in Figure 20. The concentrations are greatest near the surface but a considerable amount of material is also present in the hypolimnion. At earlier times, the contaminant is mainly restricted to the epilimnion. The contaminant is then transported to the right by surface currents. Near the shore, it is convected and mixed vertically into the hypolimnion and is then convected to the left by currents in the hypolimnion and lower part of the epilimnion.

In the second calculation, the same amount of contaminant was released at the same horizontal location but at the bottom of the lake. Figure 21 shows the concentrations at 10 days. It can be seen that the contaminant is restricted to the hypolimnion. This is because vertical mixing through the thermocline in the middle of the lake is small and horizontal hypolimnetic currents are also small. For later times, the contaminant does mix and convect vertically near shore and it then appears in the epilimnion.

SUMMARY AND CONCLUSIONS

Along with a general discussion of the factors affecting the transport of contaminants in a lake, two specific events have been analyzed: (1) sediment transport in the Western Basin of Lake Erie, and (2) the temperatures, currents, and the transport of contaminants in the Central Basin of Lake Erie during summer stratification.

Reasonable and encouraging agreement between the results of the calculations and observations was obtained. Nevertheless, it is also obvious that a great deal more needs to be done before realistic, quantitative, predictive models of contaminant transport are developed and available for use.

For sediment transport, the research needs are: (1) more qualitative and quantitative knowledge of the entrainment and deposition processes for a wide variety of sediments in lakes, (2) further investigation and verification of bottom stresses due to the combined action of waves and currents, and (3) additional calculations of sediment transport and verification of these calculations, especially for long-term events.

For stratified flow, it is necessary to further investigate, model and verify: (1) short-term events such as upwelling and downwelling due to strong winds, (2) the formation, maintenance, and decay of the thermocline and associated currents, and (3) the dispersion of contaminants during both short-term and long-term events, especially when there is coupling between the stratification, sediment-water exchange, and biochemical processes in the water column.

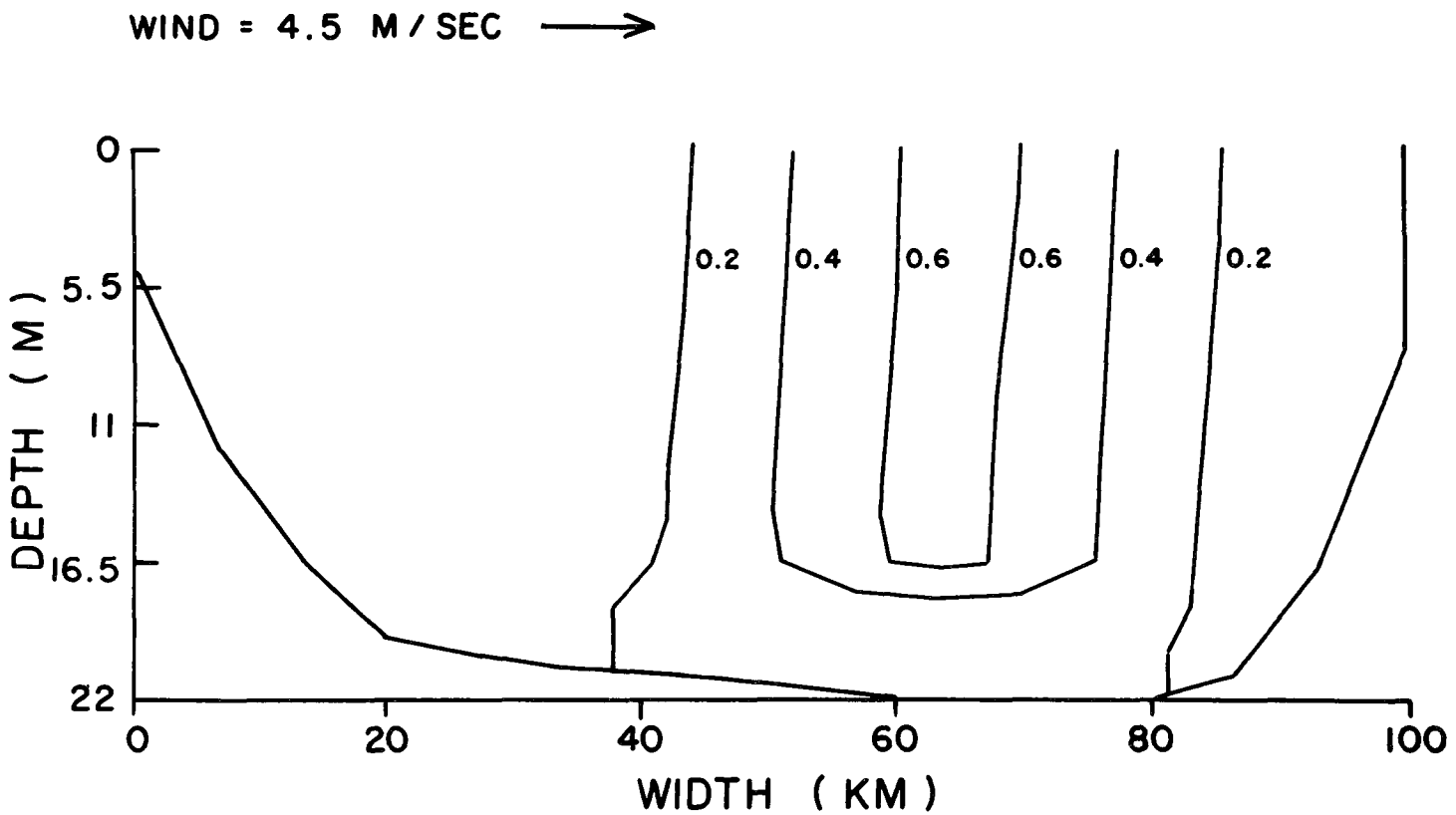

Figure 20. Contaminant concentration at 30 days after release at surface and 53 km from left side.

ACKNOWLEDGEMENTS

This research was funded by the U.S. Environmental Protection Agency. Mr. David M. Dolan was the Project Officer.

REFERENCES

Bierman, V.J., D.M. Dolan, E.F. Stoermer, J.E. Gannon, V.E. Smith. 1979. The development and calibration of a multi-class, internal pool, phytoplankton model for Saginaw Bay, Lake Huron. U.S. Environmental Protection Agency Report.

Bretschneider, C.L. 1958. Revisions in wave forecasting: Deep and shallow water. Proc. Sixth Conf. on Coastal Eng., Ch. 3, pp. 30-67.

Coastal Engineering Research Center. 1973. Shore protection manual, Vol. 1.

DiToro, D.M. and J.F. Connoly. 1979. Mathematical models of water quality in large lakes, Part II. U.S. Environmental Protection Agency Report.

DiToro, D.M. 1979. Species dependent mass transport and chemical equilibria: Application to Chesapeake Bay sediments. To be published.

Fisher, J.B., P. McCall, W. Lick, J.A. Robbins. 1979. The mixing of lake sediments by the deposit feeder, Tubifex tubifex. To be published.

Fisher, J.B. and W. Lick. 1979. Effects of tubificid oligochaetes on the flux of conservative and non-conservative solutes across the sediment-water interface. To be published.

Fukuda, M.K. 1978. The entrainment of cohesive sediments in fresh water, Ph.D. Thesis, Case Western Reserve University.

Fukuda, M.K. and W. Lick. 1979. The entrainment of cohesive sediments in fresh water. To be published.

Grant, W.D. and O.S. Madsen. 1979. Combined wave and current interaction with a rough bottom. J. Geophysical Research, Vol. 84.

Heinrich, J.C., W. Lick, and J. Paul. 1979. The temperature, currents, and the dispersion of contaminants in a stratified lake - A two-dimensional model. Presented at the Twenty-Second Conference on Great Lakes Research.

Kajiura, K. 1968. A model of the bottom boundary layer in water waves. Bull. Earthquake Res. Inst., 46.

Kang, S.W., P. Sheng, and W. Lick. 1979. Wave generation in Lake Erie. To be published.

Lee, D.Y. 1979. Resuspension and deposition of lake sediments. M.S. Thesis, Case Western Reserve University.

Lick, W., J. Paul, and P. Sheng. 1976. The dispersion of contaminants in the near-shore region. Modeling Biochemical Processes in Aquatic Ecosystems, Ann Arbor Science Publishers.

Mortimer, C.H. 1941. The exchange of dissolved substances between mud and water, I and II. J. Ecol., Vol. 29.

Mortimer, C.H. 1942. The exchange of dissolved substances between mud and water in lakes, III and IV. J. Ecol.

Mortimer, C.H. 1971. Chemical exchanges between sediments and water in the Great Lakes. Limnology Oceanography, 16.

Owen, M.W. 1978. Problems in the modeling of transport, erosion, and deposition of cohesive sediments. Vol. 6, The Sea, Ed. Goldberg.

Pierson, W.H., G. Neumann, and R.W. James. 1955. Practical methods for observing and forecasting ocean waves by means of wave spectra and statistics. H.O. Publ. 603, U.S. Navy Hydrographic Office, Washington, D.C.

Pore, N.E. 1979. Verification of automated Great Lakes wave forecasts of the National Weather Service. To be published.

Robbins, J.A. 1979. Cesium-137 in the sediments of Lake Huron. Presented at the Twenty-Second Conference on Great Lakes Research.

Robbins, J.A. and D.N. Edgington. 1979a. The distribution of Cesium-137 in Lake Erie. Presented at the Twenty-Second Conference on Great Lakes Research.

Robbins, J.A. and D.N. Edgington. 1979b. History of plutonium deposition in Lake Erie sediments. Presented at the Twenty-Second Conference on Great Lakes Research.

Sheng, P. and W. Lick. 1979. The transport and resuspension of sediments in a shallow lake. J. Geophysical Research, Vol. 84.

Sly, P.G. 1978. Sedimentary processes in lakes: Chemistry, geology, physics, Ed. A. Lerman, Springer-Verlag.

Sternberg, R.W. 1972. Predicting initial motion and bedload transport of sediment particles in the shallow marine environment. In Shelf Sediment Transport, Process and Pattern. Ed. D.J.B. Swift, D.B. Duane, O.H. Pilkey. Dowden, Hutchinson and Ross Pub., Stroudsberg, Pennsylvania.

Sverdrup, H.U. and W.H. Munk. 1947. Wind, sea, and swell: Theory of relations for forecasting. Hydrographic Office Publ. 601, U.S. Dept. of the Navy, Washington, D.C.

Terwindt, J.H.J. 1977. Deposition, transportation, and erosion of mud. In Interactions Between Sediments and Freshwater, Ed. golterman.

Thomann, R.V. 1979. A trophic length model of the fate of hazardous substances in the aquatic food chain. To be published.

Thomann, R.V., R.P. Winfield, D.M. DiToro, D.J. O'Connor. 1976. Mathematical modeling of phytoplankton in Lake Ontario, I and II. U.S. Environmental Protection Agency Report.

Thomas, R.L., A.L.W. Kemp, and C.F.M. Lewis. 1972. Distribution composition and characteristics of the surficial sediments of Lake Ontario. J. Sed. Petrol. 42.

Thomas, R.L., J.M. Jaquet, A.L.W. Kemp, and C.F.M. Lewis. 1976. Surficial sediments of Lake Erie. J. Fish. Res. Board Can. 33.

SECTION 16

SELF-ORGANIZATION OF THREE-DIMENSIONAL MODELS OF WATER POLLUTION

A.G. Ivakhnenko and G.I. Krotov[1]

SYNTHESIS OF MATHEMATICAL MODELS USING THE METHOD OF SELF-ORGANIZATION ON A DIGITAL COMPUTER

Mathematics enhances the deductive approach to the solution of problems. The construction of each solution is based on processing of an *a priori* fixed system of input axioms and initial data. The basic shortcoming of the deductive method is the need for *a priori* production of sufficiently complete and accurate information on the object. Imprecise knowledge of even a single characteristic can make the result of modeling incorrect (e.g., an output quantity may increase when it should decrease, etc.). Furthermore, the problem of the unique and optimal structure of the model is not solved. A variety of reliable models may be composed for one and the same object. In practice, this means: The number of models will be equal to the number of modeling attempts, i.e., each model is a unique invention of its author.

According to the theorem of incompleteness of Godel, the so-called internal criteria, utilized by deductive mathematics, are not suitable for selection of the structure of a model of optimal complexity. Any internal criterion leads to the false rule: "The more complex the model, the more precise it is." An example of an internal criterion might be the mean-square error calculated for all points of experimental data as well as certain other statistical criteria, including significance, elasticity, and the like (Ivakhnenko 1978).

In contrast, external criteria pass through a minimum as the model becomes increasingly complex, and this minimum defines a model of optimal complexity. The new inductive method of modeling--self-organization of models by computer--is directed toward comprehensively decreasing the volume of *a priori* information required for modeling.

The experimental points assigned in the table of initial data contain information on quite a variety of factors. For example, in modeling bodies of water, extremely complex processes of self-purification of the water and transformation of matter (which are still unclear) are reflected in the experimental data. This means that the mathematical model of such phenomena

[1]Ukranian Academy of Sciences, 252207 Kiev, USSR.

can be found by trail and error, without deep knowledge of the mechanism of self-purification and transformation.

In contrast to deductive mathematics, methods of self-organization are based on the use of external criteria: a) regularity, b) minimum bias, c) balance of variables, d) convergence of a multi-step prediction and e) combined criteria. It is the use of external criteria which enables a unique model of optimal complexity, corresponding to the minimum of the selection criterion to be obtained (Figure 1). The internal criteria play a secondary role in this case. They are used for ranking of models in a sequence for successive testing on the basis of an external criterion.

The principle of self-organization can be formulated as follows: With gradual complication of models, certain criteria (which have the property of "external supplementation") pass through a minimum. The computer, by running through the models, finds this minimum and, consequently, indicates the unique model of optimal complexity.

SELECTION CRITERIA

According to Godel's theorem of incompleteness, the task of identification of the structure and parameters of a model is not properly stated: Only with some external supplementation can a unique solution be achieved. In all works on modeling in which, by one means or another, a unique model has been achieved, certain supplementary external information has been used. The basic shortcoming of contemporary modeling is that the external, supplementary information selected is not adequate for the task at hand. The following criteria can be selected as expedient supplements for the theory of self-organization of models:

1. The criterion of regularity: The mean square error calculated at new points is not used to produce estimates of the coefficients of the model:

$$\Delta(B) = \frac{\sum_{i=1}^{N_B} (q_{tabl,i} - q_i)^2}{\sum_{i=1}^{N_B} q_{tabl,i}} \rightarrow \min \qquad (1)$$

where:

N_B is the number of points of an individual test sequence of data;
q_{tabl} are the tabular values of the output variable;
q are values calculated using the model.

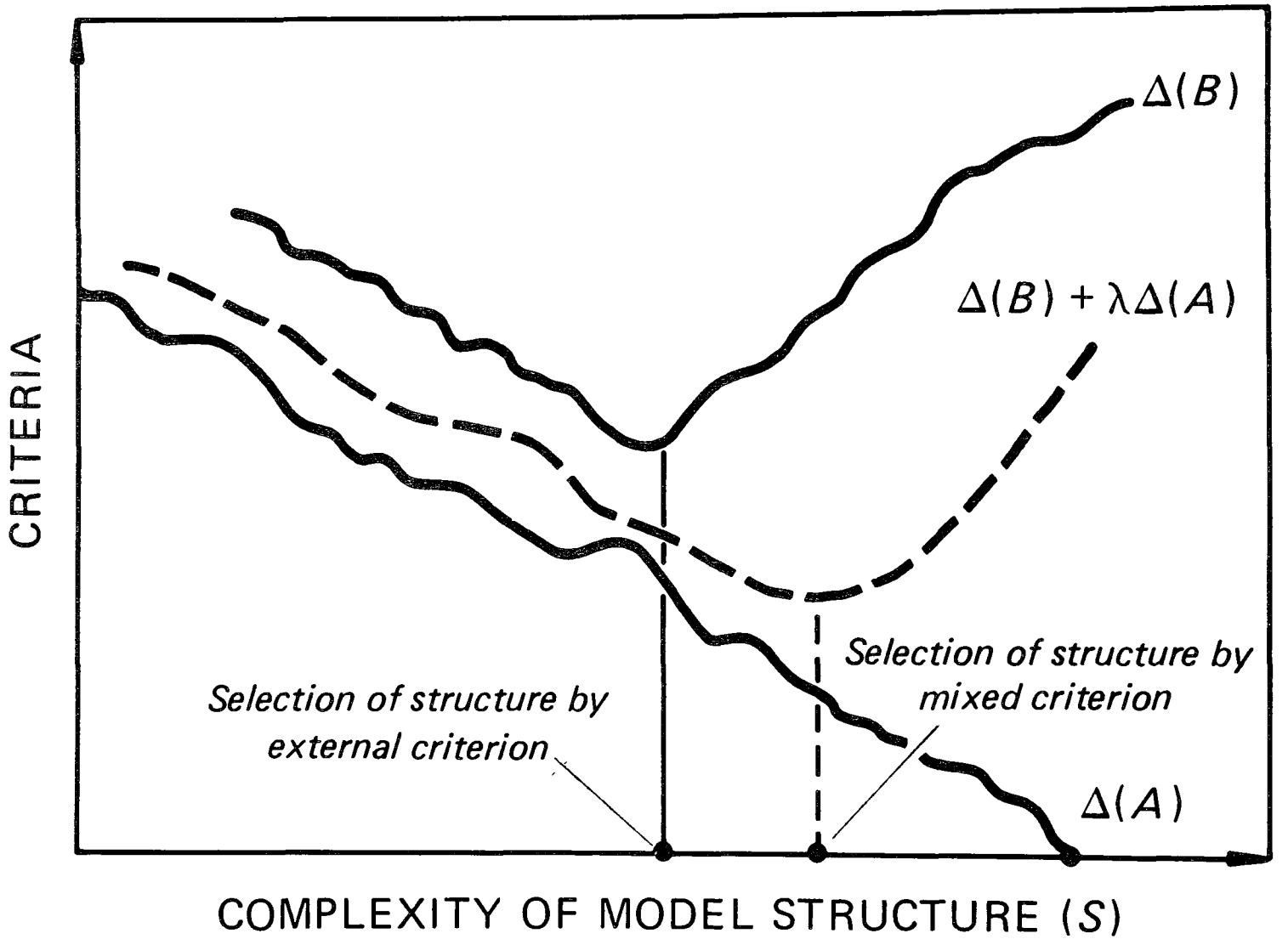

Figure 1. Characteristic curves of change of external, mixed and internal criterion with increasing complexity of model structure (No. of terms and power of polynomial).

2. The minimum bias criterion: Requires maximum agreement of the values of the output quantity of two models obtained using two different parts of the table of initial data N_A and N_B:

$$n_{cn} = \frac{\sum_{i=1}^{\alpha(N_A+N_B)} (q_{A,i} - q_{B,i})^2}{\alpha \sum_{i=1}^{N_A+N_B} q^2_{tabl,i}} \to \min \qquad (2)$$

where q_A and q_B are the values of the output quantity calculated for all $(N_A - N_B)$ points using the data of the model obtained in parts of the sample N_A and N_B, respectively; N_A and N_B are, e.g., points with even and odd ordinal indexes[1]. If the input data contain noise, it is recommended that the summation interval be increased: Coefficient α should be selected proportional to the intensity of the noise. It is taken within the limits $\alpha = 1.5 \to 3.0$.

3. Criterion of balance of variables: Used for simultaneous long-term prediction of several variables. Frequently, a certain interrelationship of variables is known a priori, and the criterion requires that this relationship be fulfilled for the future over the extrapolation interval.

Let us assume that it is known that $q = f(x_1, x_2, x_3)$.

Then the balance equation is $q - f(x_1, x_2, x_3) = 0$.

The criterion of balance of variables

---

[1]The following criterion is more resistant to interference

$$n_{cn} = \frac{\sum_{i=1}^{\alpha N} (q_{A,i} - q_{AB,i})(q_{B,i} - q_{AB,i})}{\alpha \sum_{i=1}^{N} q^2_{tabl,i}} \qquad (2)$$

where q_A, q_B, q_{A+B} are the value of the output quantity calculated using the model after training on sample N_A, N_B and N_A and N_B together. Ivakhnenko et al. (1978) compare the interference stability of various versions of the minimum bias criterion.

$$b = \frac{\sum_{i=N1}^{N2} [q_i - f(x_{1i}, x_{2i}, x_{3,i})]}{\sum_{i=N1}^{N2} q_i^2} \quad \min, \tag{3}$$

where: $N_1 = Ty - \Delta t$, $N_2 = Ty + \Delta t$

and $(N_1 - N_2)$ is the time interval, which includes the prediction point. The criterion of balance of variables frequently leads to ambiguous selection of several models; in order to assure unambiguity of selection, it is used in combination with other criteria.

In problems in which the balance of variables is unknown, it is "discovered" in advance by the use of the minimum bias criterion. In recent studies, combined selection criteria have been widely used, combinations of the individual criteria just described. The reason is that the selection of a criterion depends on the purpose of solution of the problem and should be entirely the privilege of the person who is designing the model. Usually, the motivation of statement of the modeling task is in itself not completely clear and precise. This leads to equal uncertainty in the recommendations for selection of combined criteria. Still, the following rules can be formulated:

1. For models used for short-term prediction, the combined criterion "no bias plus balance of variables" is recommended:

$$K_1 = \sqrt{n_{sm}^2 + \Delta(B)^2} \rightarrow \min; \tag{4}$$

2. For models intended for long-term prediction, the combined criterion "no bias plus balance of variables" is recommended:

$$K_2 = \sqrt{n_{sm}^2 + B^2} \rightarrow \min; \tag{5}$$

3. For differential (finite difference) models, in which long-term prediction is obtained by means of step-by-step integration, the combined criterion "no bias plus convergence of the procedure of prediction" is recommended:

$$K_3 = \sqrt{n_{sm}^2 + i^2(N)} \rightarrow \min, \tag{6}$$

where: $$i^2 = \frac{\sum_{i=1}^{N} (q_i - q_{tabl,i})^2}{q_{tabl,i}^2}$$

is the sum of the squares of deviations of the curve of the process from the curve of a repeated (multi-step) prediction, begun from the first point of the interpolation interval. N is the number of points in the table of initial data. The criterion of the minimum bias participates in all combined criteria, since bias is to be avoided in modeling.

Combined criteria not only provide a stable and unique prediction, but also make its selection "sharper". Individual criteria frequently do not provide a sufficiently sharp minimum.

Desiring to satisfy a number of requirements, other types of combined criteria may be used, containing two or three particular requirements. For example:

$$K_4 = \sqrt{n_{sm}^2 + B^2 + i^2(N)} \to \min . \tag{7}$$

All of the component criteria should be reduced to the dimensionless form with range of change from 0 to 1. This requirement is not obligatory if the criteria are applied sequentially for selection of the model.

THE PROBLEM OF MODELING OF PHYSICAL FIELDS ON THE BASIS OF EXPERIMENTAL DATA

Modeling of physical fields has as its purpose identification (construction) of a picture of the field, and estimation of its parameters. Mathematical models of the field are necessary for prediction of its subsequent development, extrapolation to neighboring areas, and for synthesis of the optimal control rule for the field. An example of a physical field to be modeled might be the field of pollution in a body of water. This example is used below to explain some very general methods of field modeling.

The number of control stations recording water pollution increases from year to year. Nevertheless, there is not yet available sufficiently precise data with a small number of measurements. This virtually eliminates the possibility of using probabilistic models based on the construction of multidimensional distributions. The possibility of modeling is related to the use of inductive methods of self-organization of models by computer, based on running a large number of models (in the form of finite-difference equations) on a computer. Actually, this method requires a relatively small number of points of measurement, and when the proper external selection criterion is used, it has significant interference resistance.

Obviously, a description of methods applicable to the problem is necessary to clarify the conduct of subsequent measurements. Thus, the peculiarities of measurement determine the selection of modeling methods, while the development of methods makes certain corrections to the process of information collection.

A field of pollution is constructed using the data from observations of control stations, and data on the location, intensity, and time of discharge of pollutant substances. The selection of the output quantity and the argu-

ments defines the "statement of the task of modeling". This depends on the purpose of modeling (interpolation, extrapolation, or prediction), and upon the availability of initial information to be used to synthesize the model.

In this work, algorithms are presented for the solution of three problems of modeling of the field of a pollutant. In the following, statements are 1) based on the data collected at control stations; 2) based on information on the discharge of pollutants, and 3) based on the two types of data, taken together.

In the first problem, the equation of turbulent diffusion (in its finite-difference form) is not assigned a priori, but rather is found from the experimental data on the principle of self-organization, by processing standard samples and their nonlinearity. The number of terms in the complete equation is usally significantly greater than the number of experimental data points. Estimates of the coefficients are found by the least-squares method. The solution is found by a multi-step integration process of the finite difference equation. It is not necessary to know its solution in analytic form.

In the second problem, the arguments of the finite-difference model are selected so that the form of the equation corresponds to the "input-output matrix" (Tamura and Kando 1977; Yurachkovskiy 1977). It is possible to refer to the area of interpolation as a portion of a space lying within a polyhedron, the points of which are the outer control stations. The area of extrapolation lies outside this three-dimensional polyhedron (Figure 2). In prediction, the area of interpolation lies within the time interval of the experimental data. The area of prediction lies in the future, outside the area of interpolation of the process.

One characteristic feature of the area of interpolation is that, according to the Weierstrass theorem, any curve described by a sufficiently complex function fits the experimental points rather well. Only in the area of extrapolation and prediction do the curves diverge rapidly, forming a "fan" of predictions. The model should correspond to the function (or solution of the differential equation) which corresponds to the future course of the process in the area of extrapolation or prediction longer than the others.

Depending on the principle of selection of arguments, three different tasks can be distinguished. The first is based on the "principle of continuity or near action"; the second on the opposite "principle of distant action"; the third task is combined, using both principles simultaneously.

The model may be a point, one-dimensional, two-dimensional, three-dimensional, multidimensional, algebraic harmonic or finite-difference (differential). If the model is constructed according to observed data in which the spatial distribution of the sensors (or control stations) is not indicated, it is called a point model, hence there is reason to act as if all data were collected at one point in space.

The model is called spatial or a field model if the initial data include information on the location of the measurement stations in space.

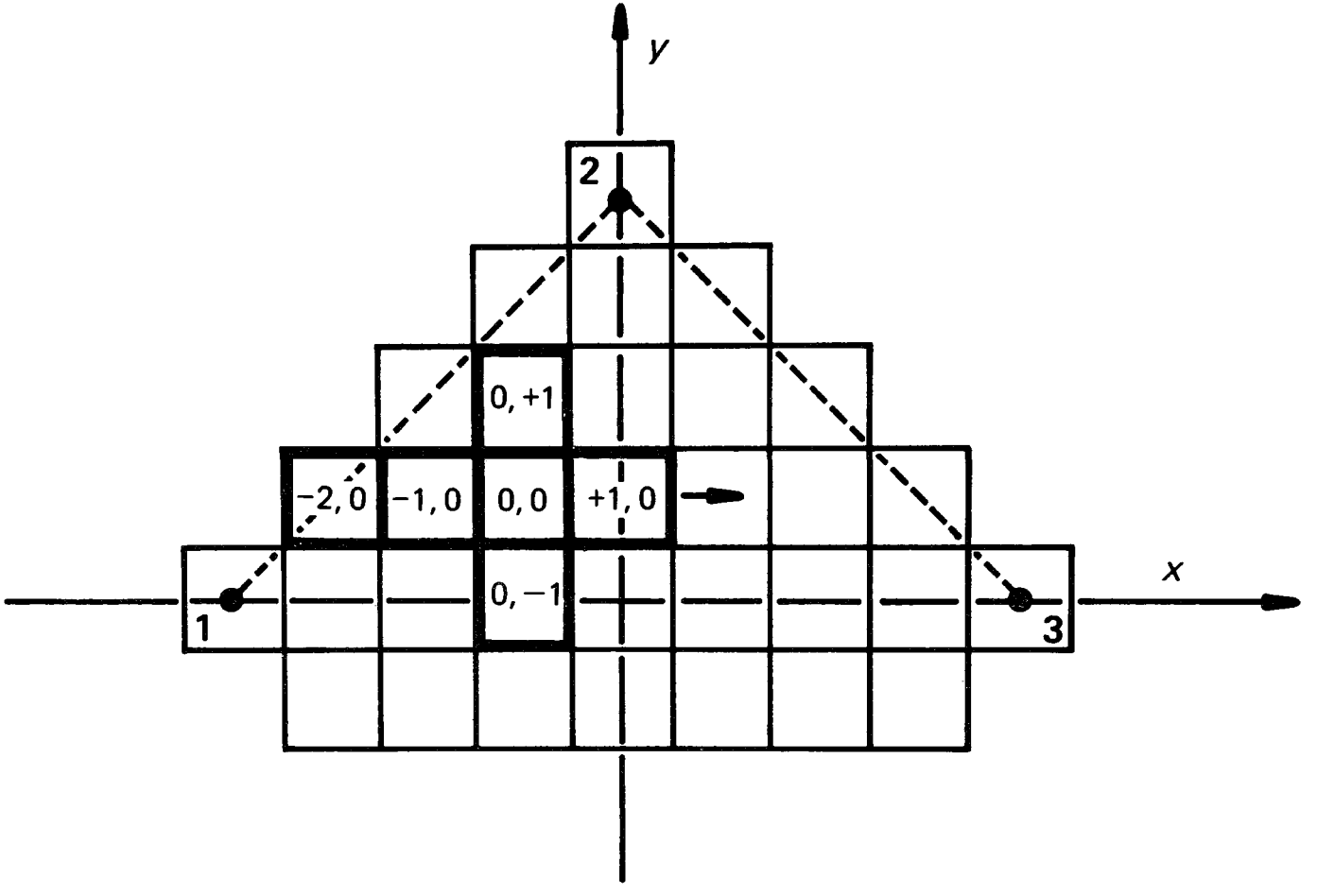

Figure 2. Use of simple models for extrapolation of the area of pollution between three measurement stations 1, 2 and 3 in the direction of the x axis.

Spatial models require at least three stations on each axis. Models with one argument are called one-dimensional, while models with several arguments are called multi-dimensional.

The same table of experimental data can be used to construct both the algebraic (or harmonic) model, e.g.,

$$q = f(t), \tag{8}$$

and the finite-difference model, e.g.,

$$q_{+1} = f(q_0, q_{-1}, q_{-2}, \ldots, q_{-\tau}).$$

The difference is only in the order of reading the data of the table. When methods of self-organization of models are used, preference must be given to the construction of finite-difference models, which are analogs of differential equations. The problem is that in problems of mathematical physics, linear differential equations correspond to nonlinear solutions. In processing models, it is easier to "guess" the linear nature of a finite-difference equation than the nonlinearity of its solution, which reduces the time required to process the reference functions. Furthermore, the solution of the finite-difference equation is more varied than the variation of curves corresponding to the same algebraic function. Therefore, further analysis will consider exclusively finite-difference models.

The symbols for the model arguments may be either the instantaneous values of the coordinates t, x, y and z, or the values of measurements of control stations $q^{(i)}_{j(\tau)}$ and discharges $\lambda^{(i)}_{j(\tau)}$ (instantaneous and delayed arguments), where:

i is the control station number;
j is the number of the pollutant;
τ is the delay in measurement of the argument in question.

Examples: $\lambda^{(1)}_{2(-3)}$ is the discharge of the second polluting component of the first source, measured only a delay of 3 time cycles;

$q^{(2)}_{1(0)}$ is the measurement of the first pollutant at the second station in the current moment of time.

If there is no subscript, this means that only one pollutant is being considered.

FIRST TASK: MODELING OF A FIELD USING FINITE-DIFFERENCE ANALOGS OF THE EQUATIONS OF TURBULENT DIFFUSION, BASED ON THE PRINCIPLE OF CLOSE ACTION

The equations of turbulent diffusion are based on the principle of continuity or close effect of neighboring particles, forming a physical field. The elementary model in the theory of finite-difference equations refers to

a geometric figure showing just which neighboring points of the field are used for construction of the equation structure. Changes in two neighboring cells (cubes) of the field are sufficient to represent the first derivative (on the axis of placement of the cells), while three cells are sufficient for the analog of the second derivative (Ivakhnenko and Krotov 1977).

Examples of the interrelations of linear differential equations, their finite-difference analogs, and elementary models are shown in Figures 3 and 4.

For physical fields, certain deterministic field models are usually known, mathematically expressed in the form of differential or integral-differential equations. These equations of the deterministic theory can be used as predictors for selection of the form of the following: a) arguments, and b) functions participating in the full description of the model (combined method). The deterministic equation of diffusion indicates a certain model which should be used as the basis of selection. The full model is produced from the model corresponding to the deterministic equation of diffusion by incrementing its dimensions by one or two cells on each axis. This means that, in any case, the order of the equation is increased by one (or two) in order to allow the algorithm to select a more general rule.

In modeling, two basic types of modeling algorithms are used:

a) a combinatorial algorithm which equates the various coefficients of the full polynomial to zero in turn, or

b) a multiple-row (threshold) algorithm.

SELECTION OF MODELS AND DEGREE OF NONLINEARITY (DOUBLE SELECTION)

When the number of components of the full polynomial is less than 20, the combinatorial algorithm is used to select the model of optimal complexity (setting all possible combinations of terms of the full polynomial equal to zero), requiring that all possible partial polynomials be considered. In this case, it is sufficient to analyze only the one, most complete, clearly sufficient model, the power of which is equal to the number of arguments; selection of models is therefore not required. When the number of components of the full polynomial is greater than 20, the multi-row (threshold) modeling algorithm is used. Testing of certain partial polynomials may be omitted in this case.

In order to expand the selection, one should use:

a) processing of particular models (composition of arguments), beginning with the simplest two-cell model (Figure 3);

b) processing of all possible polynomials for each of the simple models using the multiple-row modeling algorithm with renaming of variables, ending with a polynomial in which the highest power is equal to the number of arguments indicated in the simple model in question.

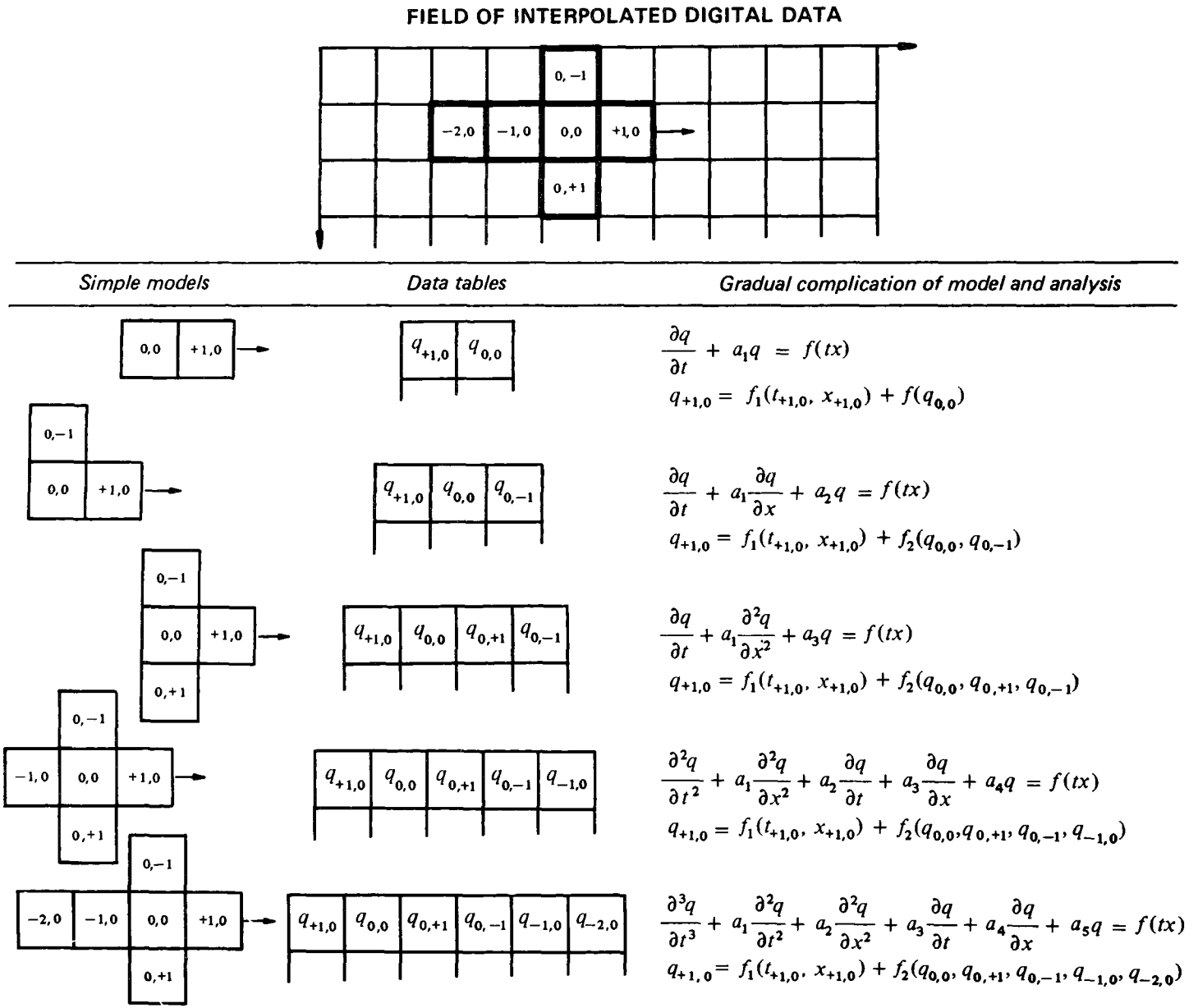

Figure 3. Run-through of simple models and production of data tables for the prediction problem $q_{+1,0} = f(t_{+1,0}, x_{+1,0}, q_{ij})$.

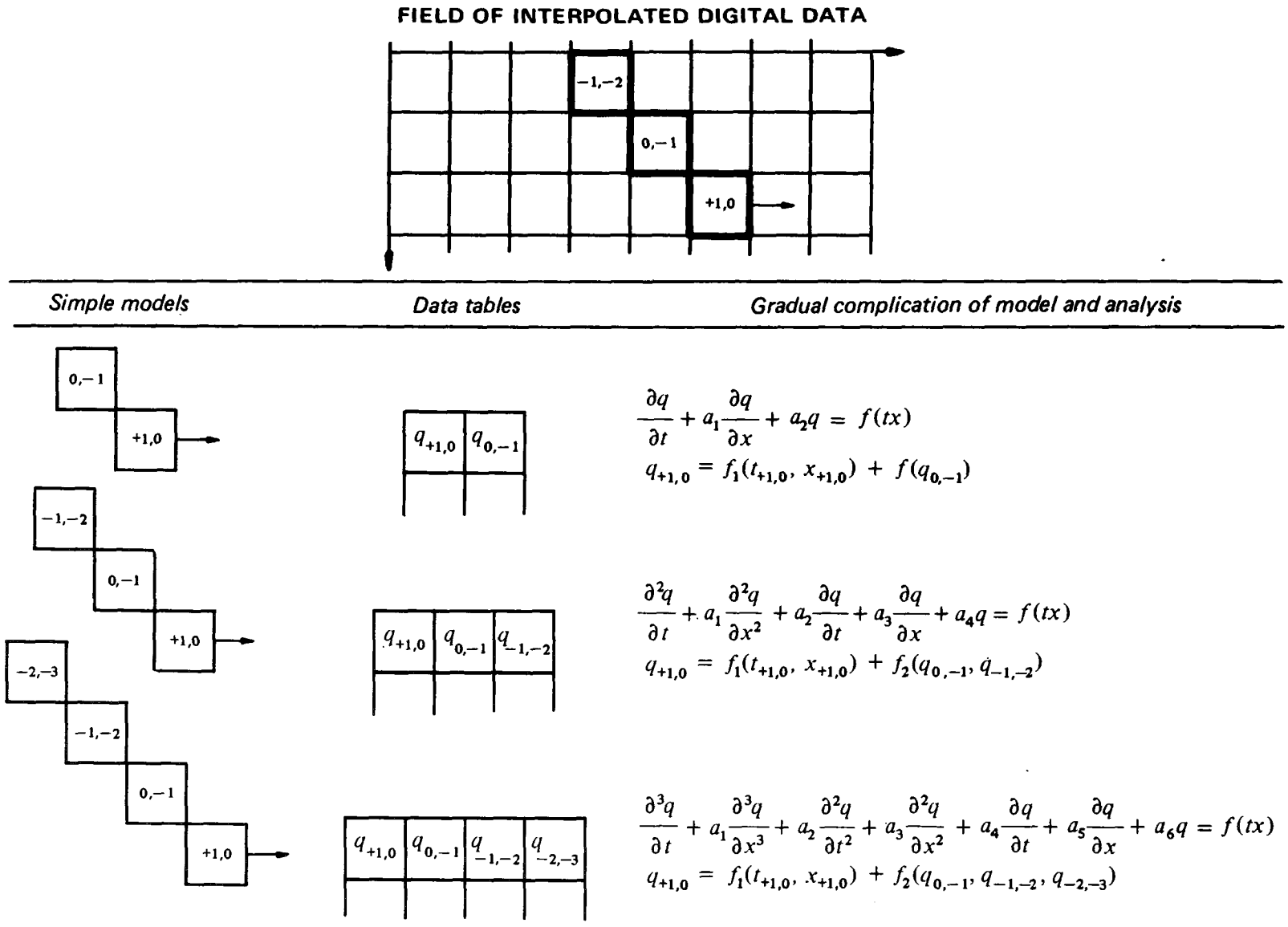

Figure 4. Run-through of simple models of diagonal shape and production of data tables for the prediction problem $q_{+1,0} = f(t_{+1,0}, x_{+1,0}, q_{ij})$.

This double processing of simple models and nonlinear polynomials provides a more complete examination of the set of possible partial polynomials in problems in which, due to the great number of arguments, it is impossible to use the simpler combinatorial modeling algorithm.

Double selection produces three types of tables of data. It is necessary to distinguish the table of initial data from the testing stations, the table of interpolated initial data, and the table of simple models, obtained as a result of shifting of the simple models over the digital field of the table (Figures 3 and 4). Each position of a simple model on the number field of interpolated data corresponds to one row (point) on the table. The points are ranked according to the dispersion of the output value (in the left part of the equation), and are used to determine the selection criterion. To do this, the row of simple model tables is divided into parts A and B.

The division into parts is performed not on the initial digital field of data, but rather on the tables obtained in the course of shifting the simple models over the field. For each simple model, a unique table of experimental data is produced. There will be as many tables as there are simple models which are compared against each other. The simple model which provides the greatest depth of the minimum of the combined criteria is best.

THE CONVERGENCE OF MULTI-STEP INTEGRATION OF FINITE-DIFFERENCE EQUATIONS

The convergence of integration may be defined as follows: Each finite-difference equation is a discrete analog of a certain differential equation with continuous derivatives. If the curve obtained as a result of step-by-step integration of the finite difference equation coincides closely enough with the curve of the analytic solution of the differential equation (or with a decrease in the discretization step--coincides with it precisely), the procedure for step-by-step integration converges. If there is no convergence, the step-by-step solution frequently becomes infinite or falls to zero.

Convergence depends on: a) the degree of bias of the estimates of the coefficients obtained by the least-squares method; b) the relationship of discretization steps of the axes; c) the form of the simple model; and d) the accumulation of computational errors (e.g., in calculation with a small number of significant digits). It is recommended that the discretization step be decreased until the accuracy of the model increases noticeably. If the steps are too small, the accuracy decreases once more.

It is known that simple models with a small number of points are more stable than branched simple models. Ivakhnenko and Krotov (1977) have suggested that the simple models be used with an "implicit" plan of step-by-step integration, as a method of increasing convergence.

All partial simple models and the full simple model are evaluated on the basis of the combined criterion "bias plus error of step-by-step integration":

$$K_3 = \sqrt{\left(\frac{n_{sm}}{n_{sm\ min}}\right)^2 + \left(\frac{i(N)}{i(N)_{min}}\right)^2}$$

where n_{sm} is the index of bias:

$$n_{sm} = \frac{\sum_{1}^{\alpha N_{A+B}} (q_A - q_{A+B})(q_B - q_{A+B})}{\alpha \sum_{1}^{N_{A+B}} q_{tabl}}, \text{ where } \alpha = 1.5 \div 3.0,$$

while i(N) is the index of stability of integration:

$$i(N) = \frac{\sum_{1}^{N_{A+B}} (q_{tabl} - q_{A+B})^2}{\sum_{1}^{N_{A+B}}}.$$

The component of the combined criterion n assures selection of an equation with minimum bias. Component i(N) is directed toward selection of a stable step-by-step procedure for construction of predictions and extrapolations. Frequently, the requirements $n_{sm} \to \min$ and $i \to \min$ are not contradictory, i.e., they lead to the selection of the same model. If there is divergence, a compromise solution must be found (Figure 5). The use of modeling algorithms does not require a priori knowledge of whether there is an algebraic solution of the differential (finite-difference) equation. Neither is it necessary to know the explicit algebraic form of this solution. The study is conducted at the level of the differential equation, and does not reach the level of its solution.

SUCCESSIVE APPLICATION OF CRITERIA WITH DOUBLE SELECTION

It has been experimentally established that models obtained for a given composition of arguments, i.e., for one simple model, differ comparatively little in the minimum value of the criterion of regularity and differ quite sharply in terms of the minimum criterion of the minimum bias. Geometrically, this is expressed in that points corresponding to the models compared form lines on a plane, similar to spectrograms. The criteria which should be used for selection of simple models are: regularity, stability of balance of variables:

$$\Delta(B) \to \min,\ i(N) \to \min,\ B \to \min,$$

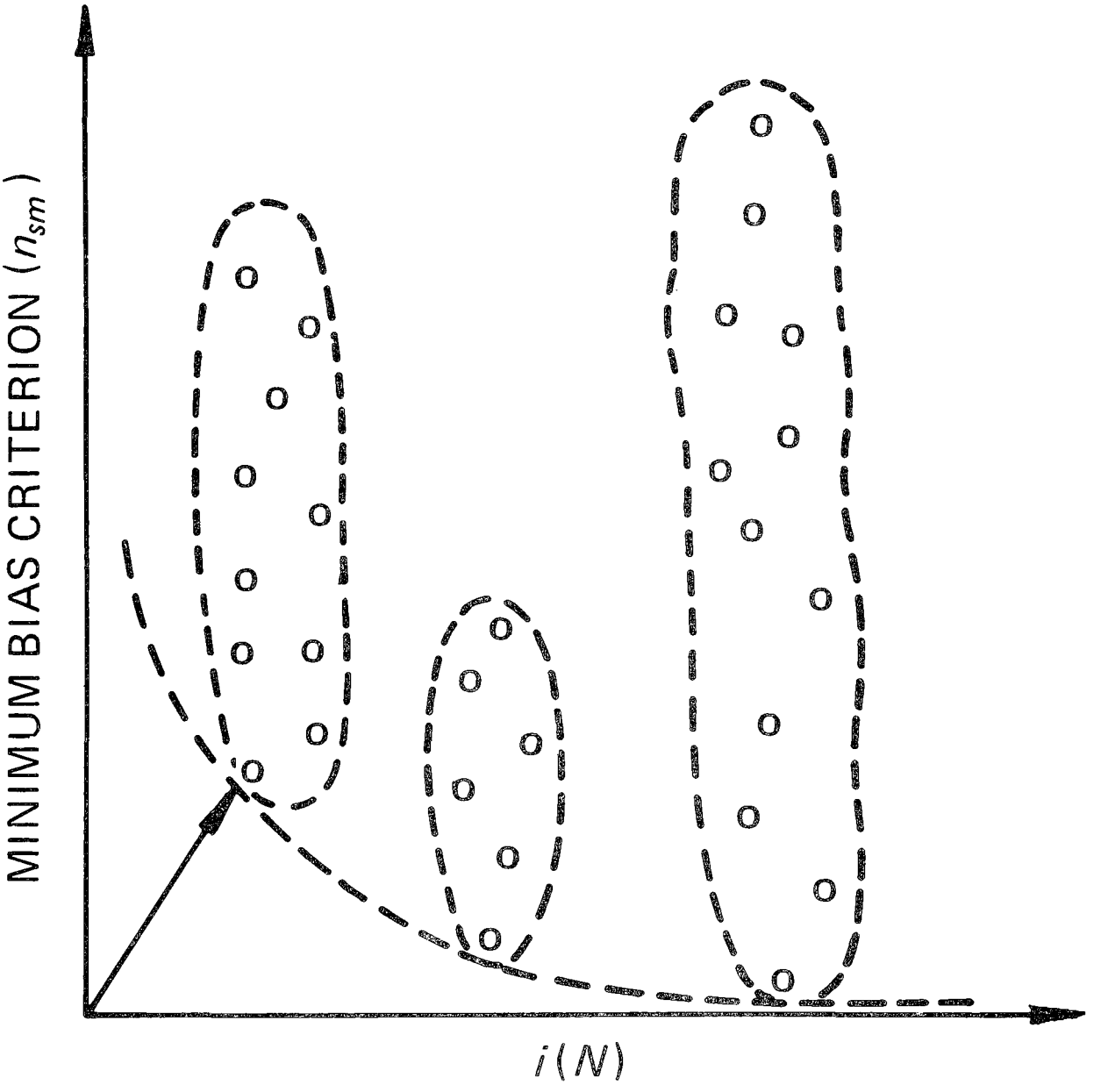

Figure 5. Selection of a model of optimal complexity based on the combined criterion

$$K_1 = \sqrt{n_{cm}^2 + i^2(N)} \rightarrow \min.$$

O = models with same composition of mean arguments.

while for selection of nonlinearity of the polynomials, the criterion of minimum bias should be used:

$$n_{sm} \to \min.$$

This recommendation leads to a reduction in program length, and to more accurate discrimination of models.

The examples show that successive application of criteria is not completely equivalent to the application of a combined criterion in all selection sequences. It yields somewhat simpler models with less variety of arguments.

Example 1. Double Selection of Point Models

For a point problem with one variable q, selection of simple models is equivalent to selection of the number of delaying arguments considered:

First simple model: $q_{+1} = f(q_0) = a_0 + a_1 q_0 + a_2 q_0^2,$

Second simple model: $q_{+1} = f(q_0, q_{-1}) = a_0 + a_1 q_0 + a_2 q_{-1} + a_3 q_0^2 + a_4 q_{-1}^2 + a_5 q_0 q_{-1},$

Third simple model: $q_{+1} = f(q_0, q_{-1}, q_{-2}) = a_0 + a_1 q_0 + a_2 q_{-1} + a_3 q_{-2} + a_4 q_0^2 + a_5 q_{-1}^2 + a_6 q_{-2}^2 + a_7 q_0 q_{-1} + a_8 q_0 q_{-2} + a_9 q_{-1} q_{-2}.$

Selection of nonlinearities in this example refers to selection of partial polynomials produced from the full polynomials using a combinational algorithm, i.e., by setting various combinations of coefficients equal to 2 , where n is the index of the last coefficient (n = 0, 5, 9, ...). As soon as the number of components of the full polynomial exceeds 20, multiple-row modeling algorithms must be used.

For a point model with two variables q and x, we have:

First simple model: $q_{+1} = f(q_0, x_0),$

Second simple model: $q_{+1} = f(q_0, x_0, q_{-1}, x_{-1}),$

Third simple model: $q_{+1} = f(q_0, x_0, q_{-1}, x_{-1}, q_{-2}, x_{-2}),$ ... etc.

Here, the transition to a multiple row algorithm occurs more rapidly, since the number of terms of the full polynomials is significantly greater. Otherwise, the processing of simple models and nonlinearities have the same form.

Example 2. Double Processing for Three-Dimensional Models

Using the principle of continuity (or similar action) for spatial models, several equations are composed (based on the number of coordinates of time and space). Furthermore, the number of arguments includes variables with different time delays and shifts in space. A two-dimensional spatial model is analyzed in detail in the following example.

BASIC STATEMENTS OF THE TASK OF MODELING (SELECTION OF ARGUMENTS)

First Task: Modeling of the Field of a Pollutant Exclusively on the Basis of Data Provided by a Few Measurement Stations

The first statement of the task of modeling of a field has as its purpose the construction of the field of a pollutant, not only in the area of interpolation (encompassed by the measurement stations), but also over a significant distance outside this area, i.e., construction of an extrapolation of the field and prediction of its development in time. It is assumed here that the emission of the pollutant changes relatively little with time and, therefore, information on the pollutant is not directly considered. It is contained indirectly in the data of the measurement stations. Therefore, in the first statement, the set of arguments contains only the data of the measurement stations. If there are few stations, the data can be interpolated within the area of interpolation in order to produce the mean values of the pollution index in all squares of the field t-x. Two-stage interpolation (Ivakhnenko and Krotov 1977) implies that first the data of the stations are interpolated (between stations) by the least-squares method. The "digital field" thus produced is used to synthesize finite-difference models suitable for prediction and extrapolation outside the area of interpolation.

For brevity of presentation of the overall method, the equations are shown below for the two-dimensional model, $q = f(xt)$, only. It is easy, by analogy, to compose similar equations for the three-dimensional (or four-dimensional) field, $q = f(x,y,z,t)$, as well.

The equation for the parameters of pollution with simple model 5 (Figure 3) can be written in vector form as follows:

a) for prediction;

$$q_{j(+1,0)} = \alpha_{jnp} \left[q_{K(0,0)}, q_{K(0,-1)}, q_{K(0,+1)}, q_{K(-1,0)}, q_{K(-2,0)}, \ldots, q_{K(-\tau,0)}\right] \tag{15}$$

b) for extrapolation:

$$q_{j(0,+1)} = \alpha_{j\ni K} \left[q_{K(0,0)}, q_{K(-1,0)}, q_{K(+1,0)}, q_{K(0,-1)}, q_{K(0,-2)}, \ldots, q_{K(0,-\tau)}\right]$$

where α_j is the vector of polynomial functions (linear, nonlinear without covariation or with incomplete consideration of covariation) of dimensionality j.

In all of the equations presented, the vector of measured external variable contained in the right portion can contain both the variables themselves, their delaying values, and covariations (in pairs), which can be considered individual variables, e.g.,

$$q_{1(0)}q_{2(0)} \cdots q_{1(-1)}q_{2(-1)} \cdots (q_{1(0)}q_{2(0)})\ (q_{1(0)}q_{1(-1)}) \cdots$$

In the equations presented below, the covariation vector will not be shown for simplicity.

q and q are vectors of the parameters of pollution with dimensionality j, k = 1, 2, 3, ... For example, to predict and extrapolate the first component of pollution, considering equations (1a) where j = 2, k = 2, τ = 2, we obtain:

a) for prediction

$$q_{1(+1,0)} = \alpha_{1np}\ [q_{1(0,0)}, q_{1(0,-1)}, q_{1(0,+1)}, q_{1(1,0)}, q_{1(-2,0)}, q_{2(0,0)}, q_{2(0,-1)}, q_{2(0,+1)}, q_{2(-1,0)}, q_{2(-2,0)}] \tag{15a}$$

b) for extrapolation

$$q_{1(0,+1)} = \alpha_{1\ni K}\ [q_{1(0,0)}, q_{1(-1,0)}, q_{1(+1,0)}, q_{1(0,-1)}, q_{1(0,-2)}, q_{2(0,0)}, q_{2(-1,0)}, q_{2(+1,0)}, q_{2(0,-1)}, q_{2(0,-2)}]$$

<u>The "Source-Functions" in the First Task (Consideration of Settling of Pollutant Particles and Lateral Influx of Pollutant, as well as External Influences of the Environment</u>

In the two-dimensional problem analyzed above, we did not consider the process of diffusion of a pollutant from layer to layer, and vertical settling of particles. In order to consider these phenomena, the "source function" or "residue" is introduced, a function of the coordinates of the square in which the output quantity is measured. Furthermore, the source function also includes the perturbing effects P of the wind, V' of current on the x axis, etc.

For the parameters of the pollutant, in the general statement, we obtain:

the prediction equation

$$q_{j(+1,0)} = Q_1(t_{+1,0}, x_{+1,0}) + Q_2(P,V') + \\ + \alpha_{jnp}\,[q_{K(0,0)}, q_{K(0,-1)}, q_{K(0,+1)}, q_{K(-2,0)}, q_{K(-1,0)}, \ldots, q_{K(-\tau,0)}] \tag{16}$$

and the extrapolation equation

$$q_{j(0,+1)} = Q_1(t_{0,+1}, x_{0,+1}) + Q_2(P,V') + \\ + \alpha_{j\ni K}\,[q_{K(0,0)}, q_{K(-1,0)}, q_{K(0,-1)}, q_{K(0,-2)}, \ldots, q_{K(0,-\tau)}] \tag{16a}$$

Simultaneous step-by-step integration of Equations (16, 16a) enables the generation of a prediction (on the t axis) or an extrapolation (on the x axis) of the field of the pollutant.

Second Task: Modeling of Fields Using Finite-Difference Equations Corresponding to the Expanded "Input-Output" Matrix (Based on the Principle of Long-Range Action)

In addition to the analogs of the equations of turbulent diffusion, the modeling of physical fields also involves equations corresponding to the functional "input-output" matrix (second task). Performance of the second task of field modeling is easy if a prediction of changes in the field of the pollutant within the area of interpolation is required when there is a change in the discharge with time. The solution of the second problem does not provide an accurate extrapolation of the field far beyond the limits of the area.

The second task has three statements:

1. Modeling by "input-output" matrix, using information of measurement stations alone:

In the first statement, the following prediction equation is used for the ith station:

$$q^i_{j(+1)} = \sum_{\substack{s=1 \\ s\neq i}}^{m} \alpha_{sj}(q^s) \tag{17}$$

where $q^s = [q^s_{1(0)}, q^s_{1(-1)}, q^s_{1(-\tau)}, \ldots, q^s_{j(0)}, q^s_{j(-1)}, q^s_{j(-\tau)}]$, $j = i,\bar{n}$;

q^s are the parameters of the pollutant;
α is the operator of the polynomial functions;
m is the number of stations.

For example, where j = 2, τ = 2, m = 3^n (n is the number of components),

$$q^{(1)}_{1(+1)} = \alpha_{21}\,[q^{(2)}_{1(0)}, q^{(2)}_{1(-1)}, q^{(2)}_{1(-2)}, q^{(2)}_{2(0)}, q^{(2)}_{2(-1)}, q^{(2)}_{2(-2)}] +$$

$$+ \alpha_{31}\,[q^{(3)}_{1(0)}, q^{(3)}_{1(-1)} q^{(3)}_{2(-2)}, q^{(3)}_{1(-2)}, q^{(3)}_{2(0)}, q^{(3)}_{2(-1)}] \qquad (17a)$$

The pollution at the ith station (or point of the field) depends directly on the value of the indexes measured from the closest neighboring stations, with various time delays.

2. Modeling by "input-output" matrix, using information on discharge of pollutants only:

In its second statement for the ith station, the prediction equation is as follows:

$$q^{i}_{j(+1)} = \sum_{s=1}^{p} \beta_{sj}(\overline{\lambda}^{s});$$

where: q are the pollution parameters,
λ is the discharge vector,

$$\lambda^s = [\lambda^s_{1(0)}, \lambda^s_{1(-1)}, \lambda^s_{1(-\tau)}, \ldots, \lambda^s_{n(0)}, \lambda^s_{n(-1)}, \lambda^s_{n(-\tau)}],$$

β_{sj} is the operator of the polynomial functions,
p is the number of sources.

For example, where n = 2, τ = 2 and p = 2, we obtain

$$q^{1}_{1(+1)} = \beta_{11}[(\lambda^{(1)}_{1(0)}, \lambda^{(1)}_{1(-1)}, \lambda^{(1)}_{1(-2)}, \lambda^{(1)}_{2(0)}, \lambda^{(1)}_{2(-1)}, \lambda^{(1)}_{2(-2)}] +$$

$$+ \beta_{21}\,[\lambda^{(2)}_{1(0)}, \lambda^{(2)}_{1(-1)}, \lambda^{(2)}_{1(-2)}, \lambda^{(2)}_{2(0)}, \lambda^{(2)}_{2(-1)}, \lambda^{(2)}_{2(-2)}]; \qquad (18a)$$

3. Modeling considering information on measurement stations and information on the discharge of sources of pollution:

In the general (third) statement of the task, the "input-output" matrix is expanded by introducing the data from the measurement of nearby stations in addition to the discharges of pollution sources.

In its general statement, the prediction equation for the ith station is:

$$q^{i}_{j(+1)} = \sum_{\substack{s=1 \\ s\neq i}}^{m} \alpha_{sj}(q^{2}) + \sum_{s=1}^{p} \beta_{sj}(\lambda^{s}) \tag{19}$$

<u>The "Source Function" in the Second Task (Consideration of External Effects)</u>

In order to consider external effects (the adjusted wind or current, temperatue, relative humidity and other physical quantities), it is recommended that Equations (17) and (18) or (19) be supplemented with the following source function in the right part:

$$Q(V', P, \ldots).$$

As a result, we produce complete descriptions, in the form of sums of polynomials:

First statement:

$$q^{(i)}_{j(+1)} = Q_1(V',P,\ldots) + \sum_{s=1}^{p} \beta_{sj}(\lambda^{s}); \tag{20}$$

Second statement:

$$q^{(i)}_{j(+1)} = Q_2(V',P,\ldots) + \sum_{\substack{s=1 \\ s\neq i}}^{m} \alpha_{sj}(q^{s}); \tag{20a}$$

or in the general (third) statement:

$$q^{(i)}_{j(+1)} = Q(V',P,\ldots).$$

The particular polynomials are produced as versions by setting various terms of these full descriptions equal to zero.

The additive introduction of "source functions" to the full equation was shown earlier. Physical fields are encountered in which this function is included multiplicatively or is mixed.

For example,

$$q_{(+1)} = Q_1(V',P) + Q_2(V',P) \left(\sum_{\substack{s=1 \\ s\neq i}}^{m} \alpha_{sj}(q^{s}) + \sum_{s=1}^{p} \beta_{sj}(\lambda^{s}) \right) . \tag{20b}$$

It is necessary to select a multiplicative or mixed version of application of the function depending on which will provide the deepest minimum of the criterion of selection, or on the basis of a priori information.

Third Task: Modeling of Fields with Simultaneous Application of the Principles of "Near" and "Distant" Action

The third task has three statements:

1. Modeling using the principle of "near" action and the "input-output" matrix, considering information from the measurement stations. In this statement, a combination of the first two problems is used.

2. Modeling using the principle of "near" action and the "input-output" matrix, considering information on discharges, a combination of the first two tasks.

3. Modeling using the principle of "near" action and the expanded "input-output" matrix, considering both data from the measurement stations and the discharges of pollutants.

Examples of Solution of Two-Dimensional Problem with Fixed Number and Position of Measurement Stations

Three variables were measured at three points in a body of water at the depth of 0.5 m: dissolved oxygen $p^k = q(t)$, biochemical oxygen demand BOD = $q(t)$ and temperature $\tau(t)$. The measurements were performed from mid-May, every two weeks, for a total of 8 times. The results are cited elsewhere (Ivakhnenko and Krotov 1977).

Two-stage interpolation:

Using quadratic interpolation, the number of measurement points was greatly increased from 3 x 8 = 24 to 16 x 16 = 256 (Ivakhnenko and Krotov 1977). The permissibility of this approach is based on the fact that the smooth functions are well approximated within the area of interpolation. However, for extrapolation (on the x axis) and prediction (on the t axis), it is necessary to use finite-difference equations derived from the modeling algorithm.

When the combined criterion k_1 is used as the external criterion, the following types of interpolating polynomials are produced:

$$q_{+1;0} = 8.109 - 0.136x + 0.033\tau + 0.061t - 8\cdot10^{-5}xT +$$

$$+ 6.54\cdot10^{-3}x^2 - 8\cdot10^{-5}t^2;$$

$$K_{3min} = 0.8728;\ \Delta(B)_{min} = 0.6500;$$

$$Z_{+1} = -13.017 + 1.725T + 0.017t + 1.8\cdot10^{-7}xt - 1.3\cdot10^{-4}x^2 -$$

$$- 0.056T^2 - 5.6\cdot10^{-4}t^2;$$

$$K_{3min} = 0.985,\ \Delta(B)_{min} = 0.362;$$

The task of prediction is performed by identification of the finite-difference equation

$$q_{+1,0} = f(x_{0,+1}, t_{0,+1}, q_{0,0}, q_{-1,0}, q_{-2,0}, q_{0,-1}, q_{0,+1},$$

$$Z_{0,0}, Z_{-1,0}, Z_{-2,0}, Z_{0,-1}, Z_{0,+1}) .$$

In order to produce the table of initial data, simple model No. 5 (Figure 3) is moved step-by-step over the digital field of the table derived from quadratic interpolation in direction t. The task of extrapolation is performed by means of identification of an equation such as

$$Z_{0,+1} = f(x_{+1,0}, t_{+1,0}, Z_{0,0}, Z_{0,-1}, Z_{0,-2}, Z_{+1,0}, Z_{-1,0},$$

$$q_{0,0}, q_{0,-1}, q_{0,-2}, q_{+1,0}, q_{-1,0}T) .$$

To produce the data table, the simple model was shifted in the direction of the x axis, using the combined criterion:

$$K_1' = \sqrt{n_{cm}^2 + \Delta^2(c)} .$$

$\Delta(c)$--the error for an individual examination sequence. The following equations were obtained for extrapolation.

$$q_{0,+1} = 9.524 + 0.094\ Z_{0,0}Z_{0,-2} + 0.003\ Z_{0,0}T_{0,0} + 0.230\ Z_{0,-1}Z_{0,-2}$$

$$- 0.140\ Z_{0,-1}Z_{+1,0} - 0.027\ Z_{0,-2} + 0.039\ Z_{0,-2}\ q_{-1,0}$$

$$- 0.140\ Z_{0,-2}Z_{0,-1} - 0.029\ Z_{-1,0} - 0.105\ Z_{-1,0}Z_{+1,0};$$

$$K_{2min} = 1.5\cdot10^{-3};\ n_{cm} = 6.95\cdot10^{-6};\ \Delta(B)_{min} = 0.38.$$

$$Z_{+1,0} = -0.18 + 1.157\ Z_{0,0} - 0.112\ Z_{0,0} + 0.01\ Z_{-1,0}T_{0,0} .$$

$$K_{2min} = 7.542 \cdot 10^{-4}; \; n_{cm} = 5.987 \cdot 10^{-4};$$

$$\Delta(c) = 4.586 \cdot 10^{-4}; \; \Delta(B)_{min} = 0.05.$$

for prediction:

$$q_{+1,0} = 12.431 - 4.648 \, Z_{0,0} + 0.162 \, q_{-2,0} Z_{0,0} + 0.840 \, Z_{0,0}^2 -$$

$$- 0.003 \, Z_{0,0} Z_{+1,0} + 0.0004 \, t_{+1,0};$$

$$K_{min} = 1.182 \cdot 10^{-3}; \; n_{cm} = 2.025 \cdot 10^{-4};$$

$$\Delta(c) = 1.165 \cdot 10^{-3}; \; \Delta(B)_{min} = 0.037.$$

$$Z_{+1,0} = 1.115 + 0.020 \, Z_{-1,0} T_{0,0} + 0.004 \, Z_{0,+1} T_{0,0};$$

$$K_{min} = 3.969 \cdot 10^{-3}; \; n_{cm} = 5.402 \cdot 10^{-4};$$

$$\Delta(B) = 0.064; \; \Delta(c) = 0.937 \cdot 10^{-3}.$$

EXAMPLE OF COMPARISON OF MODELS ON THE TEST PROBLEM OF CONSTRUCTION OF THE FIELD OF A POLLUTANT IN A BODY OF WATER

The method of using test problems to compare models requires that the field is calculated using a known, deterministic formula. The form of differential equation used to produce the formula determines the type of reference function used in the modeling algorithm.

In the present example, the field was calculated by a formula suggested by Lapshin which presumes pure diffusion of particles in space. It allows the change in pollution in space and time to be determined when there is no current:

$$q = \frac{2\tau}{\sqrt{Kx}} \int_{x = \frac{R}{\sqrt{Kt}}}^{\infty} \frac{e^{-x}}{x} \, dx$$

where k is the coefficient of turbulent diffusion,
τ is the distance of the measurement station from the source of pollution,
t is the time from the beginning of emission to the moment of measurement.

Assuming there is one source, the rule of change of emission and concentration of polluting substances with time is shown in Figure 6, according to the initial data obtained from the equation. Finite-difference models of seven types were synthesized, and compared for accuracy of step-by-step integration both inside and outside the interpolation area.

As a result, the following improved models were obtaind.

First state of problem:

Model I-1 (Figure 7)

$$q_{+1}^{(1)} = 1.06020 - 0.1779\, q_{+1,0}^{(1)} + 0.01673\, q_{-2,0}^{(1)} + 0.63904\, q_{0,-1}^{(1)}$$

$$- 0.00188\, q_{0,1}^{(1)} + 0.00054\, q_{0,0}^{(1)} q_{1,0}^{(1)} - 0.01059\, q_{0,0}^{(1)} q_{2,0}^{(1)}$$

$$+ 0.00233\, q_{0,0}^{(1)} q_{-3,0}^{(1)} + 0.00001\, q_{0,0}^{(1)} q_{0,1}^{(1)} - 0.1027\, q_{0,0}^{(1)} q_{0,+1}^{(1)}$$

$$- 0.0894\, q_{-1,0}^{2} + 0.00947\, q_{-2,0}^{(1)} - 0.0912\, q_{1,0}^{(1)} q_{-3,0}^{(1)}$$

$$+ 0.00844\, q_{-1,0}^{(1)} q_{0,-1}^{(1)} - 0.02334\, q_{-1,0}^{(1)} q_{0,+1}^{(1)} + 0.00188\, q_{-2,0}^{(1)2}$$

$$- 0.00358\, q_{-2,0}^{(1)} q_{0-1}^{(1)} + 0{,}17850\, q_{-3,0}^{(1)} q_{0,-1}^{(1)} - 0{,}25224\, q_{-3,0}^{(1)} q_{0,+1}^{(1)}$$

$$+ 0.00894\, q_{-1,0}^{(1)} q_{0,-1}^{(1)} - 0.02334\, q_{-1,0}^{(1)2} q_{0,+1}^{(1)2} + 0.00188\, q_{-2,0}^{(1)2}$$

$$+ 0.07531\, q_{0,-1}^{(1)2} - 0.0064\, q_{0,-1}^{(1)} q_{0,+1}^{(1)};$$

$$K = 0.032;\ n_{cm} = 0.017;\ \Delta(c) = 0.027;\ i = 0.182.$$

Second statement of problem:

Model II-1 (Figure 8a)

$$q_{+1}^{(1)} = 2.73520 + 0.00031\, q_{0}^{(2)} + 0.000001\, q_{-2}^{(2)} - 0.0004\, q_{-1}^{(3)}$$

$$+ 0.00001\, q_{-2}^{(3)} + 0.29626\, q_{0}^{(2)} q_{-2}^{(2)} + 0.46974\, q_{0}^{(2)} q_{-3}^{(2)}$$

$$- 0.66516\, q_{0}^{(2)} q_{0}^{(3)} + 4.86824\, q_{-1}^{(3)} q_{0}^{(2)} - 1.95950\, q_{-1}^{(2)} q_{-2}^{(2)}$$

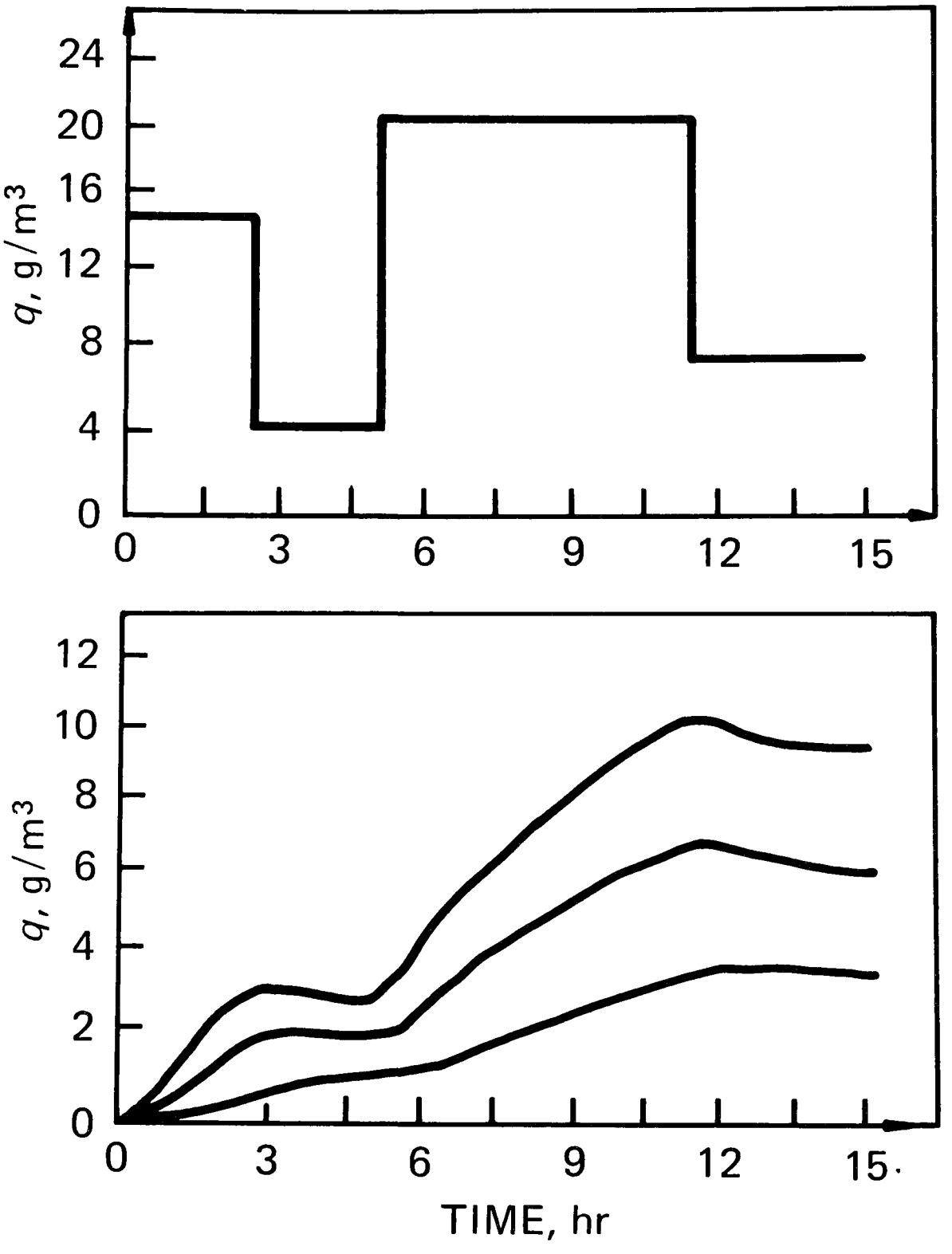

Figure 6. Change of emission and concentration of pollutants with time.

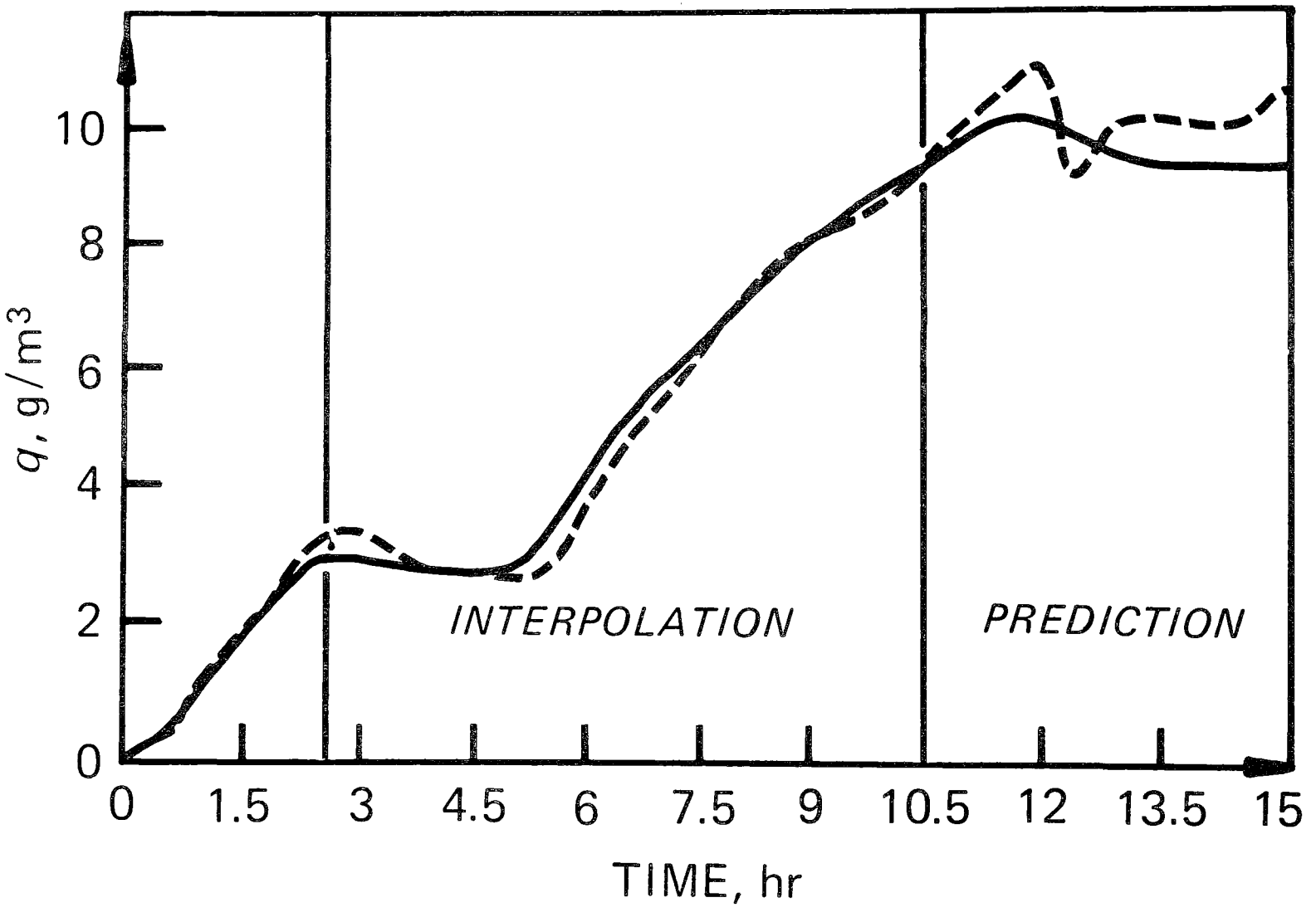

Figure 7. Model I-1.

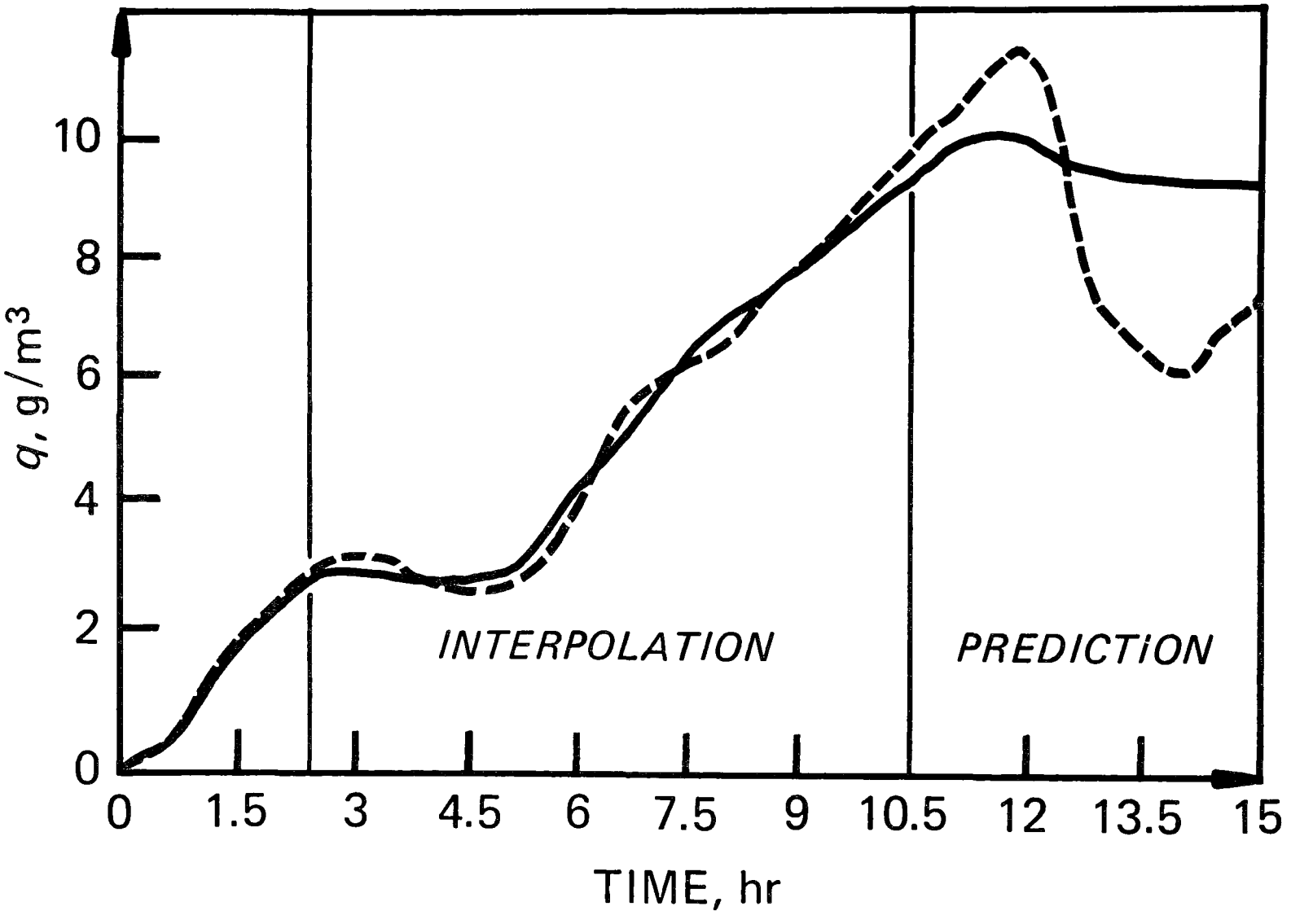

Figure 8a. Model II-1.

$$+ 1.79479\ q_{-1}^{(3)}q_{-3}^{(2)} + 1.58739\ q_{-2}^{(2)}q_{-3}^{(2)} - 1.41426\ q_{-3}$$

$$+ 1.1132\ q_{-3}^{(1)}\ q_{-3}^{(3)} + 1.513890\ q_{0}^{(3)}q_{-2}^{(3)} + 9.67937\ q_{-1}^{(3)}q_{-3}^{(3)}$$

$$- 0.10583\ q_{0}^{(3)}q_{-3}^{(2)} + 3.44364\ q_{-1}^{(3)2} - 0.38696\ q_{-1}^{(3)}q_{-2}^{(3)}$$

$$- 3.87969\ q_{-2}^{(3)}q_{-3}^{(3)};$$

$$K = 0.061;\ n_{cm} = 0.046;\ \Delta(c) = 0.040;\ i = 0.188.$$

Model II-2 (Figure 8b)

$$q_{+1}^{(1)} = 2.73090 + 0.000035\ \lambda^2 - 0.000006\ \lambda_0\lambda_{-1} - 0.00032\ \lambda_0\lambda_{-3}^2$$

$$+ 0.000394\ \lambda_{-1}\lambda_2^2 + 0.000548\ \lambda_{-2}\lambda_0^2 - 0.000548\ \lambda_{-2}\lambda_{-1}^2$$

$$- 0.000002\ \lambda_0^4 - 0.000003\ \lambda_0^2\lambda_{-3}^2 + 0.000003\ \lambda_{-1}^2\lambda_{-3}^2;$$

$$K = 0.089;\ n_{cm} = 0.082;\ \Delta(c) = 0.036;\ i = 0.169.$$

Model II-3 (Figure 8c)

$$q_{+1}^{(1)} = 2.03610 - 2.18146\ q_{-1}^{(2)} - 0.21021\ q_{-3}^{(2)} + 0.00754\ \lambda_0^2$$

$$+ 0.10985\ q_{0}^{(2)}q_{-2}^{(2)} + 0.39242\ q_{-1}^{(2)} + 0.00002\ q_{0}^{(2)2}$$

$$- 0.10895\ q_{0}^{(2)}q_{-1}^{(3)} - 0.000001\ q_{0}^{(3)2};$$

$$K = 0.08;\ n_{cm} = 0.054;\ \Delta(c) = 0.059;\ i = 0.151.$$

Third statement of problem:

Model III-1 (Figure 9a)

$$q_{+1,0}^{(1)} = 2.62225 - 0.25160\ q_{0,0}^{(1)}q_{0,0}^{(2)} + 0.12961\ q_{1,0}^{(1)2} + 0.00245\ q_{-1,0}^{(1)}q_{-2,0}^{(1)}$$

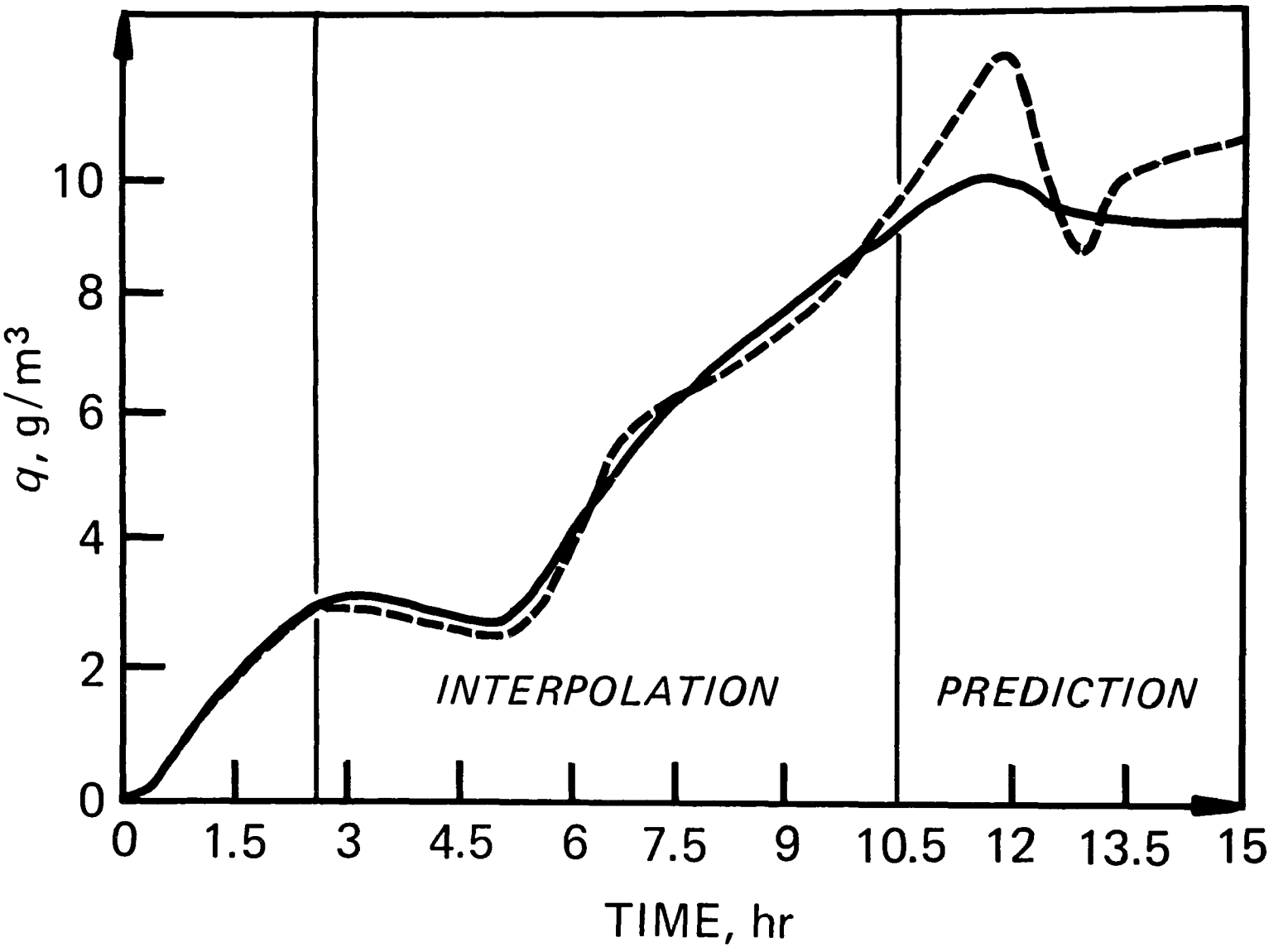

Figure 8b. Model II-2.

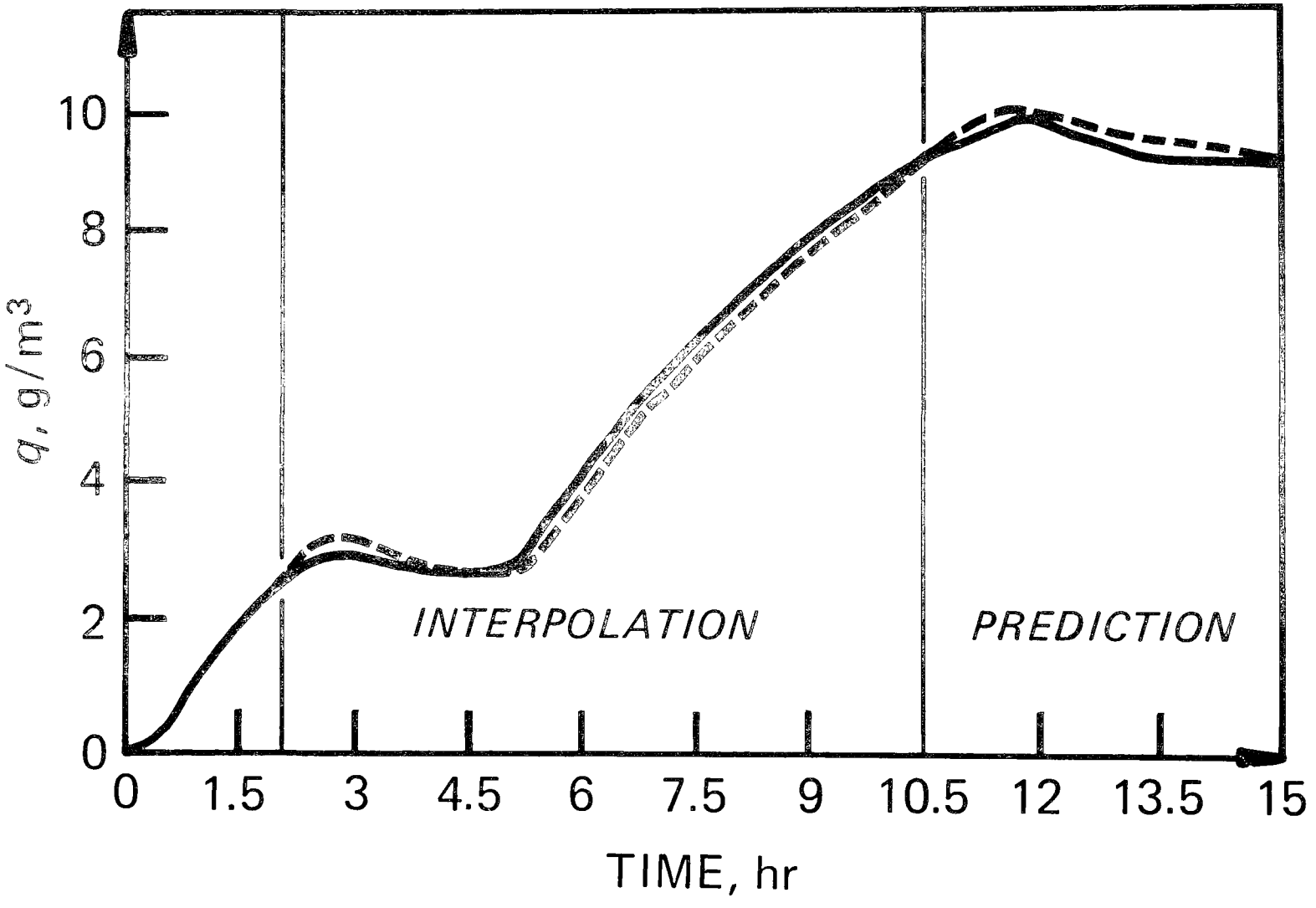

Figure 8c. Model II-3.

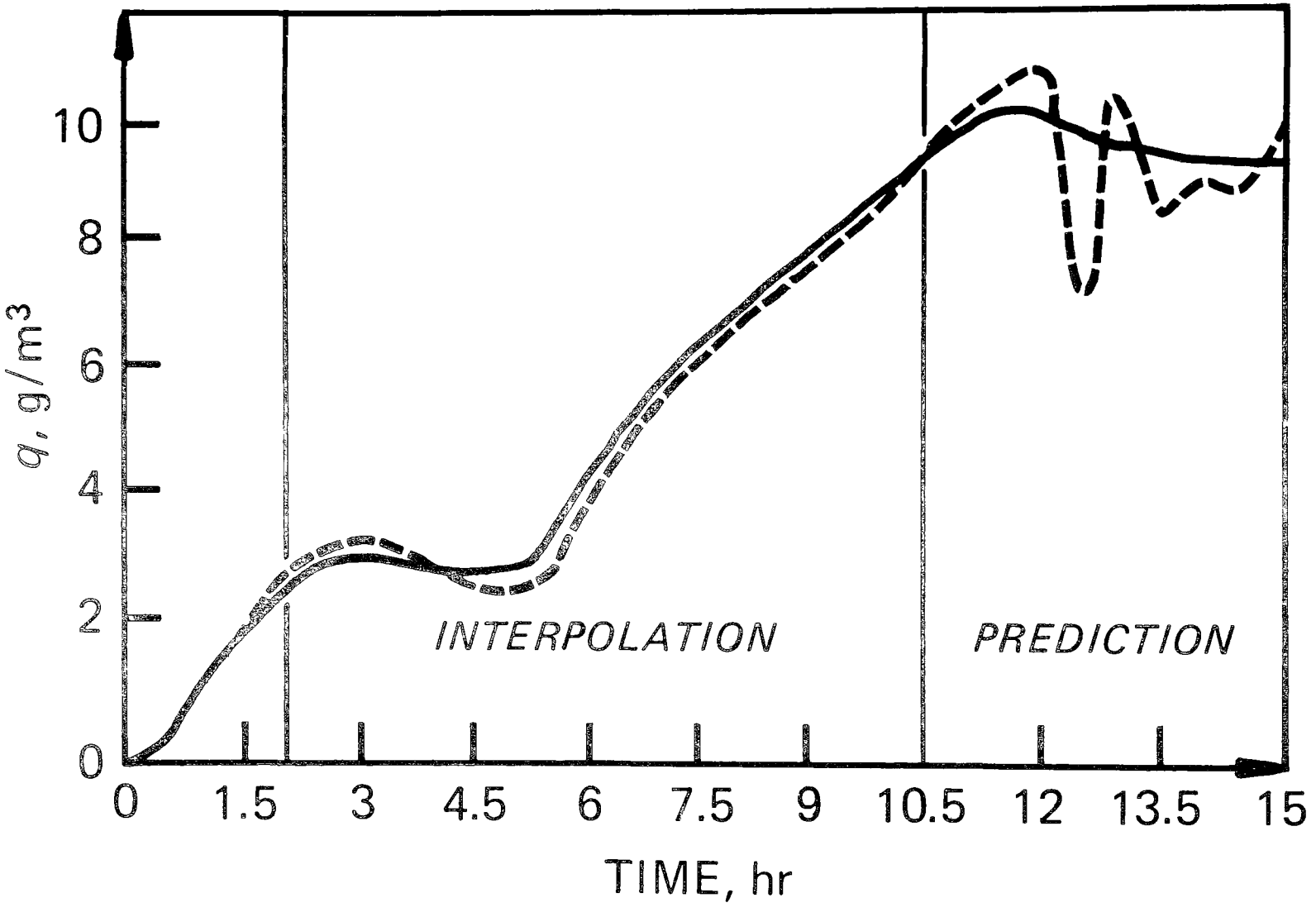

Figure 9a. Model III-1.

$$- 0.94186\ q^{(1)}_{-1,0}q^{(2)}_{-1,0} + 0.32467\ q^{(1)}_{-1,0}q^{(2)}_{-2,0} - 0.13988\ q^{(1)}_{-2,0}q^{(2)}_{0,0}$$

$$+ 0.01585\ q^{(2)}_{0,0}q^{(1)}_{0,-1} + 0.98315\ q^{(2)}_{-1,0}q^{(1)}_{0,-1} + 0.01424\ q^{(2)}_{-1,0}q^{(1)}_{0,+1}$$

$$- 0.29071\ q^{(2)}_{-2,0}q^{(1)}_{0,-1} - 2.64613\ q^{(3)}_{0,0}q^{(3)}_{2,0} + 0.78000\ q^{(3)}_{-2,0}q^{(1)}_{0,-1}$$

$$- 0.07373\ q^{(1)}_{0,-1}q^{(1)}_{0,+1};$$

$K = 0.064$; $n_{cm} = 0.063$; $\Delta(c) = 0.026$; $i = 0.176$.

Model III-2 (Figure 9b)

$$q^{(1)}_{+1} = 0.42274 - 0.77917\ q^{(1)}_{0,0} - 0.57968\ q^{(1)}_{-1,0} - 0.49081\ q^{(1)}_{-3,0}$$

$$+ 0.93996\ q^{(1)}_{0,1} + 1.15023\ q^{(1)}_{0,+1} + 0.04420\ \lambda_{-2,0} + 0.00047\ q^{(1)2}_{0,0}$$

$$+ 0.0166\ q^{(1)}_{0,0}q^{(1)}_{-1,0} + 0.00184\ q^{(1)}_{0,0}q^{(1)}_{-2,0} + 0.00739\ q^{(1)}_{-1,0}q^{(1)}_{-2,0}$$

$$- 0.02110\ q_{-1,0}q^{(1)}_{-3,0} + 0.00540\ q^{(1)}_{-1,0}q^{(1)}_{+1,0} - 0.0064\ q^{(1)}_{-2,0}q^{(1)}_{0,-1}$$

$$- 0.0021\ q^{(1)}_{-2,0}q^{(1)}_{0,+1} + 0.0184\ q^{(1)}_{-3,0}q^{(1)}_{0,-1} - 0.0032\ q_{-2,0}q^{(1)2}_{0,-1}$$

$$- 0.00196\ q^{(1)}_{0,-1}q^{(1)}_{0,+1};$$

$K = 0.033$; $n_{cm} = 0.009$; $\Delta(c) = 0.031$; $i = 0,149$.

Model III-3 (Figure 9c)

$$q^{(1)}_{+1,0} = 1.39619 + 0.03175\ q^{(1)}_{-1,0} - 0.00247\ q^{(1)}_{-2,0} + 0.03381\ q^{(1)}_{-3,0}$$

$$+ 0.46319\ q^{(2)}_{0,0} + 0.38442\ q^{(1)}_{0,-1} - 0.00115\ q^{(1)}_{0,+1} - 0.06167\ \lambda_{-3}$$

$$- 0.03674\ \lambda^2_0 - 0.0016\ q^{(1)}_{0,0}q^{(2)}_{0,0} - 0.04848\ q^{(1)}_{0,0}q^{(2)}_{-1,0}$$

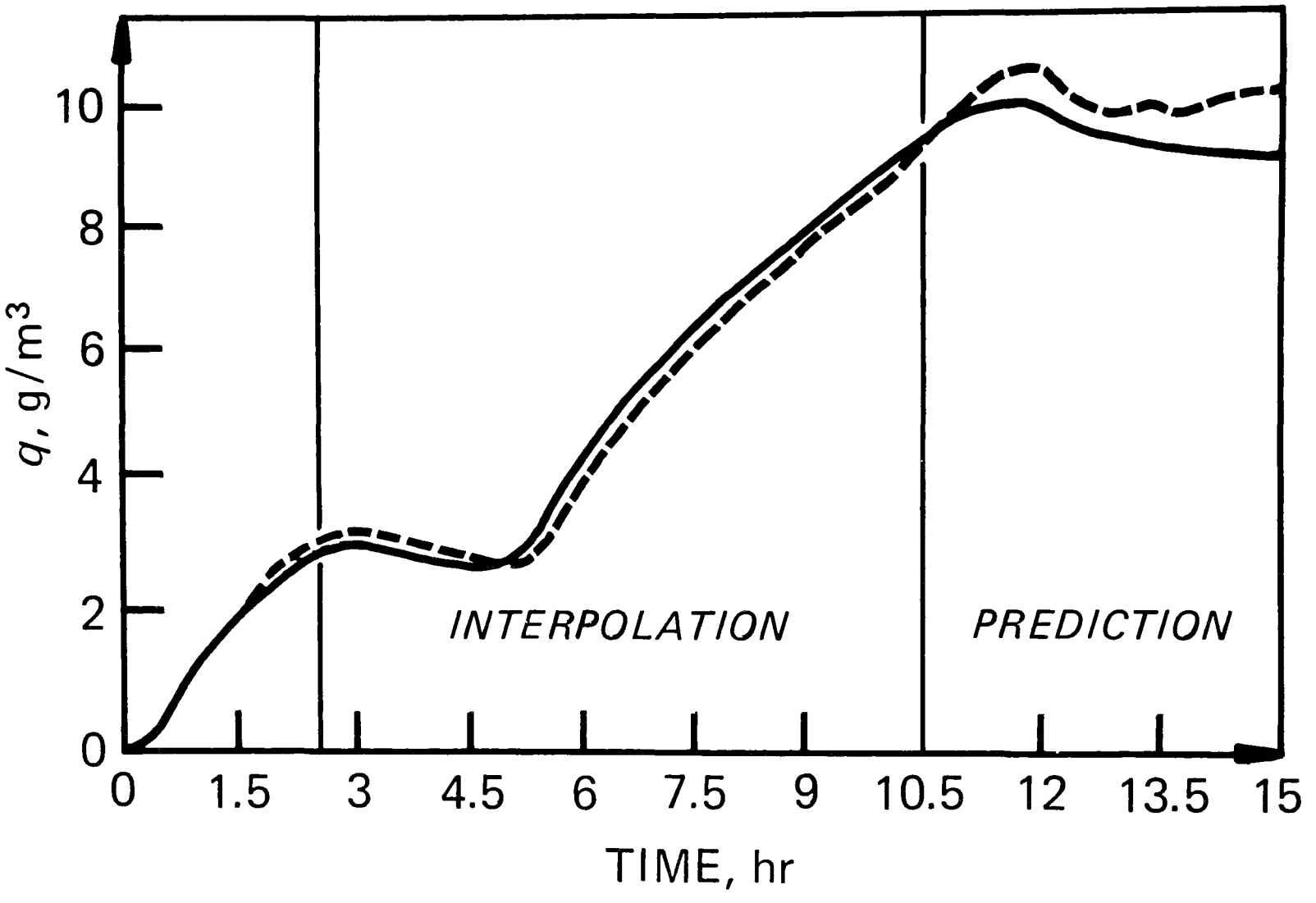

Figure 9b. Model III-2.

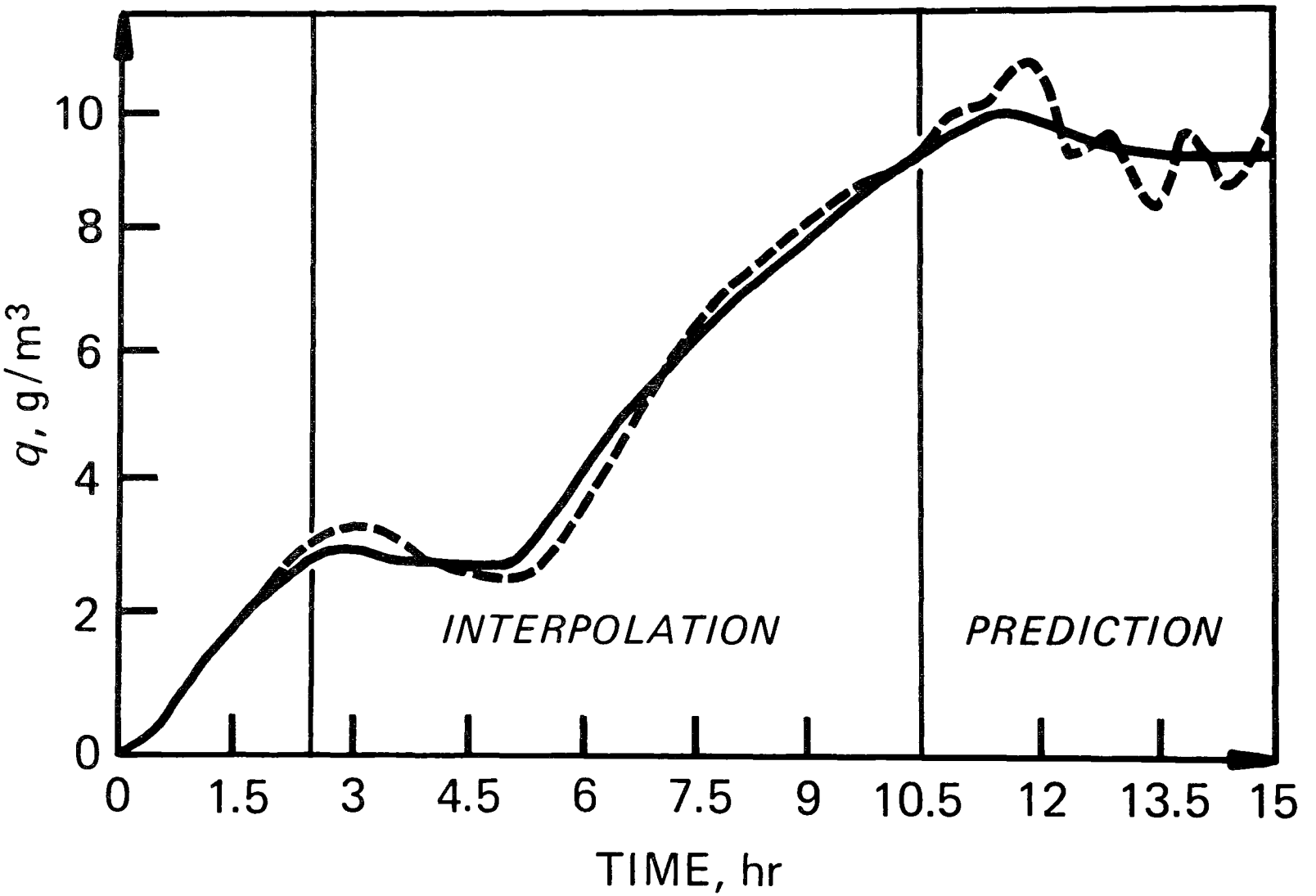

Figure 9c. Model III-3.

$$- 0.14929\ q^{(2)}_{0,0} q^{(1)}_{0,+1} + 0.08369\ q^{(2)}_{-1,0} q^{(1)}_{0,-1} + 0.22246\ q^{(3)2}_{-2,0};$$

$$K = 0.115;\ n_{cm} = 0.05;\ \Delta(c) = 0.04;\ i = 0.426.$$

The solution of the first and third problems allows construction of a picture of the field, prediction of its development with time and extrapolation of it along the spatial coordinates.

The solution of the second problem yields the value of the parameters of the pollutants at the points where the measurement stations are located. Using the data obtained, predictions can be constructed and then, by means of interpolation, the field in an area located within a polygon may be found, the points of which are the points of the measurement stations, i.e., in the interpolation area (Figure 1).

Another version of the algorithm is also possible: It is possible to first interpolate the data of the stations, and then later construct the prediction for the points in the area of interpolation of interest. Predictions can also be produced only for the area of interpolation by means of step-by-step integration of the equations along the time axis. The solution to the second problem is not suitable for extrapolation of the field into neighboring areas.

CONCLUSIONS - COMPARISON OF MODELS

The model using the principle of near action, I-1, produces less accurate predictions than improved models based on the principle of "distant" action, II-3, and the combined model, III-2, if the rate of emission of the sources of pollution change with time. The model of "distant" action, II-3, which considers both measured data at the measurement stations and information on changes in the rate of pollutant discharge, is the best of all the models.

In the future, the authors intend to use the criterion of balance of variables (Tamura and Kando 1977), which should be no worse than direct measurement of emission, for organization of models.

REFERENCES

Dyachenko, V.F. 1977. Basic concepts in computational mathematics, Mir Press, Moscow.

Ivakhnenko, A.G. and G.I. Krotov. 1977. Modeling of pollution of the environment when there is no information available on the emissions of sources of pollution. Avtomatika, No. 5, Kiev, Naukova dumka Press, pp. 14-30.

Ivakhnenko, A.G. 1978. Inductive methods of self-organization of computerized complex system models. Avtomatika, No.4, Kiev, Naukova dumka Press, pp. 11-26.

Ivakhnenko, A.G., V.N. Vysotskiy and N.A. Ivakhnenko. 1978. Basic varieties of the criterion of the minimum of displacement of a model and investigation of their interference stability. Avtomatika, No. 1, Kiev, Naukova dumka Press, pp. 32-53.

Tamura H., and T. Kando. 1977. Large-spatial pattern identification of air pollution by combined model of source-receptor matrix and revised paper presented at IFAC Symposium of Environment System, Kyoto.

Yurachkovskiy, Yu.P. 1977. Improvement of the MGUA modeling algorithm for prediction of processes (a review). Avtomatika, No. 5, Kiev, Naukova dumka Press, pp. 76-86.

SECTION 17

A SPATIALLY-SEGMENTED MULTI-CLASS PHYTOPLANKTON MODEL FOR SAGINAW BAY, LAKE HURON

Victor J. Bierman, Jr. and David M. Dolan[1]

INTRODUCTION

Saginaw Bay is a broad, shallow extension of the western shore of Lake Huron (Figure 1). The bay is oriented in a southwestward direction and is 82 km long and 42 km wide. For convenience, the bay has been divided into five spatial segments on the basis of differences in observed water quality. The average depth of the inner portion of the bay, represented by spatial segments one, two, and three, is approximately 6 m. The average depth of the outer portion of the bay, represented by spatial segments four and five, is approximately 15 m. Seventy percent of the total water volume is contained in the outer portion of the bay and the remaining 30 percent is contained in the inner portion.

The total area of the Saginaw Bay watershed is approximately 21,000 km^2. The Saginaw River is the major tributary and it accounts for over 90 percent of the total tributary inflow to the bay. The principal land use categories in the watershed are agriculture and forest. The total population of the watershed is slightly over 1.2 million. Most of the population is concentrated into four major urban-industrial centers: Bay City, Midland, Saginaw, and Flint. These centers are all situated along the Saginaw River or its major tributaries.

The principal water uses in Saginaw Bay include municipal and industrial water supply, waterborne transportation, recreation, commercial fishing, and waste assimilation. These uses are severely impacted by the considerable quantities of waste discharges and runoff to the bay as a result of human activities in the watershed. In particular, the inner portion of the bay suffers from highly degraded water quality.

The principal issue addressed in the developement of the present model was cultural eutrophication, defined as overproduction of phytoplankton biomass due to increased nutrient loadings. The purpose of the modeling effort

[1]U.S. Environmental Protection Agency, Large Lakes Research Station, Grosse Ile, Michigan 48138.

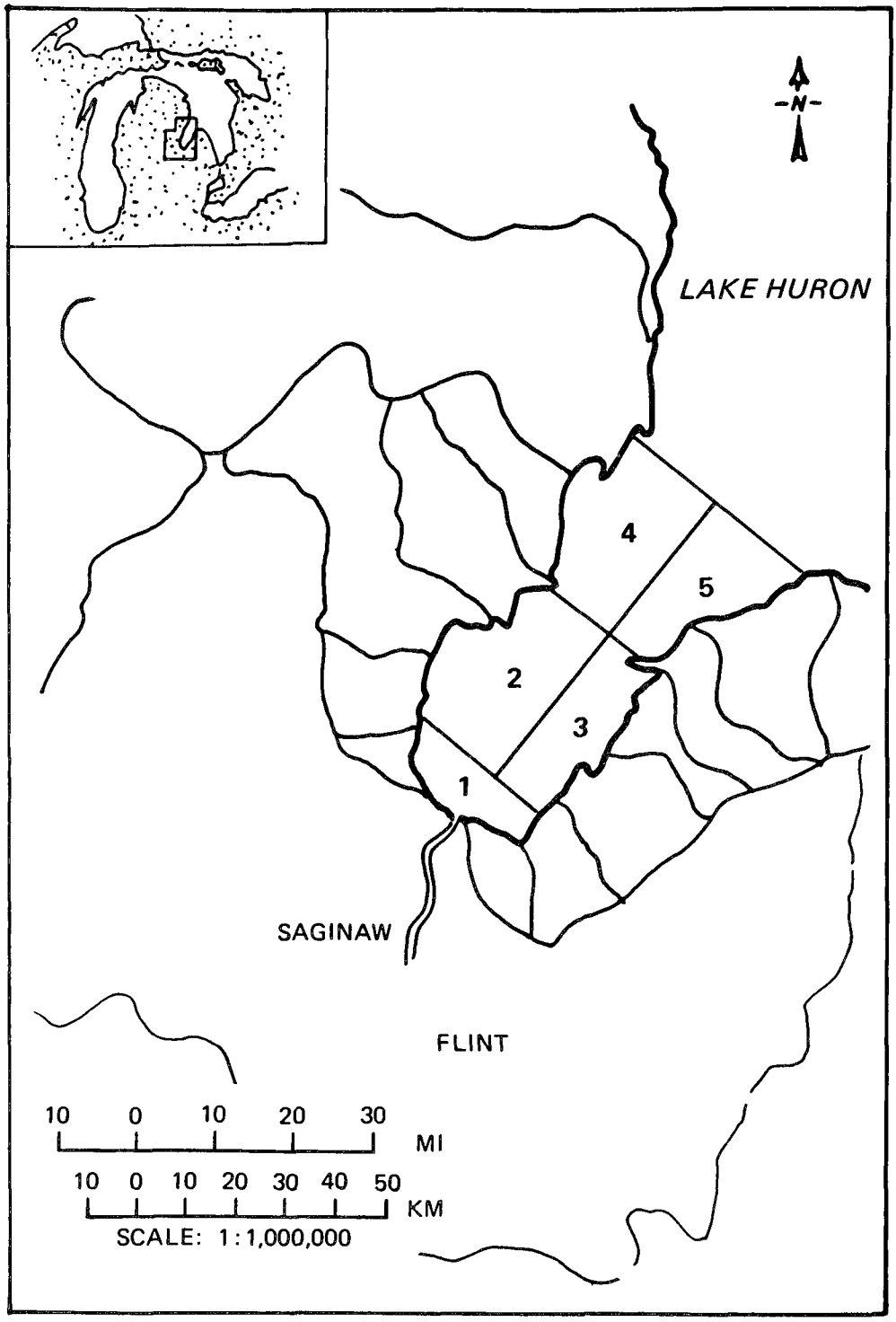

Figure 1. Saginaw Bay and the spatial segmentation scheme used for the phytoplankton model.

was to develop a deterministic phytoplankton simulation model that could describe the cause-effect connection between external nutrient loading and phytoplankton growth in Saginaw Bay. The objectives were twofold: first, to gain insight into the relevant physical, chemical, and biological processes affecting phytoplankton growth; and second, to use the model as a tool for comparing the future effects of various wastewater management strategies.

The plan of work for the study will include a calibration and a subsequent verification of the model to two independent sets of field data acquired on Saginaw Bay during 1974 and 1975. The verified model will be used to generate a set of predictions corresponding to expected reductions in external nutrient loads, principally phosphorus. These predictions will be compared to the results of a follow-up field survey to be conducted in 1980 on the Lake Huron-Saginaw Bay system.

SCOPE

The purpose of this paper is to present results of the preliminary calibration phase of the phytoplankton modeling effort. Calibration results will be presented graphically, as well as in terms of statistical tests for goodness of fit between model output and field data.

In addition to model calibration results, field data will be presented which illustrate the large gradients in water quality that exist among the five spatial segments in Saginaw Bay. These gradients have a strong impact on the model development effort because it is difficult to obtain a unified set of kinetics which can describe phytoplankton dynamics simultaneously in all five segments.

FIELD DATA

As part of the Upper Lakes Reference Study sponsored by the International Joint Commission, intensive field surveys were conducted on Saginaw Bay during 1974 and 1975 (Bratzel et al. 1977). These surveys involved several different institutions, coordinated by the Large Lakes Research Station of the U.S. Environmental Protection Agency. In each of the two years, 13 sampling cruises were conducted. In 1974, samples were taken on a 59-station grid at multiple depths (Figure 2). In 1975, samples were taken on a 37-station subset of this grid. This paper is restricted primarily to the results from 1974.

Analyses were conducted for 22 different physical-chemical variables, including phosphorus, nitrogen, silicon, chlorophyll, chloride, temperature, and Secchi depth. Biological measurements included species identification and number concentrations for both phytoplankton and zooplankton. In addition, measurements were conducted for phytoplankton cell volumes and zooplankton dry weights.

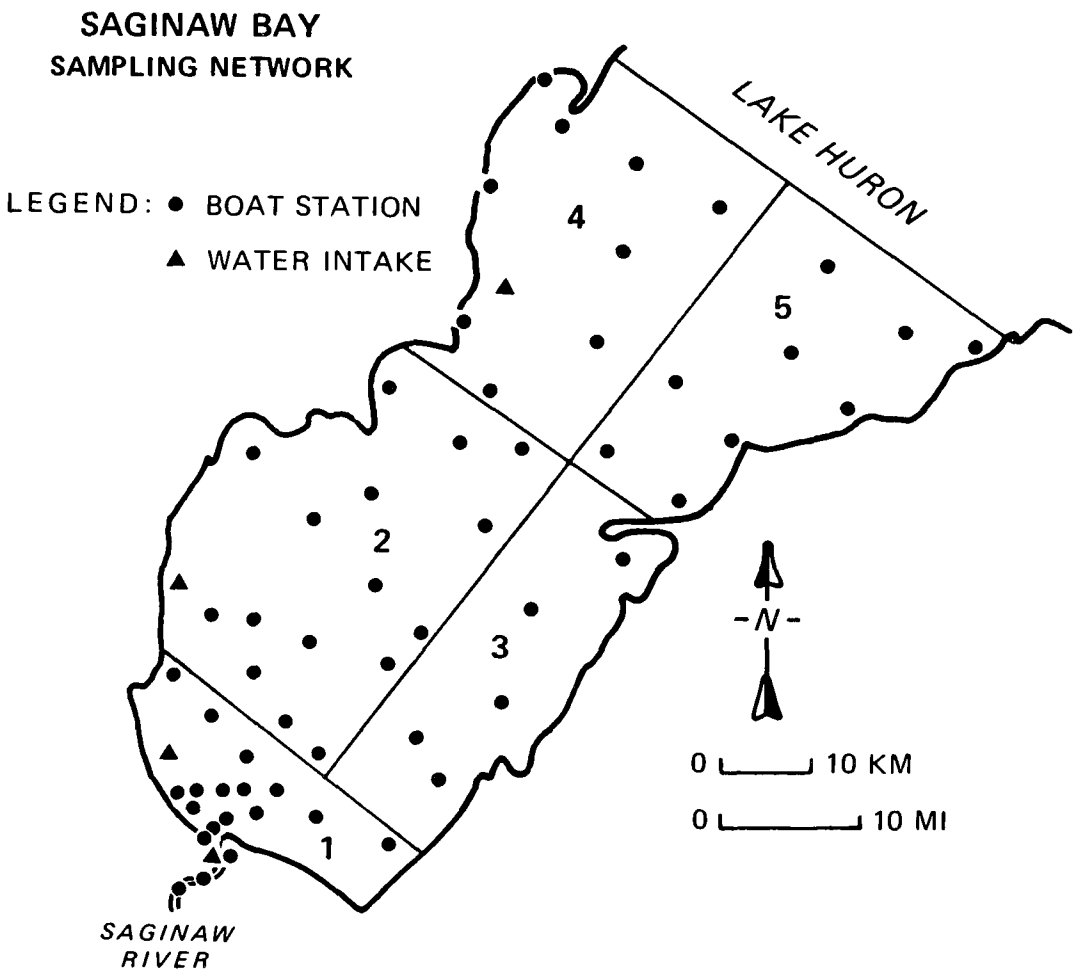

Figure 2. Sampling station network in Saginaw Bay.

Horizontal spatial gradients for several principal water quality variables are shown in Figures 3-5. All data are presented as the mean plus or minus one standard error. In general, the five spatial segments are ordered in the following manner with respect to increasing water quality: one, three, two, five, and four. The observed gradients range over a factor of five for chloride, a factor of six for total phosphorus, and a factor of ten for summer chlorophyll a.

Large spatial gradients in water quality occur in Saginaw Bay primarily because most of the external nutrient loading is from a single tributary, the Saginaw River, and because of the predominant water circulation pattern in the bay. Water circulation tends to be counterclockwise with relatively clean Lake Huron water flowing into segment four, and relatively dirty Saginaw River water flowing out through segments one, three, and five (Figure 2). Segment two is relatively dirty because of dispersion from segments one and three. Although segments one and three possess the poorest water quality of the five spatial segments, these segments together constitute less than 10 percent of the total volume of water in Saginaw Bay. The remaining three segments contain approximately equal volumes of water.

MODEL DESCRIPTION

A schematic diagram of the phytoplankton model is shown in Figure 6. The compartments represent the principal variables in the model, and the arrows represent pathways for material transport among the compartments. The reader is referred to Bierman (1976) and Bierman et al. (1979) for a detailed description of model concepts and model equations.

The model includes phytoplankton biomass in terms of five functional groups: diatoms, greens, non-N_2-fixing blue-greens, N_2-fixing blue-greens, and "others". The latter category includes primarily dinoflagellates and cryptomonads. Non-N_2-fixing blue-greens consist of those species which have an absolute requirement for dissolved combined nitrogen. N_2-fixing blue-greens consist of those species which have the capability for fixing atmospheric nitrogen, as well as for using dissolved combined nitrogen. The nutrients included in the model are phosphorus, nitrogen, and silicon.

The principal reason for this multi-class approach is that there are important physiological differences among the five groups. Diatoms are the only group with a major absolute requirement for silicon. The N_2-fixing blue-greens are the only group which can grow independently of the supply of dissolved available nitrogen. The relative maximum growth rates and temperature optima among the groups are such that a typical successional pattern during the growing season begins in the Spring with diatoms, progresses to greens and "others", and finally leads to the development of blue-greens in late Summer and Fall. An important characteristic shared by all of the groups is an absolute requirement for phosphorus.

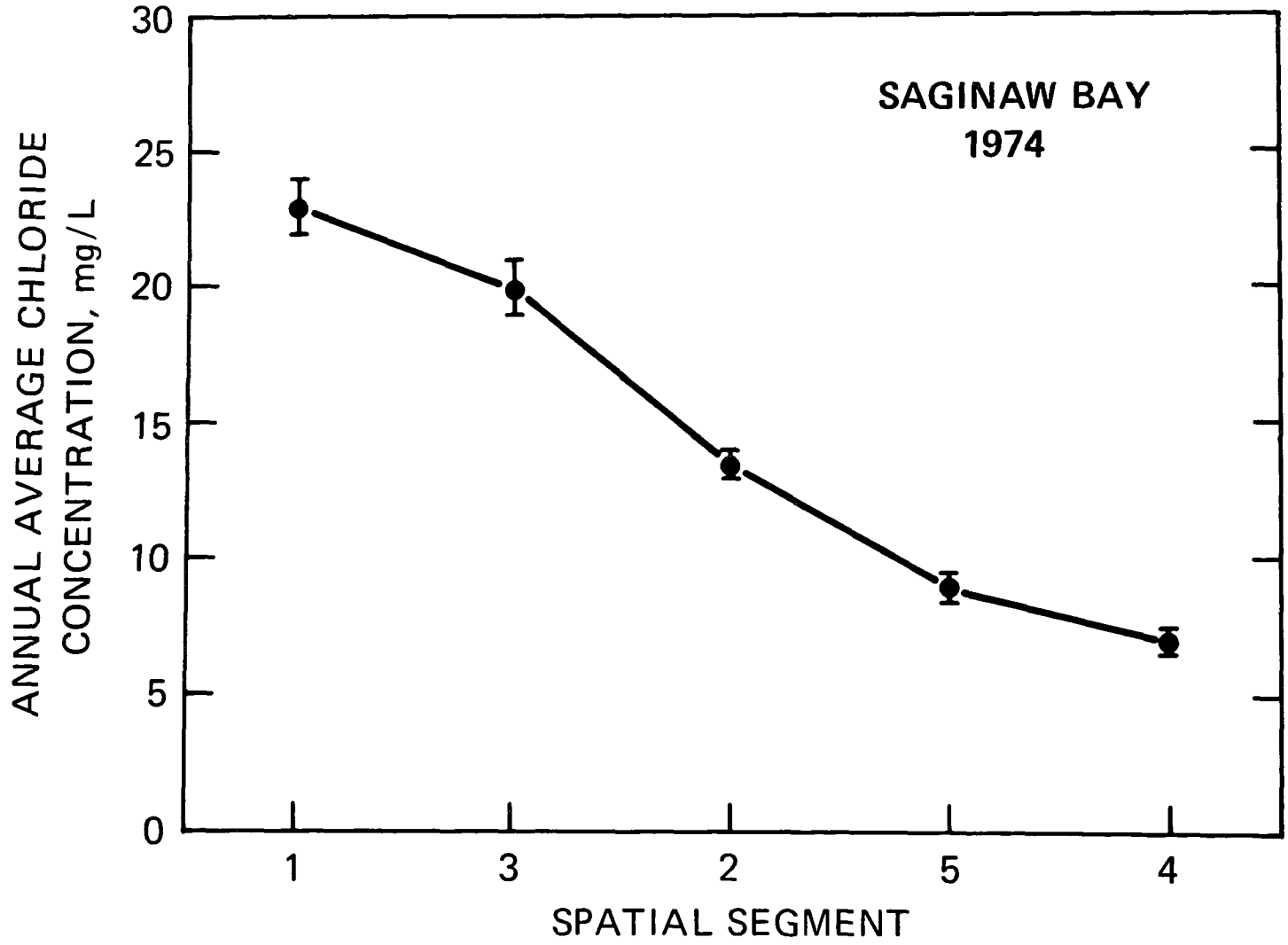

Figure 3. Gradient among spatial segments in annual average chloride concentration.

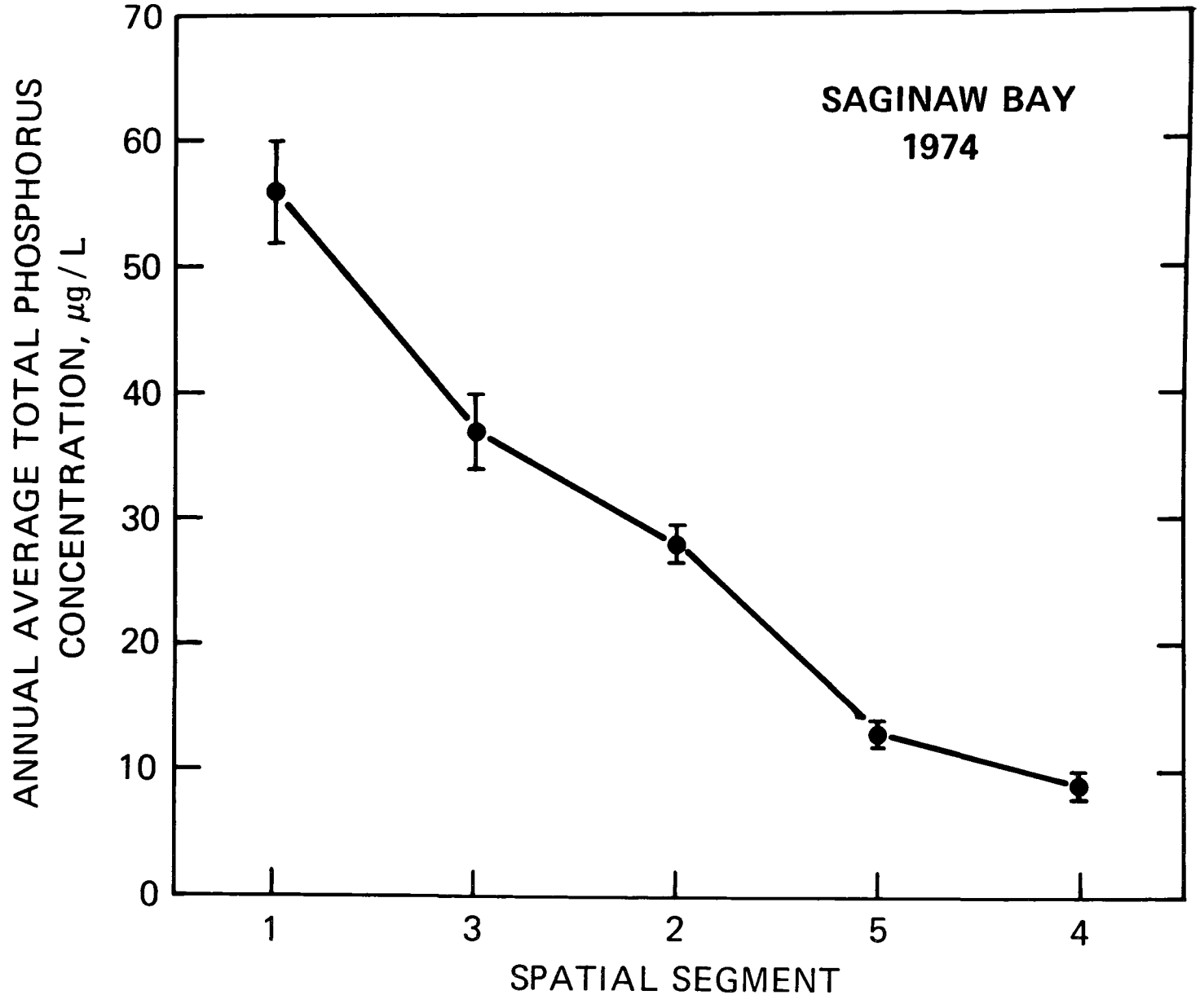

Figure 4. Gradient among spatial segments in annual average total phosphorus concentration.

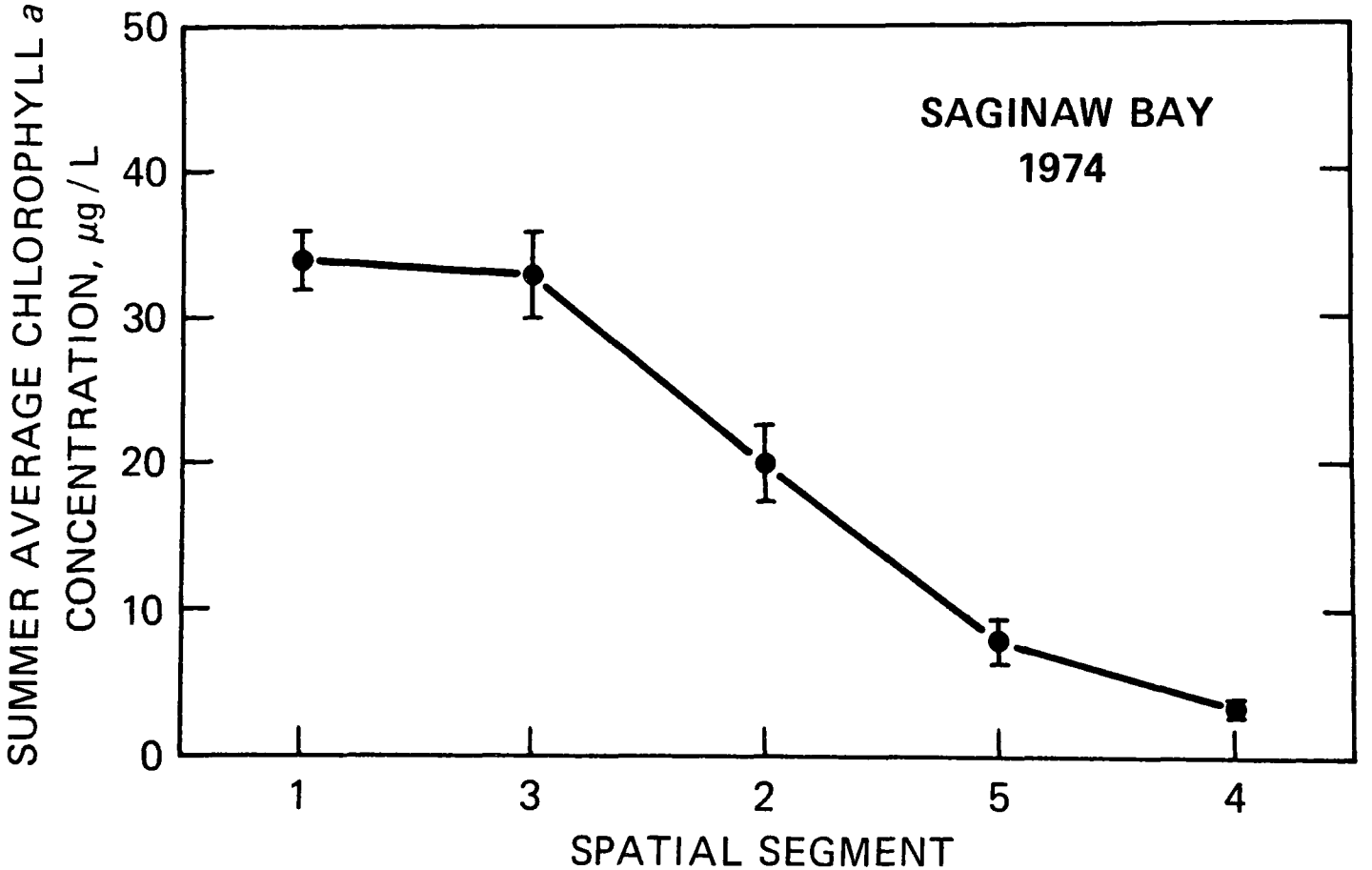

Figure 5. Gradient among spatial segments in summer average chlorophyll a concentration.

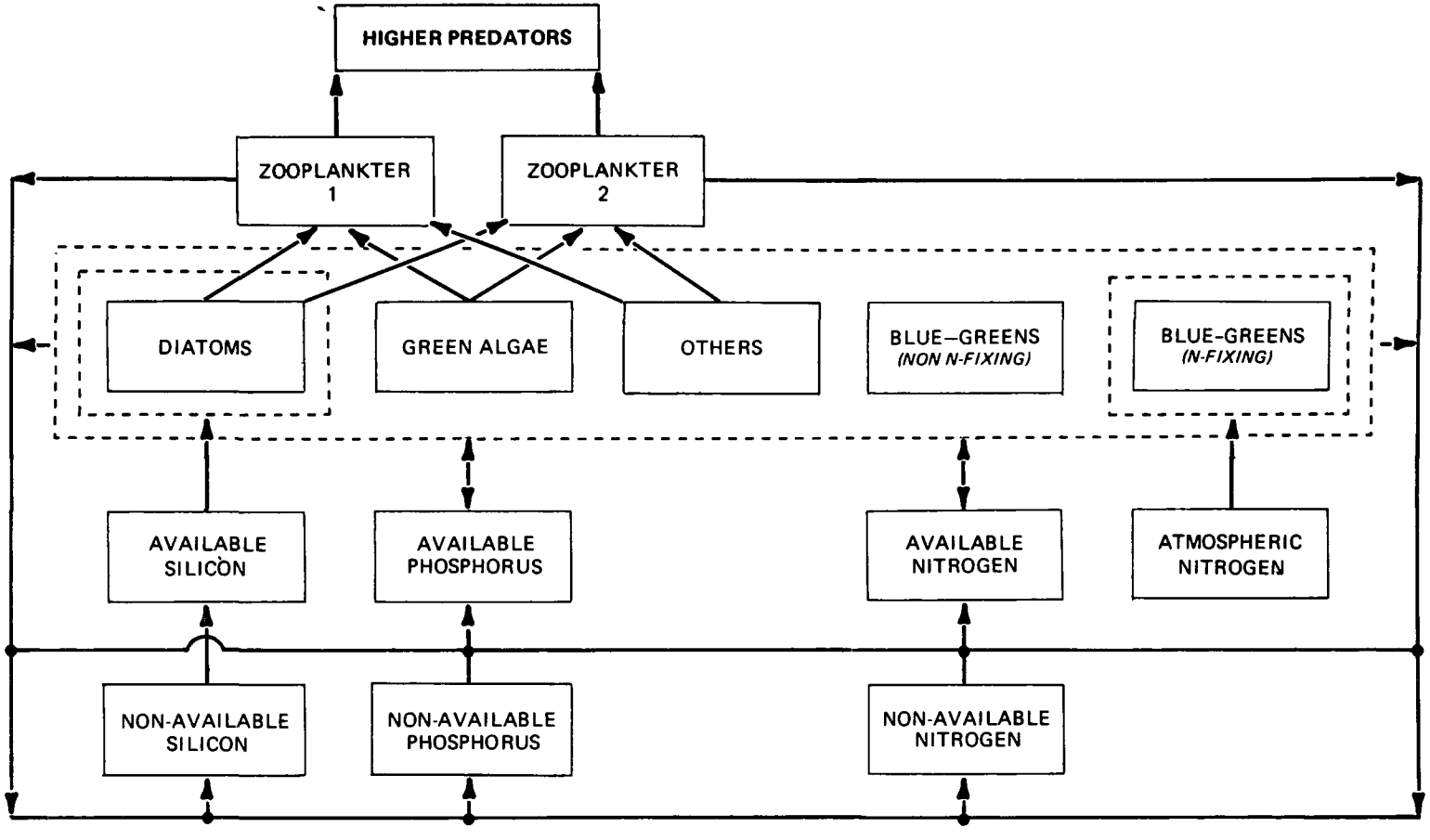

Figure 6. Schematic diagram of principal model compartments and interaction pathways.

MODEL CALIBRATION

The calibration process consists of adjusting model coefficients within their reported ranges in the literature to obtain the best possible correspondence between model output and field data. With a simple model, human intuition is usually adequate to determine the goodness of fit. With sophisticated models, it is usually necessary to resort to more systematic methods.

For the present model, there were 12 independent variables in each of five spatial segments for which field data were available. Consequently, there were 60 segment-variable combinations for each of 13 sampling cruises. It was impossible to rely completely on human intuition for model calibration.

Calibration of the model was facilitated by use of the Model Verification Program (MVP) developed by Manhattan College (Thomann and Winfield 1976; Thomann et al. 1979). The MVP is a system of statistical programs which can analyze the goodness of fit between model output and field data for each model run. Analyses can include the Student's T-test, regression tests, and tests for relative error. Only the Student's T-test has been used to date for the Saginaw Bay phytoplankton model.

MODEL RESULTS

Model results for all 12 variables and all five segments have been reported in terms of the MVP. Selected model results have been reported graphically for segments two and four. Segment four represents the volume of water in Saginaw Bay with the highest water quality, and segment two best represents the lower water quality in the inner portion of the bay because it contains the largest volume of the three inner bay segments.

Table I contains results of the MVP Student's T-test for the best calibration run to date. The T-test has been applied on a cruise-by-cruise, segment-by-segment basis for each of the 12 independent variables. Results have been reported as percent of sampling cruises for which there is no significant difference between model output and field data at the 95 percent confidence level. The overall average for the five model segments was 83 percent. In a purely statistical context, this implies that the model output for the indicated 12 variables describes the Saginaw Bay system approximately 83 percent as well as the data for these 12 variables describes the Saginaw Bay system. It should be noted that variability in the field data, as well as accuracy in the model output, will lead to favorable MVP results.

Graphical results for phytoplankton concentrations in segments two and four are shown in Figures 7-14. All field data have been presented as the mean plus or minus one standard error. A logarithmic scale has been used because it was found that the phytoplankton data followed a log-normal distribution. Such a scale causes difficulty in determining goodness of

TABLE 1. STATISTICAL COMPARISON BETWEEN MODEL OUTPUT AND FIELD DATA

Model variable	*Percent of sampling cruises not significantly different*				
	Segment number				
	1	*2*	*3*	*4*	*5*
Chloride	92	100	85	92	100
Diatoms	92	100	92	92	73
Greens	100	92	75	100	100
Others	92	92	58	92	91
Non-N_2 blue greens	69	92	92	100	100
N_2 blue greens	59	89	67	78	100
Total zooplankton	70	90	60	100	100
Total phosphorus	100	100	82	91	100
Total nitrogen	75	73	64	83	91
Dissolved phosphorus	100	77	33	42	33
Dissolved nitrogen	71	92	42	92	75
Dissolved silicon	57	92	54	77	77
Average	81	91	67	87	87

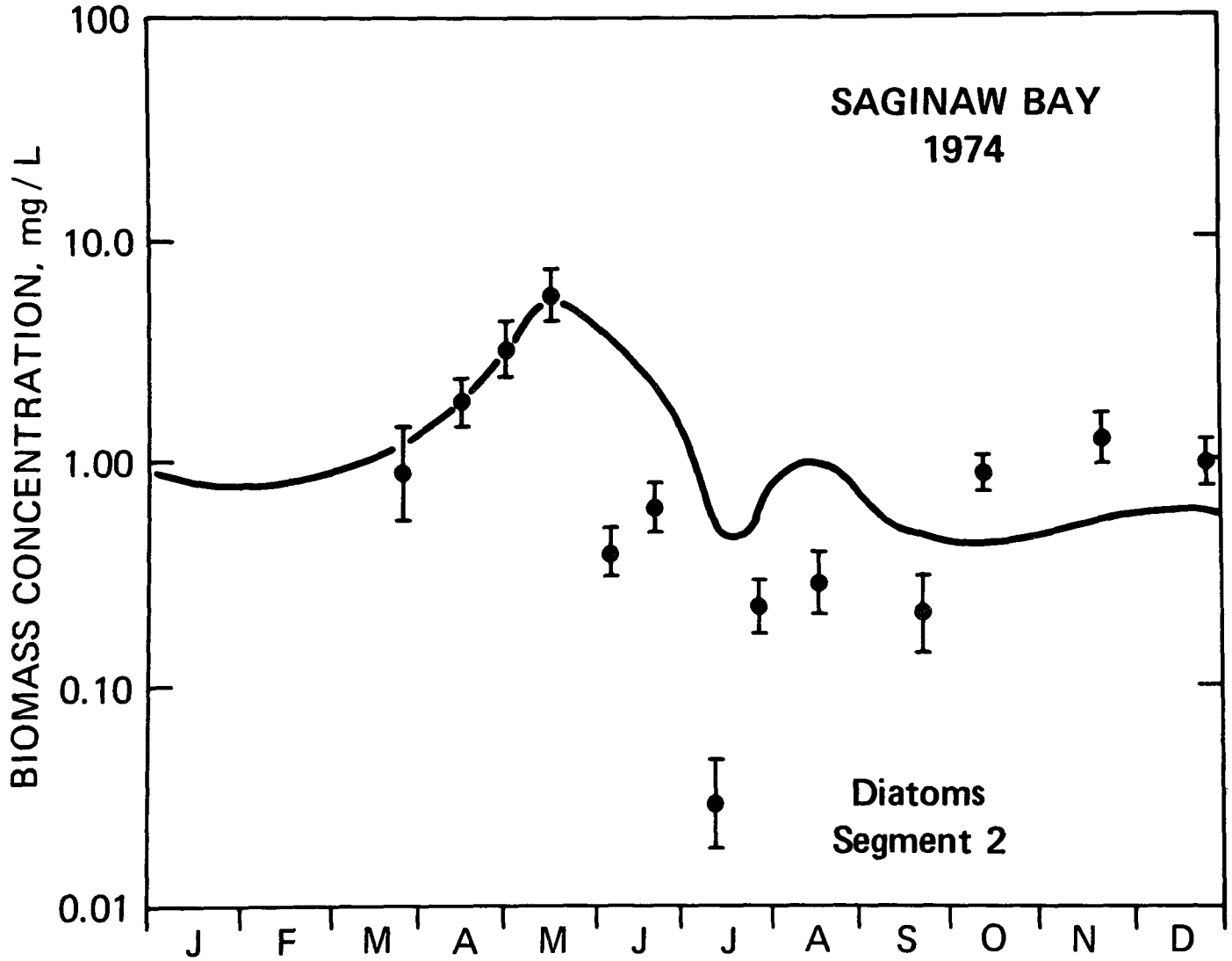

Figure 7. Comparison between model output and field data for diatom biomass in segment two.

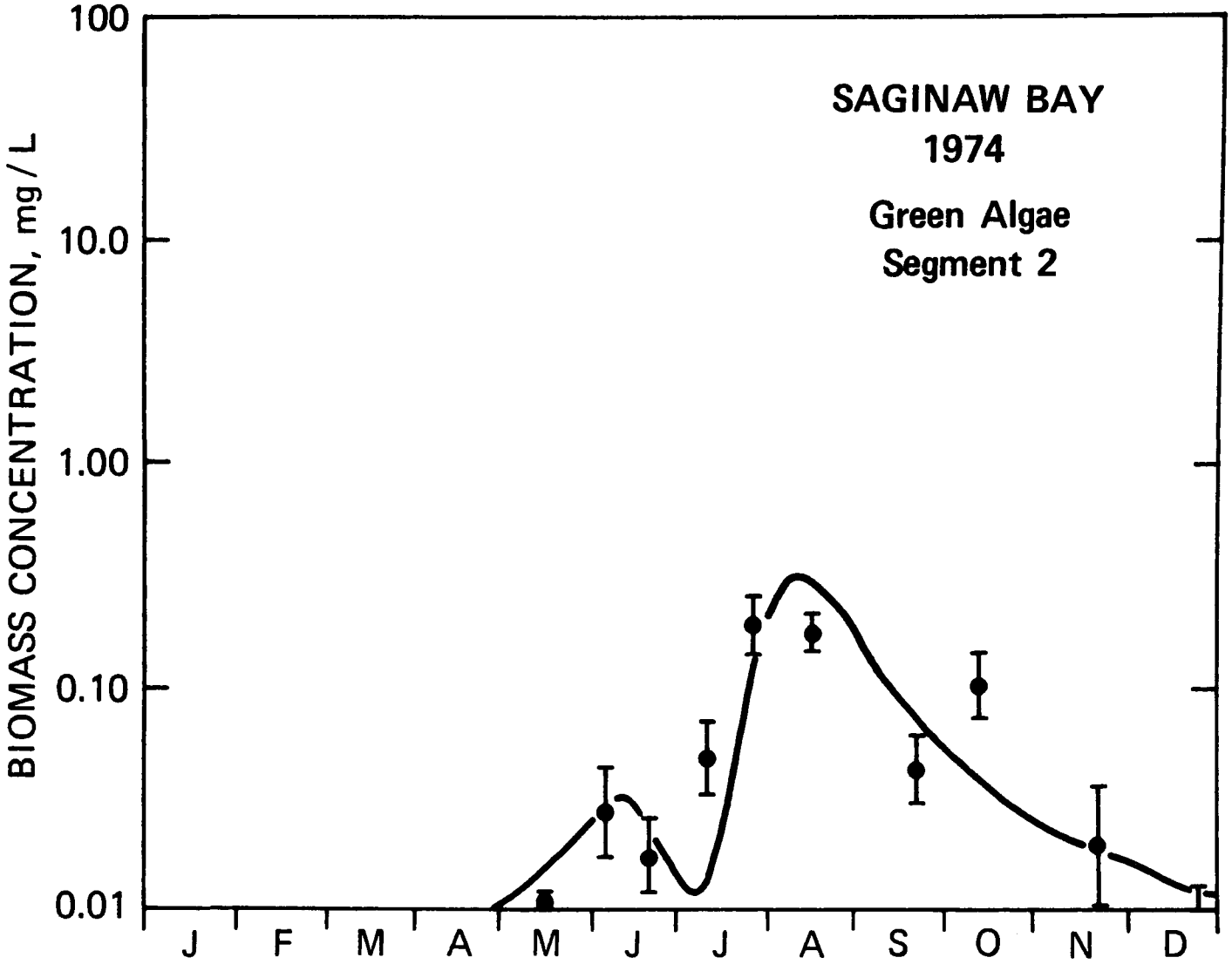

Figure 8. Comparison between model output and field data for biomass of green algae in segment two.

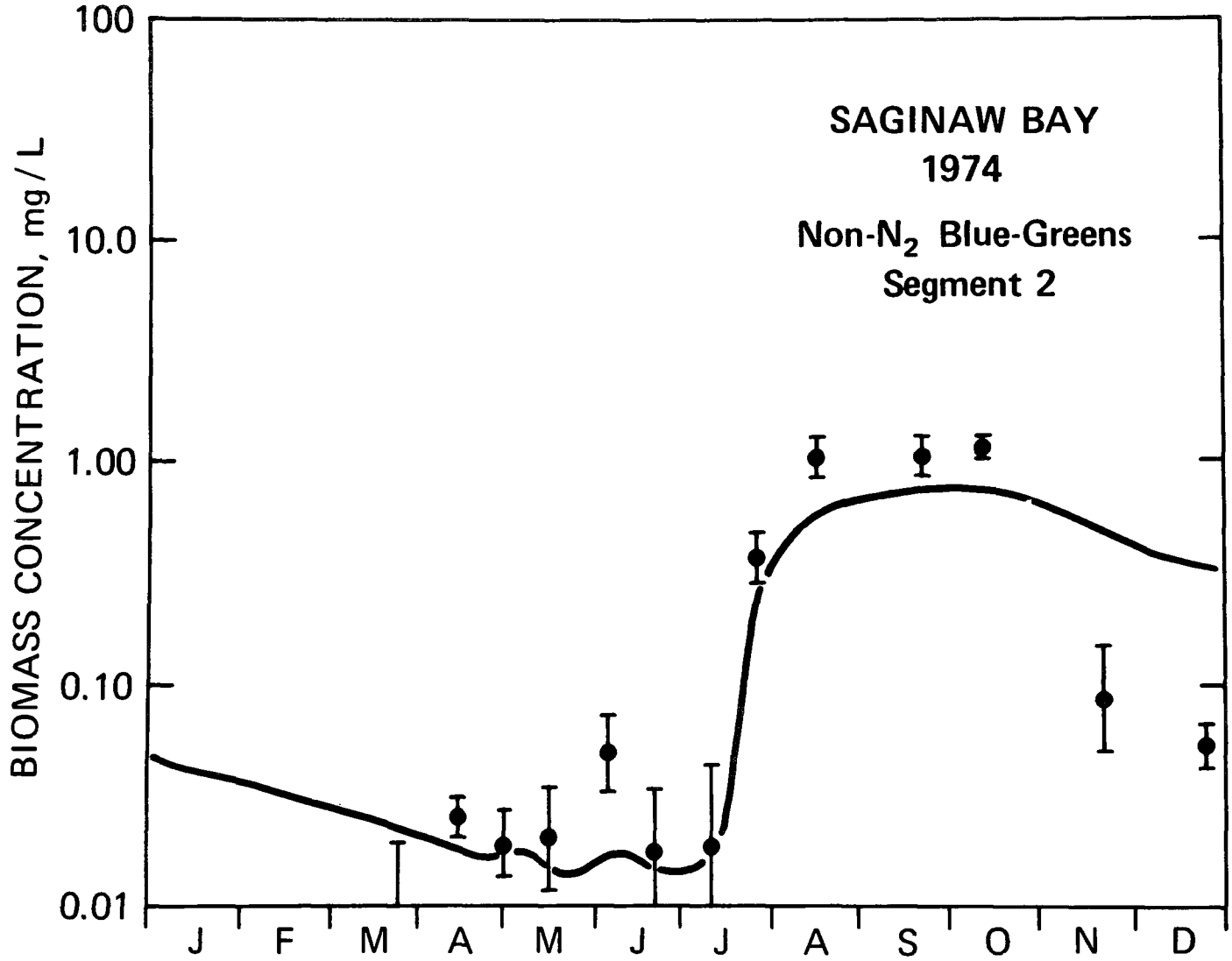

Figure 9. Comparison between model output and field data for biomass of non-N_2-fixing blue-greens in segment two.

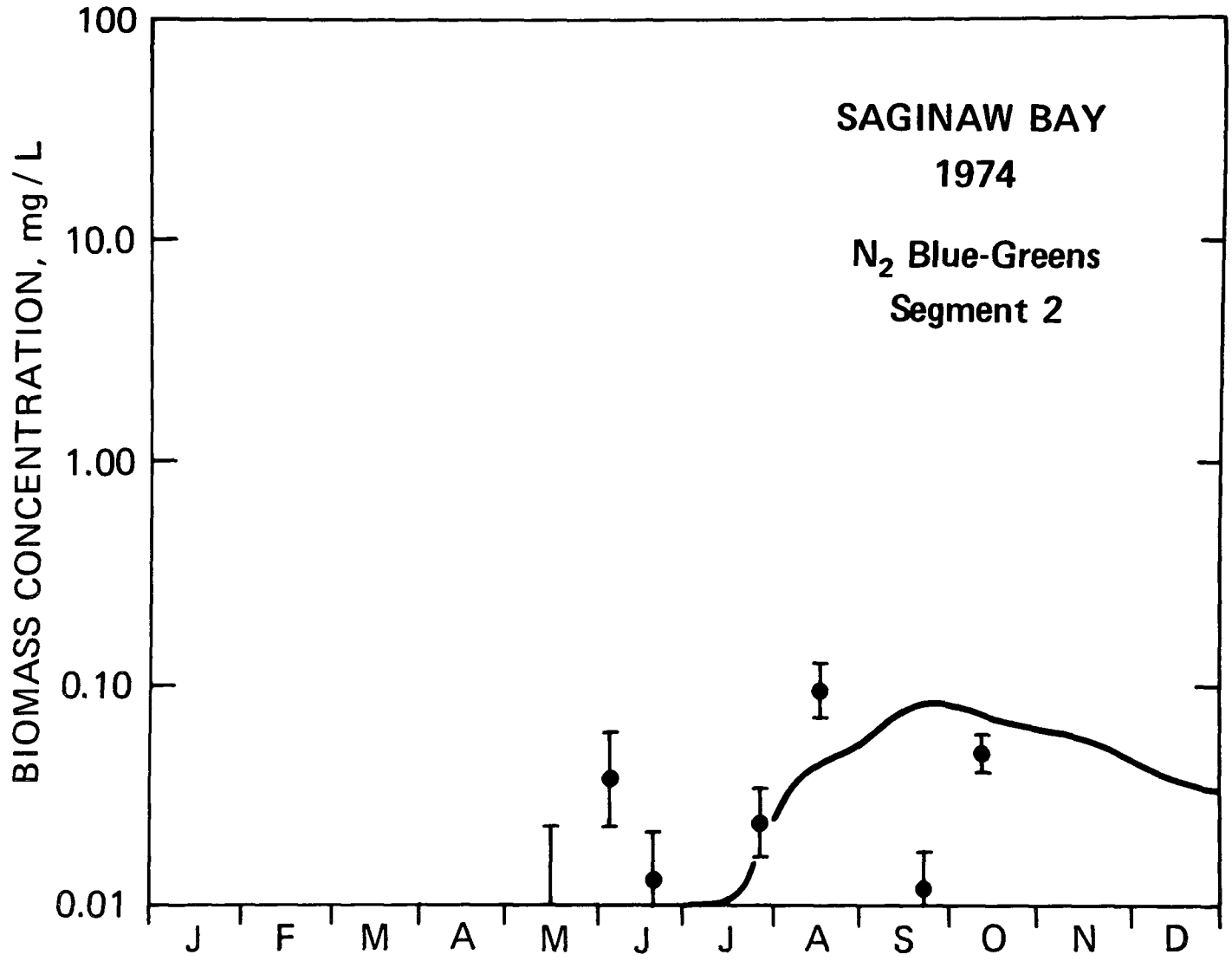

Figure 10. Comparison between model output and field data for biomass of N_2-fixing blue-greens in segment two.

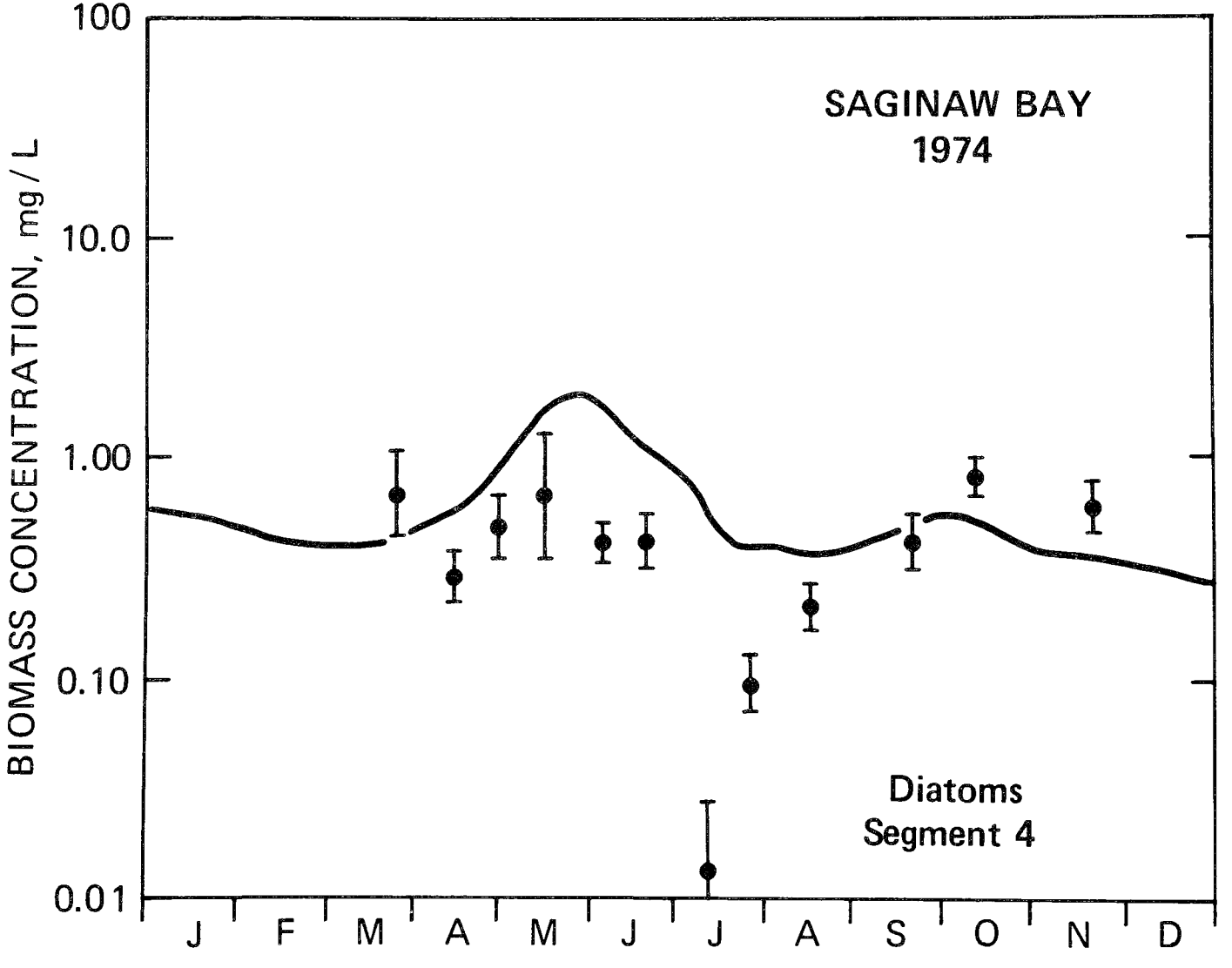

Figure 11. Comparison between model output and field data for diatom biomass in segment four.

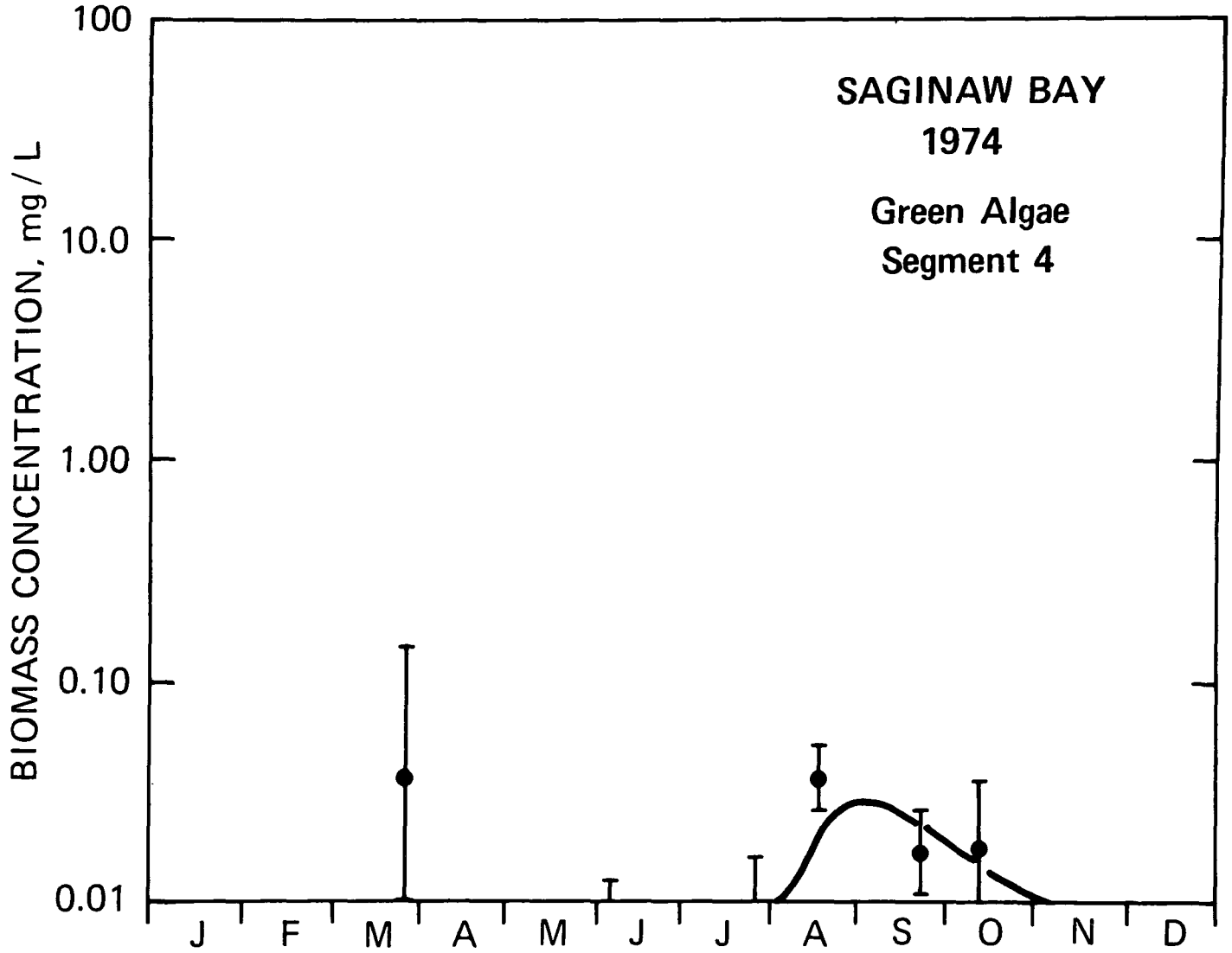

Figure 12. Comparison between model output and biomass of green algae in segment four.

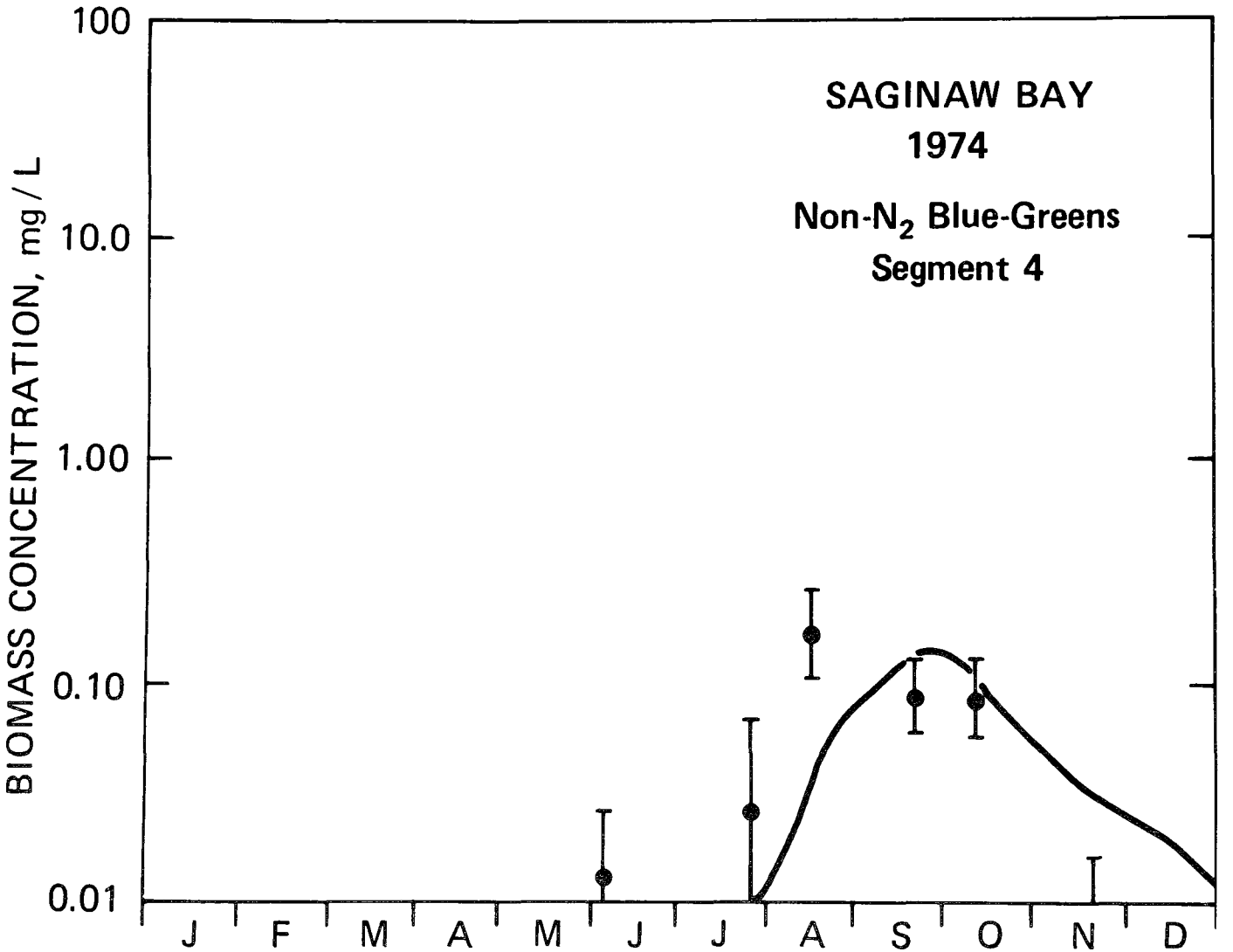

Figure 13. Comparison between model output and field data for biomass of non-N_2-fixing blue-greens in segment four.

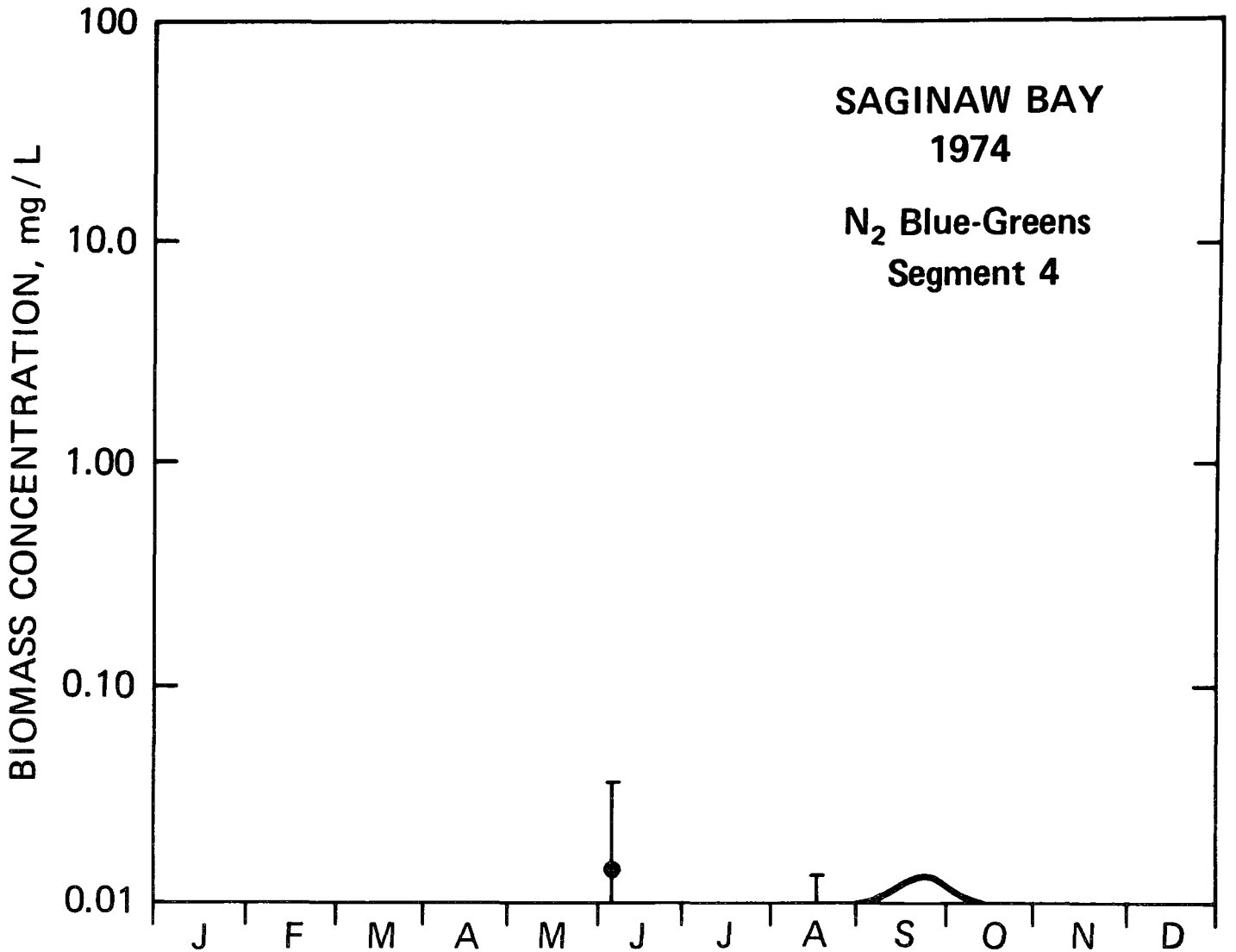

Figure 14. Comparison between model output and field data for biomass of N_2-fixing blue-greens in segment four.

fit by strictly graphical means because of its non-linearity. This was an additional reason for using the MVP.

In general, the concentrations for each phytoplankton group were approximately an order of magnitude higher in segment two than in segment four. This trend was a reflection of higher nutrient concentrations and the resulting lower water quality in the inner portion of the bay.

Model output generally followed the trends in the data for the various phytoplankton groups. Difficulties were experienced in both segments two and four with model output for diatoms during the third quarter of the year. In addition, the trend of the diatom output was somewhat high during Spring in segment four.

Results for dissolved ortho-phosphorus concentrations in segments two and four are shown in Figures 15 and 16. Phosphorus is generally considered to be the most important nutrient limiting the growth of phytoplankton in freshwater systems. The trend of the model output was low, compared to the field data, in both of the segments. The relatively poor fit for dissolved ortho-phosphorus was consistent with below-average MVP results, especially in segment four (Table I).

Initially, the poor fit for dissolved ortho-phosphorus was a matter of serious concern because it was not possible to improve the fit by adjusting any of the model coefficients. Model output for dissolved ortho-phosphorus depended heavily on the external phosphorus loading and the water circulation rates among the various segments in the bay. Both of these factors had been determined independently and then used as input to the phytoplankton model.

Subsequently, it was realized that the dissolved ortho-phosphorus data for 1974 were probably biased higher than the true concentrations. In 1975, the external phosphorus loading and the water circulation rates were essentially the same as in 1974; however, the 1975 data for dissolved ortho-phosphorus were substantially lower than the corresponding data for 1974. In fact, the trend of the model output for dissolved ortho-phosphorus in 1974 agreed closely with the trend of the dissolved ortho-phosphorus data for 1975.

The problem with the dissolved ortho-phosphorus data for 1974, especially at lower concentrations, was caused primarily by logistical difficulties. In 1974, samples were filtered immediately on shipboard, but were not analyzed until one to three days later. In addition, the analytical method used had not yet been refined to achieve maximum sensitivity. These problems were corrected in 1975 and the analyses for dissolved ortho-phosphorus were conducted on shipboard using a more refined technique. The consequences of the different approaches used for 1974 and 1975 were not readily apparent until after data had been acquired for the two years.

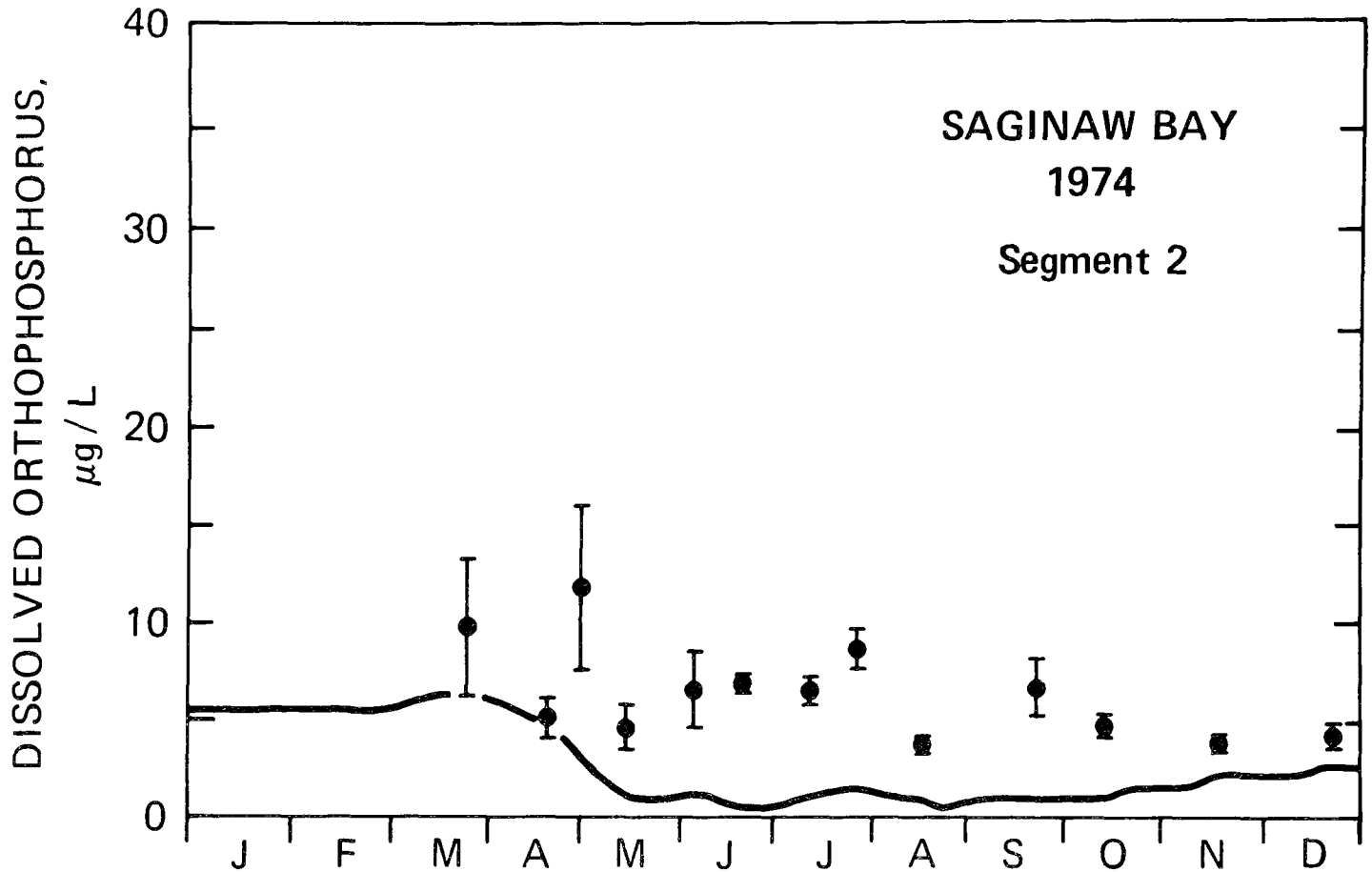

Figure 15. Comparison between model output and field data for dissolved ortho-phosphorus in segment two.

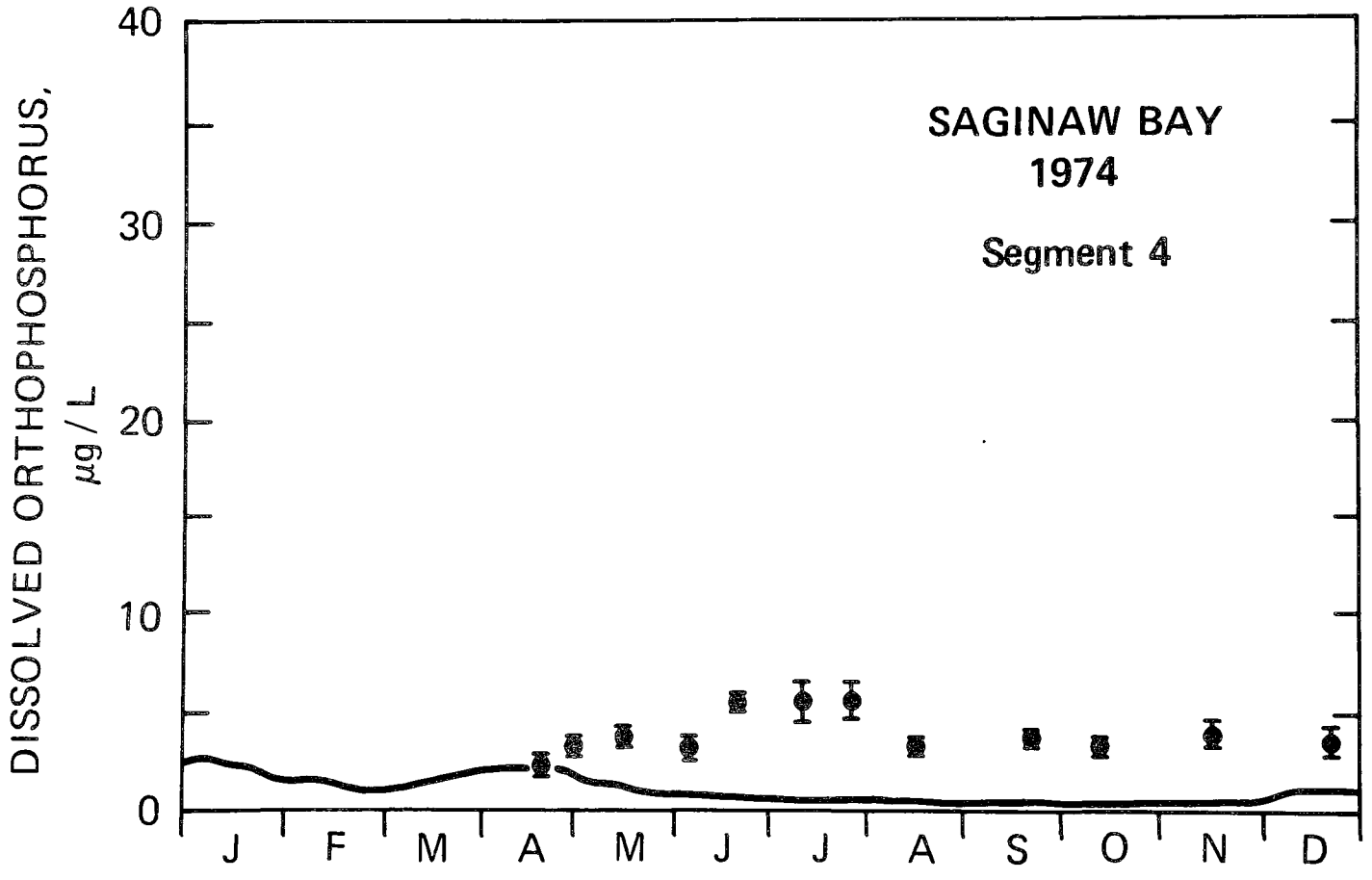

Figure 16. Comparison between model output and field data for dissolved ortho-phosphorus in segment four.

DISCUSSION

The importance of systematic quantitative methods for analyzing the correspondence between model output and field data has been emphasized. It should be pointed out, however, that such methods are not substitutes for human intuition and common sense. For example, the discrepancies in the case of dissolved ortho-phosphorus could not have been resolved strictly through the use of statistical techniques.

It has also been emphasized that phytoplankton models are not simply arbitrary systems of equations which can be curve-fitted to any set of field data. If a model is conceptually sound and internally consistent, discrepancies should be expected to arise between model output and field data in cases where anamolies exist in a given set of field data.

REFERENCES

Bierman, V.J., Jr. 1976. Mathematical model of the selective enhancement of blue-green algae by nutrient enrichment. In: Modeling Biochemical Processes in Aquatic Ecosystems ed. R.P. Canale, pp. 1-31. Ann Arbor, Michigan: Ann Arbor Science Publishers.

Bierman, V.J., Jr., D.M. Dolan, E.F. Stoermer, J.F. Gannon and V.E. Smith. The Development and Calibration of a Multi-Class Phytoplankton Model for Saginaw Bay, Lake Huron. In press in U.S. Environmental Protection Agency Ecological Research Series, 1979.

Bratzel, M.P., M.E. Thompson and R.J. Bowden (Eds.). 1977. The Waters of Lake Huron and Lake Superior. Vol. II (Part A). Lake Huron, Georgian Bay, and the North Channel. Report to the International Joint Commission by the Upper Lakes Reference Group. Windsor, Ontario. 292 p.

Thomann, R.V. and R.P. Winfield. On the Verification of a Three-Dimensional Phytoplankton Model of Lake Ontario. In: Proceedings of the Conference on Environmental Modeling and Simulation, U.S. Environmental Protection Agency, Cincinnati, Ohio, 1976. pp. 568-572.

Thomann, R.V., R.P. Winfield and J.J. Segna. Verification Analysis of Lake Ontario and Rochester Embayment Three Dimensional Eutrophication Models. In press in U.S. Environmental Protection Agency Ecological Research Series, 1979.

SECTION 18

A SEGMENTED MODEL OF THE DYNAMICS OF THE ECOSYSTEM OF LAKE BAIKAL CONSIDERING THREE-DIMENSIONAL CIRCULATION OF THE WATER

V.V. Menshutkin[1], O.M. Kozhova[2], L.Ya. Ashchepkova[2] and V.A. Krotova[2]

A model of the seasonal dynamics of the pelagic ecosystem of Lake Baikal is described, the main components of which are the phytoplankton, zooplankton, bacteria, nutrients and detritus. The surface of the lake is arbitrarily divided into 65 areas of equal size, and the volumes of water divided into two zones: the photosynthetic and destructive zones. The input functions of time include absorbed solar radiation, water temperature in both zones of the various regions of the lake, and the inputs of organic matter from the largest sources of the lake.

In calculating the status vector of an ecosystem, biologic and hydrologic processes are considered in each step. The redistribution of dissolved and suspended matter within the mass of water is performed in the model by means of horizontal advection and vertical turbulent mixing. The speed and direction of horizontal transfer in each region are constant throughout the year and correspond to the overall system of circulation of water in the lake. The turbulent flows are proportional to the vertical gradients of matter. On the whole, the dynamics of spatial distribution of plankton demonstrated by the model agrees well with the data of actual surveys made in Lake Baikal.

The ecosystem of the lake is a unique object for modeling. Some features are reminiscent of marine ecosystems in the temperate latitudes. The great length of the lake along its long axis, its extreme depths, the uniqueness of the structure and circulation of its water masses, and the influence of river runoff all create a broad range of conditions influencing the seasonal dynamics of the ecosystem.

Models of the ecosystem of Lake Baikal must consider the regionalization of the lake. In terms of horizontal distribution of plankton, a distinction

[1]Institute of Evolutionary Physiology and Biology, Academy of Sciences of the USSR, 44 Morisa Toryeza Prospect, 194223 Leningrad, USSR.

[2]Irkutsk State University, A/Y2H 24 Lenin Street, 664003 Irkutsk, USSR.

is made between shallow areas (littoral zones, shoals at the mouths of rivers, bays) and deep water regions (Kozhov 1962). In terms of the hydrometeorologic regime, there are three characteristic deep water zones in southern, central and northern Baikal, specifically the central portion of the lake and the two littoral areas adjacent to the eastern and western shores, as well as embayments, the strait of Maloye More, and the Selenga shallows.

The basis of the model consisted of two-layered segments. The water area of the lake was divided into 65 fundamental areas of equal size, so that each of them covered a region which was characteristic in its hydrometeorologic aspect (Figure 1). The size of each fundamental area was 484 km^2, selected so that a single area could cover either of the large bays, Chivyrkuyskiy and Barguzinskiy. Beneath these areas are segments consisting of two zones. The upper zone, from 0-50 m depth, is the zone of photosynthesis and the most mobile portion of the body of water. The lower, the destructive zone, extends from 50 m depth to the bottom. The shallow regions contain only the upper zones in their segments.

Exchange between the segments in the horizontal and vertical directions is achieved by advection and turbulent mixing. The system of currents in Lake Baikal is complex, variable, and insufficiently studied. Therefore, this paper seeks only to analyze the overall circulation of the waters of Lake Baikal, specifically, the large-scale movements occurring over long periods of time (Krotova 1969). The basis for the system of overall circulation (Figure 1) was the result of calculations of geostrophic currents from thermal survey data (July-October) covering the entire lake and its individual parts (Krotova 1970) and the mean multiannual dynamic topography of the surface of Lake Baikal (Figure 2). This was obtained by dynamic processing of 2256 hydrologic measurements performed for the months of August and September from 1925 to 1965. The horizontal structure of the overall circulation has been confirmed by the release of 1860 experimental drift bottles, specially designed floats (Pomytkin, 1962), and instrumented measurements from the surface to the bottom over a period of a number of days, both during the ice season and during the navigation season (Verbolov 1977a, 1977b).

The available material indicates that a single cyclonic circulation encompasses the entire lake. Movement is most intensive and continuous from south to north along the eastern shore. On the average, the summer movement is traced from Slyudyanka to Davsha (Figure 2), and reaches depths of 50-75 m. The speed of this shoreline current in southern Lake Baikal reaches 9-13 cm/sec, 5 km from the shore. In the central section, its velocity is 4 cm/sec at 5-8 km from the shore, and in the vicinity of the Svyatoy Nos Peninsula a velocity of 7 cm/sec is reached. North of Davsha, the current weakens, and its vertical thickness decreases to 10-20 m.

The current in the opposite direction - from north to south along the western shore - is not as strong. Its speed is 2-7 cm/sec, and it expands down to 20-50 m depth. In a number of places, it is complicated by an upwelling effect.

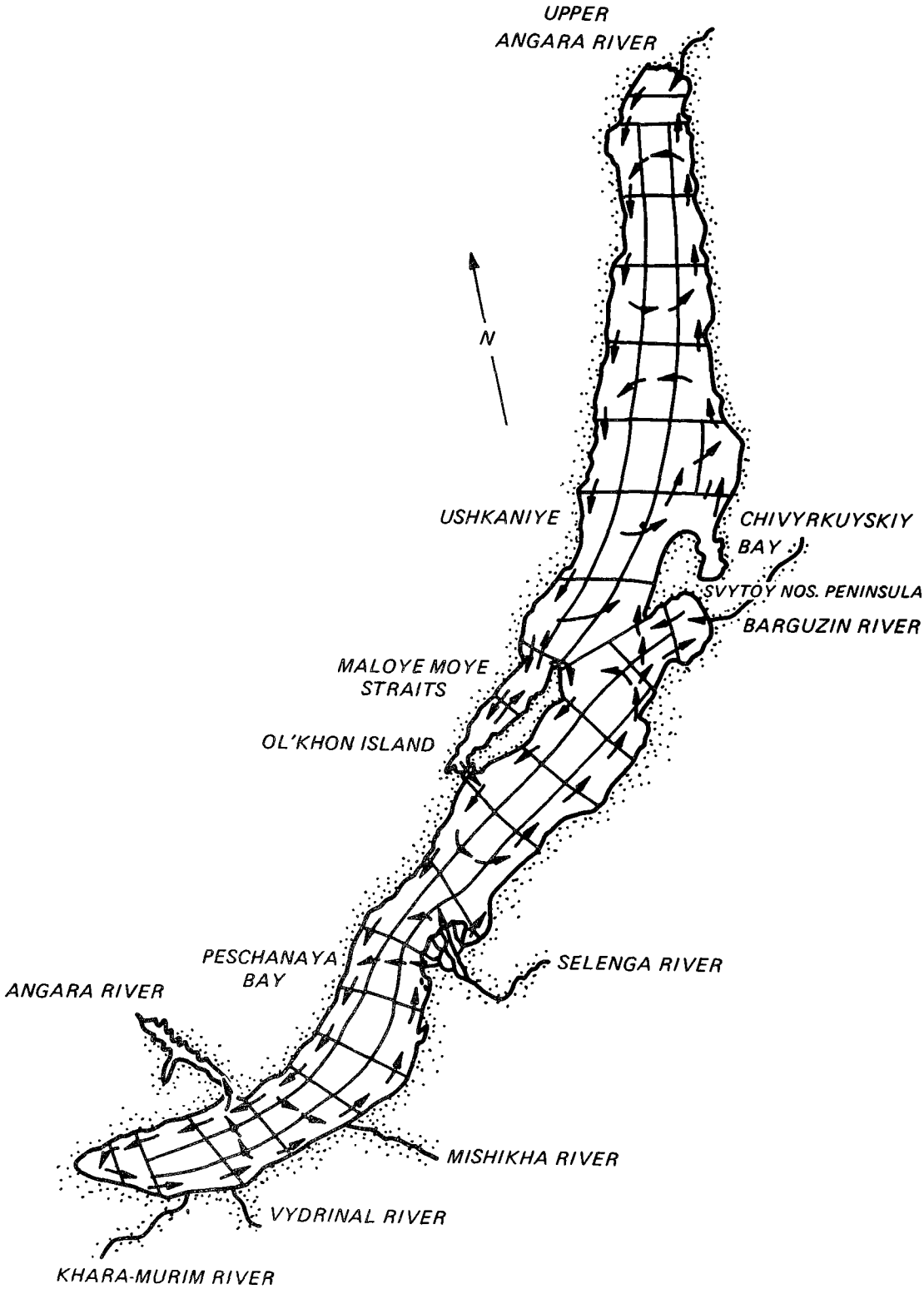

Figure 1. Regionalization of Lake Baikal in the model and direction of horizontal transfer.

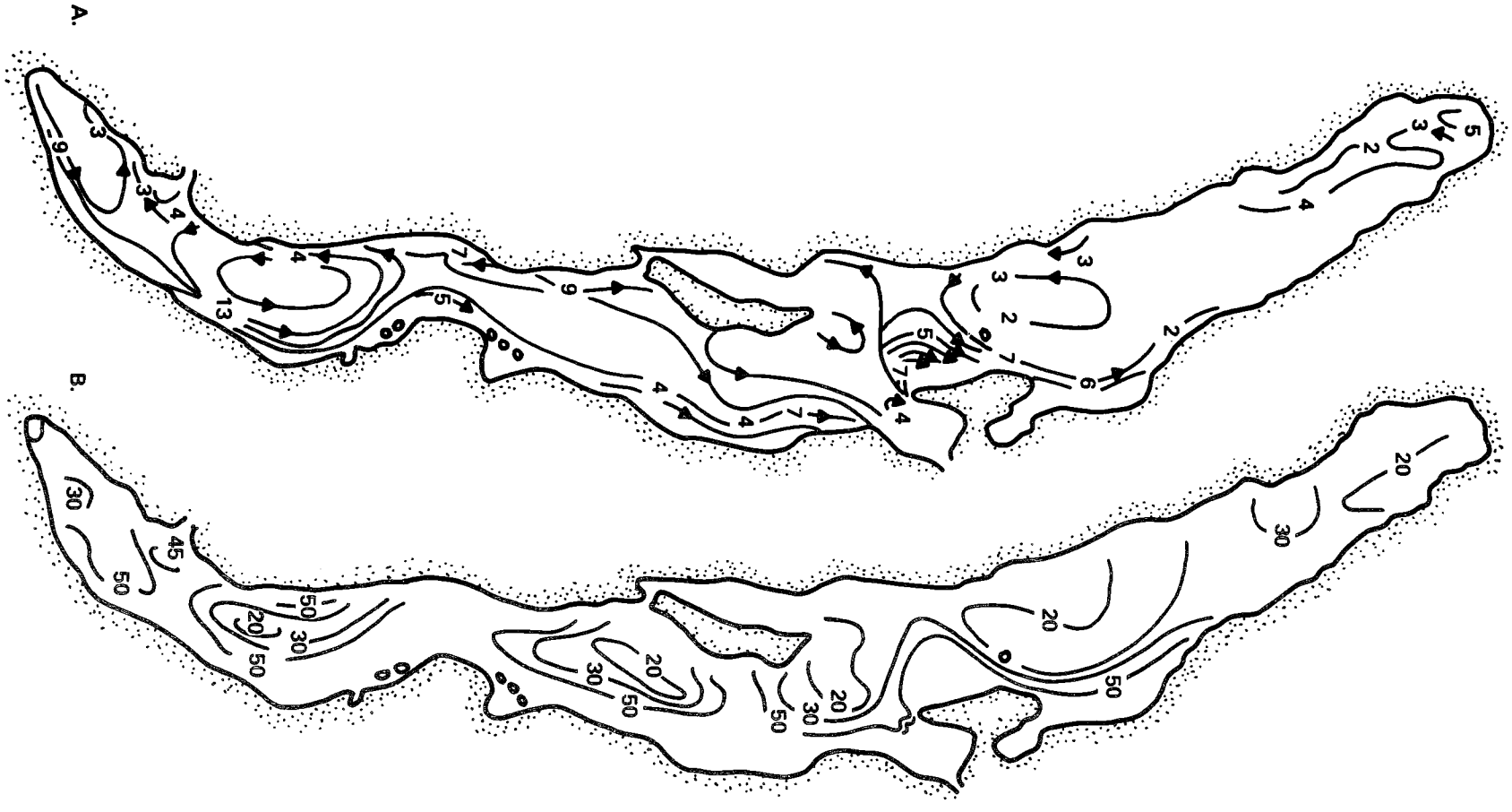

Figure 2. Geostrophic circulation on the surface of Baikal (a) and depth of circulation (b), average for August-September 1925-1965. Speed in cm/sec, vertical thickness in m.

The cyclonic formation, covering almost the entire lake, is divided into quasi-steady circular systems moving in the same direction: one in the southern extremity of the lake, another between Listvenichnyy Bay and the Selenga River delta, a third outside of Olkhon Island, a fourth north of the Ushkaniy Islands, and a fifth in the northern extremity of the lake (Figure 1). The cyclonic circulations are usually elliptical in form. Their transverse horizontal side is comparable to the width of the lake, and their longitudinal dimension reaches $7 \cdot 10^6$-$9 \cdot 10^6$ cm. In the interior, the currents extend much less deeply into the water than at the periphery; the average depth for August-September being 10-15 m. In the region of Listvenichnyy Bay, a quasi-steady anticyclonic circulation is formed, while in Maloye More, Chivyrkuyskiy and Barguzinskiy Bays cyclonic vortices measuring $1.5 \cdot 10^6$ - $4 \cdot 10^6$ cm are formed. Anticyclonic vortex formation is observed during the summer down to 75 m.

On the long axes of the cyclonic circulations are divergence zones, in which we see the highest values of the vertical components of flow speeds, directed upward. We can estimate the order of magnitude of vertical speed on the basis of the relationship of the horizontal (V) and vertical (W) components of the speed and the horizontal (L) and vertical (H) dimensions of the body of water ($V/W = L/H$). Since Lake Baikal is 636 km long and its mean depth is 700 m, the horizontal speeds of 1-10 cm/sec correspond to vertical speeds on the order of 10^{-3} and 10^{-2} cm/sec. Furthermore, we know that the variation in depth of the zero flow surface at Lake Baikal may be as great as 100 m (Krotova 1970). This surface may be wedged out in the central regions of the cyclonic formations, located near the center of the lake, or along its western shore, then drop to a depth of 100 m at the periphery, e.g., along the eastern shore. In this case, W/V is equal to the ratio of the change in thickness of the layer involved in the flow, ΔH, to the distance ΔL over which this change occurs. Assuming V, as before, to be equal to 1 and 10 cm/sec, and ΔL to be 20-40 km, where $\Delta H = 100$ m we produce vertical speeds of the same order of magnitude, 10^{-3} and 10^{-2} cm/sec.

Finally, the time of transfer of a mass of water by the vertical movement from the surface to the bottom should be of the same order of magnitude as the time required to transfer a mass through the entire body of water (Chekotillo 1965). Given the values of horizontal speeds of 1 and 10 cm/sec, and the length of the horizontal path of about 1000 km, the duration of vertical motion is approximately 3 years and 4 months.

In southern Lake Baikal, in addition to divergence zones, local areas of upwelling and downwelling of water as a result of surge phenomena are well known. Upwelling is most clearly expressed in two sections along the west coast, from Kultuk to Cape Polovinny, and from the mouth of the Angara to Cape Goloustny. In the regions of Peschanaya Bay to Cape Bolshoy Kadilny, Tosty Bay to Cape Polovinny, the Khara-Murin River to the Vydrinaya River, the Mishikha River to Istokskiy Sor, the water constantly descends (downwelling). On maps of the dynamic topography, the dynamic horizontals intersect the shoreline (Figure 2a).

In modeling Lake Baikal, it was assumed that the exchange between segments in the horizontal direction occurs as a result of advection, and in

the vertical direction as a result of turbulent diffusion. Furthermore, it was assumed that the direction and speed of the current and level of the water at each point in the lake are constant throughout the entire year. This means that in each unit of time, each segment gives its neighbors as much water as it receives from them. The condition of balance also occurs for any connected subsystem of segments.

The status of the ecosystem of Lake Baikal on each day of year t is determined in the model by the concentrations of the five primary elements: phytoplankton b_1 (k, i), zooplankton b_2 (k, i), detritus b_3 (k, i), bacteria b_4 (k, i) and nutrients b_5 (k, i), where k = 1, 2 is the number of upper and lower zones, i = 1, 2, ..., 65 is the number of each segment. The concentrations are measured in kcal/m^3. Variable b_5 (k, i) does not refer to a specific chemical element, but rather to certain hypothetical nutrients; the energy equivalent of the potential material for the creation of primary production. In the six shallow sections, mentioned earlier, are segments with only a surface zone, so that the total number of zones is 124. Thus, the status of the system is characterized by a vector with 620 components. The time interval is equal to one day.

Calculation of the system status vectors for each step is performed in two stages. In the first stage, biologic processes are simulated (growth, grazing, metabolism, death). They are reflected by the same functions as in the energy model of the Lake Baikal pelagic ecosystem constructed earlier (Ashchepkova et al. 1977). Some of them are calculated with corrections for temperature, which varies significantly in the first zone during the course of the year. It is assumed, in particular, that the optimal temperature for grazing of zooplankton is 10°C (Pomazkova 1970), for the growth of algae, 1.5°C. The daily changes in concentration $\Delta b_j(k, i)$ in this stage are determined from the equations:

$$\Delta b_1(k, i) = P^k - C^k_{12} - Q^k_1 - M^k_1,$$

$$\Delta b_2(k, i) = 0.8 \times (C^k_{12} + C^k_{32} + C^k_{42}) - Q^k_2 - M^k_2,$$

$$\Delta b_3(k, i) = 0.2 \times (C^k_{12} - 4C^k_{32} + C^k_{42}) - C^k_{34} + M^k_1 + M^k_2,$$

$$\Delta b_4(k, i) = C^k_{34} - C^k_{42} - Q^k_4,$$

$$\Delta b_5(k, i) = - P^k + Q^k_1 + Q^k_2 + Q^k_4, \qquad k = 1, 2.$$

where p^k is the rate of photosynthesis, $C^k_{j\ell}$ is the ratio of the ℓth component to the jth, Q^k_j is the cost of metabolism of the jth component, M^k_j is the death of the jth component. In the upper zone P^1 is determined in accordance with the limitation principle of Libikh, in the lower zone $P^2 = 0$.

In the second stage of calculation of the status vector, hydrologic transforms are applied to the vector produced earlier, simulating horizontal and vertical transfer. The transfer coefficients (Figure 3), representing the fraction of the volume of the upper zones of the segments which moves in a given direction during a given day, are calculated from the condition of balance, based on data on current speeds.

Detritus and the accompanying bacteria sink at a constant speed. Phytoplankton is held at the top surface of the water during the ice season. After the ice thaws, most of the algae begin to descend into the deeper layers of water, beyond the photosynthetic zone, due to the loss of floatation by the cells (Skabichevskiy 1960). Thus, the quantity of algae, detritus and bacteria sinking during the course of a day from the upper layer into the lower layer is calculated by the equation

$$V_j^k = \begin{cases} -v_j b_j(1, i), & k = 1, \\ v_j b_j(1, i)/15, & k = 2, \end{cases} \quad j = 1, 3, 4;\ i = 1, 2, \ldots, 65,$$

where v_j is the sinking coefficient:

$$v_j = \begin{cases} 0.05 \text{ for } j = 3, 4 \text{ or } j = 1 \text{ and } t > 150, \\ 0 \text{ for } j = 1 \text{ and other values of } t \end{cases}$$

where t is the time in days.

Since zooplankton can move independently, the long-term sinking of this group is not considered in the model. It is assumed that the distribution of zooplankton through the mass of the water is in accordance with the feeding and thermal conditions of the medium. The diffusion of water is interpreted in the model as exchange between vertical zones, proportional to the difference in concentration of the components they contain:

$$W_j(K, i) = \begin{cases} w_j(i) \times (b_j(2, i) - b_j(1, i)), & k = 1, \\ w_j(i) \times (b_j(1, i) - b_j(2, i)), & k = 2, \end{cases} \quad i = 1, 2, \ldots, 65$$

where $w_j(i)$ is the mixing coefficient in segment i.

Calculations were performed on an BESM-222 computer. In all segments, values of the input functions are assigned for each day of the year: absorbed solar radiation, influence of the photosynthetic processes in the surface zones of segments, and water temperature. These quantities reflect the mean indices of the sum of absorption of solar energy in the southern, middle and northern trenches of the lake over a period of many years, as well as the dynamics of effective temperature in the photosynthetic zone in all parts of the lake (Rossolimo 1957; Bufal 1966; Verbolov 1969). In the lower zones, the temperature is constant and is equal to 4°C. It is assumed

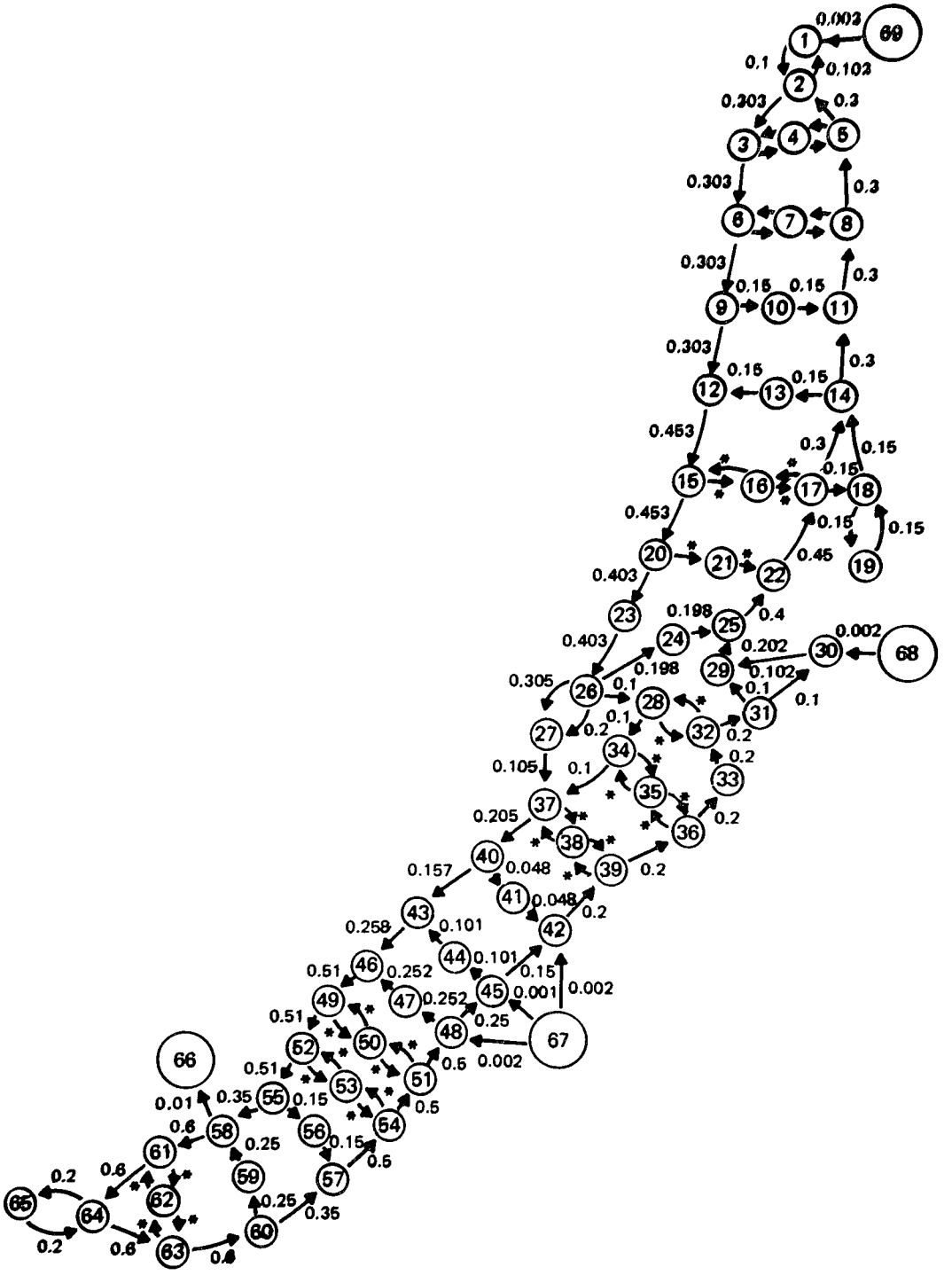

Figure 3. Diagram of horizontal exchange between segments in model. Circles show number of section, arrows show direction of flow, numbers arrows show fraction of volume of upper zone of segment moving in corresponding directions.

in the model that the annual runoff into Lake Baikal is through three rivers, the Selenga, Barguzin and Upper Angara. The Selenga brings in half of all the water, i.e,. 30 km^3/yr. Since the exchange of each of the upper segments is $242 \cdot 10^8$ m^3, the input rate of water from the Selenga into Lake Baikal is equal to about 0.005 of the volume of an upper layer during a day. The flow of water from the Barguzin and Upper Angara is 0.002 and 0.003 times the volume/day, respectively, so that the Upper Angara each day brings in 1 percent of the volume of the upper segment adjacent to its mouth. The rivers bring in more than $4 \cdot 10^5$ tons of organic matter each year, about 2/3 of the total quantity coming in with the Selenga (Votintsev, Popovskaya 1969). If we assume that the remaining quantity of organic matter is divided evenly between the Barguzin and Upper Angara Rivers, the loading to the system corresponding to these rivers will contain the following concentrations of organic matter: Selenga River, 6 g/m^3; Barguzin River, 3.75 g/cm^3; Upper Angara River, 2.5 g/m^3.

At the initial moment in time, January 1, all components of the system are evenly distributed among the segments. By the end of the first year, the transient process is completed, and beginning on January 1 of the next year, the spatial distribution of variables calculated is printed out. Information on the dynamics of the system is generated in the form of maps of the horizontal distribution of any of five components of the ecosystem in the lower or upper layer of the segments, and in the form of graphs of their change with time in the assigned layer for any selected section of the lake.

If the distribution of the concentration of phytoplankton obtained in the model in the upper layer during the course of the year (Figure 4) is examined, it may be compared with the results of observations (Figure 5). Although 1964 characteristically has the longest series of observations on the condition of the plankton, it differs significantly from an average year, primarily in the very richness of the phytoplankton. This was a so-called "mellosing" year, in which the ordinary dynamics of phytoplankton are disrupted: The spring peak of biomass of algae was very great, but there was practically no fall peak at all. Nevertheless, it is possible to compare the qualitative picture of the dynamics of distribution of plankton in the model and in Lke Baikal during the periods of formation and elimination of the spring maximum of biomass.

A comparison of the dynamics of plankton throughout the year in the model with the results of actual surveys leads to the conclusion that, on the whole, the model reflects the actual picture rather well. One major advantage of the model is the fact that it enables the tracing of the path of propagation of matter entering the lake, and considers its transformation in the biologic system. Furthermore, it enables an estimation of how changes in the status of the ecosystem at any point on the lake influence its state in other regions. For scientific purposes, the model is also useful as a research tool, revealing the key processes necessary for prediction of the behavior of the system. It enables a determination of the direction of further scientific research, outlining the contours of the problems for economic model for planning and prediction of the economic development of regions adjacent to Lake Baikal.

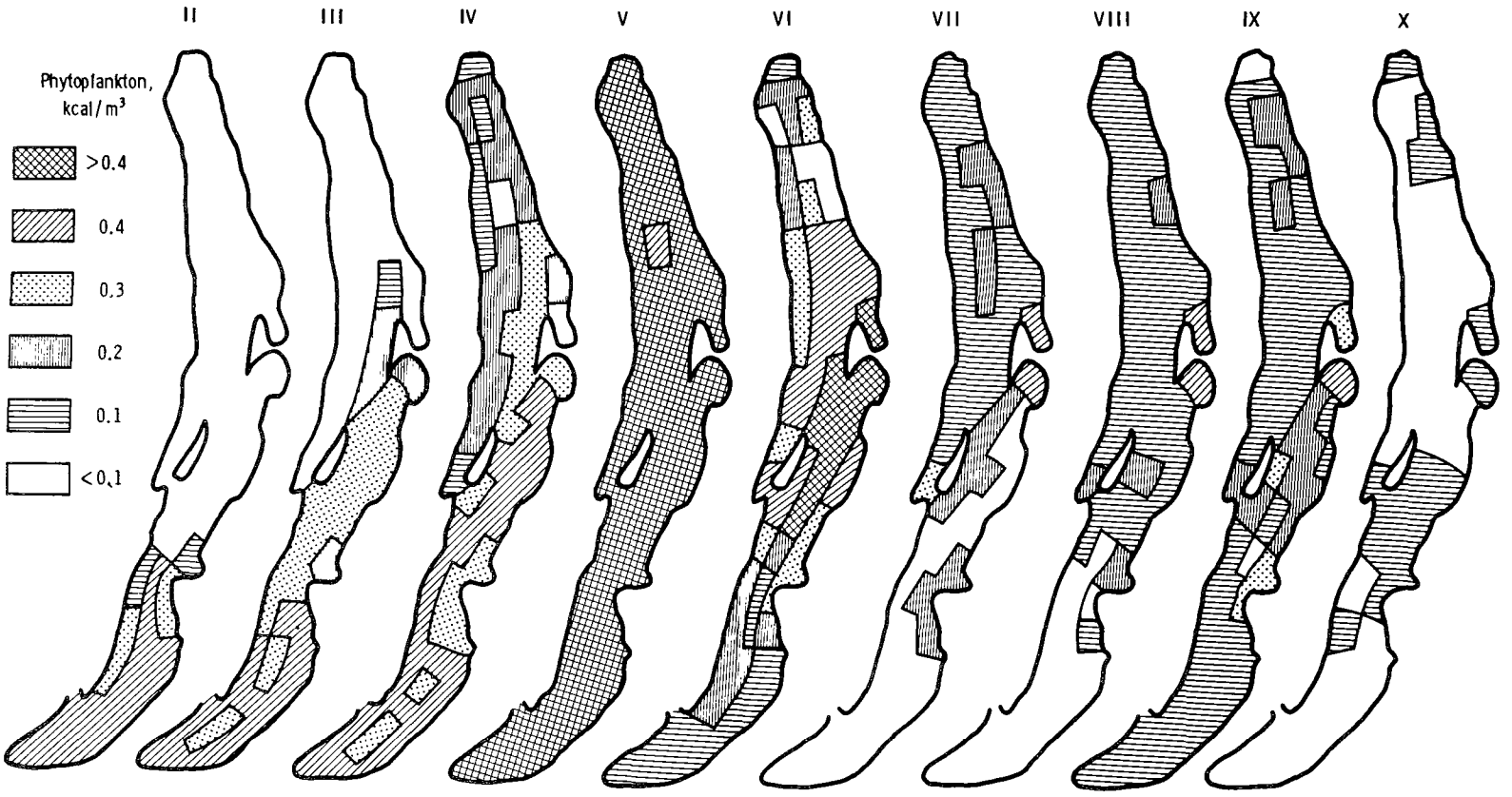

Figure 4. Horizontal distribution of phytoplankton throughout the year in the 0-50 m layer (generated by model).

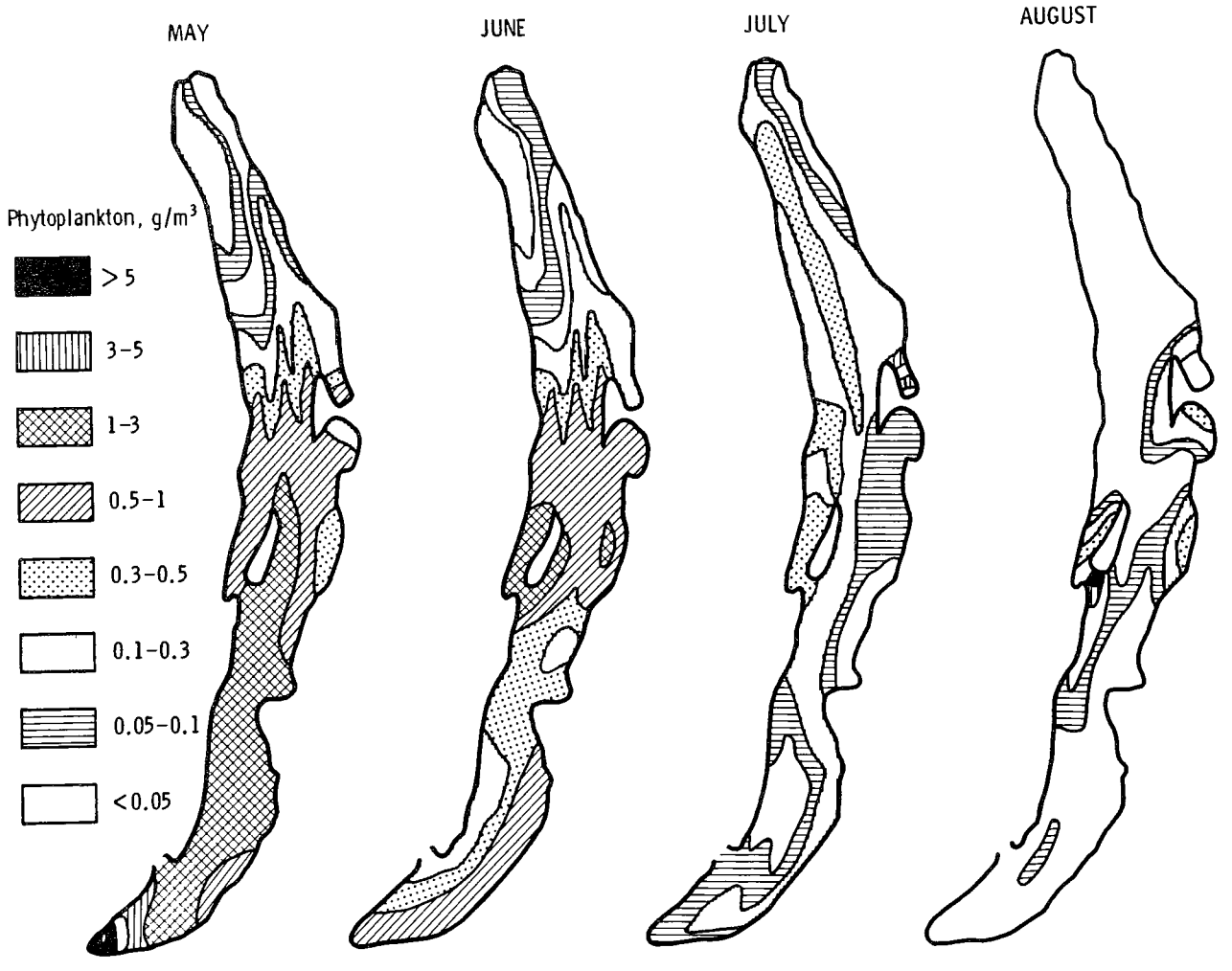

Figure 5. Distribution of phytoplankton in Lake Baikal in the 0-25 m layer in 1964 (after Votintsev, et al. 1975).

REFERENCES

Ashchepkova, L.Ya., V.I. Gurman, and O.M. Kozhova. 1978. An energetic model of the pelagic community of Lake Baikal. Modeli prirodnykh sistem. Nauka Press, Novosibirsk, pp. 51-57.

Bufal, V.V. 1966. The radiation regime of the Baikal trench and its role in the formation of climate. Klimat ozera Baykal i Pribaykalya. Nauka Press, Moscow, pp. 34-71.

Chekotillo, K.A. 1965. The time of vertical transfer of water in the ocean. Okeanologicheskiya issledovaniya, 13, pp. 24-29.

Kozhov, M.M. 1962. Biology of Lake Baikal. Acad. Sci. USSR Press, Moscow, p. 315.

Krotova, V.A. 1969. The water balance. Level. Currents. Wave action. Atlas Baykala. Main Administration for Geodesy and Cartography, Irkutsk-Moscow, pp. 12-13.

Krotova, V.A. 1970. Geostrophic circulation of the waters of Baikal during the period of direct thermal stratification. Techeniya i diffuziya vod Baykala. Nauka Press, Leningrad, pp. 11-14.

Pomazkova, G.I. 1970. Zooplankton of Lake Baikal. Auth. abst. diss. for degr. of Cand. Biol. Sci., Irkutsk, p. 22.

Pomytkin, B.A. 1962. Some information on currents in the southern portion of Baikal. Meteorologiya i gidrologiya, 11, pp. 47-49.

Rossolimo, L.L. 1957. Temperature regime of Lake Baikal. Acad. Sci. USSR Press, Moscow, p. 551.

Skavichevskiy, A.P. 1960. Planktonic diatoms of fresh waters in the USSR. Moscow State University Press, Moscow, p. 352.

Verbolov, V.I. 1969. The temperature of the surface of a lake. The radiation balance. Total absorbed radiation. Effective radiation. Atlas of Baikal, Main Administration for Geodesy and Cartography, Irkutsk-Moscow, p. 11.

Verbolov, V.I. 1977a. Horizontal currents in Baikal. The ice season. Techeniya v Baykale. Nauka Press, Novosibirsk, pp. 10-16.

Verbolov, V.I. 1977b. General characteristics of the currents during the navigation season. Techeniya v Bayale. Nauka Press, Novosibirsk, pp. 43-62.

Votintsev, K.K. and G.I. Popovskaya. 1969. Phytoplankton and water chemistry. Atlas of Baikal. Main Administration for Geodesy and Cartography, Irkutsk-Moscow, p. 20.

Votintsev, K.K., A.I. Meshcheryakova, and G.I. Popovskaya. 1975. The cycle of organic matter in Lake Baikal. Nauka Press, Novosibirsk, p. 190.

SECTION 19

THE TASK OF OPTIMAL PLANNING OF DISCHARGE OF POLLUTANTS IN A DYNAMIC MODEL OF SELF-PURIFICATION OF A BODY OF WATER

O.M. Kozhova and L.T. Aschepkova[1]

SUPPLEMENTARY RESULTS

We will be studying the vector differential equation

$$\dot{x} = f(x,w), \quad x(t\ ) = h(v) \tag{1}$$

with the parameters $w \in R^m$, $v \in R^r$. The function $h:R^r \to R^n$ is assumed continuously differentiable. The function $f:R^n \times R^m \to R^n$ is continuous along with its derivatives, with the exception of the smooth manifold

$$p_1(x,w) = 0, \ \ldots, \ p_s(x,w) = 0 \tag{2}$$

of dimensionality $n + m - 1$, on which finite discontinuities in its value are permitted. The solution of Equation (1) with the discontinuous right portion is taken from A.F. Filippov (1960). As was shown in his work, the solution exists at least in a small region of the initial values.

Let us fix the number $t_1 > t_0$ and determine the mapping $(v,w) \to I(v,w)$, assuming

$$I(v,w) = \Phi(x(t_1)),$$

where the solution $x(t)$ of Equation (1), corresponding to v,w, is defined for $t_0 \leq t \leq t_1$, and $I(v,w) = +\infty$ otherwise. Here $: R^n \to R$ is an assigned function of the class $C_1(R^n)$. In what follows, the question of derivatives of the function I is of interest. Thus, the corresponding results are presented (Aschepkov, Badam 1977).

Suppose the solution $x(t)$ of Equation (1), corresponding to fixed v,w, exists where $t_0 \leq t \leq t_1$, and at instances $t = \tau_1, \ldots, \tau_s$ it successively intersects the surfaces of Equation (2) such that

---

[1]Irkutsk State University, 1 K. Marks Avenue; 664003 Irkutsk, USSR.

$$t_0 < \tau_1 < \ldots < \tau_s < t_1,$$

$$p_i(x(\tau_i),w) = 0,\ p_j(x(\tau_i),w) \neq 0,\ i \neq j,$$

$$\dot{p}_i(x(\tau_i-),w)\ p_i(x(\tau_i+),w) > 0,\ i,j = 1, \ldots, s. \tag{3}$$

Condition (3) implies that the phase point at moment $t = \tau_i$ falls only on one surface $p_i(x,w) = 0$, approaching and departing at non-zero angles; $\dot{p}_i(x(\tau_i+), w)$ has the sense of the corresponding one-sided derivative of function $p_i(x(t), w)$ with respect to t, on the strength of Equation (1). Let us relate to $x(t)$, w the vector function $\bar{\bar{\psi}}$: $[t_0, t_1] \to R^n$, the solution of the conjugate differential equation

$$\dot{\psi} = -\ H_x(\psi,x(t),w),\ \psi(t_1) = \psi_x(x(t_1)) \tag{4}$$

with the condition of a jump at moment $t = \tau_i$:

$$\psi(\tau_i-) = \psi(\tau_i+) + \mu_i\ p_{ix}(x(\tau_i),w),$$

$$\mu_i = -\ \psi'(\tau_i+)\ \Delta\dot{x}(\tau_i)\ /\ \dot{p}_i(x(\tau_i-),w),$$

$$\Delta\dot{x}(\tau_i) = \dot{x}(\tau_i-) - \dot{x}(\tau_i+),\ i = 1, \ldots, s. \tag{5}$$

where $H(\psi,x,w) = \psi' f(x,w)$ is a Hamiltonian function, ' is the sign of transposition. Due to the linearity of Equation (4) and the unambiguity of the conditions of the jump (5), the solution of $\psi(t)$, $t_0 \leq t \leq t_1$, not only exists but is unique.

Under the assumptions made above, function I has at point v,w the partial gradients I_v, I_w, which are calculated by the equations

$$I_v(\bar{\bar{v}},\bar{\bar{w}}) = h'_v(v)\ \psi(t_0),$$

$$I_w(v,w) = \sum_{i=1}^{s} \mu_i\ p_{iw}(x(\tau_i),w) +$$

$$+ \int_{t_0}^{t_1} H_w(\psi(t),\ x(t),w)\ dt. \tag{6}$$

The procedure of calculation of the derivatives can be organized, e.g., as follows:

1. Equation (1) is integrated forward in time, and the quantities i, τ_i, $x(\tau_i-)$, $\dot{x}(\tau_i+)$ are recorded;

2. Equation (1), (4), (5) are integrated in reverse time with the known initial values $x(t_1)$, $\psi(t_1)$ and with the additional equation

$$\dot{y} = -H_w(\psi,x,w),\ y(t_1) = 0. \tag{7}$$

In the process of integration, the sum z_k of vectors $\mu_i\ p_{iw}(x(\tau_i),w)$, i=s, s-1, ..., k, is accumulated sequentially for k=s, s-1, ..., 1. The derivatives of interest to us are calculated through the values of $\psi(t_0)$, $y(t_0)$ and z_1 known up to time $t = t_0$. In particular,

$$I_w(v,w) = y(t_0) + z_1.$$

With this method of calculation, the minimum of computer memory is used and the final result is obtained with errors resulting only from the system of numerical integration and the rounding errors. However, the computation time increases due to the "extra" integration of Equation (1) in reverse time. Depending on the specifics of the problems being solved, of course, other versions of calculation of the derivatives are possible (Rozenvasser 1967; Pshenichnik and Danilin 1968).

DESCRIPTION OF THE MODEL OF SELF-PURIFICATION OF A BODY OF WATER

Consider the analysis of a certain body of water of constant depth with predominant horizontal circulation of the water. A polluting substance enters the body of water through a point source at rate u, and is carried by the currents over the water area. In terms of level of concentration x_3 of the pollutant, the various sections of the reservoir can be divided as relatively pure, moderately polluted and strongly polluted, where, respectively,

$$x_3 < c_0,\ c_0 < x_3 < c_1,\ x_3 > c_1\ (c_0,\ c_1 = \text{const}).$$

In areas with different levels of pollution, the composition of the aquatic communities are also different. In strongly polluted areas, species predominate which are capable of breaking down the pollutant (decomposers). Relatively pure areas are populated by organisms which previously inhabited the pure body of water and have adapted to the new conditions. The activity of the decomposers characterizes the self-purifying capability of the body of water.

The concentration of organisms inhabiting the pure medium before the pollutant was introduced may be represented by x_1, while x_2 represents the concentration of decomposers. The rate of change of x_1, x_2 and x_3 depends on the concentration x_3 at a given instant in time t. In the model, using certain simplifying assumptions, we assume:

$$\dot{x}_1 = x_1(a_1-a_2x_1),\ \dot{x}_2 = 0,\ \dot{x}_3 = v, \quad \text{if } x_3 \quad c_0;$$

$$\dot{x}_1 = x_1(a_3-a_4x_1-a_5\ \ x_2),\ \dot{a}_2 = a_6\ \theta\ x_2x_3,$$

$$\dot{x}_3 = -a_7 x_2 x_3, \quad \text{if } c_0 < x_3 < c_1;$$

$$\dot{x}_1 = 0, \ \dot{x}_2 = a_6 \ x_2 x_3, \ \dot{x}_3 = -a_7 \theta x_2 x_3 + v, \quad \text{if } x_3 > c_1. \tag{8}$$

Here $a_1, \ldots, a_7$ are non-negative constant coefficients; $\theta = \theta(t)$ is the water temperature at time t; v is a term resulting from water exchange. The values of v are defined as follows. The body of water is approximated by a system of k chambers. Each of them is a parallelepiped with identical top surface area, the height of which is equal to the depth of the body of water. Each number j of the jth chamber relates to a set J_j of numbers of neighboring chambers, with $|J_j| = 4$ elements, while λ_{ji} are the fractions of the volume of water carried by the current from j into chamber i per unit time. The order of numbering of the elements J_j is indicated in Figure 1. If the quantity of neighboring chambers is less than 4, the corresponding elements J_j and numbers λ_{ji} are assumed equal to zero. The values x_1, x_2, x_3 and v relating to the jth chamber are represented by x_1^j, x_2^j, x_3^j, v^j. Obviously, the sums:

$$\sum_{i \varepsilon J_j} \lambda_{ji} x_3^j, \quad \sum_{i \varepsilon J_j} \lambda_{ij} x_3^j$$

are proportional to the quantity of pollution in the outflows and inflows for the jth chamber per unit time. Then

$$v^j = -\sum_{i \varepsilon J_j} \lambda_{ji} x_3^j + \sum_{i \varepsilon J_j} \lambda_{ij} x_3^j + \delta_{qj} u, \tag{9}$$

where q is the designator for the chamber containing the source of pollution, δ_{qj} is Kroneker's delta function ($\delta_{qj} = 0$ where $j \neq q$, $\delta_{qq} = 1$). Assuming that the change in concentrations x_1^j, x_2^j and x_3^j in each jth, chamber, $j = 1, \ldots, K$, is described by the same equations (8), we obtain a simple model for self-purification of the body of water in the form of a system of 3K differential equations, the right portions of which are discontinuous on the surfaces

$$x_3^j - c_0 = 0, \ x_3^j - c_1 = 0, \ j = 1, \ldots, K. \tag{10}$$

The task of control of the process of self-purfication is formulated as follows. Suppose that with a constant rate of dumping of the pollutant $u(t) = u_0$, $t \leq 0$, the system is in equilibrium $x_i^j(t) = x_{i0}^j$, $i = 1, 2, 3$, $j = 1, \ldots, k$. During the period [0, T], the quantity of pollutant dumped into the body of water is A, and the rate of discharge is

$$u_0 \leq u \leq u_1 \qquad \left(\int_0^T u(t)dt = A\right). \tag{11}$$

We represent by $z_+ = \max\{0, z\}$, the "section" of quantity z for which the indirect index of strong pollution of the body of water is the integral

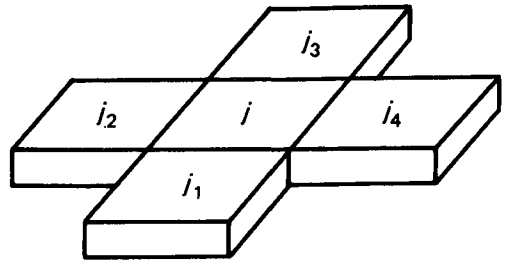

Figure 1. $j_j = (j_1, j_2, j_3, j_4)$

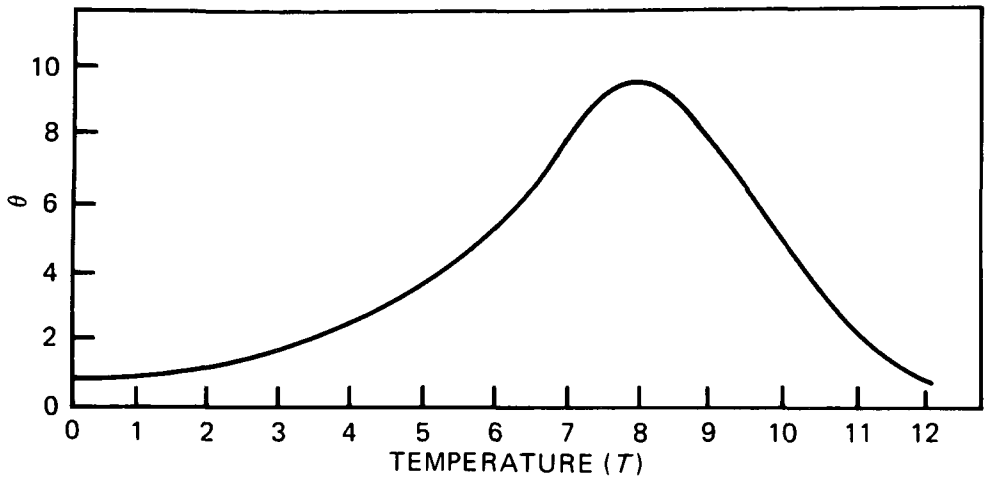

Figure 2. Temperature curve.

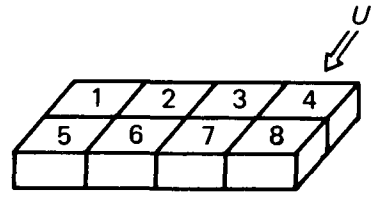

Figure 3. Subdivision of body of water into chambers.

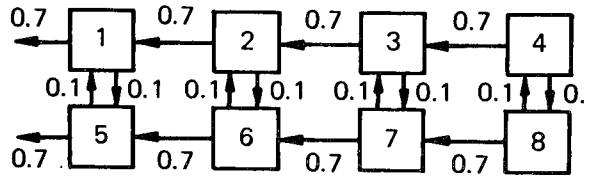

Figure 4. Diagram of water exchange.
Figures show fraction λ_{ij} of volumes of chamber carried by current per unit time.

$$I(u) = \int_0^T \sum_{j=1}^{K} [x_3^j - c_1]_+^2 \, dt. \tag{12}$$

The problem is to determine the rate of discharge of the pollutant in the form of a function of t, piecewise continuous over [0, T], satisfying limitations (11) and minimizing function (12).

With one additional assumption, this problem can be reduced to a problem with parameters. The sector [0, t] may be broken into m pairs of adjacent intervals $T_1, \ldots, T_m$ of identical length $h = T/m$. In each of these intervals, the control may be regarded as constant:

$$u(t) = w_i, \; t \in T_i, \; i = 1, \ldots, m. \tag{13}$$

The limitations (11) for Equation (13) take on the form

$$u_0 \leq u \leq u_1, \; i = 1, \ldots, m; \; \sum_{i=1}^{m} w_i = A/h. \tag{14}$$

To the equations for x_1^j, x_2^j and x_3^j, may be added the additional differential equations

$$\dot{x}_0 = \sum_{j=1}^{K} [x_3^j - c_1]_+^2, \; \dot{x}_4 = 1 \quad (x_0(0) = 0, \; x_4(0) = 0)$$

for calculation on integral (12) and time ($t = x_4(t)$). To Equation (10) for the discontinuity surfaces, additional equations may be added,

$$x_4 - ih = 0, \; i = 1, \ldots, m-1,$$

defining the moments of discontinuity of control (13). As a result, we obtain a problem of the same type as specified in the first paragraph. Find the vector of parameters $w = (w_1, \ldots, w_m)$ satisfying limitations (14) and achieving the minimum of the functional

$$I(w) = x_0(T), \tag{15}$$

assigned on the trajectory of the system

$$\dot{x}_0 = \sum_{j=1}^{K} [x_3^j - c_1]_+^2;$$

$$\dot{x}_1^j = x_1^j(a_1 - a_2 x_1^j), \; \dot{x}_2^j = 0, \; \dot{x}_3^j = v^j, \quad \text{if } x_3^j < c_0;$$

$$\dot{x}_1^j = x_1^j(a_3 - a_4 x_1^j - a_5 \, \theta \, \dot{x}_2^j), \; x_2^j = a_6 \, \theta \, x_2^j x_3^j,$$

$$\dot{x}_3^j = -a_7 \, \theta \, x_2^j x_3^j + v^j, \quad \text{if } c_1 < x_3^j < c_1;$$

$$\dot{x}_1 = 0,\ \dot{x}_2^j = a_6\ \theta\ x_2^j x_3^j,\ \dot{x}_3^j = -a_7\ \theta\ x_2^j x_3^j + v^j,$$

$$\text{if } x_3^j > c_1;\ j=1,\ \ldots,\ k;$$

$$\dot{x}_4 = 1, \tag{16}$$

with the initial conditions

$$x_0(0) = 0,\ x_4(0) = 0,$$

$$x_i^j(0) = x_{i0}^j,\ i = 1,\ 2,\ 3,\ j = 1,\ \ldots,\ k. \tag{17}$$

The right parts of system (16) have finite discontinuities on the surfaces

$$p_j = x_3^j - c_0 = 0,\ p_{k+j} = x_3^j - c_1 = 0,\ j = 1,\ \ldots,\ k,$$

$$p_{2k+i} = x_4 - ih = 0,\ i = 1,\ \ldots,\ m - 1. \tag{18}$$

The function v^j is defined by Equation (9).

METHODS OF SOLUTION OF THE CONTROL PROBLEM

In order to find the optimal parameters in Equations (13) - (18), the gradient-type iterational minimization methods may be used. Let us the equations used to calculate the derivatives of goal function (15). We compose the function

$$H = \psi_0 \sum_{j=1}^{k} [x_3 - c_1]_+^2 + \sum_{j=1}^{k} H_i + \psi_4 \cdot 1,$$

$$H_j = \psi_1^j x_1^j (a_1 - a_2 x_1^j) + \psi_3^j v^j, \qquad \text{if } x_3^j < c_0;$$

$$H_j = \psi_1^j x_1^j (a_3 - a_4 x_1^j - a_5\ \theta\ x_2^j)$$

$$+ \theta\ x_2^j x_3^j (a_6 \psi_2^j - a_7 \psi_3^j) + \psi_3^j v^j, \quad \text{if } c_0 < x_3^j < c_1;$$

$$H_j = \theta\ x_2^j x_3^j (a_6 \psi_2^j - a_7 \psi_3^j) + \psi_3^j v^j, \quad \text{if } x_3^j < c_1$$

and use it to write the conjugate equations of (4):

$$\dot{\psi}_0 = -\ H_{x_4} = 0,\ \dot{\psi}_4 = -\ H_{x_4} = 0, \tag{19}$$

$$\dot{\psi}_i^j = -\ H_{x_i} j,\ i = 1,\ 2,\ 3,\ j = 1,\ \ldots,\ k \tag{20}$$

with the initial conditions

$$\psi_0(T) = 1,\ \psi_4(T) = 0,$$

$$\psi_i^j(T) = 0,\ i = 1, 2, 3,\ j = 1, \ldots, k. \tag{21}$$

Suppose the fixed $w_1, \ldots, w_m$ correspond to the solution $x_0(t)$, $x_i^j(t)$, $x_4(t)$ of system (16)-(17), intersecting at times $\tau_1, \ldots, \tau_s$, $0 < \tau_1 < \ldots < \tau_s < T$, the surfaces (18) with numbers $i_1, \ldots, i_s$ $\{1, 2, \ldots, 2k + m - 1\}$ such that conditions such as (3) are fulfilled. This occurs, e.g., for those τ_ℓ for which $i_\ell > 2k$. Since Equation (18) of the discontinuity surfaces is independent of x_0, it follows then from the conditions of the jump (5) that function $\psi_0(t)$ is discontinuous at times $t = \tau_\ell$. Consequently, on the strength of (19) and (21), $\psi_0(t) = 1$. The conditions of the jump for the remaining conjugate variables become

$$\psi_i^j(\tau_\ell-) = \psi_i^j(\tau_\ell+) + \mu_\ell\ \partial p_{i_\ell}/\ x_i^j, \tag{22}$$

$$\psi_4(\tau_\ell-) = \psi_4(\tau_\ell+) + \mu_\ell\ \partial p_{i_\ell}/\partial x_4, \tag{23}$$

$$i = 1, 2, 3,\ j = 1, \ldots, k,\ \ell = 1, \ldots, s,$$

where

$$\mu_\ell = \begin{cases} \sum_{i=1}^{3} \psi_i^{i_\ell}(\tau_\ell+)\ \Delta\dot{x}_i^{i_\ell}(\tau_\ell)/x_3^{i_\ell}(\tau_\ell-), & 1 \le i_\ell \le k, \\ \sum_{i=1}^{3} \psi^{i_\ell-k}(\tau_\ell+)\ \Delta\dot{x}^{i_\ell-k}(\tau_\ell)/x^{i_\ell-k}(\tau_\ell-), & k < i_\ell \le 2k, \\ \sum_{i=1}^{3} \psi_i^2(\tau_\ell+)\Delta\dot{x}_i^2(\tau_\ell), & i_\ell > 2k, \end{cases}$$

$$\partial p_{i_\ell}/\partial x_i^j = \begin{cases} 1, & (i = 3,\ 1 \le i_\ell \le 2k) \vee (j = i_\ell \vee j = i_\ell - k), \\ 0, & \text{otherwise} \end{cases}$$

$$\partial p_{i_\ell}/\partial x_4 = \begin{cases} 1, & i_\ell > 2k, \\ 0, & i \le i_\ell \le 2k. \end{cases} \tag{24}$$

We can see from Equations (23) and (24) that the function $\psi_4(t)$ is piecewise continuous. At times of switching of control, i.e., at the ends of intervals T_i, it has first-order discontinuities. At these same times, the functions $\psi_i^j(t)$, as Equations (22) and (24) show, remain continuous. Writing the second equation of (6) for this problem, we produce the required values of derivatives of the functions (15) in the form

$$I_{w_i}(w) = \int_{T_i} \psi_3^2(t)dt,\ i = 1, \ldots, m. \tag{25}$$

The algorithm for calculation of derivatives described in the first paragraph can be applied to this case without significant changes. Instead of system (7) of supplementary differential equations, it is expedient to introduce the scalar equation

$$y = -\psi_3^2.$$

If we integrate this equation together with the initial and conjugate equations in sequence over sections T_i, $i = m, m - 1, \ldots, 1$ with the initial conditions $y(ih) = 0$, at times $t = (i - 1)h$ we will have

$$I_{w_i}(w) = y((i-1)h), \; i = m, m - 1, \ldots, 1.$$

Using the derivatives of (25), we can realize various gradient procedures of minimization of goal function (15) considering the limitations of (14). The theory and practice of solution of such problems is discussed in detail elsewhere (Fiacco and McCormick 1968; Himmelblau 1972; Demyanova and Rubinov 1968; Levitin and Polyak 1966).

RESULTS OF CALCULATION

Equations (13) - (18) were solved on a BESM-6 electronic computer with the following initial data:

$$K = 8, \; m = 12, \; q = 4, \; T = 12,$$

$$c_0 = 0.6, \; c_1 = 1.9; \; u_0 = 0, \; u_1 = \infty, \; A = 15;$$

$$a_1 = a_3 = 0.1, \; a_2 = a_4 = 0.001, \; a_5 = 0.01, \; a_6 = a_7 = 0.001;$$

$$x_{10}^j = 100, \; x_{20}^j = 10^{-5}, \; x_{30}^j = 0, \; j = 1, \ldots, 8.$$

The graph of function $\theta(t)$, a diagram of the subdivision of the body of water into chambers, and the values of water exchange are shown in Figures 2, 3, and 4.

The research for the optimal parameters $w^* = (w_1^*, \ldots, w_{12}^*)$ was performed by the method of the arbitrary gradient (Demyanov and Rubinov 1968) by the iterational plan:

$$w^{\nu+1} = w^\nu + \alpha_\nu(\overline{w}^\nu - w^\nu),$$

$$I'_w(w^\nu)\,\overline{w}^\nu = \min_{w \in W} I'_w(w^\nu)\,w,$$

$$I(w^{\nu+1}) = \min_{0 \le \alpha \le 1} I(w^\nu + (\overline{w}^\nu - w^\nu)), \; \nu = 0, 1, \ldots,$$

where w is the area of permissible values of parameters defined by the conditions of (14). The conditions of convergence of the method are presented

by Levitin and Polyak (1966). As the initial approximation, we can select the point w^0 with coordinates $w_i^0 = 15/12$, $i = 1, \ldots, 12$. The temperature curve was interpolated with respect to 6 shifting nodes by the method of Lagrange. The integration of the differential equations was performed by the explicit method of Euler with a step of 0.01. The optimal values of the parameters were produced in the second iteration

$$w_1^* = w_3^* = \ldots = w_{12}^* = 1.225, \; w_3^* = 1.525,$$

where $I(w^*) = 0$. The dynamics of propagation of the pollutant over the body of water, corresponding to the optimal level of discharge, are shown in Figure 5.

ACKNOWLEDGEMENTS

The authors express their gratitude to N.I. Baranchikova, who performed the calculations.

REFERENCES

Ashchepkov, L.T. and U. Badam. 1977. Theoretical and computational aspects of parametric optimization of systems with discontinuous right parts. Abstracts of reports of 4th National Conference on Problems of Theoretical Cybernetics, Institute of Mathematics, Siberian Affiliate, USSR Acad. Sci., Novosibirsk, pp. 86-87.

Demyanov, V.F. and A.M. Rubinov. 1968. Approximate methods of solution of extreme problems, Leningrad State University Press, 180 pp.

Fiacco, A.V. and Y.P. McCormick. 1968. Nonlinear programming: sequential unconstrained minimization techniques. J. Wiley & Sons, Inc., New York-London-Sydney-Toronto, 240 pp.

Filippov, A.F. 1960. Differential equations with discontinuous right part. Matematicheskii sbornik, 51(93), No. 1, pp. 99-128.

Himmelblau, D.M. 1972. Applied nonlinear programming. McGraw-Hill Book Co., 536 pp.

Levitin, Ye.S. and B.T. Polyak. 1966. Methods of minimization with limitations. Zh. vychislitel'noy matematiki i matematicheskoy fiziki, 6, No. 6, pp. 787-823.

Pshenichnyy, B.N. and Yu.M. Danilin. 1968. Differentiability of the solution of systems of differential equations with discontinuous right parts on the basis of the initial value. Teoriya optimal'nykh reshenii No. 1, Institute of Cybernetics, Ukrainian Acad. Sci., Kiev, pp. 64-68.

Rozenvasser, Ye.N. 1967. General equations of sensitivity of discontinuous systems. Avtomatika i telemekhanika, No. 3, pp. 52-56.

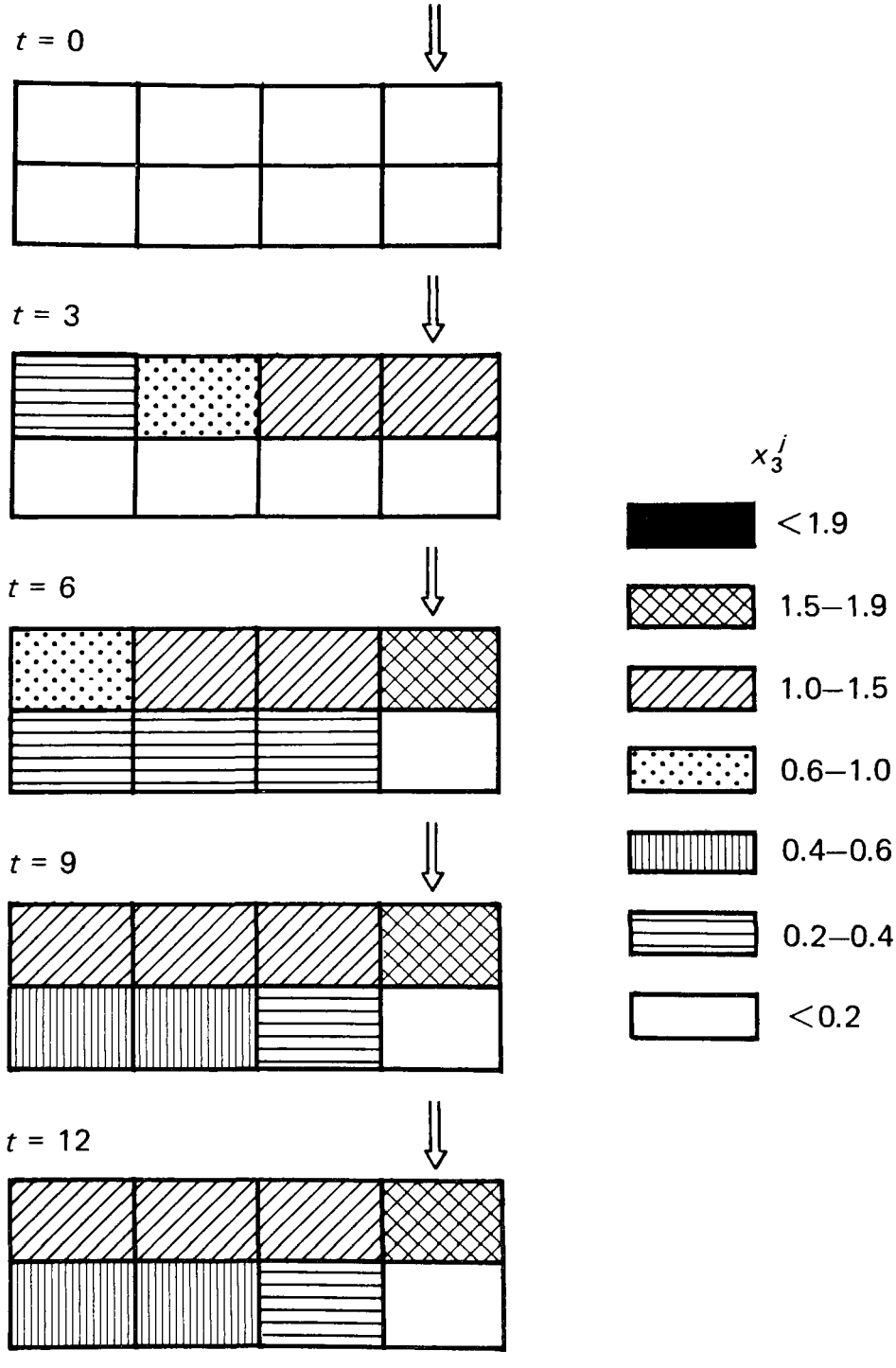

Figure 5. Propagation of a pollutant through a body of water corresponding to optimal discharge levels.

TECHNICAL REPORT DATA
(Please read Instructions on the reverse before completing)

1. REPORT NO. EPA-600/9-80-033	2.	3. RECIPIENT'S ACCESSION NO.
4. TITLE AND SUBTITLE PROCEEDINGS OF THE SECOND AMERICAN-SOVIET SYMPOSIUM ON THE USE OF MATHEMATICAL MODELS TO OPTIMIZE WATER QUALITY MANAGEMENT		5. REPORT DATE July 1980 issuing date 6. PERFORMING ORGANIZATION CODE
7. AUTHOR(S) Environmental Protection Agency - USA Institute of Mechanics and Applied Mathematics - USSR		8. PERFORMING ORGANIZATION REPORT NO.
9. PERFORMING ORGANIZATION NAME AND ADDRESS Large Lakes Research Station Environmental Research Laboratory-Duluth Grosse Ile, Michigan 48138		10. PROGRAM ELEMENT NO. A30B1A 11. CONTRACT/GRANT NO. Joint US-USSR Project 02.02-12
12. SPONSORING AGENCY NAME AND ADDRESS Environmental Research Laboratory - Duluth, MN Office of Research and Development U.S. Environmental Protection Agency Duluth, Minnesota 55804		13. TYPE OF REPORT AND PERIOD COVERED Inhouse 14. SPONSORING AGENCY CODE EPA/600/03

15. SUPPLEMENTARY NOTES
Performed as part of Project 02.02-12 (Water Quality in Lakes and Estuaries) of U.S.A./U.S.S.R. Environmental Agreement.

16. ABSTRACT

The Joint US-USSR Agreement on Cooperation in the Field of Environmental Protection was established in May of 1972. These proceedings result from one of the projects, Project 02.02-12, Effects of Pollutants on Lakes and Estuaries.

As knowledge related to fate and transport of pollutants has grown, it has become increasingly apparent that local and even national approaches to solving pollution problems are insufficient. Not only are the problems themselves frequently international, but an understanding of alternate methodological approaches to the problem can avoid needless duplication of efforts. This expansion of interest from local and national represents a logical and natural maturation from the provincial to a global concern for the environment.

In general, mankind is faced with very similar environmental problems regardless of the national of political boundaries which we have erected. While the problems may vary slightly in type or degree, the fundamental and underlying factors are remarkably similar. It is not surprising, therefore, that the interests and concerns of environmental scientists the world over are also quite similar. In this larger sense, we are our brother's brother, and have the ability to understand our fellowman and his dilemma, if we but take the trouble to do so. It is this singular idea of concerned scientists exchanging views with colleagues that provides the basic strength for this project.

17. KEY WORDS AND DOCUMENT ANALYSIS

a. DESCRIPTORS	b. IDENTIFIERS/OPEN ENDED TERMS	c. COSATI Field/Group
mathematical models lakes rivers water quality water pollution water flow	US-USSR Agreement in the Field of Environmental Protection Eutrophication Ecosystems	06/D 08/H 12/A 13/B

18. DISTRIBUTION STATEMENT Release to public	19. SECURITY CLASS *(This Report)* Unclassified	21. NO. OF PAGES 410
	20. SECURITY CLASS *(This page)* Unclassified	22. PRICE

EPA Form 2220-1 (9-73)

☆ U.S. GOVERNMENT PRINTING OFFICE: 1980—657-165/0072